An optimised THP-1 cell line model for interrogating the effects of immune complexes on macrophage polarisation

Nikki Alexandra Re

Submitted in accordance with the requirements for the degree of

Doctor of Philosophy

The University of Leeds

School of Medicine

Institute of Molecular Medicine

December, 2017

The candidate confirms that the work submitted is his/her own and that appropriate credit has been given where reference has been made to the work of others

Acknowledgements

I would like to take this opportunity to thank all the people who had a hand in the generation of data for my PhD project and those who have assisted me in the writing of this thesis.

Firstly, I would like to extend special thanks to my supervisors, Professor Ann Morgan, Dr Euan Baxter, Dr James Robinson and Dr Ian Carr whose advice and support were invaluble throughout my PhD. Additionally, I would like to thank Mrs Lubna Shafi for generating RNA-seq libraries for my project, the University of Leeds Next Generation Sequencing facility for sequencing my RNA-seq samples and Dr Agne Antanavicute for bioinformatics support and training.

I would also like to extend my gratitude to the Medical Research Council for funding my PhD project and providing me with the opportunity to contribute to knowledge; without a doubt this has been my most challenging but rewarding experience of my life.

Finally, I would like to thank all of the Molecular Rheumatology team, the staff of level 8 and all friends and family who have provided emotional support during my time at the University of Leeds. Without these people I would not have achieved what I have today, and I will always be grateful for the encouragement and motivation that they have provided.

Abstract

Macrophages are a highly plastic group of cells which polarise into inflammatory or anti-inflammatory subtypes. Independent groups define macrophage subtypes differently, creating an inherent bias for subset-specific markers in the literature. Of additional interest, macrophages express Fc-Receptors and are hence activated by immune complexes (ICs); this has implications for these cells in IC-driven conditions such as rheumatoid arthritis. The acute myeloid leukemia derived THP-1 cell line provides a genetically identical baseline for studying the effects of ICs on macrophage phenotypes. However, a lack of consistency between published protocols on how to generate macrophages from these cells introduces technical issues. Hence the aims here were to identify a panel of macrophage polarisation markers that could be used to optimise a THP-1 cell line model, and to use this system to investigate the effects of immune complexes on monocyte and macrophage transcriptomes.

M1 and M2a markers were isolated from publicly available primary macrophage datasets. THP-1 cell differentiation was optimised by titrating PMA concentration and recovery time. Concentrations of polarising cytokine and duration of cytokine exposure were varied to determine ideal polarisation conditions. RNA-seq was performed to validate the model and to test the effects of IgG1-HAGG on macrophage polarisation.

Novel and established M1 and M2 markers were identified from public datasets. These transcripts were used to develop a THP-1 macrophage differentiation protocol; 5ng/ml PMA for 24h followed by 72h rest in media and subsequent polarisation with 20ng/ml IFNγ + 250ng/ml LPS (M1) or 30ng/ml IL-4 (M2a) for 48h. Comparisons of THP-1 macrophage and MDM datasets suggested that cell line and primary macrophages were similar. Changes in gene expression upon IC treatment appeared to be consistent for monocytes but not macrophages. IC treated Monocytes appeared to be enriched for some immune related genes, and an increase in target genes for specific transcription factors was reported; The IRF3 pathway was highlighted here.

Overall, reliable macrophage polarisation markers have been identified, a THP-1 macrophage polarisation protocol mimicking primary cells has been developed and some interesting pathways have been highlighted in monocytes upon immune complex treatment.

Contents

Figure list

Table list

Abbreviations

ACPA	Anti-citrullinated peptide antibody
ADCC	Antibody-dependent cell-mediated cytotoxicity
AIM2	absent in melanoma 2 protein
AM	Alveolar macrophage
AML	Acute myeloid leukaemia
AP2	Adipocyte protein 2
APC	Antigen presenting cell
CCL	Chemokine ligand
CCR	Chemokine receptor
CD	Cluster of Differentiation
CD200R	cluster of differentiation 200 receptor
ChIP-seq	Chromatin immunoprecipitation sequencing
CNV	copy number variation
CXCL	Chemokine (C-X-C motif) ligand
CXCR	Chemokine (C-X-C motif) receptor
DAMPS	Damage-associated molecular pattern
DC	Dendritic cell
DEG	Differentially expressed gene
DHFR	Dihydrofolate reductase
dNTPs	Deoxynucleotide
DTT	Dithiothreitol
EDTA	Ethylenediaminetetraacetic acid
FCS	Foetal calf serum
FcγR	Fc-gamma receptor
FcγRI	Fc-gamma receptor I

FcγRIIa	Fc-gamma receptor Iia
FcγRIIb	Fc-gamma receptor Iib
FcγRIIc	Fc-gamma receptor Iic
FcγRIIIa	Fc-gamma receptor IIIa
FcγRIIIb	Fc-gamma receptor IIIb
FDR	False discovery rate
FITC	Fluorescein isothiocyanate
FPKM	Fragments Per Kilobase of transcript per Million mapped reads
GM-CSF	Granulate macrophage colony stmulating factor
GO	Gene ontology
GPI	Glycosylphosphatidylinositol
GTF	General Transfer Format
HAGG	Heat aggregated gamma globulin
HLA	Human leukocyte antigen
IC	Immune complex
IFNγ	interferon-gamma
IgM	Immunoglobulin M
ITAMi	Inhibitory-immunoreceptor tyrosine-based activation motif
IKZF1	Ikaros family zinc finger protein 1
IL	Interleukin
IRAK	Interleukin 1 receptor associated kinase
IRAK2	Interleukin 2 receptor associated kinase
IRF1	Interferon response factor 1
ITAM	Immunoreceptor tyrosine-based activation motif
ITIM	Immunoreceptor tyrosine-based inhibitory motif
JAK-1/2	Janus kinase 1/2
LPS	Lipopolysaccharide
M-CSF	Macrophage colony stimulating factor
MDM	monocyte derived macrophage
MHC	Major histocompatibility complex
MyD88	Myeloid differentiation primary response 88
NA1	Neutrophil antigen-1
NA2	Neutrophil antigen-2
NFκB	Nuclear factor kappa-light-chain-enhancer of activated B cells
NK	Natural killer
NLRP3	NACHT, LRR and PYD domains-containing protein 3
NO	Nitric oxide

PAMPS	Pathogen-associated molecular pattern
PBMC	Peripheral blood mononuclear cell
PBS	Phosphate buffered saline
PCR	Polymerase chain reaction
PE	Phycoerythrin
PGE2	Prostaglandin E2
PH	Pleckstrin homology domain
PI3K	Phosphoinositide 3-kinase
PMA	Phorbol myristate acetate
PMA	Phorbol myristate acetate
PPARγ	Peroxisome proliferator-activated receptor gamma
RA	Rheumatoid arthritis
RANKL	Receptor activator of nuclear factor kappa-B ligand
RF	Rheumatoid Factor
RIN	RNA integrity number
SH	Src Homology 2
SH2	Src Homology 2
SHP-1	Src Homology 2 Domain Phosphatase-1
SLE	Systemic lupus erytematosus
SLE	Systemic lupus erytematosus
SNP	single nucleotide polymorphism
SP1	Specificity Protein 1
SPI1	Spi-1 Proto-Oncogene
SPR	Surface plasmon resinance
STAT1	Signal transducer and activator of transcription 2
STAT2	Signal transducer and activator of transcription 3
STAT3	Signal transducer and activator of transcription 1
SYK	Spleen tyrosine kinase
TCA	Tricarboxylic acid
TF	Transcription factor
TGFβ	Transforming growth factor beta
Th2	T-helper cell type 2
TLR	Toll like receptor
TNF	Tumour necrosis factor
TPP	TNF, Prostaglandin E2, Pam3sk4 treated
VD3	Vitamin D3

Chapter 1: Literature review

1.1 Mononuclear phagocyte system

1.1.1 Origins and diversity

The mononuclear phagocyte system is key in maintaining immune processes along with other homeostatic events, including metabolism, angiogenesis and haematopoiesis (Zhou *et al., 20*14); (Geissmann *et al., 20*10); (Murray and Wynn, 2011a). It is made up of a group of responsive, heterogeneous cells with versatile functions. These cells may be divided into circulating monocytes, infiltrating macrophages, tissue resident macrophages and dendritic cells (DCs), each with distinct subsets demonstrating specific functions (Wermuth and Jimenez, 2015).

1.1.1.1 Circulating monocytes

Circulating monocytes originate in the bone marrow and have to ability to migrate into tissues and differentiate into macrophages in response to environmental signals, such as infection or tissue damage. Monocytes are sub classified based on expression of cluster of differentiation (CD) 14 and CD16; the classical CD14++/CD16- monocytes are considered to be inflammatory and express CCR2 bind chemoattractive chemokines) and CD62 (adhesion molecule), while the CD14+/CD16++ monocytes demonstrate weaker phagocytic ability, produce less reactive oxygen species and tend to express more CD32 and major histocompatibility complex (MHC)-II. Additionally, CD14+/CD16++ cells selectively produce tumor necrosis factor (TNF), interleukin (IL)-1β and chemokine ligand (CCL) 3 in response immune complex (IC) stimulation. CD14+/CD16++ cells have also been linked to antiviral responses (Cros *et al., 20*10). An intermediate CD14++/CD16+ phenotype has also been reported (Cros *et al., 20*10); (Geissmann *et al., 20*03); (Tacke and Randolph, 2006); these cells have been identified in rheumatoid arthritis (RA) patients, and levels appear to correlate with heat-aggregated gamma globulin (HAGG) induced TNF production (Cooper *et al., 20*12). This suggests an inflammatory function for this subtype.

1.1.1.2 Infiltrating Macrophages

Infiltrating macrophages are generated through maturation of bone marrow-derived monocytes; these cells differentiate upon exposure to agents such as Macrophage colony-stimulating factor (M-CSF) and granulate-macrophage colony-stimulating factor (GM-CSF) (Jaguin *et al., 20*13); (Vogel *et al., 20*14). Macrophages are classified based on surface marker expression, soluble factor production and response to stimuli (Sica and Mantovani, 2012); (Stout *et al., 20*05); (Zhou *et al., 20*14). Generally speaking,

macrophages polarise into inflammatory or anti-inflammatory cells in response to pathogenic and immunological stimuli. However, it should be noted that these cells are highly dynamic and reactive, and phenotypes may be altered in response to a changing environment (Stout *et al., 20*05); (Zhou *et al., 20*14).
Macrophage polarisation and details of stimuli will be discussed in greater detail in Section "1.1.2 Macrophage polarisation: The bipolar model" below.
In mice, tissue resident macrophages were determined to be mostly derived from the yolk sac during embryonic development and were found at multiple sites throughout the body (Wermuth and Jimenez, 2015); (Perdiguero and Geissmann, 2016). Using fate-mapping studies in murine models, it was reported that these cells were generally renewed by their own proliferation, but this capacity was limited, and influx of infiltrating bone marrow-derived macrophages was required for replenishment (Yona *et al., 20*13); (Wermuth and Jimenez, 2015).

1.1.1.3 Tissue resident macrophages

The phenotype of tissue resident macrophages is generally site specific; certain functions such as clearance of cellular debris (microglia), iron processing (spleen macrophages) and immune surveillance (microglia) are described for macrophages in some tissues, and it should be noted that these cells cannot necessarily be categorised as inflammatory or anti-inflammatory (Davies *et al., 20*13); (Wermuth and Jimenez, 2015). However, previous reports have found that phenotype of these macrophages is not fixed and that they may respond to environmental signals such as tissue injury or pathogens by altering their phenotype; in response to pathogen these cells may provide frontline defense roles (Sica and Mantovani, 2012); (Yona *et al., 20*13).

1.1.1.4 Dendritic cells

DCs are, generally speaking, MHC/CD11c-high cells with a high capacity for antigen presentation and phagocytosis. They are broadly divided into plasmocytoid DCs, which are long lived and highly responsive to virus, and classical DCs which are short lived, highly migratory in lymphoid tissues and are known to regulate T-cell activity (Wermuth and Jimenez, 2015), although further subtypes have been proposed (Villani *et al., 20*17).

1.1.2 Macrophage polarisation: The bipolar model

As alluded to previously, the traditional model of macrophage polarisation describes induction of cells into inflammatory or anti-inflammatory phenotypes. Standard nomenclature denotes these subtypes as M1 and M2 macrophages respectively,

following the terminology for T-helper cells. M2 cells are further divided based on stimuli used to generate the subtype, gene/protein expression profiles and functional variance; M2a, M2b and M2c cells (Zhou *et al., 20*14).

M1 macrophages are typically induced from the unpolarised state using interferon gamma (IFNγ) and Toll-like receptor (TLR) ligands such as lipopolysaccharide (LPS). There is a school of thought that GM-CSF (vs M-CSF) induces a bias towards M1 polarisation, but additional evidence suggests that induction with any colony stimulating factor will prime cells for effective stimulation with any polarising cytokine (Vogel *et al., 20*14); (Jaguin *et al., 20*13). These cells are reported to be highly inflammatory, phagocytic, tumoricidal and anti-microbial. They characteristically produce large amounts of pro-inflammatory chemokines (CXCL (Chemokine (C-X-C motif) ligand) 9, 10, 11) and cytokines (TNF, IL-6, IL1β) and exhibit strong antigen presentation and phagocytic capabilities (Zhou *et al., 20*14); (Jaguin *et al., 20*13); (Arnold *et al., 20*15); (Ambarus *et al., 20*12).

M2a cells are generated through exposure to Th2 cytokines such as IL-4 or IL-13. These cells have been linked to Th2 responses and allergy as well as tissue fibrosis, wound healing and proliferation (Fraternale *et al., 20*15); (Ambarus *et al., 20*12); (Gratchev *et al., 20*01).

M2b macrophages, induced through exposure to ICs in combination with LPS or IFNβ, are not defined very clearly for humans in the literature. In mice, these cells adopt a phenotype where IL-10 production is high and IL-12 is low hence favoring a Th2 response, despite some functional similarities with M1 cells (e.g. production of cytokines IL-6, IL-1β) (Fraternale *et al., 20*15); (Anderson and Mosser, 2002); (Edwards *et al., 20*06).

Generation of M2c cells is generally observed following exposure to IL-10, although the phenotype may also be achieved in vitro using glucocorticoids or transforming growth factor beta (TGFβ). These cells are thought to be involved in removal of cellular debris, matrix deposition and tissue remodelling, and have been described as “de-activated” macrophages (Rőszer, 2015); (Maeß *et al., 20*14); (Jaguin *et al., 20*13).

It should be noted that a poorly characterised sub-group has recently been proposed; M2d cells are generated through culture in the tumour microenvironment and are thought to have some similarities to tumour-associated macrophages. Precise stimuli are not known, but the M2d transcriptional program appears to be driven by over-expression of Fra-1 in murine monocytic cell lines. These cells are IL-10 high and IL-12 low and thought to demonstrate immunosuppressive behaviour (Wang *et al., 20*10b). These cells are not directly relevant to this project and so will not be discussed in detail in this report.

1.1.5 Macrophage polarisation: The spectral model

Although the bipolar model of macrophage polarisation is fairly well established, there is a growing body of evidence suggesting that it is far too simplistic; macrophages express a large number of receptors for various ligands that activate distinct signalling pathways and cellular functions upon receptor engagement. These stimuli modulate the macrophage transcriptome through inducing signalling cascades or by modulating pathways that are otherwise active within the cell (Mosser and Edwards, 2008); (Xue et al.); (Stout *et al., 20*05); (Martinez and Gordon, 2014). For instance, characterisation of *ex vivo* macrophages which have been exposed to a variety of stimuli are reported to exhibit a mixed phenotype. Examples of this include polarisation following exposure to the cytomegalovirus and polarisation in obese tissue in mice; in the latter case macrophages appear to adopt a pro-inflammatory state, but production of some M2-like transcripts (including arg-1, IL1ra, MMP12, ADAM8, VEGF) are seen (Chan *et al., 20*08); (Shaul *et al., 20*10). Additionally, novel subtypes are continually being identified across a number of pathological states (e.g. in obesity, chronic inflammation, atherosclerotic lesions), supporting the idea of a spectral model where macrophages can adopt a wide variety of phenotypes (Lumeng *et al., 20*07a); (Xue et al.); (Villani *et al., 20*17); (Kadl *et al., 20*10). Additionally, macrophages are subject to a number of different signals (both sy nergistic and opposing) under physiological conditions (Andrea *et al., 19*95). These conditions shift constantly, modulating macrophage phenotypes differentially at variable stages of disease progression and different cytokine exposure durations, emphasizing plasticity and heterogeneity of macrophages found under physiological conditions (Wells *et al., 20*03). For instance, indistinct, mixed phenotypes have been described for macrophages isolated from tumours (Edin *et al., 20*13) and associated ascites (Reinartz *et al., 20*14) in humans and mice (Biswas *et al., 20*08); (Biswas and Mantovani, 2010). Additionally, adipose tissue macrophage in mice appear to be altered in response to obesity signals (Lumeng *et al., 20*07a), and phenotype switches are seen during inflammation resolution (Wermuth and Jimenez, 2015). The latter event will be discussed in additional detail in Section 1.1.11 “Roles in wound healing”. Hence a spectral model is more appropriate for the study of cells isolated from healthy and pathogenic human tissue.

Despite the oversimplification of the bipolar macrophage model, it is useful for provision of certain transcriptomic “landmarks” or signatures and provides useful reference points from which comparisons can be made.

1.1.6 Polarisation subsets: Identification and definitions

One of the major obstacles for interpreting macrophage polarisation data is that there is no consensus of how these cells should be defined. This is possibly due to that fact that macrophages are isolated from different tissues and will have an inherently variable phenotype, and that a large number of groups perform characterisation studies using mouse cells (Joshi *et al., 20*14); (Fleetwood *et al., 20*09). One common approach utilizes cell surface protein expression or soluble factor production (e.g. TNF, IL-6 for M1, IL10 for M2 cells) and identification of corresponding gene transcripts. However, there is a lack of consistency in the markers used to indicate different phenotypes. Another method that has been described distinguishes macrophages based on their ability to metabolise certain molecules; arginine metabolism is reported to vary between M1 and M2 induced cells, a switch which supports the phenotype and has been well characterised in murine macrophages (Rath *et al., 20*14); (Mills, 2012). For instance, in M1 cells arginine is reportedly metabolised though activity of enzymes of the nitric oxide synthase family, leading to the production of nitric oxide (NO). This substance is important in the inflammatory response for protection against pathogens as well as contributing to a decrease in proliferation. Conversely, arginase is implicated in arginine metabolism in M2 macrophages, with subsequent production of ornithine. This metabolite assists in the tissue repair response and has proliferative properties (Mills, 2012); (Lumeng *et al., 20*07a). However, in human cells this phenomenon has not been consistently reported, with some groups detecting this change in differentially polarised macrophages (Thomas and Mattila, 2014); (Rouzaut *et al., 19*99); (Babu *et al., 20*09) and others failing to do so (Munder *et al., 20*05). Some explanations for this discrepancy have been proposed, focusing on differences in detection methods (enzyme activity versus protein and transcript detection) and source of macrophages (e.g. in vivo vs in vitro generated) (Thomas and Mattila, 2014). However, until further research is carried out and consistency is achieved, this cannot be considered a reliable standard for investigating variably polarised states in human macrophages.

More recently, attempts to characterise changes in the tricaboxylic acid (TCA) cycle between different macrophage polarisation states have been made; the TCA cycle remains intact in M2a induced cells and downstream processes such as oxidative phosphorylation occurs as expected. However in M1 treated cells, the cycle breaks in two places resulting in an accumulation of citrate and succinate and their core metabolism is carried out through glycolysis (Tannahill *et al., 20*13); (O'Neill and Pearce, 2016). The former supports the production of prostaglandins (since it generates fatty acids) and anti-microbial intermediates (via itaconate) hence promoting M1 macrophage activity (Michelucci *et al., 20*13); (Infantino *et al., 20*11). Succinate accumulations can induce some cytokines such as IL-1β

(through stabilisation of HIF-1α which targets IL1B) and these events have been linked to nitric oxide production (Tannahill *et al., 20*13); (Kelly and O'Neill, 2015). This mechanistic switch may be an interesting method to distinguish differentially polarised macrophages, although it could be argued that additional research must be performed to characterise these changes in multiple differentiation states.

One of the major issues faced when studying macrophage biology is the complete lack of consistency in markers used to define certain subtypes in different studies. Along with the problem described for the standards above, this makes it difficult to determine phenotypes experimentally. Attempts have been made to address these issues through systematic validation of cell surface markers, but these studies tend to focus on small numbers of markers, are often performed on murine cells and can be limited by existing knowledge (Ambarus *et al., 20*12); (Vogel *et al., 20*14); (Barros *et al., 20*13). Additionally, these findings are often contradictory which could be due to the source of the tissue, for instance Ambarus *et al.,* (2011) described CD163 as a robust indicator of M2c polarisation when performing experiments on peripheral blood mononuclear cell (PBMC)-derived macrophages in vitro, whereas another group found this marker to be unreliable for identifying alternative polarisation in histological Sections (Barros *et al., 20*13). Hence additional efforts must be made to define cells and to confirm which markers reliably represent different phenotypes. A summary of experiments aimed at determining macrophage function can be found in Appendix 4, Table A4.1

1.1.8. *in vitro* generation of monocyte derived macrophages and investigations of subset-specific functions

There are a number of different methods that can be used to generate polarised macrophages from monocytes isolated from PBMCs. Initial differentiation steps require addition of a colony stimulating factor, such as M-CSF or GM-CSF to mature monocytes into macrophages (Fleetwood *et al., 20*09); (Wang *et al., 20*14b); (Vogel *et al., 20*14). This alone has been found to induce differences in gene expression of these cells; GM-CSF has been reported to induce a more inflammatory (M1) phenotype whereas M-CSF supports M2 (anti-inflammatory) polarisation (Hamilton *et al., 20*14); (Mahdavi *et al., 20*17); (Jaguin *et al., 20*13). However, it should be emphasised that these agents do not induce polarisation phenotypes to the same extent as polarising cytokines, and instead adopt a more intermediate/primed M1 or M2 phenotype (Vogel *et al., 20*14). For instance, upregulation of M2 factor IL-10 has been reportedly higher for M-CSF treated cells (versus GM-CSF treated), and M1 associated agents IL-6, TNF, IL-18 and IL-1β were found to be higher in GM-CSF primed cells. Beyond this, these cells were

considered to be in an unpolarised state; for instance, M1 macrophages required stimulation from IFNγ in addition to GM-CSF for induction of IL-12 (Hamilton *et al., 20*14); (Verreck *et al., 20*04). Additionally, it should be noted that cells primed with either colony stimulating factor appear to upregulate some subtype specific markers in response to additional cytokine polarisation stimuli (e.g. CD40 and CD64 for M1 cells following IFNγ stimulation and CD163 for M2c cells following glucocorticoid treatment), suggesting a degree of redundancy for these factors. However, it should be noted that there are differences in gene expression in these cells which must be considered when designing experiments (Hamilton *et al., 20*14); (Fleetwood *et al., 20*09); (Vogel *et al., 20*14).

Cell polarisation occurs through interaction of macrophages with agent in their local environment. This is discussed in more detail in Section 1.1.2:
Macrophage polarisation: The bipolar model.

1.1.9 Response to tissue damage/inflammation

Upon inflammation, damage associated molecular patterns (DAMPS) and pathogen associated molecular patterns (PAMPS) including various cytokines and chemokines are released from necrotic cells or derived from bacteria respectively (Kawai and Akira, 2010). Circulating monocytes are recruited to the site and differentiate into inflammatory “M1”-like cells. Once induced, M1 macrophages release pro-inflammatory cytokines (e.g. TNF, IL-6) and chemokines (e.g. CXCL9,10,11), produce reactive oxygen species and other damage molecules such as metalloproteases, serine and cysteine proteases and elastases (Bryan *et al., 20*12); (Wermuth and Jimenez, 2015); (Reichner *et al., 19*99). This contributes to destruction and subsequent removal of the offending pathogen. Interestingly, mouse models have demonstrated cell populations analogous to the CD16+ monocyte (i.e. Gr-1- monocyte) subset patrolling the endothelium that become recruited to sites of IC deposition (Auffray *et al., 20*07). Similarly, in humans CD16+ cell infiltrates are found in the inflamed joints of auto-antibody positive RA patients, suggesting a role for these cells in IC mediated inflammation (Kawanaka *et al., 20*02).

Additionally, macrophages stimulate apoptosis of invading neutrophils and endocytose the cellular debris (Korns *et al., 20*11). Extracellular matrix degradation is a consequence of this destructive inflammatory processes and results in release of a number of agents; growth factors (e.g. TGFβ) and chemokines stimulate endothelial cell and fibroblast proliferation, and prepare the tissue for repair and angiogenesis (Horiguchi *et al., 20*12); (Butterfield *et al., 20*06). Immune resolution is triggered; pro-inflammatory transcription factors such as interferon response factor

(IRF)1 and NFκB are reportedly downregulated, and wound healing related factor IRF4 is induced here (DiDonato *et al., 20*12); (Tamura *et al., 20*05).

1.1.11 Roles in wound healing

To promote inflammation resolution, macrophages either switch from the M1 to the M2 phenotype in the tissue, or additional M2 cells are recruited through differentiation and polarisation of infiltrating monocytes. Studies into the mechanisms of inflammation resolution in mice used labelled monocytes and cytokine profiling to demonstrate this; classical Ly6C positive monocytes infiltrated tissue during active inflammation, where they matured into M1 macrophages which switched to the M2 state during tissue repair (Arnold *et al., 20*07), and Ly6C negative cells were reported to infiltrate repairing tissue and differentiate into M2-like cells (Nahrendorf *et al., 20*07). Here, M2 cells aid immune resolution by producing growth factors and proliferative cytokines, promoting the survival of endothelial cells and supporting the generation of myofibroblasts (increased collagen production) from fibroblasts for wound healing (Mosser and Edwards, 2008); (Koh and DiPietro, 2011); (Wermuth and Jimenez, 2015).

1.1.12 Roles in disease

Macrophages are frequently observed in many different tissues and their population size is found to increase drastically during a number of conditions including infection, cancer, obesity, autoimmunity and chronic inflammatory diseases (Laria *et al., 20*16b). The diverse role of macrophages in these different pathological conditions, highlights their heterogeneous and dynamic nature, and subsequent consequences in disease. Macrophages have some regulatory roles in adipose tissue that are disrupted during obesity; under physiological conditions, adipose macrophages adopt an M2-like phenotype under the influence of Peroxisome proliferator-activated receptor gamma (PPAR-γ) (Lumeng *et al., 20*07b); (Odegaard *et al., 20*07); (Murray and Wynn, 2011b). These cells secrete IL-10, which supports glucose tolerance and insulin signalling in adipocytes (Weisberg *et al., 20*03); (Murray and Wynn, 2011b). However, during obesity, low level inflammation is seen. Here, danger signals lead to NACHT, LRR and PYD domains-containing protein 3 (NLRP3) inflammasome activation along with an increase in number of tissue macrophages (Weisberg *et al., 20*03); (Chawla *et al., 20*11). These cells are converted to more of an M1-like phenotype under these conditions, and subsequent production of pro-inflammatory cytokines (TNF, IL-6, Monocyte Chemoattractant Protein-1) reportedly promotes insulin resistance in adipose tissue (Lumeng *et al., 20*07b); (Chawla *et al., 20*11). This supports the development of a diabetic state (Murray and Wynn, 2011b).

M2a polarised cells have been reported to be involved in allergic responses in addition to their roles in the attenuation of inflammation (Anthony *et al., 20*06); (Bhatia *et al., 20*11). There is, however, some disagreement as to the exact functioning of macrophages in these conditions; some reports suggest that they suppress inflammation (Lee *et al., 20*15) whilst others that these cells drive the type-2 response (Mathie *et al., 20*15b); (Murray and Wynn, 2011b). Although this could be to some degree dependent on disease phase and location of the macrophages. For instance, in asthma macrophages found in different lung compartments have been observed to have pro and anti-inflammatory functions, although the data surrounding this is not completely clear; alveolar macrophage (AM) depletion was found to induce a Th-2 allergic response in mouse asthma models which was reversed by adoptive transfer of AMs from healthy mice (Mathie *et al., 20*15a); (Lauzon-Joset *et al., 20*14); (Jiang and Zhu, 2016). Conversely, other studies described attenuation of allergic (Th-2) inflammation in mouse asthma models upon AM depletion (Lee *et al., 20*15). It has been suggested that this could related to the origin of the macrophages; (Zasłona *et al., 20*14) reported that increased infiltrating monocytes in the lung contributed to inflammation in murine models, and that this was decreased upon depletion of circulating monocytes. Hence different groups of macrophages in the lung may have distinct functions.

Macrophages appear to have altered phenotypes in some autoimmune and inflammatory diseases; for instance, SLE macrophages are reported to demonstrate defective clearance of apoptotic cells. Evidence for this includes results from SLE lymph node biopsies where increased apoptotic cell bodies were found near the germinal centers (Ren *et al., 20*03), and experiments where sera from SLE patients decreased phagocytic capacity of healthy control macrophages in vitro (Baumann *et al., 20*02). Additionally, the macrophage phenotype identified in this disease is associated with increased production of factors such as TNF, IL-6, IL-10 and type 1 interferons which can in turn increase auto-antibody production by B cells (Laria *et al., 20*16a); (Kavai and Szegedi, 2007).

Investigations of macrophages in the spondyloarthropathies revealed an increase in number of cells in peripheral joints. Interestingly, a larger fraction of macrophages expressing M2 associated markers (such as CD200R and CD163) were identified in these conditions, versus reports for disorders such as RA. Hence M2 cells and their pro-fibrotic functions are implicated in pathogenesis of spondyloarthritis (Baeten *et al., 20*02); (Laria *et al., 20*16b).

Involvement of macrophages in RA will be discussed in detail in Section 1.4.5: Roles of macrophage and other cells in RA**.**

1.2 Macrophage cell lines as in vitro model systems

1.2.1 Different cell line models

As mentioned previously, macrophages are characteristically heterogeneous cells with phenotypes that vary depending on their origin, location and exogenous signals. It should be noted that any variation in genetic background of monocytes from different donors may alter responses to stimuli and risk masking any functional changes that occur on exposure to different stimuli; variants in genes coding for cytokine receptors or FcγRs may affect how cells respond to cytokine or IC stimuli. For instance, interferon-γ (IFNγ) polymorphisms have been reported to alter susceptibility to infections in Chinese cohorts (Ding *et al., 20*08). Additionally, physiological factors such as diet, exercise and exposure to infectious agents may alter the phenotype of CD16+ monocytes (Poitou *et al., 20*11); (Timmerman *et al., 20*08); (Kwissa *et al., 20*14). Additionally, only limited numbers of tissue macrophages can be isolated from human subjects and procedures to do so are by necessity invasive (Daigneault *et al., 20*10); (Gordon *et al., 20*00). In terms of PBMC monocytes, 0.2-0.9 x 10^6 cells can be isolated from 1ml of blood
(source: https://www.stemcell.com/media/files/wallchart/WA10006-Frequencies_Cell_Types_Human_Peripheral_Blood.pdf) with 2.2 million being required for a 100mm tissue culture plate (according to thermos-fisher scientific, source: https://www.thermofisher.com/us/en/home/references/gibco-cell-culture-basics/cell-culture-protocols/cell-culture-useful-numbers.html). If primary MDMs from healthy donors were used, to ensure replicability of experiments, blood from the same donor would be required for all experiments to ensure that no genetic variability was present to confound results. As approximately 750mls of blood can be drawn every 8-16 weeks (source: http://www.redcrossblood.org/donating-blood/donation-faqs), this would be a major limiting factor when considering experimental feasibility. One way to address these inherent challenges in the use of primary cells is to use monocytic cell lines as model systems for multiple, replicable experiments with genetically identical baselines (Chanput *et al., 20*13).

A number of human cells lines have been characterised for the study of human monocytes and macrophages; HL-60, U937, KG-1, HEL, ML-2, Mono MAC 6 and THP-1 are some examples (Auwerx, 1991). Different cell lines are at different stages of maturity, dictating their applicability and protocols required to induce a macrophage-like state (Chanput *et al., 20*13). For instance, HL-60 cells are promyelocytic and require differential stimuli to achieve a monocyte or macrophage-like phenotype (Collins, 1987); (Rovera *et al., 19*79). Conversely THP-1 cells were monocytes derived from the blood of an acute myeloid leukemia (AML) patient (Tsuchiya *et al., 19*80) and U937 monocytes were originally isolated from tissue and are at a much more mature stage of

development (Chanput *et al., 20*13). Some evidence suggests that Mono MAC 6 cell line (isolated from blood of a monoblastic leukaemia patient) is most suitable for the study of mature monocytes due to their mature marker expression (not found on other cell lines) and abilities to phagocytose opsonised erythrocytes and mycobacteria (Friedland *et al., 19*93); (Ziegler-Heitbroc *et al., 19*88); (Shattock *et al., 19*94). However, there has not been a great deal of research performed on these cells (including induction into macrophages) so reliability for certain assays is unclear, particularly with regard to the experiments planned for this project. THP-1 cells appear to be the most commonly used line in the literature, followed by U937 cells (Qin, 2012); (Chanput *et al., 20*13); (Chanput *et al., 20*12). Upon stimulation, THP-1 cells are reported to adopt a phenotype more closely related to that of PBMC macrophages when scrutinised for morphology, gene expression, certain antigens and flow cytometry characteristics and will be the cell line of focus here (Chanput *et al., 20*13); (Chanput *et al., 20*14); (Chanput *et al., 20*15). It is important to emphasize that these are cancer cell lines and that the malignant phenotype has been introduced through different types of mutations; generally relating to proliferative capacity or inhibiting a key pathway (Adati *et al., 20*09); (Sharif *et al., 20*07). Hence specific mutations in cell lines of interest must be considered if the study is aimed at examining a particular pathway; for instance, the KG-1 cell line has a very high p-Syk/Syk (involved in Immunoreceptor tyrosine-based activation motif phosphorylation, and therefore activating FcγR signalling) ratio at rest, suggesting that these cells have a mutation which will constitutively activate downstream pathways; for instance those related to cell cycle (Hahn *et al., 20*09). Hence use of these cell lines would be inappropriate in any studies examining signalling through related receptors (e.g. activating FcγRs). It should be noted that although HL-60 cells were isolated from a promyeocytic leukaemia patient, these cells resemble banded neutrophils rather than fully multilobulated polynuclear cells. Hence, they will not be the most appropriate cell line for the study of macrophage differentiation and polarisation (Collins, 1987). Cell line advantages and disadvantages are summarized in Appendix 4, Table 4.2.

1.2.2 THP-1 cell features and comparisons with primary cells

THP-1 cells tend to mimic the phenotype of primary macrophages upon differentiation; an increase in cytoplasm and number of mitochondria and ribosomes have been described (Daigneault *et al., 20*10) along with expression of some macrophage receptors (e.g. CD11b, CD14 and CD36) (Schwende *et al., 19*96); (Park *et al., 20*07); (Zhou *et al., 20*10), reports of morphological similarities and cell adherence (Tsuchiya *et al., 19*82); (Schwende *et al., 19*96). THP-1 cells also adopt some macrophage-related functions such as phagocytosis, lipid accumulation and

antigen presentation (Schwende *et al., 19*96). As with primary macrophages, THP-1 cells may polarise upon exposure to cytokines; a feature that will be discussed in more detail below (Caras *et al., 20*11); (Spencer *et al., 20*10).

Some differences in responsiveness of these cells have however been reported; decreased responsiveness to LPS (potentially due to lower CD14 expression) and other compounds have been described and must be held in consideration when examining macrophage function using these cells experimentally (Heil *et al., 20*02); (Bosshart and Heinzelmann, 2016). However, as some of these responses have been found to vary following different culture conditions, it is unclear whether this is an effect of experimental variance or a cell line limitation.

Despite the numerous reports highlighting advantages of their use, the malignant origin of THP-1 cells should be emphasised and genetic variances between these AML cells and MDMs from health donors should be highlighted. A number of leukaemia related aberrations were identified in this cell line. For instance, AML related fusion of *MLL* and *MLLT3* genes was identified for THP-1 monocytes. The resulting protein is documented to prevent the normal maturation of haematopoietic cells which implies differences in the maturation of THP-1 monocytes and MDMs, which is likely to affect their functioning (Adati *et al., 20*09); (Odero *et al., 20*00); (Mueller *et al., 20*09).

Deletions in a number of regions have also been reported; cyclin dependant kinase coding genes *CDKN2A* and *CDKN2B* are credited as tumour suppressing genes, due to the involvement of their relative proteins in cell cycle regulation. As in AML, THP-1 cells are described to have deleterious changes in these regions (Adati *et al., 20*09).

Deletions in PTEN have also been identified; as this protein regulates activity of Akt, disruption of function will promote cell survival and hence contribute to the immortalised THP-1 phenotype (Dahia *et al., 19*99); (Adati *et al., 20*09).

Some additional deletions have also been described for some regions of chromosome 1 which contain portions of genes KIAA0495 and TP73. The latter is a homologue for TP53 which codes for P53, a well-documented protein involved in cell cycle and cell death that is linked to numerous cancers (Adati *et al., 20*09); (Pluta *et al., 20*06). Hence the protein coded by TP73 may have a similar function in malignant cells.

It is important to consider how immune pathways commonly seen in primary cells are represented in THP-1 monocytes; for instance, signalling through the immunoreceptor tyrosine-based activation motif (ITAM) (via ICs) (Ghazizadeh *et al., 19*94) and TLR4 (via LPS) has been reported for THP1 cells. For the former, co-precipitation studies and in vitro kinase activity assays revealed kinase activity compatible with tyrosine phosphorylation of FcγRIIa along with engagement and activity of Src protein tyrosine kinases. In terms of LPS signalling, luciferase assays were used to examine NFκB activity (used as a reporter of LPS signalling) in a series of THP-1 cells

with a number of signalling molecules knocked out; as in primary cells, myeloid differentiation primary response 88 (MyD88), interleukin 1 receptor associated kinase (IRAK) and interleukin 2 receptor associated kinase (IRAK2) were found to be essential for activation of nuclear factor kappa-light-chain-enhancer of activated B cells (NFκB) via LPS (Zhang *et al., 19*99). As discussed previously however, cytokine release as a product of LPS ligation is lower in THP-1 macrophages versus monocyte derived macrophages (MDMs) (Schildberger *et al., 20*13). It should be noted that the U937 monocytic cell line have comparatively poor responses to LPS, and would hence be less desirable for studies aiming to polarise macrophages into an inflammatory phenotype (Sharif *et al., 20*07). The MAP3K7 pathway, involved in differentiation of monocytes to macrophages has been reported in THP-1 cells; here the cell line was used to study signalling events through this pathway
using kinomics and phosphoproteomic technicues (Richter *et al., 20*16). As these pathways appear to reliably represent PBMC macrophages, it is reasonable to use THP-1 cells in studies examining macrophage polarisation.

1.2.3 Differentiation protocols

Due to their frequent use, there is a large amount of information available on the culture conditions and methods that can be used to transform THP-1 cells into differentially polarised macrophages. One consideration is the agent that should be used to differentiate these monocyte-like cells; Phorbol-12-myristate-13-acetate (PMA), M-CSF and 1,25-dihydroxyvitamin D3 (VD3) have all been reported to induce a macrophage-like phenotype in THP-1 cells (Schwende *et al., 19*96); (Park *et al., 20*07); (Daigneault *et al., 20*10). These agents activate separate pathways to induce monocyte differentiation and so have variable effects on the cells; when treated with PMA (a diacylglycerol analogue which activates protein kinase C), THP-1 cells appear to adopt a phenotype that more closely resembles PBMC-macrophages. For instance, macrophage-like characteristics such as adherence, phagocytic capability, decreased proliferation and expression of surface molecules (CD14, CD11b) were all more strongly induced using PMA compared with VD3 (Schwende *et al., 19*96); (Daigneault *et al., 20*10); (Qin, 2012). Due to its low efficacy, M-CSF tends not to be used as a stimulus for cell lines unless in combination with IFNγ, which would only allow induction of M1-like cells (Chanput *et al., 20*14).
PMA is generally considered the most effective agent for differentiating monocytes. Reports have claimed that macrophage differentiation characteristics such as cytoplasmic to nuclear ratio, mitochondrial and lysosomal numbers and differentiation-dependent cell surface markers are induced in a manner similar to that of MDMs (Chanput *et al., 20*14); (Daigneault *et al., 20*10). Thus, this agent is frequently

used in THP-1 differentiation studies. However, there is no standardised protocol with respect to the concentration of PMA that should be used and duration of time that cells should be exposed to it for. For instance, huge ranges of PMA have been used to induce differentiation that range from 2.5-400ng/ml (Park *et al., 20*07); (Genin *et al., 20*15); (Daigneault *et al., 20*10); (Lund *et al., 20*16); (Jiang *et al., 20*16a); (Jiang *et al., 20*17); (Kohro *et al., 20*04); (Feng *et al., 20*04); (Tulk *et al., 20*15); (Hirakata *et al., 20*04); (Maeß *et al., 20*14). In addition, exposure times ranging from 3-72 hours have been applied (Chanput *et al., 20*14); (Daigneault *et al., 20*10). This will increase inter-experimental variability as PMA induces a strong activation signal which can lead to production of protein kinase C products, not related to macrophage polarisation state (Zeng *et al., 20*15); (Park *et al., 20*07). Previous reports have concluded that concentrations of PMA exceeding 100ng/ml are not physiologically relevant, and that applications of high quantities of this agent can induce an M1 bias in macrophages (Park *et al., 20*07); (Maeß *et al., 20*14). Importantly, some studies have reported that reduced PMA induction can render cells more responsive to additional stimuli, suggesting a more plastic phenotype (Maeß *et al., 20*14). Taken together, this implies that differentiation by PMA is not consistent, and that the variability affects the phenotype; an issue that has provided obstacles when identifying an optimal protocol in the past.

Rest period following initial differentiation is another important aspect of THP-1 differentiation protocols; the longest described appeared to be 10 days (Solberg *et al., 20*15) and some protocols eliminated recovery time completely (Chanput *et al., 20*10); (Tulk *et al., 20*15). Rest period tends to be useful for reducing undesirable effects of PMA, but care must be taken not to de-differentiate the cells; due to the dynamic nature of these cells, culture in stimulus-free media for extended periods of time may result in cells losing their phenotype and becoming detached, particularly if initial stimuli were not sufficient to induce a robustly differentiated phenotype (Park *et al., 20*07); (Chanput *et al., 20*13); (Spano *et al., 20*13); (Solberg *et al., 20*15).

Another discrepancy in THP-1 protocols is that of polarisation treatments. As with primary monocytes, M1 polarisation is generally achieved through addition of LPS and IFNγ, M2a via IL-4 and M2c with IL-10. However, the concentrations of polarising agents are not always consistent; for M1 cells, the majority of protocols tend to keep levels of IFNγ consistent at 20ng/ml, but LPS concentrations vary widely; some studies exclude this TLR4 agonist completely, whereas others use it in concentrations of up to 250ng/ml (Genin *et al., 20*15); (Chanput *et al., 20*13); (Sun *et al., 20*16); (EngstrÖM *et al., 20*14). As LPS induces some pathways that are not implicated in interferon signalling, it is likely that its presence as a stimulus would alter

the macrophage transcriptome. IL-10 and IL-4 are generally used at 20ng/ml for M2c and M2a cells, respectively (Chanput *et al., 20*13); (Qin, 2012).
In terms of cytokine exposure duration for macrophage polarisation, times have been found to vary between protocols, which may also affect the expression profile of genes in these cells, since transcription of different markers will be under variable levels of regulation, and hence be affected by degree and duration of cytokine exposure (Chanput *et al., 20*12); (Daigneault *et al., 20*10); (Solberg *et al., 20*15); (Park *et al., 20*07). Type of plasic used should also be noted as this affects macrophage growth and activation (Murray *et al., 20*14).

1.2.4 M2 polarisation and THP-1 cells

Generally speaking, reports have suggested that it is more difficult to polarise THP-1 macrophages into the M2 state than that for the inflammatory M1 cells; reports demonstrated decreased induction of cell surface markers and cytokines (including CCL1, 16, 17, 18, 22, 24 and CCR (chemokine receptor) 2, CXCR (Chemokine (C-X-C motif) receptor) 1 and 2) upon IL-4 stimulation versus primary cells (Chanput *et al., 20*13). This could, however, be linked to increased activity of PMA; this agent has been found to induce M1 cytokine CCR7 at 100ng/ml, suggesting M1 macrophage activation (Maeß *et al., 20*14). Reduction of this stimulant reportedly increases responsiveness of THP-1 cells to a number of different polarising signals, including IL-10 (an M2 polarising molecule), so the M2 polarisation issue may reflect deficiencies in current protocols rather than cell line used (Maeß *et al., 20*14); (Park *et al., 20*07).

1.2.5 Myeloid cell differentiation in the presence of immune complexes

Changes in macrophage phenotypes in response to an IC stimulus have not been studied in a great deal of detail; most of the literature focuses on the phenotype of M2b cells, originally characterised by Anderson and Mosser (Anderson and Mosser, 2002). Here, FcγR ligation is described to reverse the TH1-like phenotype in mouse macrophages and induce production of IL-10. Additional studies have interrogated the transcriptome of human cells induced in this manner, and have characterised this phenotype, but not looked in any detail as to how other stimuli interact with this signal (Xue et al.).
Differentiation of FcγR expressing myeloid cells is reportedly influenced by ICs. More specifically, introduction of ICs into an in vitro system reportedly affects dendritic cell and osteoclast differentiation pathways. In dendritic cells, FcR crosslinking seemingly induces more macrophage-like phenotypes, or DCs with reduced antigen presentation cell (APC) activity and greater T-cell activating capabilities (Jancar and Crespo,

2005); (Laborde *et al., 20*07); (Köller *et al., 20*04); (Tanaka *et al., 20*09). Interaction of IC with FcR on myeloid precursor cells has been implicated in osteoclastogenesis in studies on mice; increased osteoclast generation has been reported for cells treated with IC (Seeling *et al., 20*13). Dysregulation of osteoclast generation was particularly interesting in RA as this may be related to early bone loss and articular erosions (Grevers *et al., 20*13); (Seeling *et al., 20*13). Some reports claim that stimulation of macrophages with ICs cause shifts in cytokine production and even expression of some protein markers (Clavel *et al., 20*08), (Ambarus *et al., 20*12); (Barrionuevo *et al., 20*03), implying a polarising function of ICs.
Conversely, other studies have examined how engagement of FcγRs affects soluble factor production under a variety of conditions, but have only considered a small number of chemokines and cytokines (Sironi *et al., 20*06); (Stone and La Flamme, 2016); (Ambarus *et al., 20*12). For instance, one study described production of CCL1 (a chemokine found in rheumatoid synovium) upon FcγRII (a and b) ligation, in the presence of LPS or IL-1β (i.e. M2b stimuli). Additionally, enhanced production of IL-4 induced CCL22 was also described with FcγRII engagement (Sironi *et al., 20*06). More recently, Stone and Flamme (2016) described an LPS+IC driven induction of IL-17A which was not perturbed by addition of IL-10 (M2c cytokine) or IL-12 (a cytokine driving the type 1 inflammatory response). Immobilised HAGG may be used as an in vitro surrogate for immune complexes bound to tissue (such as the cartilage pannus junction in RA); macrophages spread over the surface of these IgG-bound “targets” and upon failure to phagocytose them release lytic granules onto the region. This process is known as frustrated phagocytosis (Bainton *et al., 19*89); (Takemura *et al., 19*86); (Wright *et al., 20*14). Ambarus *et al.,* (2012) investigated the effect of HAGG and immobilised IgG on production of some agents in murine macrophages; HAGG appeared to enhance TLR induced IL-10 production, and a modest increase was recorded for TNF and IL-6 secretion. All three of these cytokines were significantly increased upon exposure to immobilised IgG. As described above, strength of signalling is affected by avidity, i.e. degree of crosslinking. Hence, depending on size of HAGG molecules, immobilized IgG could be binding more receptors, driving the differences in cytokine production (in addition to generation of substances as a consequence of frustrated phagocytosis).
Early reports attempting to characterise the THP-1 cell line described expression of FcγRI and FcγRII, but not FcγRIII on these cells, with and without PMA or VD3 as differentiation stimuli (Fleit and Kobasiuk, 1991). Polarisation was not examined in this experiment, however, and efforts to distinguish the activating FcγRIIa and inhibitory FcγRIIb were not made. Additional reports have suggested that FcγRIIa recruits Src and induces protein kinase activity upon cross-

linking (Ghazizadeh *et al., 199*4). This is the same method of signalling reported for primary monocytes, suggesting that this pathway is not perturbed in THP-1 cells.

1.3 Fc-gamma Receptors

Non-classical monocytes and macrophages are known to express all activating Fcγ receptors (except FcγRIIIb) along with the inhibitory FcγRIIb (CD32b). Classical monocytes, as described above, do not express FcγRIIIa (CD16a) but this receptor is upregulated upon macrophage differentiation (Gordan *et al., 20*15). Taken together with the data indicating that ICs influence macrophage polarisation (in Section 1.2.5), it may be suggested that signalling through FcγRs can have some influence on macrophage development. Therefore, these receptors must be considered when studying how macrophages are activated under physiological conditions.

1.3.1 Fc receptor subtypes and signalling pathways

Fc receptors are a family of proteins that bind immunoglobulins and are found on a number of immune cells, including monocytes, macrophages, eosinophils, DCs, mast cells, natural killer (NK) cells, B cells and T-cells (Barrionuevo *et al., 20*03); (Hogarth and Pietersz, 2012); (Chauhan *et al., 20*15). Expression profiles of these receptors on different immune cells are summarised in Table 1.3.1.

The Fc receptor subgroup of interest here is that of Fc gamma receptors (FcγRs), which bind IgG antibodies by the Fc region and are implicated in modulating inflammation and are genetically associated with a number of autoimmune diseases such as RA and SLE (Vogelpoel *et al., 20*15); (Hargreaves *et al., 20*15). There are six different FcγR subtypes in humans (FcγRI/CD64, FcγRIIa/CD32A, FcγRIIb /CD32B, FcγRIIc/CD32C, FcγRIIIa/CD16A, and FcγRIIIb/CD16B) which can be classified according to affinity for IgG and signalling activity.

FcγRI is a high affinity receptor and can bind both monomeric immunoglobulin G (IgG) and IgG-containing ICs (Hargreaves *et al., 20*15). Conversely, the other receptors are low affinity and will hence only bind IC in a multivalent fashion (Nimmerjahn and Ravetch, 2010); (Nimmerjahn and Ravetch, 2008).

With respect to signalling, most of the receptors (FcγRI, FcγRIIa, FcγRIIc and FcγRIIIa) are activating; these receptors initiate cellular signalling through the ITAM, which is either integral to the cytoplasmic domain of the receptor protein (FcγRIIa, FcγRIIc) or through an accessory signalling chain such as the common gamma chain or zeta chains (FcγRIIIa, FcγRI) (Guilliams *et al.,* 2014); (Hargreaves *et al., 20*15).

ITAM signalling triggers downstream responses via Syk that contribute to various inflammatory functions, such as cytokine release, production of reactive oxygen species and increased phagocytosis. It should be noted, however, that responses are dependent on cell type and the precise FcγR cross-linked (Nimmerjahn and Ravetch, 2008); (Hargreaves *et al., 20*15). Furthermore, these receptors vary in their binding preferences for different IgG subclasses according to flow cytometry and surface plasmon resonance (SPR) data produced by Bruhns *et al.,* (2009) (Bruhns *et al., 20*09); these differences are summarised in Table 1.3.2.

FcγRIIb is the only inhibitory receptor, which signals through an immunotyrosine based inhibitory motif (ITIM) in its cytoplasmic tail. Generally speaking, Src protein tyrosine kinase will phosphorylate the tyrosine residue in the ITIM sequence.

The phosphotyrosine subsequently recruits either inositol phosphatase SHIP or SH2 domain containing protein tyrosine phosphatases SHP-1 and SHP-2. Recruited SHIP hydrolyses membrane phosphoinsitide and releases membrane pleckstrin homology domain (PH domain) containing molecules. Consequential decreases in calcium release from intracellular stores results in a decrease in calcium signalling. SHP-1 removes phosphate groups from substrate proteins, preventing signalling through these molecules. Additionally, upon phosphorylation of FcγRIIb associated ITIM, PH domain containing molecule Akt is recruited and interacts with Dok (RasGAP binding protein), hence inhibiting Ras and Erk signalling (Billadeau and Leibson, 2002); (Long, 2008).The overall paradigm is that the ratio of activating and inhibitory receptors on Fc receptor expressing cells dictates the threshold for activation and thus cellular functions (Nimmerjahn and Ravetch, 2008); (Hargreaves *et al., 20*15). This is summarised in Figure 1.3.1.

FcγRIIIb is a glycosylphosphatidylinositol (GPI)-linked receptor found on neutrophils and eosinophils lacking activating/inhibitory signalling domains; there has been some discussion surrounding the function of this receptor; it is possible that it acts as a decoy receptor which acts to reduce IgG bound to the activating receptors. Alternative theories describe this protein as a molecular trap for ICs in the vicinity of activating receptors, hence enhancing their signalling (Kurosaki and Ravetch, 1989); (Guilliams *et al., 20*14); (Nagelkerke and Kuijpers, 2014). Earlier reports have also suggested that this receptor can signal through complement receptor 3 (Galon *et al., 19*96), through FcγRIIa (Chuang *et al., 20*00) or via lipid rafts (Fernandes *et al., 20*06).

Paradoxical inhibitory signalling has recently been reported to be generated through ITAM receptors (Ben Mkaddem *et al., 20*14); (Pfirsch-Maisonnas *et al., 20*11). This can be induced following the binding of monomeric IgG or specific F(ab)2 fragments. The high avidity binding with immune complexes, described above, stimulates complete phosphorylation of tyrosine residues and subsequent Syk activation (Hirsch *et al., 20*17). Inhibitory signals are generated through low avidity binding;
here, monophosphorylation of the membrane distal tyrosine leads to transient recruitment of Syk, actin depolymerisation and translocation of phosphatases SHIP and SHP1 into the lipid rafts (Ivashkiv, 2011); (Pfirsch-Maisonnas *et al., 20*11). These enzymes deactivate high-avidity signalling by dephosphorylating signalling molecules related to activating pathways (Barrow and Trowsdale, 2006); (Hirsch *et al., 20*17). Furthermore, iITAM signalling induces the formation of large intracellular inhibitory complexes, termed inhibisomes, which have the potential to deactivate multiple membrane receptors following internalisation. Hence FcγR signalling is under multiple complex levels of control that are ultimately dependent on IC composition and local environmental factors.
There are 4 distinct subclasses of IgG which are given in Table 1.3.2; these subclasses have variable affinities for the different FcγRs (Bruhns *et al., 20*09) and some are induced by specific stimuli. Examples are given here; production of IgG1 can be triggered by soluble and membrane protein antigens, viruses and allergens. The latter also induces production of IgG4 (Vidarsson *et al., 20*14); (Aalberse *et al., 19*83); (Ferrante *et al., 19*90). IgG2 is induced by bacterial capsular polysaccharide antigens (as well as in response to increased levels of IgG1 and 3) (Barrett and Ayoub, 1986); (Vidarsson *et al., 20*14), and IgG3 release can be triggered by viral infection (Ferrante *et al., 19*90).

As different FcγR subtypes are only expressed on certain cell types (Table 1.3.1, Smith and Clatworthy *et al., 20*10), presence of specific IgG subclasses will to some degree dictate which cells are activated. For example, as IgG2 is induced by bacterial capsular polysaccharides (Barret and Agoub, 1986) and does not preferentially
bind FcγRIIb,(Bruhns *et al., 20*09), cells expressing FcγRIIb only (such as basophils (Smith and Clatworthy *et al., 20*10)) will not be as strongly affected by infections with pathogens containing this antigen. Additionally, as IgG2 appears to trigger activating receptors (Table 1.3.2), it would be logical to assume that this subtype would drive a highly inflammatory response.
IgG glycosylation further controls antibody responses through the FcγRs; glycosylation of N297 of the CH2 domain of the IgG-Fc region has been described. Various
IgG glycoforms have been identified, and confer structural changes which in turn have

an impact on antibody effector function. For instance, natural killer (NK) cells treated with IgG engineered to have lower levels of fucose or higher levels of bisecting N-acetylglucosamine (inhibits addition of fucose) in vitro demonstrated increased antibody dependent cell cytotoxicity activity (Shields *et al., 20*02); (Umaña *et al., 19*99). Additionally, removal of terminal galactose from IgG antibodies reduced classic complement activation (Boyd *et al., 19*95), and mouse models demonstrated that sialylated IgG may increase expression of FcγRII (orthologue of human FcγRIIb) (Anthony and Ravetch, 2010). However, the latter example must be considered with caution as there are a number of differences between human and mouse FcγRs.

Differences in glycosylation patterns have been reported for different isotypes (Keusch *et al., 19*96), age differences (Yamada *et al., 19*97), during pregnancy (KIBE *et al., 19*96) or in the case of infection (Ackerman *et al., 20*13) and inflammation (Irani *et al., 20*15); (Malhotra *et al., 19*95). Of interest here, a distinct glycoform of IgG is reportedly increased in RA patients; circulating IgG glycoforms which lack galactose and terminate with N-acetyl glucosamine are described, where the N-acetyl glucosamine residue appears to be more accessible for interactions with mannose binding protein. Subsequent activation of complement is seen, a factor which may further promote inflammation in this condition (Malhotra *et al., 19*96).

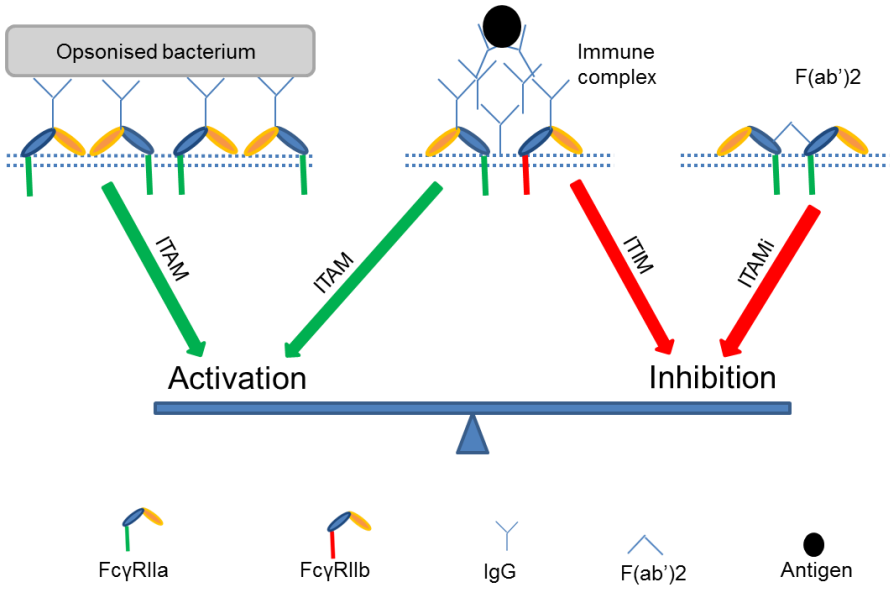

Figure 1.3.1. A simplified schematic of how the balance between activating and inhibitory signals dictates the threshold for immune complex-driven activation in cells. FcγRIIa = Fc gamma receptor IIa, FcγRIIb = Fc gamma receptor IIb, IgG= immunoglobulin G, ITAM = Immunoreceptor tyrosine-based activation motif, ITAMi = inhibitory Immunoreceptor tyrosine-based activation motif, ITIM = Immunoreceptor tyrosine-based inhibitory motif, F(ab')2 = fragment antigen binding 2

Table 1.3.1. Table of expression of different FcγRs on different immune cells, adapted from a Figure by Smith and Clathworthy (2010) (Smith and Clatworthy, 2010)

	FcγRI	**FcγRIIa**	**FcγRIIb**	**FcγRIIc**	**FcγRIIIa**	**FcγRIIIb**
Lymphoid cells	N/A	N/A	B cells, plasma cells	NK cells	NK cells, T cells	N/A
Myeloid cells	Monocytes, dendritic cells, macrophages	Monocytes, dendritic cells, macrophages, platelets	Monocytes, dendritic cells, macrophages	N/A	Monocytes, dendritic cells, macrophages	N/A
Granulocytes	Neutrophil, eosinophil	Neutrophil	Neutrophil, basophil and mast cell	N/A	N/A	Neutrophil, mast cell, eosinophil

Table 1.3.2. Table comparing differences in binding preferences for FcγRs in relation to the different isotypes of IgG (formed into immune complexes) using CHO transfectants, adapted from a Figure by Bruhns *et al.,* (2009). Here, - indicates no binding, + low levels of binding, ++ intermediate binding and +++ high levels of binding. This was determined using indirect immunofluorescence.

	IgG1	**IgG2**	**IgG3**	**IgG4**
FcγRI	+++	-	+++	+++
FcγRIIa (H131)	+++	++	+++	++
FcγRIIa (R131)	+++	+	+++	++
FcγRIIb	+	-	++	+
FcγRIIc	+	-	++	+
FcγRIIIa (F158)	++	-	+++	-
FcγRIIIa (V158)	+++	+	+++	++
FcγRIIIb (NA1)	+++	-	+++	-
FcγRIIIb (NA2)	+++	-	+++	-
FcγRIIIb (SH)	+++	-	+++	-

1.3.2 Genetic variants and disease

FcγRs are a highly homologous family of receptors. Single nucleotide polymorphisms (SNPs) and copy number variants (CNVs) have been reported for the genes, some of which are reported to have a functional impact on IgG interactions. As emphasised previously, the balance between activating and inhibitory signalling dictates the threshold for IC-driven activation (Figure 1.3.1), and subsequent activity of the cell. Hence, variants affecting this balance can influence susceptibility to autoimmunity, responses to pathogens and determine response to biologic therapies (i.e. monoclonal

antibody treatments) (Willcocks *et al., 20*08); (Mueller *et al., 20*13); (Machado *et al., 20*12); (Mellor *et al., 20*13); (Weng and Levy, 2003).

One example for *FCGR2A* is the 131H allotype; this is reported to have a higher affinity for IgG2 versus the 131R allotype. Expression of genes containing this variant alters the FcγR activating/inhibitory balance, and lower the threshold for inflammation and onset of autoimmunity (Hargreaves *et al., 20*15); (Clark *et al., 19*91); (Duan *et al., 20*14); (Lee *et al., 20*08). This could be the reason for association of this allotype with autoimmune conditions such as lupus nephritis (Song *et al., 19*98) in some populations. The absence of the 131H allotype would also reduce immune activation in response to IgG2 driven inflammation (e.g.in response to bacterial capsular polysaccharides), increasing susceptibility to some infections (Barrett and Ayoub, 1986).

For *FCGR2B*, the 232T allotype produces a protein that does not migrate into signalling rafts. As this is an inhibitory receptor, this variant would reduce the level of IC signalling required for immune cell activation, hence rendering subjects more susceptible to conditions such as SLE (Su *et al., 20*04); (Bolland and Ravetch, 2000).

One example for FCGR2C is the Q57X variant; protein is absent when genotype is 57X as this change generates a premature stop codon, which can alter the activating/inhibitory ratio on immune cells (Van der Heijden *et al., 20*12); (Hargreaves *et al., 20*15).

For *FCGR3A*, the 158 V SNP has been reported; this variant demonstrates higher affinity for IgG1 and 3 and binds IgG4 (versus the 158F allotype), lowering the threshold for cell activation upon antibody binding. The 158V allele has been associated with RA in some populations, and an increased susceptibility to inflammatory signals could be the mechanism here (Bournazos *et al., 20*09) (Li *et al., 20*13); (Hargreaves *et al., 20*15). Additionally, *FCGR3A* copy number correlates with protein expression, and increased expression of this protein confers risk for RA and SLE. Again this through lowering the threshold for activating signalling in FcγR expressing immune cells (Hollox *et al., 20*09).

There are allotypic variants reported for *FCGR3B*; neutrophil antigen (NA)1, NA2 and SH, where SH is seen in the presence of the NA2 allele. NA1 is reported to have a higher affinity for IgG and 3 (Salmon *et al., 19*90). The functional impact of this variant will depend on whether FcγRIIIb acts as a decoy receptor or as part of a molecular trap (as described previously). A low copy number of FCGR3B is associated with SLE and RA; copy number correlates with degree of protein expression and pathology is thought to be related to decreased uptake of IC, hence aggrevating auto-antibody driven

conditions such as RA and SLE (Willcocks *et al., 20*08); (Robinson *et al., 20*12); (Chen *et al., 20*14b).

1.4 Rheumatoid Arthritis

1.4.1 Pathophysiology

RA is a chronic inflammatory disease affecting approximately 1% of the population. This condition is characterised by synovial inflammation, synovial hyperplasia, and production of autoantibodies such as rheumatoid factor (RF) and anti-citrullinated peptide antibodies (ACPA) (Choy, 2012); (McInnes and Schett 2011).

Although the exact cause of RA is unknown, genetic and environmental factors are thought to contribute to disease susceptibility. There are a number of genes associated with RA, the most prominent being *HLADRB1*, followed by *PTPN22* (Burton *et al., 20*07). The association with *HLA-DRB1* risk alleles is well established, with increased susceptibility found in patients with alleles containing a "QKRAA" motif, referred to as the shared epitope (Burton *et al., 20*07); (McInnes and Schett 2011). (Konda Mohan *et al., 20*16) recently examined these genes in more detail and determined that *HLA-DRB1* *01, *04 and *10 alleles confer risk for RA, were other allotypes are protective (*HLA-DRB1* *03, *07, *11, *13). Mechanisms have been suggested for this link that relate to the role of human leukocyte antigen (HLA)-DRβ in the presentation of antigens to T helper cells, triggering an inflammatory response (De Almeida *et al., 20*10); (Holoshitz, 2013); (Choy, 2012); (Okada *et al., 20*14); (McInnes and Schett 2011). Recent investigations have attempted to correlate these risk alleles with responses to TNF inhibitor therapy but found no associations, even when stratified for ACPA status (Jiang *et al., 20*16b). However, associations have been reported between certain *HLADRB1* alleles and levels of ACPA; for instance *HLADRB1* *04:04, *04:01 and *01:01 alleles are associated with a significant increase in ACPA in RA patients (Gerstner *et al., 20*16).

PTPN22 codes for lymphoid protein tyrosine phosphatase (Lyp), a protein tyrosine phosphatase which is expressed exclusively in immune cells (Burn *et al., 20*11). Lyp has been reported to act as a regulator of B and T-cell activation and variants in the corresponding gene have been linked to RA along with a number of other autoimmune diseases (including SLE, autoimmune thyroid disease, type 1 diabetes, idiopathic juvenile arthritis) (Hinks *et al., 20*05). This again places B and T-cells as central to the pathogenesis of RA. Additionally, distinct isoforms of Lyp have been identified in tissue from patients with inflammatory diseases, which may indicate one mechanism for how these mutations contribute to pathogenesis (Diaz-Gallo and Martin, 2012).

Over 100 RA associated genes have been identified at genome wide significance levels; polymorphisms in agents involved in STAT4 and IL-10 signalling and in *PSOR1C1, PTPN2, MIR146A, CCR6* and *ICAM1* have been reported. Additionally, SNPs in *PSOR1C1*, *PTPN2*, and *MIR146A* are seemingly associated with a severe phenotype (Angelotti *et al., 20*17); (Ciccacci *et al., 20*16); (Lee and Bae, 2016); (Li *et al., 20*16). Of interest to this project, genes coding for the FcγRs were reported to be associated with RA, as was discussed in Section 1.3.2 genetic variants and disease.

It is possible that environmental factors trigger disease in genetically predisposed individuals; environmental triggers such as smoking have been linked to citrullination of proteins and by extension generation of autoimmunity and ACPAs (Klareskog *et al., 20*09);(Klareskog *et al., 20*11). This is supported by recent findings from a study looking at gene-environmental interactions in RA patients using an immunochip array; here gene variation patterns involved in gene-smoking interactions were identified for ACPA positive but not negative patients, and HLA-DRB1 alleles (along with other genes in the MHC II regions) were found to be associated with exposure to cigarette smoke (Jiang *et al., 20*16c). Thus supporting the suggestion that cigarette smoke-modified proteins can act as immunogenic antigens resulting in ACPA.

Infection has also been suggested as a trigger for RA. For instance, peptidyl-arginine deiminase, an enzyme released by bacteria in periodontitis converts arginine to citrulline, recognised by ACPAs. Relationships described between RA and periodontitis, implicate the process described above as a mechanism (Arunachalam, 2014); (Koziel *et al., 20*14). Additional infectious agents such as Epstein-Barr virus, cytomegalovirus and Escherichia coli have also been associated with RA. The evidence here is not completely clear; these pathogens are known to produce heat shock proteins which reportedly induce T-cell responses in cells isolated from juvenile RA patients. Molecular mimicry of these bacterial products may therefore be a mechanism for disease pathogenesis (McInnes and Schett 2011); (Kamphuis *et al., 20*05). Another factor associated susceptibility to RA is the gut microbiome. Some microbiome signatures have been reported to correlate with auto-antibody positive RA, for instance diversity of microbiota are found to be decreased in patients and expansions of some species (e.g. Actinobacter) are reported. However there are numerous environmental and genetic associations linked with RA, and the pathogenesis of this condition is likely to involve more factors than just gut microbiome (Scher and Abramson, 2011); (Chen *et al., 20*16); (Angelotti *et al., 20*17).

Synovial inflammation is characterised by local leukocyte infiltration, supported by a number of physiological changes; synovial microvessels are activated, permitting cell migration, which is also supported by increased expression of endothelial adhesion

molecules (intergrins, selectins) and chemoattractive cytokines (McInnes and Schett 2011). Additionally, hypoxia promotes angiogenesis. Increased inflammatory synovial tissue is a consequence of these changes and fibroblast activity (Szekanecz and Koch, 2007); (Polzer *et al., 20*08). Bringing in ICs, many ACPA Recognise matrix proteins or secreted enzymes in the joint, thus lending to soluble and fixed ICs that may lead to a vicious cycle by activating FcγR expressing immune cells.

Associations with the HLADRB1 shared epitope and autoantibody production suggest cells related to adaptive immunity are important for RA pathophysiology, specifically when considering that auto-reactive ACPA-specific cells are detecTable in this disorder (McInnes and Schett 2011). However, the inefficacy of T-cell targeting drugs (such as ciclosporin) seems contradictory (Panayi, 2006). It should be noted that CD28 blocking agents (abatacept) that interfere with MHC II costimulation are effective drugs, supporting importance of T-cells in perpetuating inflammation following the initial breakdown of immune tolerance (Vital and Emery, 2006); (Schiff, 2011); (McInnes and Schett 2011)). The presence of autoreactive antibodies (ACPA and RF) in this condition suggest B cells are important in RA pathophysiology, supported by efficacy of biologics targeting these cells as a therapy (e.g. anti-CD20 rituximab).

The presence of innate immune cells and macrophage-derived cytokines in the rheumatoid synovium, together with the fact that a number of cells of the innate immune system are activated by ICs implicates innate immunity in RA inflammation (Gierut *et al., 20*10). Involvement of these cells will be discussed in detail in the later Section “1.4.5 Macrophage and other cell involvement”.

Bone erosion is a central feature of RA where synovitis leads to bone destruction. It reportedly occurs when there is a misbalance between bone resorption by osteoclasts and formation via osteoblasts. In RA, production of TNF is thought to support migration of osteoclast precursors (i.e. monocytes) to the synovium (Li *et al., 20*04). Here differentiation is triggered by M-CSF and receptor activator of nuclear factor KB ligand (RANKL) to form mature osteoclasts (Firestein, 2003); (Schett and Gravallese, 2012). Additional disease mediators, including some ACPAs (targeting vimentin), are thought to enhance osteoclast differentiation (Harre *et al., 20*12). Targeting of RANKL therapeutically was found to halt bone resorption, but not prevent inflammation, whereas treatments aimed to reduce synovitis by targeting cytokines also reduced bone destruction. This supports the involvement of cytokines in promoting these destructive processes. However it is important to emphasize that treatments aimed at decreasing synovitis to effectively reduce bone destruction are not unique to anti-cytokine therapies; other treatments such as methotrexate and rituximab are also

effective for this and will be discussed in Section 1.4.2 Treatments (Schett and Gravallese, 2012); (Cohen *et al., 20*08); (Schett *et al., 20*08).

Cartilage damage is another pathological feature in RA; synovial inflammation increases production of MMPs and other proteases. Subsequent disruption of cartilage collagen network is supported by inability of TIMPs to inhibit the effects and cytokine mediated apoptosis of chondrocytes, which regulate matrix formation under physiological conditions (Sabeh *et al., 20*10); (McInnes and Schett 2011).

1.4.2 Treatments

The drugs used to modulate the immune system for the treatment of RA are referred to as disease modifying anti rheumatic drugs (DMARDs). Methotrexate is the first line treatment for RA and this is also commonly used in combination with other drugs. Methotrexate inhibits an enzyme (dihydrofolate reductase) involved in the synthesis of RNA and DNA, hence blocking proliferation of the rapidly dividing B and T-cells. It is also thought to decrease binding of IL-1β (inflammatory cytokine) and cellular adhesion molecules (Cutolo *et al., 20*01). Leflunomide works in a similar way, inhibiting pathways required for rapid proliferation (Breedveld and Dayer, 2000); sulphasalazine and hydroxychloroquine are also used in some therapeutic combinations (Clements, 2011). Some biologics available include numerous TNF inhibitors (golimumab, entanacept, infliximab, adalimumab), anti CD20 drugs (rituximab) and cytokine blockers (anakira and tocilizumab which are antagonists for IL-1 and IL-6 respectively). Corticosteroids and cyclooxygenase inhibitors can also be used as adjunctive therapies to treat RA, but have a significant toxicity burden (Lipsky and Isakson, 1997); (Saag *et al., 19*94); (Clements, 2011).

It should be noted that limited numbers of RA patients improve in response to any single therapy (Seymour *et al., 20*01), emphasizing the heterogeneity in pathophysiological mechanisms and clinical need for ongoing target identification, drug development and therapeutic stratification.

1.4.3 Role of immune complexes

The presence of auto-antibodies and consequent production of immune complexes (ICs) in the presence of auto-antigens are important pathological processes detectable in the majority of RA subjects (Lorenz, 2001). The major auto-antibodies found in RA are RF (largely of the immunoglobulin M (IgM) class but IgG and IgA RF are present, but not routinely analysed) and ACPAs (largely IgG and to a lesser extent IgA); RF

recognises the Fc region of IgG, and ACPA recognise a variety of peptides that have undergone citrullination. Some examples in the rheumatoid synovium include citrullinated fibrinogen, vimentin and α-endolase (Cantaert *et al., 20*06); (Willemze *et al., 20*12). Presence of ACPA is strongly associated with disease severity, and is linked to increased disease activity, bone destruction, patient disability and reduced frequency of remission with treatment (Humphreys *et al., 20*14); (Hecht *et al., 20*14); (Sokolove *et al., 20*14).

ICs exert their effect through ligation of Fc Receptors (FcR), rendering cells expressing these receptors sensitive to IC stimulation. IC stimulation of FcR expressing myeloid cells (macrophages, monocytes, dendritic cells) induce various responses including cell activation, phagocytosis of opsonised pathogens, antibody-dependent cellular cytotoxicity (ADCC), release of pro-inflammatory mediators and reactive oxygen intermediates, and production of chemokines and cytokines (Laborde *et al., 20*07). Fc gamma receptors (FcγRs), the IgG binding class of FcRs, have been implicated in a number of autoimmune diseases characterised by IC accumulation, such as RA (also ANCA-associated vasculitis, systemic lupus erythematosus (SLE)) (Cooper *et al., 20*12); (Willcocks *et al., 20*08); (Jancar and Crespo, 2005); (Laborde *et al., 20*07); (Morgan *et al., 20*05); (Morgan *et al., 20*06). Additionally, FcγR ligation by IC can affect differentiation of some cell types, alter cell cytokine profile, induce different phenotypes, be involved in cross-talk with other receptors and modulate signalling pathways induced by other ligands and effector molecules.

1.4.4 Fc receptors in RA

FcγRs are implicated in the pathogenesis of RA. APCA are often IgG and will form ICs that bind FcγRs resulting in immune cell stimulation. IgG binding RF also exists as IgG but mainly in the IgM isotype, with their pentameric structure contributing to formation of large IgG-containing ICs that may crosslink multiple FcRs. Release of inflammatory mediators that propagate inflammation (such as TNF and IL-6) by activated cells is one consequence of FcγR ligation (Clavel *et al., 20*08); (Magnusson *et al., 20*14). Several studies demonstrated that activating FcγRs are essential for development of IC-mediated experimental arthritis in murine models; FcγRI, II, III and IV are described for mice, with I, III and IV being activating and II being inhibitory. The inhibitory mouse FcγRII has suppressed arthritis in these models (Magnusson *et al., 20*14); (Nimmerjahn and Ravetch, 2008). Protection against arthritic disease has also been reported for mice deficient in the FcRγ chain, further implicating activating FcγRs (I, III and IV in mice) in arthritis disease pathogenesis, as these receptors cannot induce downstream signalling without this accessory signalling chain (Kleinau, 2003). FcγRII

has a well-established protective role, highlighted by knock-out studies in mice where deficiency of this receptor was associated with increased risk of developing collagen induced arthritis (Yuasa *et al., 19*99). Interestingly, it has recently been reported that mice with B cell specific FcγRII knockout are less susceptible to CIA than myeloid cell specific and full FcγRII knock-out, suggesting B cell FcγRs are less involved in disease susceptibility (Yilmaz-Elis *et al., 20*14). However, in addition to controlling signalling through inflammatory receptors, the human orthologue, FcγRIIb, has a role in inducing tolerance in B cells (Sun *et al., 20*13). Hence decreased expression or functioning of FcγRIIb may lead to impaired toleragenic mechanisms; this has been reported in B cells derived from SLE patients, emphasising the relevance of this phenomenon in auto-immune disease (Mackay, 2008).

When considering murine literature, it must be stressed that FcγRs in mice are evolutionarily distinct from those in humans and so data produced using murine receptors can only be used to give an overall idea of how this class of receptors contributes to disease rather than implicating a specific FcγR. As described in Section 1.3.2 (Genetic variants and disease) a number of FcγR polymorphisms and haplotypes have been linked to RA, supporting their involvement in RA pathology.

1.4.5 Macrophage and other cell involvement

A number of cells are implicated in the pathophysiology of RA; the fibroblast-like synoviocytes of the joint interact with cells of both the innate (neutrophils, macrophages, NK cells and dendritic cells, mast cells) and adaptive immune system (B cells and T-cells) involved in disease onset and progression (Angelotti *et al., 20*17).

Neutrophils in the joint are known to produce of a number of agents lending to destructive processes that occur in RA including proteases, prostaglandins and reactive oxygen species (McInnes and Schett 2011); (Cascao *et al., 20*10). Additionally, increased numbers of mast cells are found in the joints of RA patients and they are thought to have roles in disease given their TLR-mediated production of inflammatory agents (chemokines, cytokines, proteases) (McInnes and Schett 2011); (Nigrovic and Lee, 2007).

Macrophages are thought to occupy a central role in RA pathophysiology. Accumulations of macrophages are seen in the synovial lining and cartilage-pannus junction during active disease, a feature which can be used to predict patient responses to immune modulating therapies and has been associated with disease activity score (Lebre and Tak, 2010). Additionally, macrophage-derived cytokines are strongly associated with ongoing inflammation, cartilage destruction, remodelling and

destructive processes; notably macrophage levels have been found to correlate with degree of joint erosion (Kennedy *et al., 20*11); (Kinne *et al., 20*07); (Mulherin *et al., 19*96); macrophages contribute significantly to extracellular matrix degradation in RA through production of proteinases (cathepsins and matrix metalloproteinases) (Szekanecz and Koch, 2007); (Nagase and Murphy, 2013). Some reports describe the macrophages found in the rheumatoid synovium as “M1” cells due to the high levels of GM-CSF in the synovium and production of pro-inflammatory cytokines and reactive oxygen species by these cells along with the demonstration of increased phagocytosis and antigen presentation capabilities (Laria *et al., 20*16b); (McInnes and Schett 2011). It has also been suggested that this phenotype is reversed into the M2 state upon treatment with glucocorticoids (Laria *et al., 20*16b). However, this view is over simplistic and does not take into account the presence of polarising molecules such as ICs in the synovium. Overall, these observations highlight macrophages as therapeutic targets in this disorder, but gaps in the literature surrounding their activation limits therapeutic application.

1.5 Next generation sequencing technology

1.5.1 RNA-seq

Next generation RNA-sequencing (RNA-seq) technology is a powerful tool for uncovering important functional aspects of the genome through an in depth interrogation of cell transcripts (Wang *et al., 20*09). Generally speaking, this method utilizes next generation sequencing (NGS) techniques to profile RNA-derived cDNA, to discover and quantify genes expressed in a given cell or population of cells (Conesa *et al., 20*16); (Guo *et al., 20*13). Here, given expression levels are determined by the number of reads mapped and length of the transcript (Young *et al., 20*10). In addition to providing higher coverage and greater resolution than previous methods, this technology additionally allows the user to investigate splice variants, allele-specific expression and RNA editing (Young *et al., 20*10). It should also be noted that microRNA, small non-coding and long noncoding RNA may also be detected using this method, which may give further insights into the post-transcriptional landscape and additional levels of regulation in certain cell types (Wang *et al., 20*09).

1.5.2 Practical considerations

Broadly speaking, library preparation involves isolating RNA from cells, converting them to cDNA fragments which are then ligated to adaptors and sequenced to produce short reads (Wang *et al., 20*09). However, there are a number of factors that must be

considered at different stages of this process which have an impact on the data produced. Some of these may vary depending on the depth of sequencing and coverage required in the experiment and others are essential for production of high quality data (Kukurba and Montgomery, 2015). For instance, when considering RNA extraction, it is important to ensure high quality RNA is entered into library preparation stages. One way to do this is to check RNA integrity number (RIN) following extraction using a piece of equipment such as a bioanalyser or tape station; here software generates an electropherogram representing the RNA sample (Schroeder *et al., 20*06). This estimates the quality of RNA by looking at a complete RNA trace, determining ratio of ribosomal bands and detecting degradation products, and assigns the sample a score between 1 and 10; here 10 represents the highest integrity and 1 the lowest. Values less than 6 are considered to be of poor quality, which may give rise to certain biases such as uneven coverage or bias towards the 5' or 3' regions (Gallego Romero *et al., 20*14); (Schroeder *et al., 20*06); (Kukurba and Montgomery, 2015). It should be noted that it is not always possible to collect samples with high integrity (e.g. from fixed or paraffin embedded samples), but this method is useful as a consistent, reproducible way to determine quality of RNA between different laboratories (Kukurba and Montgomery, 2015).

There are a number of different types of RNA that are isolated during extractions. Messenger RNA is usually of interest in these experiments, but ribosomal RNA is much more abundant in the cell (constitutes 90-95% of total RNA) (Conesa *et al., 20*16); (Kukurba and Montgomery, 2015). Other types of non-coding RNA include transfer RNA, small nuclear RNA, small nucleolar RNA, micro RNA and piwi-interacting RNA (Stefani and Slack, 2008); (Kukurba and Montgomery, 2015). If not removed, ribosomal RNA will constitute the bulk of reads, reducing the read depth for all other RNA types and thus reduced sensitivity. Hence RNA-seq library preparation methods commonly use ribosomal depletion of poly(A) selection to remove ribosomal RNA. Poly(A) enrichment involves using poly(T) oligonucleotides attached to a substrate which will bind the poly(A) tail before isolation steps. This method is optimal for experiments only interested in mRNA, but tends to require RNA input with a high RIN score, which as previously described is not always possible. Additionally this will not be appropriate for samples of bacteria for instance which do not have poly(A) tails (Kukurba and Montgomery, 2015); (Conesa *et al., 20*16). Ribosomal depletion is useful for looking at expression of lower abundance non-coding RNA and pre-mRNA (not post-transcriptionally modified) in addition to mRNA. However, it should be noted that variances in efficiency of ribosomal depletion and coverage of small transcripts have been reported between different kits, which must be considered as part of the experimental design (Huang *et al., 20*11); (Kukurba and Montgomery, 2015). It should

be noted that specific protocols have been developed to study expression of small non-coding RNA species, but these methods are not the focus of this report.

Depending on the methodology, sequencing can be stranded or non-stranded (i.e. information is given on whether reads are derived from sequencing a sense or anti-sense strand). Non-stranded methods make it impossible to distinguish between reads from both orientations which can cause issues when attempting to analyse the data (for instance, overlapping reads from alternative strands are required for identification of novel transcripts) (Kukurba and Montgomery, 2015). Stranded methods commonly incorporate deoxy-UTP labels into the reaction during second strand synthesis followed by ligation of "Y-adaptors" which inform on strand orientation. An additional step involving degradation of this molecule prior to subsequent PCR amplification allows identification of coding strands (Parkhomchuk *et al., 20*09).

During sequencing, reads can be paired or single-ended. Paired end reads refer to a scenario where both ends of a sequence are read as opposed to just one (i.e. in both directions). This is beneficial when sequencing transcripts that will be mapped to poorly understood transcriptomes, but may not be essential for differential expression analysis on sufficiently annotated genomes (Kukurba and Montgomery, 2015).

Coverage has been referred to as number of reads, given an assumed number of reads of a certain length, and the supposition that the reads are randomly distributed across all the genes being sequenced (Sims *et al., 20*14). Depth of sequencing is the redundancy of coverage and these factors are also determined by the methodology used. As different samples can be tagged with distinct adaptors (genetic barcodes), which may be used to identify them, it is possible to pool different conditions onto one lane of the sequencer. There are a number of reads generated per sequencing run for different platforms, and so coverage will be dependent on technology used, amount of genetic material being sequenced and length of reads produced (Sims *et al., 20*14).Hence depth of sequencing required depends strongly on the aims of the experiment; for instance if large changes are being detected in overall transcriptome, the number of reads per sample does not need to be as high. However, if low abundance transcripts are of interest or highly complex regions, a greater depth of sequencing is required to ensure accurate detection (Conesa *et al., 20*16). There is also some discussion as to whether deep sequencing may lead to an increase in the number of off target transcripts and increase noise (Tarazona *et al., 20*11).

A number of different platforms are currently available for RNA-seq, but the majority of experiments are currently performed using Illumina based technology.

1.5.3 Analysis and applications

Preparation of RNA-seq libraries are extensive, intricate processes, and issues at numerous stages can introduce errors that would affect the quality of the data. Subsequent biases and problems with mapping would reduce integrity of results. Hence, introduction of a quality control step prior to downstream analysis is essential (Li *et al., 20*15). Raw reads generated by the sequencer can be analysed using different bioinformatic programs for quality scores (Conesa *et al., 20*16); FASTQC, TileQC and PIQA are useful programs that can be used to investigate quality of reads generated using an Illumina platform and NGS QC is a cross platform tool, i.e. it can be used to calculate quality of output from Illumina, Roche and Applied Biosystems technologies (Dai *et al., 20*10); (Patel and Jain, 2012). Different tools can be used to remove poor quality sequences from read files; Trimmomatic, FASTX toolkit and Btrim are some examples (Chen *et al., 20*14); (Bolger *et al., 20*14); (Conesa *et al., 20*16). It should be noted that these technologies tend to determine data quality based on similar metrics such as duplication of reads (indicates likelyhood of contamination or PCR artefacts for instance), *k*-mer content, GC levels, sequence quality, sequence depth and presence of adaptor sequences (Conesa *et al., 20*16); (Li *et al., 20*15). The latter may be improved using programs designed to remove adaptor sequences from reads such as Cutadapt and SeqPurge, and through applying some of the other tools mentioned above that were described to remove low quality sequence reads (e.g. Trimmomatic, Btrim) (Chen *et al., 20*14); (Sturm *et al., 20*16).

Counts are produced through mapping reads to a reference genome or transcriptome and normalising the output. Generally speaking the choice depends on applications; as alignments to a reference transcriptome (versus a reference genome) relies on previous knowledge of known exon boundaries and splice variants, this protocol would be considered unsuitable for studies interested in identifying novel splice variants (Garber *et al., 20*11). There are a number of factors that require consideration prior to this process such as choice of reference genome and software used to perform mapping. Choice of alignment software may depend on other aspects of experimental design, for instance unspliced aligners (do not allow large gaps) such as Stampy, Bowtie, MAQ and BWA may be sui1able for alignment to a reference transcriptome, but spliced aligners such as STAR, Tophat, and MapSplice would be required for alignment to a genome (Yang and Kim, 2015); (Li and Durbin, 2009); (Langmead and Salzberg, 2012); (Trapnell *et al., 20*09); (Wang *et al., 20*10a); (Dobin *et al., 20*13). Some differences between these could include factors such as mapping speed, mapping biases and error rates and limitations in terms or read length, all of which must be considered at the experimental design phase (Dobin *et al., 20*13). Hence

selection of an aligner will depend on complexity of transcriptome being investigated and experimental aims. Different reference genomes are available for human samples and may vary slightly in terms of annotations, one example of a recent assembly being Hg38, which includes annotations from databases such as GENCODE, ClinVar, ClinGene and more (Speir *et al., 20*16).

Technical differences between RNA-seq and previous technologies required advances in analysis techniques to ensure maximal amounts of data could be interpreted from outputs of this method (Young *et al., 20*10). Various software packages have been designed to perform various analyses and will be discussed here. It should be clarified that there are a number of different ways to analyse RNA-seq data and only some options for the more fundamental approaches will be considered in this Section.

Identification of differentially expressed genes between conditions is one of the main analyses performed on RNA-seq data, and is often required for downstream investigations. Many packages in R based on different mathematical models can be used to identify these gene lists and some of the most popular choices include edgeR and DESeq (Robinson *et al., 20*10); (Anders and Huber, 2010).

Although differentially expressed gene (DEG) analysis gives an idea of changes that are occurring in the transcriptional landscape between different conditions, context is required to draw any conclusions or give indications of a direction in which to carry out further research. Gene ontology (GO) enrichment analysis can provide insight into biological functions that vary between samples from different tissues or with different treatments. A number of packages are available to determine which biological processes are enriched in different conditions, some commonly used examples being the following; ClusterProfiler, BinGO (Yu, 2012); (Maere *et al., 20*05). These packages tend to rely on databases summarising genes annotated for specific terms. Enrichment of genes from specific pathways can also be distinguished from a list of DEGs. Some commonly used databases to identify genes in the same pathways are KEGG and REACTOME (Jin *et al., 20*14).

It is possible to plot expression levels of genes which are related to one another as networks. This can give insight into functional interactions between similarly expressed of counter regulated genes.

Depending on the experimental design and methods used to map reads, it can be possible to identify transcript variants or gene fusions within samples using RNA-seq data. These are useful applications but are not directly relevant for this project so will not be discussed in detail here; please see Conesa *et al.,* (2016) for detailed summaries.

1.5.4 Comparisons with microarrays

Although gene expression profiles generated through both microarray and RNA-seq methods show high correlation, a number of differences have been described. Some variations between standard microarray and RNA-seq experiments have been summarised in Table 1.5.1.

Table 1.5.1. comparison of microarray and RNA-seq experiments in terms of technical and analytical issue and performance. References are also given for the source of information

	RNA-seq	Microarray	Reference(s)
Identification of novel transcripts	No issues with annotation redundancy	Limited by current knowledge of transcripts Tiling arrays face problems with cross-hybridisation affecting reliability	(Zhao *et al.*, 2014) (Wang *et al.*, 2009)
Differential gene expression	Detection of more differentially expressed genes due to greater dynamic range	Limited detection range of individual probes	(Zhao *et al.*, 2014) (Nookaew *et al.*, 2012) (Wilhelm and Landry, 2009)
Low abundance transcripts	More sensitive detection of low abundance transcripts	Less effective at detecting low abundance transcripts vs RNA-seq More correlation for longer exons	(Zhao *et al.*, 2014) (Guo *et al.*, 2013) (Wang *et al.*, 2014a)
Splice variants	Mapping of intron/exon boundaries can identify splice variants	Limited by current knowledge- some isoforms may be ignored	(Zhao *et al.*, 2014) (Nookaew *et al.*, 2012) (Piskol *et al.*, 2013)
Background signal/off target effects	Little background as no probe effect	Probe cross-hybridisation or non-specific-hybridisation cause off target effects and higher background	(Zhao *et al.*, 2014)
Cost	Higher cost of sequencing	Less expensive experiment	(Zhao *et al.*, 2014)
Technology	More complex analysis vs microarray	Less complicated analysis	(Zhao *et al.*, 2014) (Garber *et al.*, 2011)

1.5.5 Additional technical issues to be considered when analysing RNA-seq data

Intrinsic bias towards selecting longer or more highly expressed transcripts as differentially expressed may be an issue when analysing RNA-seq data; due to increased amounts of mapping to these regions, they will be represented by higher statistical power and are hence more likely to be identified through differential expression analyses. Normalisation and rescaling are not effective in removing this data artefact (Oshlack and Wakefield, 2009); (Young *et al., 20*10).

During library construction, some biases can be introduced based on different fragmentation methods. For instance, this can be carried out on either RNA or cDNA. When performed on RNA there appears to be little bias over the transcript body, but depletion at the sequence ends may occur when contrasted with other methods. Conversely, cDNA fragmentation creates a bias towards the 3-prime region during poly(A) purification (Wang *et al., 20*10a); (Mortazavi *et al., 20*08); (Nagalakshmi *et al., 20*08).

Other problems may occur when there is high expression of a short read; this phenomenon may accurately represent expression of the mapped gene in the transcriptome, but could also occur as a PCR artefact. Replicates are important here for such investigations (Wang *et al., 20*10).

Another limitation is presented when mapping output sequences to a reference; multi-mapping can occur where some reads recognise multiple sites on the genome. This may be compensated for by proportionally assigning reads based on mapping to adjacent sequences, dividing read counts over multiple sites or disregarding multi-mappers completely (Wang *et al., 20*10); (Mortazavi *et al., 20*08). As paired end reads detect longer sequences they are less likely to produce this issue, hence steps can be taken during experimental design stages to improve this. Additionally, it should be noted that complex mutations may create problems with mapping (Wang *et al., 20*10). One problem that may be encountered in this project is mapping-specificity when looking at differential expression of the different Fc Receptors; corresponsing gene sequences are highly homologous and so only reads mapping to distinctive regions may be considered for giving an estimate of expression (Li *et al., 20*09).

1.6 Aims and objectives

The overall objective of this project was to dissect the role of immune complexes in modulating the transcriptome and polarisation state of macrophages using next generation sequencing technology. To achieve this a number of smaller objectives were required:

1. To identify a panel of polarisation markers that reliably indicated different human macrophage polarisation states

2. To generate an optimised THP-1 cell line model to study the effects of ICs

3. Validation of this cell line model using next generation sequencing and comparisons with primary cells

4. Ultimately to examine changes in macrophage transcriptomes following exposure to ICs

These objectives were sequentially addressed in my PhD project.

Chapter 2: Analysis of differentially polarised macrophage transcriptomes using publicly available datasets

2.1 Introduction

Macrophages are a highly heterogeneous group of cells that respond to a variety of stimuli; PBMC derived macrophages differentiate from monocytes following activation signals from colony stimulating factors, and may polarise variably depending on the local cytokine milieu (Zhou *et al., 20*14). These cells are also reported to demonstrate high plasticity in response to environmental changes under physiological conditions (Zhou *et al., 20*14); (Wynn *et al., 20*13); (Moore *et al., 20*13); (Murray *et al., 20*14). Traditionally macrophages are classified into the more inflammatory M1 phenotype and the anti-inflammatory/wound healing/allergy associated M2 state which is sub-typed into M2a M2b and M2c cells (Martinez *et al., 20*06); (Chinetti-Gbaguidi and Staels, 2011). Details of polarisation stimuli can be seen in Figure 2.1.1.

Although these subtypes are frequently referred to in the literature, there is no consensus on how to define them; characteristic functions and metabolic differences are unclear for human macrophage populations. One explanation for this variability could be that experiments are carried out on both peripheral and tissue macrophages in human and murine cells and are activated with variable agents (i.e. M-CSF, GM-CSF) prior to polarisation (Joshi *et al., 20*14); (Fleetwood *et al., 20*09). For instance, one of the original standards for distinguishing M1 and M2 cells involves examination of arginine metabolism in murine cells, but this paradigm does not translate to human macrophage phenotypes (Bogdan, 2001); (Murray and Wynn, 2011). More recently, alterations in the Krebs cycle were reported for inflammatory macrophages (vs M2 cells) but again this research was performed using murine macrophages, and is not a reliable model for classifying human macrophages (O'Neill *et al., 20*16).

For this reason, protein and RNA markers have been adopted as the gold standard for distinguishing these cell types in humans. However, different studies tend to use different marker panels, which again makes it difficult to define individual subtypes, as marker recommendations are often contradictory (Barros *et al., 20*13); (Murray *et al., 20*14). Hence it was deemed necessary to develop a strategy to produce a list of markers that can be used to define specific cells types, and subsequently be utilised in experiments to optimise monocytic cell line models.

Next generation RNA sequencing produces vast datasets which can be mined for both specific genes and general expression signatures. Generation of lists of potential

marker transcripts can be identified in a less biased manner (i.e. not using a marker that an individual experiment determined to be accurate) using this methodology than if replicating panels used in a specific study.

However, if genes have frequently been reported as effective markers in different studies, it is possible that they may demonstrate robust performance and reliability; identification of these markers in this public dataset analysis may be considered as an extra level of validation for their use as subset-specific transcripts in experiments. Additionally, it may be possible to identify novel markers that may outperform those already reported.

There was no in-house production of *ex-vivo* macrophage datasets at the time of this analysis, so publicly available RNA-seq and microarray datasets were used as a preliminary data source.

In summary, the primary aims of this Chapter were to identify sequencing datasets for appropriate macrophage subtypes and isolate potential polarisation markers, some of which may be novel.

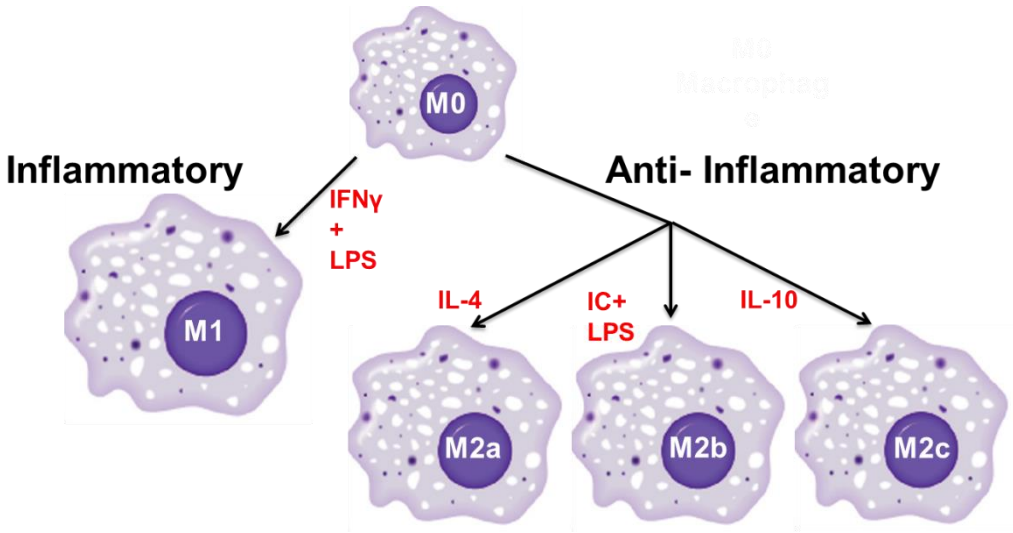

Figure 2.1.1. Basic bipolar model of macrophage differentiation using standard polarising agents: interferon gamma (IFNγ), interleukin-4 (IL-4), immune complexes (IC), lipopolysaccharide (LPS), interleukin-10 (IL-10).

2.2 Materials and Methods

2.2.1 Marker literature review

Markers frequently used to define different macrophage subsets were identified from the literature. Experimentally validated and frequently used genes from the literature were summarised into a Table (along with key references) for cross comparison with lists produced through public dataset analysis.

2.2.2 Identification of suitable datasets

Array Express (source: https://www.ebi.ac.uk/arrayexpress/) was searched for both RNA-seq and microarray datasets which looked at different macrophage conditions in humans, with a primary focus on the classical M1 (IFNγ and LPS) and M2a (IL-4)-induced cells. Experiments where other basic polarisation conditions such as M2b (LPS and ICs) and M2c (IL-10) were included were also searched for.

2.2.3 Analysis of publicaly available RNA-seq data to identify markers

Datasets E-GEOD-36952 and E-GEOD-37769 which were obtained using Illumina HiSeqSQ and Illumina HiSeq2000 platforms, respectively, (in the original studies) were selected for analysis (Beyer *et al., 20*12). Raw, unprocessed data was extracted for in-house analysis; i.e. for identification and selection of optimal established/novel markers

2.2.3.1 Quality control of public data and adaptor removal

A pair of gzipped fastq sequence files for each sample were downloaded from Array Express. While data for read 1 and read 2 sequences were stored in the different files, their order was maintained such that the sequences for each end of an insert could be determined. The quality of the base calling for each position and the amount of sequencing adaptor present in each file was determined using FASTQC (Andrews, 2010). Adapter sequences and positions with a low-quality base calling score were removed using CUTADAPT (Martin, 2011), which was run using the following command line:

```
cutadapt -q 10,10 -m 30 -b $read1_adaptorseq -B $read2_adaptorseq -o $trimmed_read1 -p $trimmed_read2 $read1 $read2
```

Where $read1 and $read2 represent the names of the paired input sequence files, $trimmed_read1 and $trimmed_read2 represent the paired files to which the processed

data was saved too. The input for $read1_adaptorseq identifies the sequence of the sequencing adaptors to be removed from the data (the preceding flags –b indicates that $read1 should be scanned for the following sequence, while –B indicates $read2 is the target). The –m 30 parameter results in read pairs with a read less than 30 bp in length being discarded. Finally, the –q 10,10 parameter indicates that both the 5' and 3' ends of each read will be trimmed of base calls with a quality score of less than 10. The command simultaneously processed a sample's read 1 and read 2 data files such that the link between an insert's read 1 and read 2 sequence data was maintained in the exported fastq files. The processed files were screened a second time with FASTQC to access the efficiency of the quality trimming and adaptor removal, with the process reiterated until the data contained no significant amounts of poor quality sequence data.

2.2.3.2 Read alignment and production of counts Tables

Sequencing reads were aligned to the reference human genome GRChg19/hg19. Sequence and annotation GTF (general transfer format) files were downloaded from the Genome browser web page (http://genome.ucsc.edu/cgi-bin/hgTables). Indexing of reference genome was performed using the following command:

```
STAR --runThreadN 12 --runMode genomeGenerate --genomeDir STAR_genome/ --
genomeFastaFiles $hg19 --sjdbGTFfile $hg19 --sjdbOverhang 150
```

A key of parameters for the command is given in Table 4.2.1

Table 2.2.1. Key of parameters for STAR genome alignment command

Star flag, parameter pair	Description of the option or flag
--runMode genomeGenerate	directs STAR to create a genome index
--runThreadN	number of threads to be used for the genome index generation (number of cores)
--genomeDir	path to the directory where the genome indices are stored
--genomeFastaFiles	specifies one or more FASTA files containing the genome reference sequences
--sjdbGTFfile	path to the file containing transcripts annotation in the standard GTF format
--sjdbOverhang	specifies the length of the genomic sequence around the annotated junction to be used in constructing the splice junctions database

Alignment of the read data to the indexed reference sequences was performed using the STAR software (Dobin *et al., 20*13) to produce output BAM files, using the following command:

STAR --runMode alignReads --genomeDir $StarIndex --runThreadN 4 --readFilesIn $read1 $read2 --readFilesCommand zcat --outFileNamePrefix $outDir --outSAMtype BAM SortedByCoordinate

--outFilterMultimapNmax 50 --sjdbGTFfile hg19.gtf --sjdbOverhang 150 --outReadsUnmapped Fastx --outSAMstrandField intronMotif

The functions for each of the parameters are listed in Table 2.2.1

Table 2.2.2. Function key for STAR software command

Star flag, parameter pair	**Description of the option or flag**
--runMode alignReads	Instructs STAR to align reads to the genome
--runThreadN 4	Instructs STAR to run 4 threads when aligning the data.
--genomeDir $StarIndex	Identifies the location of genome index files that are used to align the data.
--readFilesIn $read1 and $read2	Identifies the read 1 and 2 fastq files.
--readFilesCommand zcat	Indicates that the sequence files are compressed using gzip algorithm.
--outFileNamePrefix $outDir	Gives the 'base' name and path to use when saving the alignment and associated meta data.
--outSAMtype BAM SortedByCoordinate	These tell STAR to make a sorted BAM file
--sjdbGTFfile hg19.gtf	Name of the annotation file that describes the location of known exon positions
--sjdbOverhang 150	Specifies the length of the genomic sequence around the annotated junction to be used when constructing the splice junction's database.
--outReadsUnmapped Fastx	Saves unmapped reads to a fasta file
--outSAMstrandField intronMotif	Reads with inconsistent and/or non-canonical introns are filtered out

Read 1 and read 2 sequences from each insert were alignment together so their ultimate location in the genome was based on the quality of the sequence alignment and the location of its matched pair mate.

As described in the key, the parameter --outSAMtype BAM SortedByCoordinate instructed STAR to give the output as sorted BAM files. BAM files underwent further processing to produce normalised counts Tables. The cufflinks suite (source: http://software.broadinstitute.org/cancer/software/genepattern/modules/docs/Cufflinks.cuffmerge) was used for data normalisation. Cufflinks was used to assemble the bam files into transcriptomes; GTF files were formed for each BAM file containing all the genes expressed in each sample.

cufflinks --g hg19.gtf -- M / rRNA_tRNA.gtf --b hg19.fa -u -o $output_directry -p 4 $input.bam

Command functions are summarised in Table 2.2.2

Table 2.2.3. Function key for Cufflinks software command

Star flag, parameter pair	Description of the option or flag
cufflinks	Tell the HPC to run cufflinks
-g	Reference gene annotation in GTF file format, used to guide transcriptome assembly
-M	Masked (i.e.) ignored gene annotation in GTF file format
-b	Tells the program the location of multi-fasta reference sequence file that contains the genome sequences the reads were aligned to.
-u	An option to more accurately weight reads mapping to multiple locations in the genome
-p	The number of cores/threads to execute on
-o	Output directory to export the results to
BAM file	Input BAM format file

Cuffmerge combined GTF files generated for each BAM file using the following command:

cuffmerge -s $hg19.fa -g $hg38.gtf -p 10 -o $path to output directory

Command functions are summarised in Table 2.2.3

Table 2.2.4. Function key for Cuffmerge software command

Star flag, parameter pair	Description of the option or flag
-s	Input reference fasta file that the read data was aligned too.
-g	Input GTF file containing gene annotations (original downloaded from UCSC)
-o	Output directory to put the results in.
-p	Number of cores/threads to run the program on.

Cuffdiff was used to produce a counts Table from the merged GTF file. Output counts file gave counts as FPKM (fragments per kilobase per million mapped reads). The following command was used:

cuffdiff -p 10 -o $hg38.fa -u -v -M $rRNA_tRNA.gtf -g $merged.gtf -L affected,control $affected1.bam,$affected2.bam, $control1.bam,$control2.bam -o $path to output file

Command functions are summarised in Table 2.2.4

Table 2.2.5. Function key for Cuffdiff software command

Star flag, parameter pair	Description of the option or flag
cuffdiff	Tells the HPC to run the program
-p	Number of cores/thread to execute on
-b	Tells the program the location of multi-fasta reference sequence file that contains the genome sequences the reads were aligned too.
-u	An option to more accurately weight reads mapping to multiple locations in the genome
-M	GTF file for masking rRNA and tRNA
-g	Assembled merged.gtf file from cuffmerge
-L	Comma separated list of conditions (i.e. groups)
Control1.bam,control2.bam,control3.bam	Comma separated list of bams (from the first condition
S1.bam,S2.bam,S3.bam	Comma separated list of bams from the second condition
-o	Output directory for storing files in

Normalised counts (as FPKM) were imported into R using the readr package and merged with gene name identifiers using data found in the org.Hs.db package (Carlson, 2017). Functions from the annotationDBi and clusterProfiler packages were also used here (Yu *et al., 20*12); (Pagès *et al., 20*17); please refer to complete script in Appendix 3 (Script A3.7). Subsequent data was then exported from R for manual analysis.

2.2.4 Refining gene lists for marker identification

Gene Tables were imported into Microsoft Excel for further analysis. Using the data functions, potential marker genes were refined prior to analysis according to the following criteria:

-genes with no expression were removed

-genes where average counts were <10 in both M1 and M2a conditions were discounted

-if read count was highest in untreated condition, then gene was removed

-Lower threshold for FPKM counts of genes in the condition of interest was set at 40; transcripts with lower read counts were eliminated

For M1 marker selection, genes were ordered by average M1 count/ average M2a count and the top 150 markers were isolated. Similarly, genes were ordered by average M2a/ average M1 count to identify the top 150 potential M2a markers. These lists were combined and read into R using the readr package, and plotted as heatmaps using the heatmap2 package

Using lists produced in the literature review, established markers appearing in the top 30 gene lists for M1 and M2a cells were selected as suiTable candidates for marker panels in various cell pathways. Additionally, previously unknown genes following a similar pattern in these lists were flagged as potential novel markers.

2.2.5 Identification of markers from microarray datasets

A dataset generated in a study by Xue *et al.,* (Xue *et al*. 2014) (Array Express accession number: E-GEOD-46903) was selected for marker validation, and identification of additional subset-specific transcripts.

Pre-processed (normalised) gene expression data files for all conditions of interest (monocytes, M0, M1, M2a, M2b and M2c) were downloaded from Array Express (source: https://www.ebi.ac.uk/arrayexpress/) in a zipped folder. Individual sample text files were extracted manually and imported into R. Data were then merged and gene expression Tables were exported as text files at this point. The complete script used here can be found in Appendix 3, Script A3.4, along with annotations describing command functions.

The Tables exported as text files were analysed manually in Microsoft Excel using data analysis functions, and fold change was used to identify markers that were high in one condition only. Genes were then ordered using the ratio of expression for a specific treatment vs expression in M0 cells. M1 and M2a cells were also contrasted using fold change in the same way using Microsoft Excel.

2.2.6 Comparison of RNA-seq and microarray gene lists

Lists of genes identified following relative selection criteria were ordered and ranked according to fold change in Microsoft Excel using the data manipulation functions. Ranking for genes of interest were isolated and noted.

2.2.7 Tracking changes in subset specific gene expression over different time points

Microarray data for various cytokine treatment times were identified from supplementary data provided by Xue *et al.,* (2014), read into R using functions in the readr package, and combined into Tables. Heatmaps were generated using the the heatmap2 package. The complete script for this can be found in Appendix 3, Scripts A3.9.

2.3 Results

2.3.1 Markers identified through literature review

A large number of genes have been used in previous protocols to define macrophage polarisation. Some genes which have previously been linked to the M1 or M2 macrophage phenotypes were identified here by literature review and were summarised for further consideration; Tables 2.3.1 and 2.3.2 (M1 and M2 macrophage markers, respectively). The efficacy of these genes as subset markers is unclear, and some reports describing specificity of certain transcripts have been contradictory (e.g. in the case of *CD163* where some groups refer to this marker as M2a-specific and others describe it as M2c-specific or even a pan-macrophage marker) (Barros *et al., 20*13); (Murray *et al., 20*14, Hu *et al., 20*17). Hence these markers were set aside for comparisons with transcripts highlighted in the analysis of transcriptome data (described in subsequent Sections), and for potential validation.

Table 2.3.1. Commonly used M1 markers identified through searching the literature. Details of publications of where use of these markers can be seen is also given in the "Reference" column. M1 refers to M1 macrophages

Gene	Polarisation state	Reference
TNF	M1	(Soler Palacios *et al*., 2015); (Martinez *et al*., 2006); (Arnold *et al*., 2015)
IL23A	M1	(Soler Palacios *et al*., 2015)
MMP1	M1	(Chizzolini *et al*., 2000)
MMP2	M1	(Chizzolini *et al*., 2000)
MMP7	M1	(Chizzolini *et al*., 2000)
MMP9	M1	(Chizzolini *et al*., 2000)
MMP12	M1	(Chizzolini *et al*., 2000); (Soler Palacios *et al*., 2015)
EGLN3	M1	(Soler Palacios *et al*., 2015)
INHBA	M1	(Soler Palacios *et al*., 2015)
CCR2	M1	(Soler Palacios *et al*., 2015)
SLC2A1	M1	(Soler Palacios *et al*., 2015)
CCR7	M1	(Soler Palacios *et al*., 2015); (Martinez *et al*., 2006); (Kittan *et al*., 2013); (Jaguin *et al*., 2013)
IRF1	M1	(Günthner and Anders, 2013)
IRF5	M1	(Krausgruber *et al*., 2011); (Günthner and Anders, 2013)
IRF8	M1	(Günthner and Anders, 2013)
IL12B	M1	(Kittan *et al*., 2013)
CXCL10	M1	(Jaguin *et al*., 2013); (Ambarus *et al*., 2012); (Martinez *et al*., 2006); (Donlin *et al*., 2014)
CXCL9	M1	(Martinez *et al*., 2006); (Donlin *et al*., 2014)
CXCL11	M1	(Martinez *et al*., 2006); (Jaguin *et al*., 2013); (Vogel *et al*., 2014)
SOCS3	M1	(Arnold *et al*., 2015); (Wilson, 2014)
STAT1	M1	(Wilson, 2014)
HLA-DR	M1	(Arnold *et al*., 2015)
CD80	M1	(Ambarus *et al*., 2012); (Wermuth and Jimenez, 2015)
CD86	M1	(Wermuth and Jimenez, 2015)
CD64	M1	(Ambarus *et al*., 2012); (Vogel *et al*., 2014)
CD40	M1	(Vogel *et al*., 2014)
CD180	M1	(Vogel *et al*., 2014)
CCL19	M1	(Martinez *et al*., 2006)
BCL2A1	M1	(Martinez *et al*., 2006)
INDO	M1	(Martinez *et al*., 2006)
PTX3	M1	(Martinez *et al*., 2006)
IL12P35	M1	(Jaguin *et al*., 2013)
CCL5	M1	(Jaguin *et al*., 2013)
IDO1	M1	(Jaguin *et al*., 2013)
CXCL5	M1	(Günthner and Anders, 2013)
IL1B	M1	(Günthner and Anders, 2013)
NKG7	M1	(Günthner and Anders, 2013)
IL6	M1	(Arnold *et al*., 2015)
GBP5	M1	(Fujiwara *et al*., 2016)

Table 2.3.2. Commonly used M2a markers identified through searching the literature. Details of publications of where use of these markers can be seen is also given in the "Reference" column. M2 refers to M2a macrophages

Gene	Polarisation state	Reference
IGF1	M2	(Soler Palacios *et al., 20*15)
HTR2B	M2	(Soler Palacios *et al., 20*15)
IFR4	M2	(Günthner and Anders, 2013)
STAB1	M2	(Soler Palacios *et al., 20*15)
SLC40A1	M2	(Soler Palacios *et al., 20*15)
CMKLR1	M2	(Soler Palacios *et al., 20*15)
SERPINB2	M2	(Soler Palacios *et al., 20*15)
HMOX	M2	(Soler Palacios *et al., 20*15)
IL10	M2a	(Soler Palacios *et al., 20*15); (Kittan *et al., 20*13); (Nakamura *et al., 20*15)
FOLR2	M2/M2a	(Soler Palacios *et al., 20*15); (Kittan *et al., 20*13)
CD36	M2/M2a	(Soler Palacios *et al., 20*15); (Martinez *et al., 20*06)
CD200R	M2a	(Ambarus *et al., 20*12)
SOCS1	M2a	(Whyte *et al., 20*11)
CISH	M2a	(Arnold *et al., 20*15)
KLF4	M2a	(Liao *et al., 20*11)
STAT6	M2a	(Wilson, 2014)
CCL17	M2a	(Kobayashi *et al., 20*10)
MRC1	M2a	(Martinez *et al., 20*06); (Kittan *et al., 20*13)
CHD1	M2a	(Kittan *et al., 20*13)
ALOX15	M2a	(Kittan *et al., 20*13)
CCL23	M2a	(Chistiakov *et al., 20*15); (Walker and Lue, 2015)
CCL26	M2a	(David and Kroner, 2011); (Kong and Gao, 2017)
TGM2	M2a	(Rőszer, 2015)

2.3.2 Datasets were identified through searching Array Express

As described previously, although some macrophage subset markers appear to be consistently and reliably used in the literature, the specificities of some proteins and transcripts are contradictory between reports (Ambarus *et al., 20*11); (Barros *et al., 20*13). Hence it was considered essential to identify a number of genes that could be used confidently to indicate the polarisation state of macrophages. Here, sequencing data generated using primary macrophages was selected as a potential source for subset-marker identification. However, there were no primary polarisation and differentiation datasets for macrophages available in-house at the start of my PhD. Hence publicly available data was chosen as a suitable source for validating the use of existing markers and for identifying novel polarisation markers. Two suitable datasets were identified through searching the Array Express databases; one RNA-seq dataset which was generated before the start of my study and a microarray dataset released at a later time point. Both datasets were generated using human blood MDMs. The RNA-seq data included reads from both M1 and M2a polarised PMBC macrophages (Beyer *et al., 20*12). A separate RNA-seq dataset representing untreated monocytes was also identified and included as a baseline (Pena *et al., 20*13). The microarray dataset comprised 30 different macrophage treatment protocols, including those of the basic model (M0, M1, M2a, M2b, and M2c) which were selected for use in these analyses (Xue *et al., 20*14). The different datasets and some methodological details are summarised in Table 2.3.3.

Table 2.3.3 Different publicly available datasets identified for analysis. Details of the dataset, associated publication as well as details of the method used to generate the cells and sequencing platform used in the experiment are given.

Data Set	Associated paper	Reference cell types	Differentiation method used	Platform
E-GEOD-36952	Beyer *et al., 20*12	PBMC derived M1 macrophages	RPMI1640 media + 10% FCS + GM-CSF (500 U/ml) for 72h followed by IFNγ (200 U/ml)	Illumina HiSeqSQ
E-GEOD-36952	Beyer *et al., 20*12	PBMC derived M2a macrophages	RPMI1640 media + 10% FCS + GM-CSF (500 U/ml) for 72h followed by IL-4 (1000 U/ml)	Illumina HiSeqSQ
E-GEOD-40131	Pena *et al., 20*13	PBMC Monocytes	Maintained in RPMI media	Illumina Genome Analyser IIx platform
E-GEOD-46903	Xue *et al., 20*14	PBMC derived macrophages (various)	RPMI1640 media + 10% FBS, 72h M-CSF, 72h cytokine	Illumina iScan or HiScanSQ system

PBMC= peripheral blood mononuclear cells, FCS= foetal calf serum, M1=M1 macrophages, M2 = M2a macrophages, M-CSF= macrophage colony stimulating factor, GM-CSF= granular monocyte stimulating factor, IFNγ= interferon-gama, IL-4= interleukin-4

2.3.3. M1 versus M2a Fold change analysis of RNA-seq data produced a list of potential marker genes

RNA-seq datasets can be vast and produce counts for a large number of transcripts, hence it was necessary to develop a list of criteria identifying markers that demonstrated the largest changes between conditions being contrasted. Thus, aligned and processed RNA-seq data was analysed using an M1 versus M2a fold change method to produce a shortlist of filtered transcripts with elevated expression in either the M1 or M2a condition. The top 300 differentially expressed genes according to this method can be seen in Figure 2.3.1; clusters of transcripts that were high in one condition and low in others are seen. This indicated that groups of genes specifically enriched for one of the given conditions (M1 or M2a) were present within the gene list.

Although fold change allows data to be organised, it eliminates some information, such as individual replicate expression values and averages. Therefore, it was necessary to manually inspect the data for a shortlist of transcripts. Additionally, inspection of lists containing gene names allowed cross-referencing with genes that appeared most frequently in the published literature (Tables 2.3.1 and 2.3.2).

To inspect these candidate genes in more detail, the top 30 transcripts for M1 and M2a conditions according to the previously described selection criteria were isolated; triplicate averages are summarised in Tables 2.3.4 and 2.3.5 for M2a and M1 markers, respectively.

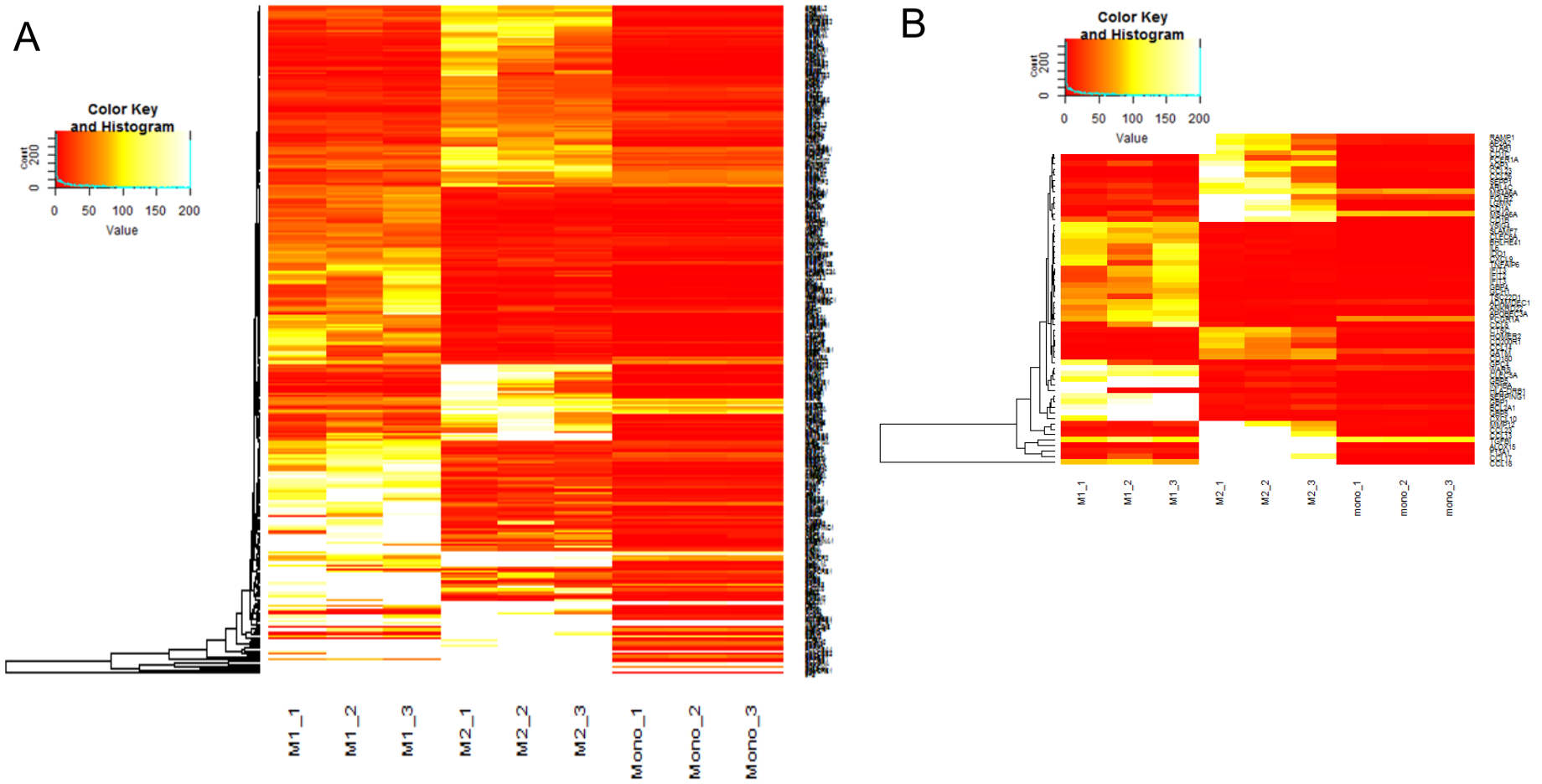

Figure 2.3.1. Genes identified from publicly available RNA-seq data through analysis. (A) Top 300 genes (top 150 M1 and top 150 M2a genes) and (B) top 60 genes (top 30 M1 and M2a genes). Note that top 300 genes here are given in appendix 1. M1 = M1 macrophage, M2 = M2a macrophage, Mono= monocyte

2.3.4 Analysis validated the use of a number of some frequently used literature markers

As mentioned previously, isolation of the top hits allowed closer inspection of markers, including those that are regularly used in published protocols for defining macrophage polarisation into the M1 and M2a states. It could be suggested that macrophage subtype markers that are frequently described to be effective experimentally in published studies should be considered more reliable if they are also identified as one of the top hits in the analyses performed here.

Some genes that appeared frequently in the literature as subset-specific markers also appeared in the list of top 30 differentially expressed transcripts for M1 or M2a macrophages (e.g. *CXCL9, CXCL10* and *CCL17*) (Tables 2.3.4 and 2.3.5 for M2a and M1, respectively- these genes are highlighted in red). Scrutiny of exact expression levels of these genes in different polarisation states confirmed enrichment in one condition alone, i.e. the condition of interest (Figures 2.3.2 and 2.3.3); this validated their use as lineage markers. Other genes that have previously been associated with specific conditions, but are not commonly used as marker genes (such as *CCL26*), were also selected. A number of these genes were incorporated into a marker panel to be used in the optimisation of a cell-line macrophage model, and are detailed in Figures 2.3.2 and 2.3.3.

2.3.5 Potential novel marker genes were identified through the analysis

It would be beneficial to identify novel markers of macrophage polarisation from publicly available datasets which may out-perform those which are currently in use.

Potential novel marker genes for specific macrophage lineages were also identified in the top 30 lists (Tables 2.3.4-5 highlighted in green). These transcripts followed a similar expression pattern to the validated genes from literature; i.e. they were high in the M1 or M2a samples only, and some transcripts (*ANKRD22*, *TSC22D1*, *HOMER2*, *AP2A2*, and *SERPING1*) were selected to be incorporated into a panel of potential markers to be tested experimentally.

Table 2.3.4. Top 30 M2a marker genes identified through analysis of the Beyer et al., (2012) RNA-seq dataset. Established markers of interest are highlighted in red and novel markers of interest are highlighted in green. Other markers in table have been identified previously but are not frequently used. M1=M1 macrophages, M2 = M2a macrophages, Mono=monocytes. _1, _2, _3 indicate replicates.

Gene	M1_1	M1_2	M1_3	M2a_1	M2a_2	M2a_3	Mon_1	Mon_2	Mon_3	M1 average	M2a average	Mon average
ALOX15	0	0.082574	1.05614	996.167	716.234	1263.92	0.090445	0.102125	0.091069	0.379571	992.107	0.094546
CCL23	5.96E-05	0.573597	0.000204	256.319	97.7472	24.5817	1.37431	1.49923	2.59475	0.191287	126.216	1.822763
CCL26	0.449102	0	0	219.127	52.2089	22.4549	0.042593	0.051528	0.049484	0.149701	97.93027	0.047868
FCER1A	0.120236	0.15483	0.396306	148.704	18.7862	28.9389	0	0	0	0.223791	65.47637	0
CCL14	0.345806	0.09049	0	80.2579	35.8545	10.2569	0	0	0	0.145432	42.1231	0
HOMER2	0.509863	0.114831	0.445949	87.2222	59.7023	37.4435	0.528955	0.588332	0.505528	0.356881	61.456	0.540938
F13A1	6.67721	10.4013	7.78903	2076.47	929.137	776.338	3.05371	3.0103	2.48538	8.28918	1260.648	2.849797
CD1A	2.03199	0.995397	0.999075	320.832	156.097	89.721	0.015832	0.019153	0.036787	1.342154	188.8833	0.023924
CCL23	1.6805	4.01201	1.83122	636.099	233.333	66.2203	1.81962	1.29915	0.987952	2.50791	311.8841	1.368907
CCL17	2.64758	23.9477	0.851574	2044.84	343.609	146.404	0	0.04475	0.042976	9.148951	844.951	0.029242
CCL13	6.02629	7.10657	5.47598	1337.76	252.417	116.51	0.046655	0.112885	0.081307	6.202947	568.8957	0.080282
CCL18	67.32	81.4315	49.9553	11243.1	2911.25	506.328	0	0.031694	0	66.2356	4886.893	0.010565
GATM	0.473876	0.236224	1.36467	44.1619	37.102	48.262	18.7918	22.0884	18.9657	0.69159	43.1753	19.94863
STAB1	1.76206	3.07738	0.76412	163.888	100.1	18.763	0.036712	0.021048	0.026958	1.867853	94.25033	0.028239
CD1C	2.78649	1.41386	1.59376	123.318	42.4808	78.0207	0.018788	0.02273	0.021828	1.93137	81.27317	0.021116
RAMP1	0.161194	6.21645	0.10552	129.733	92.6806	23.9388	7.74181	7.08913	8.82059	2.161055	82.11747	7.883843
MMP12	9.55144	4.42684	12.0452	826.411	109.79	49.1342	2.06921	2.65502	1.39455	8.674493	328.4451	2.039593
CD180	1.08941	1.69269	1.04344	47.6039	40.6228	51.3975	2.58446	2.17569	1.95795	1.27518	46.5414	2.239367
SEPP1	3.74337	5.6889	1.08719	179.126	164.426	25.3901	0.039426	0.066946	0.024233	3.506487	122.9807	0.043535
MS4A6A	1.59776	7.9065	5.13136	130.593	131.305	123.412	43.0828	52.3239	49.7184	4.87854	128.4367	48.37503
CD200R1	2.19182	1.33136	1.737	68.0757	38.0938	22.6107	0.203397	0.201306	0.188542	1.753393	42.92673	0.197748
MS4A6A	2.40239	19.8152	6.45633	222.293	230.108	159.361	71.445	69.4715	62.1907	9.557973	203.9207	67.7024
FOLR2	8.80038	16.3841	6.61767	303.844	213.023	33.2313	11.9214	10.5122	11.7392	10.60072	183.3661	11.39093
LGMN	7.8122	8.36477	19.931	256.354	180.035	60.9606	0.315069	0.342067	0.272172	12.03599	165.7832	0.309769
CTSC	4.84339	4.33776	4.16168	69.5734	74.5863	32.8247	4.07916	4.45109	3.80848	4.44761	58.9948	4.11291
AP2A2	5.42514	7.81371	5.15305	105.657	82.7821	34.7024	7.95012	5.88479	7.70993	6.130633	74.3805	7.181613
AQP3	7.67052	23.05	5.64041	179.934	86.6908	97.5289	1.94068	2.39129	2.30689	12.12031	121.3846	2.212953
ARL4C	11.0959	16.83	6.73914	99.0296	167.87	70.0301	0.412279	0.460761	0.187614	11.55501	112.3099	0.353551
TGFBI	90.207	155.852	106.447	791.493	1679.99	921.019	127.713	118.736	110.204	117.502	1130.834	118.8843
CD1B	28.0714	8.99305	24.5962	264.163	159.955	165.726	0	0	0	20.55355	196.6147	0

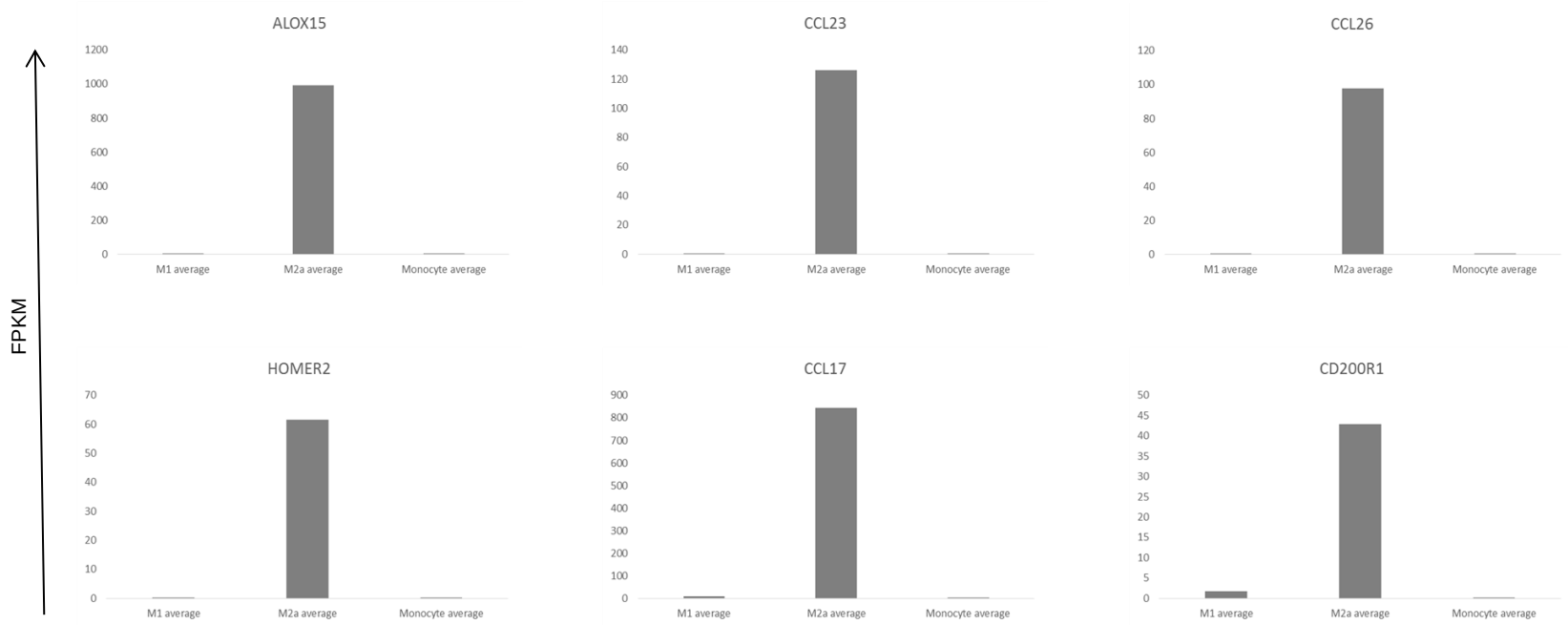

Figure 2.3.2. Bar charts showing expression of genes selected as candidates for M2a macrophages in primary PBMC monocytes and differentially polarised macrophages, isolated from the original RNA-seq datasets. All genes selected from top 30 transcripts according to the selection criteria. M1=M1 macrophages, M2 = M2a macrophages, Mono=monocytes

Table 2.3.5. Top 30 M1 marker genes identified through analysis of the Beyer et al., (2012) RNA-seq dataset. Established markers of interest are highlighted in red and novel markers of interest are highlighted in green. Other markers in table have been identified previously but are not frequently used. M1=M1 macrophages, M2 = M2a macrophages, Mono=monocytes. _1, _2, _3 indicate replicates.

Gene	M1_1	M1_2	M1_3	M2a_1	M2a_2	M2a_3	Mon_1	Mon_2	Mon_3	M1 average	M2a average	Mon average
CXCL10	107.69	281.177	861.426	1.79202	0.416124	0.032246	1.36587	1.59853	1.3799	416.7643	0.746797	0.001792
HLA-DRB1	426.638	1.23048	0.062848	0.086242	1.3743	0.002685	0.000153	0.000299	0.000388	142.6438	0.487742	0.003419
TSC22D1	41.3375	15.3121	70.4267	0.056714	0.159106	0.373654	1.26347	1.35686	1.4643	42.35877	0.196491	0.004639
GBP5	251.341	451.218	403.912	3.08278	2.23301	2.1935	0.559967	0.509536	0.790299	368.8237	2.503097	0.006787
GBP5	115.281	264.544	197.922	0.480696	2.55045	1.28925	0.430556	0.524487	0.217214	192.5823	1.440132	0.007478
FCGR1A	52.2494	107.834	124.114	0.136527	0.494163	1.62048	42.805	41.2033	41.9941	94.73247	0.75039	0.007921
GBP4	35.2075	41.1778	73.185	0.770246	0.390562	0.289375	0.702675	0.845426	0.765199	49.85677	0.483394	0.009696
CXCL9	92.7828	40.2041	121.242	2.70597	0	0	0.011943	0.014449	0.013876	84.74297	0.90199	0.010644
APOBEC3A	43.5218	101.964	86.6154	1.34666	0.77216	0.86217	0.242593	0.000381	5.44E-05	77.36707	0.993663	0.012843
ANKRD22	35.8616	76.8642	120.79	1.1452	1.77323	0.307414	0	0	0	77.8386	1.075281	0.013814
IFIT3	20.6442	60.3144	116.973	1.04347	0.780144	1.31643	1.04153	1.27238	0.157003	65.9772	1.046681	0.015864
VSIG4	113.184	88.733	74.815	1.93915	0.002544	2.68223	0.408541	0.199093	0.245126	92.244	1.541308	0.016709
GBP1	141.464	191.645	384.115	5.25309	3.16792	3.63323	0.036764	0.034946	0.067121	239.0747	4.01808	0.016807
GPC4	141.56	19.9414	7.54365	1.15304	0.875254	0.981892	3.04319	3.01222	2.85816	56.34835	1.003395	0.017807
GCH1	44.2795	44.2618	53.8455	1.06617	1.04472	0.544262	0.292449	0.536584	0.386893	47.46227	0.885051	0.018647
CLEC6A	90.1562	73.6359	47.8994	0.864738	1.97433	2.07396	0	0	0.024722	70.56383	1.637676	0.023208
BCL2A1	186.73	220.232	603.667	2.05582	5.70122	16.6259	6.12866	8.22964	6.5906	336.8763	8.127647	0.024126
TNFAIP6	100.478	12.8638	77.0597	1.65455	1.56851	1.51373	0.073791	0.089271	0.028577	63.46717	1.57893	0.024878
IFIT2	18.2387	55.2071	102.204	1.4304	1.16555	2.22651	0.867165	0.928248	0.749018	58.54993	1.607487	0.027455
CCL8	3.21555	45.1612	176.148	5.4913	0.605015	0.250079	0.201042	0.191099	0.166837	74.84158	2.115465	0.028266
IDO1	71.2926	24.7994	109.946	2.17125	3.62097	0.058165	0.027252	0.002623	0.041136	68.67933	1.950128	0.028395
SERPING1	168.883	175.323	367.611	6.14985	4.07482	10.8063	3.33093	3.1855	3.26148	237.2723	7.010323	0.029545
IL6	69.4293	31.1049	134.596	4.07499	1.07229	2.32624	0	0	0.017817	78.37673	2.491173	0.031785
INHBA	326.922	208.259	247.087	4.95908	12.1404	9.21566	0.045559	0.009186	0.026466	260.756	8.771713	0.03364
SLAMF7	118.245	50.3432	67.0071	3.66281	1.66064	2.78307	4.79E-05	0.446626	0.373208	78.53177	2.702173	0.034409
BHLHE41	69.974	65.1468	63.0827	0.620325	3.56025	2.7682	0.121147	0.1314	0.116482	66.06783	2.316258	0.035059
IFIT3	19.588	36.0833	94.4043	2.33319	0.002503	2.93197	0.874855	0.576356	1.64406	50.0252	1.755888	0.0351
WARS	200.712	164.655	164.999	6.67935	2.74266	9.28729	15.1984	13.6599	11.8973	176.7887	6.236433	0.035276
CLEC5A	169.939	148.235	129.808	2.44515	8.54676	5.89636	0.00024	0.00029	0.000282	149.3273	5.629423	0.037699
ADAMDEC1	54.2774	64.986	102.627	1.71957	3.26977	4.74198	8.44646	9.16031	6.5274	73.96347	3.243773	0.043856

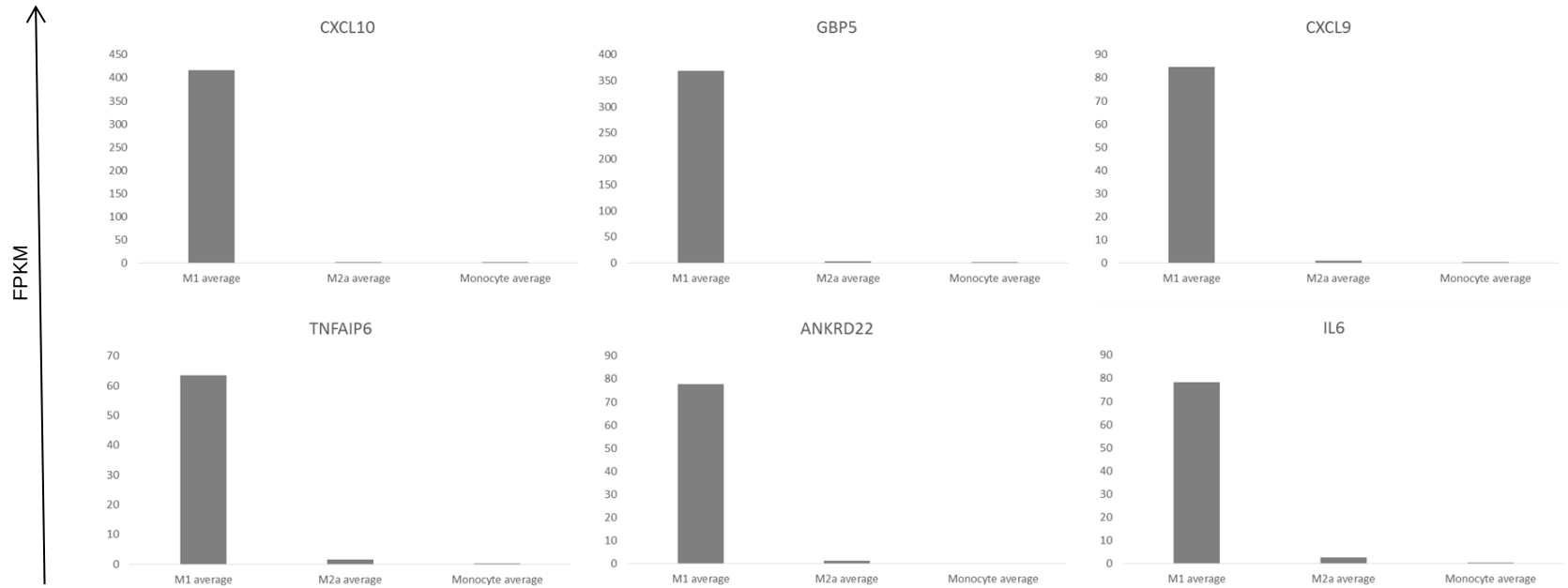

Figure 2.3.3. Bar charts showing expression of genes selected as candidates for M1 macrophages in primary PBMC monocytes and differentially polarised macrophages, isolated from the original RNA-seq datasets. All genes selected from top 30 transcripts according to the selection criteria. M1=M1 macrophages, M2 = M2a macrophages, Mono=monocytes

2.3.6 Some markers identified through analysis of RNA-seq data were validated following cross reference with results from microarray analysis

As the microarray dataset was not available at the start of my study, marker panels for practical investigations were generated using the RNA-seq data only (note that this dataset was the only one available with multiple treatments during my PhD). However, it was considered useful to investigate the markers in a separate dataset to examine reproducibility, and also to determine how markers were expressed in a wider range of conditions. These two datasets were generated using different techniques (microarray and RNA-seq), using macrophages of unknown quality which were grown under variable tissue culture conditions. Hence it was reasonable to suggest that there may be some inherent differences in top candidate markers identified between the two datasets.

For the microarray data, two-way comparisons between M1 (IFNγ and LPS treated) and M2a (IL-4 induced) datasets (using a manual fold change analysis), produced lists of transcripts which were further filtered through removing genes which were more highly expressed in the M0 condition to ensure subset-specificity. Subsequent lists could be compared to the marker panels suggested from the RNA-seq (Beyer *et al., 20*12) dataset analysis. Gene lists produced here may be found in appendix 1 (Tables A1.4 and A1.5) and visualised using the heatmaps in Figure 2.4.3. It was clear from the heatmaps that genes which are highly expressed in one condition only (i.e. M1 versus M2a and M0 or M2a versus M1 and M0) were present in the filtered gene lists.

As with the RNA-seq dataset, genes were ordered by fold change following filtering. Rank of genes in different datasets were compared; Figure 2.3.5 demonstrated that markers suggested from the RNA-seq data analysis were expressed most strongly in the corresponding (M1 or M2a) condition in the microarray dataset. However, some genes (*IL6* for M1 and *CCL23* for M2a) were not ranked in the top 150 microarray hits for the macrophage subset of interest, and may therefore not be as reliable as the other markers. This was considered important to have in mind when using these markers in Chapter 3 to optimize the THP-1 cell line model.

M1, M2a, M2b and M2c specific genes were also identified from the dataset by filtering for transcripts which were more highly expressed in the condition of interest versus others. Top markers (ranked versus M0) can be found in appendix 1, Table A1.5. Top M1, M2a, M2b and M2c genes (versus M0) may also be visualised using the heatmaps in Figure 2.3.6. Some marker specificity is demonstrated for the different cell types here.

Lists of M1 and M2a specific genes (filtered for transcripts more highly expressed in M2b, M2c and M0 conditions) were also ranked (according to M1 versus M2a expression) and compared to the gene rankings generated through analysis of the RNA-seq dataset (please refer to Figure 2.3.7). Some of the transcripts used as markers in the literature, henceforth known as “literature transcripts” were present as top hits in both microarray and RNA-seq gene lists (such as *GBP5* and *CXCL10*, ranked 4/4 and 1/28 in RNA-seq/microarray datasets respectively) providing further validation for their use as subset-specific markers experimentally. Additionally, the presence of novel markers, such as *ANKRD22* in the top hits for both proposed panels (ranked 10 in RNA-seq data and 16 in stringently filtered microarray data) increased confidence in the reliability of the methods used, and highlighted these transcripts for *in vitro* validation as subset-specific genes. However, *TNFAIP6* and *IL6* which were originally described as an M1 marker in the bivalent M1/M2a analysis were found to be more highly expressed in M2b cells when this additional condition was taken into account. Interestingly the heatmaps in Figure 2.3.6 demonstrated some similarities in expression of M1 and M2b transcripts, and so there may be some overlap in transcriptional profile of these cell types. This is not necessarily surprising since LPS is used in the generation of both of these subtypes and transcripts activated downstream of TLR4 (binds LPS) signalling pathways may be similarly induced. *CCL23* was also found to be M2b-high, rather than M2a-specific, as previously thought. It should be noted that markers which were not identified as highly specific (when considering an increased number of conditions) may still be useful as part of a panel, or when distinguishing M1 and M2a cells only.

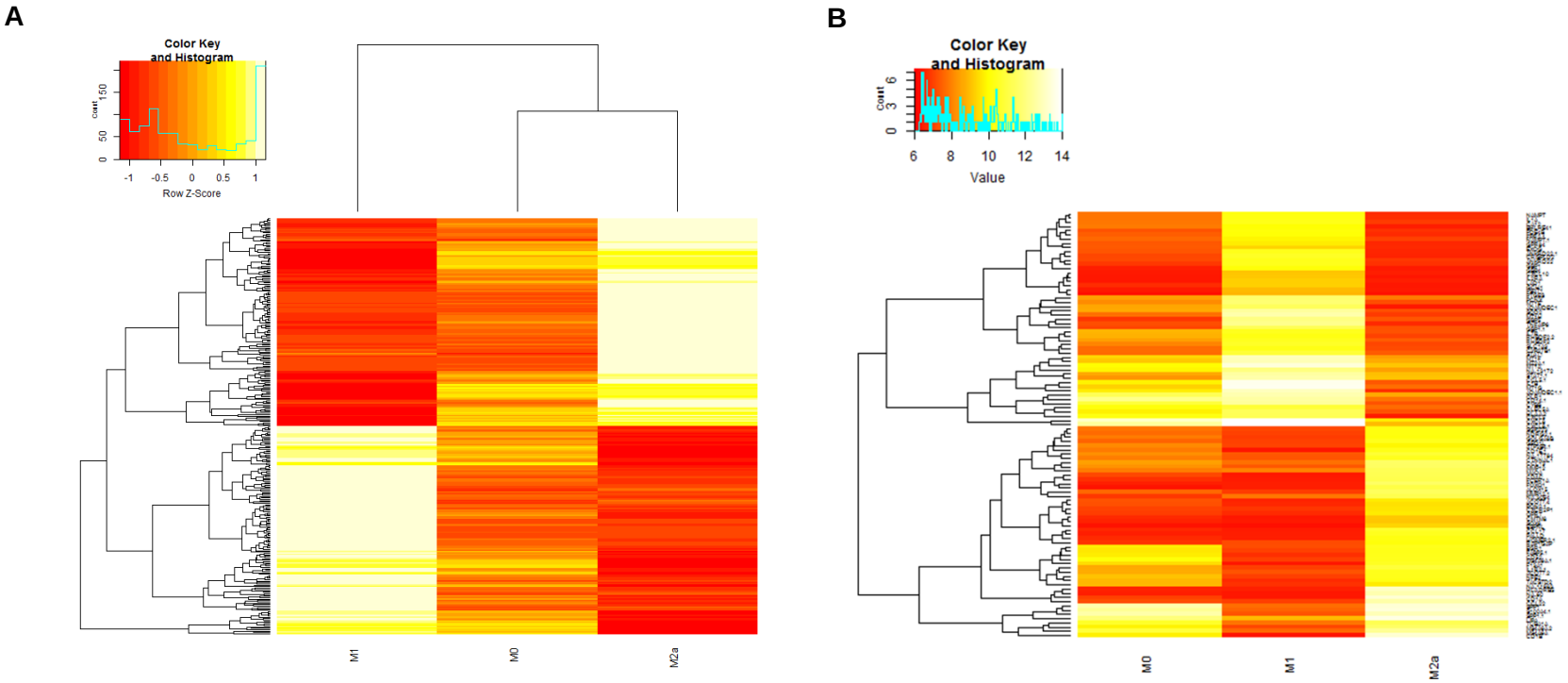

Figure 2.3.4. Heatmap showing gene expression according to publicly available microarray data for M1, M2a and M0 macrophages. (**A**) Top 300 genes according to M1 (LPS and IFNγ) vs M2a (IL-4) fold change, filtered for transcripts more highly expressed in M0 (differentiated, unpolarised) macrophages. (**B**) Top 30 M1/M2a genes according to same criteria. Note that top 300 genes are given in appendix 1. M1=M1 macrophages, M2a = M2a macrophages, M0= unpolarised macrophages

A

Gene	Polarisation state	Rank in RNAseq dataset	Rank in microarray dataset (fold change)
CXCL10	M1	1	46
GBP5	M1	4/5	10
CXCL9	M1	8	122
ANKRD22	M1	10	16
TNFAIP6	M1	18	4
IL6	M1	23	>150
ALOX15	M2a	1	12
CCL23	M2a	2/9	>150
CCL26	M2a	3	134
HOMER2	M2a	6	21
CCL17	M2a	10	15
CD200R	M2a	21	100

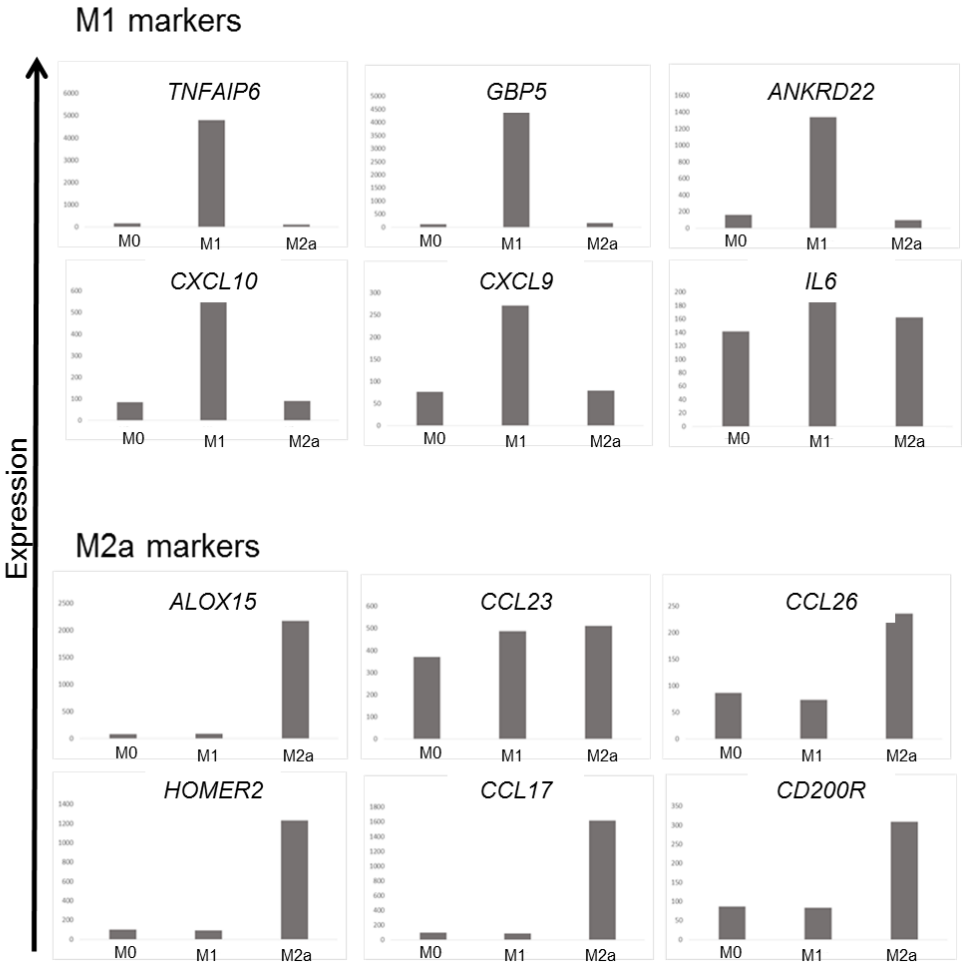

Figure 2.3.5. Genes identified in the initial analysis; rankings in both RNA-seq and microarray datasets (**A**) expression of M1 markers selected from the Beyer et al (2012) dataset in differentially polarised PBMC macrophages and monocytes, where expression levels are isolated from the Xue et al., (2014) microarray dataset; M0, M1 and M2a cells (**B**), expression of M2a markers selected from the Beyer et al (2012) dataset in differentially polarised PBMC macrophages and monocytes, where expression levels are isolated from the Xue et al., (2014) microarray dataset; M0, M1 and M2a cells (**C**). M1=M1 macrophages, M2a = M2a macrophages, Mono=monocytes

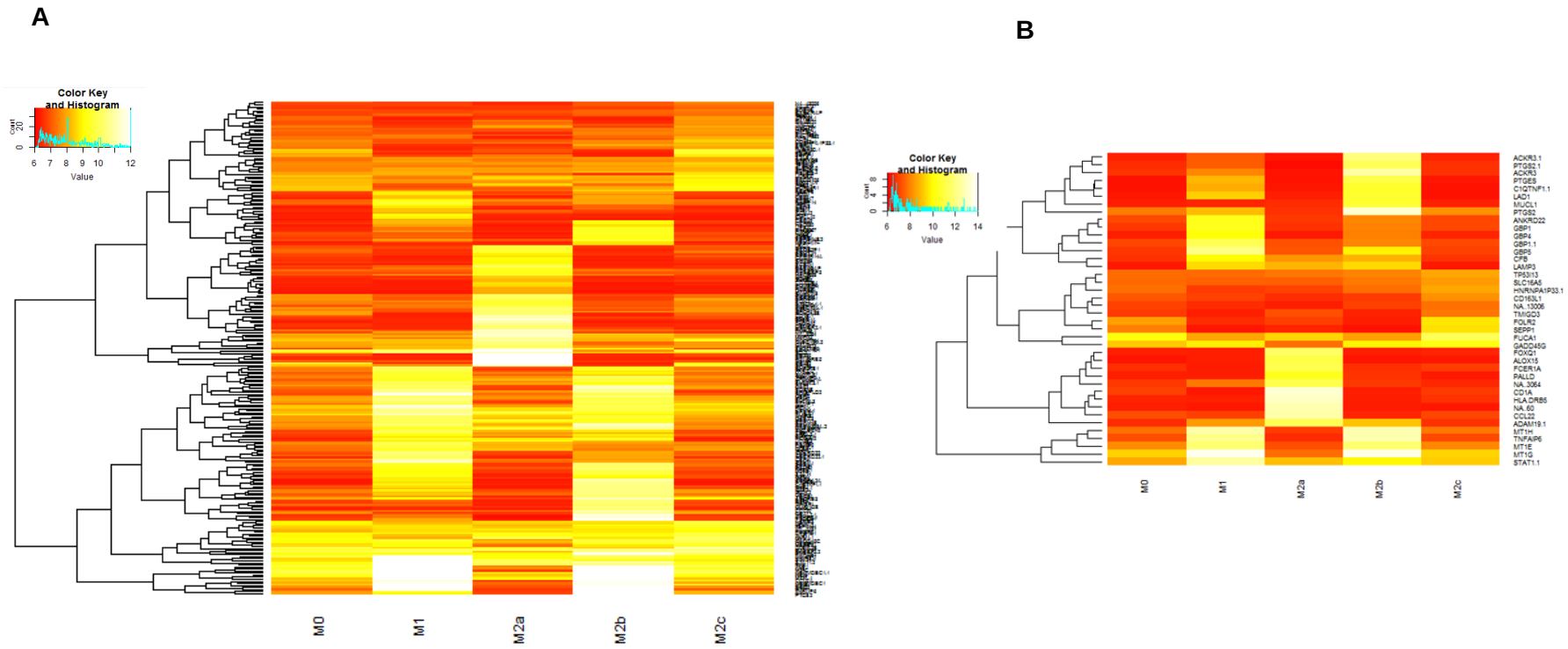

Figure 2.3.6. Heatmap showing gene expression according to publicly available microarray data generated by Xue et al., (2014) for M1, M2a, M2b, M2c and M0 macrophages. (**A**) Top 300 genes according to condition of interest (i.e. M1, M2a, M2b, M2c) vs M0 fold change, filtered for genes higher in any condition other than the one of interest (**B**) Top 10 M1/M2a/M2b/M2c genes (combined) according to same criteria. Note that top 300 genes here are given in appendix 1. M1=M1 macrophages, M2a = M2a macrophages, M2b= M2b macrophage, M2c=M2c macrophage, M0= unpolarised macrophages

A

Gene	Polarisation state	Rank in RNAseq dataset	Rank in filtered microarray dataset (fold change)
CXCL10	M1	1	28
GBP5	M1	4/5	4
CXCL9	M1	8	70
ANKRD22	M1	10	15
TNFAIP6	M1	18	M2b high
IL6	M1	23	M2b high
ALOX15	M2a	1	13
CCL23	M2a	2/9	M2b high
CCL26	M2a	3	124
HOMER2	M2a	6	21
CCL17	M2a	10	15
CD200R	M2a	21	95

B

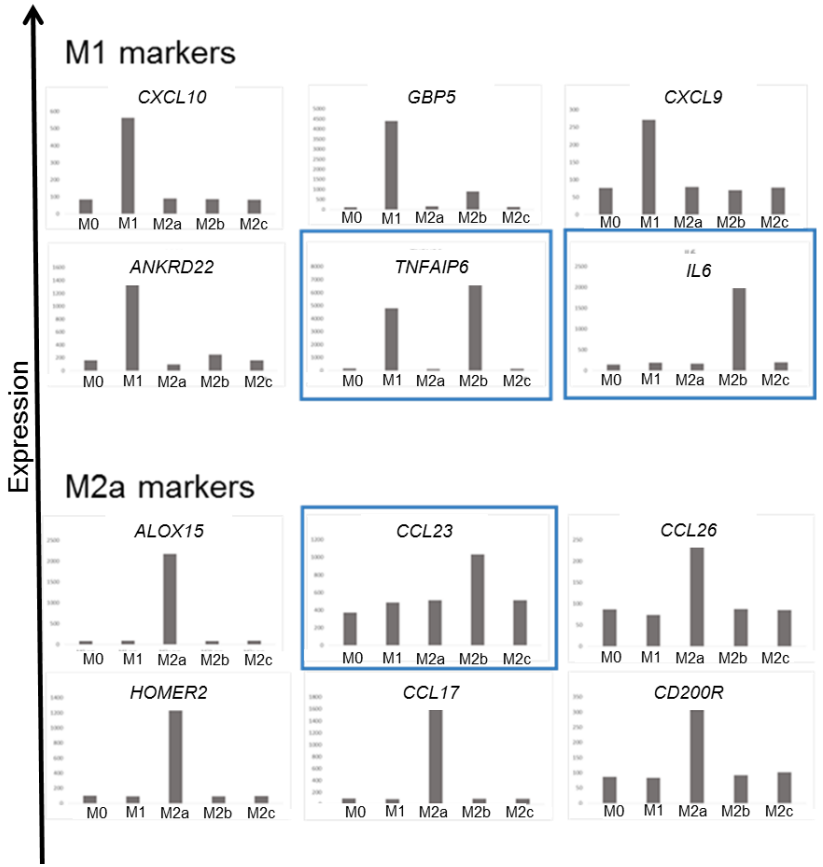

C

Figure 2.3.7. Genes identified in the initial analysis examined in an extended number of polarisation states using microarray datasets; (**A**) rankings in both RNA-seq and microarray datasets. (**B**) expression of M1 markers selected from the Beyer et al (2012) dataset in differentially polarised PBMC macrophages and monocytes, where expression levels are isolated from the Xue et al., (2014) microarray dataset; M0, M1, M2a, M2b and M2c cells, (**C**) expression of M2a markers selected from the Beyer et al (2012) dataset in differentially polarised PBMC macrophages and monocytes, where expression levels are isolated from the Xue et al., (2014) microarray dataset; M0, M1, M2a, M2b and M2c cells. M1=M1 macrophages, M2a = M2a macrophages, M2b= M2b macrophage, M2c=M2c macrophage, M0= unpolarised macrophages. Blue boxes highlight markers that do not follow the pattern of expression indicated by the RNA-seq dataset analysis.

2.3.7 Multiple time points of microarray dataset allowed changes of potential markers to be tracked over time course

As the ultimate aim here was to use the genes selected as subset-specific markers to optimise a THP-1 macrophage polarisation protocol, it was considered useful to inspect changes in expression of these transcripts between different cytokine exposure times. The microarray data produced by Xue *et al.,* included a number of cytokine exposure time points for IFNγ and IL-4 conditions (ranging from 30 minutes to 72 hours). IFNγ-only treated cells were used to examine changes in gene expression for the M1 subtype as multiple time points for macrophages polarised using both IFNγ and LPS were not available (please see appendix 1 Table A1.5 for raw counts). Based on the heatmaps (Figure 2.3.8), some genes (such as *ANKRD22* and *CXCL10*) were expressed relatively consistently at different time points. However, other transcripts were up-regulated to a greater extent at later exposure times (e.g. *IL6*). It should be noted that some genes in the microarray dataset were represented by more than one probe, and separate probes may correspond to different splice variants; hence one may be upregulated and another may not be (e.g. *TNFAIP6*). M2a (IL-4)-induced cells also express some genes consistently (e.g. *CCL23*) and others are upregulated at later time points only. Taken together this data suggests that marker expression fluctuates with polarisation time. Hence in an experimental system, cytokine exposure times will need to be titrated to determine the optimal exposure time of these agents for inducing their particular phenotypes.

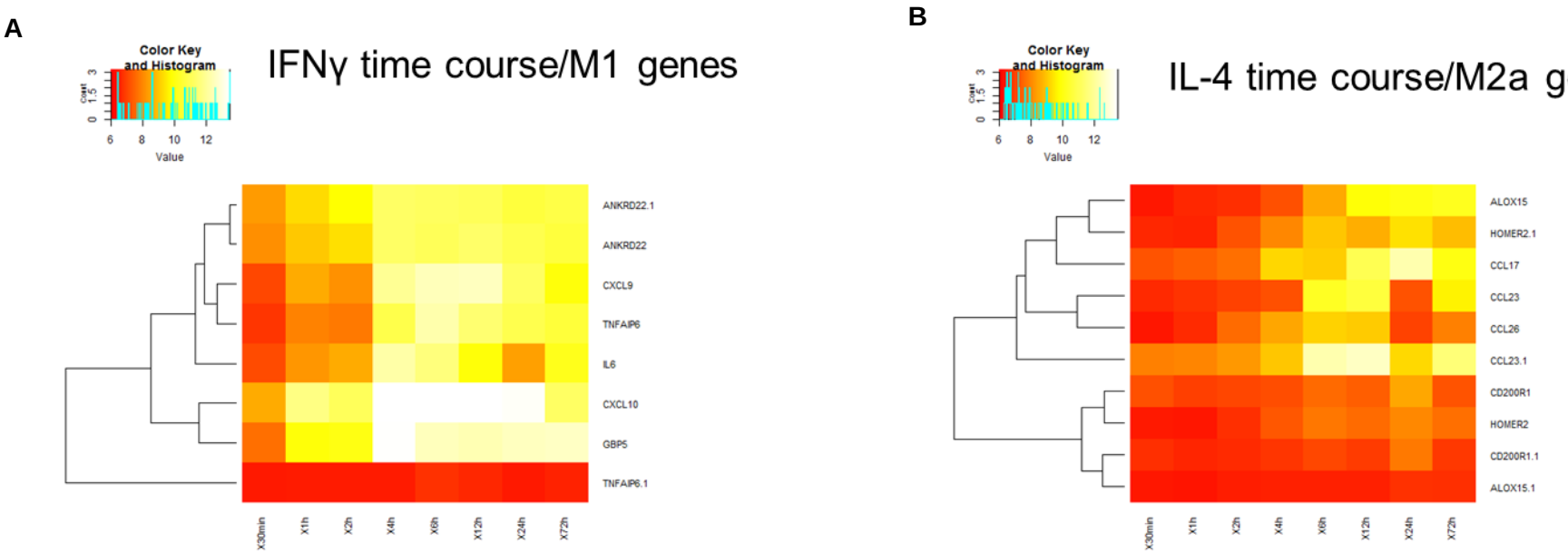

Figure 2.3.8. Heatmaps and line graphs showing changes in gene expression of cells exposed to polarising cytokine for increasing lengths of time, isolated from data generated by Xue et al., (2014): (**A**) M1 markers in macrophages polarised using IFNγ for increasing periods of time, shown by heatmap and (**B**) M2a markers in macrophages polarised using IL-4 for increasing periods of time, according to heatmap. M1=M1 macrophages, M2a = M2a macrophages, IL-4=interleukin-4, IFNγ=interferon-gamma

2.3.8 Final marker panel

The main aim of this analysis was to identify a marker panel that could be used to optimise a monocytic cell line model for macrophage differentiation and to identify potential novel markers of M1 and M2a macrophage polarisation. The final marker panel is given in Table 2.3.6. The majority of transcripts selected for this list were genes that have been frequently used as markers in the literature and validated using this approach (appeared as the top hits); identification through both *in silico* analyses and literature search increased confidence in suitability of these genes as polarisation markers. Novel transcripts following similar expression patterns were also included in the panel (e.g. *ANKRD22* for M1 and *HOMER2* for M2a). Frequently used literature genes that did not appear in the top 30 list but demonstrated an appropriate expression pattern according to data analysis were also included (*IRF1* ranked at 32*, TGM2* ranked at 330).

An additional list of novel markers identified that may be validated experimentally but were not included in the final panel are given in Table 2.3.7.

Table 2.3.6 Final marker panel identified from Beyer *et al.,* (2012) dataset and examined in Xue *et al.,* (2014) dataset M1=M1 macrophages, M2a = M2a macrophages

Marker	Subtype	Type of marker
CXCL10	M1	Literature: validated
CXCL9	M1	Literature: validated
GBP5	M1	Literature: validated
ANKRD22	M1	Novel
TNFAIP6	M1	Literature: validated
IRF1	M1	Literature: NON-validated
ALOX15	M2a	Literature: validated
CCL17	M2a	Literature: validated
CCL23	M2a	Literature: validated
CCL26	M2a	Literature: validated
HOMER2	M2a	Novel
TGM2	M2a	Literature: NON-validated

Table 2.3.7 Additional novel markers to be validated experimentally identified from Beyer *et al.,* (2012) dataset and examined in Xue *et al.,* (2014) dataset, M1=M1 macrophages, M2a = M2a macrophages

Marker	Subtype
SERPING1	M1
TSC22D1	M1
AP2A2	M2a

2.4 Discussion

Data generated using different methods were combined to generate candidate marker panels. RNA-seq was used to assemble initial panels and microarray data then allowed expression of these genes to be analysed in the context of an increased number of conditions. Studies have generally found high correlation between differentially expressed genes when comparing data generated through both of these methods. Hence combining findings from these separate experiments was deemed accepTable (Zhao *et al., 20*14, Wang *et al., 20*14). Generally, discordance is observed when examining low abundance transcripts, which were not of interest here (Vinciotti *et al., 20*16); (Zhao *et al., 20*14). It should be noted, however, that RNA-seq has been reported to outperform microarray in terms of differentially expressed gene verification by qPCR; validated genes proportions were given at 93% and 75% for RNA-seq and microarray, respectively (Wang *et al., 20*14), potentially due to technical limitations of microarray (probe redundancy and annotation issues). Therefore, when looking at these datasets it was considered optimal to use the RNA-seq dataset for the initial analysis, and supplement using microarray.

Discordant results between datasets could also be due to protocols used to generate macrophage polarisation. For instance, M-CSF was used to prime cells in the microarray experiment and GM-CSF was the differentiation stimulus for the RNA-seq cells. Although these two agents are reported to prime macrophages effectively for polarisation (Vogel *et al., 20*14), they induce distinct transcriptional events which, in addition to methods of sequencing, could account for the inconsistencies in the top differentially expressed genes between the subsets (Jaguin *et al., 20*13); (Vogel *et al., 20*14).

A number of frequently used markers in the literature were not well defined as subset-specific markers. For instance, *CD80* and *CD86* are frequently used to differentiate M1 from M2a cells in published protocols, but these markers were not identified as top hits in the analysis here; *CD80* was filtered out in the analysis of Bayer *et al.,* (2012) data as expression was lower than FPKM of 10 in all conditions and *CD86* was ranked as 313 for potential M1 marker genes and was hence not considered to be a top hit. Additionally, expression of the gene coding for CD163 is frequently used as a marker of M2a polarisation. However, this gene did not appear in the top 30 panel for these cells and there is a growing body of evidence that this gene is induced by a variety of agents and may be more indicative of the M2c state; considering the Beyer *et al* conditions (M1 and M2a only), expression of this marker did appear to be higher for M2a cells. However, *CD163* was ranked at 346, suggesting that there are better markers available

for identifying M2a cells. Hence this analysis is useful for identifying literature genes which have not been misused in previous reports, or are superior to those available.

Some of the proteins relating to M1 markers described in the literature that were validated using RNA-seq data have well defined roles in inflammatory functioning; *CXCL9* and *CXCL10* are potent chemoattractants for a number of immune cells, and signalling through their target CXCR3 may promote a Type 1 T-helper cell response (Thapa *et al., 20*08); (Hardison *et al., 20*06). *GBP5* has been reported to promote NLRP3 inflammasome assembly and is required for activation of the absent in melanoma 2 protein (AIM2) inflammasome in the presence of certain pathogens (Man *et al., 20*15); (Shenoy *et al., 20*12). IL-6 is a well-defined pro-inflammatory cytokine with roles in T-cell activation, acute phase protein production and more (Tanaka *et al., 20*14). Hence it reasonable to assume that all of the corresponding genes for these agents are reliable candidates for M1 macrophage markers.

Conversely, it is clear how some of the markers identified for the M2a state would correspond to anti-inflammatory functions and wound healing; ALOX15 is a lipoxygenase that is reportedly involved in clearance of apoptotic cell bodies, an important aspect of tissue repair (Kwon *et al., 20*16). CCL26 and CCL17 interact with CCR3 and CCR4, respectively; receptors involved in inducing Th2 responses and activating other cells implicated in allergy (Mackay, 2008); (Berin, 2002).

In summary, the work in this Chapter provided a panel of M1 and M2a macrophage markers from literature and publicly available sequencing datasets that are likely to reflect the relevant phenotype under experimental conditions. Hence these markers may be used to optimise tissue culture experiments in future work.

Chapter 3: Optimisation of *in vitro* macrophage differentiation and polarisation protocols

3.1 Rationale for development of a macrophage cell line model system

Although PBMC derived macrophages are frequently used in research, studying specific cellular functions can be problematic without a genetically identical baseline. Limited numbers of monocytes can be isolated from individual donors, with multiple blood draws putting stress on the bone marrow and affecting cell phenotype. This is an issue when studying conditions where common allelic variants are known to alter disease susceptibility and responsiveness to therapies. Hence monocytic cell lines are useful in providing robust, homogenous models for studying macrophage physiology and pathology in certain diseases. There are a number of human monocytic cell lines available that can be differentiated into a macrophage-like state when exposed to certain stimuli; the THP-1 cell line was isolated from an acute myeloid leukaemia patient and is the most commonly used immortalised model for *in vitro* representation of monocytes. According to reports, induced THP-1 cells resemble primary MDMs when scrutinised for morphology, gene expression, certain antigens and flow cytometry characteristics, hence their frequent use in *in vitro* studies. Additionally it should be noted that these cells were isolated from blood rather than tissue (unlike the U937 line), lending to their plasticity and susceptibility to polarising stimuli (Chanput *et al., 20*12); (Feng *et al., 20*04); (Auwerx, 1991); (Tsuchiya *et al., 19*80); (Koeffler, 1986); (Park *et al., 20*07).

Upon treatment with PMA, these monocytic cells differentiate into a more mature macrophage-like state according to defining characteristics (such as adherence and phagocytic capacity) and surface marker expression (CD14, CD11b) (Schwende *et al., 19*96); (Lund *et al., 20*16); (Park *et al., 20*07); (Aldo *et al., 20*13).

Although the literature broadly agrees that THP-1 macrophages are induced through an initial PMA spike and polarisation occurs with relevant cytokines, similarities between published protocols end there. There is little agreement on what concentration of PMA should be used, length of time required for differentiation, whether a rest period should be given after this induction, duration of this rest and cytokine exposure times and dosage (Chanput *et al., 20*12); (Spencer *et al., 20*10).

PMA concentrations ranging from 2.5ng/ml to 400ng/ml have been used in published protocols (Park *et al., 20*07); (Genin *et al., 20*15); (Daigneault *et al., 20*10); (Lund *et al., 20*16); (Jiang *et al., 20*16); (Jiang *et al., 20*17); (Kohro *et al., 20*04); (Feng *et al., 20*04);

(Tulk *et al., 20*15); (Hirakata *et al., 20*04); (Maeß *et al., 20*14). PMA is a diacylglycerol (DAG) analogue, so higher concentrations will upregulate products downstream of protein kinase C, some of which are undesirable and may skew the transcriptome; PMA reportedly induces an M1 polarisation bias. Some groups have reported difficulty in generating M2a macrophages from THP-1 cells following treatments with high concentrations of PMA; reduced upregulation of M2a transcripts following cytokine stimulation, or a failure to induce this phenotype altogether were described (Chanput *et al., 20*13); (Spano *et al., 20*13); (Park *et al., 20*07)**.** Hence a lower concentration of PMA should be used, wherever possible, to induce M2a polarisation. However, the lowest concentration at which undesired effects of PMA are minimised whilst macrophage polarisation and expression of subset-specific markers are retained has not previously been explored.

The effects of PMA may also be reduced through culture in stimulant free media following the PMA spike (Park *et al., 20*07); (Chanput *et al., 20*12). Again, the challenge remains in identifying a rest duration that would reduce non-specific PMA effects whilst allowing cells to retain macrophage-like adherence, and as before there is little consensus in the literature on the duration of "rest period" (Chanput *et al., 20*12); (Daigneault *et al., 20*10); (Solberg *et al., 20*15).

As with other aspects of the protocol, cytokine exposure time varied between reports. As some genes are up-regulated for limited periods of time following cytokine induction it is necessary to identify a point at which most markers are most strongly induced, to confirm the phenotype and identify optimal conditions (Chanput *et al., 20*12); (Daigneault *et al., 20*10); (Solberg *et al., 20*15); (Park *et al., 20*07).

The aim of the work described in this Chapter was to determine the optimal protocol for generation of M1 and M2a THP-1 macrophages (using the workflow in Figure 3.1.1), that may also be used to validate subset-specific novel markers identified in previous analyses. The workflow used here may be seen in Figure 3.1.1.

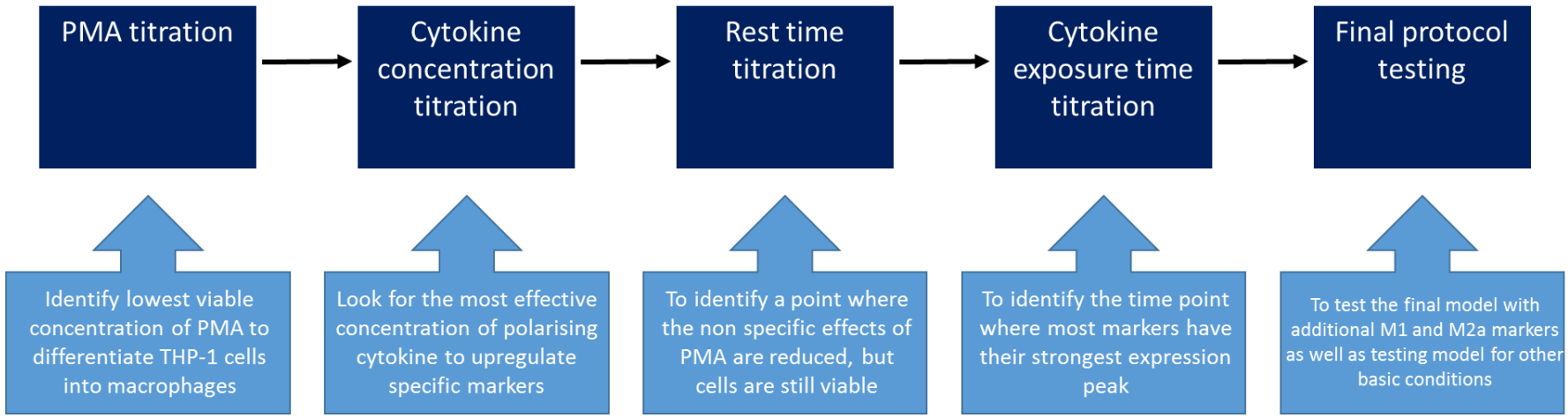

Figure 3.1.1 workflow for optimisation of THP-1 cell line model to produce M1 and M2a polarised macrophages. PMA=phorbol myristate acetate

3.2 Materials and methods

3.2.1 Marker panel selection

The majority of genes used in the panel were selected through analysis of public datasets and appeared in the top 30 differentially expressed gene list according to fold change (see Chapter 2, Table 2.3.6). A frequently used literature marker was also included for each condition that did not appear in the top 30 transcript list: *IRF1* for M1 and *TGM2* for M2a (Xie *et al., 20*16); (Martinez and Gordon, 2014). A summary of the panel is seen in Table 3.2.1. *RPL37A*, a gene coding for a ribosomal protein was included as a loading control (Maeß *et al., 20*10).

3.2.2 Cell culture

THP-1 cells (European Collection of Authenticated Cell Cultures, Sailsbury, UK) were counted and seeded at a concentration of 300,000 cells/ml in antibiotic-free RPMI (Roswell Park Memorial Institute) media + 10% foetal calf serum (FCS) (Sigma-Aldrich, Steinheim, Germany) and maintained at 37ºC, 5% carbon dioxide in a humidified tissue culture incubator (product code MCO20AIC, Sanyo, Osaka, Japan). All centrifugations were performed in an Eppendorf 5810 R centrifuge (Eppendorf, Hamburg, Germany). THP-1 cells underwent mycoplasma testing as a quality control measure, and short tandem repeat profiling (a method used to compare loci on DNA samples) was performed to confirm cell type prior to experiments.

3.2.3 PMA exposure

The initial protocol considered required addition of 50ng/ml PMA (Sigma-Aldrich, Steinheim, Germany) to RPMI media (Sigma-Aldrich, Missouri, USA) + 10% FCS (Sigma-Aldrich, Missouri, USA) for 24 hours to mature the THP-1 monocytes into macrophage-like cells, 24h rest period in fresh media and exposure to polarising cytokines for a further 24h; 20ng/ml IFNγ (Peprotech, NJ, USA) and 250ng/ml LPS (Peprotech, NJ, USA) were used for M1 and 20ng/ml of IL-4 (R&D Systems, Minnesota, USA) for M2a cells.

To identify the lowest, effective concentration of PMA that would ensure specificity and sensitivity of markers in the protocol, a titration was performed; cells destined to be M1 and M2a macrophages were incubated at 37ºC in 6 well plates (Corning, New York, USA) (1 million cells per well, 3ml RPMI media) and differentiated with 2.5, 5, 10, 20, 50ng/ml PMA for 24h before rest period and polarisation (as described above).

3.2.4 Cytokine titration

THP-1 cells were differentiated here with 5ng/ml PMA (Sigma-Aldrich, Steinheim, Germany) for 24h. Initial cytokine concentrations of 250ng/ml LPS (Peprotech, NJ, USA) and 20ng/ml IFNγ (Peprotech, NJ, USA) for M1, 20ng/ml IL-4 (R&D Systems, Minnesota, USA) for M2a and 20ng/ml IL-10 (R&D Systems, Minnesota, USA) for M2c were deduced from the literature.

For M1 cells, IFNγ concentrations were kept consistent whilst those for LPS were varied between 0 and 250 ng/ml, at 50ng/ml increments for the 24h cytokine exposure time.

Potential M2a cells were treated with IL-4 concentrations of 20, 25 and 30ng/ml for the 24h polarisation period.

3.2.5 Rest period

A PMA (Sigma-Aldrich, Steinheim, Germany) concentration of 5ng/ml was given for 24 hours to differentiate cells. Post PMA-spike rest time was increased incrementally to include 24h, 48h, and 96h periods.

Subsequently, polarising cytokines (20ng/ml IFNγ (Peprotech, NJ, USA) and 250ng/ml LPS (Peprotech, NJ, USA) were used for M1 and 30ng/ml of IL-4 (R&D Systems, Minnesota, USA) for M2a cells) were given for 24h.

3.2.6 Cytokine exposure time

Cells were again differentiated with 5ng/ml PMA (Sigma-Aldrich, Steinheim, Germany) for 24h and rested in cytokine free media for 72h. THP-1 cells incubated with polarising agents for the various sub-types were tested at different time points: 24, 48, 72 and 96h. Cytokine concentrations of 20ng/ml IFNγ (Peprotech, NJ, USA) and 250ng/ml LPS (Peprotech, NJ, USA) were used for M1 and 30ng/ml of IL-4 (R&D Systems, Minnesota, USA) for M2a cells

3.2.7 Final tissue culture protocol

THP-1 monocytes were treated with 5ng/ml PMA (Sigma-Aldrich, Steinheim, Germany) for 24h, rested in cytokine free RPMI media (Sigma-Aldrich, Steinheim, Germany) + 10% FCS (Sigma-Aldrich, Steinheim, Germany) for 72h, and then polarised for 48h

with the following; for M1 cells, 20ng/ml IFNγ (Peprotech, NJ, USA) and 250ng/ml LPS (Peprotech, NJ, USA), for M2a cells 30ng/ml of IL-4 (R&D Systems, Minnesota, USA), for M2c cells 30ng/ml IL-10 (R&D Systems, Minnesota, USA) and for TPP cells, 800IU/ml TNF (Sigma-Aldrich, Steinheim, Germany), 100ng/ml Prostaglandin E2 (Sigma-Aldrich, Steinheim, Germany), 100ng/ml Pam3SK4 (Invitrogen, Carlsbad, USA).

3.2.8. Extraction, polarisation and culture of primary peripheral blood derived monocytes for use as positive controls

Blood was drawn from healthy volunteers using lithium-heparin containing vacuette tubes (Greiner Bio-One, Kremsmünster, Austria) and mixed at a 1:1 ratio with Dulbecco's Phosphate Buffered Saline (PBS) (Sigma-Aldrich, Missouri, USA) (formulation for 1 litre is 8 g Sodium Chloride, 0.2 g Potassium Phosphate, monobasic, 1.15 g Sodium Phosphate, dibasic, and 0.2 g Potassium Chloride). Lymphoprep (Stemcell Technologies, Vancouver, Canada) was added to SepMate tubes (Stemcell Technologies, Vancouver, Canada) and blood/PBS was layered on top of lymphoprep. Sepmate tubes were centrifuged at 1200xg for 10 minutes with the brake set to 4. Red blood cells were removed here by density gradient centrifugation and remaining blood components were decanted and further diluted using PBS. Samples were centrifuged at 300xg for 10 minutes to pellet cells. Supernatant was discarded and cells were resuspended in fresh PBS and the step was repeated. Cell pellets were subsequently resuspended in RPMI media (Sigma-Aldrich, Missouri, USA) and plated into T75 tissue culture plates (Corning, New York, USA) which had previously been coated in a 10µg/ml solution of fibronectin (Sigma-Aldrich, Missouri, USA) at a concentration of 3 million cells per flask. Monocytes were left to adhere overnight before a media change (fresh RPMI) and 72h rest. As with the THP-1 cells, macrophages were polarised for 72h with the same cytokine concentrations of 250ng/ml LPS (Peprotech, NJ, USA) and 20ng/ml IFNγ (Peprotech, NJ, USA) for M1 cells, 30ng/ml IL-4 for M2a cells (R&D Systems, Minnesota, USA) and 30ng/ml IL-10 (R&D Systems, Minnesota, USA) for M2c macrophages. Use of healthy controls was approved by Leeds Research ethics committee (reference number 04/Q1206/107).

3.2.9 RNA extraction

Cells were washed in PBS and lysed using the Qiagen RLT plus buffer according to the Qiagen RNeasy plus kit protocol. Briefly, lysate was added to a genomic DNA exclusion column and centrifuged at 10,000xg to remove any genomic DNA. Lysate

was then diluted at a 1:1 ratio with 70% ethanol and added to a mini-spin column before another 10,000xg centrifugation, adhering the RNA to the column membrane and removing the buffer. RNA was then washed once with RW1 buffer (removed carbohydrates, protein, fatty acids) and twice in RPE buffer to remove residual salts from other buffers. RNA was then eluted using RNase free deionised water, checked for purity using the nanodrop and then stored at -20ºC prior to use; here a 260/280 ratio of approximately 2.0 is considered pure for RNA.

3.2.10 Cell viability and RNA yield

Once the polarisation protocol was complete, cells were washed with PBS (Sigma-Aldrich, Steinheim, Germany) and removed from flasks using Trypsin-EDTA (Sigma-Aldrich, Steinheim, Germany).

Following resuspension in media, cells were stained with trypan blue (Invitrogen, Carlsbad, USA) at a 1:1 ratio and injected into a countess slide chamber. This slide was subsequently loaded into the countess where cell counting and viability assessment were performed (Invitrogen, Carlsbad, USA).

3.2.11 cDNA synthesis

cDNA was produced according to the Invitrogen superscript II protocol. Briefly 2.5 µg RNA template was mixed with oligo dT (0.5 µg) (Invitrogen, Carlsbad, USA) and deoxynucleotides (dNTPs) (Bioline, London, UK) and heated to 65^0C to remove secondary structures. Reactions were put on ice while First Strand buffer and dithiothreitol (DTT) (all Invitrogen, Carlsbad, USA) were added, and the mixture was heated to 42^0C for 2 minutes so primers could anneal to RNA template. 1-unit Superscript II enzyme (Invitrogen, Carlsbad, USA) was added and the reactions were heated to 42^0C for 50 minutes. The reaction was ended by heating to 70ºC for 15 minutes.

3.2.12 Marker panel Polymerase chain reaction

3.2.12.1 Primer design

Primers producing an amplicon of minimum 100bp were designed for genes identified as potential markers in RNA-seq analysis (Chapter 2, Tables 2.3.4 and 2.3.5). Primers were designed to span exon junctions so any genomic contamination produced a larger amplicon. Primers were designed to have a GC content of around 50%, Tm of

approximately 60^0C, and a GC clamp at the 5' end. Primers were checked for secondary structures using the basic Northwestern oligocalc (http://www.basic.northwestern.edu/biotools/oligocalc.html) and specificity was verified using the UCSC *in silico* polymerase chain reaction (PCR) tool (https://genome.ucsc.edu).

Details of primer lengths and sequences can be found in Tables 3.2.3-5.

3.2.11.2 PCR

See Table 3.2.2 for details of reagents used. All PCRs were run using the M1 and M2a primers listed in Tables 3.2.3-5, and using cycling conditions described in Table 3.2.6. Generally speaking, template and relevant primers were combined on ice with PCR buffer, magnesium, dNTPs and *Taq* polymerase. Initial denaturation was performed at 95ºC to remove secondary structures. A short denaturation was included at the start of each cycle. An annealing step at a temperature where the primers could bind to the cDNA and an elongation phase at 72ºC where the polymerase enzyme amplified the target region of the template followed. Generally, 25-30 cycles were used for each reaction, i.e. enough cycles to allow expression of a positive control.

3.2.12.3 Agarose gel electrophoresis

All PCR products were run on a 3% agarose/TAE (W:V) (Sigma-Aldrich, Steinheim, Germany) gel for 75 minutes at 120V in TAE buffer, using a Bio rad Laboratories (California, USA) electrophoresis system. Gels were imaged using ImageLab software and a Bio rad gel doc system (Bio rad Laboratories, California, USA).

3.2.13 Flow cytometry

Trypsin-ethylene-diaminetetraacetic acid (EDTA) (Sigma-Aldrich, Steinheim, Germany) was added to flasks until cells became detached and 10x the volume of RPMI media + 10% FCS was added to neutralise the effects of the enzyme. The cell suspension was centrifuged at 400xg for 5 minutes and resuspended in a lower volume of media (generally around 2mls from a T75 tissue culture flask). Cell number was determined using the Countess as described above. 200,000 cells were added on to a 96 well plate for each sample, blocked in 2ng/ml IgG1 for 30 minutes on ice and stained with anti-CD14 fluorescein isothiocyanate (FITC)-conjugated (VIM12, Thermo Fisher Scientific, Massachusetts, USA) and anti-CD11b allophycocyanin (APC)-conjugated (M5E2, BD Biosciences, California, USA) clones in the dark for 1 hour. Cells were subsequently

washed in FACS buffer (PBS, 2% FCS, 2mM EDTA) and fixed in FACS fix (50% FACS buffer, 10% methanol, 2% formaldehyde). Flow cytometry was performed using the plate reader arm of a BD Biosciences Cytoflex (California, USA) and data was recorded for the APC (785nm) and FITC (520nm) channels. All analyses were performed using FlowJo software (flowJo, Oregon, USA).

Table 3.2.1. Panel of M1 and M2a macrophage transcriptional markers identified in Chapter 2 (Table 2.3.4) from public datasets or published studies, selected for optimisation of the THP-1 cells line model, M1= M1 macrophage, M2a= M2a macrophage

Gene	**Subtype**	**Source**
CXCL10	M1	public datasets
CXCL9	M1	public datasets
GBP5	M1	public datasets
ANKRD22	M1	public datasets
TNFAIP6	M1	public datasets
IRF1	M1	Literature marker (Xie *et al., 20*16)
ALOX15	M2a	Analysis marker
CCL17	M2a	Analysis marker
CCL23	M2a	Analysis marker
CCL26	M2a	Analysis marker
HOMER2	M2a	Analysis marker
TGM2	M2a	Literature marker (Rőszer, 2015)

Table 3.2.2. Details of PCR reagents used in all reactions described in this Chapter. dH2O=water, Mg2+=magnesium ions, dNTPs=deoxynucleotides

Reagent	**Concentration**	**Volume in 20µl reaction**
dH2O	N/A	14.43 µl
Taq Buffer	20x	2 µl
Mg2+ (Applied Biosystems, CA, USA)	50mM	1.2 µl
dNTPs (Bioline, London, UK)	0.4 µM	0.4 µl
Forward primer (IDT, CA, USA)	0.2µg/ml	0.4 µl
Reverse primer (IDT, CA, USA)	0.2µg/ml	0.4 µl
Template	2.5 µl	1 µl
***Taq* polymerase**	1 unit	0.17 µl

Table 3.2.3. M1 transcript marker primer sequences to be used in THP-1 PCR experiments. Details of length in base pairs are also given here. Bp= base pairs

Gene	Forward primer sequence	Reverse primer sequence	Product length (bp)
CXCL10	dCCTTATCTTTCTGACTC TAAGTGG	dCTAAAGACCTTGGAT TAACAGG	107
CXCL9	dGCTGGTTCTGATTGGA GTGC	dGAAGGGCTTGGGGC AAATTG	124
GBP5	dCCAGCTATGAACTCCT TCTCC	dCTTTGGAATCTTCTC CTGGGG	118
ANKRD22	dGAAGGACCAGCATGG GAATC	dGTTGGCATAGCTGCT GTCTTC	110
TNFAIP6	dGGGATGCCTATTGCTA CAACC	dCGTACTCATTTGGGA AGCCTG	99
IL6	dCCAGCTATGAACTCCT TTCC	dCTTTGGAATCTTCTC CTGGGG	118
IRF1	dGGAAGGGAAATTACCT GAGG	dCTCCAGGTTCATTGA GTAGG	101
RPL37A	dTTCCGCTCGTCCGCCT AATAC	dGGCCAGTGATGTCTC AAAGAG	89

Table 3.2.4. M2a transcript marker primer sequences to be used in THP-1 optimisation PCR experiments. Details of length in base pairs are also given here. Bp= base pairs

Gene	**Forward primer sequence**	**Reverse primer sequence**	**Product length (bp)**
ALOX15	dCAGATGTCCATCACTTGGCAG	dCTCCTCCCTGAACTTCTTCAG	123
CCL17	dCTTCTCTGCAGCACATCCAC	dCAGATGTCTGGTACCACGTC	117
CCL23	dGAAGCATCCCGTGTTCACTC	dCTTATCACTGGGGTTGGCAC	119
CCL26	dGAAGGGCCTGATTTGCAGCATC	dCAGGTCTTGGATATGTCACTCC	120
HOMER2	dCCTCAGCTCATGTCAGAGTGC	dGCTCTTCAACTCCACCTTCAGG	153
TGM2	dGCAGTGACTTTGACGTCTTTGCCC	dGTAGCTGTTGATAACTGGCTCCACG	269
CD200R1	dCTGTACATAGAGCTACTTCCTGTTCC	dGCATTTCATCCTCCTCAACAACTGG	187

Table 3.2.5. Sequences and lengths of other primers; additional M1 and M2a marker to further test the final optimised protocol, and TPP and M2c primers to test these polarisation states using PCR experiments. Details of length in base pairs are also given here. Bp= base pairs

Gene	Forward primer sequence	Reverse primer sequence	Product length (bp)
ABHD	dAACCTCTACGCCGACATCGAC	dGACAGTCCCAATGCTCTGACC	102
LAMP3	dGCAGAGATGGGGATACAGCTG	dAGTTCCCAGAGGCTTGCGTTG	103
STAT4	dACAATGGGCTCGACCAGCTTC	dGCATTGGAATGGGATCACCTTC	132
STAT1	dCAATGCTTGCTTGGATCAGC	dGTGATAGGGTCATGTTGCTAGG	130
INHBA	dGATCATCACGTTTGCCGAGTC	dGGGACTTTTAGGAAGAGCCAG	120
SERPING1	dGATGTCCAAGTTCCAGCCCAC	dCAGCCCACACAGGTTAAGGTC	130
TSC22D1	dCTCTGGTGCAAGTGTGGTA	dCCTCCACTTCTTCTCTGACC	98
CD163			214
CXCL13	dGTATCCATTCAGCTTGAGGG	dAAATCTTGCCCCGTGGGAATG	99
SEPP1	dGTGGAGCTGCCAGAGTAAAG	dCCAGGCTTCTCCACATTGCTG	86

F13A1	dATGTCAGAAACTTC CAGGACCG	dAGAAACTCTTGCAGG TTGACGC	137
CD206	dCGAGGAAGAGGTT CGGTTCACC	dGCAATCCCGGTTCTC ATGGC	84
AP2A2	dGGAGCTGGAATCAT CCACACG	dGCTTCCTTACTTGTG CGCAG	110

Table 3.2.6. Summary of cycling conditions used in marker panel PCR experiments in this Chapter

Gene	**Cycling conditions**	**Annealing temperature (ºC)**	**Number of cycles**
CXCL10	**Initial denaturation:** 2 minutes/95ºC **Denaturation:** 30s/95 ºC **Annealing:** 30s **Elongation:** 30s/72 ºC **Final elongation:** 3 minutes/72 ºC	55	25
CXCL9		63	25
GBP5		60	25
ANKRD22		60	30
TNFAIP6		60	25
IRF1		55	25
ALOX15		60	30
CCL17		58	30
CCL23		60	30
CCL26		63	25
HOMER2		60	25
TGM2		63	25
RPL37A		63	25

3.3 Results

3.3.1 Phorbol-12-myristate-13-acetate titration identified the lowest viable concentration that could be used for generation of macrophages as 5ng/ml

PMA is an effective agent for differentiating THP-1 monocytes into adherent, macrophage like cells. However, the interactions of this DAG analogue with elements of intracellular signalling pathways may result in the induction of additional, undesirable transcriptional events, which may be impossible to account for (Zeng *et al., 20*15); (Park *et al., 20*07). To address this, PMA concentrations were titrated down to identify the lowest concentration where the differentiated state could still be achieved (i.e. adherent, viable cells expressing appropriate markers) whilst reducing non-specific effects. Some evidence implies that PMA concentrations upwards of 100ng/ml exceed physiological concentrations for the *in vitro* study of macrophages, so an upper limit of 100ng/ml PMA (previously found to be effective) was selected for experiments on M0 cells, which could be reduced to 50ng/ml for other experiments if no differences in viability or marker expression could be seen between the two increments (Park *et al., 20*07).

M0 THP-1 cells were tested using trypan blue staining to determine the independent effect of PMA on macrophage viability (Figure 3.3.1); the scores appeared to be consistent throughout the range of concentrations tested with no significant differences detected (Figure 3.3.1 A-B), suggesting that healthy cells could be obtained through any degree of PMA priming. Once viability was established other parameters (such as cellular adherence and marker expression) were then used to determine the lowest suiTable concentration of PMA, as all of the experimental conditions were accepTable based on viability alone.

Considering the lowest concentration of PMA used; although the THP-1 cells appear to be viable at 2.5ng/ml PMA, compared to higher concentrations (Figure 3.3.2 B-C) cellular adherence was affected (Figure 3.3.1); considerably fewer cells remained attached to the flask following the PBS wash for both M0 and M2a cells, suggesting an unreliable adherence and weaker macrophage phenotype. It should be noted that M1 cells remained adherent for all PMA titration conditions, possibly due to LPS and IFNγ upregulating adhesion molecule expression. Unsurprisingly, lowering the PMA concentration appeared to have a detrimental effect on RNA yield of the inherently less adherent M2a induced THP-1 cells. For these reasons 2.5ng/ml of PMA was discounted as a viable treatment.

Cell attachment appeared to be improved for concentrations of 5ng/ml PMA upwards, and degree of adherence was comparable between these different conditions.

Morphologically speaking, M0 and M2a cells have the characteristic rounder appearance at the lower concentrations of PMA (5-10ng/ml), but become more spindle-like at high concentrations, suggesting that they may be becoming more inflammatory, although this was difficult to tell based on cell images alone.

End-point PCRs were performed in this study as transcripts that were induced in one condition and completely absent in another were selected as markers, so to give an indication of how this expression pattern may correspond to that of protein markers.

Looking at subset markers, there appeared to be little difference in specific and non-specific gene expression for both M0 and M2a-polarised cells at different PMA concentrations (Figures 3.3.3 and 3.3.6 respectively); in fact, using these initial conditions, overall expression of M2a markers appeared quite weak for all given PMA concentrations, which was possibly due to cytokine concentration or cytokine exposure time factors. Non-specific expression of M2a markers *HOMER2* and *TGM2* was seen for both M1 (Figure 3.3.4) and M0 (Figure 3.3.3) conditions, and M1-specific transcript *TNFAIP6* was weakly upregulated in M0 and M2a phenotypes at this stage; their induction did not appear to be strongly affected by changes in PMA concentration for the preliminary protocol.

M1 markers did not appear to be as strongly up-regulated in M1 cells treated with 2.5ng/ml PMA compared to other concentrations tested. When the concentration was increased to 5ng/ml of PMA, M1 marker expression in LPS/IFNγ treated cells was stronger, and consistent with expression seen with higher concentrations of PMA. Therefore, 5ng/ml was selected as a suitable level of PMA to be used for downstream experiments.

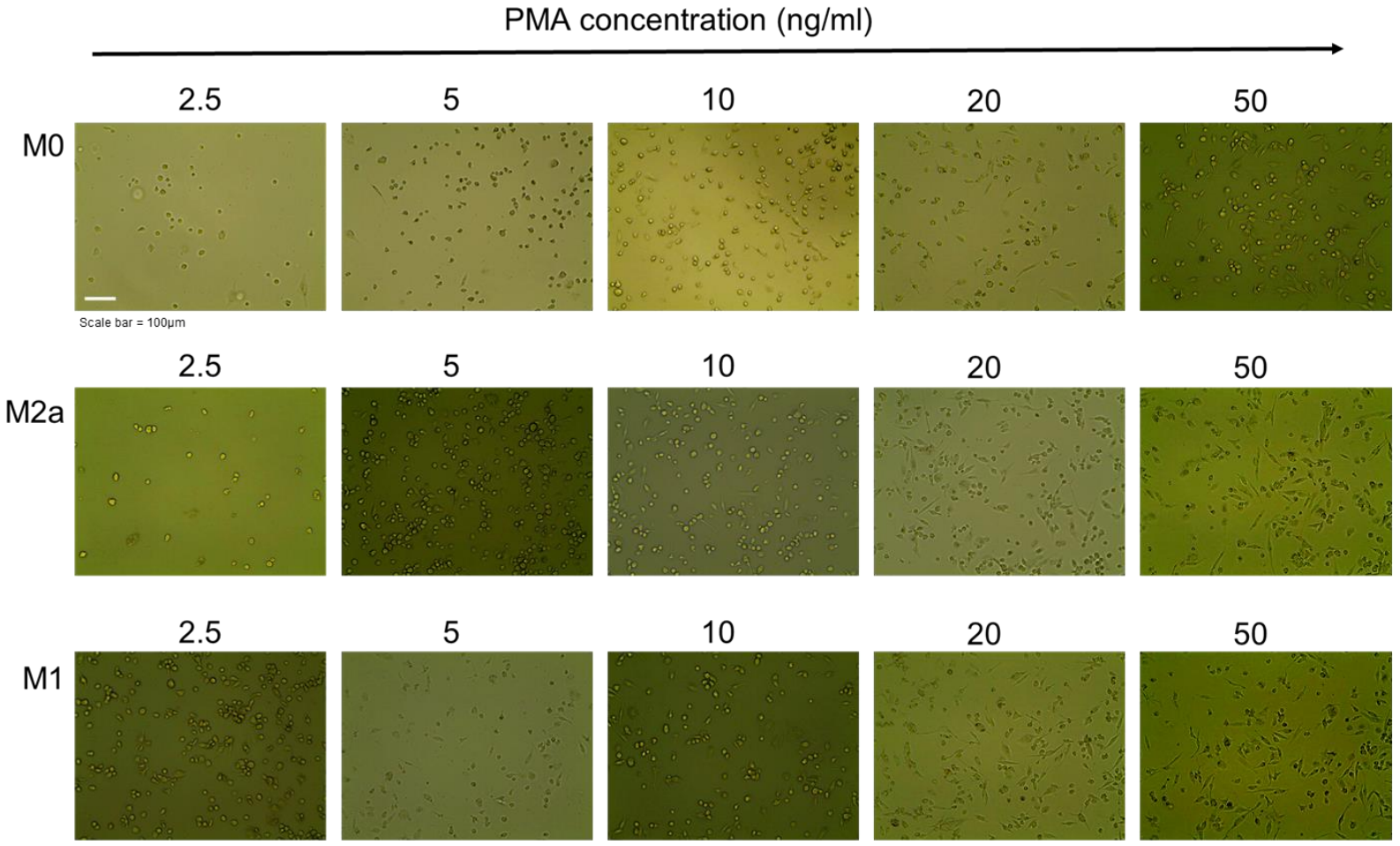

Figure 3.3.1. Light microscope images (taken at magnification x20) of THP-1 cells treated with different concentrations of PMA and then rested (M0) or polarised using IFNγ and LPS (M1) or IL-4 (M2a). Note that scaling is identical for all images and scale bar is given in bottom left corner of top left box as a white bar. PMA = phorbol 12-myristate 13-acetate. M1= M1 macrophage, M2a=M2a macrophage, M0=unpolarised macrophage

A

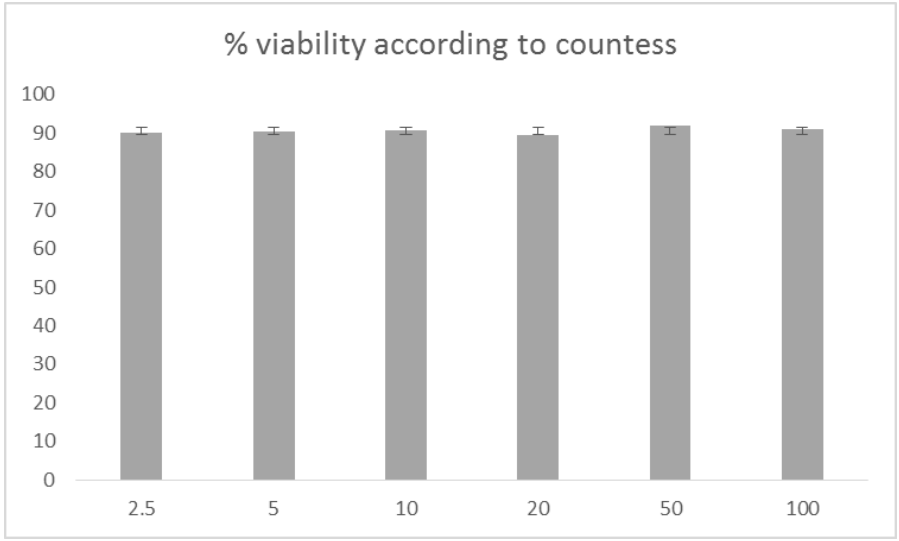

B

PMA conc (ng/ml)	% average viability	Standard deviation	Cell count according to countess (x10^6/ml)
2.5	90.0	3.0	3.3
5	90.3	3.2	2.6
10	90.7	5.5	3.5
20	89.3	3.2	2.9
50	92.0	2.0	2.6
100	91.0	3.6	3.0

Figure 3.3.2. Viability experiments for THP-1 cells treated with various concentrations of PMA; according to trypan blue staining using a countess (**A**). A summary of trypan blue viability data (where % average viability refers to an average of percentage viability according to trypan blue staining across three replicates) and cell counts of samples treated with different concentrations of PMA is also given (**B**) PMA = phorbol 12-myristate 13-acetate

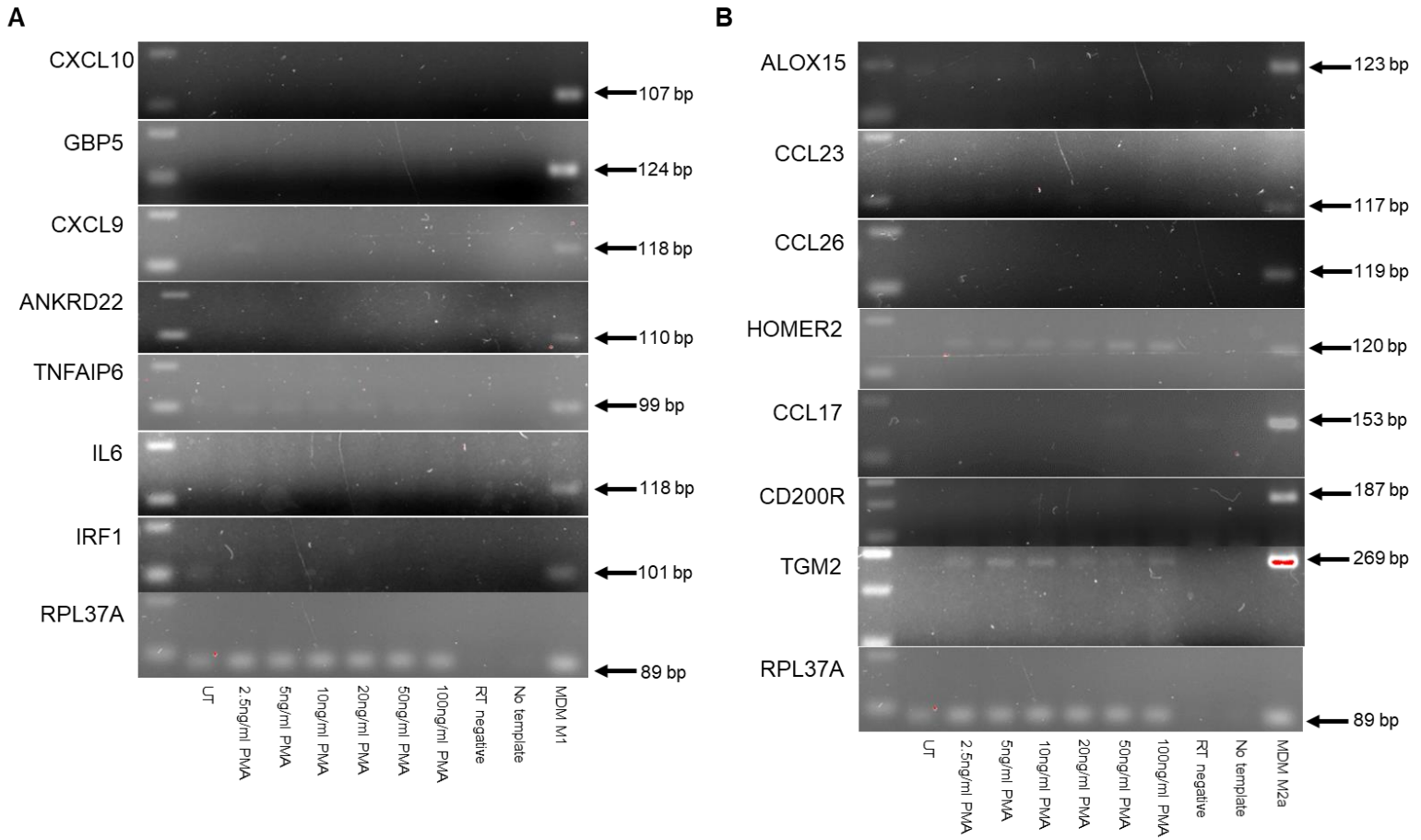

Figure 3.3.3. M0 PMA titration; cDNA derived unpolarised THP-1 cells treated with different concentrations of PMA tested for expression of M1 specific genes using PCR (**A**) and tested for expression of M2a marker genes using PCR (**B**). For both subsets (M1 and M2a) differentially polarised monocyte derived macrophages (MDMs) were used as a positive control. For each gel, size of PCR product is given in bp (base pairs) and amplicon is indicated by arrow. Left-most lane is DNA ladder where bottom band is 100bp mark. Bp= base pairs, PMA = phorbol 12-myristate 13-acetate. RT negative= reverse transcriptase negative, MDM=monocyte derived macrophage, UT=untreated

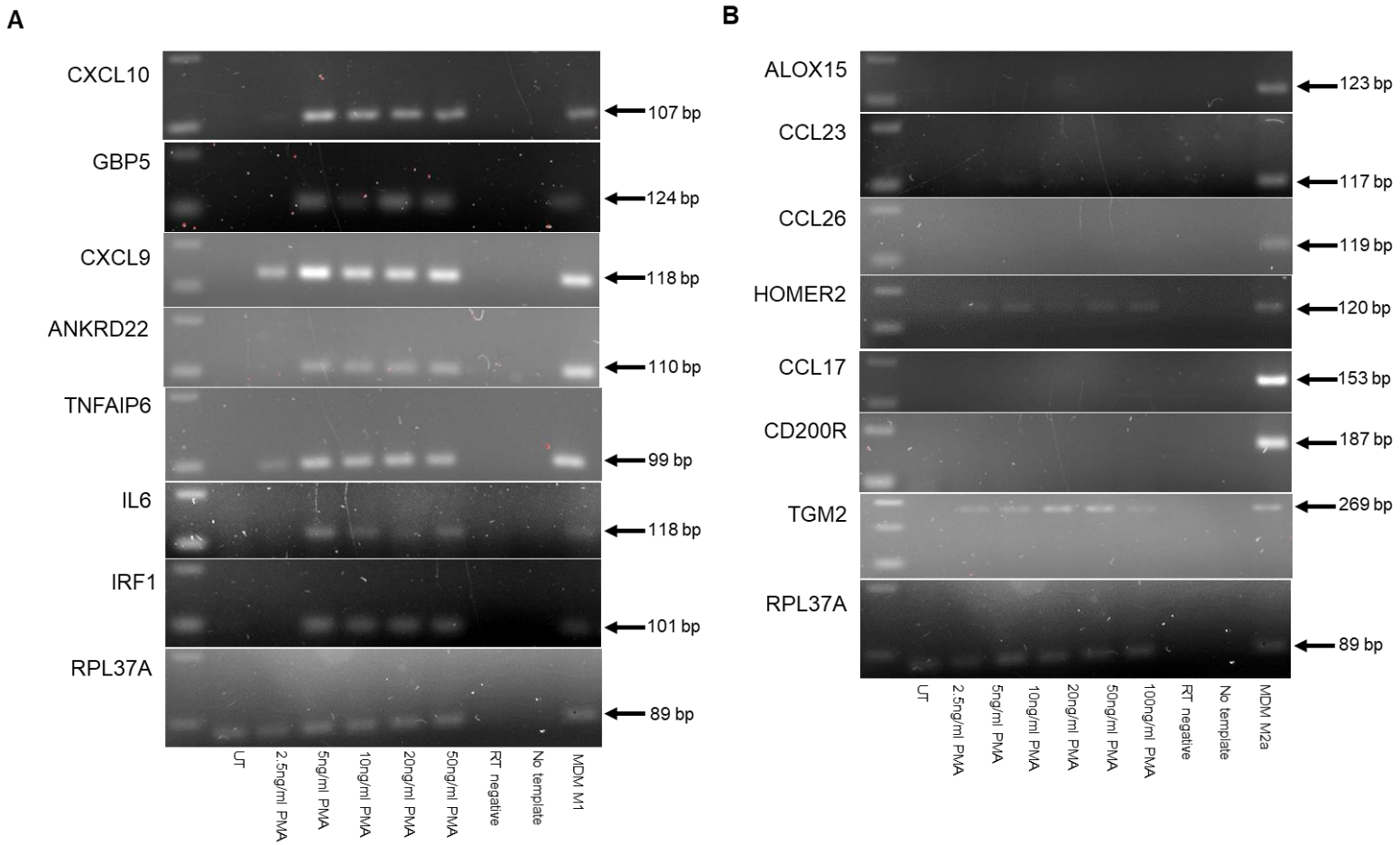

Figure 3.3.4. M1 PMA titration; cDNA derived from LPS and IFNγ polarised (M1) THP-1 cells treated with different concentrations of PMA tested for expression of M1 specific genes using PCR (**A**) and tested for expression of M2a marker genes using PCR (**B**). For both subsets (M1 and M2a) differentially polarised monocyte derived macrophages (MDMs) were used as a positive control. For each gel, size of PCR product is given in bp (base pairs) and amplicon is indicated by arrow. Left-most lane is DNA ladder where bottom band is 100bp mark. Bp=base pairs, PMA = phorbol 12-myristate 13-acetate. RT negative= reverse transcriptase negative, MDM=monocyte derived macrophage, UT=untreated

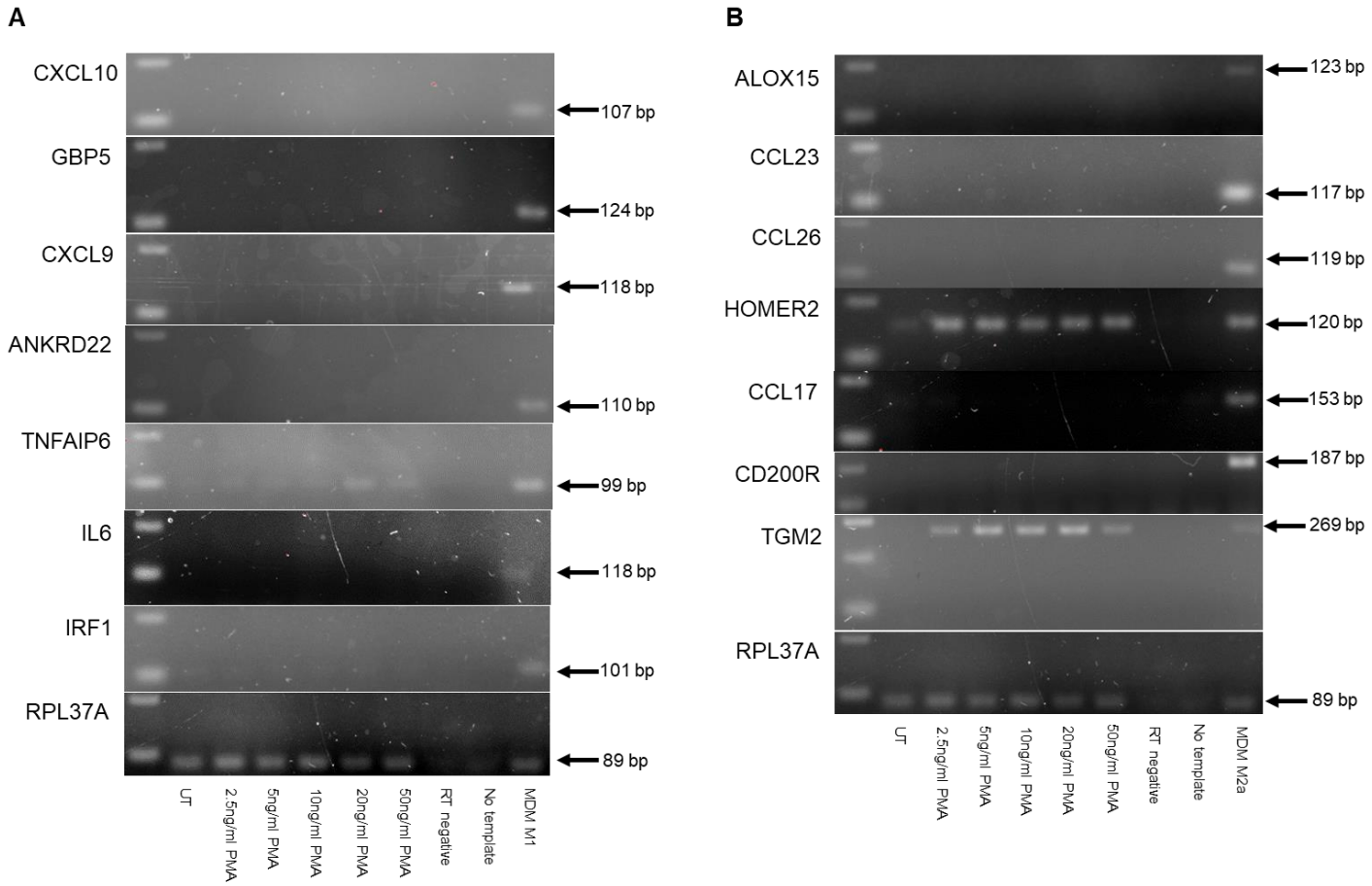

Figure 3.3.5. M2a PMA titration; cDNA derived from IL-4 polarised (M2a) THP-1 cells treated with different concentrations of PMA tested for expression of M1 specific genes using PCR (A) and tested for expression of M2a marker genes using PCR (B). For both subsets (M1 and M2a) differentially polarised monocyte derived macrophages (MDMs) were used as a positive control. For each gel, size of PCR product is given in bp (base pairs) and amplicon is indicated by arrow. Left-most lane is DNA ladder where bottom band is 100bp mark bp= base pairs, PMA = phorbol 12-myristate 13-acetate. RT negative= reverse transcriptase negative, MDM=monocyte derived macrophage, UT=untreated

Table 3.3.1. RNA concentration values taken using a nanodrop-1000 spectrophotometer for RNA extracted from cells stimulated with different concentrations of PMA and polarised into the M1 (IFNγ + LPS) (**A**), M2a (IL-4) (**B**) and M0 (IL-10) (**C**) state. PMA = phorbol 12-myristate 13-acetate

A

PMA conc ng/ml	Nanodrop conc (ng/ul) M1
2.5	145.6
5	274.2
10	127
20	130
50	167

B

PMA conc ng/ml	Nanodrop conc (ng/ul) M2a
2.5	175.2
5	282.5
10	276.6
20	279
50	331.6

C

PMA conc ng/ml	Nanodrop conc (ng/ul) M0
2.5	155
5	144
10	131
20	111
50	124

3.3.2 Optimal cytokine concentrations for gene expression were identified

Suggested concentrations of IFNγ were relatively consistent in the literature at 20ng/ml, but amount of LPS used varied between protocols depending on the assay and whether or not cell lines or MDMs were used (Genin *et al., 20*15); (Chanput *et al., 20*13); (Sun *et al., 20*16); (EngstrÖM *et al., 20*14). To address this variability, LPS was titrated to determine which concentration was ideal for upregulation of M1 markers (Figures 3.3.7 and 3.3.8). Although the majority of markers were expressed fairly consistently across the range, some genes (*IL6, TNFAIP6*) were only weakly induced where LPS concentrations were reduced to levels below 100ng/ml. Additionally some markers appear to be upregulated more strongly where the concentration of LPS was highest (*IL6, CXCL9*). Hence, the highest concentration of LPS tested (at 250ng/ml) was selected to carry forwards for further experiments and the finalised protocol. All M1 markers tested were induced at this concentration so potentially toxic higher increments of LPS were not tested. IL-4 concentrations were titrated from 20-30ng/ml (Figures 3.3.9 and 3.3.10); generally speaking, most published protocols use 20ng/ml of this cytokine, but as M2a cells are considered difficult to induce from THP-1 macrophages, higher concentrations were tested (Chanput *et al., 20*13). As some of the transcripts in the panel were not up-regulated strongly at the 24h time point (*ALOX15, CCL26, CCL23*), no distinctive pattern was identified. Bands for some markers (*TGM2* and *CCL17*) however, appeared to become slightly brighter with higher IL-4 concentrations, although this was subtle and difficult to judge without quantitative measurements. There was no visible change in M1 lineage markers for all of the tested IL-4 concentrations; M1 marker *TNFAIP6* was weakly expressed for all IL-4 conditions tested. The different concentrations of IL-4 did not appear to alter the morphology of the cells and in all three conditions tested a rounded morphology was adopted, typical of an M2a cell. Based on the subtle changes seen in the gels and as M2a cells are reportedly difficult to generate from THP-1 cells, the highest concentration of IL-4 was selected.

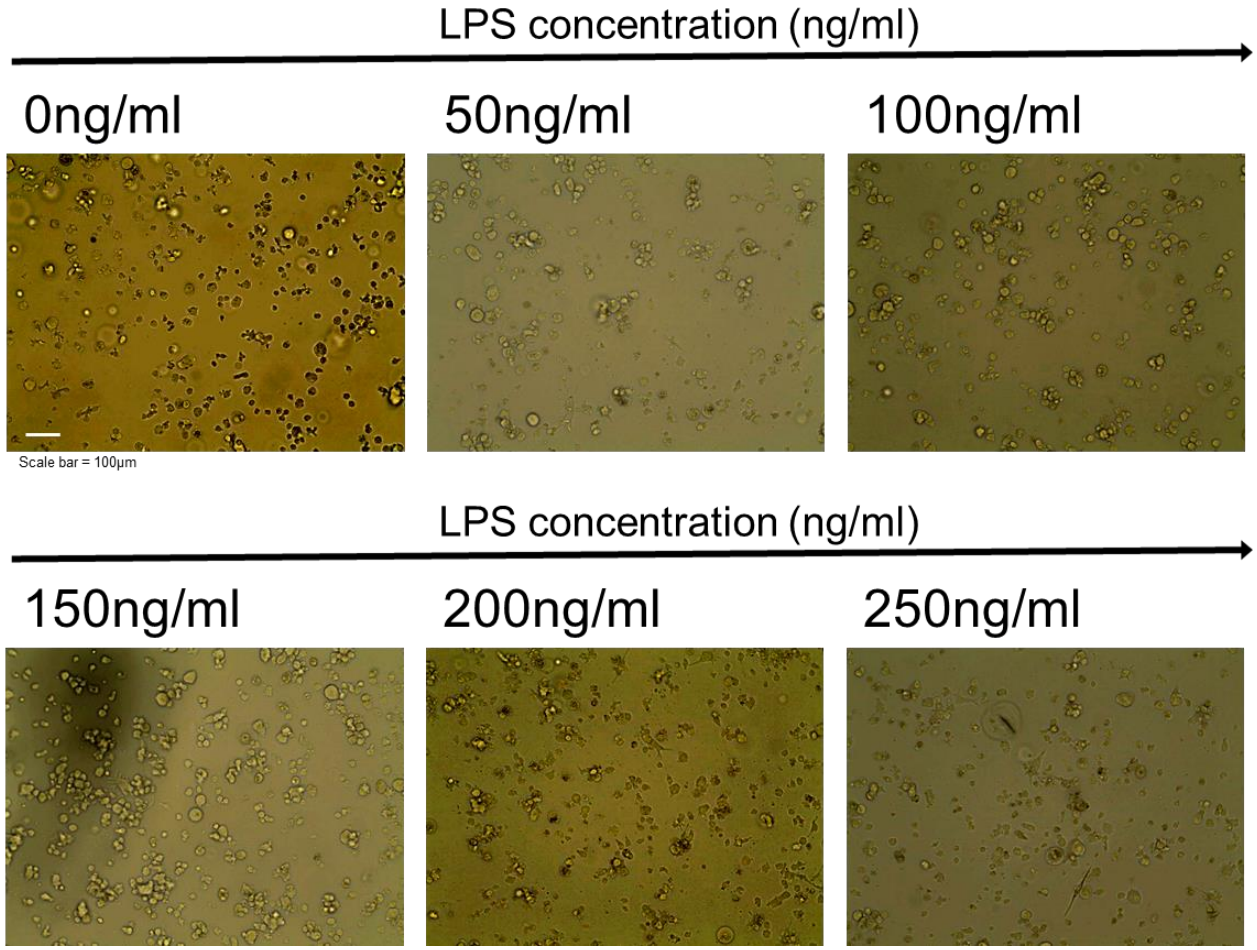

Figure 3.3.7. Light microscope images (taken at magnification x20) of THP-1 cells treated with different concentrations of LPS and a constant concentration of IFNγ, to examine differences in morphology and cellular adherence between treatments. Note that scaling is the same for all images (scale bar is given in the bottom left corner of top, left box as a white bar) PMA = phorbol 12-myristate 13-acetate, LPS=lipopolysaccharide

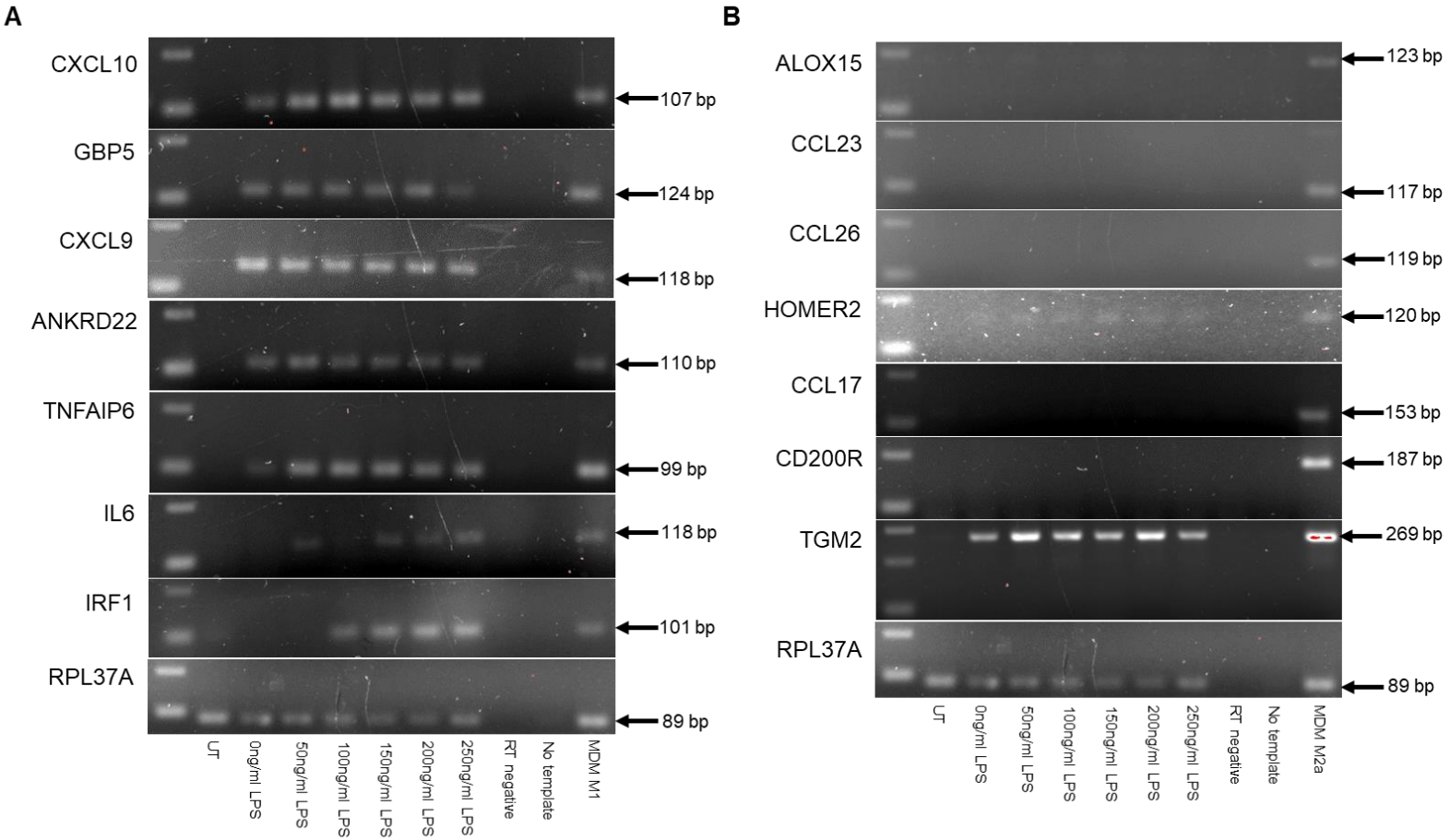

Figure 3.3.8. LPS titration; cDNA derived from LPS and IFNγ polarised (M1) THP-1 cells treated with different concentrations of PMA tested for expression of M1 specific genes using PCR (**A**) and tested for expression of M2a marker genes using PCR (**B**). For both subsets (M1 and M2a) differentially polarised monocyte derived macrophages (MDMs) were used as a positive control. For each gel, size of PCR product is given in bp (base pairs) and amplicon is indicated by arrow. Left-most lane is DNA ladder where bottom band is 100bp mark, LPS=lipopolysaccharide. RT negative= reverse transcriptase negative, MDM=monocyte derived macrophage, UT=untreated

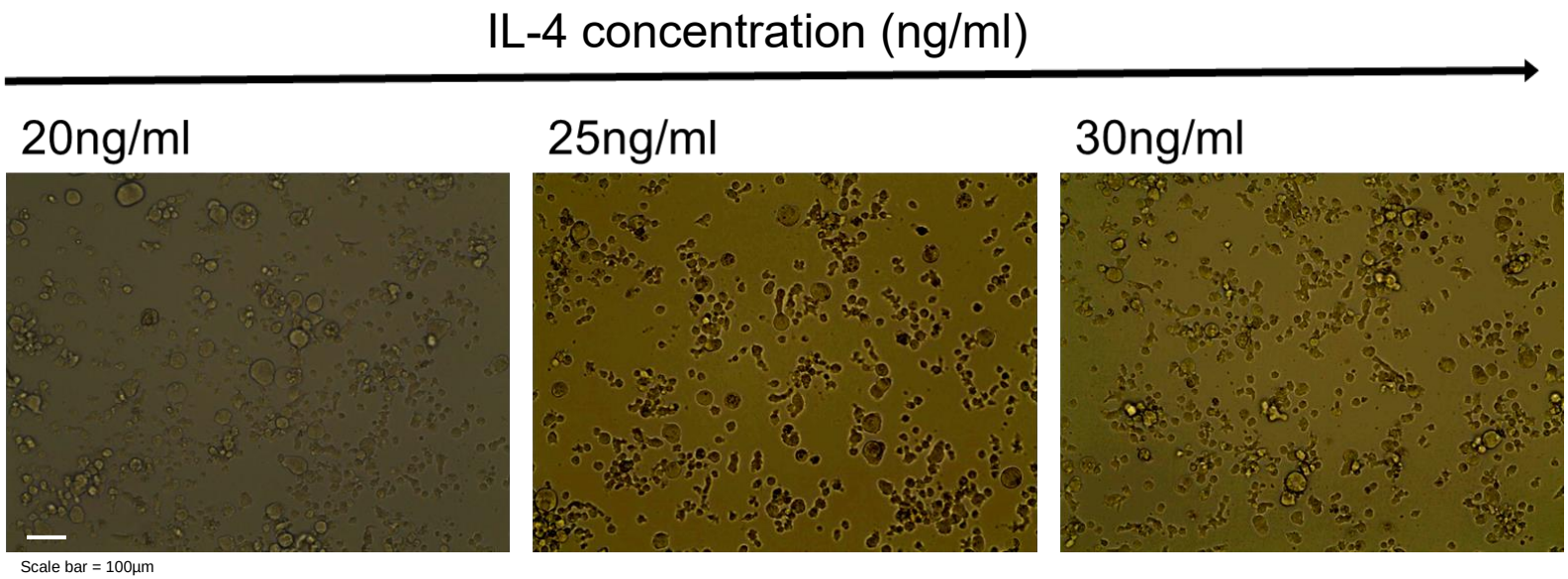

Figure 3.3.9. Light microscope images (taken at magnification x20) of THP-1 cells treated with different concentrations of IL-4, to examine changes in cell morphology and adherence between treatments. Note that scaling is the same for all images (scale bar is given in the bottom left corner of left box as a white bar). IL-4=interleukin-4

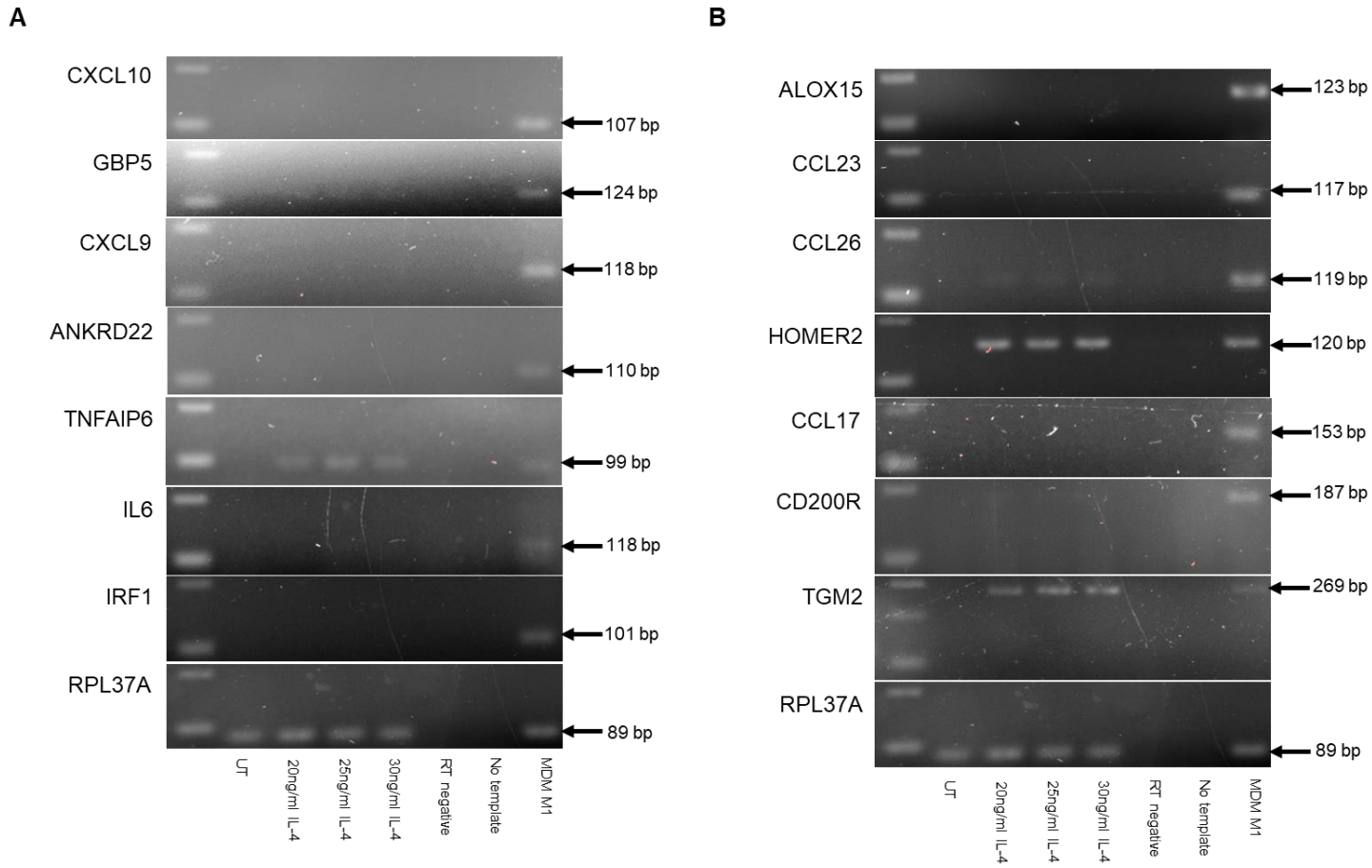

Figure 3.3.10. IL-4 titration**;** cDNA derived from THP-1 cells primed with PMA and treated with different concentrations of IL-4, tested for expression of M1 specific genes using PCR (**A**) and tested for expression of M2a marker genes using PCR (**B**). For both subsets (M1 and M2a) differentially polarised monocyte derived macrophages (MDMs) were used as a positive control. For each gel, size of PCR product is given in bp (base pairs) and amplicon is indicated by arrow. Left-most lane is DNA ladder where bottom band is 100bp mark, IL-4=interleukin-4, RT negative= reverse transcriptase negative, MDM=monocyte derived macrophage, UT=untreated

3.3.3 A 72h rest period was required for the reduction of non-specific expression of certain markers, whilst retaining sub-set specific expression and sufficient cell and RNA yield

The non-specific expression of lineage markers as a result of PMA exposure could potentially be reduced by resting the cells for increased periods of time (versus the 24h window used in earlier experiments) following the initial priming step. As lengthy rest times may result in cells losing their phenotype and becoming detached from culture flasks, a range of rest periods were tested.

Morphologically speaking, M1 cells rested for longer periods of time became rounder and lost some of their characteristic spindle-like morphology. Changes in cell shape were less apparent in M0 and M2a macrophages between different rest periods (Figure 3.3.11).

Cellular detachment did not seem to be an issue for any rest time for M1-induced cells. However, for the M0 and M2a conditions fewer cells appeared to remain attached to flasks after a 96h rest, so nothing longer than 72h rest was used in downstream experiments.

Not all markers were directly affected by PMA and so the issue of non-specific induction did not affect their expression patterns. Therefore, *HOMER2* (an M2a marker which appeared to be upregulated by PMA as seen in Figure 3.3.5) was used for this Section of this report as a representative example when discussing non-lineage-specific expression of transcripts. For both M1 and M0 conditions (Figures 3.3.12 and 3.3.13), *HOMER2* expression was seen following 24h and 48h rest, but dropped off when cells were rested for extended times of 72 or 96h. Additionally, although expression of *HOMER2* decreased between 48h and 72h rest time for M2a cells (Figure 3.3.14), induction of this M2a marker was still seen, suggesting the presence of this transcript was more M2a-specific for these given conditions. The M1 marker *TNFAIP6* also seemed to be downregulated in M2a and M0 sub-types, although some non-specific expression was still seen. It should also be noted that when rest periods in M2a cells were increased to 48 or 72h, expression of some M2a markers that were not previously upregulated (*CCL26, CCL23, ALOX15*) was seen.

For M1-like THP-1 cells, there did not appear to be any consistency when considering which rest time was optimal; some markers appeared to be more strongly induced with increased rest times (*ANKRD22* and *GBP5*) whereas others seemed to be slightly downregulated (*IL6*). However, expression of two lineage markers (*ANKRD22* and *GBP5*) was much stronger at 48 h and 72h whereas *IL6* gene expression was slightly

reduced, so 72h was chosen, since this rest time was also better considering cell morphology and adherence.

3.3.4 CCL26 expression is induced following increased rest periods when PMA spike is at 5ng/ml versus 50ng/ml

The potential detrimental effect of PMA on M2a macrophage polarisation was determined by directly comparing cells treated with 5ng/ml and 50ng/ml of PMA followed by various rest periods (Figures 5.3.14 and 3.3.15 respectively). As movement into the M2a state is reportedly blocked by higher levels of PMA, it could be argued that decreasing the concentration of this polarising agent and resting the cells for longer periods of time may render the cells more susceptible to M2a polarisation. The M2a marker *CCL26* appeared to be inducible following a rest period of 48h or 72h, and the upregulation appeared to be much stronger when the concentration of PMA was reduced to 5ng/ml versus 50ng/ml. This supported the use of the lower concentration of PMA that was more favourable for alternative activation states. Few markers appeared to persist after resting for 96h; as these cells are highly plastic it is possible that they require consistent cytokine stimulation to retain expression of certain transcripts. Alternatively, these genes could be under tight regulated by cellular machinery, and are thus only briefly induced following polarisation challenge.

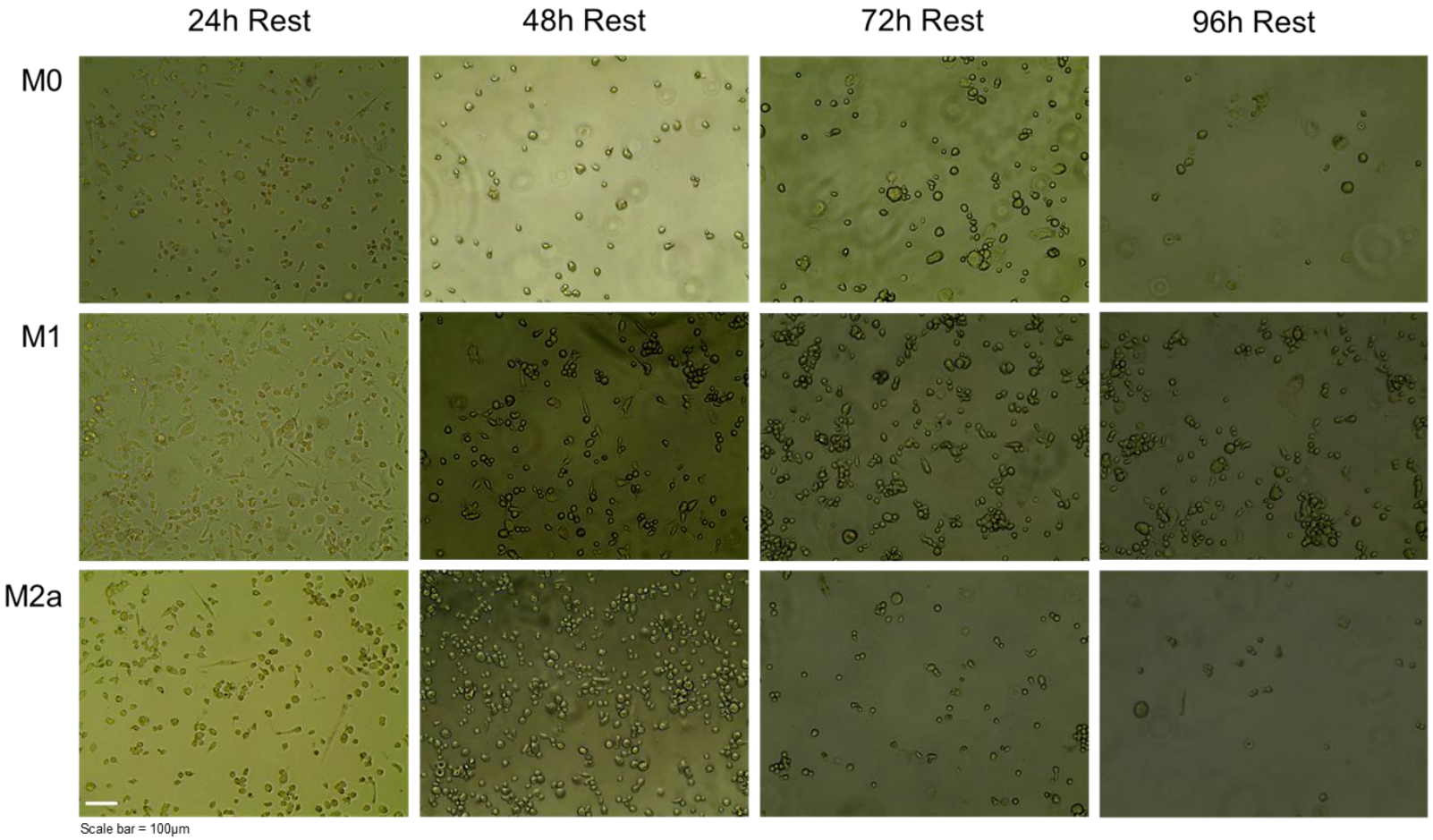

Figure 3.3.11. Light microscope images taken at x20 magnification of THP-1 cells rested for different amounts of time following initial PMA spike and then stimulated using IFNγ and LPS (M1) or IL-4 (M2a), or left unpolarised (M0). Note that scaling is identical for all images and scale bar is given in bottom left corner of bottom left box as a white bar. M1= M1 macrophage, M2a=M2a macrophage, M0=unpolarised macrophage

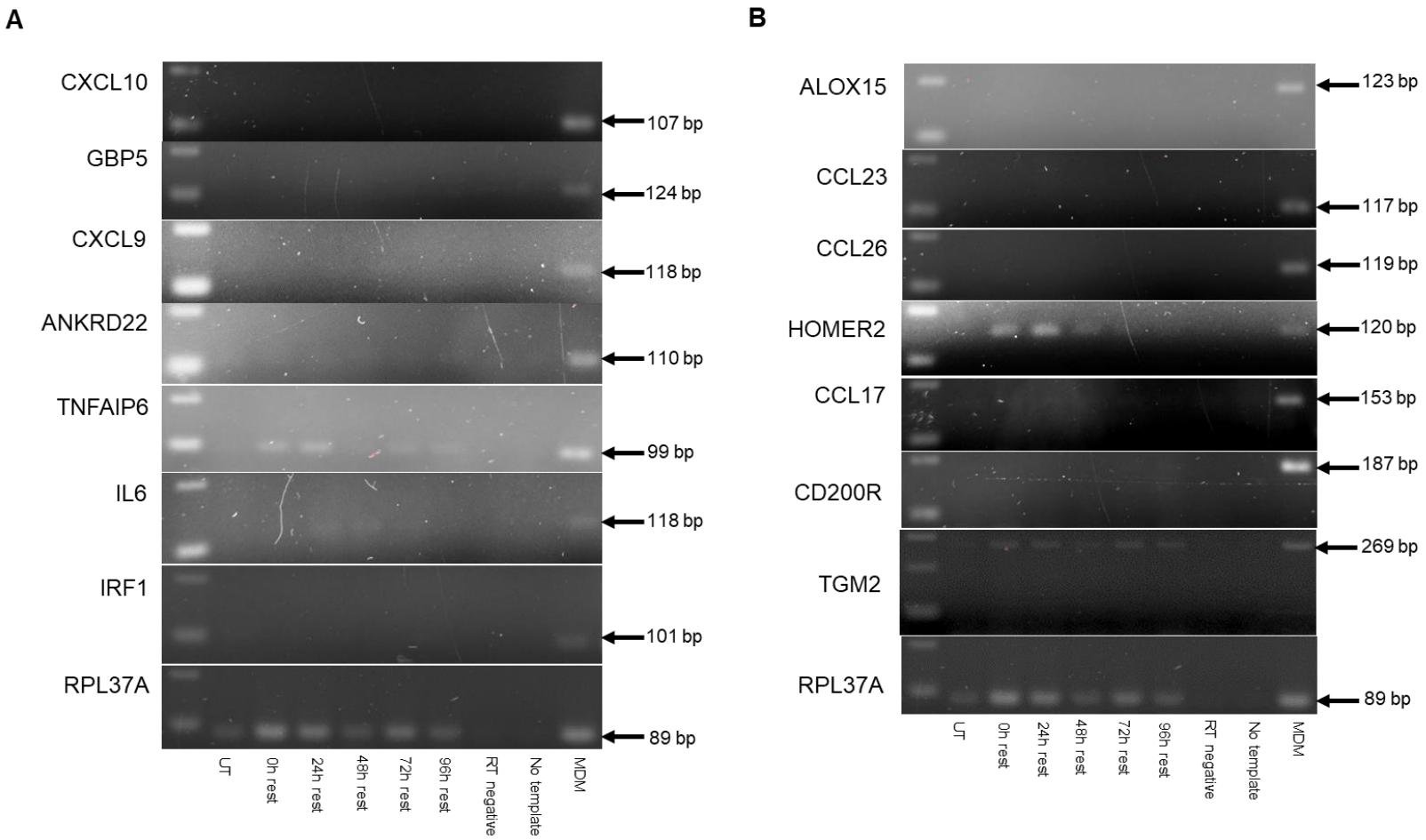

Figure 3.3.12. M0 cell rest titration; cDNA derived from un-polarised (M0) THP-1 cells treated with PMA and rested for different amounts of time, tested for expression of M1 specific genes using PCR (**A**) and tested for expression of M2a marker genes using PCR (**B**). For both subsets (M1 and M2a) differentially polarised monocyte derived macrophages (MDMs) were used as a positive control. For each gel, size of PCR product is given in bp (base pairs) and amplicon is indicated by arrow. Left-most lane is DNA ladder where bottom band is 100bp mark. RT negative= reverse transcriptase negative, MDM=monocyte derived macrophage, UT=untreated

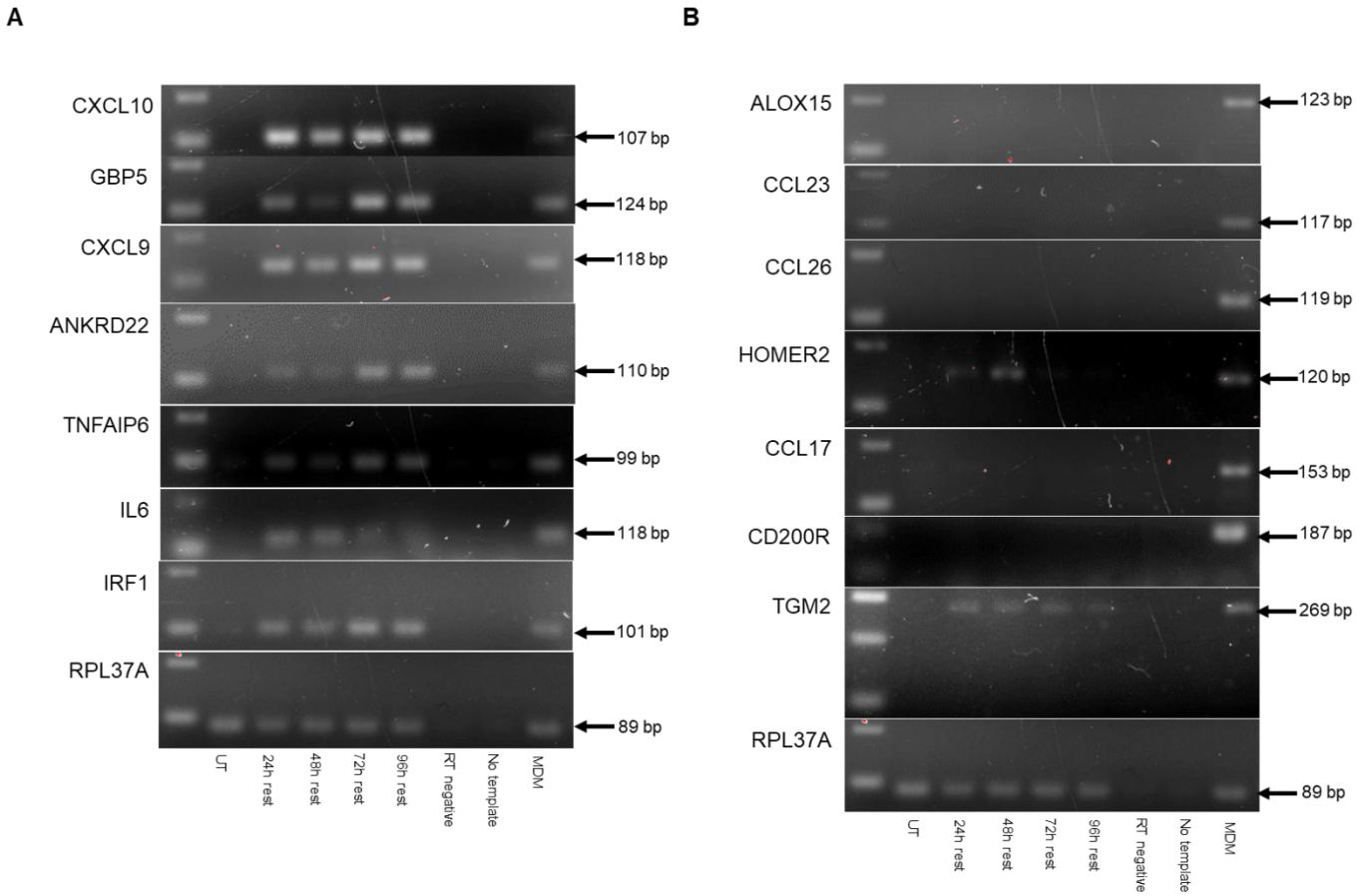

Figure 3.3.13. M1 cell rest titration; cDNA derived from LPS and IFNγ polarised (M1) THP-1 cells treated with PMA and rested for various amounts of time, tested for expression of M1 specific genes using PCR (**A**) and tested for expression of M2a marker genes using PCR (**B**). For both subsets (M1 and M2a) differentially polarised monocyte derived macrophages (MDMs) were used as a positive control. For each gel, size of PCR product is given in bp (base pairs) and amplicon is indicated by arrow. Left-most lane is DNA ladder where bottom band is 100bp mark. RT negative= reverse transcriptase negative, MDM=monocyte derived macrophage, UT=untreated

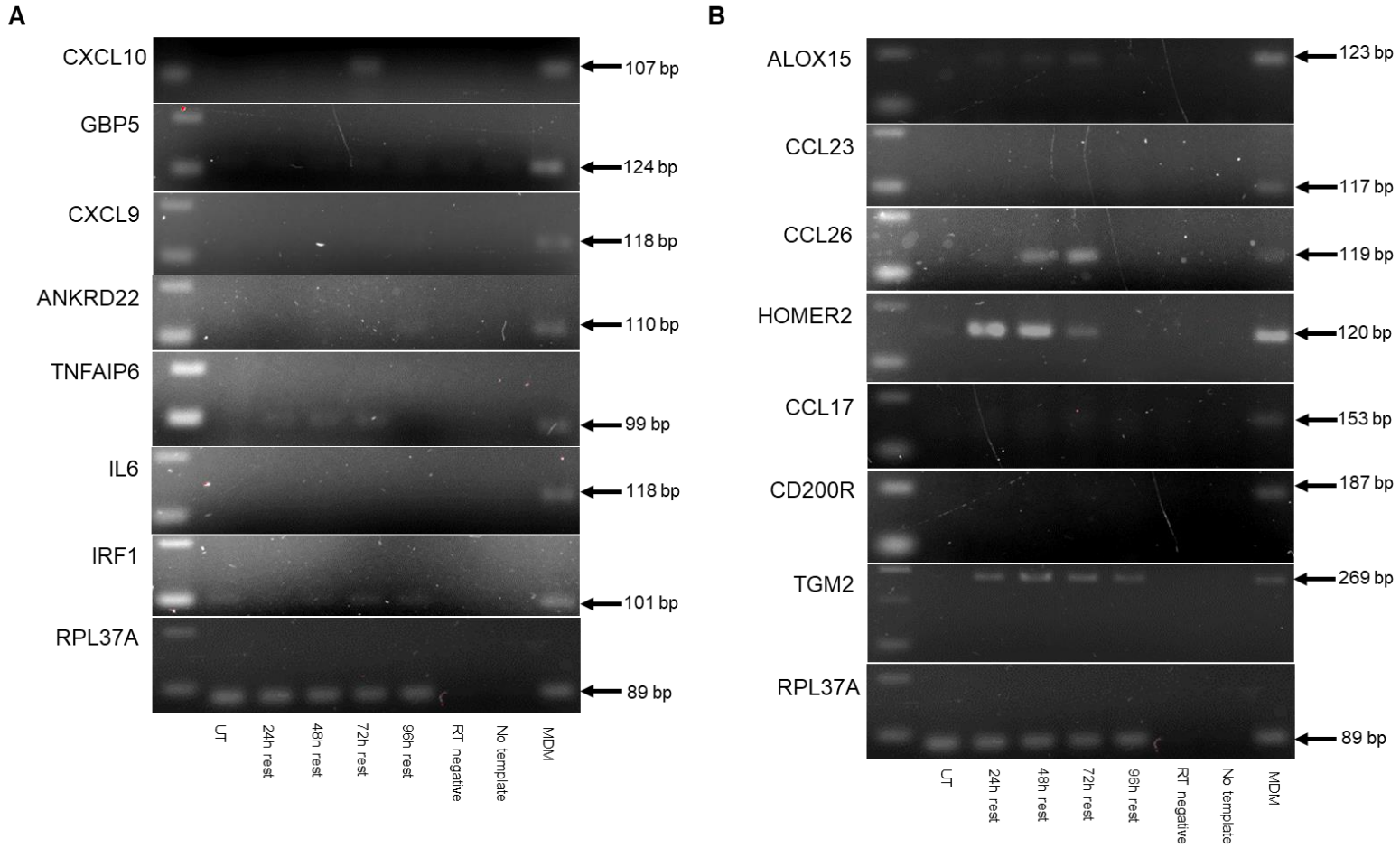

Figure 3.3.14. M2a cell rest titration; cDNA derived from IL-4 polarised (M2a) THP-1 cells treated with PMA and rested for various amounts of time, tested for expression of M1 specific genes using PCR (**A**) and tested for expression of M2a marker genes using PCR (**B**). For both subsets (M1 and M2a) differentially polarised monocyte derived macrophages (MDMs) were used as a positive control. For each gel, size of PCR product is given in bp (base pairs) and amplicon is indicated by arrow. Left-most lane is DNA ladder where bottom band is 100bp mark, RT negative= reverse transcriptase negative, MDM=monocyte derived macrophage, UT=untreated

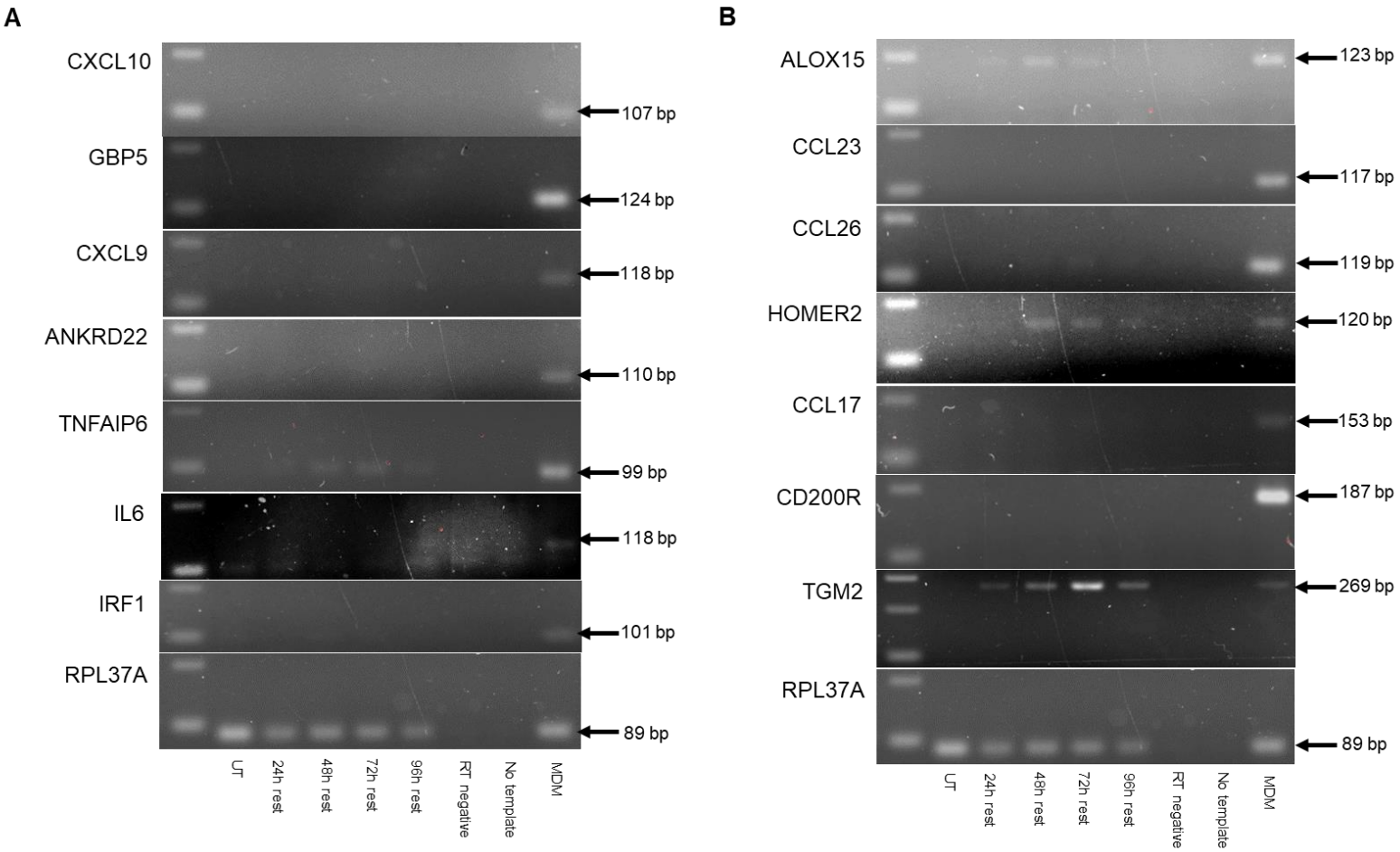

Figure 3.3.15. M2a cell rest titration (50ng/ml PMA); cDNA derived from IL-4 polarised (M2a) THP-1 cells treated with **50ng/ml** PMA and rested for various amounts of time, tested for expression of M1 specific genes using PCR (**A**) and tested for expression of M2a marker genes using PCR (**B**). For both subsets (M1 and M2a) differentially polarised monocyte derived macrophages (MDMs) were used as a positive control. For each gel, size of PCR product is given in bp (base pairs) and amplicon is indicated by arrow. Left-most lane is DNA ladder where bottom band is 100bp mark. RT negative= reverse transcriptase negative, MDM=monocyte derived macrophage, UT=untreated

3.3.5 Marker expression varied between cytokine exposure times with a 48h exposure providing the most consistent upregulation for each marker

Different transcripts will have expression peaks at different time points following exposure to the polarising cytokine. Although panel markers were identified from a dataset where macrophages were polarised for 72h, the cells used were MDMs; this together with the fact that THP-1 cells have a slightly different transcriptional profile and are already established under culture conditions mean that it is reasonable to consider the possibility that the cell line will respond slightly differently to stimuli (Kohro *et al., 20*04). For the M1 polarised cells (Figures 3.3.16 and 3.3.17), only one of the panel markers (*CXCL9*) was up-regulated at a 96h IFNγ/LPS exposure time. Most of the markers were induced at 24h, but expression appears to be weaker compared to other time points where marker transcription was induced. All of the markers were present at the 48h and 72h time points, but expression appeared to be higher for the former. There did not appear to be any difference in non-specific expression of M2a markers in the M1 polarised cells other than *TGM2*, and expression of this transcript appeared to be much greater in M2a cells (Figure 3.3.18). Not all M2a markers were upregulated at the 24h time point (e.g. in *CCL17* and *CD200R*), and expression of the other subset-specific genes for this condition appeared to be weak versus 48 and 72h IL-4 treatments. This is consistent with the findings from previous optimisations which included 24h polarisations. Mirroring the pattern observed for M1 cells, M2a markers appeared to be most strongly up-regulated at 48h (i.e. for *CCL17, CCL26* and *TGM2*) and seemed to drop off at 96h exposure times (*CCL26, CCL17*). Based on these findings 48h was selected as the most suiTable cytokine exposure time for both M1 and M2a cells.

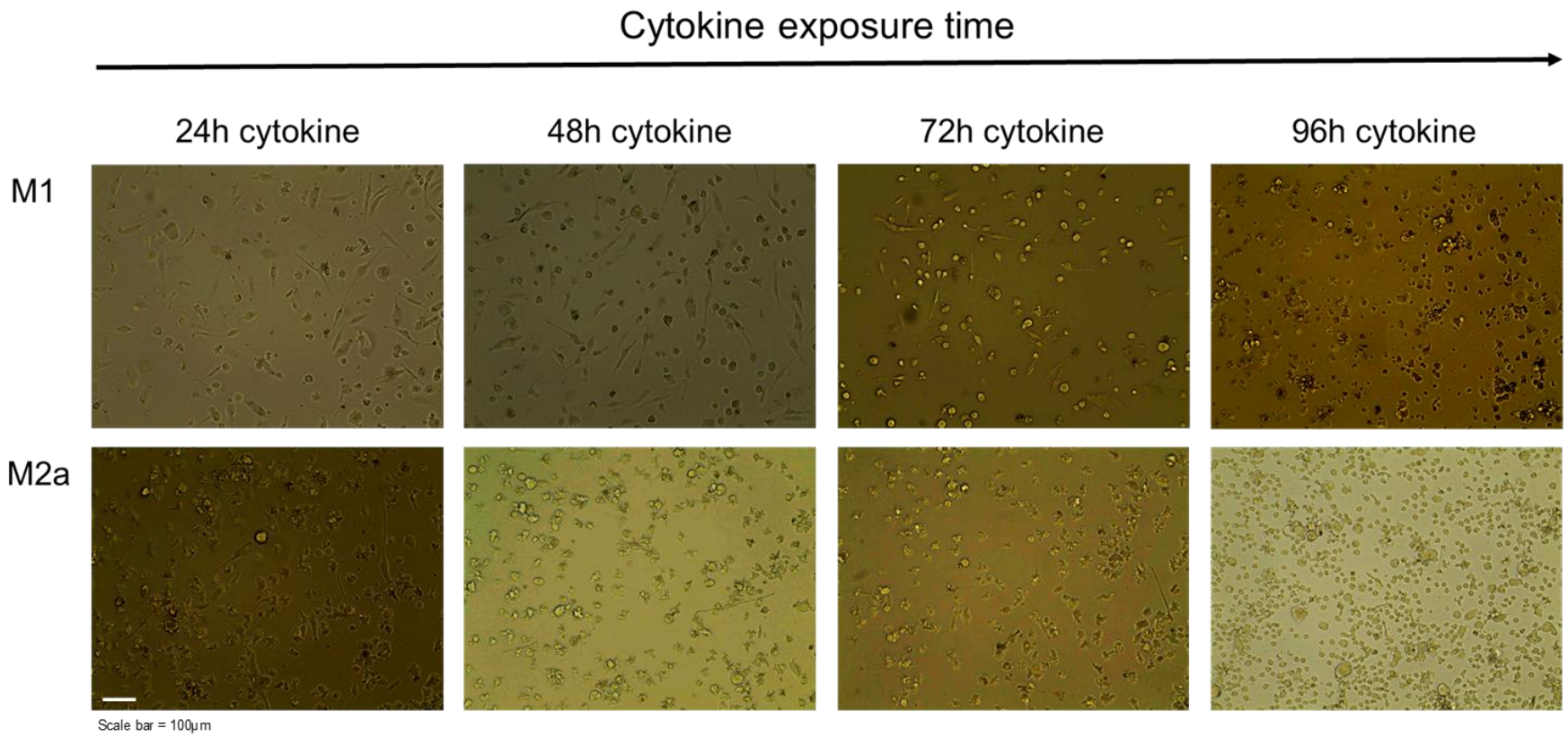

Figure 3.3.16. Light microscope images taken at x20 magnification of THP-1 cells polarised for different amounts of time using IFNγ and LPS (M1) or IL-4 (M2a), demonstrating cell morphology and cellular attachment under these conditions. Note that scaling is identical for all images and scale bar is given in bottom left corner of bottom left box as a white bar. M1= M1 macrophage, M2a=M2a macrophage

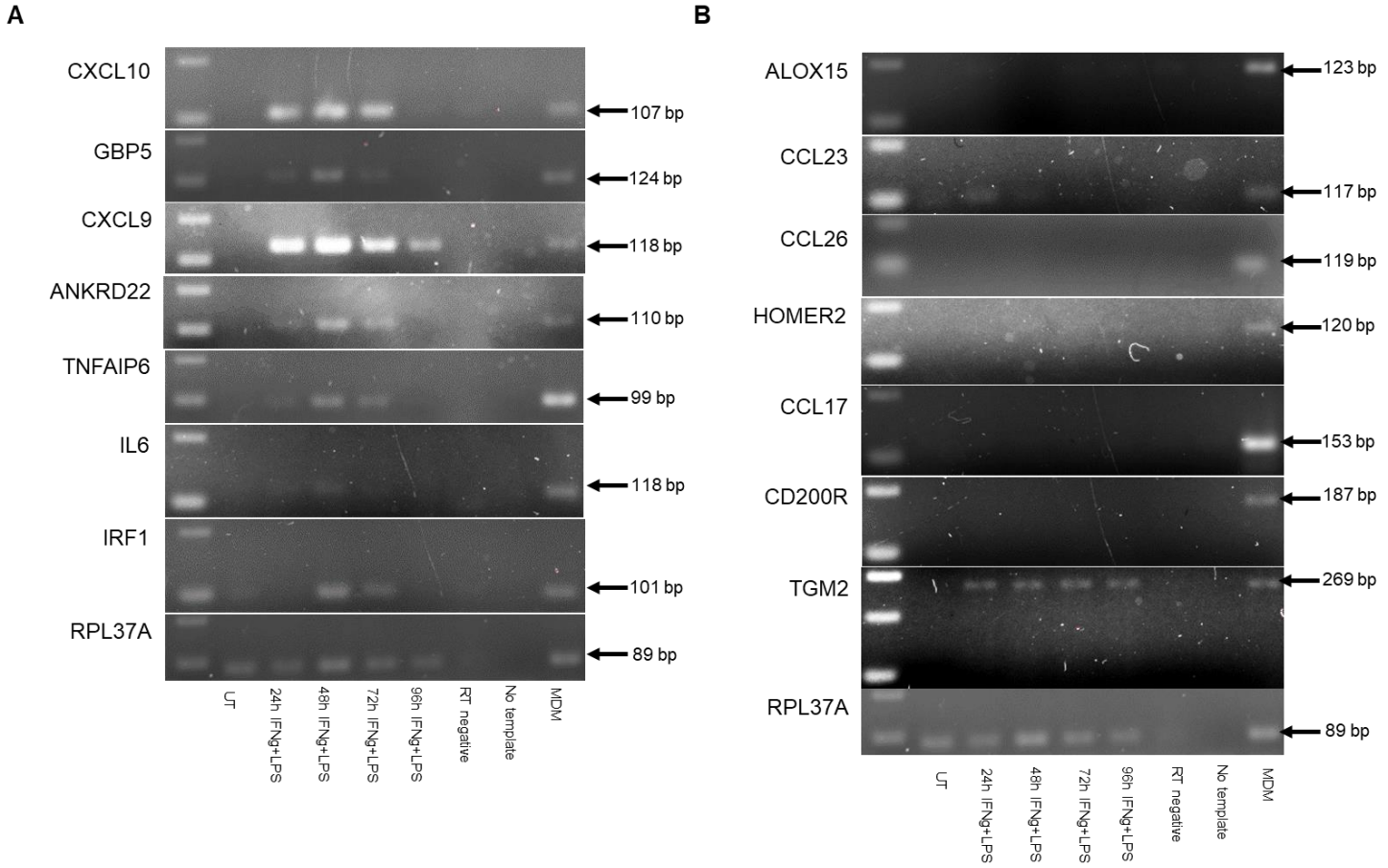

Figure 3.3.17. M1 cell cytokine exposure titration; cDNA derived from LPS and IFNγ polarised (M1) THP-1 cells treated with PMA and polarised with cytokine for various time periods, tested for expression of M1 specific genes using PCR (**A**) and tested for expression of M2a marker genes using PCR (**B**). For both subsets (M1 and M2a) differentially polarised monocyte derived macrophages (MDMs) were used as a positive control. For each gel, size of PCR product is given in bp (base pairs) and amplicon is indicated by arrow. Left-most lane is DNA ladder where bottom band is 100bp mark. IFNγ=interferon-gamma, LPS=lipopolysaccharise. RT negative= reverse transcriptase negative, MDM=monocyte derived macrophage, UT=untreated

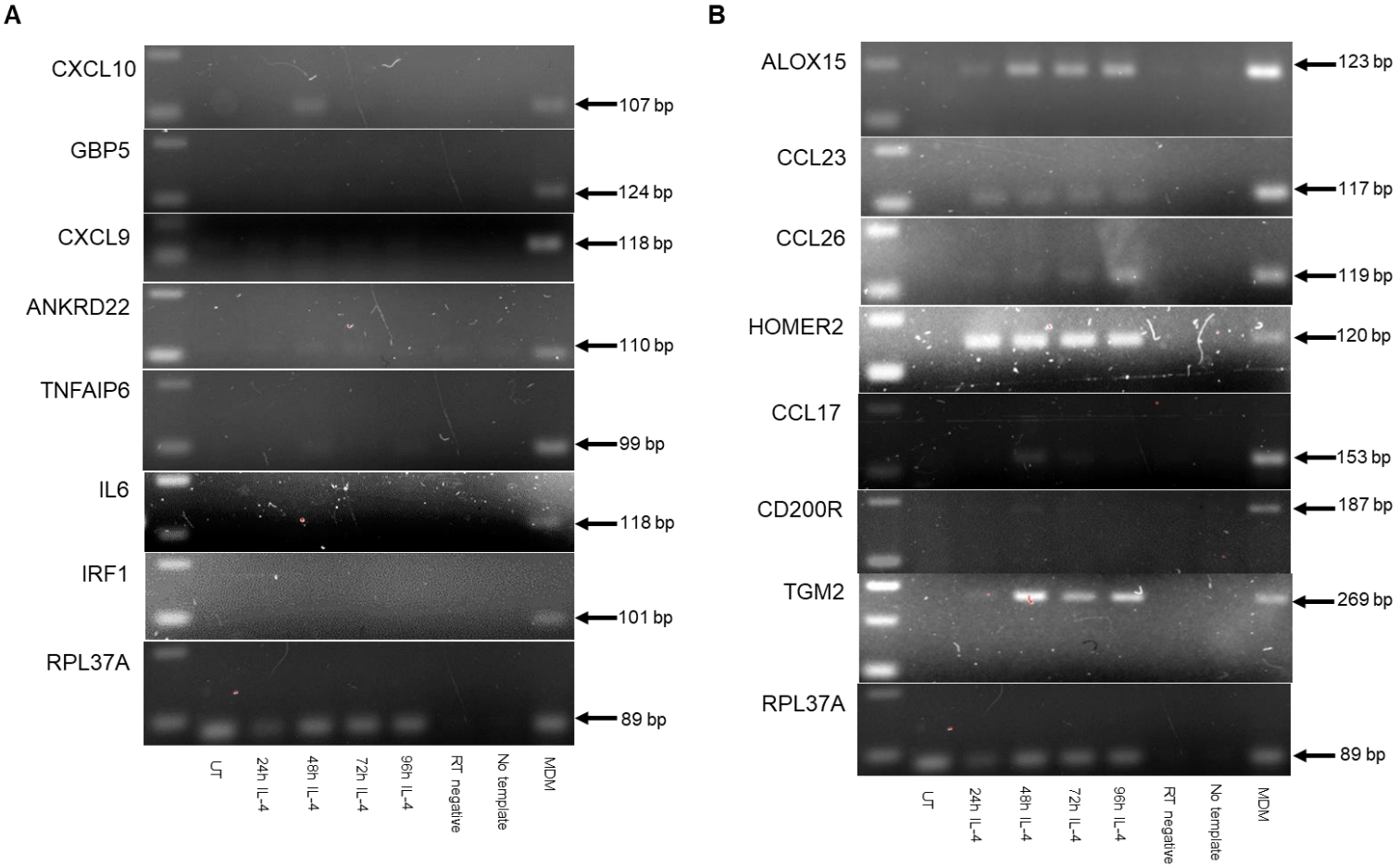

Figure 3.3.18. M2a cell cytokine exposure titration; cDNA derived from IL-4 polarised (M2a) THP-1 cells treated with PMA and polarised with cytokine for various time periods, tested for expression of M1 specific genes using PCR (**A**) and tested for expression of M2a marker genes using PCR (**B**). For both subsets (M1 and M2a) differentially polarised monocyte derived macrophages (MDMs) were used as a positive control. For each gel, size of PCR product is given in bp (base pairs) and amplicon is indicated by arrow. Left-most lane is DNA ladder where bottom band is 100bp mark. IL-4=interleukin-4. RT negative= reverse transcriptase negative, MDM=monocyte derived macrophage, UT=untreated

3.3.6 Final optimised protocol allows specific up regulation of subset specific markers

To summarise, the final protocol involved 5ng/ml PMA for 24h, followed by a media change and 72h rest. Cells were then polarised in respective cytokines for a further 48h (Figure 3.3.19 A). Macrophages generated using this protocol adopted the characteristic morphology for their phenotype; M1 induced THP-1 cells were classically spindle-like and stellate in appearance, versus the alternatively-activated M2 cells which were much rounder and typically “fried egg” shaped (Figure 3.3.19 B). The M1 markers were specifically upregulated for the M1 induced cells for the finalised protocols, with no non-specific up regulation in the other conditions. Similarly, up-regulation of M2a markers was seen for M2a cells generated according to the finalised protocol (Figure 3.3.21). Low level expression of some M2a markers (*TGM2, HOMER2, CCL23*) and M1 marker *TNFAIP6* could be seen in other polarisation states, but transcript induction was stronger in the relevant condition suggesting that polarisation to inflammatory and anti-inflammatory states had been achieved. It should be noted that for *CCL23* in particular, expression seemed to be almost as high for the M2c and M0 conditions as the M2a conditions, so although the phenotype has been achieved, this may not be an ideal marker for alternative activation in THP-1 cells.

3.3.7 CD14 and CD11b expression was seen on macrophages generated using the final protocol

CD11b and CD14 (an intergrin alpha-M which regulates leukocyte adhesion and LPS binding co-receptor for TLR-4 respectively) are frequently described macrophage surface markers (3.3.20) (Mittar *et al., 20*11). To test cell maturity these proteins were detected on the surface of cells generated using the final optimised protocol by flow cytometry. CD14 is also found on monocytes, so some expression would also be expected for untreated cells. Expression of both markers was seen for all cell types tested, suggesting that my final protocol produced a mature macrophage phenotype. It should be noted that some expression of CD11b was also recorded for non-PMA stimulated monocyte-like THP-1 cells, although this was low versus macrophage like cells.

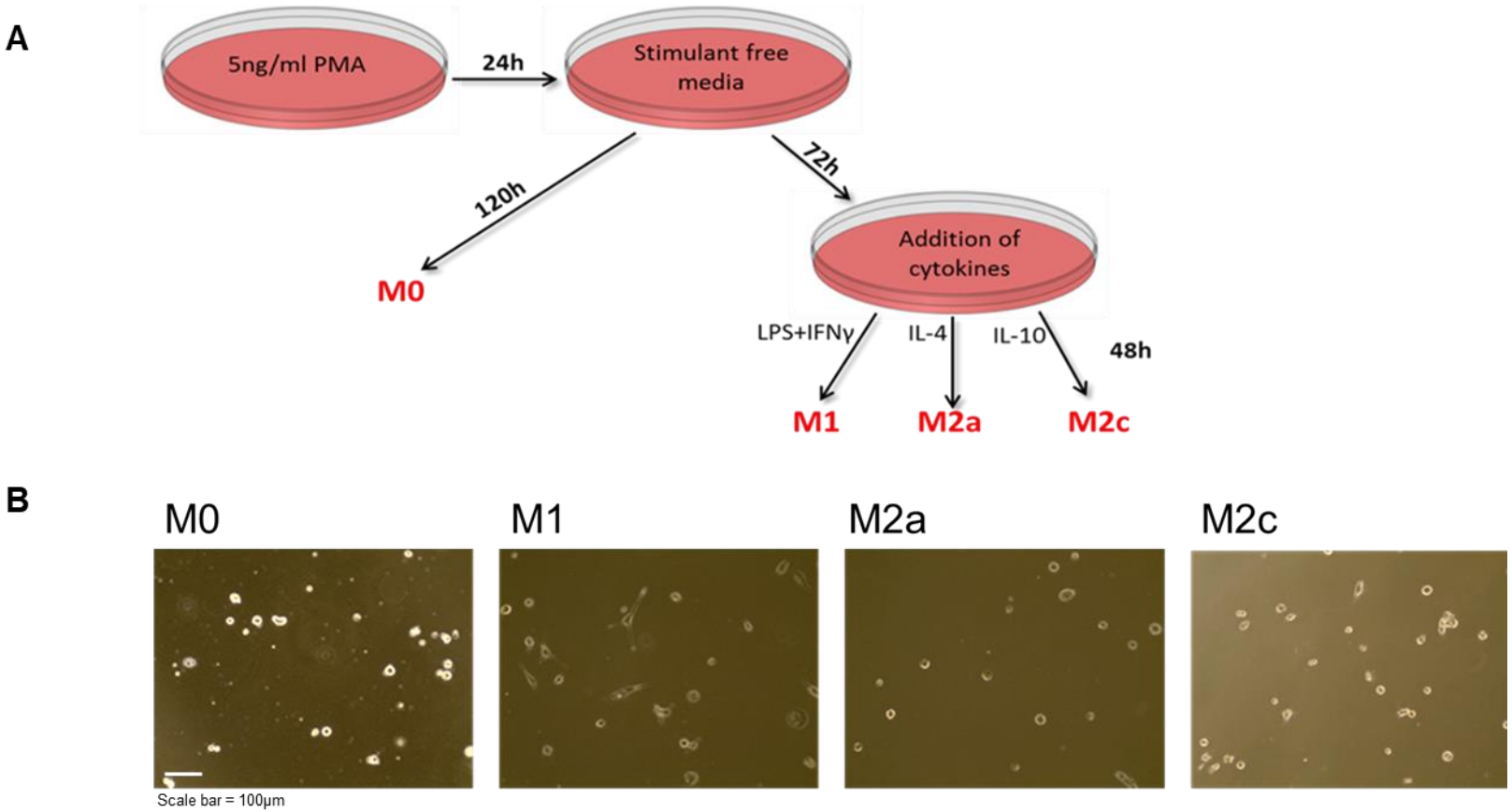

Figure 3.3.19. (**A**) Details of the final optimised protocol for generating polarised macrophages from THP-1 cells and (**B**) 20x magnification of THP-1 cells developed using the final protocol demonstrating cellular morphology of these phenotypes. Note that scaling is identical for all images and scale bar is given in bottom left corner of left box as a white bar. M1= M1 macrophage, M2a=M2a macrophage, M0=unpolarised macrophage. IL-4=interleukin-4, IL-10=interleukin-10, LPS-lipopolysaccharide, IFNγ=interferon-gamma, PMA = phorbol 12-myristate 13-acetate

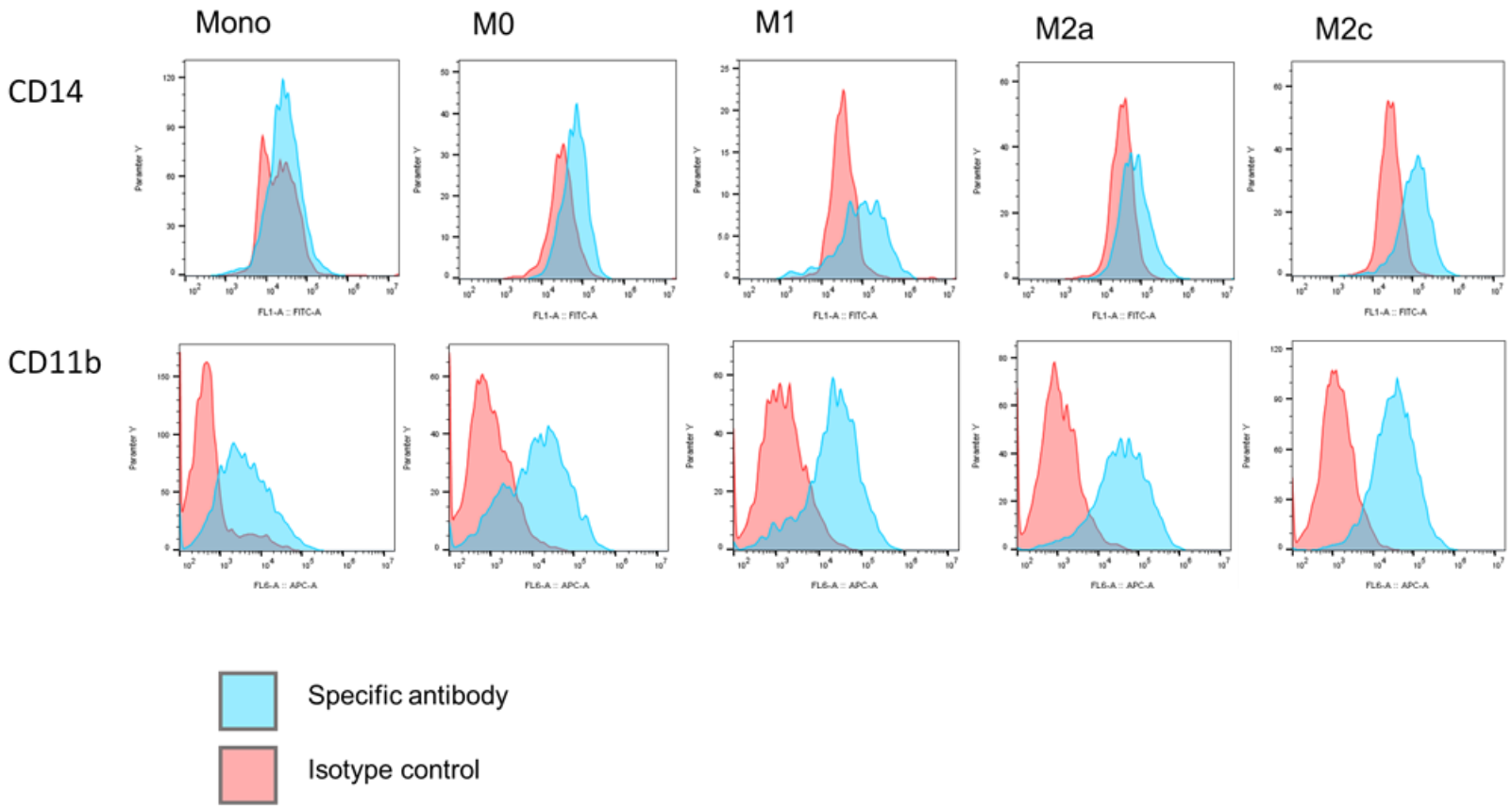

Figure 3.3.20. Flow cytometry histograms for surface expression of CD14 and CD11b on monocytes (Mono) and differentially polarised macrophages; LPS + IFNγ treated (M1), IL-4 treated (M2a), IL-10 treated (M2c) and unpolarised (M0). Staining antibodies for CD14 and CD11b are shaded in blue and isotype control histograms are given in pink. PMA = phorbol 12-myristate 13-acetate

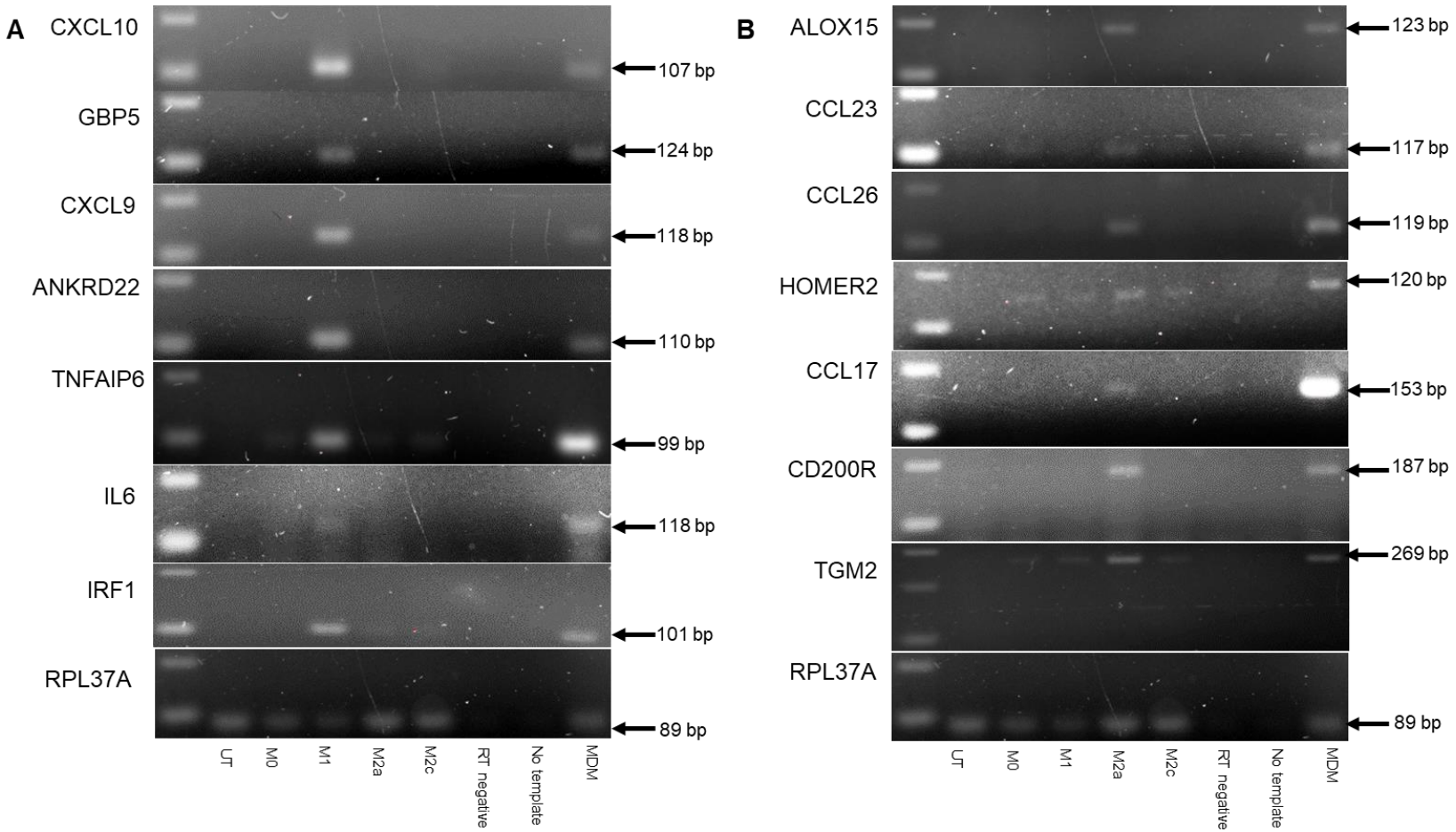

Figure 3.3.21. Final protocol; cDNA derived from THP-1 cells developed using the final optimised protocol tested for expression of M1 specific genes using PCR (**A**) and tested for expression of M2a marker genes using PCR (**B**). For both subsets (M1 and M2a) differentially polarised monocyte derived macrophages (MDMs) were used as a positive control. For each gel, size of PCR product is given in bp (base pairs) and amplicon is indicated by arrow. Left-most lane is DNA ladder where bottom band is 100bp mark. MDM=monocyte derived macrophage. UT=untreated, RT negative= reverse transcriptase negative

3.3.8 M2c and TPP cells generated using the optimised protocol also show upregulation of specific markers along with additional M1 and M2a markers

Some M2c markers identified both from the literature and through the analysis performed in Chapter 2 were tested against cells generated using the optimised protocol, where IL-10 (typical M2c inducer) was used to polarise the cells. *CXCL13* (a common literature marker) was strongly expressed in M2c cells, although high levels of transcription were also seen for other conditions (Figure 3.3.23 C); it was difficult to determine whether expression was highest in M2c cells without quantitative assessment of transcript expression. Based on these observations, *CXCL13* could not be considered lineage-specific. *SEPP1* was upregulated in both M0 and M2c cells, which may be expected due to the description of M2c cells as “de-activated” macrophages, which is arguably the phenotype of M0 cells. *CD163* is a marker commonly used to describe M2c cells in the literature, however, this transcript did not appear in the top genes list for this polarisation state (Chapter 2). In my final protocol *CD163* appeared to be strongly expressed for M2c cells, but was also weakly expressed in other polarisation conditions.

Additional M1 and M2a markers tested in the final protocol appeared to follow the same pattern as those used to optimise the protocol (Figure 3.3.23 A-B). Some of these markers (e.g. *STAT1*) appeared to be transcribed in conditions other than the one of interest, but non-specific expression was generally low and may have been discriminated using quantitative methods.

TPP polarised macrophages, originally described by Xue *et al.,* (2014) were generated through addition of prostaglandin E2 (PGE2), Pam3SK4 (a toll-like receptor II agonist) and TNF at the point of polarisation, and are thought to represent macrophages found in the chronic inflammatory state (Figure 3.3.22 A-B). Morphologically speaking, these cells appeared to be spindle-shaped (showing some resemblance to M1 macrophages) as may be expected for an inflammatory phenotype. However, although TPP-specific markers were expressed in these cells it did not appear to be a lineage-specific up-regulation. As this is a newly described phenotype there are limited literature resources from which to identify transcripts and for corroboration of my results.

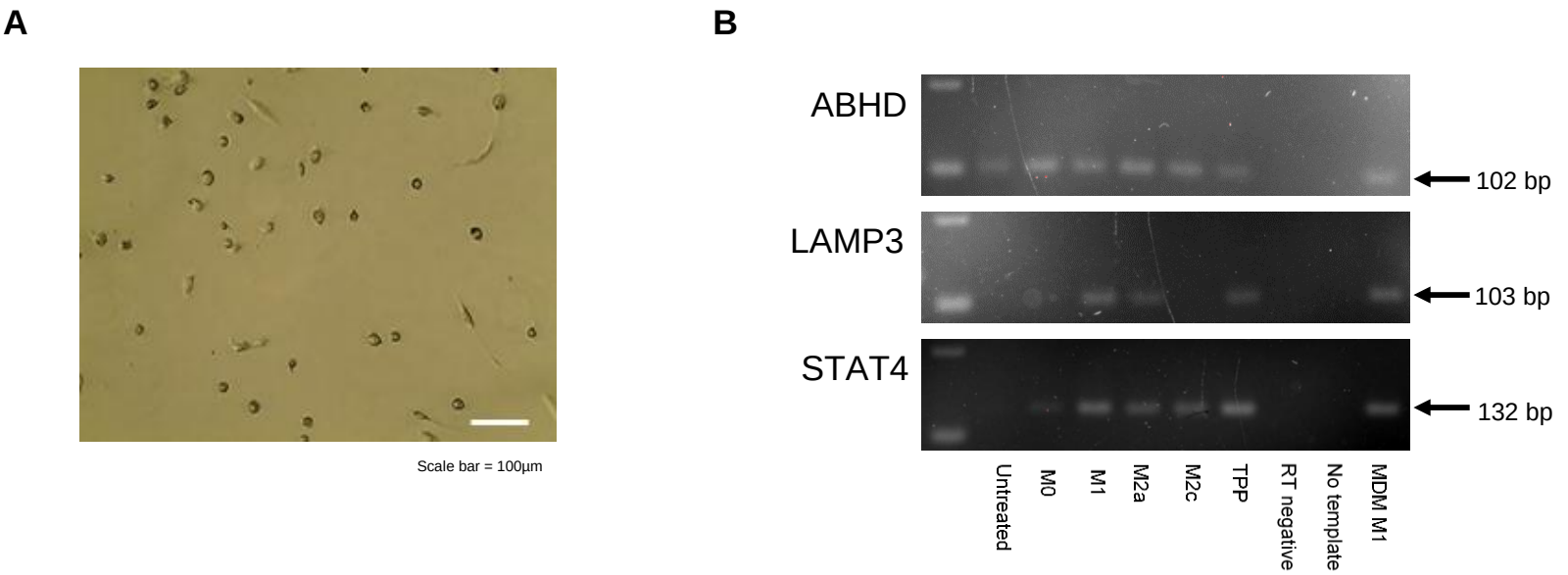

Figure 3.3.22. Macrophages developed using the optimised protocol, and polarised using TNF, PGE2 and Pam3sk4, imaged at 20x magnification to examine cell morphology (scale bar is given in bottom left corner of box as a white bar). (**A**) cDNA extracted from these cells run against TPP markers identified from literature using PCR techniques (Xue et al., 2014) (**B**). For both subsets (M1 and M2a) differentially polarised monocyte derived macrophages (MDMs) were used as a positive control. For each gel, size of PCR product is given in bp (base pairs) and amplicon is indicated by arrow. Left-most lane is DNA ladder where bottom band is 100bp mark, RT negative= reverse transcriptase negative, MDM=monocyte derived macrophage

3.3.9 Finalised protocol could be used to validate additional markers

Additional novel M1 and M2a markers that had been identified from publicly available datasets were tested against the protocol descried above for validation (Figure 3.3.23 A-B). M1 markers *SERPING1* and *TSC22D1,* identified in the dataset analysis showed a similar expression pattern to the marker panel genes used to optimise the protocol; i.e. these genes were up-regulated specifically in the M1 protocol, and may therefore be considered appropriate markers of macrophage polarisation. Novel M2a marker *AP2A2* appeared to be expressed more highly in M2a cells, but some transcription was seen for other conditions.

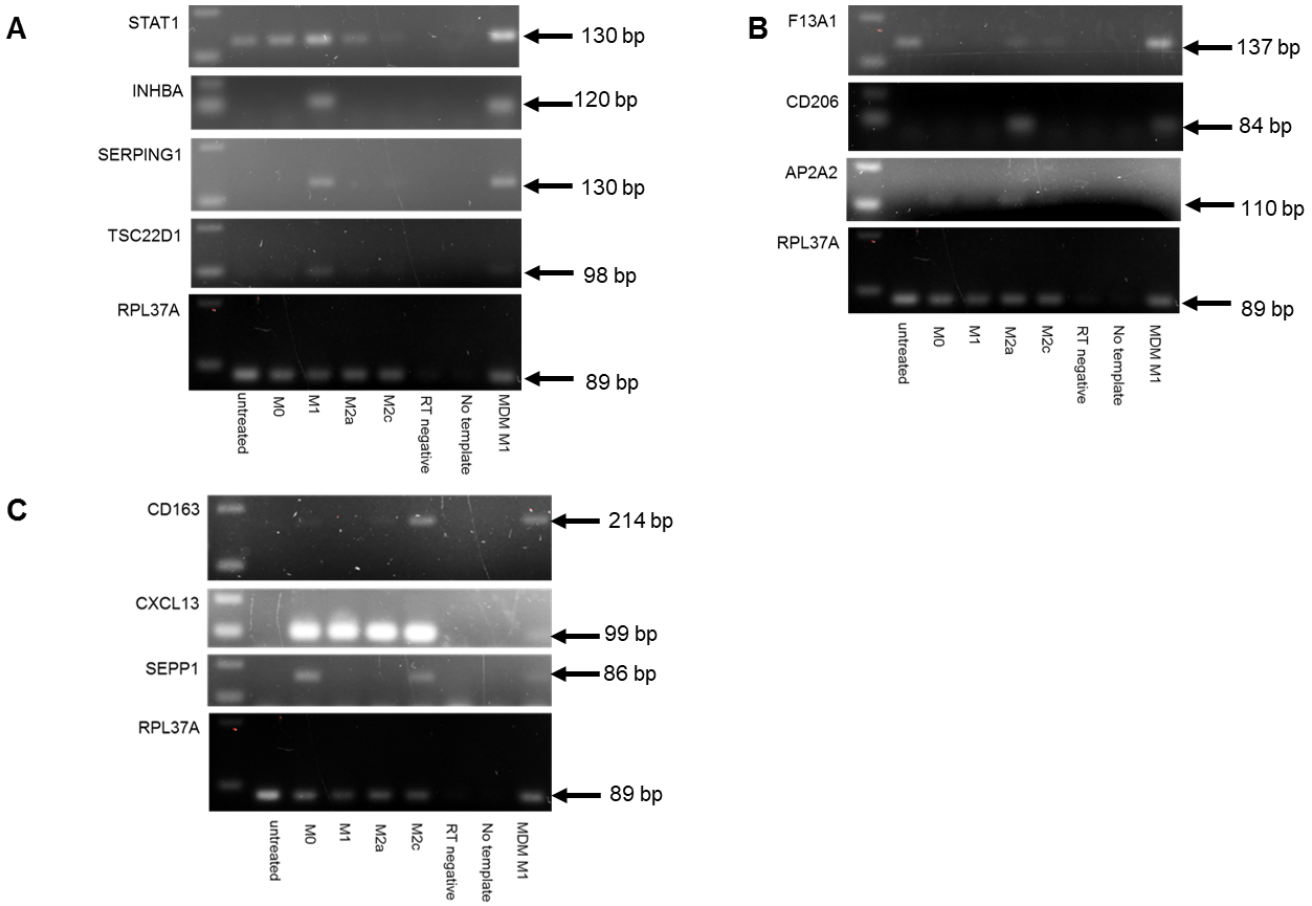

Figure 3.3.23. cDNA derived from THP-1 cells developed using the final optimised protocol run against (**A**) additional established and novel M1 markers (Beyer et al., 2012) using end point PCR, (**B**) novel and additional established M2a markers using end point PCR (**C**) and established M2c markers using end point PCR. For all subsets (M1, M2a and M2c), differentially polarised monocyte derived macrophages (MDMs) were used as a positive control. For each gel, size of PCR product is given in bp (base pairs) and amplicon is indicated by arrow. Left-most lane is DNA ladder where bottom band is 100bp mark, RT negative= reverse transcriptase negative, MDM=monocyte derived macrophage

3.4 Discussion

This cell line model showed phenotypic features consistent with primary MDM polarised under the same experimental conditions; based on viability, cell surface marker expression, morphological features and transcriptomic profile (Daigneault *et al., 20*10); (Lund *et al., 20*16); (Park *et al., 20*07); (Chanput *et al., 20*12). This is the first time a THP-1 protocol has been described that included optimisation of PMA concentration and rest time (to reduce non-specific transcript expression), whilst titrating cytokine concentration for both M1 and M2a polarisation states. This unified protocol will provide a robust system that may be used to study macrophage behaviour in a more consistent fashion than was previously possible.

Non-specific effects of PMA are effectively reduced by decreasing PMA concentration and increasing rest times*. HOMER2* has been linked to Phosphoinositide 3-kinase (PI3K) signalling and *TNFAIP6* is activated downstream of protein kinase C which could be why these transcripts appear to be induced by PMA alone (Maier *et al., 19*96); (Cozzoli *et al., 20*12). The fact that these markers are reduced or absent when the concentration of PMA is decreased and when cells are rested for extended periods of time implies that the effect of PMA signalling through this pathway is minimalised using my finalised protocol.

It has been reported that THP-1 cells become less adherent if PMA concentrations are too low; as this is a characteristic feature of macrophage-like cells, detachment from flasks suggests de-differentiation (Lund *et al., 20*16); (Auwerx, 1991); (Schwende *et al., 19*96). Reduction in cellular adherence was seen here at 2.5ng/ml, hence the lowest concentration of PMA tested in this study was not adequate for generation of macrophages, supporting previous findings (Park *et al., 20*07).

Although inclusion of a rest following PMA spike reportedly generates THP-1 macrophages with lysosomal and granularity properties more similar to MDMs, these cells may again become detached from the flask if cultured in PMA free media for extended periods of time (Kohro *et al., 20*04); (Daigneault *et al., 20*10); (Lund *et al., 20*16). Hence, a similar effect was seen in this report for 5ng/ml PMA using rest periods exceeding 72h in some subtypes. These combinations of conditions were therefore not sufficient for a THP-1 differentiation protocol; although cells may be more susceptible to polarising stimuli, they are not in a sTable macrophage-like state.

The THP-1 cell line has some genetic differences to human circulating monocytes and they can respond differently to stimuli; this may be why a 48h cytokine exposure time was deemed to be optimal for up-regulation of appropriate transcripts, when most markers in the panel were identified from a study where MDMs were polarised for 72h

(Khoro *et al., 20*04). Marker expression in THP-1 cells was not as strong using that time scale. Although, it should be noted that the 48h time point was not closely scrutinised in other protocols and so it cannot be confirmed that 72h polarisation is ideal for MDMs, and must therefore be optimised for other studies.

The induction of M2a-specific markers on THP-1 cells using IL-4 refuted any previous conclusions that this subtype could not be induced from THP-1 monocytes. The increase in rest time in particular appeared to render the cells more susceptible to M2a polarising stimuli. However, consistent with previous findings, it was much harder to induce expression of most M2a markers versus those for M1, and overall M2a transcript expression seemed comparatively weaker (Shiratori *et al., 20*17); (Chanput *et al., 20*13). It is reasonable to assume that this is due to the inflammatory bias of PMA; although this effect is reduced by reducing the concentration it cannot be completely removed and further reduction of concentration would result in loss of macrophage defining properties, as discussed previously (Park *et al., 20*07).

Both M2c and TPP cells were generated from THP-1 cells using the optimised protocol. M2c cells demonstrated up-regulation of some subset-specific markers. Some degree of overlap with the M0 transcriptome was expected as this subtype is often referred to as “de-activated” (Maeß *et al., 20*14). TPP marker expression was not specific for cells polarised to this subtype. This could again result from the confounding effects of PMA, genetic differences between THP-1 cells and MDMs or subtle changes in transcript levels that are not seen using the end-point PCRs that were employed in this study. As this subtype has only recently been defined and supporting literature is limited, it is difficult to speculate the reasons for this observation without quantitative studies and close comparisons with primary MDM (Xue *et al., 20*14).

Novel M1 (*TSC22D1, ANKRD22* and *SERPING1*) and M2a (*AP2A2*) markers identified in Chapter 2 were validated using this THP1 model. *ANKRD22*, a gene recently associated with tumour progression was found to be induced in whole blood samples following some immunisations along with some inflammatory genes, suggesting a role in immunity (Matsumiya *et al., 20*14); (Yin *et al., 20*17). *TSC22D1* codes for a tightly regulated transcription factor that regulates cellular senescence, a process involving interactions with some inflammatory genes (*IL6, IL8*), as well as having a role in C-type natriuretic peptide induction, hence describing the complexity of its interactions (Hömig-Hölzel *et al., 20*11); (Mendonça *et al., 20*10). *SERPING1* is a complement activation inhibitor so has clearer roles in immune regulation (Wagenaar-Bos and Hack, 2006). *AP2A2* codes for a subunit of adipocyte protein 2 (AP2), a protein involved in clathrin-mediated endocytosis so may also have specific roles in the immune system; efferocytosis is a feature of M2a polarised cells which may require upregulation of

phagocytic machinery, such as the protein coded for by this transcript (Garrison *et al., 20*13).

Chapter 4: Validation of THP-1 cell line polarisation protocol using RNA-seq data

4.1 Background

Although THP-1 cells appear to represent primary monocytes closely in terms of morphology, cell surface expression molecules and general functions (e.g. phagocytosis, cytokine production upon stimulation) (Auwerx, 1991); (Tsuchiya *et al., 19*82), there are some genetic and functional aspects that are reported to vary between these cell types, which need to be considered when establishing a new cellular model for translational research studies.

THP-1 cells were originally isolated from a patient with acute myeloid leukaemia (AML) and oncogenic changes are expected. For instance, when this cell line was subject to high resolution genomic analysis, some cancer specific variants were identified. Fusion of *MLL* and *MLLT3* genes has been verified (Odero *et al., 20*00); (Adati *et al., 20*09) and deletions of *CDKN2A*, *CDKN2B* and *PTEN* have also been described (Ogawa *et al., 19*94); (Guo *et al., 20*00); (Adati *et al., 20*09). Any pathways downstream of these variants will consequently be altered when compared with non-AML monocytes, but this may not necessarily have a detrimental impact on cell polarisation and differentiation. However, validation through comparison with primary cells will improve confidence in the use of the THP-1 cell line for immunological studies, in light of these mutations.

In terms of functional differences, decreased responsiveness to LPS has been described for THP-1 cells compared with primary monocytes from healthy controls. This was suggested to be related to low expression levels of CD14 (constitutes part of the LPS receptor) on THP-1 cells versus primary monocytes (Bosshart and Heinzelmann, 2016); (Schildberger *et al., 20*13). However, some reports have suggested the level of CD14 expression on THP-1 monocytes is more likely to be a consequence of experimental factors, such as the pre-culture density of these cells and duration of incubation prior to stimulation (Aldo *et al., 20*13). Thus, it is unclear whether this observation is genuine or a consequence of tissue culture techniques used.

In spite of the discrepancies between the THP-1 cell line and primary monocytes mentioned above, it was demonstrated in the previous Chapter that certain inflammatory and anti-inflammatory markers were expressed in THP-1 macrophages following exposure to the same stimuli used to polarise primary cells. Therefore, it may be suggested that although some genes and pathways may be altered in THP-1 cells

due to their malignant origin, those relating to inflammatory functioning may be retained. This is supported by some RNA sequencing experiments; for example a recent study by Hu *et al.,* (Hu *et al., 20*16) used THP-1 cells to examine effects of *candida albicans* on these cells using microarray experimentally and identified some promising targets. However, it should be noted that this experiment is still awaiting experimental validation.

To determine whether these cells accurately represent monocytes in terms of inflammatory/anti-inflammatory functioning, I compared public RNA-seq datasets for primary monocytes and macrophages (Beyer *et al., 20*12) with data from polarised THP-1 cells that was produced specifically for this study. Such investigations, using RNA-seq data to compare macrophage polarisation in primary cells and THP-1 cell line models had not previously been carried out. Hence this study is the first of its kind.

4.2. Materials and Methods

4.2.1 Cell culture

THP-1 cells were cultured using the optimised protocol described in Chapter 3 Section 3.2.7 Final protocol; briefly, cells were plated at a concentration of 300,000 cells/ml in RPMI (+ 10% FCS) media (Sigma-Aldrich, CA, USA) and activated with 5ng/ml PMA for 24h. Cells were then washed and incubated in stimulant free media for 72h before polarising cytokines were added for a further 48h. Each sample was produced in triplicate; individual replicates were generated on different days in three batches from the same stock of cells. Details of stimuli for different samples generated are given in Table 4.2.1. In addition to the conditions described in Chapter 3, Section 3.2.7, cells treated with 250ng/ml LPS (Peprotech, NJ, USA) were generated with and without treatment with IC; here HAGG was generated and used; see Section 4.2.1.1.

4.2.1.1 Generation of HAGG

CAMPATH 1H IgG1 antibody (3.8mg/ml) (Therapeutic Antibody Centre, Oxford, UK) was heated to 62ºC for 20 minutes. Samples were then aliquotted and centrifuged for at 10,000 x g for 10 minutes with the temperature at 4ºC, and insoluble material was discarded. Supernatants were collected and stored at -20ºC for future use.

Table 4.2.1. Monocyte and macrophage samples with details of sample name, which replicate samples belong to and conditions used to generate the cell type

Condition	Treatment	Replicate number	Sample name
Monocyte	N/A	1	Mono_1
		2	Mono_2
		3	Mono_3
M0	PMA	1	M0_1
		2	M0_2
		3	M0_3
M1	IFNγ+LPS+PMA	1	M1_1
		2	M1_2
		3	M1_3
M2a	IL-4+PMA	1	M2a_1
		2	M2a_2
		3	M2a_3
M2c	IL-10+PMA	1	M2c_1
		2	M2c_2
		3	M2c_3
LPS	LPS+PMA	1	LPS_1
		2	LPS_2
		3	LPS_3
M2b	LPS+PMA+	1	LPS_IC_1
	HAGG	2	LPS_IC_2
		3	LPS_IC_3
TPP	TNF+PGE2+	1	TPP_1
	Pam3SK4+PMA	2	TPP_2
		3	TPP_3

4.2.2 RNA extraction

RNA extractions were performed using the Qiagen (Netherlands, Venlo) RNeasy mini plus kit and the corresponding program on a Qiacube (Qiagen, Netherlands, Venlo).

Briefly, samples were lysed from tissue culture flasks using RLT plus lysis buffer (Qiagen, Netherlands, Venlo). Samples were then placed into a gDNA exclusion column (Qiagen, Netherlands, Venlo) and centrifuged for 1 minute at 10,000 x g. following this samples were loaded into the Qiacube. Here, samples were combined with 70% ethanol (Sigma-Aldrich, Missouri, USA) at a 1:1 ratio (V:V), before being transferred into an RNeasy spin column (Qiagen, Netherlands, Venlo) and centrifuged for 1 minute at 10,000 x g to adhere RNA to the column membrane. Volumes of RW1 wash buffer (Qiagen, Netherlands, Venlo) were added to the columns to remove biomolecules carbohydrates, fatty acids from the RNA before a 1-minute centrifugation at 10,000 x g. following this RPE buffer (Qiagen, Netherlands, Venlo) was added before another 1-minute centrifugation at 10,000 x g to remove salt traces. This was repeated for a 2-minute centrifugation at 10,000 x g. Concentration and quality of RNA samples were determined using a nanodrop-1000 spectrophotometer (Thermo-Fisher Scientific, Waltham, Massachusetts). Ratio of absorbance at 260/280nm and 260/230nm were determined here to indicate purity (with a 260/280 ratio of approximately 1.8 being required for pure RNA), and concentration was given as ng/µl.

4.2.3 PCR

Reactions were performed as described in Chapter 3, Section 3.3.12 with the same primers and cycling conditions (Chapter 3 Tables 3.2.1-3.2.5). This was carried out as a quality control step for samples prior to sequencing.

4.2.4 RNA library preparation and RNA quality checking

Library preparation was performed by the group's research assistant using the Illumina TruSeq stranded sample preparation kit (Illumina, California, USA; all reagents mentioned here were purchased from this manufacturer), using the Low Sample Protocol. Please refer to https://support.illumina.com/downloads/TruSeq_stranded_total_rna_sample_preparation_guide_15031048.html.

A schematic for this protocol is given in figure 4.2.1 and highlights 8 major steps. Firstly, ribosomal (r) RNA was removed from 200 ng of total RNA followed by RNA. Firstly, ribosomal (r) RNA was removed and RNA was fragmented; RNA was added to plates and diluted with nuclease free water, and rRNA binding buffer to the desired concentration. The samples were combined with the rRNA removal mix and incubated at 68^{o}C for 5 minutes in a sealed plate before a further incubation at room temperature for 1 minute. Following the addition of the rRNA removal beads, the samples were

incubated at room temperature. The rRNA removal beads and any bound rRNA were then separated from the sample by placing the plate on a magnetic plate holder and decanting the sample solution to a fresh plate. RNA binding RNAClean XP beads were added to the rRNA depleted samples and incubated at room temperature for 15 minutes, after which the samples were place on the magnetic stand for 5 minutes to separate the RNAClean XP beads and bound RNA from the supernatant which was discarded. The beads were washed with 70% ethanol before drying for 15 minutes at room temperature. The beads were resuspended in elution buffer and incubation at room temperature for 2 minutes, followed by 5 a minute separation of beads from the supernatant on magnetic stand. The supernatants containing RNA were incubating at 94ºC for 8 minutes in sealed plates to fragment the RNA.

For first stand cDNA synthesis, a master mix of SuperScript II enzyme and the First Strand Synthesis Act D Mix tube combine at a 1:9 ratio was added to each sample, mixed and incubated in a thermal cycler at 25ºC for 10 minutes, 42ºC for 15 minutes and 70ºC at 15 minutes.

Next second stand synthesis was performed by the mixing 5µl of resuspension buffer and Second Strand Marking Master Mix to each sample and incubating at 16ºC for 1 hour before equilibration to room temperature. The cDNA was purified using AMPure XP beads which were mixed with each sample and before incubating for 15 minutes at room temperature and separation using a magnetic stand for 5 minutes. Beads were washed with 80% ethanol, resuspended in resuspension buffer and supernatants were collected after another separation step on a magnetic stand.

The 3’ ends of the cDNA were adenylated by mixing the samples with A-Tailing Mix and incubation at 37ºC for 30 minutes followed by 5 minutes at 70ºC.

Indexed, Illumina sequencing compatible adapters where ligated to the cDNA by incubation at 30ºC for 10 minutes following the addition of the ligation mix and appropriate adapters to each sample. The Stop ligation mixture was added to each sample to terminate the ligation process before the unligated adapters and adapter dimers were removed from the unamplified library by preforming two rounds of using AMPure XP beads sample justification as described for the second strand synthesis step.

Finally, the library was amplified by PCR to select for inserts to which the adapters were correctly ligated. This was done after the addition of the PCR Primer Cocktail and PCR Master Mix using the following PCR conditions: 98ºC for 30 seconds, 15 cycles of 98ºC for 10 seconds, 60ºC for 30 seconds and 72ºC for 30 seconds, and completed

with a final 5 minutes elongation at 72ºC. The samples were purified by two rounds of AMPure XP beads selection as described.

Library insert size and distribution were determined using an Agilent Bioanalyser TapeStation 2200 instrument (Agilent Technologies, California, USA) by comparing each sample to a reference ladder (Agilent Technologies, California, USA). The concentration of each library was determined by comparing their fluorescence at room temperature in the appropriate Qubit working solution (Thermo-Fisher Scientific, Massachusetts, USA) to a known control samples using a Qubit fluorometer (Thermo-Fisher Scientific, Massachusetts, USA).

The libraries were diluted in Tris-HCl 10mM, pH 8.5 with 0.1% Tween 20 and combined in equimolar quantities to form the required sequencing library pools.

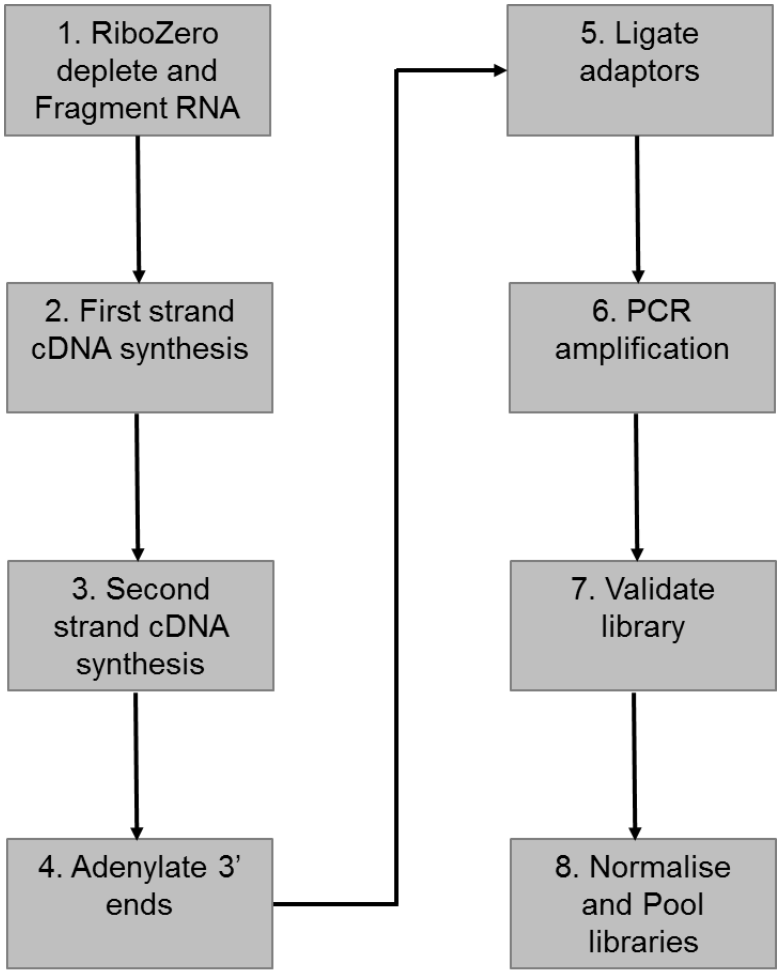

Figure 4.2.1. Basic workflow for generating cDNA libraries from RNA for application in RNA-seq experiments using the Illumina low sample protocol, detailed in the manual here: https://support.illumina.com/downloads/truseq_stranded_total_rna_sample_preparation_guide_15031048.html Figure adapted from Figure 2 in the manual.

4.2.5 Next generation sequencing

All samples in independent replicates were pooled, bound to different lanes of a flow cell (i.e. onto 3 lanes) and subsequently analysed using an Illumina HiSeq 3000 next generation sequencer to generate 151bp paired end data, by the University of Leeds's Next Generation Sequencing Facility. Sample names can be found along with the treatment details in Table 4.2.1.

4.2.6 Assessment of read quality

The complete data analysis pipeline is summarised in Figure 4.2.2. Initial data quality control and sequence analysis was performed in a LINUX environment. Briefly, the NGS Facility supplied the sequence data as a pair of gzipped fastq sequence files for each sample. While data for read 1 and read 2 sequences were stored in the different files, there order was maintained such that the sequences for each end of an insert could be determined. The quality of the base calling for each position and the amount of sequencing adaptor present in each file was determined using FASTQC (Andrews, 2010). Adapter sequences and positions with a low-quality base calling score were removed using CUTADAPT (Martin, 2011), which was ran using the following command line:

```
cutadapt -q 10,10 -m 30 -b GTATCAACGCAGAGTAC -B GTATCAACGCAGAGTAC -o $trimmed_read1 -p $trimmed_read2 $read1 $read2
```

where $read1 and $read2 represent the names of the paired input sequence files, $trimmed_read1 and $trimmed_read2 represent the paired files to which the processed data was saved too. GTATCAACGCAGAGTAC identifies the sequence of the sequencing adaptors to be removed from the data (the preceding flags –b indicate that $read1 should be scanned for the following sequence, while –B indicates $read2 is the target). The –m 30 parameter results in read pairs with a read less than 30 bp in length being discorded. Finally, the –q 10,10 parameter indicates that both the 5' and 3' ends of each read will be trimmed of base calls with a quality score of less than 10. The command simultaneously processed a sample's read 1 and read 2 data files such that the link between an insert's read 1 and read 2 sequence data was maintained in the exported fastq files. The processed files were screened a second time with FASTQC to access the efficiency of the quality trimming and adaptor removal, with the process reiterated until the data contained no significant amounts of poor quality sequence data.

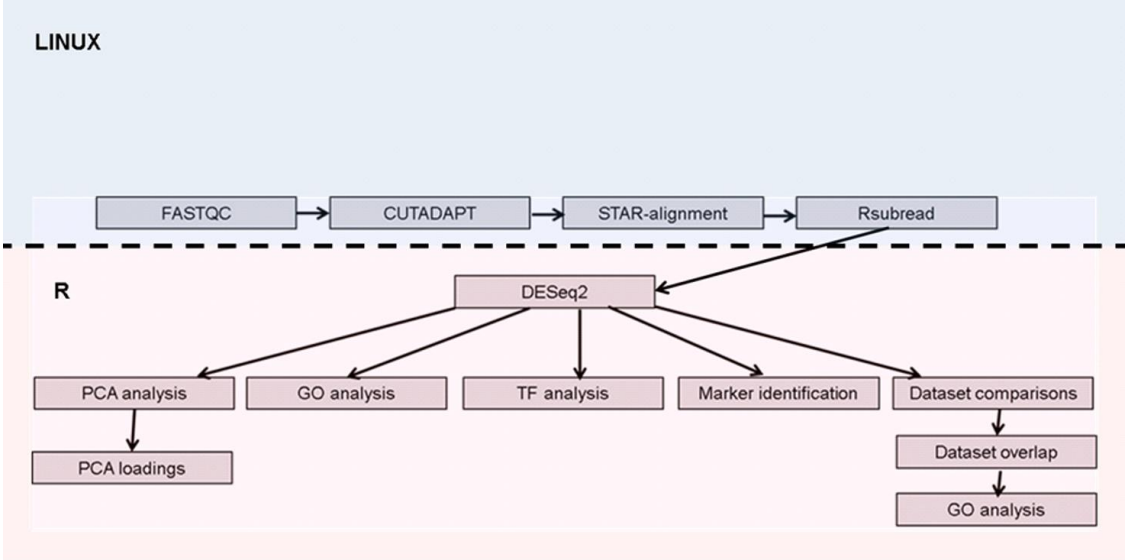

Figure 4.2.2. Overview of RNA-seq data analysis pipeline. Steps performed in a LINUX environment can be found in the blue shaded region and steps performed in R are given in the pink shaded region. PCA=principle component analysis, GO=gene ontology, TF=transcription factor.

4.2.7 Read alignment

Sequencing reads were aligned to the reference human genome GRChg38/hg38 with reference to the splice junctions as descripted in the assembly matched GTF annotation file, with both the reference sequences and annotation file downloaded using the UCSC Table Browser tool (Karolchik *et al., 20*04). Indexing of reference genome was performed using the following command:

STAR --runThreadN 12 --runMode genomeGenerate --genomeDir STAR_genome/ --genomeFastaFiles $GRCh38.fa --sjdbGTFfile $hg38.gtf --sjdbOverhang 150

A key of parameters for the command is given in Table 4.2.1

Table 4.2.2. Key of parameters for STAR genome index command

Star flag, parameter pair	Description of the option or flag
--runMode genomeGenerate	directs STAR to create a genome index
--runThreadN	number of threads to be used for the genome index generation (number of cores)
--genomeDir	path to the directory where the genome indices are stored
--genomeFastaFiles	specifies one or more FASTA files containing the genome reference sequences
--sjdbGTFfile	path to the file containing transcripts annotation in the standard GTF format
--sjdbOverhang	specifies the length of the genomic sequence around the annotated junction to be used in constructing the splice junctions database

Alignment of the read data to the indexed reference sequences were performed using the STAR software (Dobin *et al., 20*13) to produce output BAM files, using the following command:

```
STAR --runMode alignReads --genomeDir $StarIndex --runThreadN 4 --readFilesIn $read1
$read2 --readFilesCommand zcat  --outFileNamePrefix $outDir --outSAMtype BAM
SortedByCoordinate --sjdbGTFfile hg38.gtf --sjdbOverhang 150 --outReadsUnmapped Fastx --
outSAMstrandField intronMotif
```

The function of each of the parameters is listed in Table 4.2.2

Table 4.2.3. Key of parameters for STAR genome alignment command

Star flag, parameter pair	**Description of the option or flag**
--runMode alignReads	Instructs STAR to align reads to the genome
--runThreadN 4	Instructs STAR to run 4 threads when aligning the data.
--genomeDir $StarIndex	Identifies the location of genome index files that are used to align the data.
--readFilesIn $read1 and $read2	Identifies the read 1 and 2 fastq files.
--readFilesCommand zcat	Indicates that the sequence files are compressed using gzip algorithm and a UNIX zcat command, which decompresses the data, should be used to read the input
--outFileNamePrefix $outDir	Gives the 'base' name and path to use when saving the alignment and associated meta data.
--sjdbGTFfile hg38.gtf	Name of the annotation file that describes the location of known exon positions
--sjdbOverhang 150	Specifies the length of the genomic sequence around the annotated junction to be used when constructing the splice junction database prior to read alignment. This effectively determines how much an aligned read can 'overhang' when aligning to a splice junction.
--outReadsUnmapped Fastx	Saves unmapped reads to a fasta file
--outSAMstrandField intronMotif	Marks splice-junction alignments in the output file with the orientation of the donor and acceptor site for canonical junctions. Required for compatibility with some downstream software.
--outFilterMismatchNmax	controls maximum number of mismatches
--outFilterMismatchNoverLmax	controls proportion of mismatches over read length
--outFilterMultimapNmax	controls maximum multi-mapping reads

Read 1 and read 2 sequences from each insert were alignment together so their ultimate location in the genome was based on the quality of the sequence alignment and the location of it matched pair mate.

Alignment was performed to be stringent; ideally a cut off of 0 mismatches could be set, but STAR parameters allow mismatches based on read length (longer read allows more mismatches) and sequencing quality (more mismatches for lower quality). Trimming of reads for adaptors and quality results in variable read length by default,

which would have been the case here. The parameters described in Table 4.2.2 to control this included –outFilterMultimapNmax (sets a maximum for multimapping reads) which was set as 50 here, --outFilterMismatchNoverLmax (controls proportion of mismatches over readlength) which was set at 0.01 and –outFilterMismatchNmax (controls maximum number of mismatched bases) which was set at 1. For a complete example of the script please refer to appendix 2, Script A2.3.

4.2.8 Generation of gene and exon counts Tables

As described in Table 4.2.4, the parameter --outSAMtype BAM SortedByCoordinate instructed STAR to give the output as sorted BAM files. Gene expression data was extracted from BAM files and summarised into raw read counts using the Rsubread package (Liao *et al., 20*13). Simply, this package counted alignments to genes and gene overlaps to produce gene and exon count Tables. Some non-default parameters were applied here; multimapping reads were set to be counted as fractions. The same reference genome annotation file (i.e. hg38) was used here as for splice junction database during alignment. Tables were transferred into Rstudio for further analyses. The script used here along with descriptive annotations may be found in appendix 2, script A2.4.

4.2.9 Differential expression analysis

It should be noted that examples of R scripts used with descriptive annotation may be found in Appendix 3.

Genes which are differentially expressed between conditions of interest were identified through pairwise comparisons, performed using the DESeq2 package; the raw counts Table generated by Rsubread was imported into R, and a metadata matrix was created as a key to subset data. The DESeq command from the DESeq2 was then used to generate a Table of normalised DEGs; the raw read counts isolated from BAM files using Rsubread are noramlised between samples here. Briefly, a negative binomial generalised linear model (takes into account estimates of dispersion, log fold change and data-driven prior distributions) is used to generate the data Tables; i.e. Deseq2 does not use normalised counts, but it incorporates a normalisation factor that is used to generate normalised counts. Genes with an adjusted p-value of less than 0.05, and a log2 fold change greater than absolute 1 were selected as significant hits (Love *et al., 20*17). Heatmaps were drawn to visualise the data using the pheatmap function from the pheatmap package. Any data re-formatting was performed using reshape2 and all

other plots were drawn using ggplot2 package. Genes were annotated with symbols through switching Refseq identifiers with gene names using clusterProfiler functions and the org.Hs.eg.db database as a key.

4.2.10 Principle component analysis (PCA)

The DESeq2 package was used for generating PCA plots for the data. Briefly, the complete dataset was summerised into a DeseqDataset object, rlog transformed (shrinks values towards gene mean to account for data dispersion) and stored as a matrix (for compatibility with downstream functions). PCA plots were then drawn with the plotPCA function, using the 1000 most variable genes in the dataset. If only certain conditions were of interest, subsets of the data were created using the meta data table as a key for selection.

Proportion of explained variable was calculated and visualised as scree plots using the pcascree function. Top loading (i.e. most variable) genes for each principle component were also identified from this object and plotted as graphs. Top loading genes were summarised into a Table and enriched biological processes were determined using the clusterProfiler package, and plotted as dot plots. Database org.Hs.eg.db was used as a source for annotations and a Benjamini-Hochberg was used as a multiple testing correction method for these analyses. Adjusted p-value of 0.01 and q-value cut-off of 0.05 were selected here (Yendrek *et al., 20*12).

4.2.11 Gene enrichment analysis

Lists of significantly differentially expressed genes were identified in the analyses described in Section 4.2.9 were analysed further here. As described above enriched GO terms (biological processes, cellular components, and molecular functions) were determined using functions of the clusterProfiler and AnnotationDBi packages (Yu *et al., 20*12); (Pagès Herve, 2017) by comparing genes with significant changes to the entire gene list. Bioconductor database org.Hs.eg.db was used as a source for annotations (Carlson, 2017) and Benjamini-Hochberg adjustment was used for multiple testing correction. Adjusted p-value of 0.01 and qvalue cut-off of 0.05 were selected here. Data were summarised as dot plots. KEGG and reactome pathway enrichment analyses were performed in a similar way (Carlson, 2016); (Yu and He, 2016), but both involved a change of gene identifiers from symbols to entrez ID. As with the gene ontology enrichment, adjusted p-value of 0.01 and qvalue cut-off of 0.05 were used.

4.2.12 Transcription factor analysis

A Table of transcription factors and targets derived from various ChIPseq experiments (ENCODE_TF_ChIP-seq_2015) was downloaded from http://amp.pharm.mssm.edu/Enrichr/#stats and read into R. Lists of genes differentially expressed between conditions of interest were generated as described in Section 4.2.9. For each TF, the number of target DEGs were counted along with the number of genes regulated by TF of interest in a background control set. Enrichment was tested for by contrasting these counts using Fisher's exact test; here, p-value was adjusted using the Benjamini-Hochberg method and an FDR cut-off of 0.05 was applied.

4.2.13 MA plotting

These plots were used to ensure that data for samples from different datasets were similarly normalised. BAM files generated from the alignments performed in Chapter 2, Section 2.2.3.2 "Read alignment and production of counts Tables", were analysed by Rsubread as described in Sections 4.2.8 to generate a second gene counts Table. The two gene expression counts Tables corresponding to two different datasets were read into R. Both counts Tables were combined into one large matrix using Refseq identifiers as a key. MA plots were plotted between every pair of samples in the Table, where M is the logarithm of the intensity ratio and A is the average count for any given dot in a plot. The plotMA function was used from the geneplotter package for this. Plot demonstrating contrasts of interest were selected.

4.3.14 Venn diagram plotting

As above, two gene expression counts Tables corresponding to two different datasets (one generated from BAM files produced through analysing public datasets in Chapter 2 and another from data generated in this Chapter) were read into R. Metadata Tables were generated for each dataset. Both counts Tables were combined into one large matrix using Refseq identifiers as a key, so only genes listed in both datasets were considered. Metadata Tables were also combined. Differentially expressed genes between M1 and M2a conditions were identified for both publicly available data and that generated in this Chapter. These genes were selected as described in Section 4.2.10 (Differential expression analysis) with adjusted p-value cut-off set to 0.01 (P-adjust method used was Benjamini Hochberg). Overlapping genes were identified and a Venn diagram was plotted using the VennDiagram package. Lists of genes in each

segment were isolated for downstream enrichment analysis which was performed as in Section 4.2.11 (Gene enrichment analysis).

4.3 Results

4.3.1 Quality Control of THP-1 polarisation was performed prior to next generation sequencing

Prior to performing next generation sequencing, it was considered important to confirm that the THP-1 cells had undergone polarisation. This would ensure that the input RNA accurately represented the culture conditions which were being investigated. Hence samples for each replicate used to generate RNA-seq libraries were tested against a small number of M1 and M2a markers that were previously used to optimise the protocol. Specific upregulation of markers for appropriate conditions (i.e. *CXCL9* and *GBP5* for M1 induced cells and *ALOX15* and *TGM2* for M2a cells) indicated that polarisation had been achieved and that the samples could be used to generate reliable RNA libraries and thus were used for sequencing reactions (Figure 4.3.1)

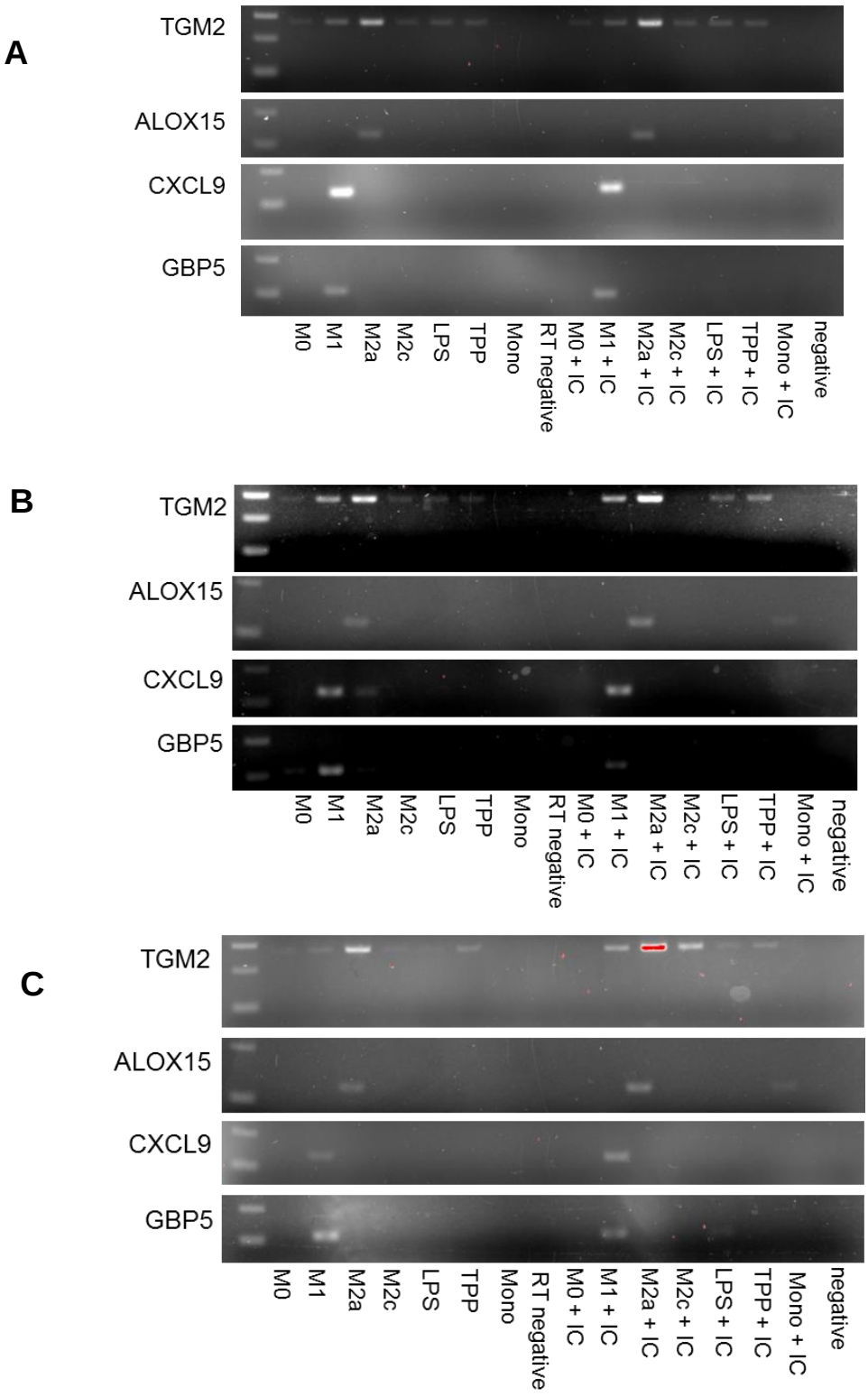

Figure 4.3.1. PCRs of cDNA derived from RNA-seq samples prior to library preparation to examine M1 (CXCL9 and GBP5) and M2a (ALOX15 and CCL17) marker expression in cDNA synthesised from RNA, generated for RNA-seq experiments; gene expression for replicates 1 (**A**), 2 (**B**), and 3 (**C**) was examined. Red band indicates light saturation. IC= immune complex, RT= reverse transcriptase, Mono= monocyte. Lane on far left of all gells represents ladder with lowest band at 100bp

4.3.2. Principal component analysis highlighted samples from second replicate to be outliers

PCA plots cluster data bases on the most variable factors in the dataset, i.e. principle components 1 and 2. This gives an indication as to which samples are most similar in terms of gene expression and provides some information as to whether replicates are consistent within conditions. The plot of all three experimental replicates highlights the samples from replicate 2 as outliers (Figure 4.3.2, A); they do not cluster with other samples generated using the same experimental conditions, and appear to align at the same point on the x-axis. As each of the replicates were run on separate sequencing lanes, it is likely that a lane effect skewed the output. For this reason, this replicate was excluded from further analyses in this Chapter. Samples were re-plotted without replicate 2 (Figure 4.3.2, B); repeats of conditions clustered together appropriately here. On these plots, monocytes appeared to separate from the macrophage-like cells along the x-axis; scrutinisation of loading components for the x-axis on Figure 4.3.3, C (i) + (ii) revealed transcripts involved in the immune response (e.g. *IDO1*, *ACOD1*, *SERPINB7*), which may indicate differences in differentiation functions between these cells (Figure 4.3.3, C (i)). The PMA-activated cells (macrophages) were divided in a linear fashion by the y-axis, with M1 and M2a polarised THP-1 macrophages at either end of the spectrum. Other subtypes were found at intermediate points. It is also clear based on this analysis that both M2a and M2c cells have similar transcriptomic profiles to M0 cells as they cluster fairly closely together. M1 cells appear to be differentiated much further from M0 (baseline) macrophages based on this analysis. LPS and TPP-induced cells were clustered at intermediate points between the M0 and M1 samples. One of the “M2b” (treatment with LPS +HAGG) samples mapped with the LPS conditions, and the other near the M1 cluster. This could imply a varying response to the addition of ICs. Top loading genes for this axis appeared to be inflammatory-related (e.g. *CXCL9, CXCL10, GBP5, SERPING1*), suggesting that y-axis separated samples by polarisation state (Figure 4.3.3, D (i)).

Although the samples appeared to map in a polarisation/differentiation manner, additional investigations were performed for confirmation; analysis of most significant loading genes for principal component 1 revealed enrichment of functions relating to cell activation and migration, implying that this category may separate samples by degree of activation, i.e. differentiation state (Figure 4.3.3, D (i) + (ii)). Analysis of top loading genes from principle component 2 revealed enrichment of functions relating to IFNγ signalling and pathogen responses. This lends to the theory that the y-axis separates samples according to polarisation state (Figure 4.3.3, C (i) + (ii)). Hence the M2b sample that is skewed further from the LPS conditions may have responded

differently to IC (e.g. cells may have adopted some M1-like transcriptomic signatures). Varying responses to ICs will be explored in more detail in Chapter 5.

4.3.3. MDM and THP-1 datasets were found to be comparable

Comparisons between the THP-1 RNA-seq data generated in this Chapter, and publicly available MDM RNA-seq data identified in Chapter 2 were considered to be useful for validating the THP-1 cell line model as a surrogate for studying the activity of primary cells. However, comparing datasets generated in two separate experiments can be problematic. MA plots (where M is the binary logarithm of the gene expression count ratio and A is the average expression for a dot in the plot) can be used to investigate the distribution of genes between two datasets; as x-axis corresponds to average expression and y-axis to fold change, a directional skew of data points on the y-axis would imply transcriptional or technical bias for one of the samples, making any further comparisons unreliable. Thus, MA plots were used here to determine whether RNA-seq data derived from publicly available MDM studies (identified and analysed in Chapter 2) and that produced in this THP-1 experiment were comparable. Symmetry of plots between M1 and M2a samples in both datasets suggested that the samples were similarly normalised and could therefore be compared to one another to identify parallels in gene expression (Figure 4.3.4, A and B).

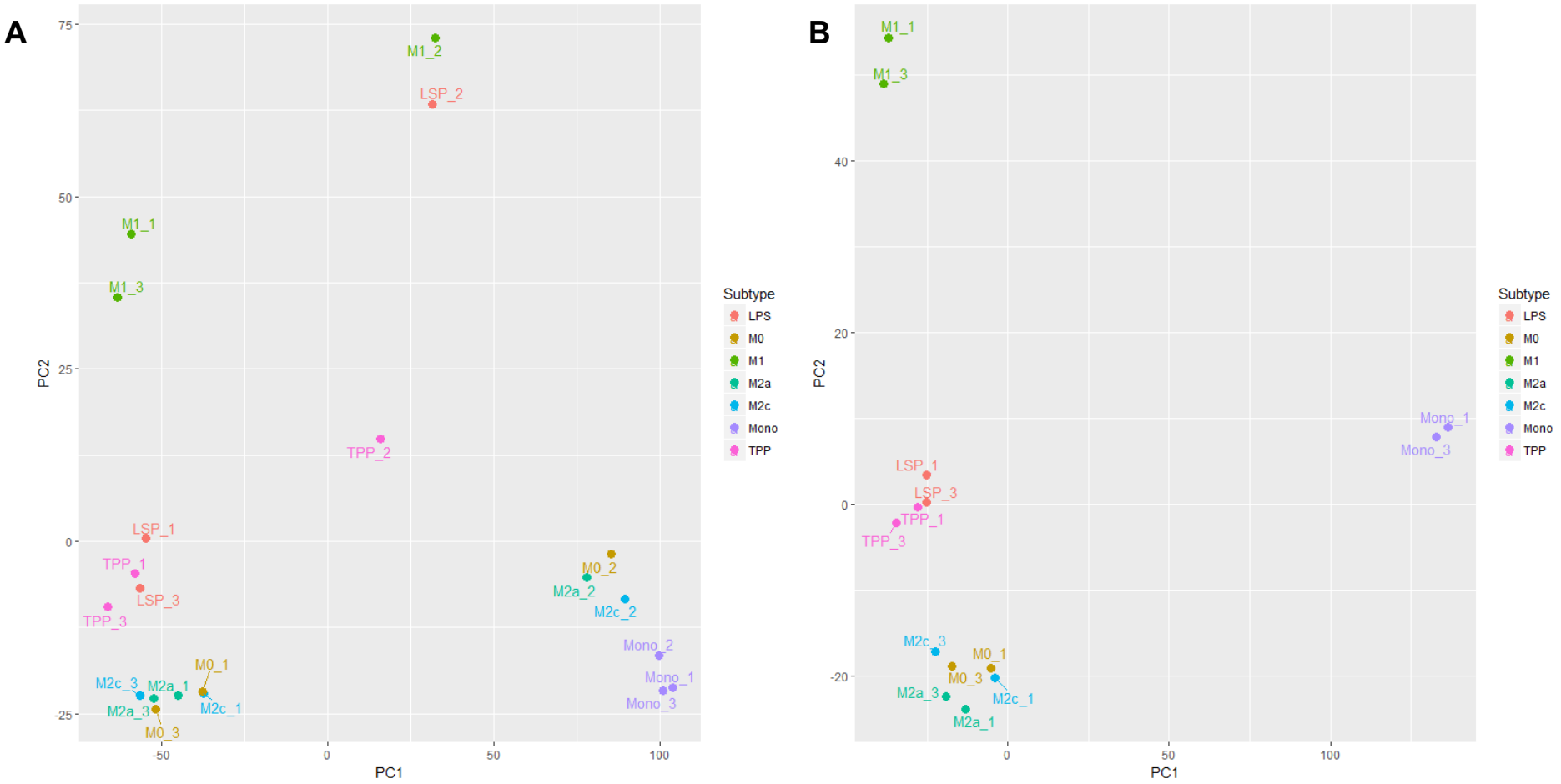

Figure 4.3.2. Principle component analysis plots using top 1000 most differentially expressed genes to examine clustering of all macrophage samples from all replicates (**A**) and all macrophage samples in the replicates 1 and 3 (**B**), i.e. run on lanes 4 and 6 of the sequences respectively. PC=principle component

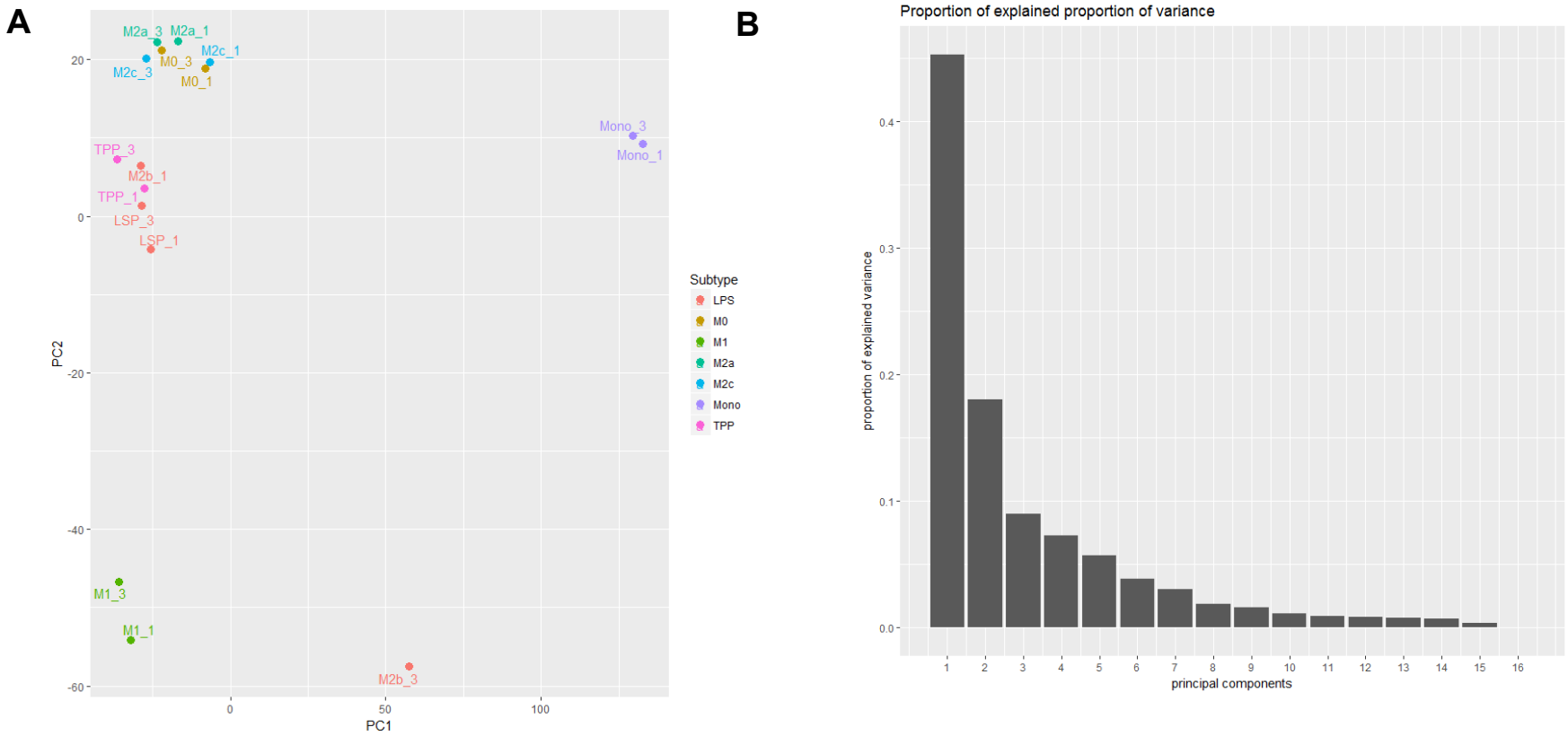

Figure 4.3.3. PCA demonstrating how samples plot according to 1000 most variable genes with LPS+HAGG (M2b) samples and no LPS only conditions, and no samples from replicate 2 (**A**). Bar chart for contributions of each principle component of top 1000 variable genes (**B**). loading gene analysis (**C**), see next page; x-axis (principle component 1) top ten up and down-regulated loading genes (**i**) top 50 enriched biological processes for all genes in x-axis (principle component 1)(**ii**), (**D**), see next page; y-axis (principle component 2) top ten up and down-regulated loading genes (**i**) top 50 enriched biological processes for all genes in y-axis (principle component 2) (**ii**). PC=principle component

C **i)**

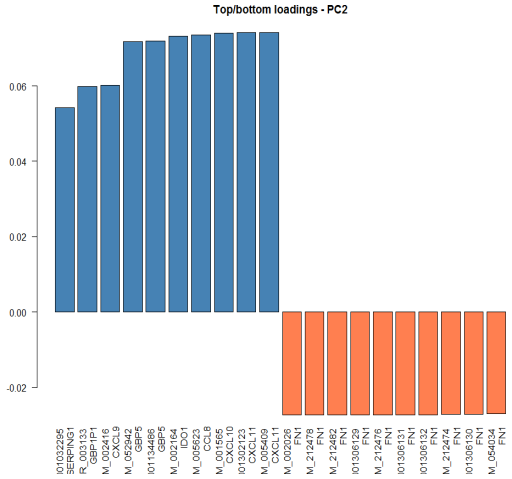
Top/bottom loadings - PC2
0.06
0.04
0.02
0.00
-0.02
IDO1
CXCL9
GBP5
CXCL10
CXCL11
FN1
CCL8

ii)

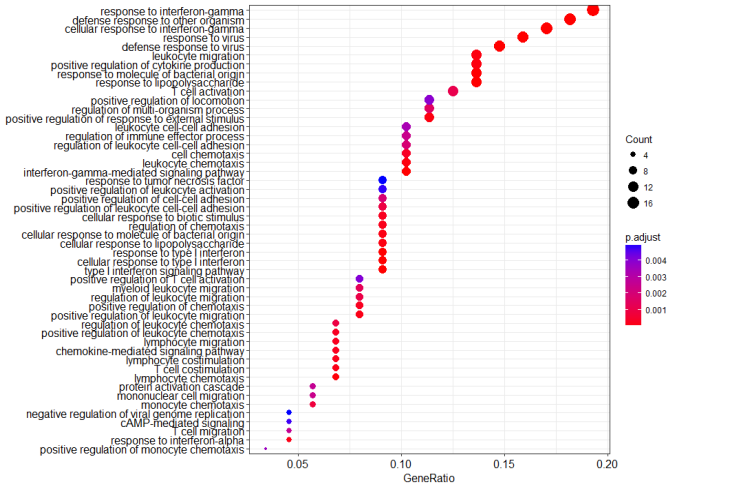
response to interferon-gamma
defense response to other organism
cellular response to interferon-gamma
response to virus
defense response to virus
leukocyte migration
positive regulation of cytokine production
response to molecule of bacterial origin
response to lipopolysaccharide
T cell activation
positive regulation of locomotion
regulation of multi-organism process
positive regulation of response to external stimulus
leukocyte cell-cell adhesion
regulation of immune effector process
regulation of leukocyte cell-cell adhesion
cell chemotaxis
leukocyte chemotaxis
interferon-gamma-mediated signaling pathway
response to tumor necrosis factor
positive regulation of leukocyte activation
positive regulation of cell-cell adhesion
positive regulation of leukocyte cell-cell adhesion
cellular response to biotic stimulus
regulation of chemotaxis
cellular response to molecule of bacterial origin
cellular response to lipopolysaccharide
response to type I interferon
cellular response to type I interferon
type I interferon signaling pathway
positive regulation of T cell activation
myeloid leukocyte migration
regulation of leukocyte migration
positive regulation of chemotaxis
positive regulation of leukocyte migration
regulation of leukocyte chemotaxis
positive regulation of leukocyte chemotaxis
lymphocyte migration
chemokine-mediated signaling pathway
lymphocyte costimulation
T cell costimulation
lymphocyte chemotaxis
protein activation cascade
mononuclear cell migration
monocyte chemotaxis
negative regulation of viral genome replication
cAMP-mediated signaling
T cell migration
response to interferon-alpha
positive regulation of monocyte chemotaxis
0.05
0.10
0.15
0.20
GeneRatio
Count
4
8
12
16
p.adjust
0.004
0.003
0.002
0.001

D **i)**

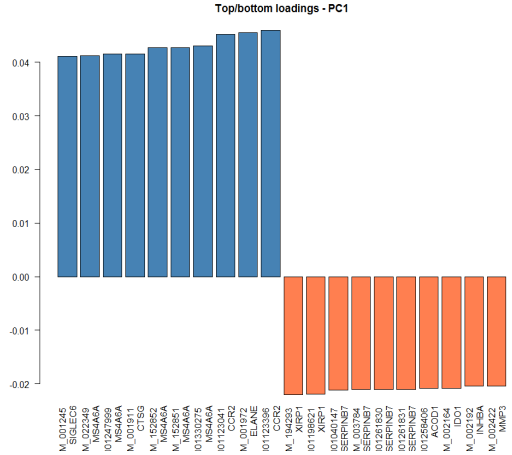
Top/bottom loadings - PC1
0.04
0.03
0.02
0.01
0.00
-0.01
-0.02
CCR2
ELANE
CCR2
XIRP1
SERPINB7
SERPINB7
SERPINB7
SERPINB7
ACOD1
IDO1
INHBA
MMP3

ii)

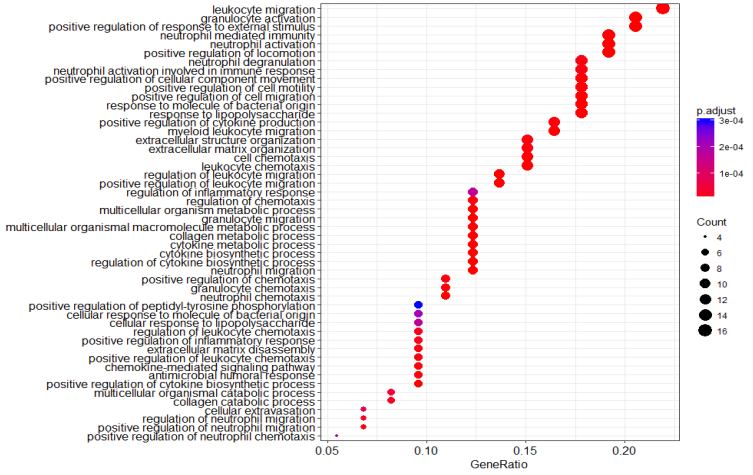
leukocyte migration
granulocyte activation
positive regulation of response to external stimulus
neutrophil mediated immunity
neutrophil activation
positive regulation of locomotion
neutrophil degranulation
neutrophil activation involved in immune response
positive regulation of cellular component movement
positive regulation of cell motility
positive regulation of cell migration
response to molecule of bacterial origin
response to lipopolysaccharide
positive regulation of cytokine production
myeloid leukocyte migration
extracellular structure organization
extracellular matrix organization
cell chemotaxis
leukocyte chemotaxis
regulation of leukocyte migration
positive regulation of leukocyte migration
regulation of inflammatory response
regulation of chemotaxis
multicellular organism metabolic process
granulocyte migration
multicellular organismal macromolecule metabolic process
collagen metabolic process
cytokine metabolic process
cytokine biosynthetic process
regulation of cytokine biosynthetic process
neutrophil migration
positive regulation of chemotaxis
granulocyte chemotaxis
neutrophil chemotaxis
positive regulation of peptidyl-tyrosine phosphorylation
cellular response to molecule of bacterial origin
cellular response to lipopolysaccharide
regulation of leukocyte chemotaxis
positive regulation of inflammatory response
extracellular matrix disassembly
positive regulation of leukocyte chemotaxis
chemokine-mediated signaling pathway
antimicrobial humoral response
positive regulation of cytokine biosynthetic process
multicellular organismal catabolic process
collagen catabolic process
cellular extravasation
regulation of neutrophil migration
positive regulation of neutrophil migration
positive regulation of neutrophil chemotaxis
0.05
0.10
0.15
0.20
GeneRatio
p.adjust
3e-04
2e-04
1e-04
Count
4
6
8
10
12
14
16

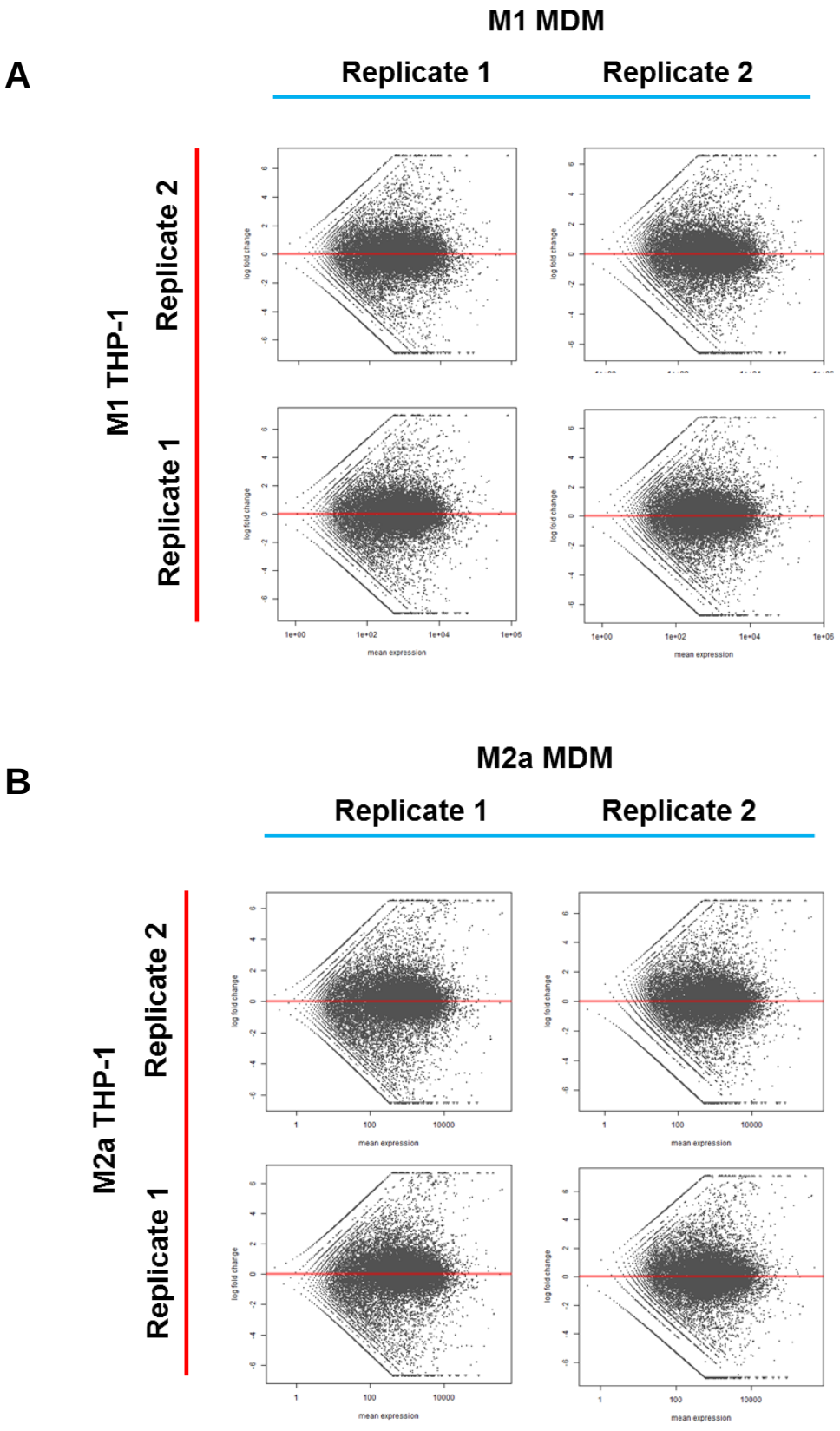

Figure 4.3.3. MA plots demonstrating the distribution of monocyte derived macrophages (MDM) samples versus THP-1 cells for M1 macrophages (**A**) and distribution of monocyte derived macrophages (MDM) samples versus THP- in M2a induced cells (**B**)

4.3.4. Inflammatory genes were found to be similarly expressed in THP-1 and monocyte derived macrophage datasets

After ensuring that the datasets were comparable in Section 4.3.3, it was necessary to determine whether gene expression followed a similar pattern in THP-1 macrophages and MDMs, with a particular focus on inflammatory functions. Differences in gene expression between M1 (inflammatory genes) and M2a macrophages (immune resolution related genes) are well documented. Therefore, as a way to normalise genes (a factor that may vary between data generated in different experiments), lists of transcripts that were significantly differentially expressed between M1 and M2a conditions were produced for both THP-1 macrophage and MDM datasets. These gene lists were then compared; overlapping and non-overlapping transcripts (between datasets) were subject to GO enrichment analyses to inform on which functions were similar and different between the two datasets (Figure 4.3.5). The overlapping region (containing genes which were differentially expressed in both THP-1 and MDM datasets) was heavily enriched for a large number of inflammatory terms, suggesting that the markers that are similarly regulated in THP-1 macrophage and MDM datasets are involved in immune functioning (Figure 4.3.6, B). Hence these functions are represented similarly in both datasets, and THP-1 cells can be considered a reliable surrogate for studying these processes. The DEGs that were present in the THP-1 cells, but not the MDMs were mostly enriched for GO terms related to cell cycle checkpoints (4.3.6, A). As the macrophage cell cycles were not synchronised prior to RNA extraction, it is possible that the M1 and M2a cells were undergoing different cellular processes relating to this cycle, hence the DEGs being enriched for those terms. Some of the GO terms enriched for genes only found in the MDM dataset were immunity related. However, the gene ratio of enriched terms was fairly low compared to the ones seen for the overlap region category, and adjusted P-value was higher for overlapping region. For instance, the gene ratio for top enriched terms in the overlap region were between 0.1 and 0.15 (10-15%) compared to approximately 0.06 (6%) for the MDM only region (figure 4.3.6, B and C respectively), and maximum adjusted P-value for MDM-only region was around 0.005-0.01 whereas for overlap section was less than $2X10^{-9}$. Additionally, it is important to bear in mind that the methods used to differentiate the THP-1 and MDMs differ; M-CSF was used to generate macrophages from PBMC monocytes versus the use of PMA for THP-1 cells, and cytokine exposure time was 72h for primary macrophages in contrast with 48h used for THP-1 macrophages. Therefore, some changes in gene expression profile along these lines should be expected. In support of this, the ontology terms in the MDM only category appeared to be related to leukocyte development and motility versus top hits in the

cross-over section, which were directly associated with response to pathogen (figure 4.3.6, C).

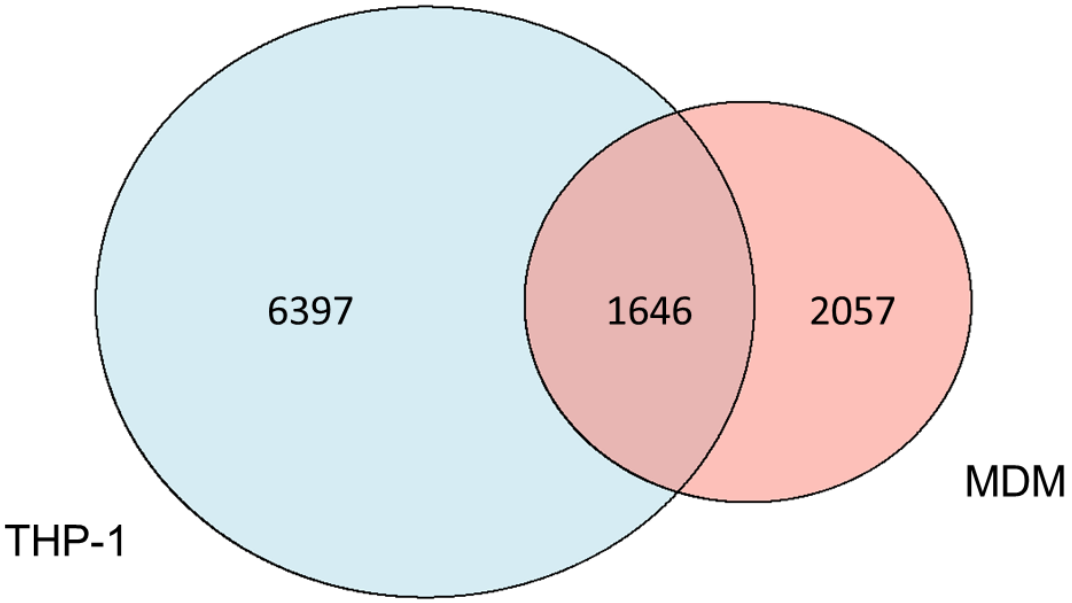

Figure 4.3.5. Lists of genes that were differentially expressed between M1 and M2a cells were generated for both THP-1 cells and MDMs. Lists were contrasted to determine whether there was any overlap between them. Overlapping and outlying genes were plotted as a Venn diagram, with THP-1 cell outlier genes in blue segment, overlapping region representing genes found in both lists of differentially expressed genes (THP-1 and MDM) and non-overlapping pink region corresponding to genes found in the MDM differentially expressed gene list only. Numbers refer to number of genes represented by the segment. MDM=monocyte derived macrophage.

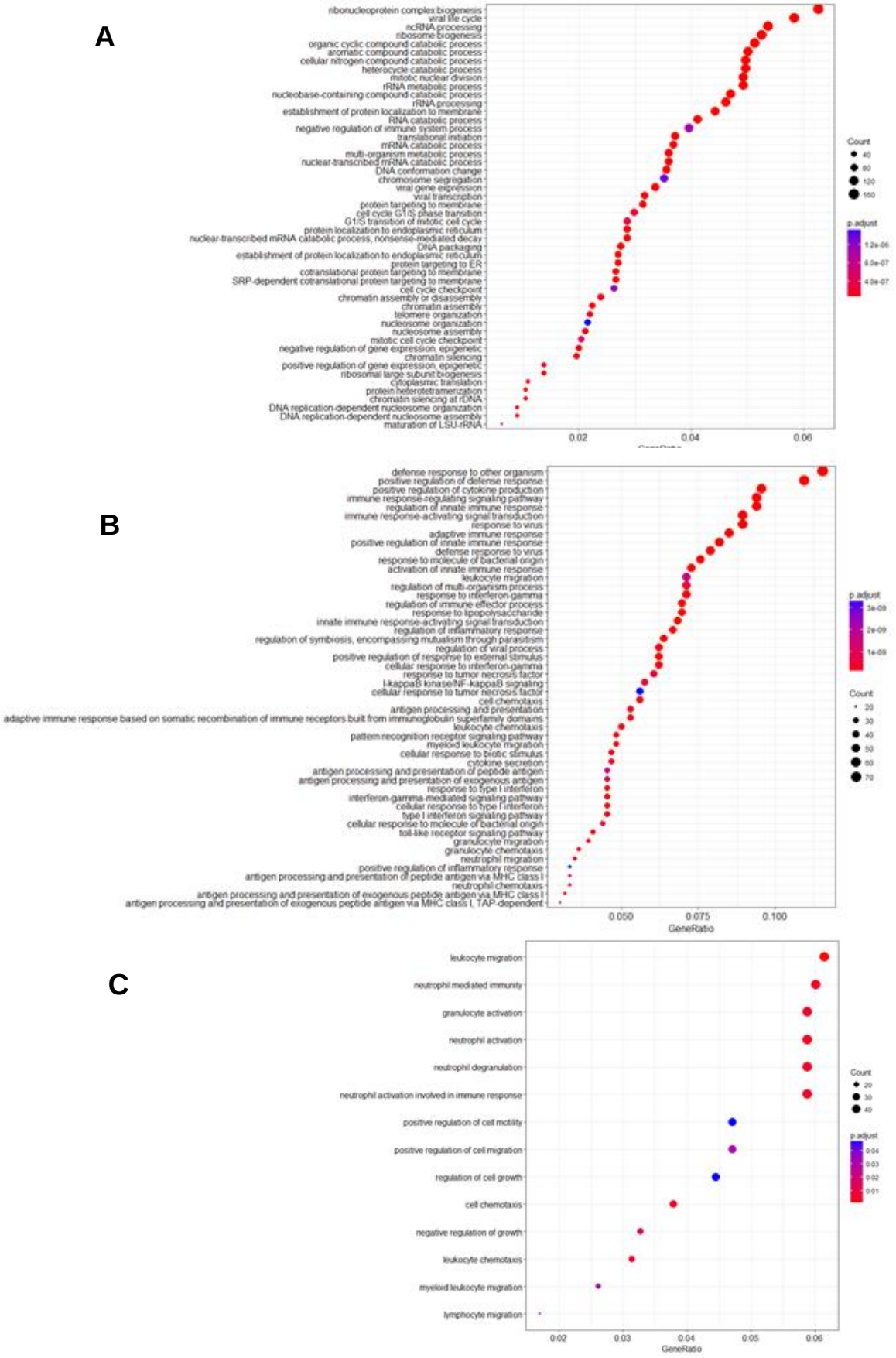

Figure 4.3.6. Dot plots showing biological process gene ontology enrichment terms for transcripts appearing in different regions of the venn diagram (Figure 4.3.5.); THP-1 only region (**A**), overlap region (**B**) and MDM only region (**C**)

4.3.5. Marker panel indicated polarisation into M1 and M2a phenotypes was achieved

Transcripts for markers used to optimise the polarisation model in Chapter 3 (Tables 3.2.3 and 3.2.4) were isolated from the dataset to examine expression quantitatively in the different macrophage conditions. Generally speaking, the markers followed the same pattern for this data that was seen experimentally, with M1 and M2a markers being up-regulated specifically for their respective conditions (Figure 4.3.7). The exceptions appear to be *CCL17, CCL23* and *HOMER2*. *CCL17* did not appear to be consistently up-regulated for any of the conditions looking at these data (Figure 4.3.7); this transcript only appeared to be weakly induced according to PCR studies, so it is possible that it is an unreliable marker that is not consistently and reliably up-regulated. *CCL23* and *HOMER2* did not appear to be M2a specific; this is not necessarily surprising as some non-specific up-regulation was seen for these markers (Chapter 3 Figure 3.3.21). Experimental variability and the fact that PCR products were not actually sequenced may also account for this; off target amplification may be an issue for the PCR results described in Chapter 3. The remaining transcripts appeared to be specific for their respective conditions (Figure 4.3.7). Novel markers identified in the previous analysis were also quantified. *SERPING1* and *AP2A2* appeared to be specific for the M1 and M2a conditions, respectively, and may therefore make effective markers (Figure 4.3.8, B). *TSC22D1* was up-regulated for all macrophage conditions, but was highest for M1, making it a marker that may be useful as part of a signature or when using quantitative techniques. *TSC22D1* was also modestly up-regulated in TPP cells versus other conditions tested. As TLR agonists are used to generate both M1 and TPP cell types (LPS for M1, Pam3SK4 for TPP), it is unsurprising that there are some similarities in terms of transcripts induced.

M2c and TPP markers which were identified from literature and through data mining publicly available microarray sources were also examined in this dataset. Relative, quantitative expression of these markers was not possible when using end-point assays in Chapter 3 (Figures 3.3.22, A and 3.3.23, C) and so this investigation was considered to be essential in these datasets. TPP markers *ABHD17C*, *LAMP3* and *STAT4* were expressed in TPP induced THP-1 cells here, but expression was also reported in M1 cells (Figure 4.3.8, A). This is not necessarily surprising as these cells are reported to be both inflammatory in nature and may have some similar gene expressions and functions.

The reported M2c marker *CD163* was expressed in M2c cells but also in M2a and M0 subsets, and another marker, *CXCL13* was seen to be expressed in M2c and M0 cells as well as the more inflammatory macrophage (M1 and TPP subtypes) (Figure 4.3.8,

A). Additionally, no expression of M2c marker *SELENOP* (*SEPP1*) was observed for M2c cells; this was only up-regulated in M1 cells and monocytes (Figure 4.3.8, A), suggesting that this is a poor M2c marker. Similarities between M2c and M0 cells are expected as the former subset is described to be “de-activated”. However, non-specific expression of some “M2c markers” in other conditions make it difficult to determine whether induction of this subtype was successful (Maess *et al., 20*14).

Additional M2a markers which were tested included *MRC1* and *F13A1*, which were highly expressed in M2a macrophages, but also in monocytes (Figure 4.3.8, A). Hence these markers may be most useful when incorporated into a panel containing markers which can distinguish monocytes and macrophages.

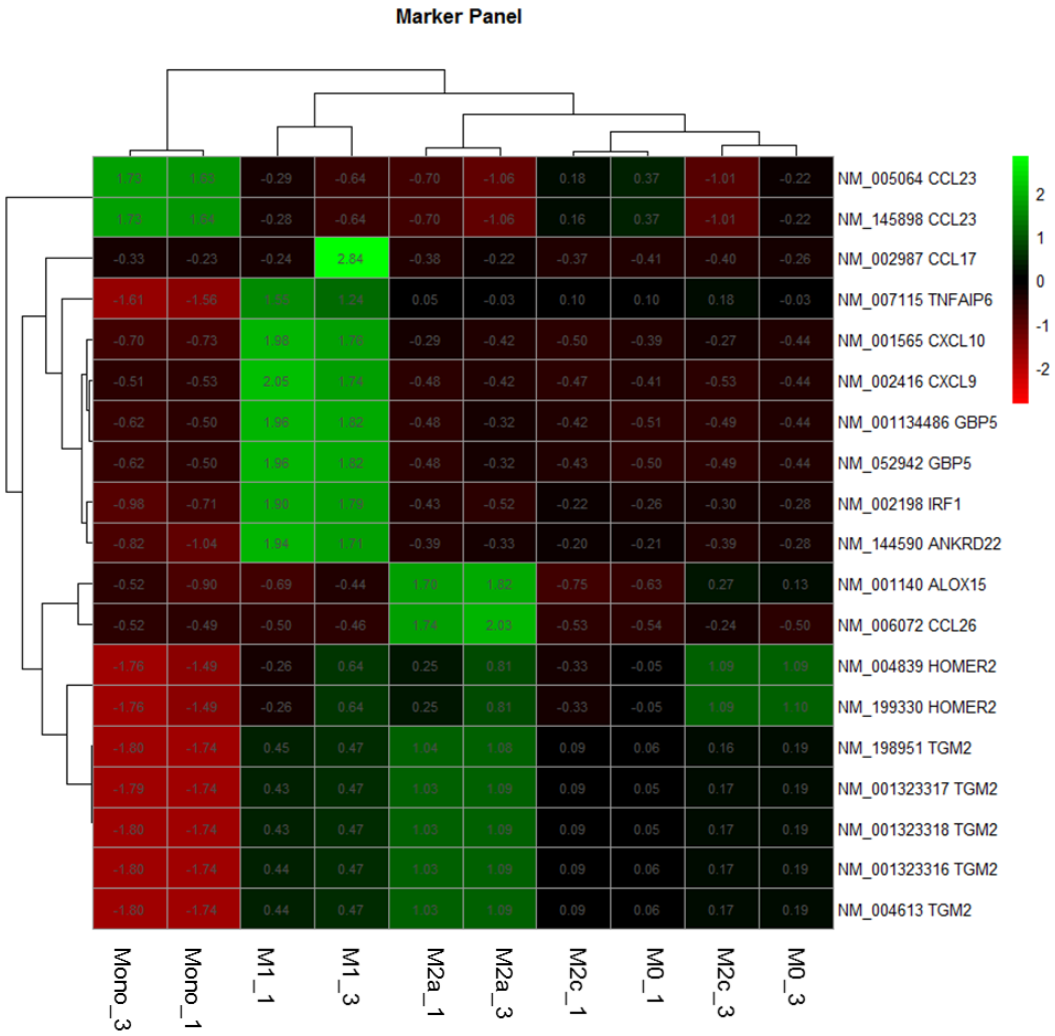

Figure 4.3.7. Heatmap showing expression of M1 and M2a marker genes identified in Chapter 2 (Table 2.3.4) for all THP-1 cell subtypes. Refseq identifiers (NM_ keys) are given alongside gene names for transcripts with more than one identifier

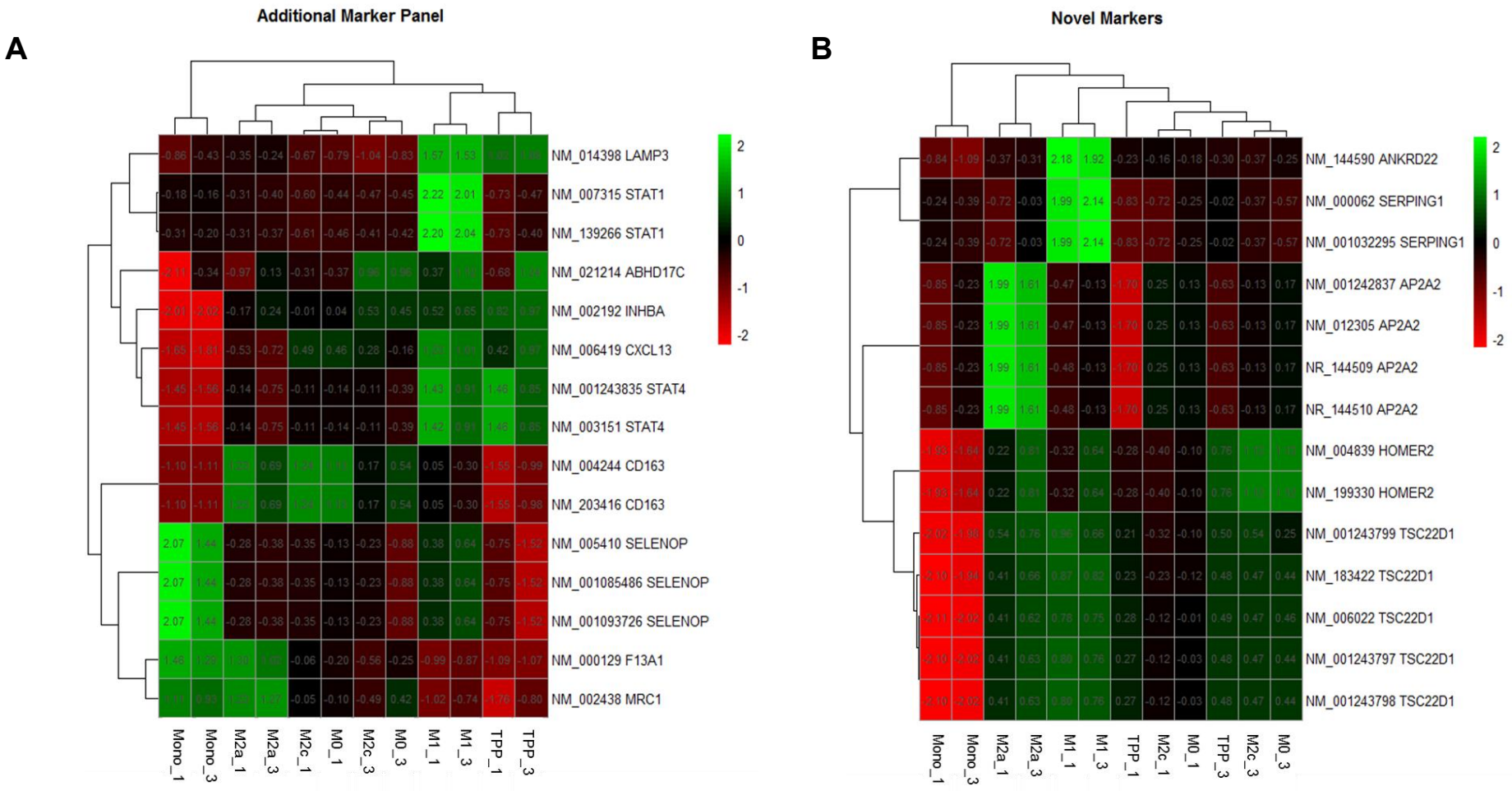

Figure 4.3.8. Heatmap of additional known markers used in Chapter 3 to investigate THP-1 cell differentiation (**A**) and heatmap of novel markers of M1 and M2a polarisation identified in Chapter 2 and tested experimentally in Chapter 3. Again, Refseq identifiers (NM_ keys) are given alongside gene names for transcripts with more than one identifier and additional identifiers showing consistent patterns may increase confidence that the differences are genuine

4.3.6. Pairwise comparisons demonstrated differentially expressed genes in certain subtypes which were enriched for subtype specific functions

As stated previously, the most well-defined expression pattern in macrophage polarisation exists through contrasting M1 and M2a subsets. Hence these two conditions were used for pairwise comparisons and differential gene expression analyses to determine whether the pattern observed followed that to be expected; i.e. with M1 conditions demonstrating enrichment in more inflammatory pathways and M2a showing enrichment for immune resolution and tissue repair pathways. Looking broadly at the dataset using heatmaps of all DEGs (Figure 4.3.9), it is clear that there is a large distinction in gene expression between the two conditions. When transcripts up-regulated in the M1 condition were passed through the Gene Ontology enrichment pipeline, functions relating to the immune response and pathogen removal were highly represented (Figure 4.3.10, A), e.g. defence response to other organism, T cell activation response to interferon-gamma are examples of terms given. Conversely, genes induced in M2a cells in this comparison were not enriched for biological processes relating to typical M2a functions; enriched terms were more cell cycle related. The cell cycle is reportedly halted in M1 macrophages and not M2a cells (Xaus *et al., 19*99), but it is impossible to determine whether this difference is responsible for these observations as cell cycle of macrophages was not synced prior to cell stimulation in this experiment.

Examining changes in the expression of a small number of genes between macrophage subtypes (as in Chapter 3) does not holistically define functional differences that occur in response to polarising stimuli. Hence this report aimed to discriminate transcriptomic signatures in the cell-line model, by passing genes isolated from an M1 versus M2a contrast through a transcription factor enrichment pipeline. TFs STAT1, STAT2 and STAT3 are renowned for up regulating inflammatory genes in response to signalling through the interferon pathways (Au-Yeung *et al., 20*13). Targets for these factors were found to be enriched in M1 DEGs (vs M2a) (Figure 4.3.11, A), suggesting that the THP-1 cells used for this experiment achieved M1 polarisation. Targets for MYC (also known as c-MYC) were enriched for M2a genes (Figure 4.3.11, B); this TF has been linked to IL-4 signalling and M2a polarisation, hence supporting conversion of THP-1 cells into the M2a state in this experiment (Pello *et al., 20*12).

DEG and analyses were performed for all other subtypes through pairwise comparisons with M1 and M0 cells (Table 4.3.1). Pairwise comparisons with M1 cells were included as the anti-inflammatory conditions (M2a, M2c) were clustered closely to the M0 cells in the PCA analysis (Figure 4.3.3, A), and so comparisons with these cells as a baseline alone may not clearly highlight the most differentiating phenotypic

features. It should be noted that although M0 and M2c cells demonstrated patterns of differential expression when contrasted against M1 induced cells, no genes were found to be significantly different between these two conditions (p-value given at 0.05, Table 4.3.1). It is possible that M2c cells did not respond to the IL-10 stimulus and therefore did not adopt the appropriate phenotype. However, cells of this subtype have been described as de-differentiated macrophages, which could be the reason for transcriptional similarities between M2c and M0 cells.

It should be noted that significantly differentially expressed genes were identified for all other comparisons (Table 4.3.1). Tables listing genes which are differentially expressed between conditions may be found in Appendix 1.

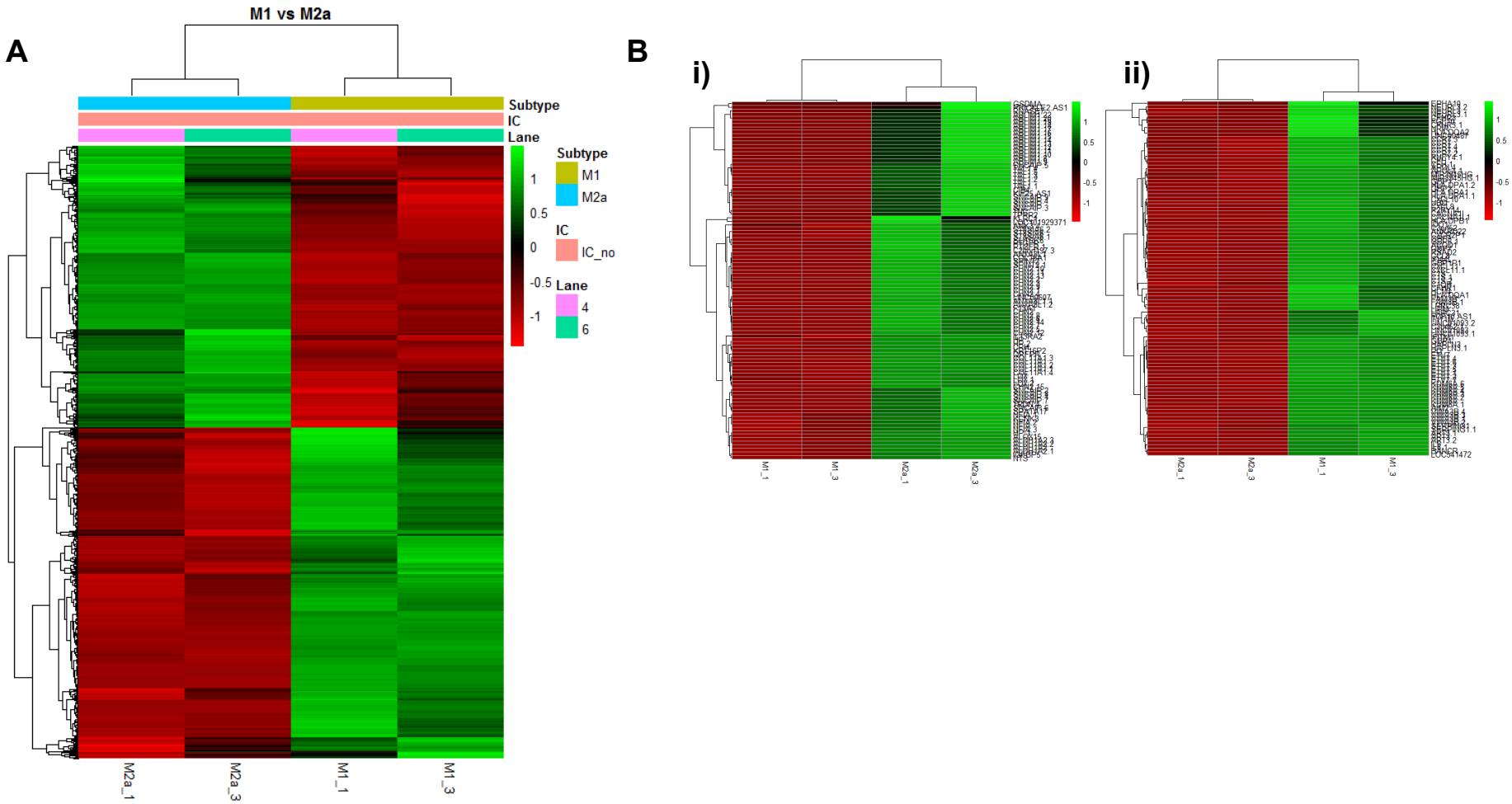

Figure 4.3.9. Heatmap of differentially expressed genes between M1 and M2a induced THP-1 cells (**A**), top 100 genes which were found to be significantly up-regulated in for M2a cells versus M1 cells (**B. i**) and top M1 genes significantly up-regulated for M1 versus M2a comparison (**B. ii**)

A

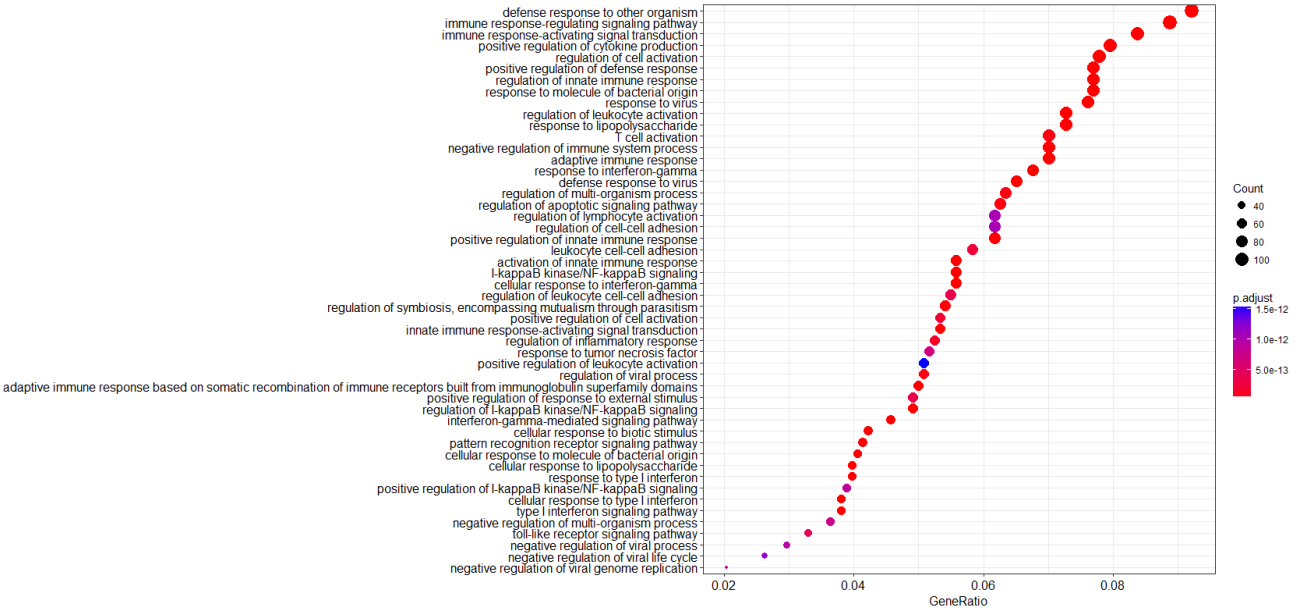

B

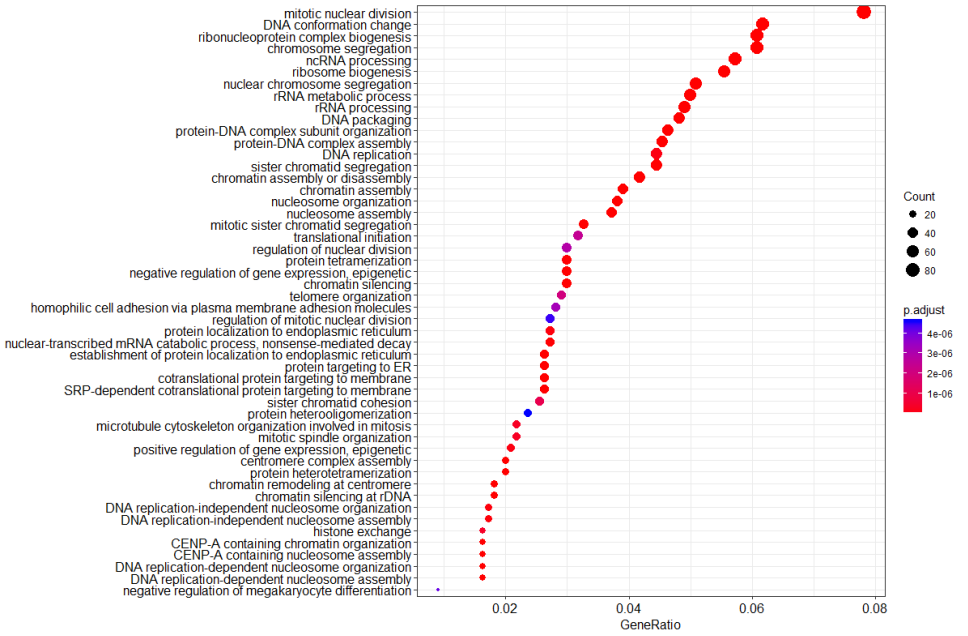

Figure 4.3.10. Dot plots for biological process related gene ontology enrichment for differentially expressed transcripts up-regulated in M1 condition versus M2a (**A**) and for transcripts up-regulated in M2a condition versus M1

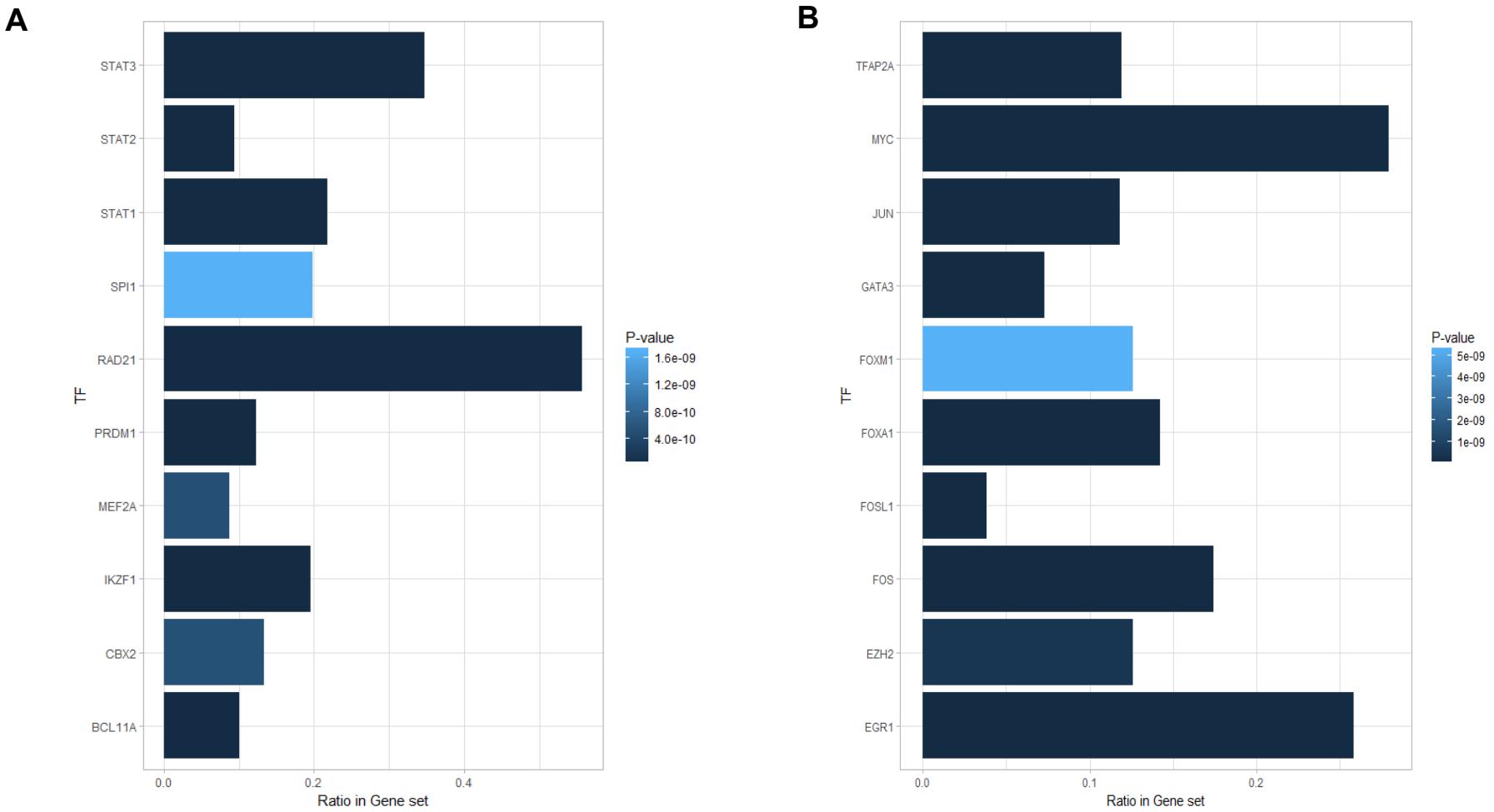

Figure 4.3.11. Bar charts demonstrating gene ratios and respective p-values for transcription factors in lists of genes; those elevated in M1 condition versus M2a (**A**) and for those elevated in the M2a condition versus the M1 condition (**B**). Top ten transcription factors were selected for each condition when ordered according to p-value

Table 4.3.1. Conditions in which pairwise comparisons produced a list of differentially expressed genes; Green indicates that a list of significantly differentially expressed genes (p-value threshold set at 0.05) was identified between conditions, red indicates that no significantly differentially expressed genes were identified between the different conditions (p- value at 0.05). Grey boxes indicate when the same condition is given on both axes

	Monocytes	**M0**	**M1**	**M2a**	**M2b**	**M2c**	**TPP**
M0							
M1							

4.3.7. Top 30 most differentially expressed transcripts for THP-1 macrophage subsets were identified

Some of the transcripts identified through the analysis of public datasets in Chapter 2 were not considered to be particularly robust markers in THP-1 cells (Chapter 3 Figure 3.3.21). In addition, it should be noted that there were some differences in the transcripts identified as strong candidate markers between both the RNA-seq and microarray datasets in Chapter 2 (Figure 2.3.7). Hence efforts were made here to identify more reliable marker genes in these datasets that were strongly up-regulated in one condition only. Candidates were selected through a pairwise comparison that broadly speaking involved contrasting one subtype against all other conditions (e.g. M1 versus not-M1).

For the M1 subtype, there were clear distinctions between the top markers and most of the other conditions used in the contrasts (Figure 4.3.12, A). Some of the top 30 transcripts (*GBP5*, *SERPING1*) were identified in the MDM dataset analysis in Chapter 2 (Table 2.3.4), increasing confidence in this approach. There did appear to be some overlap between gene expression in the M1 and M2b (LPS+HAGG) samples. These cells are both induced using LPS (along with other agents), and subsequent overlaps in transcriptomic profiles are to be expected (as seen for *SERPING1* and *ETV7* in Figure 4.3.13, A. ii). As some of the genes selected were not expressed in both conditions, it is possible that all markers here may be included as part of a panel to identify macrophages expressing an M1-like signature; for instance *SERPING1* which is seen for both M1 and M2b (Figures 4.3.12, A and 4.3.13, A respectively) could be included in a panel *GBP5* which is highly specific for M1 cells (Figure 4.3.12, A. ii). It should also be noted that the expression of these genes in the M2b condition was not consistent

between the two replicates, and so up-regulation of the M1 markers in this subtype may not be a reliable observation and further verification would be needed.

On contrasting M2a induced genes with all other conditions, a list of significantly differentially expressed genes were produced as potential markers for this subtype (Figure 4.3.12, B); some M2a markers identified through this analysis were also highly ranked in the analyses performed in Chapter 2, although some of these markers (*F13A1, FCER2*) were also highly expressed in THP-1 monocytes, so would need to be used in conjunction with other markers as part of a panel. Overall there appeared to be a number of potential M2a markers that may be cross validated in a MDM dataset.

As mentioned previously, the two M2b-like conditions were not consistently polarised, and so markers identified through contrasting these conditions with the other samples should be considered with caution. As expected from other contrasts, there were some overlaps with genes identified for the M1 conditions, but others that were high in one replicate of the M2b treated cells (versus all other conditions) only (Figure 4.3.13, A); these could be considered as candidate markers to be cross-validated in MDM datasets. It could be suggested that one of the samples did not react as strongly to IC as the other, or polarised differentially in response to the LPS leading to differences in transcript expression. Explanations would require validation or repeats of experiments to determine correct gene expression profile.

As there were no significantly different genes expressed between M2c and M0 cells in the pairwise analyses, these two conditions were combined in an attempt to identify markers relating to these two subsets (Figure 4.3.13, B). A small number of hits (27 separate refseq identifiers) were identified using this method that appeared to represent this subset, although differences between expression in subsets of interest and other conditions were not as clear as those seen for M1 and M2a markers (for instance) (Figure 4.3.14, B). It was particularly important for these markers to be examined in other datasets, as they were isolated through an analysis spanning two different polarisation states (Figure 4.3.16, C).

Isolation of potential markers for the TPP subtype was of particular interest as these cells have only recently been described and relatively little gene expression information is available for them (Xue *et al., 20*14). Upon inspection (Figure 4.3.14, A), some of the genes isolated appeared to be related to immunological functioning (e.g. *IL23A*). However, as this list of genes was produced by contrasting with all other conditions (including M1 samples which according to the PCA plot shared some similarities with TPP cells) some genes relating to characteristic inflammatory patterns may have been discounted because of overlapping expression with M1 cells.

Monocytic markers were also identified using similar contrast methods (Figure 4.3.14, B); *SIGLE6C* (codes for sialic acid binding Ig-like lectin) (von Gunten and Bochner, 2008) and *MS4A3* (member of a family of four-transmembrane proteins responsible for cell surface signalling) (Kutok *et al., 20*11) were among the top hits for this analysis. It is clear when looking at the marker plots (Figure 4.3.13, A) that one of the M2b conditions shares some similarities with monocytes. Additionally, according to the PCA this sample does not appear to align with other macrophage-like conditions on the x-axis (previously proposed to relate to differentiation) and is at an intermediate stage between these cells and the monocytes. Hence it is possible that cells grown for this sample did not effectively differentiate and become macrophage-like, making the markers more specific for the monocyte state versus other conditions. However, an alternative explanation is that this set of conditions reverses differentiation of macrophages to some degree, resulting in a more intermediately activated phenotype. Further investigation is required to confirm or rule out either hypothesis. As an additional point, the fact that this M2b sample appears to be an outlier in terms of both differentiation and polarisation begs the question, does failure to differentiate render cells more susceptible to the influence of HAGG or vice versa. As with the previous point, more information is required to hypothesize reliably.

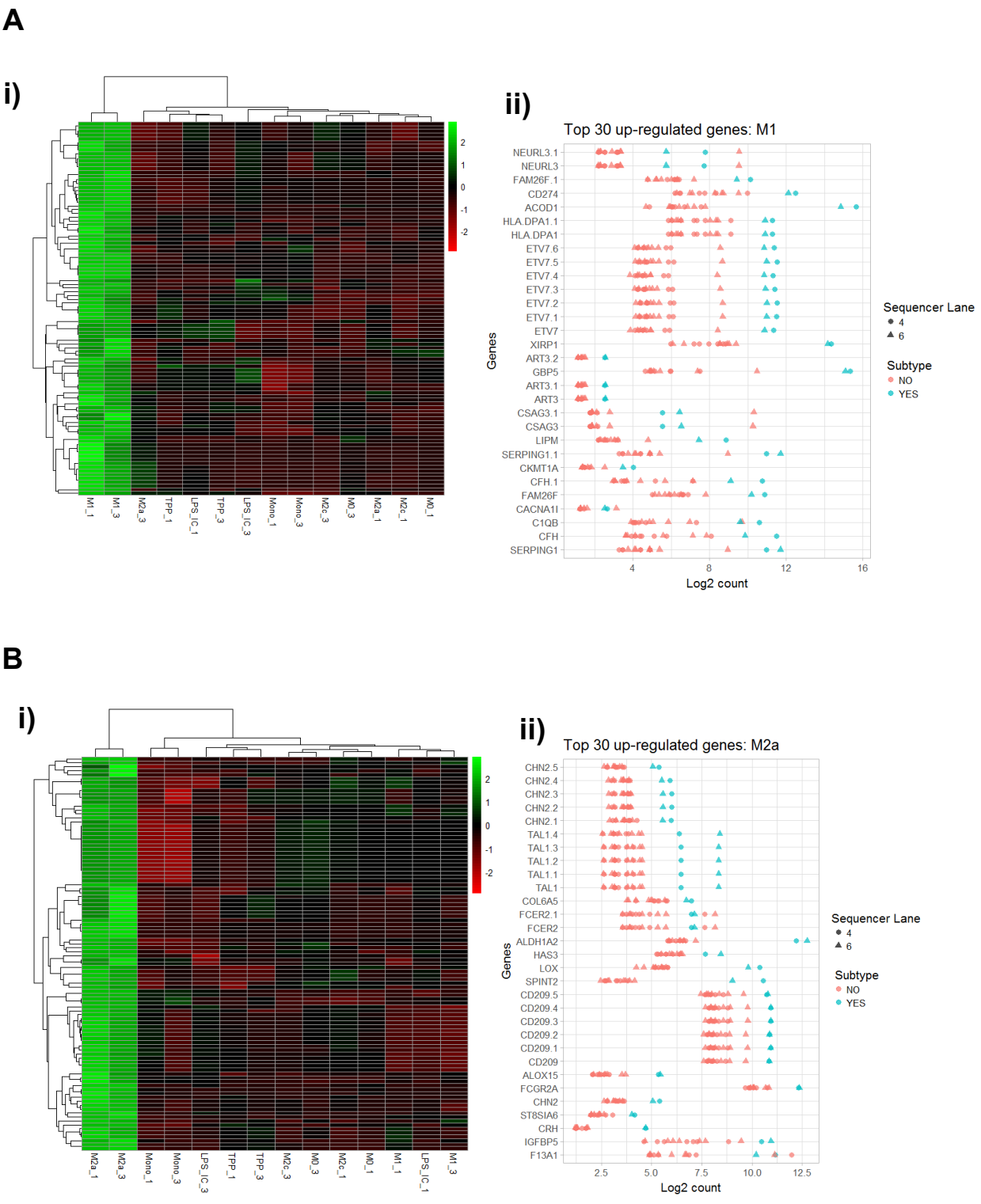

Figure 4.3.12. Heatmap showing potential markers up-regulated in condition of interest, and dotplot showing top marker expressions for condition of interest (blue) versus other samples (pink) for M1 subtype (**A**) and M2a subtype (**B**)

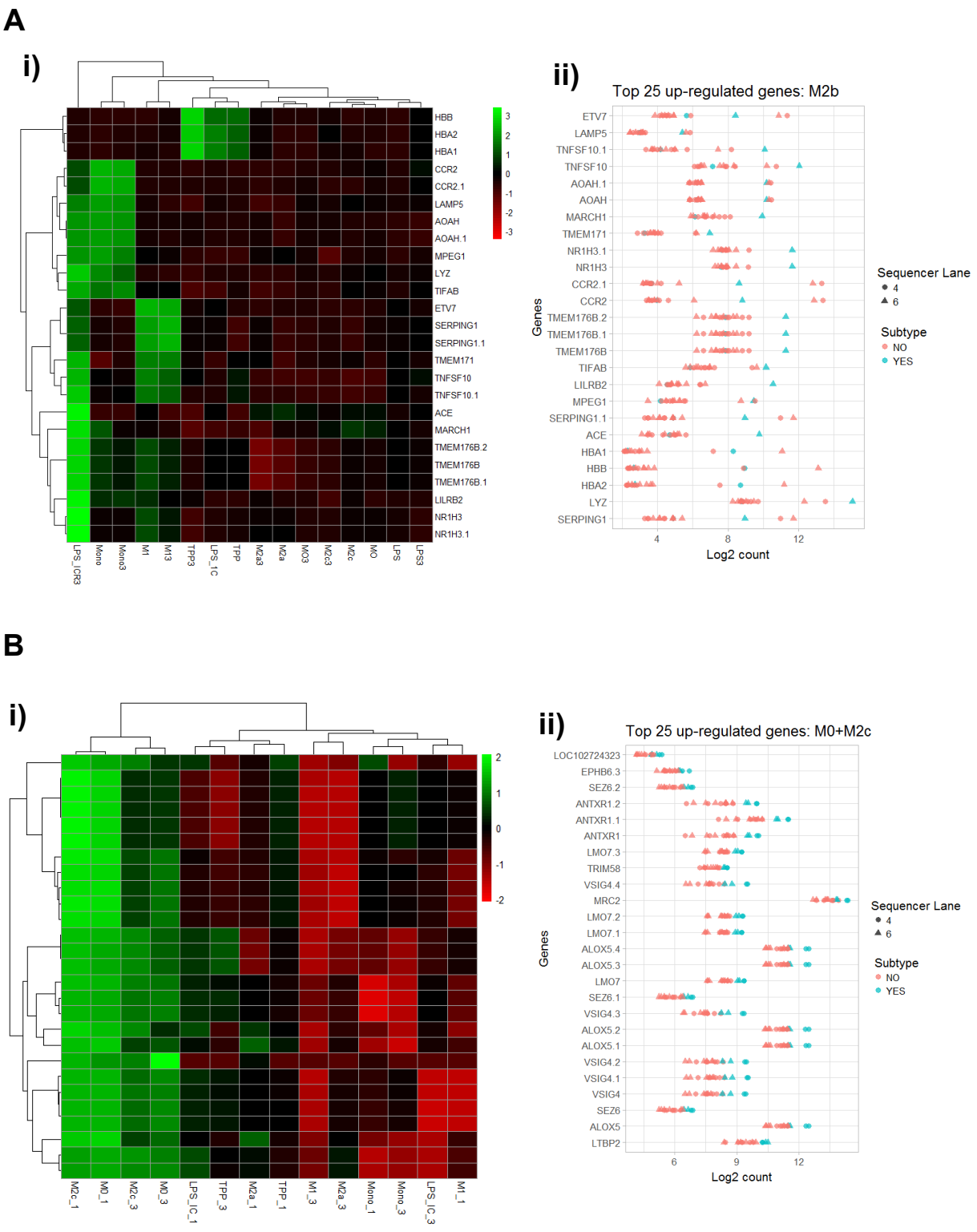

Figure 4.3.13. Heatmap showing potential markers up-regulated in condition of interest and dotplot showing top marker expressions for condition of interest (blue) versus other samples (pink) for M2b subtype (**A**) and M0/M2c subtypes (**B**)

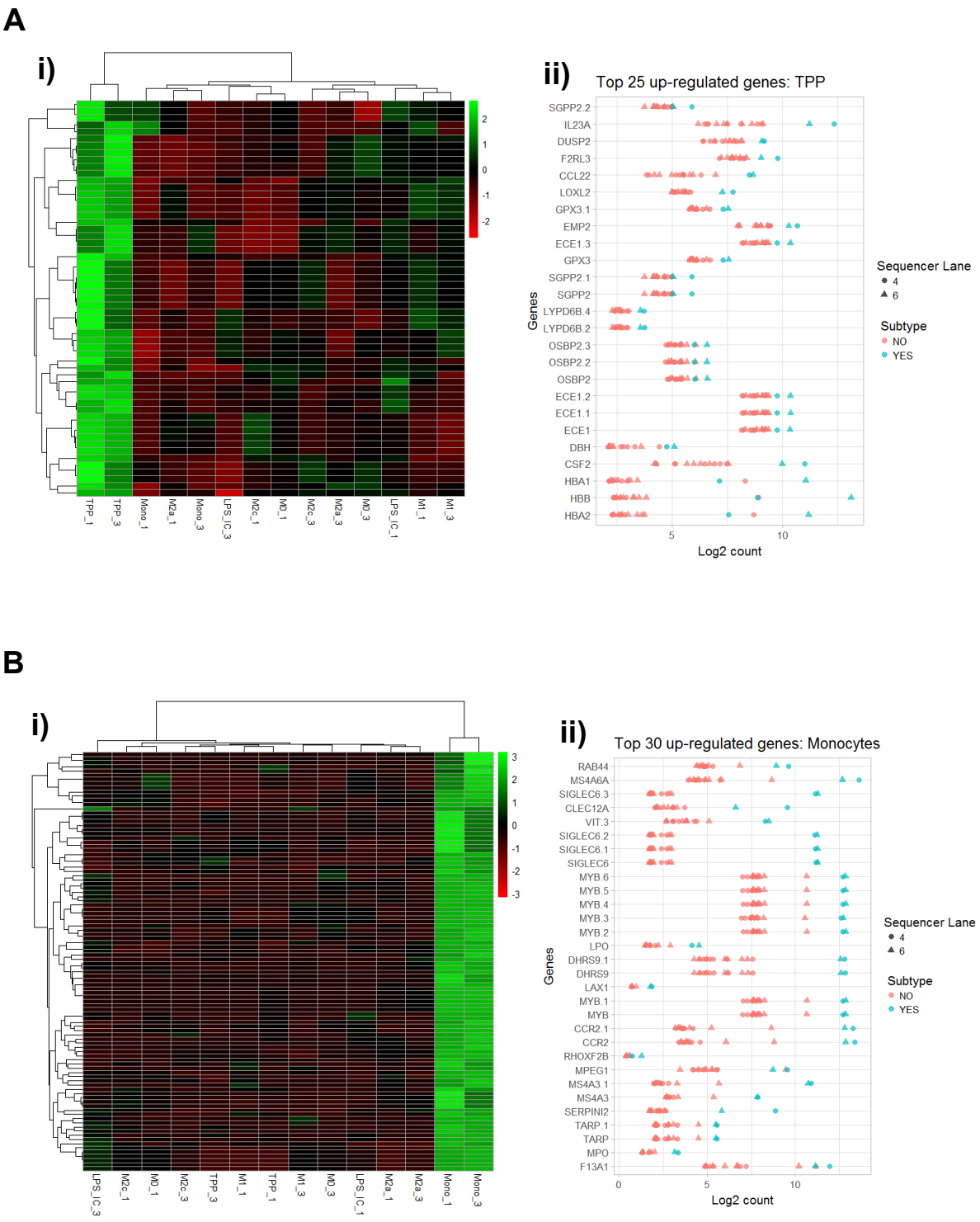

Figure 4.3.14. Heatmap showing potential markers up-regulated in condition of interest and dotplot showing top marker expressions for condition of interest (blue) versus other samples (pink) for TPP subtype (**A**) and monocyte subtype (**B**)

4.3.8. Some THP-1 markers were validated using MDM datasets

As stated previously, some differences have been described for markers derived from MDM and THP-1 datasets due to inherent protocol variations (e.g. use of PMA to differentiate THP-1 cells versus M-CSF). Consequently, any markers identified using THP-1 cells must be cross validated in primary cell datasets. As comparisons between data generated using the same method is more reliable, validations were made by cross-referencing THP-1 RNA-seq data with MDM RNA-seq data (identified in Chapter 2) where possible, i.e. for M1, M2a and monocyte conditions (Beyer *et al., 20*12). For M2c, M2b and TPP subsets RNA-seq data were not available, so findings from microarray experiments (identified in Chapter 2) were used to validate potential marker transcripts identified from these samples. For the M1, M2a and monocyte conditions, a number of genes are specific according to both datasets. These transcripts may be tested experimentally to validate their use as marker genes that may be applied to distinguish polarisation states in both MDMs and THP-1 macrophages. Transcripts of interest for M1 included *ETV7* (coding for a transcription factor that has previously been associated with LPS signalling), *NEURL3* (ubiquitin protein ligase gene which undergoes activity change upon cholesterol accumulation) and *CD276* (a member of the B7 costimulatory family of receptors) (Bobryshev *et al., 20*16); (Baillie *et al., 20*17); (Mao *et al., 20*17). Some genes that may make useful markers for the M2a polarisation state if validated include *HAS3* which codes for hyaluronan synthase-3, a protein involved in production of hyaluronic acid, *CHN2* (chimerin 2) which codes for a protein involved in proliferation and migration and *LOX* which has been found to be associated with atherosclerosis in studies performed on murine macrophages (Chang *et al., 20*14); (Chen *et al., 20*14); (Ding *et al., 20*13).

A number of the transcripts identified for the M2b condition in THP-1 cells were not found to be specific in MDM cells. The differences in cytokine exposure time between the different cell types (48 in THP1 cells and 72 in MDMs) may contribute to this as well as reagents used to induce the formation of macrophages (PMA in THP-1 cells and M-CSF in MDMs). The transcripts which were expressed in M2b cells had similar expression patterns to the M1 polarised primary cells (e.g. expression of *ETV7*, *SERPING1*). This could be due to use of LPS in cell culture protocols for both of these macrophage subtypes. These markers may therefore be used as part of a panel to distinguish M2b cells from other phenotypes when combined with M1 specific transcripts to negatively select the phenotype (using M1 markers such as *GBP5* and *CXCL10*).

As was the case with the M2b genes, a number of the TPP markers were not specific in MDM datasets, which again could be attributed to differences in experimental timings

(for instance cytokine exposure times) or other differences in experimental differences (PMA versus M-CSF in THP-1 cells and MDMs respectively). Some however looked specific (*DBH, CSF2*) and may be tested experimentally.

Very few of the M2c/M0 markers identified for THP-1 cells were reflected in the MDM dataset, possibly due to the fact that these cells are deactivated/unpolarised and may reflect baseline changes between cell lines and primary cells most sensitively. There were some markers identified that could be used in combination to deduce cell type; *ALOX5* and *VSIG4* were both present in MDM M0/M2c cells, but also M1 and M2b phenotypes. Another M0/M2c marker, *EPHB6*, was not induced in M1 and M2b cells but was present for M2a and monocyte subtypes. Therefore, this panel of markers may be used to identify the deactivated sub-type.

It must be noted that the quality of the MDM datasets is not completely known as they were isolated from previously published studies.

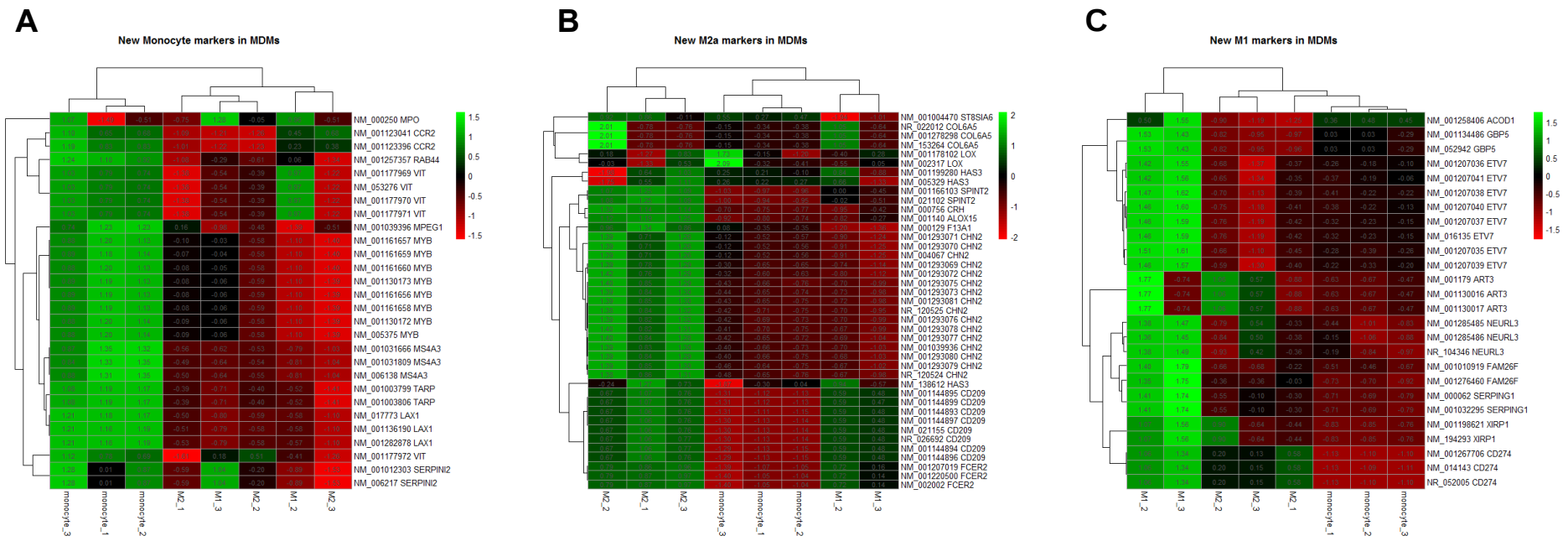

Figure 4.3.15. Previously identified THP-1 polarisation markers identified in MDM RNA-seq dataset for monocytes (**A**), M1 cells (**B**) and M2a macrophages (**C**)

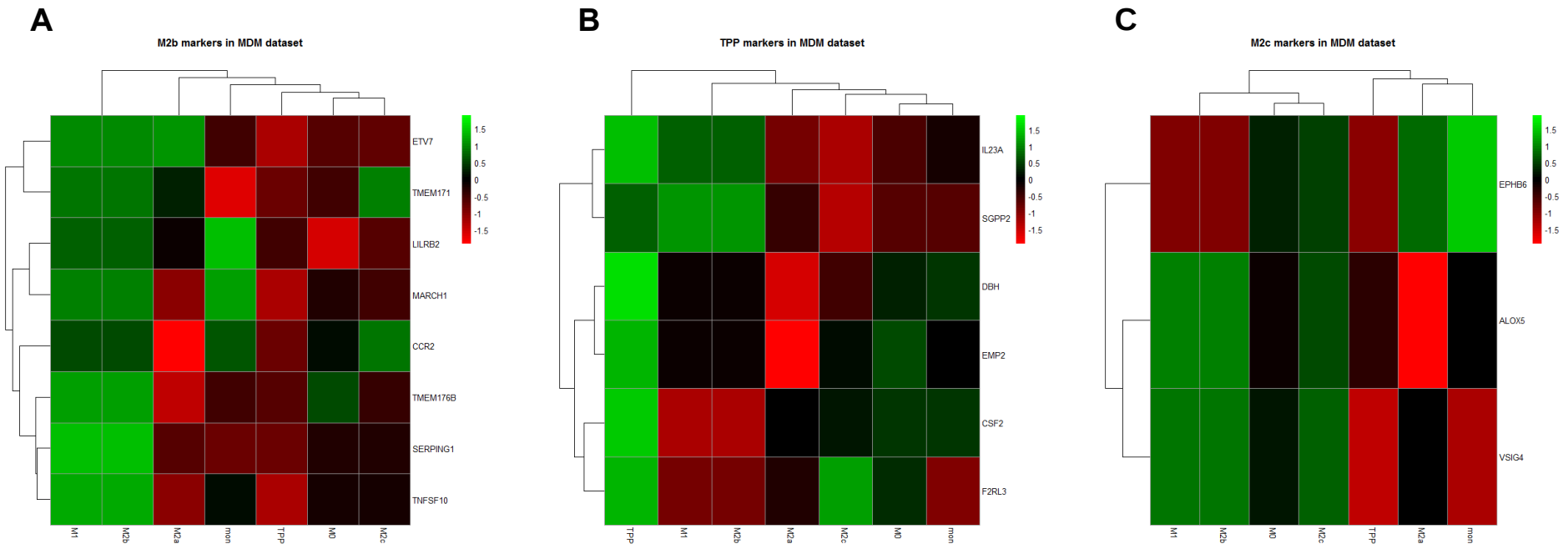

Figure 4.3.16. Previously identified THP-1 polarisation markers identified in MDM microarray dataset for M2b cells (**A**), TPP cells (**B**) and M0/M2c macrophages (**C**)

4.4. Discussion

It appears, based on comparative transcript analyses performed in Section 4.3.4, that monocytes derived from THP-1 cells and PBMCs polarise into M1 and M2a macrophages in similar manners. It should be noted, however, that actual numerical values were not used for this analysis, rather a comparison between lists of genes generated by identifying transcripts that were significantly differentially expressed. Although this method may exclude some detail, it should be emphasised that a more rigorous analysis may not be possible without introducing additional issues; traditionally, comparing RNA-seq datasets generated at different times using different protocols can be problematic. For instance, issues such as laboratory batch effects, variance in methods used to prepare libraries and divergences in bioinformatics processing pipelines can have a profound effect on read values, and normalisation may not completely correct for this (Danielsson *et al., 20*15); (Leek *et al., 20*12). Hence, despite limitations, the methods discussed here give a general indication that primary macrophages and THP-1 cells generated using the optimised cell line protocol polarise comparably.

The previous Chapter demonstrated upregulation of M1 and M2a markers in relevant subsets, but this was restrictive in that only a small number of genes were examined and little functional information could be inferred from these findings. Here, however, it is clear from the comparative analyses (described above), PCA mapping and gene ontology enrichment analysis, that macrophages at apposing ends of the polarisation scale (i.e. M1 and M2a cells) can be generated. For instance, some of the transcription factors (STAT1, STAT2) highlighted in the analysis of M1 induced genes (versus M2a) are strongly associated with interferon signalling (Au-Yeung *et al., 20*13); (Ivashkiv and Donlin, 2014); (Blaszczyk *et al., 20*16). Additionally, functions such as bacterial killing are characteristic for inflammatory macrophages and so presence of biological terms relating to this activity (such as “defense response to other organisms”) in enriched gene ontology terms increases confidence in this phenotype being achieved (Fraternale *et al., 20*15); (Martinez and Gordon, 2014); (Lam *et al., 20*16); (Benoit *et al., 20*08). Specifically, some transcripts up-regulated in M1 but not M2a cells constitute the GO term “defense response to other organisms”. Examples include *CXCL9* and *CXCL10* which are M1-high and M2a-low, and code for proteins that contribute to bacterial killing, as shown by Egesten *et al*, (2007) who demonstrated the bactericidal effects of CXCL9 and CXCL10 on *Streptococcus pyogenes in vitro* (Egesten *et al., 20*07). Follow up functional experiments to test these M1-specific functions (e.g. bacterial removal assays) would be beneficial.

When samples skewing data with a strong lane effect (lane 5/replicate 2) were removed from the analysis, it could be seen that polarisation effects of the cells were replicable, suggesting that this model can be used to generate cells of these subtypes in future experiments.

It should be noted that M1 cells appeared to diverge further from the M0 cells than those of the M2a phenotype. It was previously observed in Chapter 3 that the M2a markers did not appear to be as strongly induced as those for the M1 condition; it was discussed that previous reports have described difficulty inducing the anti-inflammatory subtype and that this may be a limitation of THP-1 cells (Chanput *et al., 20*13); (Park *et al., 20*07). This could be the reason for the observations described here.

Some M2c markers from the literature have been examined in this dataset; *CXCL13* was expressed in M0 and M2c cells, but upregulation was strongest in the M1 condition; although some studies describe this transcript as an M2c marker, other reports have demonstrated its induction in M1 cells, in support of the findings here (Martinez *et al., 20*06); (Wang *et al., 20*14). *CD163* is reportedly up-regulated by both IL-4 and IL-10 in macrophages, and was originally described as a marker for all M2 cells (Zeyda *et al., 20*07). However, more recent studies have found expression of *CD163* to be higher in IL-10 induced macrophages, and classified this transcript as an M2c marker (Olmes *et al., 20*16). Some reports have also found this transcript to be highly expressed in M0 PBMC macrophages compared to M1 and M2a induced cells (Lathrop *et al., 20*15). According to the data generated for this report, expression of this marker was high in M2c and M0 cells, and some expression was seen for the M2a condition, corroborating the reports describing PMBC macrophage activity in the literature.

It should be emphasised that no significantly different genes were detected between M0 and M2c cells in this study and the latter has previously been described as a “deactivated” subtype (Maeß *et al., 20*14). It currently remains unclear whether IL-10 induces a transcriptional profile distinct from that of M0 cells; some reports have described a separate gene expression profile for this phenotype, but a number of studies simply compare M2c cells to M1 and M2a induced macrophages rather than M0 cells (Bai *et al., 20*15); (Yuan *et al., 20*15); (Jetten *et al., 20*14); (Szulzewsky *et al., 20*15). In these cases it is more difficult to determine whether IL-10 merely reverses the effects of other stimuli and restores up-regulation of M0 genes, or induces specific pathways. The fact that some transcripts reported to be M2c markers (*CD163*) are up-regulated in both M2c and M0 samples in this data supports the idea that these phenotypes are very similar. However, the complete absence of some M2c markers in these experiments (*SEPP1*/*SELENOP*) could indicate failure to induce this phenotype.

Some additional experiments could be performed to investigate whether M2c polarisation failed or not. In addition to examining larger number of M2c associated transcripts, it would be interesting to inhibit some components of the IL-10 signalling pathway to determine whether this affects transcript expression. Other experiments may include co-stimulating M1 induced cells with IL-10, to determine whether this agent will “de-activate” this subtype to a more M0-like state. Comparisons with TGFβ and dexamethasone (other agents reported to induce M2c polarisation) may also clarify whether this is a separate subtype (Rőszer, 2015). Examination of some of the functions described for M2c cells (e.g. Tissue remodelling using scratch assays) between IL-10 and unpolarised macrophages may provide further insight into the similarities of these cells (Ferrante and Leibovich, 2012); (Jetten *et al., 20*14). It may have been beneficial to test an increased number of IL-10 exposure times to generate some clearer conclusions on whether distinct M2c cells are generated here. Additionally, a repeat of this experiment may be useful, as a low number of significant hits could be a result experimental and technical variability between samples.

It should be noted that combining the M0 and M2c conditions could bias the selection of markers. However as no significantly differentially expressed genes could be detected between these two subtypes, it would not be possible to identify any markers in an analysis that included all conditions. Additionally, if both of these subsets represent a “de-activated” state, if may be considered beneficial to identify transcripts which could be used to indicate this combined phenotype. If this is determined to be a case of failure to induce the M2c phenotype, then additional efforts must be made in future experiments to identify markers for this subtype.

Based on the PCA plotting and marker panel generation, despite mapping in the same direction as M1 cells on the PCA plot (compared to M0 samples) it appeared that macrophages treated with LPS and TPP stimuli generated distinct sub-populations and so should be considered as independent phenotypes for further study. This may be of particular interest for TPP cells when studying chronic inflammatory diseases characterised by macrophage infiltration such as atherosclerosis, asthma and some cancers (Liu *et al., 20*14).

All markers identified in these studies require experimental validation to confirm their efficacy before being applied in further investigations. One way to do this would be to perform qPCR for quantitative gene expression in differentially polarised THP-1 and MDM macrophages. BioMark HD Systems assays from Fluidigm (qPCR based methods) may be used to look at a large number of markers, but sensitivity may be compromised here (Livak *et al., 20*13); (Rajkumar *et al., 20*15).

Some of the markers identified in the initial analysis of primary macrophage gene expression data were also found in top 30 transcripts (according to Refseq identifiers) for polarised THP-1 cells. As changes between different cell culture and sequencing protocols can have effects on macrophage transcriptomes (as seen in Chapter 2 with microarray versus RNA-seq data) as well as genetic differences between the cell types, it was promising to see markers identified from THP-1 data validated in public primary cell data. Additionally, it can be suggested from this data that the transcripts cross-validated in both datasets can be used to indicate polarisation for both PBMC and THP-1 derived macrophages.

Treatment of LPS cells with ICs did not appear to generate consistent results. One potential explanation for this could be that there were different sizes of IC in the mixture formed by heat aggregated IgG1. This is demonstrated by the coomassie brilliant blue R-250 stained gel in Appendix 4 (Figure A4.1) which demonstrates two distinct bands. As different sized IC have differential effects on macrophage activity, an uneven distribution of different molecular weight complexes between different aliquots could have adversely affected the consistency of this experiment (Lux *et al., 20*13); (Jarvis *et al., 19*99).

One potential downstream application for these markers is to look at expression of these markers at the protein level to investigate macrophage polarisation in healthy and disease tissue. This would require validation of marker expression at the protein level using techniques such as western blotting or flow cytometry. Another consideration for this is whether expression is specific for macrophages in tissues, as this would dictate their use. For instance, according to the human protein atlas (source: https://www.proteinatlas.org), the corresponding protein for the potential M1 marker *NEURL3* is also highly expressed in cell lines derived from B lymphocytes and pancreatic cells (RPMI-8226 and CAPAN-2 respectively) (Thul *et al., 20*17). Hence when considering macrophage polarisation in any diseases where these cell types are also present (e.g. macrophage infiltration in pancreatic cancer, rheumatoid synovium where B cells and macrophages are present), it is important to consider the likelihood of this marker being cross-expressed. Similarly, the protein for potential M2a marker *HAS3* is strongly expressed in prostate and urinary bladder tissue cell lines (PC-3 and RT4 respectively) (Thul *et al., 20*17). Hence this may not be the ideal marker for identifying M2a macrophages in urinary tissue and male reproductive tissue samples if a single specific marker is required. If expression is not specific in a tissue sample then it would be necessary to co-stain with a pan-macrophage marker such as CD68 (Stöger *et al., 20*12).

Chapter 5: Effect of Immune Complexes on Macrophage Polarisation

5.1 Rationale for investigating effects of immune complexes on monocytes and macrophages

As described in previous Chapters, macrophages are known to polarise into a variety of activation states depending on the stimuli they receive, the most commonly discussed subtypes being given in the bipolar (M1 vs M2) paradigm (Barros *et al., 20*13); (Murray and Wynn, 2011); (Stöger *et al., 20*12). More recently a spectral macrophage activation model has been described which suggests that these cells will respond to any agent that they express a receptor for (Xue *et al*.); (Edwards *et al., 20*06); (Stout *et al., 20*05); (Martinez and Gordon, 2014). Since macrophages are subject to an array of stimuli under physiological conditions they may adopt a more intermediate phenotype or differentiate into a different subs*et al*together (Lumeng *et al., 20*07); (Xue *et al*.); (Villani *et al., 20*17); (Kadl *et al., 20*10). Hence the spectral model of polarisation may be more representative when considering the phenotypes of these cells in disease models and *in vivo*.

As monocytes and macrophages are known to express a variety of Fc gamma receptors (FcγRs), it is possible that they respond to both monomeric IgG (via the high affinity FcγRI) and ICs through binding the low affinity FcγRs (FcγRIIa/b/c and FcγRIIIa) (Jungi and Hafner, 1986). This may have implications for inflammatory diseases where macrophages are key effector cells, and autoantibodies (forming ICs with their cognate antigen) are a pathological feature, such as in RA and SLE.

It should be noted that myeloid cells have been reported to respond to IgG stimuli; effects of ICs on both osteoclast and dendritic cell differentiation have been investigated previously; IC stimulation was described to induce a more macrophage-like phenotype in mouse dendritic cells and reduce antigen presentation capabilities whilst increasing T-cell activating functions (Jancar and Crespo, 2005); (Laborde *et al., 20*07); (Köller *et al., 20*04); (Tanaka *et al., 20*09). Additionally, interaction of ICs with FcγR on myeloid precursor cells has been implicated in osteoclastogenesis in mouse studies (Grevers *et al., 20*13); (Seeling *et al., 20*13).

In terms of macrophages, one study looked at the effect of IgG1-opsonised sheep red blood cells on FcγRI knock out in murine monocytes *in vitro*; some transcriptional profiles were retained but others were reportedly altered under these conditions

(Bezbradica *et al., 20*14). Myeloid cells have been reported to release TNF and other inflammatory stimuli in response to HAGG or anti-Fc receptor antibodies in previous studies, suggesting that an IgG-containing stimulus may drive the inflammatory state to some extent; a theory that requires further examination (Clavel *et al., 20*08); (Ambarus *et al., 20*12); (Barrionuevo *et al., 20*03); (Stout *et al., 20*05). Different sized ICs have variable effects on activation of FcγR expressing cells. For instance, IL-1β and IL-8 production is reportedly upregulated in monocytes treated with larger ICs, and binding of IC to cells also appears to depend on molecule size (Lux *et al., 20*13); (Jarvis *et al., 19*99). Presence of complement and IgG glycosylation can also have an effect (Jarvis *et al., 19*99); (Lux *et al., 20*13). This is particularly relevant for diseases such as RA where patients are found to have pentameric IgM RF targeting IgG, smaller IgG ACPA ICs or both (Song and Kang, 2010). The latter state is associated with increased systemic inflammation and higher disease activity, and *in vitro* treatment of macrophages with both antibodies has been found to induce greater production of cytokines (Sokolove *et al., 20*14).

Some reports have described frustrated phagocytosis in response to immobilised IgG; this occurs when a macrophage (or another phagocytic cell) cannot engulf its IgG-bound target, and so spreads over its surface and releases secretory granules containing lytic substances (Bainton *et al., 19*89); (Takemura *et al., 19*86, Bainton *et al., 19*89). Subsequent degradation of the ICs and adherent surface occurs. This can occur *in vivo*, where ICs are bound to tissue and can be replicated *in vitro* by adhering antibodies to plastic tissue culture flasks (Labrousse *et al., 20*11). This phenomenon has been reported in RA at the cartilage-pannus junction, where deposition of IC was found to induce frustrated phagocytosis in neutrophils, which release reactive oxygen species, cartilage degrading enzymes and other destructive substances, contributing to the damage seen in this condition (Wright *et al., 20*14).

Macrophages treated with ICs (generally IgG1-HAGG) have been studied in the presence of LPS stimuli, i.e. M2b cells. However, the effects of this agent as both an independent signal and in the context of additional immune phenotypes has not been dissected (Xue *et al*.). Although marker panels are useful in identifying presence of phenotype-specific pathways, effects of multiple stimuli are better investigated through analysis of the entire transcriptome; to identify novel gene signatures. Hence the aim of this Chapter was to interrogate the effects of IgG1 HAGG (as a surrogate for IC) on the transcriptomes of monocytes and differentially polarised monocytes using next generation sequencing techniques. IgG1 was used to generate the ICs as different subclasses of IgG have variable affinities for the different FcγR, and use of one subclass only in this study was considered essential for making direct comparisons

between some conditions. Additionally, IgG1 has been found to bind all 6 FcγRs (see Chapter 1, Table 1.3.2). The main hypothesis to be tested here was that IC stimulation of monocytes can skew the transcriptome or phenotype of these cells, and that these changes may contribute to pathologies in auto-antibody driven conditions where macrophages contribute to destructive processes, such as RA and SLE.

5.2 Materials and Methods

5.2.1 Cell culture

THP-1 cells were cultured using the optimised protocol described in Chapter 3; briefly, cells were plated at a concentration of 300,000 cells/ml in RPMI (+ 10% FCS) media (Sigma-Aldrich, CA, USA) and activated with 5ng/ml PMA (Sigma-Aldrich, CA, USA) for 24h. Cells were then washed and incubated in stimulant free media for 72h before polarising cytokines were added for a further 48h. HAGG was prepared as described in Chapter 4 Section 4.2.1.1 and added at the same time point as polarising cytokines for relevant samples. Details of stimuli for different phenotypes generated are given in Table 5.2.1.

Table 5.2.1. Details of all samples sequenced, including treatments which replicate the sample was included in and sample name

Condition	Treatment	Replicate number	Sample name
Monocyte	N/A	1	Mono_1
		2	Mono_2
		3	Mono_3
Monocytes +HAGG	HAGG	1	Mono_IC_1
		2	Mono_IC_2
		3	Mono_IC_3
M0	PMA	1	M0_1
		2	M0_2
		3	M0_3
M0+HAGG	PMA+HAGG	1	M0_IC_1
		2	M0_IC_2
		3	M0_IC_3
M1	IFNγ+LPS+PMA	1	M1_1
		2	M1_2

		3	M1_3
M1+HAGG	IFNγ+LPS+PMA+	1	M1_IC_1
	HAGG	2	M1_IC_2
		3	M1_IC_3
M2a	IL-4+PMA	1	M2a_1
		2	M2a_2
		3	M2a_3
M2a+HAGG	IL-4+PMA+HAGG	1	M2a_IC_1
		2	M2a_IC_2
		3	M2a_IC_3
M2c	IL-10+PMA	1	M2c_1
		2	M2c_2
		3	M2c_3
M2c+HAGG	IL-10+PMA+HAGG	1	M2c_IC_1
		2	M2c_IC_2
		3	M2c_IC_3
LPS	LPS+PMA	1	LPS_1
		2	LPS_2
		3	LPS_3
LPS+HAGG	LPS+PMA+	1	LPS_IC_1
	HAGG	2	LPS_IC_2
		3	LPS_IC_3
TPP	TNF+PGE2+	1	TPP_1
	Pam3SK4+PMA	2	TPP_2
		3	TPP_3
TPP+HAGG	TNF+PGE2+	1	TPP_IC_1
	Pam3SK4+PMA+	2	TPP_IC_2
	HAGG	3	TPP_IC_3

5.2.2 RNA extraction

This was performed as described in Chapter 4 Section 4.2.2 RNA extraction.

5.2.3 Endpoint Polymerase Chain Reaction

Reactions were performed as described in Chapter 3 with the same primers and cycling conditions (Tables 3.2.3, 3.2.4 and 3.2.6).

5.2.4 Flow Cytometry

Cells were digested from tissue culture flasks using trypsin-EDTA solution (0.05% trypsin, 0.02% EDTA) (Sigma-Aldrich, Steinheim, Germany), and once detachment has occurred, the enzyme was neutralised with RPMI media + 10% FCS (Sigma-Aldrich, Steinheim, Germany) at a 1:10 ratio. Cells were subsequently centrifuged at 400 x g for 5 minutes to a pellet before resuspension in fresh RPMI media. 10µl aliquots of cells were then combined with 10µl trypan blue before being loaded onto an Invitrogen countess slide, and counted using an Invitrogen countess (Invitrogen, Carlsbad, USA). Cells were added into wells of a 96 well plate at a concentration of 200,000 cells per well. On ice, cells were blocked with monomeric human IgG1 at a concentration of 2ng/ml for 20 minutes before staining antibody at a concentration on 1:100 (antibody to media, (V:V) was added and kept in the dark for 1 hour. Details of antibodies can be found in Table 5.2.2. Following staining, cells were washed in FACS buffer (PBS, 2% FCS, 2mM EDTA) and finally resuspended in FACS fix buffer (50% FACS buffer, 10% methanol, 2% formaldehyde). Cells were run on a Cytoflex flow cytometer (BD Biosciences, California, USA) using the plate reader arm, set to record data for forward and side scatter as well as on the FITC (520nm) and phycoerythin (PE) (578nm) channels.

5.2.5 Analysis of flow cytometry data

FlowJo software (FlowJo, Oregon, USA) was used to gate living cells and plot data into histograms. Median fluorescent intensities (MFI) of the appropriate channel for all receptors and isotype controls were extracted for the different cell types. This was done for three independent (biological) replicates. MFI was selected as this metric represents the data more closely. The fluorescence for each receptor was normalised for background through subtracting the MFI of the appropriate isotype control from the MFI of the marker. ANOVA statistical tests were used to determine whether there were any significant changes in expression of a specific protein between different cells types using these values. Averages of MFI/isotype control were used to plot bar charts.

Table 5.2.2 details of antibodies used in flow cytometry experiments to stain THP-1 monocytes and macrophages for FcγR phenotyping experiments.

Antibody clone	Fluorescent conjugate	Isotype	Target	Manufacturer details	Isotype control details
IV.3	FITC	IgG2b	FcγRIIa	Stem cell technologies, Vancouver, Canada	IgG2b-FITC BD (Biosciences, California, USA)
3D3	FITC	IgG1	FcγRIIb	BD Biosciences, California, USA	IgG1-FITC BD (Biosciences, California, USA)
DJ130	FITC	IgG1	FcγRIIIa	Merk Millipore, Massachusets, USA	IgG1-FITC BD (Biosciences, California, USA)
Anti-CD64	PE	IgG1	FcγRI	Bio-Rad, California, USA	PE BD (Biosciences, California, USA)

5.2.6 RNA library preparation, sequencing, alignment to reference genome, adaptor removal, quality checking and production of count Tables

These processes were performed as described in Chapter 4, Sections 4.2.4-4.2.8.

5.2.8 Differentially expressed gene identification

Differentially expressed genes between IC treated and non-IC treated samples were identified through pairwise comparisons performed using DESeq2 package as described in Chapter 4, Section 4.2.9.

5.2.7 Principle component analysis

As highlighted in Chapter 4, all R scripts with annotations describing commands may be found in Appendix 3. This was performed as described in Chapter 4 Section 4.2.10 but with additional conditions included as input, i.e. IC treated samples.

5.2.9 Analysis of individual replicates

For samples where replicates were not consistent, a script was used that determined differential expression between two conditions in the same replicate. Here, samples of interest were selected from the counts Table. An exact test was used to determine significant differential expression in this list using an arbitrary variance estimate of 0.2. Further analyses of DEG lists were performed in the same ways as gene list produced using replicates, i.e. as in Chapter 4, Section 4.2.9.

5.2.10 Gene ontology enrichment analysis

Lists of significantly differentially expressed genes identified in Sections 5.2.5 and 5.2.6 were analysed here. Analysis of these gene lists were performed as described in Chapter 4 Section 4.2.11.

5.2.11 Transcription factor enrichment analysis

This was performed as described in Chapter 4 Section 4.2.12, using gene lists produced through contrasting IC treated and non-IC treated samples (through processes described in Sections 5.2.8 and 5.2.9).

5.2.12 Network visualisation

TFs of interest were entered into STRING app on Cytoscape as a network, and a cut-off of top 30 interactors was set. A count Table for transcripts which contained columns for gene symbols (generated during the steps in Section 5.2.7), log2 fold change and –log10 adjusted p value was imported. Node parameters were adjusted so colour reflected –log10 adjusted p-value and size represented log2 fold change, and gene symbols were used as identifiers. Network plots were then exported as images.

5.2.13 Identifying reads specifically mapping to *FCGR* genes

Discriminating regions were identified for the different *FCGR* genes using pre-existing sequencing data (Robinson *et al., 20*12). For *FCGR2* a region of exon 3 was used; there are confirmed paralogous sequence variants (PSVs) specific for *FCGR2A* (when compared to *FCGR2B* and *FCGR2C)* in this region. There are no confirmed differences in the reference sequences of *FCGR2B* and *FCGR2C* in this region, but there are confirmed single nucleotide polymorphisms (SNPs) for *FCGR2C*. As THP-1 cells are homozygous for a *FCGR2C* SNP (rs10917661) which differs from *FCGR2B*, it was possible to use this region to distinguish transcripts from these two genes. SNPs and PSVs which were targeted are demonstrated in the alignment in Figure 5.2.1. Regions of exon 5 in *FCGR3A* and *FCGR3B* and the *FCGR3B* untranslated region (3' UTR) were used to distinguish these two regions. Genomic co-ordinates are given in Table 5.2.3 and nucleotide differences between the genes that were targeted by this analysis are highlighted in Figure 3.2.2. Co-ordinates for these regions were incorporated into the hg38 GTF file, which was used as a modified genome annotation file. Details of these regions are given in Table 5.2.3. Mapping was performed using STAR alignment software (Dobin *et al., 20*13) as described in Chapter 4 Section 4.2.7, to produce output BAM files. As before, alignment was performed with stringent parameters controlling mismatches between read sequences and reference genome (see Chapter 4, Section 4.2.8). As in Chapter 4, Section 2.4.8, raw counts were added into a Table using Rsubread (as in Chapter 4, Section 4.2.8) and read into R for analysis. Counts were normalised using functions in the DESeq package and by dividing the read count by length of the reference region. Figures were plotted for expression using ggplots2 and pheatmap packages in R. One-way ANOVA statistical tests were performed in Microsoft Excel using the "Data Analysis" add-on to identify any significant changes in gene expression in different cell types and subtypes.

Table 5.2.3 Genomic coordinates (Hg38 assembly) for specific regions of different *FCGR* genes, used to differentiate them and used as targets when reads were mapped to give expression counts.

Gene	Chromosome	Start	End	Length (bp)	Strand
FCGR2A	1	161506333	161506474	142	+
FCGR2B	1	161671388	161671546	159	+
FCGR2C	1	161589562	161589701	140	+
FCGR3A	1	161541771	161543240	1470	-
FCGR3B	1	161623138	161624731	1594	-

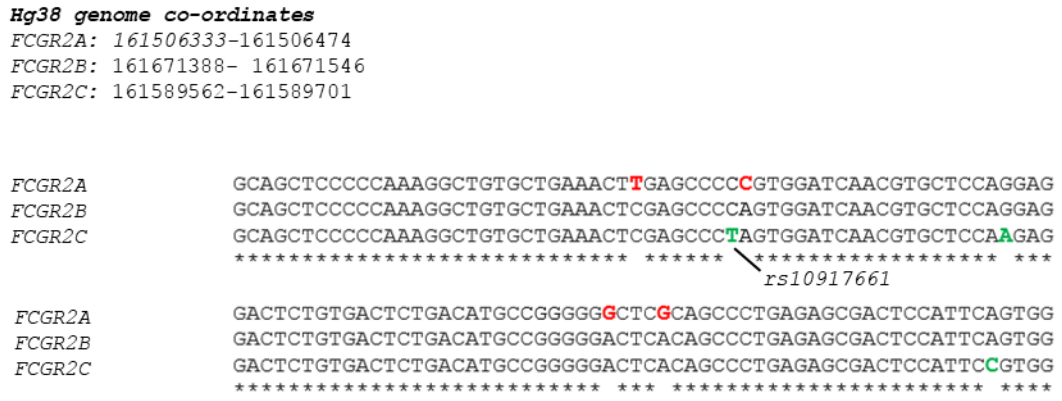

Figure 5.2.1. Alignments of target regions of *FCGR2A, FCGR2B* and *FCGR2C* demonstrating homology between regions and highlighting differences in sequences; SNPs are highlighted in green and conserved differences between the genes are in red.

Figure 5.2.2. Genomic DNA alignments of regions of *FCGR3A* and *FCGR3B* which were used for the remapping analysis, demonstrating homology between regions and highlighting differences in sequences that differentiate the genes; PSVs are highlighted in red. PSV=paralogous sequence variant, SNPs are in green and indels are blue. All non-highlighted regions are in exon 5 of *FCGR3A* or *FCGR3B*. Grey box indicates 3' untranslated region of *FCGR3B.* Genome co-ordinates are given on top left-hand side. PSV=paralogous sequence variant, SNP=single nucleotide polymorphisms.

5.3 Results

5.3.1 Fc-gamma Receptor expression is variable between different macrophage subtypes

To investigate the effects of IgG-ICs on different macrophage sub-types, it was important to profile the expression levels of FcγR on these cells. Thus, any differences in polarisation or gene signatures observed may be linked to FcγR signalling pathways. Flow cytometry was therefore performed to investigate FcγR expression on cell membranes (where the interactions with ICs occur) (Figure 5.3.1), and RNA-seq data were extracted from a larger dataset to quantify abundance of FcγR transcripts (Figure 5.3.2). Due to the high homology of the different subtypes of *FCGR* genes, a stringent analysis was performed where reads mapping to specific variable regions only were counted. It must be noted that due to the selective nature of this experiment, counts were an underestimation of expression for these genes. However, this analysis provided an indication of how these transcripts were expressed relative to one another.

Flow cytometry data demonstrated expression of FcγRI on monocytes and all macrophage subtypes (Figure 5.3.1, A). It should be noted however, that the expression levels appeared to be lower on the less inflammatory cells (M2a and M2c) (Figure 5.3.1, A, left hand side panel) and TPP cells did not appear to express high levels of this receptor (Figure 5.3.1, A, bottom left histogram). This could indicate distinct functioning in macrophages found in chronic and acute inflammation in terms of FcγR responsiveness. ANOVA tests performed on corresponding fluorescent values (corrected for isotype control fluorescence) for 3 flow cytometry experiments demonstrated a significant difference (p-value <0.05) in the expression of FcγRI between the different cell types (Figure 5.3.2). Generally speaking, bar charts of averages of fluorescent values (for the 3 experimental replicates) demonstrated a similar pattern to histograms, with lowest expression levels of FcγRI seen for M2a, M2c and TPP induced cells. Please note that raw fluorescent data for analyses performed can be found in appendix A5.

Comparisons of staining antibodies with isotype controls demonstrated expression of FcγRIIa on all cell types (Figure 5.3.1, A). Upon examination of the histograms in Figure 5.3.2, A, there was no clear visual difference in the expression levels of FcγRIIa between most macrophage subtypes, although the right-shift (of staining antibody versus isotype control) appeared to be greatest for M2a cells. Bar charts plotting fluorescent values (reflecting protein levels) of 3 experimental repeats also indicated increased expression of FcγRIIa on M2a cells (Figure 5.3.2, B). It should also be noted here that comparison of FcγRIIa levels between all the samples demonstrated a

significant difference (p-value <0.01) in protein expression according to ANOVA (Figure 5.3.1, B).

The genotype of THP-1 cells allows distinction of FcγRIIa (131H-corresponding SNP in THP-1 cells) and FcγRIIb (131R-corresponding PSV) cells using the 3D3 anti-CD32 antibody which recognises 131R specifically. Expression of the inhibitory FcγRIIb was not found to be significantly different between distinct cell types (Figure 5.3.1, B). However, upon inspection of flow cytometry histograms, there did appear to be an increase in expression of FcγRIIb on M2a cells (Figure 5.3.1, A). This was reflected on the bar chart containing data for the 3 experimental replicates (Figure 5.3.2, A); this is interesting as this is an inhibitory receptor and M2a cells are anti-inflammatory. Hence this observation may relate to the anti-inflammatory functions of these cells. Future experiments with an increased number of replicates may increase statistical power for comparisons and reveal a difference in significance of this change.

Histogram presentation of FcγRIIa revealed consistent lack of FcγRIIIa expression on all cells (Figure 5.3.1, A). This was unexpected as this receptor is generally reported to be expressed on macrophages (Bhatia *et al., 19*98); (Albright *et al., 20*04); (Guilliams *et al., 20*14). However, it should be considered that high levels of background fluorescence from presence of the IgG binding FcγRI protein was observed despite blocking with monomeric IgG1 antibodies or Fc block. It is possible that high levels of this protein on the cell surface may mask any subtle changes in FcγR expression. Alternatively, the THP-1 cells may have accumulated mutations preventing the expression of this protein.

RNA-seq data for replicates 1 and 3 (run on lanes 4 and 6 of the sequencer respectively) were analysed together as they have previously been shown to be consistent (Chapter 4, Figure 4.3.2). Replicate 2 (lane 5) transcript expression was provided separately, so FcγR expression in this experiment could be considered, without skewing the clustering of samples run on the other lanes. *FCGR1A* expression was high for all conditions (Figure 5.3.2, A), supporting observations for the protein surface expression experiment (Figure 5.3.1, C).

Some finding from the original alignment (non-stringent alignment) of RNA-seq reads to reference genome corroborated findings from the flow cytometry experiment; *FCGR2A* expression was reported for all subtypes and was seen to be in M2a cells (Figure 5.3.2). However, as described previously, additional methods were required to differentiate these highly homologous transcripts (Figure 5.3.2, B and C). Normalised counts from the stringent alignment experiment were analysed for each region using ANOVA tests; Expression levels of *FCGR2A* were found to be significantly different (p-

value <0.05) between the different cell types tested. This was not the case for *FCGR2B* and *FCGR2C* trannscripts (Figure 5.3.2, C). In agreement with the flow cytometry data, expression of the *FCGR2A* transcript appeared to be most highly expressed in M2a macrophages (Figure 5.3.2, C (i) and D (ii)).

FCGR2C protein is not found on THP-1 macrophages as they are homozygous for the STP allele that prevents translation. However, the possibility that non-coding transcripts were produced under certain experimental conditions was considered; expression of *FCGR2C* transcripts appeared to be relatively lower than *FCGR2B*, and *FCGR2B* expression seemed to be decreased when compared to *FCGR2A* in all conditions (Figure 5.3.2, C (i) and D (ii)). This analysis also demonstrated that it is possible to distinguish between *FCGR2A*, *FCGR2B* and *FCGR2C* transcripts in these cells.

Using the stringent realignment method, no significant difference was found in expression of *FCGR3A* or *FCGR3B* between monocytes and macrophage subtypes (Figure 5.3.2, C). As *FCGR3B* encodes a neutrophil-specific receptor (Smith and Clatworthy, 2010) no expression was expected in these myeloid cells. This was reflected in the alignment data for this transcript in Figure 5.3.2, D (ii); in terms of relative expression, *FCGR3B* was low versus *FCGR3A* transcripts in all conditions. When comparing these two transcripts, it appeared that there may be some transcription of *FCGR3A,* as normalised counts were higher versus those for *FCGR3B* (Figure 5.3.2, D (ii)). However, when compared to the *FCGR2* genes which were normalised in a similar way, expression of both *FCGR3* transcripts appeared to be lower (Figure 5.3.2, C). Hence it is possible that *FCGR3A* was only expressed at a very low level, which may lend an explanation as to why no protein expression was reported for the flow cytometry data.

It must be emphasised that for the stringent analysis, it was only possible to use small (distinguishing) regions of the gene. Hence number of reads mapping would be inherently lower, and small changes in receptor expression between the different *FCGR* transcripts are less likely to be identified or considered as statistically significant. Therefore, this method may underestimate variance between receptor expressions on different cells. However, due to the highly homologous nature of the *FCGR* transcripts, use of larger regions would reduce specificity and confound results.

Overall expression of FcγRs appears to vary between monocytes and different macrophage subtypes, suggesting that these cells may respond differently to treatment with IC. Raw data for flow cytometry statistics may be found in appendix 5.

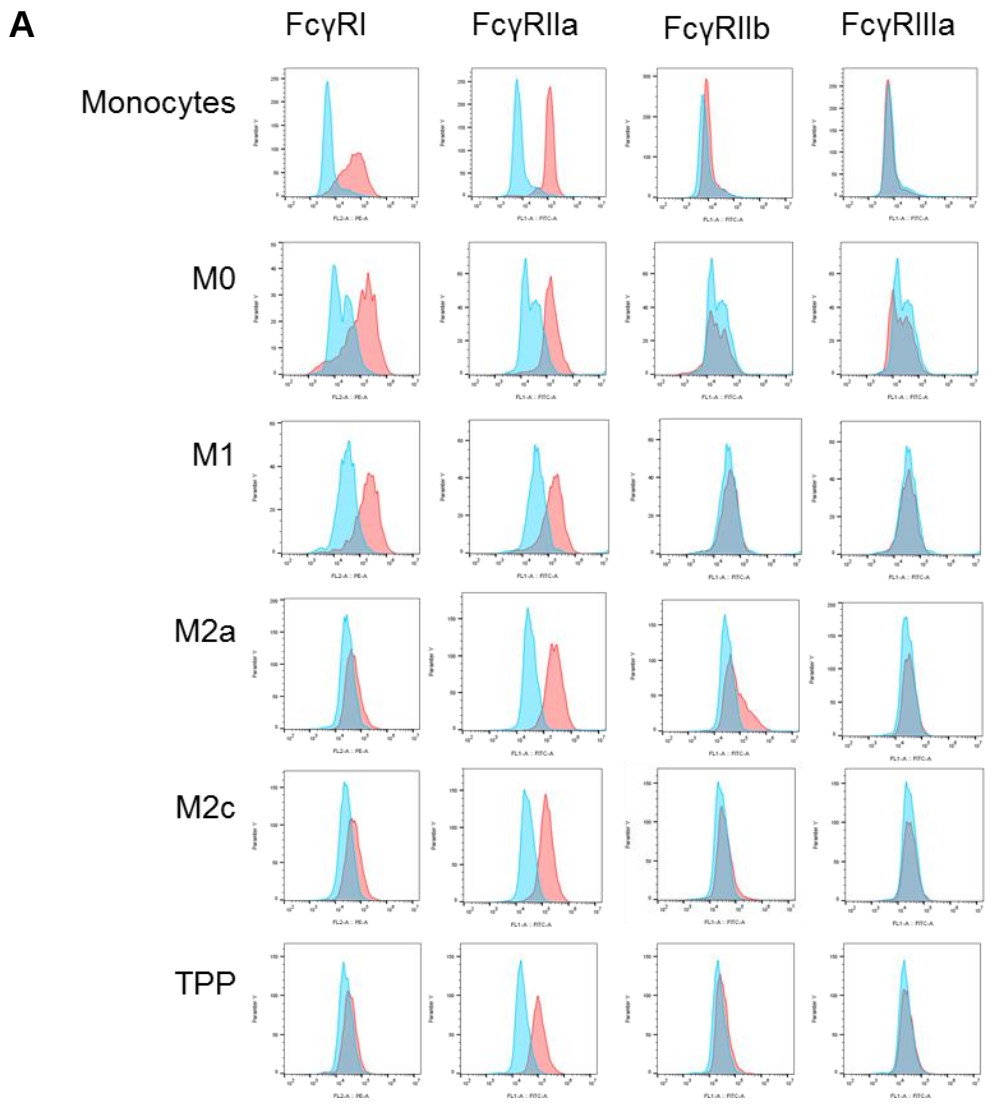

Figure 5.3.1. Part 1. Histograms showing surface expression of Fcγ receptors in monocytes and different macrophage subsets using flow cytometry; staining antibody (pink) versus isotype control (blue). Monocytes (top panel), baseline M0 macrophages (panel 2) and differentially polarised macrophages (panels 3-6) were tested. The latter included TPP macrophages differentiated using tumour necrosis factor, prostaglandin E2 and toll-like receptor 2 agonist Pam3SK4. examples shown are representative of three repeats. Please see Appendix 1 for replicates 2 and 3. **(A)**. Vertical axis corresponds to cell frequency, horizontal axis represents mean fluorescence intensity.

B (i)

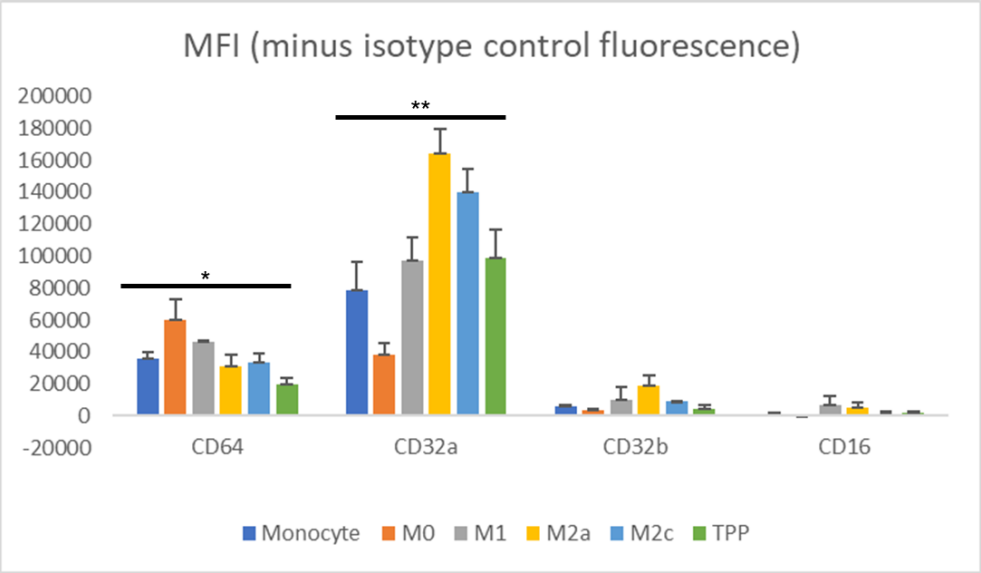

(ii)

ANOVA	
Receptor	p-value
CD64	0.015705922
CD32a	0.000966197
CD32b	0.182754706
CD16	0.552795545

Figure 5.3.1. Part 2. Bar charts illustrating averages (means) of flow cytometry median fluorescent intensities (MFIs) of three independent replicates, corrected for background by subtracting fluorescence of isotype control. * indicates that a p-value less than 0.05 was found when comparing samples using ANOVA tests and ** indicates a p-value of less than 0.01 when comparing samples by ANOVA. Error bars represent standard error of the mean **(B (i)).** Results of ANOVA test for each receptor are also given **(B (ii)).**

C i)

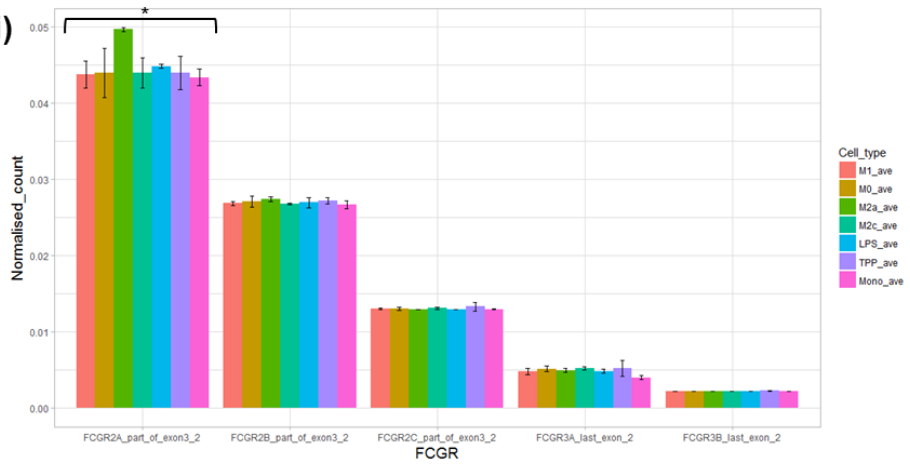

ii)

ANOVA	
Gene	**P-value**
FCGR2A_part_of_exon3_2	0.04789
FCGR2B_part_of_exon3_2	0.604478
FCGR2C_part_of_exon3_2	0.641035
FCGR3A_last_exon_2	0.271063
FCGR3B_last_exon_2	0.321162

iii)

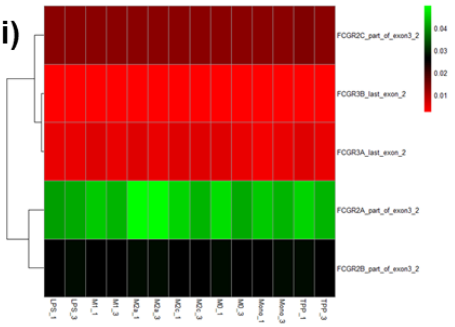

D i)

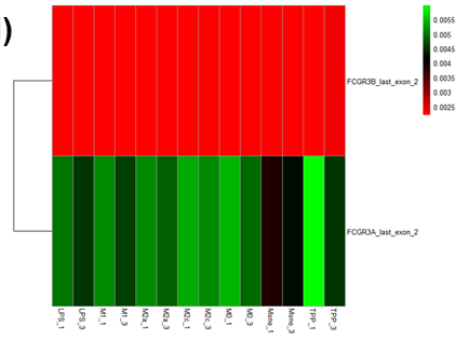

ii)

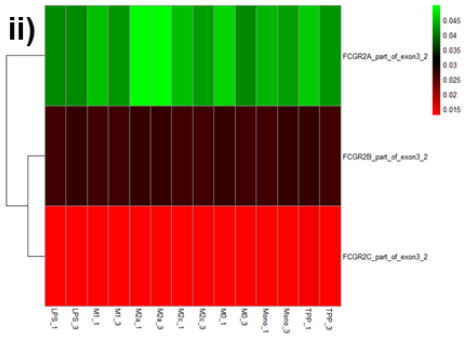

Figure 5.3.2. Part 3. Mean expression of various *FCGR* transcripts (normalised by dividing by length) in variably polarised macrophages, grouped by receptor. . * significant difference < p=0.05 was found between samples according to ANOVA statistical tests (**C (i)**). P values for ANOVA tests performed for expression of the different receptors between groups are given (**C (ii)**). Heatmap of relative expressions of *FCGR2* and *FCGR3* transcripts (**C (iii)**). Heatmap of relative expressions of *FCGR2* transcripts only (**D (i)**), heatmap of relative expressions of *FCGR3* transcripts only (**D (ii)**).

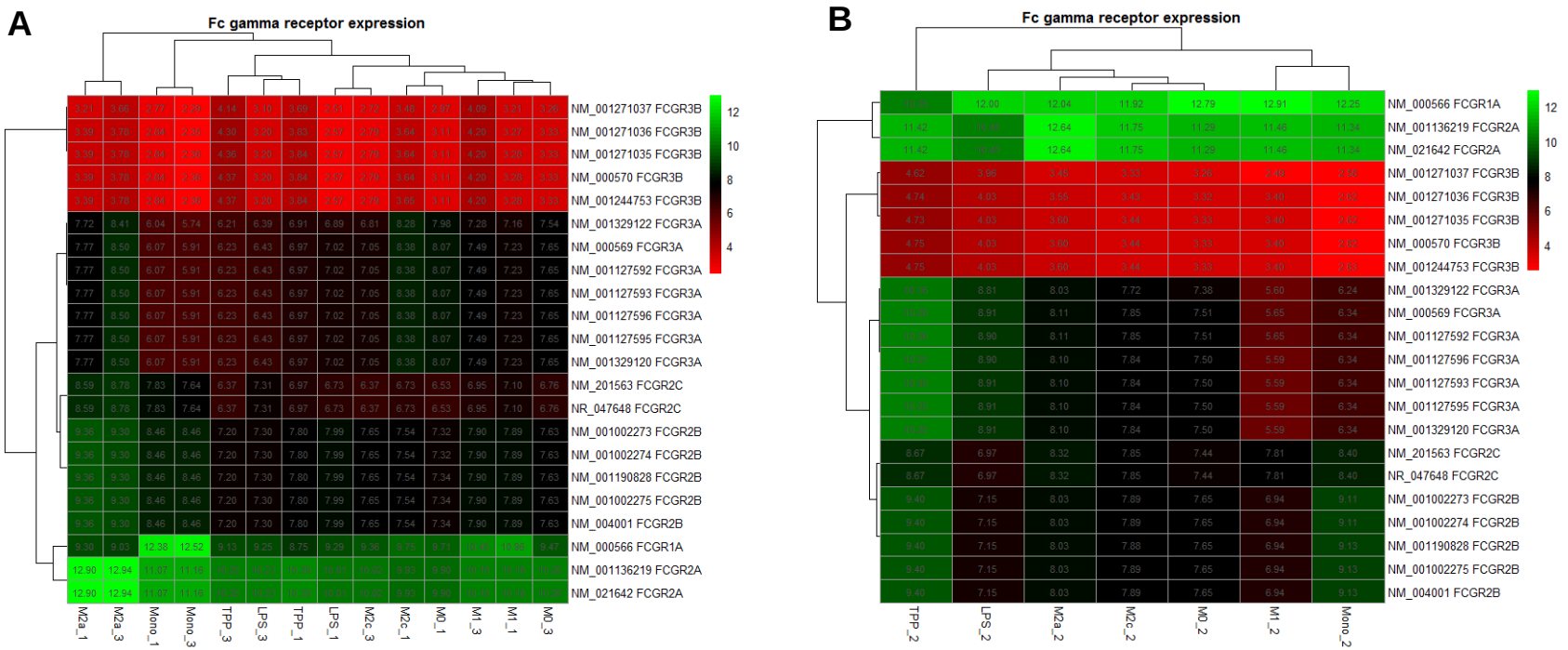

Figure 5.3.2. Expression of different Fcγ receptor transcripts in monocytes and various macrophage subtypes according to RNA-seq data; expression is given in the more consistent replicates 1 and 3 (**A**) and in replicate 2 separately (**B**). Refer the reader to the description of transcripts.

5.3.2 Macrophage morphology and adherence upon addition of immune complexes

Macrophage morphology for inflammatory and anti-inflammatory subtypes has been described consistently in the literature, with the former reported as being more spindle-like and the latter rounder in shape. Hence morphology may be used to infer the polarisation status of cells. As seen in Figure 5.3.3, upon treatment with HAGG the different polarisation states appear to retain their subset-specific morphology, but it should be noted that a larger number of cells were adhered to the tissue culture flask, despite seeding densities of cells and other treatments remaining consistent. It is possible that the cells were activated to a more adherent state, or that the HAGG coated the plastic allowing more cells to attach to the flask via FcγRs. However, the latter is less likely as ICs were not added to the flask first, and instead to the media covering the cultured cells. To validate this finding, cell counts following completion of the protocols should be performed.

5.3.3 Many macrophage polarisation transcripts retain subset-specific expression when treated with immune complexes

Prior to the sequencing, cells were cultured using the protocol described in Chapter 3 for the M1, M2a and M2c subtypes, but with an addition of HAGG (IC) at the polarisation stage. The aim was to identify any obvious changes in macrophage transcriptional profiles in response to IgG1 IC; one isotype was used for simplicity, and IgG1 was selected as it is able to bind all classes of FcγR (Bruhns *et al., 20*09). End-point PCR did not highlight any major changes in these lineage specific genes (Figures 5.3.4-5.3.6); some transcripts appeared to be more strongly induced but overall expression pattern was not altered. One possible change was in the IC-treated “M1” cells; CD163, an M2c marker demonstrated non-specific up regulation in the non-IC treated subtype, which was completely abrogated upon IC treatment.

When examined using RNA-seq data, the different macrophage subtypes appeared to follow the same patterns for marker gene expression, regardless of whether IC were added for the 48h polarisation phase of the tissue culture experiment or not (Figure 5.3.7).

Overall it appears that IC-treatment does not drastically alter polarisation, as expression of transcription markers is retained following addition of this stimulus.

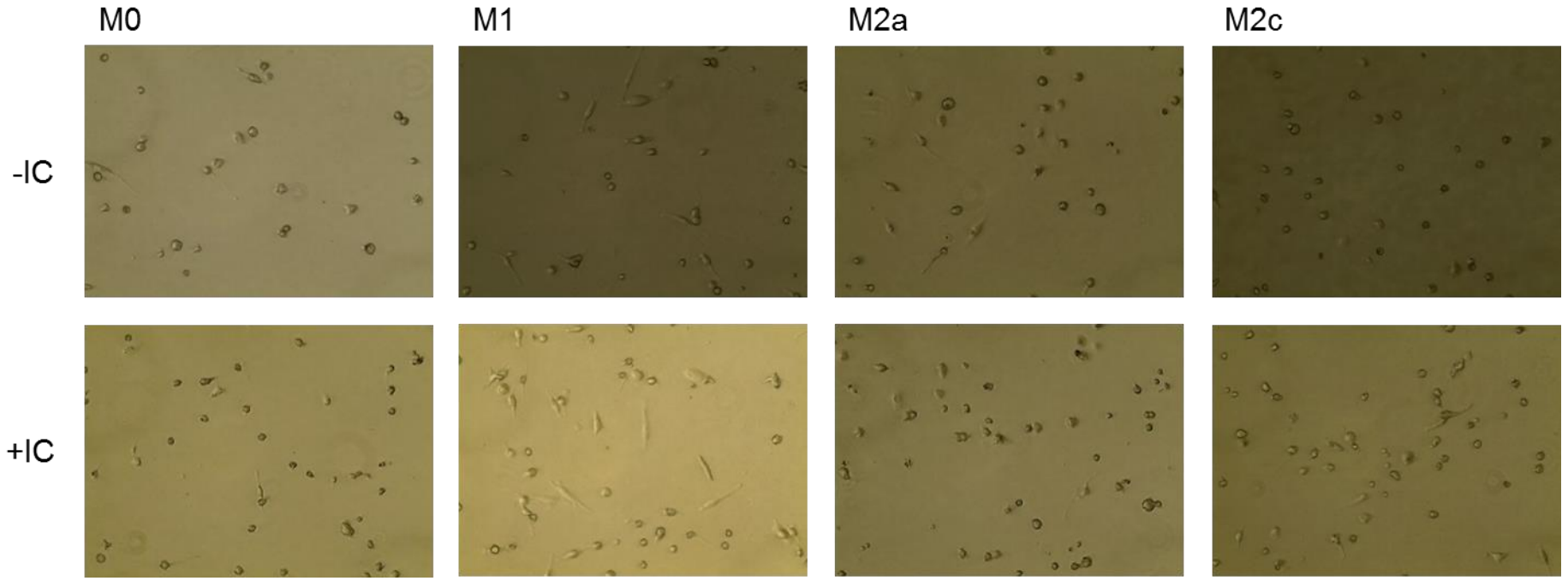

Figure 5.3.3. Morphology of different macrophage subtypes with and without immune complex addition taken at 20x magnification on an EVOS light microscope

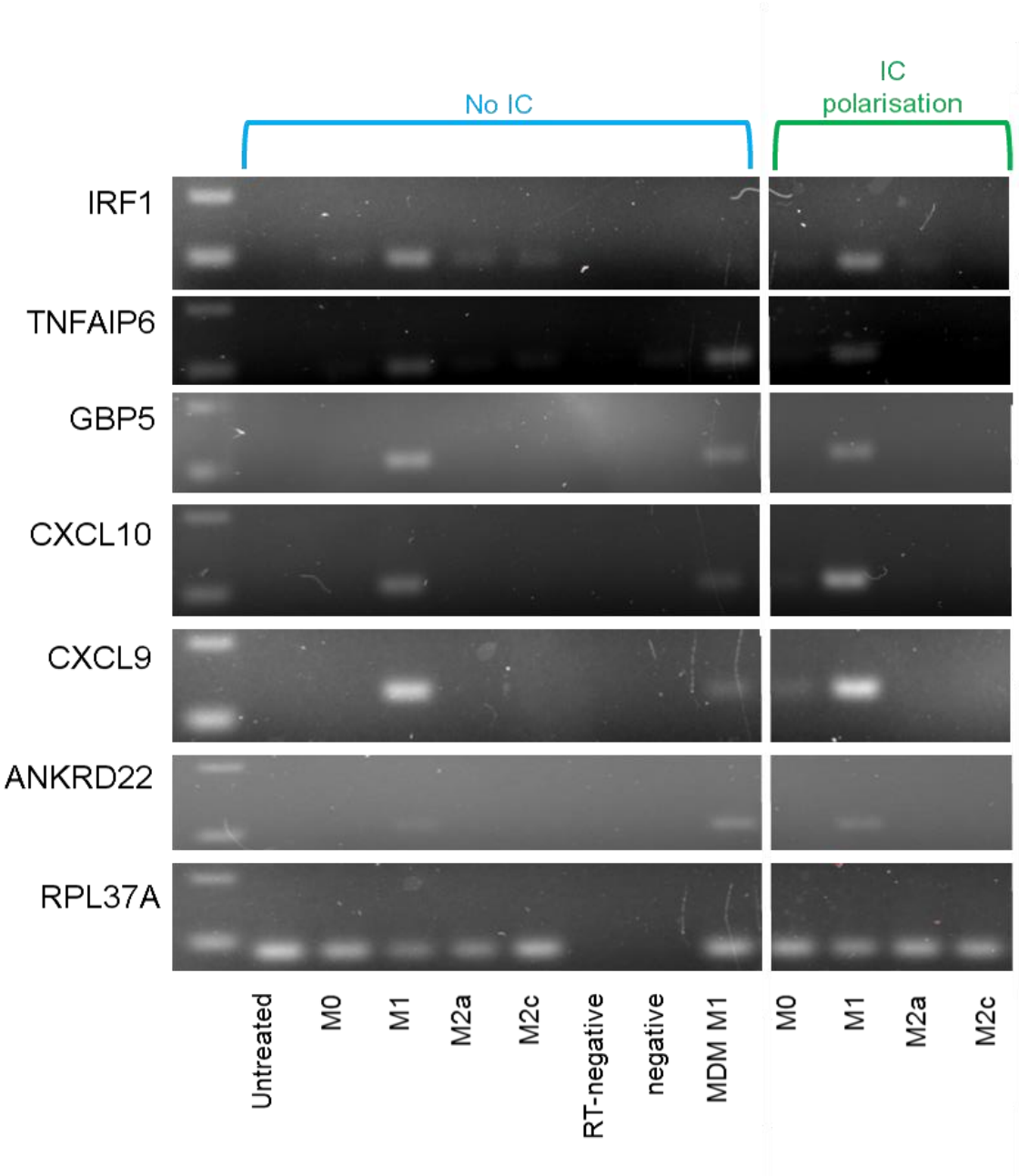

Figure 5.3.4. Expression of M1 marker panel genes in differentially polarised macrophages upon addition of heat aggregated gamma globulin (HAGG, as an experiment surrogate for physiological IC) according to PCR analysis. No IC referred to differentially polarised cells which were not supplemented with IC and IC polarisation indicated that the cells were treated with HAGG/IC during the 48h polarisation stage of the tissue culture experiment.

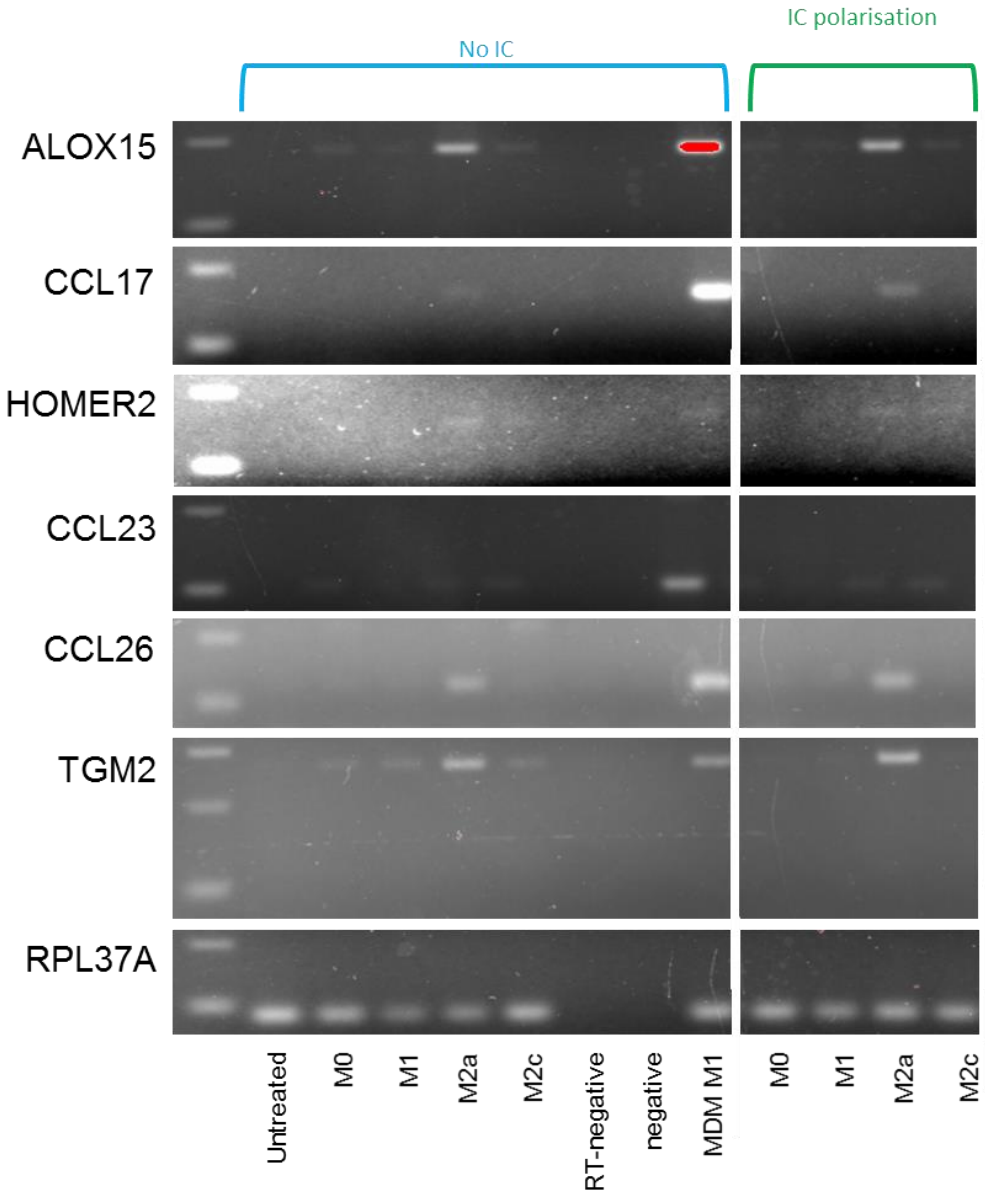

Figure 5.3.5. Expression of M2a marker panel genes in differentially polarised macrophages upon addition of heat aggregated gamma globulin (HAGG, as an experiment surrogate for physiological IC) according to PCR analysis. No IC referred to differentially polarised cells which were not supplemented with IC and IC polarisation indicated that the cells were treated with HAGG/IC during the 48h polarisation stage of the tissue culture experiment.

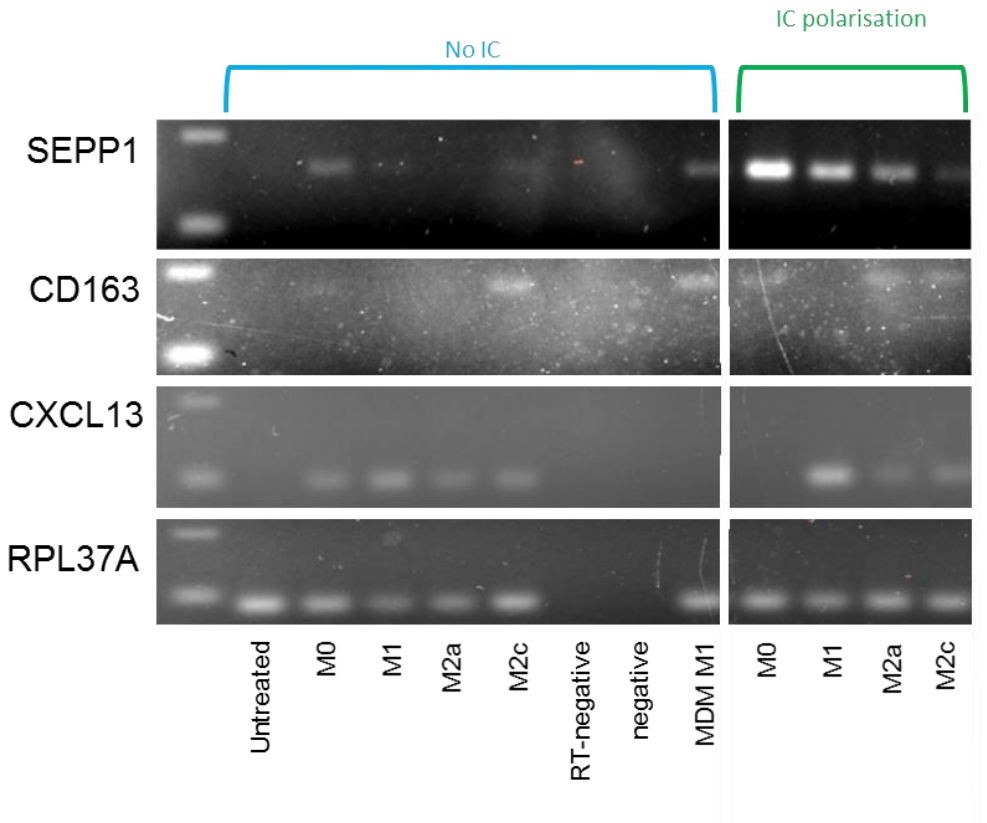

Figure 5.3.6. Expression of M2c marker panel genes in differentially polarised macrophages upon addition of heat aggregated gamma globulin (HAGG, as an experiment surrogate for physiological IC) according to PCR analysis. No IC referred to differentially polarised cells which were not supplemented with IC and IC polarisation indicated that the cells were treated with HAGG/IC during the 48h polarisation stage of the tissue culture experiment.

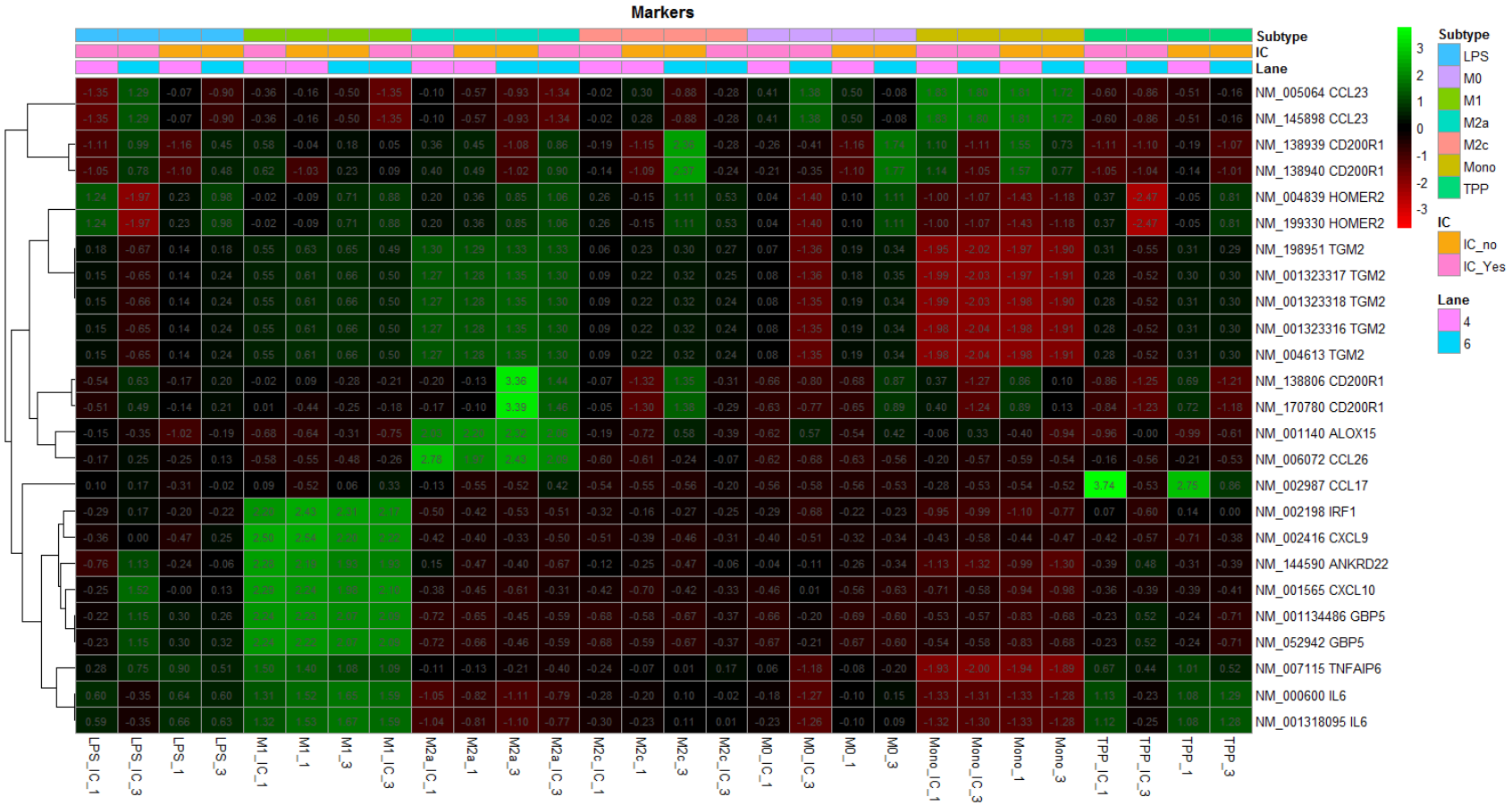

Figure 5.3.7. Quantitative expression of M1 and M2a marker panel transcripts in differentially polarised macrophages upon addition of heat aggregated gamma globulin (HAGG) according to RNA-seq data

5.3.4 Principle component analysis examined how differentially polarised cells with and without immune complex treatment clustered according to most variable genes

As with the differentially polarised subsets in Chapter 4, PCA plotting was used to examine dispersion of samples based on the top 1000 most differentially expressed genes. As replicate 2 was previously determined to be an outlier (Chapter 4, Figure 4.3.2), analyses in this Section were performed separately for samples in this replicate and those in replicates 1 and 3, which were combined.

In the PCA plot corresponding to replicates 2 and 3, when the samples treated with ICs were added, the overall mapping of differentially polarised cells did not seem to change compared to that seen in Chapter 4 (with the non-IC treated samples only, Figure 4.3.3), but there did appear to be some additional outliers (Figure 5.3.8, A). When scrutinised for top loading genes and biological process enrichment terms, it appeared that principle component 1 (x-axis) strongly represented cell migration (Figure 5.3.8, C (i) and (ii)). As this function discriminates monocytes and macrophages (Tuomisto *et al., 20*05), it could be put forward that this axis represents cell differentiation, as was the case with the first principle component in the absence of IC treated samples (Chapter 4, Figure 4.3.3). Principle component 2 loading genes appeared to be more inflammation related, and enriched biological processes highlighted response to pathogens (Figure 5.3.8, D (i) and (ii)). Hence this axis separates cells by inflammatory state (i.e. polarisation status), as was the case with basic conditions discussed in Chapter 4 (Figure 4.3.3).

Figure 5.3.8, B indicates how the samples in replicate 2 cluster according to the 1000 most differentially expressed genes for these samples. Mapping of these genes varied greatly from that seen for replicates 2 and 3; here x-axis still demonstrated separation of M1, LPS and TPP samples from monocytes (irrespective of IC treatment), but M0 and M2 conditions appeared to cluster more closely to the monocytes. Analysis of loading genes for this component revealed some inflammatory markers (*CXCL10, CXCL11, CCR7*) which would explain this pattern (Figure 5.3.8, E (i)). Some of the enriched biological terms referred to functions separating monocytes from macrophages (e.g. cell migration, cell chemotaxis), but some were linked to inflammatory polarisation (e.g. response to LPS, positive regulation of cytokine production) (Figure 5.3.8, E (ii)). Hence this axis may separate samples by both cell maturity and whether or not treatments included an inflammatory stimulus. This is supported by the fact that inflammatory samples map distinctly from all other samples

here, and that monocytes are the cells plotted furthest from M1/LPS/TPP samples along the x-axis.

Based on Figure 5.3.8, B, the y-axis (principle component 2) appeared to separate M1 cells from those of the TPP and LPS subtype, both of which are inflammatory conditions. Monocytes, M0 and M2 conditions appeared to map around the same point as the LPS (with and without IC) samples here. Top loading genes again contained inflammation-related transcripts (e.g. *CXCL9, CXCL10, CXCL11*) suggesting again that this axis separated samples to some degree by polarisation (Figure 5.3.8, F (i)). This was supported by enrichment of biological processes that again related to cell migration and polarisation (e.g. leukocyte migration, response to LPS) (Figure 5.3.8, F (ii)).

Overall this mapping appears to reflect how either M1 or TPP conditions (with or without IC) relate to other treatments. Hence it is possible that the most differentially expressed genes in this replicate may relate to how transcripts are up/downregulation in M1/TPP samples versus others.

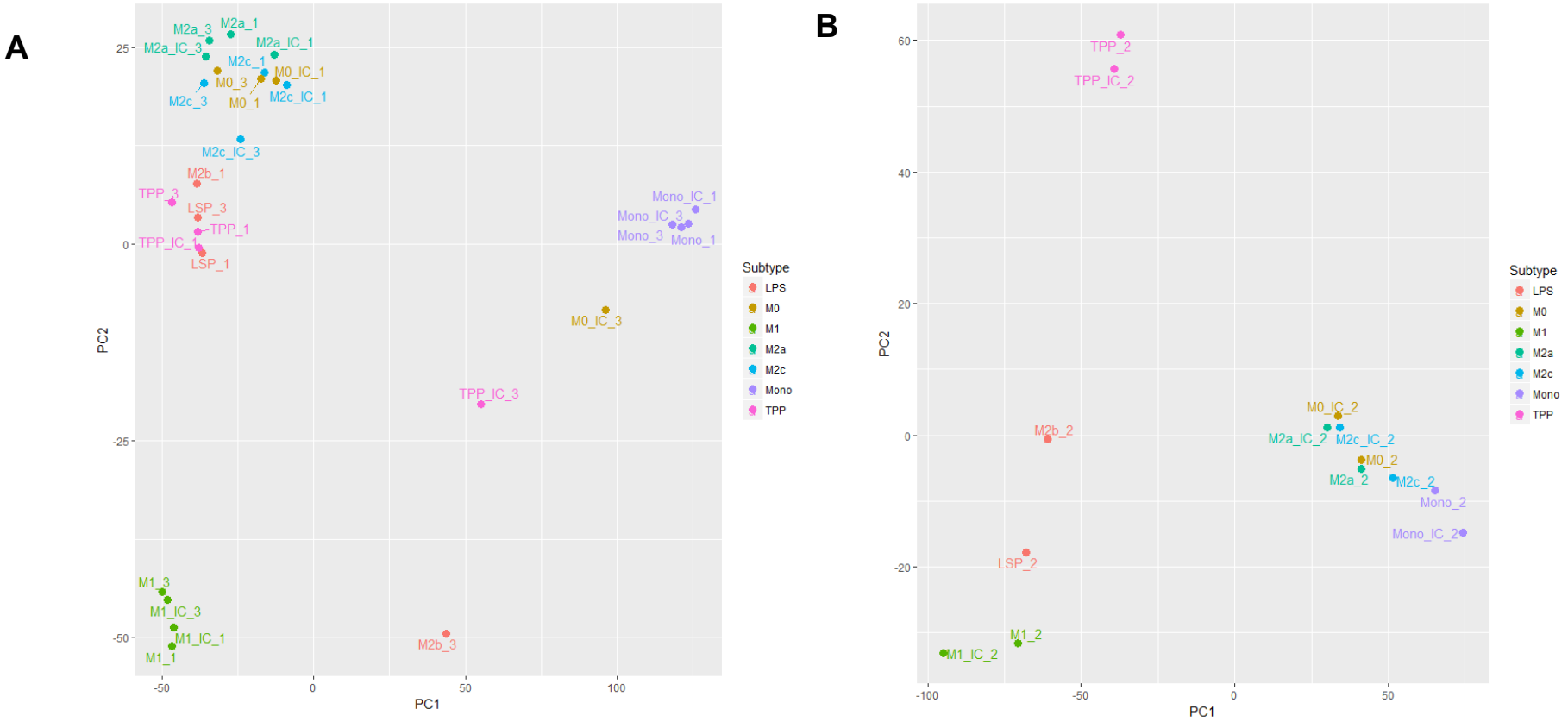

Figure 5.3.8. (part 1) PCA plot indicating how differentially polarised macrophages with and without immune complexes cluster according to 1000 most variable genes (**A**) for replicates 1 and 4 combined (**B**) for replicate 2 only

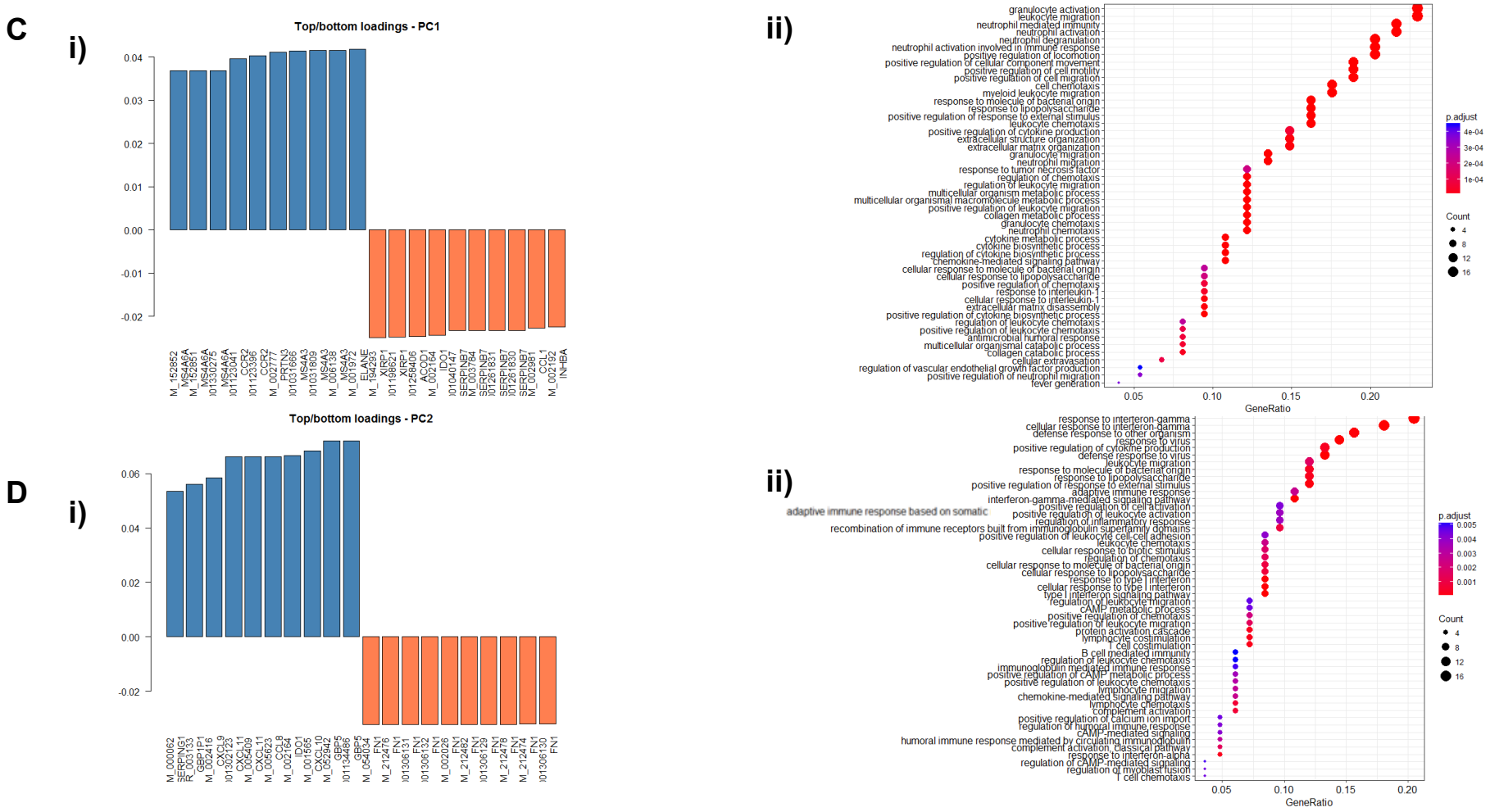

Figure 5.3.8. (part 2) Analysis of PCA loading genes; (**C**) for replicates 1 and 3 combined **(i)**, top 10 and bottom 10 loading genes in principle component 1 (**i**) and top 50 enriched biological processes for principle component 1 (**ii**); (**D**) for replicates 1 and 3 combined **(i)**, top 10 and bottom 10 loading genes in principle component 2 (**i**) and top 50 enriched biological processes for principle component 2 (**ii**)

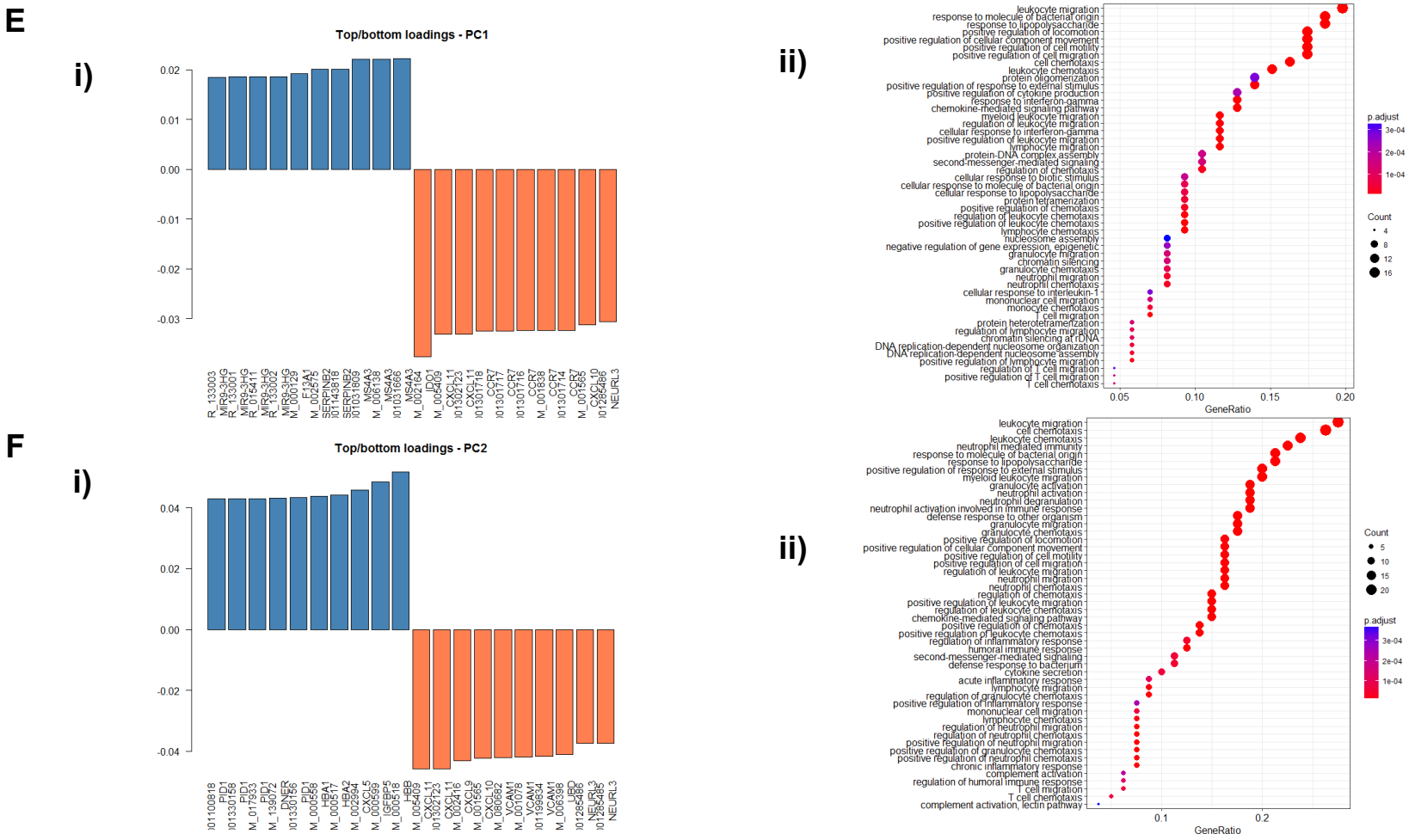

Figure 5.3.8. (part 3) Analysis of PCA loading genes; (**C**) for replicate 2 **(i)**, top 10 and bottom 10 loading genes in principle component 1 (**i**) and top 50 enriched biological processes for principle component 1 (**ii**); (**D**) for replicate 2 **(i)**, top 10 and bottom 10 loading genes in principle component 2 (**i**) and top 50 enriched biological processes for principle component 2 (**ii**)

5.3.5 Clustering varied between different replicates for macrophage samples

As described previously, PCA plotting gives an indication of how samples relate to one another; this is helpful for inferring functional changes between different samples. As the changes seen upon addition of ICs are not consistent, mapping of samples was examined for individual replicates (Figure 5.3.9).

All subtypes in replicate 1 (both with and without IC treatment) appear to follow a similar pattern to original PCA plots (discussed for Chapter 4, Figure 4.3.2); principal component 1 (x-axis) separates the monocytes from the differentiated macrophage samples and principal component 2 (y-axis) discriminates conditions by polarisation state, i.e. with M1 and M2a at opposing ends of the scale. This implies that either the samples in this experiment did not respond strongly to the IC stimulus or that addition of IgG1-IC does not skew polarisation.

Replicates 2 and 3 show less consistent clustering; it is unclear how the samples in these plots map in terms of differentiation and polarisation, but plots do give some indication of how similar IC-treated cells are to those of non-IC conditions. For instance, subtypes of the same polarisation state +/- IC appeared to map similarly in replicate 2, although LPS and M2b conditions show some separation. For replicate 3, LPS, TPP and M0 macrophages treated with ICs appear to map completely differently to respective parent subtypes. Hence the subtypes in this replicate may have responded more to IC-treatment. Other subtypes in this experiment tended to cluster together regardless of whether IC was added or not. It is therefore likely that the most variable factors between the samples were results of batch effects which arose from conducting the experiment at different time points rather than polarisation state of IC addition.

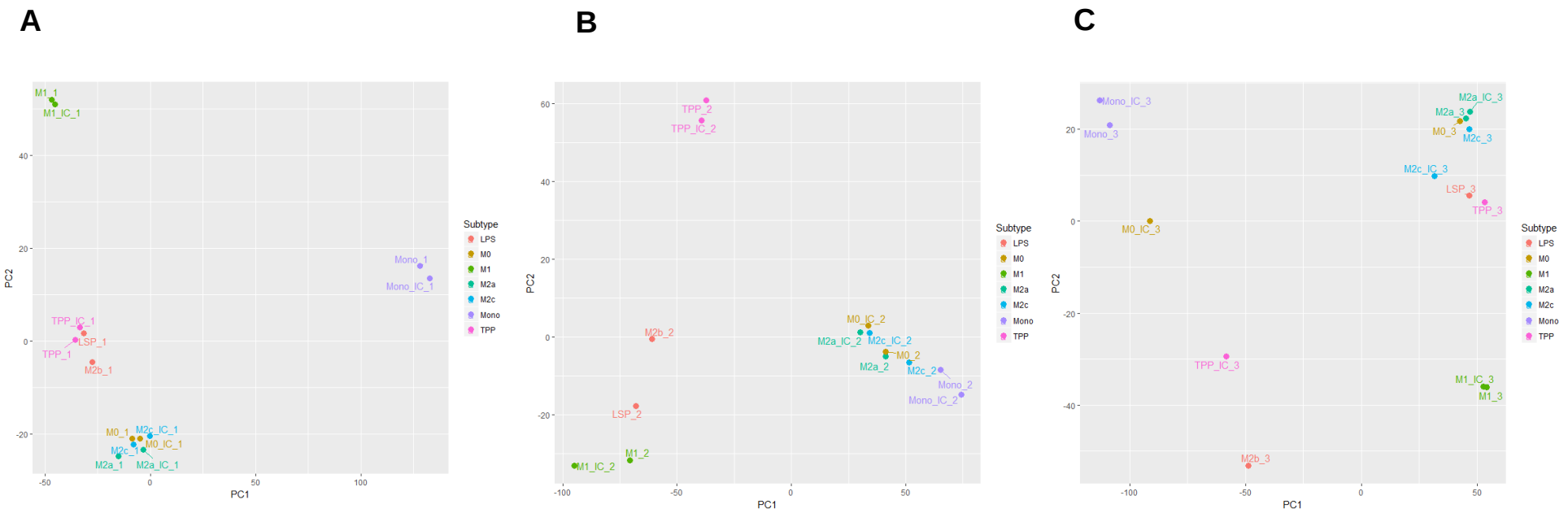

Figure 5.3.9. PCA plots demonstrating how samples cluster in individual replicates, including treatments with and without immune complexes; replicate 1 (**A**), replicate 2 (**B**) and replicate 3 (**C**)

5.3.6 Some genes are differentially expressed between baseline monocytes and those treated with immune complexes

s stated previously, not all of the macrophages appeared to cluster consistently when treated with IC, but monocytes in replicates 1 and 3 did (Figure 5.3.8, A). Hence these samples were selected as the primary focus for downstream analyses; as in Chapter 4 the second replicate was not included due to the presence of a strong lane effect. Differential gene expression analysis was performed to determine whether there were changes upon addition of IC, and to interrogate the inferred functional impact of these changes on the cells. A number of genes were found to be high in one condition and low in the other (Figure 5.3.10). The top genes found to be significantly differentially expressed in monocytes upon the addition of IC were identified. These could potentially be used as markers to indicate that the IC driven state has been achieved.

Examination of differentially induced transcripts has the potential to provide a preliminary insight into functional changes in these cells upon IC stimulation. The top 50 transcripts found to be elevated in the monocytes treated with IC were plotted, and upon examination some of these genes were found to be related to immune functioning (Figure 5.3.11); *CXCR3*, a gene coding for a receptor of the same name, is a receptor able to recognise pro-inflammatory chemokines (CXCL9, CXCL10 and CXCL11 and has been implicated in chemotactic migration (Costa *et al., 20*16). Another gene featured in this list is *HSD11B1*, a gene coding for an enzyme implicated in the activation of cortisol, an agent known to affect immune system functions (Jefferies, 1991). Although these transcripts can imply changes, it was difficult to draw conclusions based on functions of individual markers.

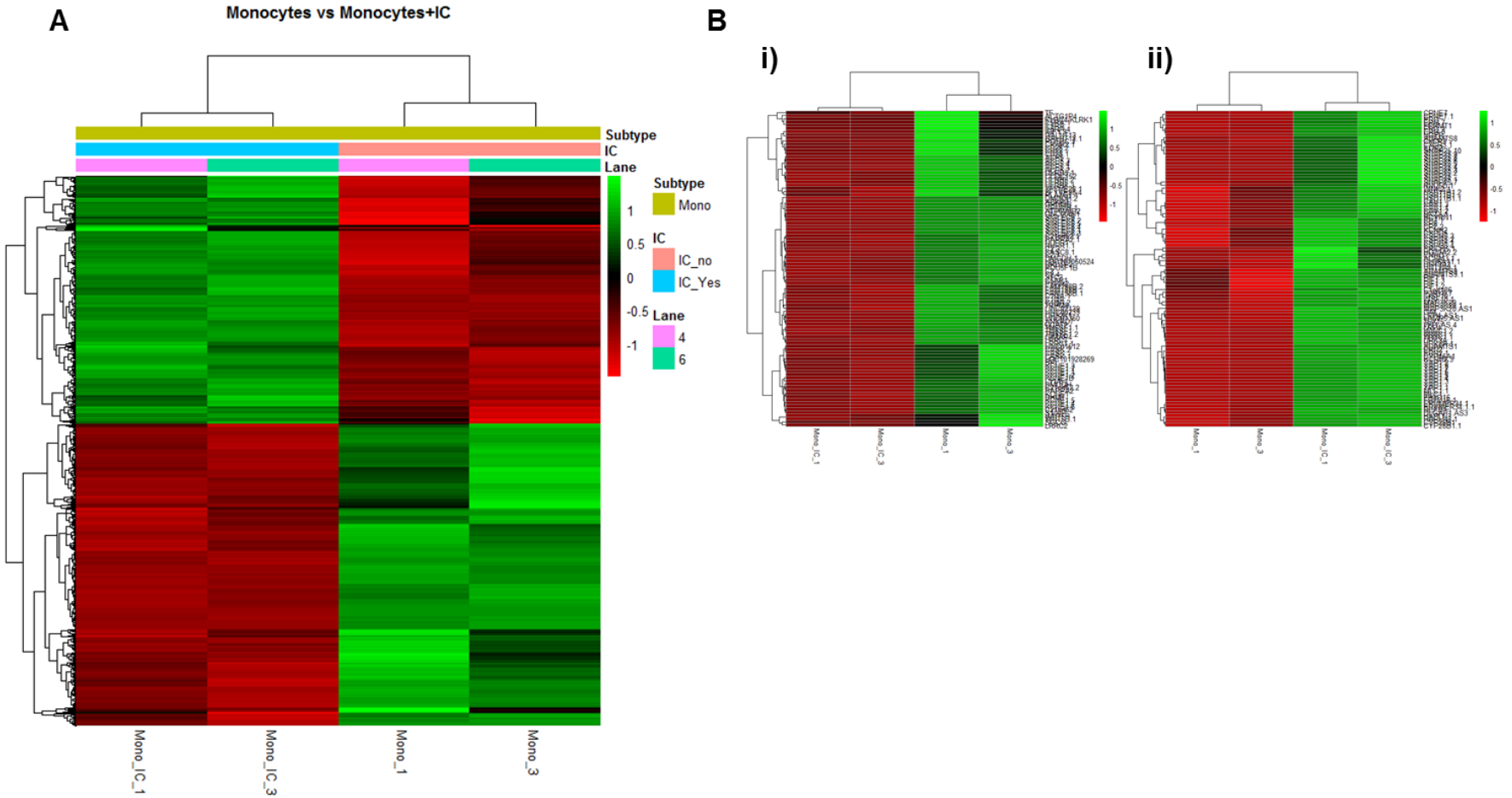

Figure 5.3.10. Heatmaps visualising all differentially expressed genes between monocytes and monocytes treated with immune complexes (**A**), top 100 down regulated genes upon immune complex addition (**B(i)**) and top 100 up regulated genes upon immune complex addition (**B(ii)**)

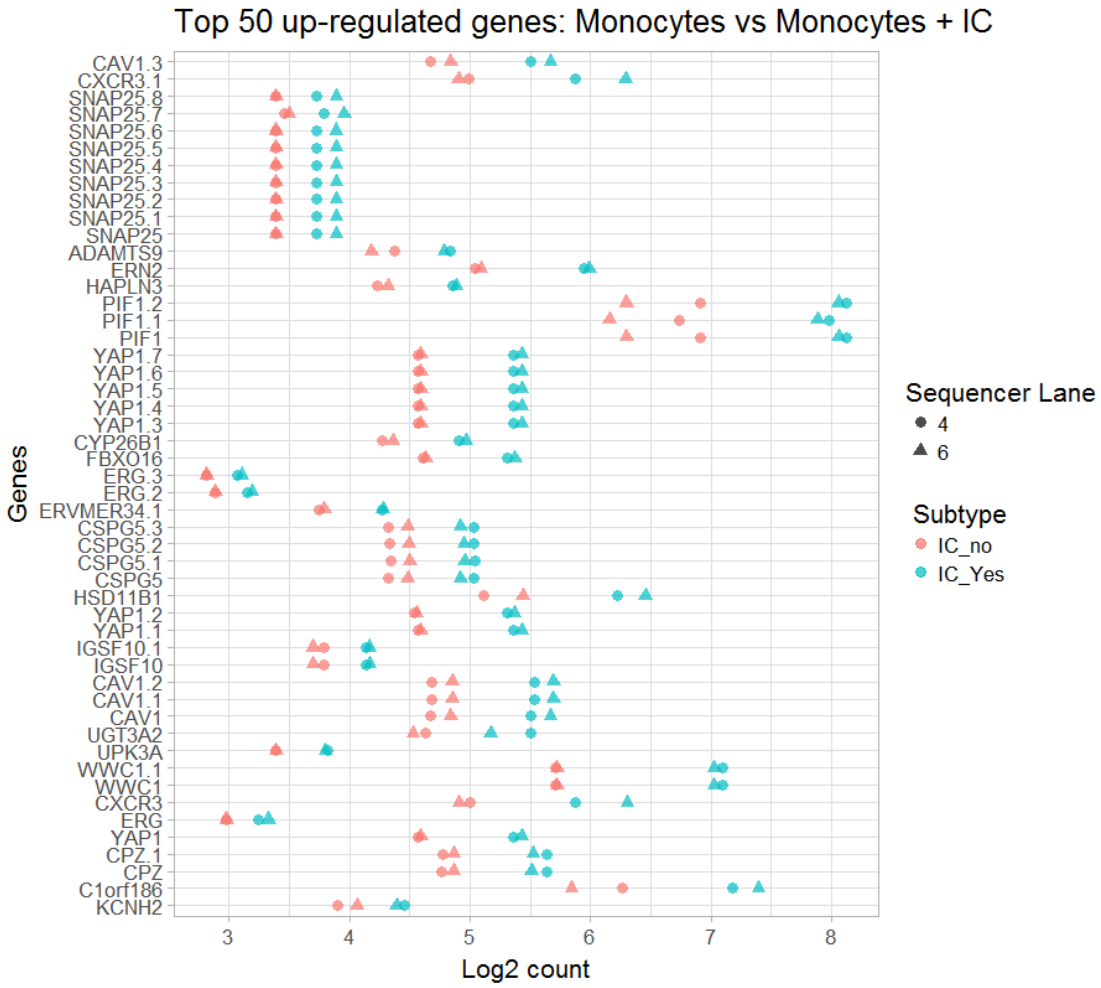

Figure 5.3.11. Dot plot detailing the top 50 transcripts found to be induced when monocytes are treated with immune complex

5.3.7 Enrichment analysis for genes differentially expressed between monocytes with and without immune complex treatment were immunity related

GO enrichment analysis and pathway enrichment studies (KEGG, REACTOME) can give a clearer overview of global changes in the behaviour of different cell types. GO analyses are performed by identifying genes that are differentially expressed between two conditions in a pairwise analysis, and isolating GO terms that are enriched in that list. Functions identified from this investigation can be divided into biological processes, molecular function and cellular components. Here, these aspects were investigated separately to examine differences between monocytes with and without ICs (Figure 5.3.12); some of the top hits relating to biological processes included changes in neutrophil and granulocyte function; although this is not a monocyte specific term, there are some overlaps of ontology functions with different cell types, and this term implies immune-related transcriptional changes. Additionally, processes relating to antigen processing and presentation are highlighted here, although the gene ratio and p-value are not as high as for the granulocyte activity functions. For molecular function, ontology terms relating to microtubules and protein binding are given; this could indicate changes in certain immune cell functions, such as migration, antigen recognition and phagocytosis that are dependent upon rearrangements of the cytoskeleton. However, the fact that the gene ratios and p-values for these terms are low, and that no other details are given to put these functions into context make it difficult to draw firm conclusions without additional experimental data.

The top cellular components enriched for the monocyte versus monocyte + HAGG comparison were not clearly related to immune functioning; this was surprising considering the association between FcγRs signalling and activation of immune pathways (Hargreaves *et al., 20*15). However, there were some terms in the list that may be linked to the inflammatory response; vesicle lumen and MHC II protein complex are detailed here and could imply changes relating to pathogen removal and antigen presentation. Both of these functions are typical for myeloid cells responding to activation signals.

KEGG analysis is useful as there are a number of pathways relating to specific disease states stored in this database, as well as some for functional signalling. A number of the hits on the list of pathways altered between monocytes with and without HAGG were related to the immune system and immune disease; the top pathway identified was for SLE, an IC-driven, autoimmune disease. RA was also on the list along with phagosome function, antigen processing and presentation and other functions and

disorders (e.g. graft versus host disease, Type 1 diabetes mellitus) that could be related to immune system modulation.

Reactome is another pathway enrichment analysis database, with less focus on pathologies and a keener interest on pathways relating to cell functioning. A number of the top 50 hits detailed in Figure 5.3.12 (a) were not related to immunity, but those that were appeared to corroborate the biological process gene ontology terms; there were details of neutrophil induction and acti vity as well as antigen presentation on the list.

Figure 5.3.12. enriched terms for genes differentially expressed between monocytes with and without HAGG relating to Reactome pathways (**A**), cellular components (**B**), KEGG pathways (**C**), biological processes (**D**) and molecular functions (**E**)

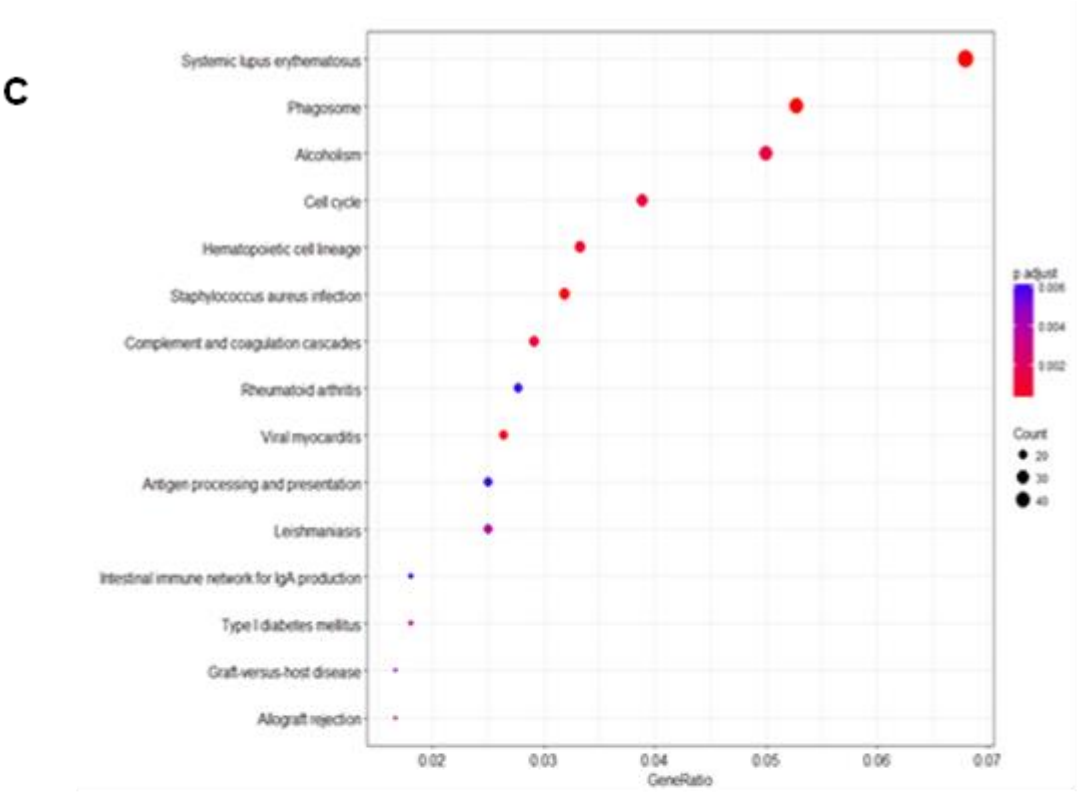
C
Systemic lupus erythematosus
Phagosome
Alcoholism
Cell cycle
Hematopoietic cell lineage
Staphylococcus aureus infection
Complement and coagulation cascades
Rheumatoid arthritis
Viral myocarditis
Antigen processing and presentation
Leishmaniasis
Intestinal immune network for IgA production
Type I diabetes mellitus
Graft-versus-host disease
Allograft rejection
0.02
0.03
0.04
0.05
0.06
0.07
GeneRatio
p.adjust
0.006
0.004
0.002
Count
20
30
40

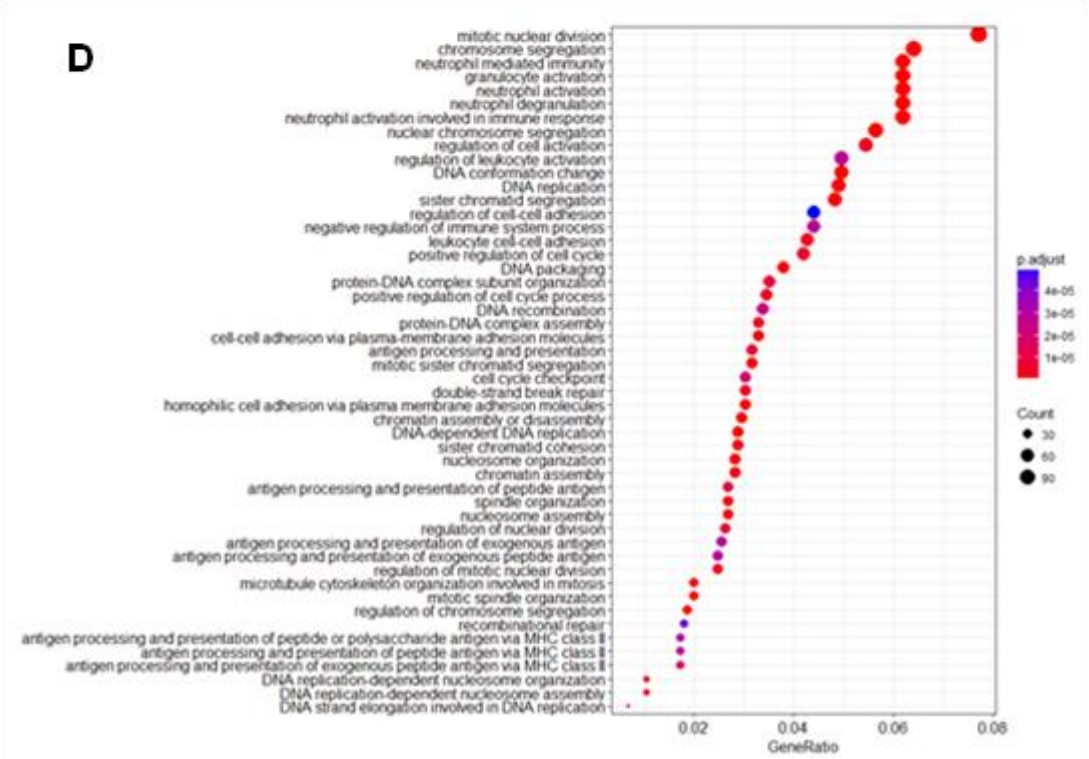
D
mitotic nuclear division
chromosome segregation
neutrophil mediated immunity
granulocyte activation
neutrophil activation
neutrophil degranulation
neutrophil activation involved in immune response
nuclear chromosome segregation
regulation of cell activation
regulation of leukocyte activation
DNA conformation change
DNA replication
sister chromatid segregation
regulation of cell-cell adhesion
negative regulation of immune system process
leukocyte cell-cell adhesion
positive regulation of cell cycle
DNA packaging
protein-DNA complex subunit organization
positive regulation of cell cycle process
DNA recombination
protein-DNA complex assembly
cell-cell adhesion via plasma-membrane adhesion molecules
antigen processing and presentation
mitotic sister chromatid segregation
cell cycle checkpoint
double-strand break repair
homophilic cell adhesion via plasma membrane adhesion molecules
chromatin assembly or disassembly
DNA-dependent DNA replication
sister chromatid cohesion
nucleosome organization
chromatin assembly
antigen processing and presentation of peptide antigen
spindle organization
nucleosome assembly
regulation of nuclear division
antigen processing and presentation of exogenous antigen
antigen processing and presentation of exogenous peptide antigen
regulation of mitotic nuclear division
microtubule cytoskeleton organization involved in mitosis
mitotic spindle organization
regulation of chromosome segregation
recombinational repair
antigen processing and presentation of peptide or polysaccharide antigen via MHC class II
antigen processing and presentation of peptide antigen via MHC class II
antigen processing and presentation of exogenous peptide antigen via MHC class II
DNA replication-dependent nucleosome organization
DNA replication-dependent nucleosome assembly
DNA strand elongation involved in DNA replication
0.02
0.04
0.06
0.08
GeneRatio
p.adjust
4e-05
3e-05
2e-05
1e-05
Count
30
60
90

E

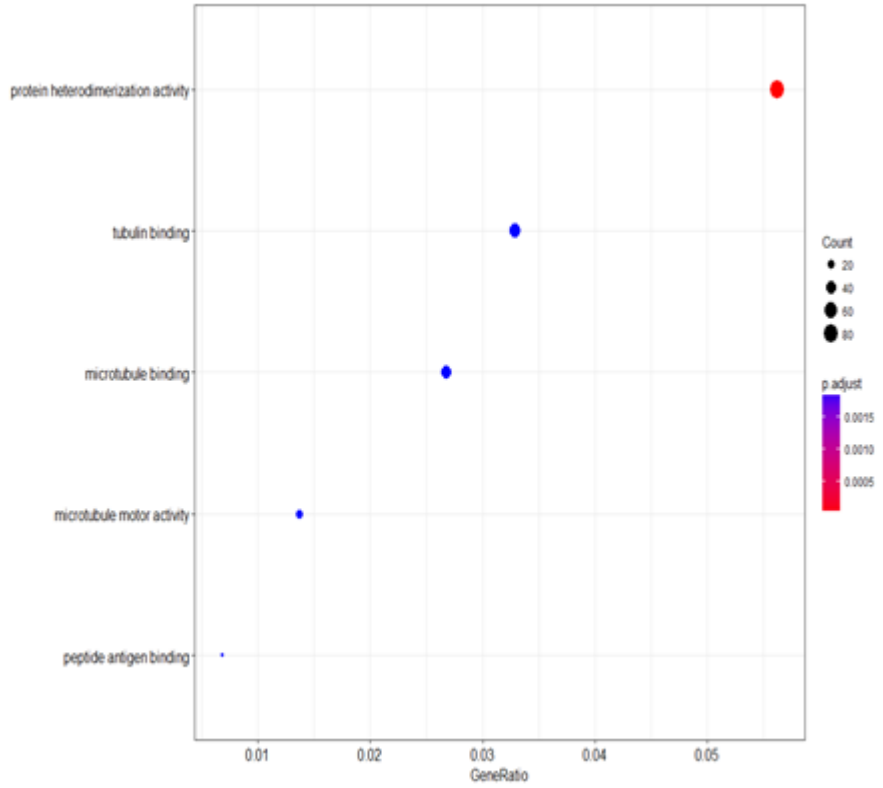
protein heterodimerization activity
tubulin binding
microtubule binding
microtubule motor activity
peptide antigen binding
0.01
0.02
0.03
0.04
0.05
GeneRatio
Count
20
40
60
80
p.adjust
0.0015
0.0010
0.0005

5.3.8 Some autoimmune disease related transcription factor target genes are enriched in monocytes treated with immune complexes

Although the GO analyses provide a broad overview of how the cells treated with different stimuli may vary in function, it does not give specific information as to what changes are happening in the cell. Additional investigations can be performed to link changes in transcripts which appear to be similarly regulated, but do not have any obvious functional links. One possible connection is that some groups of genes may be induced by the same TF; investigations were performed here using lists of TFs and target genes, derived from ChIP-seq experiments. Analysis of the genes up-regulated in the condition where monocytes treated with ICs (versus unstimulated cells) revealed a number of TFs for which target gene ratio was high, versus background (according to Fishers exact test with FDR set as a threshold of 0.05). Please refer to Figure 5.3.13. The top ten given TFs include some regulatory elements that are implicated in the pathophysiology of autoantibody-driven inflammatory conditions such as RA and SLE. For instance, interferon response factor (IRF3), was identified; this TF has previously been found to influence gene expression in RA synovial cells (Angiolilli *et al., 20*16); (Sweeney *et al., 20*10). STRING network plots of proteins (intersected with gene expression Tables derived from monocyte versus monocyte + IC pairwise analysis) were generated (Figure 5.3.14). Please note that Tables containing raw data corresponding to these plots can be found in appendix 6. These network plots demonstrated interactions of IRF3 with other proteins (Figure 5.3.14, A); transcription of genes corresponding to proteins PRKDC, HERC5, IKBKE and IFIT2 appeared to be significantly upregulated in the monocyte + IC condition. Interestingly these factors all appear to post-translationally regulate the activity of IRF3; PRKDC enhances phosphorylation of IRF3, increasing its time in the nucleus and aids in resistance of this TF to degradation (Karpova *et al., 20*02). HERC5 catalyses the conjunction of IRF3 with ISG15 hence preventing binding of Pin1 (a peptidyl-prolyl isomerase) and subsequent polyubiquitinylation and removal (Shi *et al., 20*10). IKBKE is involved in IRF3 signalling and IFIT2 in IFR3 phosphorylation (Siegfried *et al., 20*13); (Fitzgerald *et al., 20*03). This is a potential explanation as to why an increased number of targets for this TF are found in monocyte + IC samples; although the gene expression levels are not significantly different; the activity is enhanced post-translationally. Changes in activity at the protein level would not be detected using RNA-seq analysis (Figure 5.3.14, A).

Specificity protein-1 (SP1) was another TF identified through this analysis which is reported to activate expression of certain genes in rheumatoid joints; in RA synovial fibroblasts, this TF is instrumental in activation of angiogenic and arthritogenic

phosphorylases (gliostatin/thymidine phosphorylase) through proliferation and chemotactic migration of endothelial cells, as well as inducing peptidylarginine deaminase-coding genes in other cells which induce citrullination. This protein modification is strongly linked to RA pathology (Ikuta *et al., 20*12); (Dong *et al., 20*08). Therefore, increased activity of these proteins as a result of IC exposure may contribute to the pathologies seen in RA. As with IRF3, expression patterns of genes relating to proteins interacting with SP1 were plotted as a network (Figure 5.3.14, B); it is less clear how expression of these proteins affects cell functioning. Most significantly increased genes which interact with SP1 are DHFR (dihydrofolate reductase) and HDAC1 (Histone deacetylase 1). The DHFR promoter is a target for SP1 so it follows that the transcript for this protein is upregulated where the activity of SP1 is increased (Dynan *et al., 19*86). This molecule has been linked to production of nitric oxide through tetrahydrobiopterin which may have some implications for monocyte functioning (Chalupsky and Cai, 2005). Additionally this protein is targeted and reduced by methotrexate, a drug commonly used to treat RA, emphasizing the relevance of SP1 as a TF in this disease (Rajagopalan *et al., 20*02). Reports suggest that in addition to its role as a TF, SP1 interacts with HDAC1 to repress activation of gene expression at other sites, with targets associated with cell cycle, cell death and anti-viral immunity (Jiang *et al., 20*07); (Waby *et al., 20*10); (Won *et al., 20*02).

As a control, the same analysis was performed on the genes upregulated in the unstimulated monocytes versus monocytes treated with HAGG. No overlapping TFs were identified for the top 10 hits in both lists. It should be noted that overall FDR and P-values indicated lower levels of significance for the results of the unstimulated monocyte (versus monocyte + IC) gene analysis (Figure 5.3.13, B). Of interest, STAT3, a TF induced by either IL-10-related or inflammatory signalling appears to be enriched in lists of genes increased in monocytes vs monocytes + IC (Nakamura *et al., 20*15). However, it is unclear which signalling mechanism is represented here based on this data alone.

It is possible that the activation of these TFs is either supported by or solely due to IC stimulation in the RA synovium. However, laboratory experiments must be carried out to validate these results experimentally and determine the degree to which this stimulus is responsible for the activation of the TFs of interest.

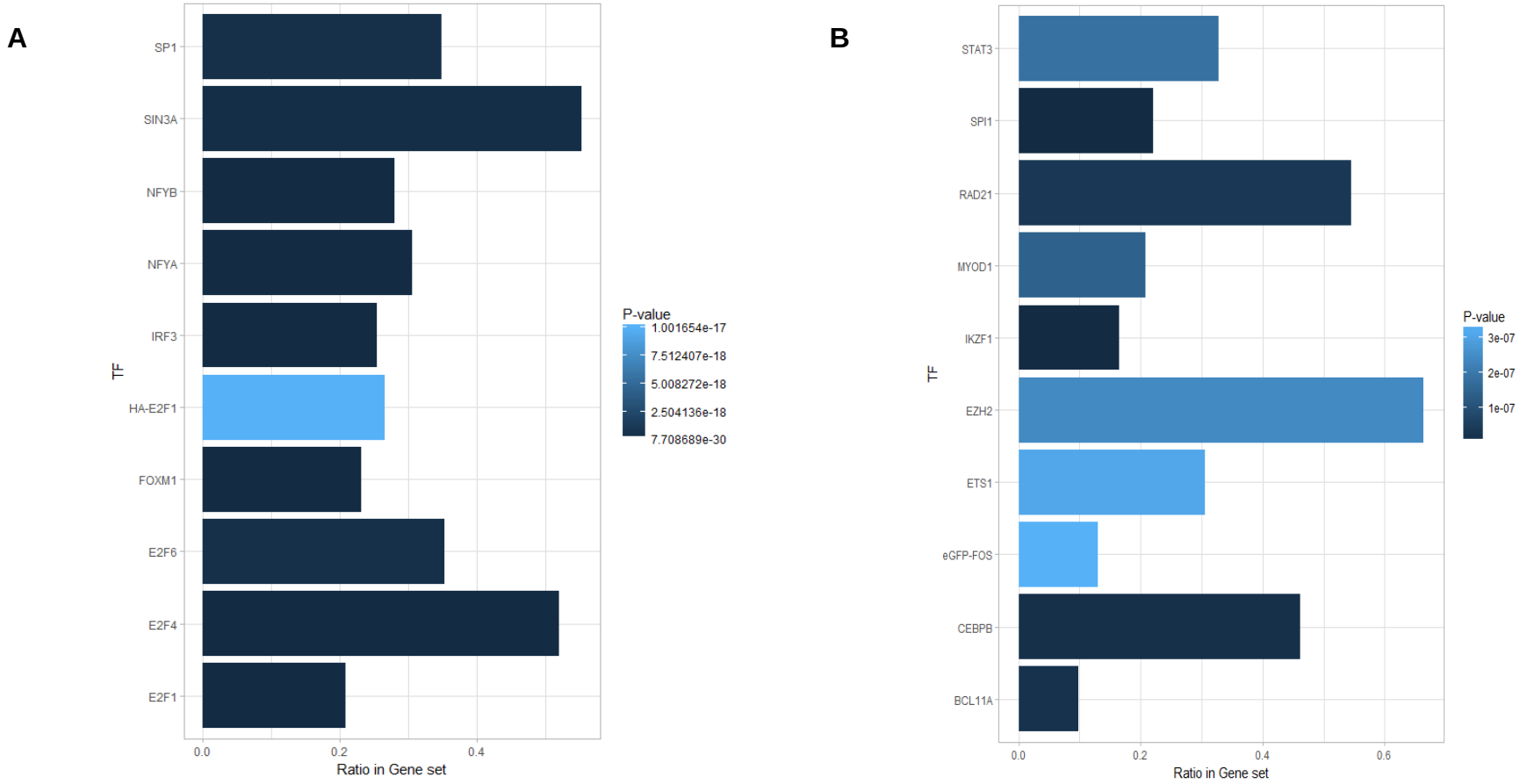

Figure 5.3.13. Transcription factors with a significantly increased number of targets in lists of genes that are upregulated upon addition of immune complexes to monocytes (**A**) and genes that are significantly downregulated upon addition of immune complexes to monocytes (B)

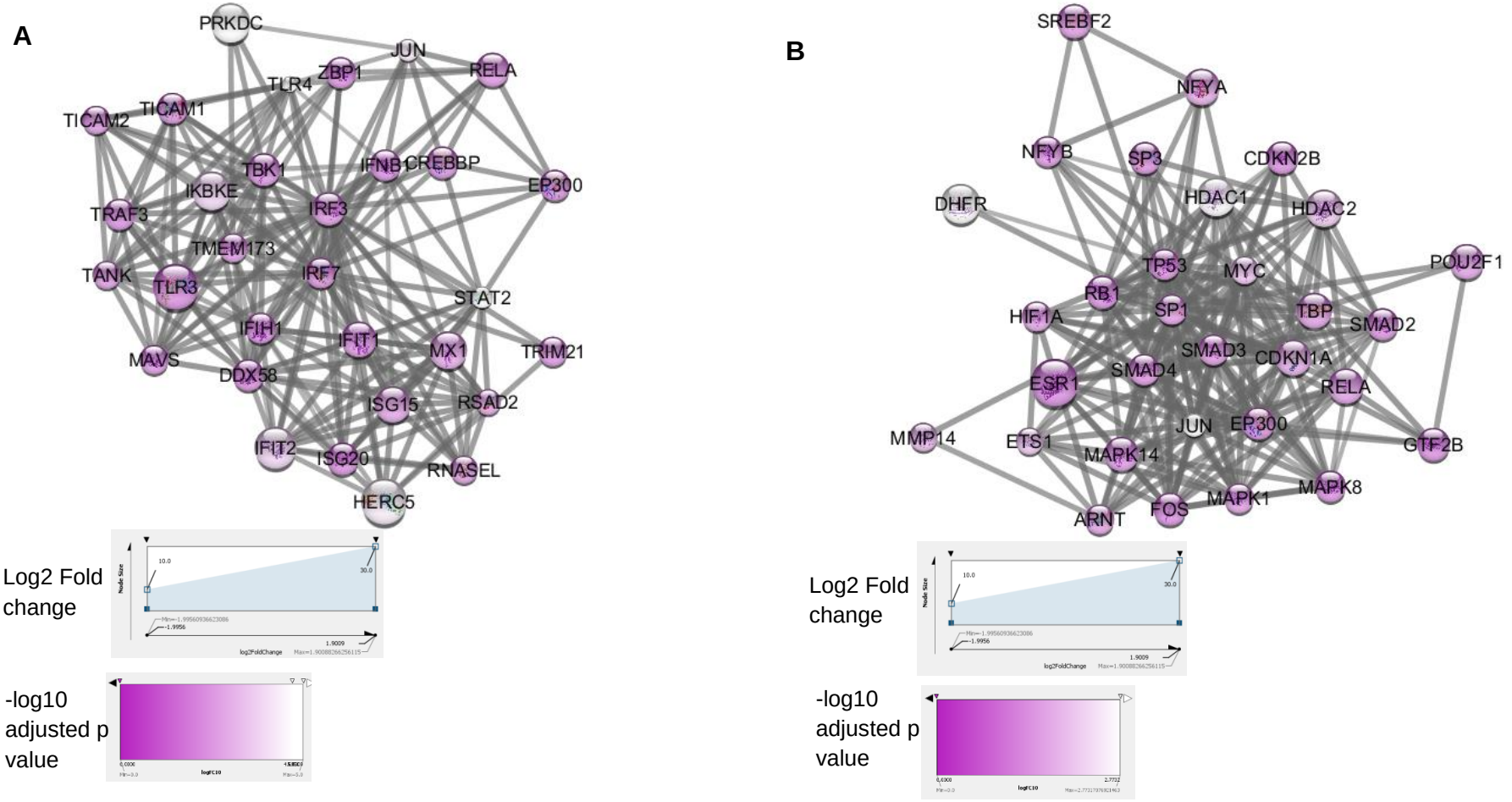

Figure 5.3.14. STRING plots showing protein interactions for transcription factors IRF3 (**A**) and SP1 (**B**) with top 30 associated proteins according to the Cytoscape STRING database. Node size corresponds with Log2 fold change, with an increase in size representing an increase in fold change upon addition of immune complexes and colour corresponding to –log10 adjusted p value where pink represents lower significance and white is higher significance

5.3.9 Some differences in transcript expression between monocytes and monocytes treated with immune complexes are observed for disease specific transcript lists

As changes in gene expression have been observed in monocytes upon addition of IC, it is reasonable to consider the possibility that these observations are also present in IC-driven diseases. The Broad Institute has generated curated lists of genes identified through microarray analysis for a variety of conditions that are freely accessible for download and analysis (http://software.broadinstitute.org/gsea/msigdb/genesets.jsp?collection=C7). Transcripts upregulated in macrophages isolated from SLE and RA patient tissue were compared with genes differentially expressed between monocytes and monocytes treated with IC. Heatmaps comparing expression of these gene lists in the presence and absence of IC demonstrated some clustering (Figure 5.3.15, B and C); there do appear to be some consistent changes in gene expression in the transcriptomes of monocytes upon IC-stimulation, but overall expression does not appear to be higher in one condition versus the other.

It must be noted that the SLE and RA gene lists were generated from experiments using blood myeloid cells and synovial macrophages respectively, and the comparisons here are made using monocytes only; some of the genes induced in this list may therefore be macrophage-specific. Another factor that needs to be considered is that the cells isolated from diseased tissue will be under the influence of a number of stimuli, and individual contributions of certain agents (e.g. IC) to this phenotype can only be teased out using additional experiments. This could be the reason why some genes were upregulated in these conditions and expression of others were found to be reduced.

Genes relating to the inflammatory response (i.e. genes that are induced and depleted during this process) were also isolated using GO terms, and plotted (Figure 5.3.15, A); as with the disease-specific gene lists some clustering was seen between monocytes treated with immune complexes and unstimulated cells. Hence transcription of genes relating to the inflammatory response are altered in monocytes upon addition of IC.

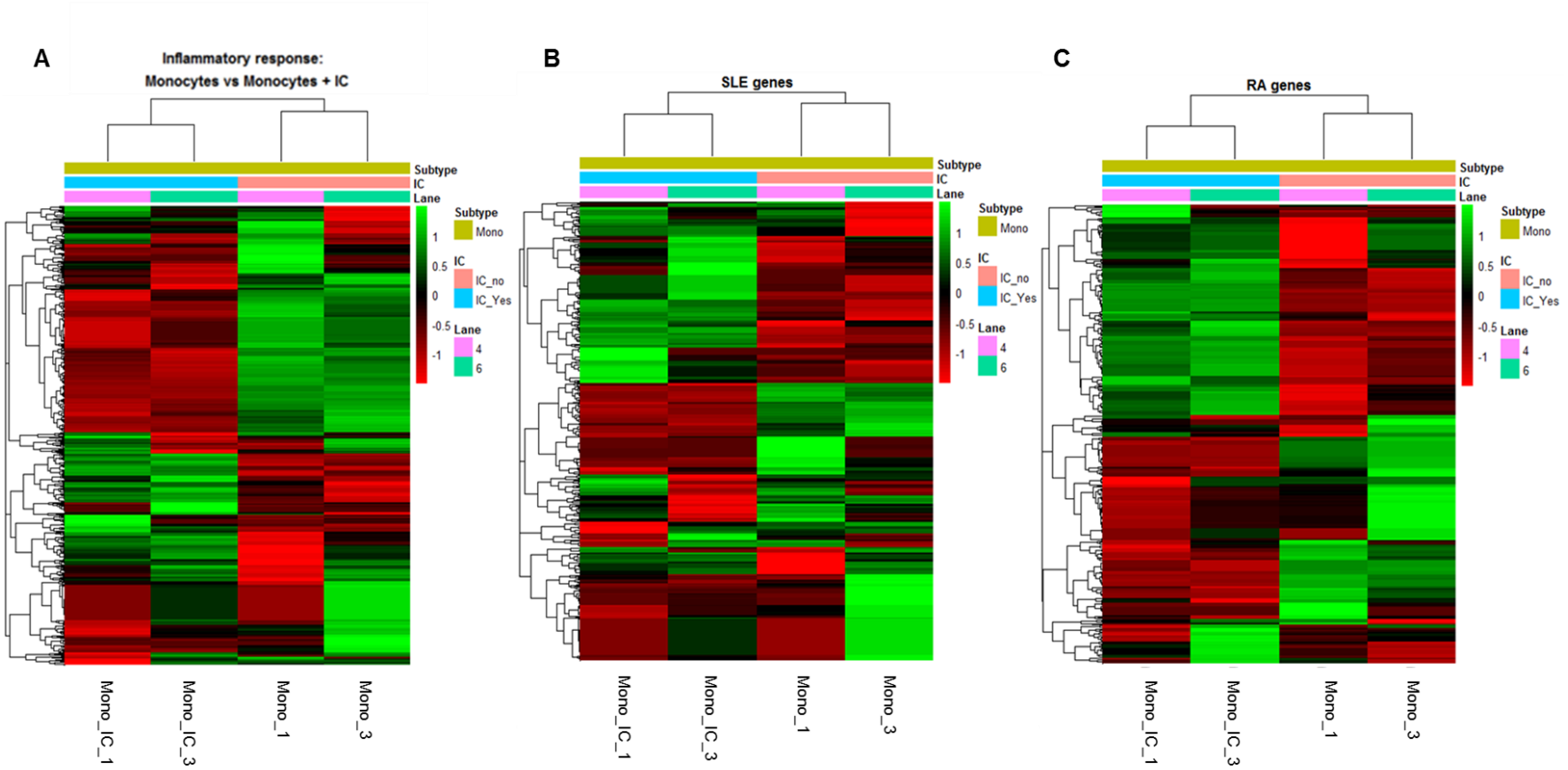

Figure 5.3.15. Heatmaps showing differences in gene expression for monocytes with and without immune complexes for different gene lists; those inked to the inflammatory response (**A**), those found to be increased in SLE (**B**) and genes upregulated in RA (**C**)

5.3.10 Changes in transcript expression do not appear to be consistent between macrophage replicates

As demonstrated by the PCA plots, there is little consistency between the replicates treated with IC, making comparisons between gene-averages for these conditions problematic; when differential gene expression is calculated between specific macrophage subsets with and without IC using all of the replicates, no significant changes are detected between the groups. Based on the PCA plots, one possible explanation is that baseline polarisation and thus transcriptome was variable prior to IC addition. Thus, cell phenotypes may have been slightly different, causing the cells to respond differently to stimuli.

When taken as individual experiment (samples with and without ICs from the same replicate/lane of sequencer), it appears that some replicates respond to addition of IC, demonstrating differential gene expression and some do not. A summary of the samples that react to HAGG addition are summarised in Figure 5.3.16

	Replicate 1	Replicate 2	Replicate 3
M0	Yes	Yes	Yes
M1	No	Yes	No
M2a	No	Yes	Yes
M2b (LPS)	Yes	No	Yes
M2c	No	Yes	No
TPP	Yes	No	Yes

Figure 5.3.16. Table indicating which replicates of various macrophage subsets demonstrated differential expression upon addition of immune complexes; those that responded are labelled as “Yes” (pink) and those that did not as “No” (blue)

5.3.11. Some macrophage replicates were found to have changes in gene expression relating to inflammatory functioning

As mentioned previously due to high variability between samples, comparisons between macrophages with and without ICs were made by examining separate replicates as individual experiments. The samples that did respond to IC stimulation were fed through a pipeline to identify DEGs which were subsequently subject to GO enrichment analysis. Biological processes which appeared to be significantly changed through this analysis were explored for immunological relevance (Figure 5.3.17).

Although the M0 cells appeared to respond to immune complexes in all experiments, the changes observed were not consistent; when subject to enrichment analysis for biological processes, different replicates highlighted different terms. For instance, the DEGs for these conditions in replicate 1 were related to cell adhesion, developmental processes and RNA events. The terms in replicate 2 referred to cell-cell adhesion only. More terms were enriched for the differentially regulated genes in replicate 3; there were some overlaps with terms mentioned in other replicates but inflammatory response was given as one of the top hits. Hence this condition was selected as interesting for further investigation. Note that only small numbers of DEGs (<100) were identified between conditions with and without IC when triplicates were contrasted (data not shown).

For M1 cells, only replicate 2 demonstrated differential gene expression in the presence and absence of IC; enrichment analysis of this DEG list also indicated inflammatory response, along with other immunity related terms, including response to bacterium, leukocyte migration and more.

M2a samples treated with IC in both replicates 2 and 3 appeared to respond; inflammatory response and other immune related functions were among top hits for both experiments when biological process enrichment analysis was performed. As these terms were enriched with the highest gene ratios and lowest p-values in replicate 2, this experiment was selected for use in further investigations.

For M2c cells, a change upon IC addition was only detected in replicate 2 and inflammatory functions were amongst highly enriched terms when differentially expressed genes were fed through a gene ontology biological process analysis.

LPS gene expression was significantly altered in both replicate 1 and 3 upon IC induction. However, the enriched biological processes for DEGs in replicate 1 were linked to non-specific terms such as cell adhesion and system development. Conversely, top enriched processes in replicate 3 referred to immunological functions,

thus this experiment was applied in downstream analyses to investigate effects of IC on LPS induced cells.

DEGs were identified between TPP cells with and without immune complexes for replicates 1 and 3. However, only those in the former replicate responded in an inflammatory fashion according to GO enrichment investigations. As was the case previously, the inflammatory sample was selected as the condition of interest.

These samples were not investigated in as much detail as the monocytes; the high degree of variability between the samples suggested that the IC stimulation may have failed for some of the samples, or that technical variability lead to induction of non-specific genes which may have masked any relevant changes. Hence rigorous downstream investigations would not be appropriate for these samples. Selection of samples demonstrating immune changes was deemed acceptable as induction of TNF and other pro-inflammatory cytokines upon IC ligation has been reported for myeloid cells (Ambarus *et al., 20*12; Santeogets *et al., 20*14). It should be noted however, that the replicates responding in an inflammatory manner may not have necessarily worked and may in fact be an instance of experimental failure. However, further investigations could not be carried out on cells that did not appear to respond to IC and any interesting observations must be tested experimentally for validity.

A i)

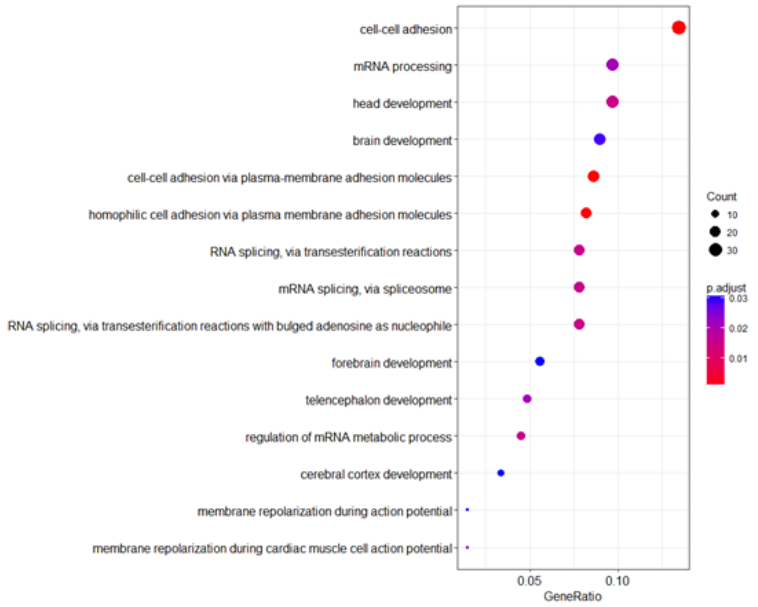

ii)

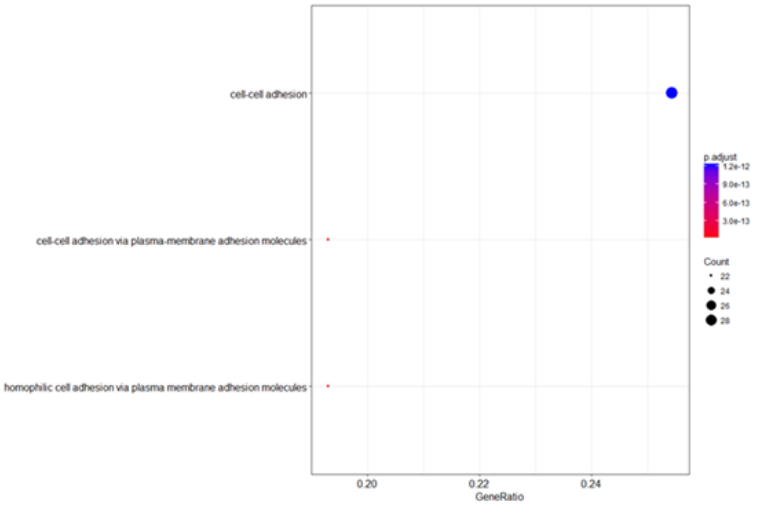

iii)

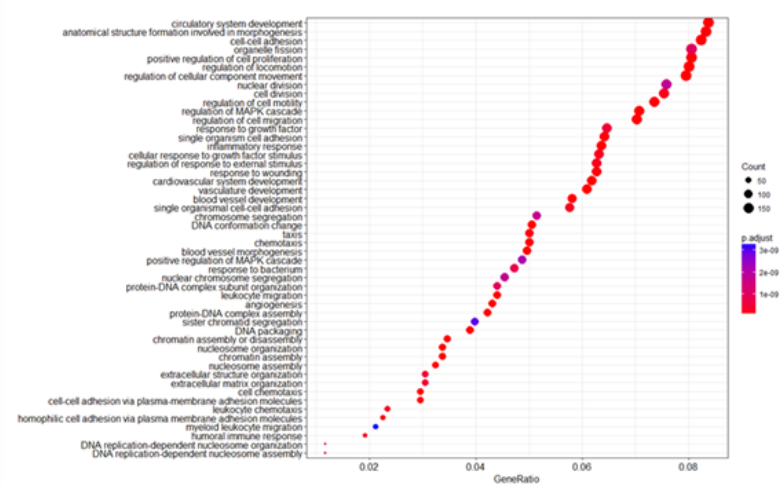

Figure 5.3.17. (Part 1) enriched biological processes for individual replicates that responded to addition of immune complexes; replicates 1, 2 and 3 for M0 cells (**A (i), (ii) and (iii)** respectively)

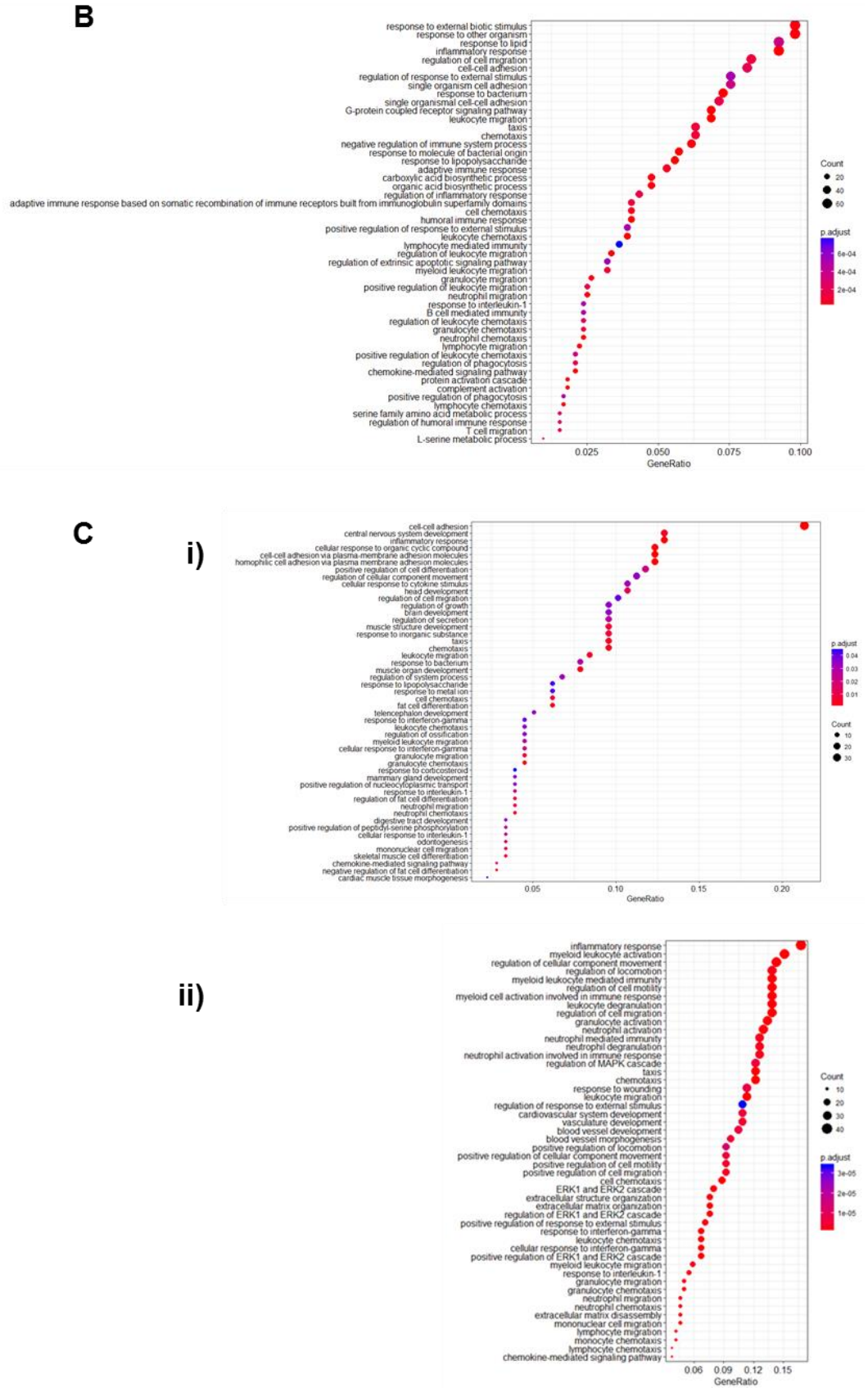

Figure 5.3.17. (Part 2) enriched biological processes for individual replicates that responded to addition of immune complexes; replicate 2 for M1 cells (**B**) and replicates 2 (**C(i)**) and 3 (**C(ii)**) for M2a cells

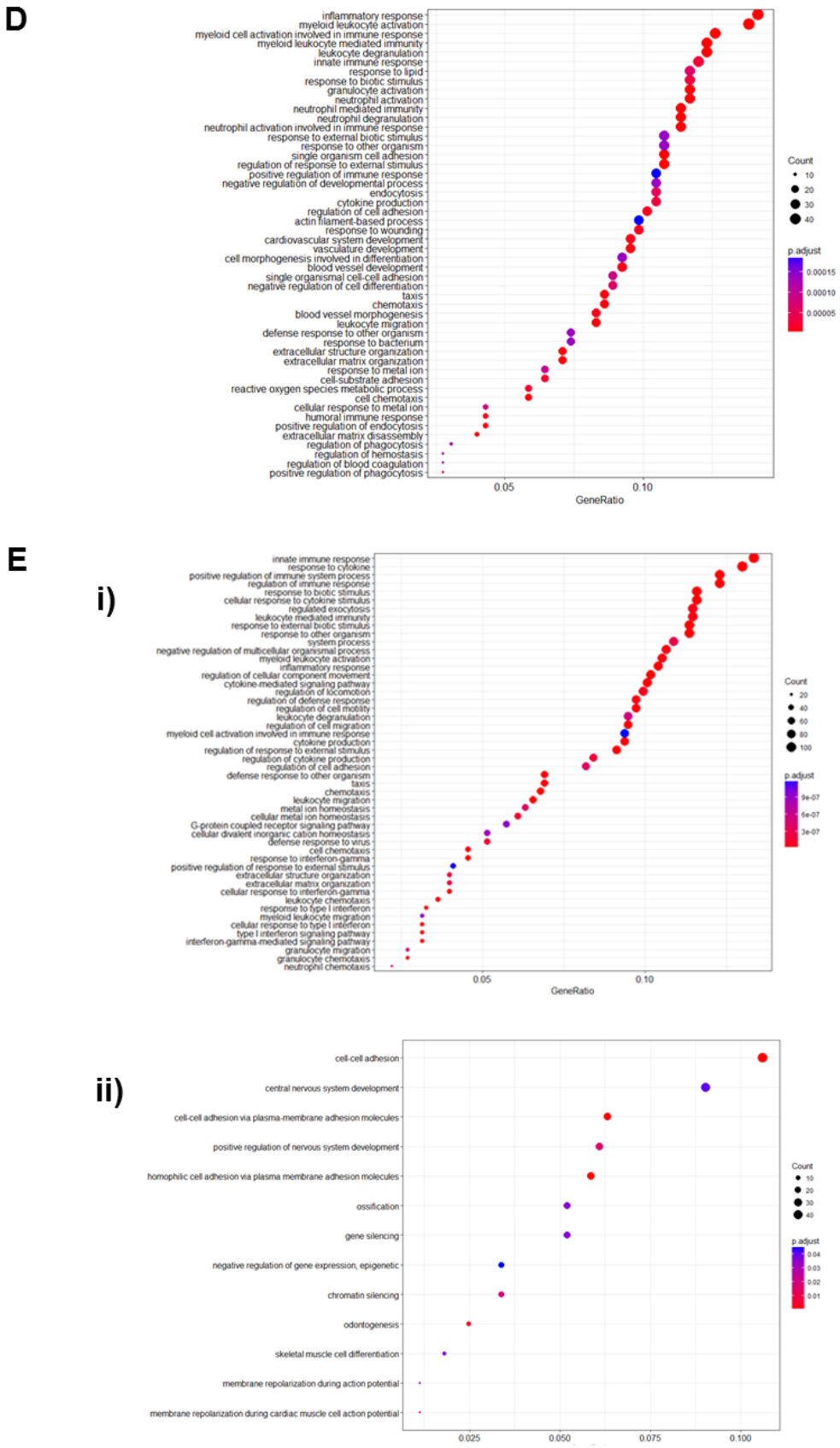

Figure 5.3.17. (Part 3) enriched biological processes for individual replicates that responded to addition of immune complexes; replicate 2 for M2c cells (**D**) and replicates 1 (**E(i)**) and 3 (**E(ii)**) for LPS cells

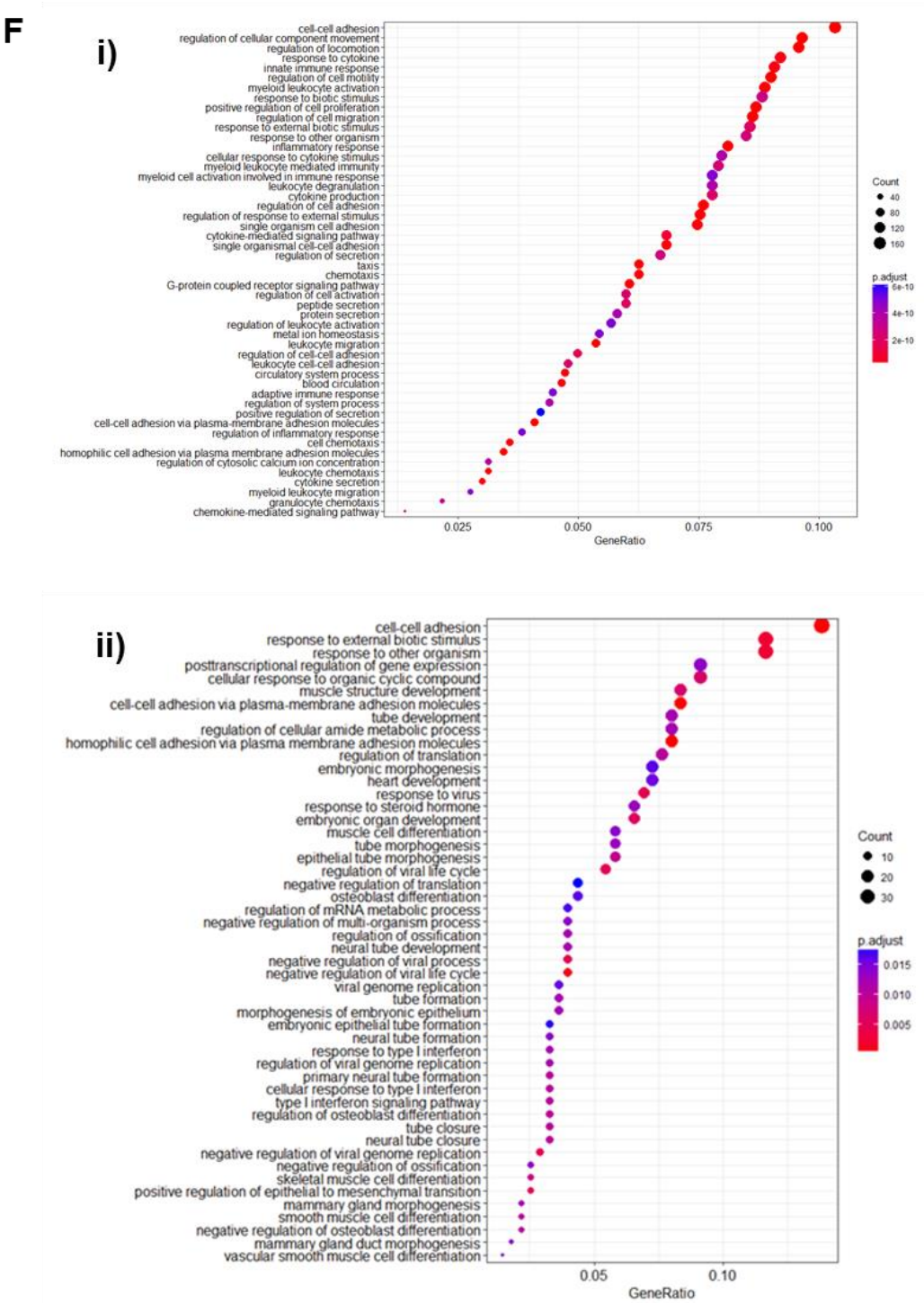

Figure 5.3.17. (Part 4) enriched biological processes for individual replicates that responded to addition of immune complexes; replicates 1 (**F(i)**) and 3 (**F(ii)**) for TPP cells

5.3.12 Replicates with inflammatory changes demonstrate enrichment for some disease specific transcription factors

As with the monocytes, TF analysis gives a more insightful indication of the changes occurring in IC treated cells; as consistency between replicates was an issue, individual experiments were scrutinised for changes using GO analysis. The biological process enrichment investigation indicated that only some of the replicates responded to IC in an inflammatory or immunity-related fashion. Differences between IC +/- conditions in other replicates appeared to be non-specific and could be related to changes in the cell cycle. Hence, samples with these enrichments were discounted as it is possible that the differences seen were due to not synchronising the THP-1 cells cycle prior to stimulation. Given the associations seen with M1/M2a macrophage polarisation and cell cycle (that it is halted upon M1 stimulation), it is possible that additional treatments (including IC) alter cell cycle-related processes, particularly as ERK-mediated cell cycle progression was found to be induced via FcR ligation in murine macrophages (Luo *et al., 20*10). However, this was impossible to determine without synchronisation prior to cell induction. As with the monocytes, genes significantly downregulated upon addition of IC were subject to TF enrichment as a control.

For M1 treated cells, it was the second replicate that appeared to respond to IC-stimulation in an inflammatory manner; inflammatory response was a top hit for GO-biological process enrichment analysis. Thus, genes elevated in M1 cells + HAGG (versus M1 cells) in replicate 2 were selected for TF enrichment analysis (Figure 5.3.18). One of the most significant hits here was PU.1 (coded for by spi-1 Proto-Oncogene (SPI1)); this factor has been associated with gene expression during myeloid cell development (stimulates expression of the M-CSF coding gene) (Delgado *et al., 19*98), so may influence macrophage phenotypes if activated in disease states. It should be noted that this macrophage subtype is the most inflammatory due to induction with LPS and IFNγ. Hence activity of inflammatory TFs in these cells will naturally be high compared to other polarisation states. Therefore, pro-inflammatory changes induced by IC stimulation in this subtype may be masked by a highly inflammatory background.

M2a and M2c cells in replicate 2 cells also demonstrated an enrichment of targets for the SPI1 TF upon IC treatment (Figure 5.3.18). Genes upregulated in M2c cells upon IC treatment were also linked to ikaros family zinc finger protein 1 (IKZF1), a TF that reportedly regulates aspects of the immune response and has been linked to SLE (Cunninghame Graham *et al., 20*11). Hence induction of this factor in the disease state could potentially be partly driven by the presence of IC. No significant TF hits were

identified from significantly downregulated genes in these macrophage subsets, compared to IC treated cells using a cut off 0.05 for FDR (control experiment) (Figure 5.3.19).

The M0 cells from replicate 3 responds to IC in the most inflammatory manner for all of the replicates from that condition (Figure 5.3.18). The changes seen in this experiment are relatively similar to those described for monocytes stimulated with IC; RA-related TFs IRF3 and SP1 are implicated and are not identified in the reverse analysis (Figure 5.3.19). As M0 cells are subject to the least stimuli of all the macrophages subtypes, they are most closely related to monocytes in terms of polarisation. Hence it is unsurprising that these cells would respond in a similar way when exposed to ICs.

LPS-treated cells are subtyped into M2b macrophages when IC is included as a stimulus. The most responsive sample for this condition was found to be in replicate 3, and so this experiment was scrutinised for TF activity (Figure 5.3.18). As with some other subtypes, SPI1 and IKZF1 were found to be enriched for genes elevated in the IC-treated condition, although the latter TF was also a top hit for genes significantly downregulated genes, so this TF may just be elevated in this subset generally (Figure 5.3.19). In addition to this, certain TFs that are known to be involved in regulation of inflammatory genes were identified as top hits; STAT1, STAT2, and IRF1 were listed (Au-Yeung *et al., 20*13); (Ivashkiv and Donlin, 2014); (Blaszczyk *et al., 20*16). If these TFs are activated downstream of IC binding, this interaction could contribute significantly to perpetuation of inflammation.

TPP cells in replicate 3 were identified as samples responding to HAGG in the most inflammatory manner. TFs implicated in this investigation included SPI1 and STAT2; both have been linked to inflammation or immune system driven disease as discussed previously in this Section (Figure 5.3.18). IKZF1 was identified in both IC and non-IC treated differentially expressed gene lists, suggesting that (as with LPS treatment) this factor is induced in all TPP cells.

It is important to highlight that any findings discussed here were identified from individual experiments and were not reproducible; findings may therefore be invalid. It is possible that there were variations between batches of IC used to treat the cells which may have caused some samples to respond to this stimulus more strongly than others. However, this does not completely eliminate the possibility of the findings discussed in this Section being valid; it is simply not possible to identify the samples that represents responses to immune complexes most accurately from this data. This study would need to be repeated with experimental efforts to validate any inflammatory changes seen between samples with and without IC, identified here.

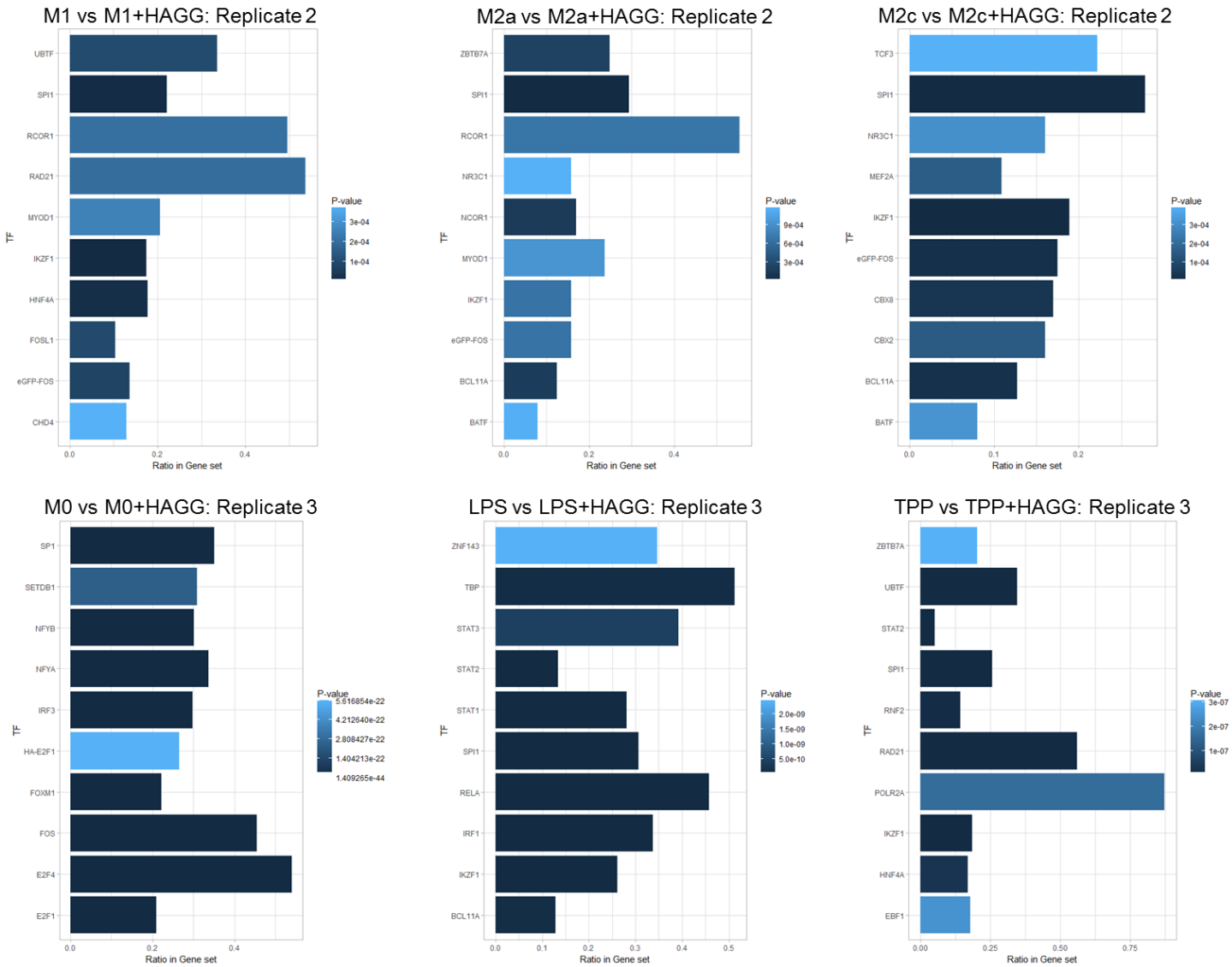

Figure 5.3.18. Transcription factors with significantly increased expression of target genes upon addition of immune complexes to macrophage subsets; data from replicates showing the most inflammatory changes

M1 vs M1+HAGG: Replicate 2

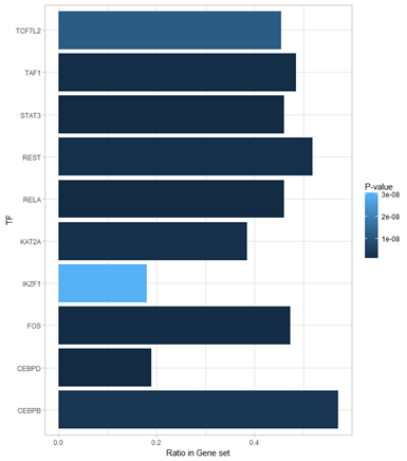

M2a vs M2a+HAGG: Replicate 2 (top 5)

TF	Ratio list	Ratio universe	in_list	total_list	Total in_universe	Total universe	pvalue	FDR
EZH2	0.71875	0.502995	46	64	13269	26380	0.041533	0.668301
ZC3H11A	0.28125	0.149659	18	64	3948	26380	0.017348	0.668301
RXRA	0.109375	0.045527	7	64	1201	26380	0.035141	0.668301
TAF1	0.421875	0.262472	27	64	6924	26380	0.028935	0.668301
USF2	0.421875	0.271569	27	64	7164	26380	0.039336	0.668301

M2c vs M2c+HAGG: Replicate 2 (top 5)

TF	Ratio list	Ratio universe	in_list	total_list	Total in_universe	Total universe	pvalue	FDR
EZH2	0.773913043	0.502995	89	115	13269	26380	0.00164	0.291886
POLR2A	0.869565217	0.671304	100	115	17709	26380	0.034794	0.502484
CTCF	0.834782609	0.650644	96	115	17164	26380	0.042371	0.502484
CEBPB	0.452173913	0.325967	52	115	8599	26380	0.032972	0.502484
RAD21	0.556521739	0.396361	64	115	10456	26380	0.019565	0.502484

M0 vs M0+HAGG: Replicate 3

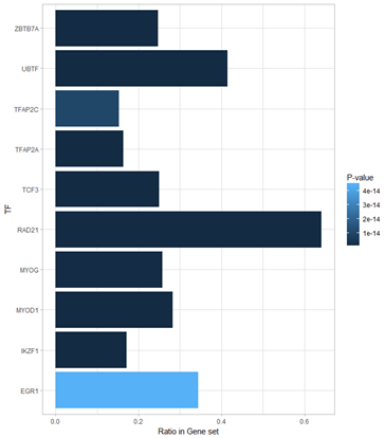

LPS vs LPS+HAGG: Replicate 3

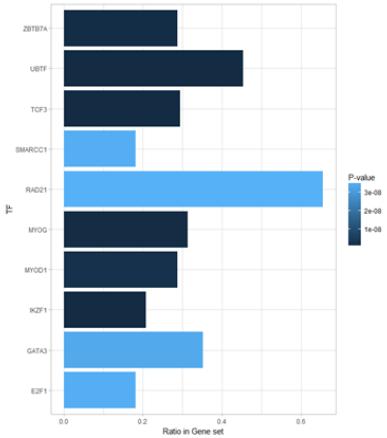

TPP vs TPP+HAGG: Replicate 3

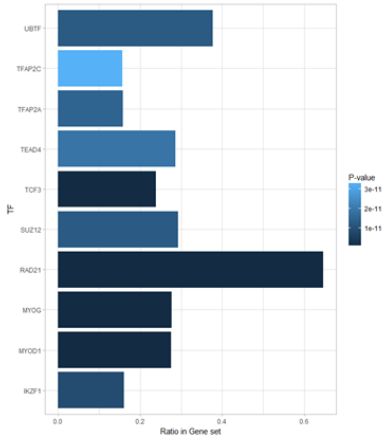

Figure 5.3.19. Transcription factors with a significantly increased number of targets in conditions without immune complexes vs those with; samples that showed inflammatory changes. Note M2a and M2c data are shown in tables as no significant hits.

5.4 Discussion

Based on flow cytometry analysis and RNA-seq data, expression of FcγRIIb appeared to be increased for M2a cells compared with other conditions, although the change did not appear to be statistically significant (Figures 5.3.1 and 5.3.2). If an increased number of repeats for the flow cytometry experiment (providing higher statistical power) demonstrate a more significant change, then this would be an interesting observation; FcγRIIb is an inhibitory receptor, known to regulate the activity of immune cells, and M2a macrophages are reportedly involved in regulation of the immune response and inflammation resolution (Nimmerjahn and Ravetch, 2008); (Fraternale *et al., 20*15). Hence it is possible that the activity of these cells is in part regulated by signalling through this receptor. One way to test this may be to perform an M2a activity assay (e.g. production of anti-inflammatory cytokines) where IC are present and signalling through FcγRIIb is blocked in one condition. If this inhibition alters the functionality of M2a macrophages then it would be possible to suggest that the anti-inflammatory activity demonstrated by these cells is in part due to FcγRIIb signalling (Bartosh and Ylostalo, 2014). Although the stringent *FCGR* gene alinment allowed transcripts corresponding to the different receptors to be distinguished, it meant that reads mapping to the more homologous regions were discounted. Hence counts given were an underestimation of expression. This meant that although transcription of different receptor subclasses could be compared to one another, they could not be compared to that of other genes. If this information is required, future studies may use qPCR, with primers targeted to PSVs and CSVs, described in this Chapter. Note that in the case of *FCGR2C* the region targeted was a SNP (THP-1 cells were homozygous for this allotype) and so may not be applied in cells which do not have the appropriate genotype.

Based on the findings in this Chapter, it can be suggested that although the addition of IC to a myeloid culture system does not block or induce any of the polarisation states previously described, they do appear to modulate the transcriptional profile of monocytes, and perhaps macrophages. In the analyses described here, GO terms such as “Neutrophil activation” and “Granulocyte activation” have been highlighted as top hits when comparing genes differentially expressed between unstimulated monocytes and cells treated with IC. As monocytes and neutrophils share a common myeloid origin, it is not necessarily surprising that there are some overlaps in gene expression between these phagocytic cell types (Kumar *et al., 20*16); (Naranbhai *et al., 20*15). Some of the genes significantly differentially expressed in monocyte + IC samples (versus unstimulated monocytes) relating to the neutrophil enrichment terms

described above include *C3* and *CD55* which contribute to and regulate the complement pathway respectively (Terstappen *et al., 199*2); (Shimizu *et al., 199*2). Other genes include *NEU1* and *FUCA1*, which translate to lysosomal proteins in phagocytes (Stamatos *et al., 20*05); (Panmontha *et al., 20*16). *CYBB* is another DEG contributing to the neutrophil enrichment terms; this genes codes for a super oxide generating enzyme which contributes to the formation of reactive oxygen species, which has microbicidal properties (Okura *et al., 20*15). Expression of these genes and subsequent proteins, and respective functions have also been reported in myeloid cells, which could be an explanation for why “neutrophil” functions are enriched between different populations of monocytes (Stamatos *et al., 20*05); (Verdugo *et al., 20*13); (Terstappen *et al., 199*2); (Shimizu *et al., 199*2); (Okura *et al., 20*15). More detailed investigations supplemented with experimental data would be required to determine the relevance of expression of these genes in this cell type.

Myeloid cells are key effectors in auto-antibody driven inflammatory disease, so it is possible that the transcriptional changes identified in this chapter are consequences of pathological events and may contribute to disease progression. For instance, the TFs identified which were linked to autoimmune disease (where autoreactive antibodies are a characteristic feature) could be at least in part activated or cooperatively induced by ICs (Ikuta *et al., 20*12); (Dong *et al., 20*08); (Angiolilli *et al., 20*16); (Sweeney *et al., 20*10). An interesting next step would be to investigate expression of transcripts and related pathways downstream of these TFs binding experimentally, and investigate whether this gene signature can be induced using ICs isolated from RA or SLE patients. Considering up-regulation of TF IRF3 target genes, string network plots for IRF3 interactors revealed an interesting pattern; transcription of genes for some proteins which increase the activity of IRF3 at the post-translational level was upregulated in monocytes treated with IC (versus unstimulated monocytes). As transcriptional expression of *IRF3* was not increased upon the addition of ICs, these findings suggest a mechanism by which activity of the respective protein could be increased under these conditions. Links between activity of this TF and RA are also interesting as ICs are reportedly found in these patients (Angiolilli *et al., 20*16). Hence it would be a logical step to question the involvement of IC ligation on activating monocytes in this way in RA. A potential next step would be to look at promotor regions for these genes to identify any common binding sites for agents inducing transcription. If this reveals a common activator then chromatin immunoprecipitation could be performed to verify this, and further experiments could be performed to link this agent to FcγR signalling. These findings highlight another interesting point; a number of

changes induced through treatment with immune complexes may actually occur at the protein level, which may be indicated by aspects of sequencing data but not clearly demonstrated. Hence follow up experiments and additional studies focusing on protein changes may be necessary to get a clearer picture of how myeloid cells respond to immune complexes.

Technical issues between repeats were likely to be responsible for lack of consistency between macrophage replicates treated with immune complexes; due to the size of the experiment, different replicates were prepared separately and run on different lanes of the sequencer flow cell. Batch effects are common in samples prepared on different days and can be attributed to a number of issues, some as simple as hardware differences (Leek *et al., 20*12). For instance, fluctuations in temperature in a tissue culture incubator may alter cell transcriptomes and work towards masking any biological differences; there are reported cases of biological variables relating strongly to technical variance and normalisation is not always possible (Petricoin *et al., 20*02); (Johnson *et al., 20*07); (Leek *et al., 20*12). This could be the case here, so any attempts to repeat this experiment should include scaling the experiment down to a size at which all samples could be prepared at the same time. Another factor that may have contributed to the differential transcriptomes upon immune complex treatment is size of IC molecule used. As interactions between FcγRs and IgG are highly co-operative; size of immune complex is a crucial factor in determining binding strength and activation of subsequent signalling pathways (Lux *et al., 20*13); (Jarvis *et al., 19*99). When run on a polyacrylamide gel, two distinct bands were identified, suggesting the presence of IgG aggregates of different molecular weights in the IC fractions. Although the IC was prepared as a batch, it is possible that upon aliquotting, the quantities of different sizes of immune complexes added to each sample were not consistent. One way to ensure this issue is avoided in the future would be to mix the batch well prior to aliquotting, and run a small amount of each aspirate on a polyacrylamide gel to ensure consistency.

One important consideration here is the lack of expression of FcγRIIIa on the THP-1 macrophages according to flow cytometry data; tissue macrophages isolated from patients with IC driven conditions such as RA are found to express these receptors, and subsequent signalling is likely to induce changes in the cell (Laurent *et al., 20*11). As this receptor is important in IC-mediated activation *in vitro*, it is likely that its absence would influence the results generated for this experiment (Nimmerjahn and Ravetch, 2008). It could be that the absence this protein in THP-1 macrophages is due to a problem with the cell line or is a consequence of experimental factors or a result of

a mutation that has been acquired. This could be addressed by purchasing a new batch of THP-1 cells or further optimisation of the flow cytometry experiment, aimed at reducing background and maturing the macrophages. If further optimisation fails, it may be possible to virally transfect these cells to induce production of FcγRIIIa in the absence of stimuli. This could be used as model to examine how ligation of this receptor with IC influences macrophage functioning.

Despite the lack of consistency between macrophages replicates, immune changes were observed in some samples. Although no definitive conclusions can be drawn from this particular analysis, a number of experiments can be designed to interrogate gene expression profiles and pathways based on this data. It should also be noted that any phosphorylation events which may change cell activity at the protein level would not necessarily be detected here; different experiments would be required to investigate these changes, such as western blotting (to detect phosphorylation by size change), or functional assays to detect changes in activities of enzymes downstream of FcγRs. There are other factors that may have compromised replicability of macrophage-IC+ conditions including strong cytokine stimuli masking the effects of IC, different fractions of HAGG having variable effects on samples, responses being protein related (making transcription changes unrelated to polarisation) and type of antibody (anti-CD52) having variable effects on cells. One way to help determine whether changes are genuine rather than non-specific would be to measure kinetics changes upon IC addition (e.g. using a Ligand tracer) alongside other experiments to discern whether an interaction has taken place.

One alternative approach to the analysis may have been to look for DEGs between all macrophage subtypes (as a group) with and without IC; consistant differences may have been identified this way. However, any co-operative signalling-related or subtype-specific changes that occur upon FcγR ligation would have been missed. Additionally, if any IC-specific gene expression profiles are masked through specific cytokine treatments (e.g. IFNγ), this approach may have prevented detection of relevant DEGs in the other treatments.

Notably, effects of FcR pathways are modified through interactions with other signalling pathways (e.g. complement) and this may drive the RA macrophage phenotype. Hence the absence of other cells and inflammatory agents may be responsible for any limited responses from IC ligation compared to pathological states (Del Rio *et al., 19*99). However, testing of individual agent is essential before progression to more complex systems, and so the experiments described in this chapter are necessary.

Chapter 6: General Discussion and future work

6.1. Macrophage polarisation and in vitro models

6.1.1 The spectral model of macrophage polarisation is represented *in vitro*

Overall, the data generated in this thesis supports the paradigm that macrophage polarisation is a diverse and flexible process, with differentially stimulated macrophage phenotypes appearing on a spectrum. For instance, there is a great deal of evidence that the macrophage transcriptome, and possibly overall phenotype, is dictated by more than just the classical stimuli (IFNγ and LPS for M1, IL-4 and IL-10 for M2a and M2c, respectively). In Chapter 3 of this report, changes could be seen when cells were stimulated with additional stimuli; i.e TNF, PGE2, Pam3sk4, to generate chronic inflammatory-like TPP macrophages (Chapter 3, Figure 3.3.22). This subtype was not described in the original bipolar paradigm, but was observed here. Chapter 4 confirmed a distinct transcriptional profile for these cells when compared to M0 and M1 subtypes; significantly DEGs were identified through pairwise comparisons with both of these cell types, demonstrating changes in gene expression in response to the TPP stimuli into a phenotype distinct from that of the classical inflammatory cells (for DEGs please refer to Appendix 1, Tables A1.1 and A1.2). Additionally, transcriptional changes were identified for macrophages in Chapter 5 when ICs were included as an additional stimulus. However, as described in Chapter 5 these changes were not consistent and so it is unclear whether observations are valid markers of IC-skewing, given the large amount of variability in the dataset.

Other studies have demonstrated changes in transcription profiles of macrophages in response to non-classical stimuli. For example, novel subtypes have been described for cells isolated from adipose tissue in obese mice, for macrophages found during chronic inflammation and for cells isolated from atherosclerotic lesions (Lumeng *et al., 20*07); (Xue *et al*.); (Villani *et al., 20*17); (Kadl *et al., 20*10).

It should be noted that although the subtypes of the bipolar model of macrophage polarisation may be over simplistic, they are useful as reference points when testing the effects of other stimuli. For instance, it is interesting to examine the effect of a previously untested stimulus on unpolarised cells to examine which pathways are upregulated, but it is also useful to determine how gene expression under these treatments relate to that on (for instance) M1 cells. This could be beneficial in giving an indication of macrophage function.

Taken together these data suggest that macrophages are incredibly versatile and may adopt a large number of states. This is particularly relevant when considering macrophages in disease and healthy tissue, since these cells will express cell surface receptors for many agents present under physiological and pathophysiological conditions. It should hence be considered that an increased number of macrophage subtypes than those already established may be present in tissue, and (as alluded to previously) that physiological subsets should be considered as positions on a continuum.

6.1.2 Intermediate phenotypes

A growing body of evidence suggests that when exposed to two or more different stimuli, monocytes and macrophages will demonstrate a combined transcriptional profile for these agents (Chan *et al., 20*08); (Shaul *et al., 20*10). Multiple signals may be co-operative, opposing or independent depending on the stimuli given.

Some macrophage signals are additive; for instance, M1-THP-1 macrophages were induced with both LPS and IFNγ. In Chapter 3 an LPS titration was performed where concentrations were increased from 0ng/ml to 250ng/ml (Chapter 3, Figure 3.3.8). Here it could be seen that when LPS was added, an increased number of markers was seen compared to those expressed when exposed to IFNγ only. Transcription of other M1 markers (e.g. *CXCL9* and *TNFAIP6*) was consistent upon LPS addition. Hence these cells demonstrate a transcriptional profile relating to both of these agents. Additionally, in Chapter 4 where LPS only and M1 (LPS+IFNγ) samples were plotted on the PCA plot, the y axis appeared to represent polarisation (please see Chapter 4, Figure 4.3.2); here LPS-treated samples mapped between M1 and M0 cells, suggesting that LPS cells had an intermediate M1/M0 phenotype.

It should also be noted that in Chapter 5 (Figure 5.3.7), differentially polarised macrophages retain expression of subset-specific markers, even upon administration of ICs. Although changes in IC-treated samples are inconsistent, the transcriptional changes are present. Hence any change in transcriptional profile appears to be in addition to polarisation response. Given this, phenotypes identified following the addition of ICs may be considered as intermediate or mixed.

Under physiological conditions macrophages will be exposed to multiple, variable stimuli, and so identifying combined phenotypes is highly relevant when considering healthy or disease-tissue macrophages.

Previous reports have taken changes in transcriptional profiles of cells to be indicative of an altered monocyte or macrophage phenotype. Terms relating to these two aspects

have hence been used synonymously in some reports. Some papers have recently veered away from using terms such as M1 and M2a, and instead describe the cells as having a specific signature; for instance, a pro-inflammatory IFNγ signature or anti-inflammatory IL-4 signature. Given that expression of certain cytokine-specific markers does not change upon addition of other molecules (e.g. addition of ICs or LPS to IFNγ as described earlier in this Section), this may be more appropriate nomenclature to use in the future; M1 macrophages may be described as having a combined IFNγ and LPS signature for instance.

6.2. Fluidity of macrophage markers

A large number of studies consider phenotype-specific markers to be absolute. However, gene expression is highly dependent on the length of time for which the cells are cultured with the polarising stimuli. This appears to be true for both THP-1 cells and primary macrophages; for instance, PBMC macrophage microarray datasets published by Xue *et al.* (2014) were analysed in Chapter 2 (Figure 2.3.8), and gene expression levels were seen to vary between the shortest (30 minutes) and longest (72h) cytokine incubation times. Additionally, THP-1 cells were cultured with M1 and M2a stimuli (IFNγ+LPS and IL-4, respectively) for different lengths of time, and this appeared to have an effect on gene expression (Chapter 3, Figures 3.3.18 and 3.3.19). Hence, it must be emphasised that macrophage markers are considered for a specific time point rather than immediately and consistently once a polarising cytokine signal has been given.

6.3. THP-1 cells as a model for primary monocytes and macrophages

6.3.1. Cell lines as *in vitro* models for studying macrophage polarisation

The use of cell line models in the study of human disease is a hotly debated topic. On one hand, there is an argument that mutations in the cell line will have an effect on the results, but homogenous genetic background is essential for running multiple, replicable, comparable experiments. This is not always feasible using primary human cells and so cell lines have a place when exploring immunological and pathological processes. One way to increase confidence in the cell line is to develop a model which demonstrates high levels of similarity with primary cells. This study aimed to develop a THP-1 cell-line model to these specifications. In Chapter 3 it was clear that M1 and M2a THP-1 macrophages expressed some subset-specific markers (Figure 3.3.21) identified from a public available dataset generated using PMBC monocytes in Chapter 2 (Table 2.3.4), suggesting that in terms of polarisation, these cell types followed a

similar pattern. This was corroborated in Chapter 4 when genes differentially expressed between M1 and M2a cells in both THP-1 and PBMC macrophages were correlated, and overlapping genes between the two cell types were found to be related to immune signalling (Chapter 4, Figures 4.3.5 and 4.3.6). Hence this cell line model would be useful when studying immune pathways.

Biological processes that vary between M1 and M2a macrophages are fairly well established and relate to functions of these cells. Hence gene ontology analysis focusing on biological functions was used to indicate polarisation state; functions traditionally relating to M1 cells were enriched for lists of significant DEG upregulated in M1 cells. Examples of terms which were found in the top ten hits include defense response to other organisms, positive regulation of cytokine production, and regulation of innate immune response. These functions relate to M1 activities such as bacterial killing, cytokine production and activation of macrophage immune responses respectively (Arango Duque and Descoteaux, 2014). The terms enriched for the M2a genes did not appear to reflect traditional M2a functions to the same degree as those identified for the M1 gene list. For instance, top hits generally related to cell cycle processes and included terms such as mitotic nuclear division or ribosomal biogenesis. In mice, cell cycle is reportedly halted in IFNγ and LPS treated macrophages which may account for these findings (Xaus *et al., 19*99). However, it could be the case that transcription of M2a specific genes was not extensive enough due to incomplete M2a polarisation (reported to be the case in THP-1 cells), or that there is some redundancy of GO annotations. Additionally, as annotations are based on literature there are some limitations; for instance, novel ontologies reflecting these phenotypes would not be identified here.

Transcription factor (TF) target analysis provided a method to group transcripts that may otherwise appear unassociated. In the analysis of genes upregulated in M1 cells versus M2a, enrichment of transcripts induced by STAT1, 2 and 3 TFs was reported. M1 polarisation is linked with the activity of STAT1; IFNγ reportedly induces JAK-1/2 mediated tyrosine phosphorylation and subsequent STAT1 dimerisation and phosphorylation. For LPS induced M1 cells, signalling through TLR-4 results in NFκB activation and subsequent transcription of IFNβ. Autocrine activity of this cytokine results in STAT2 phosphorylation and activation. As described in previous Chapters, STAT3 can be induced by IL-10 signalling and subsequently drives an anti-inflammatory phenotype. Conversely, this TF can also be activated by IFNβ (as with STAT2) and promote an inflammatory macrophage phenotype (Tugal *et al., 20*13). Taken together, the activation of the TFs described above supports transition of macrophages into an inflammatory, M1-like phenotype.

For the genes upregulated in the M2a condition, enrichment of targets for TF MYC was observed. MYC (or c-MYC) is a TF known to be induced by IL-4 in macrophages and is reportedly responsible for induction of around 45% of M2a associated genes (Pello *et al., 20*12). Specifically, this TF increases transcription of *ALOX15* and *CD206*; two genes strongly associated with alternative macrophage activation which were also induced in THP-1 M2a macrophages (in Chapters 3 and 4). Additionally, MYC is indirectly linked to transcription of *CD209*, a gene found to be M2a specific in the analysis aimed at identifying subset-specific transcripts (Figure 4.3.12) (Pello *et al., 20*12). Hence enrichment of targets of this TF is in support of the M2a state being achieved by THP-1 macrophages using the protocol developed in Chapter 3.

6.3.2 M1 and M2a specific functions for THP-1 macrophages generated using the optimised polarisation protocol

Although gene expression and morphology suggested that accurate M1 and M2a macrophage phenotypes had been achieved, functional assays demonstrating subset specific activities in differentially polarised cells would be beneficial for confirmation. TNF release assays may be useful for distinguishing M1 and M2 cells as TNF production is reportedly higher in the former following subset-specific cytokine exposure (Bartosh and Ylostalo, 2014). Conversely, wound healing assays and efferocytosis studies can be performed to test M2a functions; wound healing (e.g. scratch assays) and removal of cellular debris (assays focused on measuring endocytosis of non-bacterial cell bodies), respectively (Zizzo *et al., 20*12); (Jetten *et al., 20*14).

6.4.Macrophage markers: novel and validated

6.4.1. Marker validation

As described in previous Chapters, certain transcripts were highlighted as robust macrophage polarisation markers. Established M1 markers such as *CXCL10*, *CXCL9*, *IL6*, *TNFAIP6* and *GBP5* were identified from public datasets generated through experiments using primary macrophages (Chapter 2 Figure 2.3.2), and were similarly upregulated in the M1 condition (versus M0 and M2a) in THP-1 cells according to end-point PCR (Chapter 3 Figure final). Additional quantitative analysis of gene expression using RNA-seq data derived through sequencing differentiated and polarised THP-1 macrophage transcriptomes confirmed these observations. Hence these markers appear to be highly robust for identifying M1 cells in both the THP-1 cell line and primary macrophages, suggesting that they strongly reflect the polarisation status of

the cells. This is further supported by the functions of proteins translated from these transcripts in immunity; CXCL9 and CXCL10 are credited as chemoattractants for immune cells via their target receptor, CXCR3, and have roles in promoting a type 1 T-helper cell response (Thapa *et al., 20*08); (Hardison *et al., 20*06), GBP5 promotes NLRP3 inflammasome assembly and is required for activation of the AIM2 inflammasome in the presence of certain pathogens (Man *et al., 20*15); (Shenoy *et al., 20*12), IL-6 is a pro-inflammatory cytokine involved in T-cell activation and acute phase protein production (Tanaka *et al., 20*14) and TNFAIP6 protein interacts with mediators of the protease network involved in inflammation (Wisniewski *et al., 19*96).

Similarly, Novel markers M1 *ANKRD22* and *TSC22D1* were identified from primary macrophage data and validated in differentiated THP-1 cells using PCR and RNA-seq experiments. Interestingly, the functions of proteins coded by these genes are not well studied and so it is unclear how expression of these transcripts relates to macrophage functioning. Some studies have linked the activity of ANKRD22 to tumor progression, and expression has been demonstrated in human whole blood samples following immunisation, suggesting a potential role in immunity (Matsumiya *et al., 20*14); (Yin *et al., 20*17). However, the role of this gene remains unclear and additional investigations (e.g. siRNA knockdown studies in THP-1 macrophages during M1 polarisation) would be required to further elucidate its roles in inflammation and macrophage physiology. The function of *TSC22D1* is more studied; this gene codes for a TF that regulates cellular senescence, which (as described in Chapter 3) is a process involving interactions with some inflammatory genes (*IL6, IL8*) (Hömig-Hölzel *et al., 20*11); (Mendonça *et al., 20*10). However, as with *ANKRD22*, further investigations must be carried out to determine the role of this gene in macrophage polarisation.

It should be noted that in Chapter 5 (Figure 5.3.7), examination of marker panel transcripts in an increased number of conditions revealed some overlap between gene expression in M1, M2b and TPP conditions; for instance, genes *IL6* and *TNFAIP6* were found to be highly expressed in these polarisation states compared with others. As M1 and M2b conditions share LPS as a common stimulus (a TLR4 agonist) and TPP cells include treatment with Pam3SK4 (a TLR2 and TLR4 ligand), it is possible that genes upregulated by all of these subtypes are induced by TLR signalling. In fact, expression of *IL6* has previously been associated with TLR4 signalling in murine T-cells, suggesting this is a plausible hypothesis (Wu *et al., 20*15).

Interestingly, these markers appeared to retain their expression pattern across the different subtypes when all samples were supplemented with ICs in Chapter 5. Hence these markers may be used in experiments where macrophages have been exposed to ICs to determine whether an M1 signature is present. This may be useful when

studying cells isolated from patients with autoimmune diseases, characterised by the presence of ICs (SLE, RA) or infections with associated antibody responses.

In terms of protein expression, markers such as *IL6*, *CXCL9* and *CXCL10* may be of limited use in histology studies as they are generally secreted. They may, however, be useful in experiments involving biochemical examination of macrophage derived media or some tissue samples (e.g. synovial fluid or blood or RA patients) to give an indication of inflammatory status of cells. Tissue specificity must be considered when selecting markers that may be used in studies on patient tissue; although strongly expressed by macrophages, these factors can be expressed by other immune-related cells (Villiger *et al., 19*91); (Ohtani *et al., 20*09); (Spurrell *et al., 20*05). Therefore, it would be necessary to use other means to identify macrophages if examining a mixed cell population (e.g. in tissue samples).

According to the human protein atlas (source: http://www.proteinatlas.org), proteins corresponding to *GBP5*, *TNFAIP6*, *ANKRD22* and *TSC22D1* are intracellular and so may be detected in tissue or cell lysates, or fixed, permeabilised cells. Tissue specificity should also be considered in these cells; GBP5 protein appears to be the most specific marker for myeloid cells, although it can be expressed in endothelial cells upon IFNγ stimulation (Tripal *et al., 20*07); (Shenoy *et al., 20*12). Little information is available for ANKRD22 reducing confidence in its use as a tissue specific marker.

As with the M1 markers, established M2a specific transcripts highlighted in the analysis of primary macrophage subtypes in Chapter 2 were tested experimentally using PCR and RNA-seq experiments on differentiated and polarised THP-1 cells. Transcripts such as *ALOX15*, *CCL26* and *CD200R1* were found to be specific when examined using both of these techniques in THP-1 cells, emphasising their efficacy. The commonly used literature marker *TGM2* was also found to be effective for demonstrating M2a polarisation in THP-1 cells. Novel transcript *HOMER2* was specific for M2a cells in the PBMC macrophage dataset and in THP-1 cells. However, in the quantitative RNA-seq experiment it appeared to be expressed to some degree in M2c and M0 cells. It was also observed to be upregulated for one of the M1 samples, but this was not consistent. The lack of consensus between the conditions suggests that these reads are not as reliable as for the other genes. The reliability of this marker must therefore be determined through additional experiments. *CCL23* expression was reportedly higher in monocytes versus other cell types, and *CCL17* was increased in TPP conditions versus other samples (Chapter 5 Figure 5.3.7); this did not correlate with the MDM dataset examined in Chapter 2 (Table 2.3.4) and the PCR experiments in Chapter 3 (Figure 3.3.21). However, an increased number of conditions were used in this analysis versus those in Chapters 2 and 3 which may have confounded the results.

It should also be noted that expression of *CCL17* did appear to be quite weak in the PCR experiments in Chapter 3 so it is possible that this is not a robust marker. However, in Chapter 4 Figure 4.3.7, *CCL17* did appear to be more specific when less conditions (i.e. no TPP or M2b cells) were considered. Based on this data *CCL23* and *CCL17* cannot be considered reliable M2a markers (the latter when TPP cells are included in the analysis) and further investigations should be performed to determine whether they could be used reliably in macrophage polarisation studies or not.

As with M1 markers, expression of transcripts *ALOX15*, *CCL26*, *CD200R1* and *TGM2* does not appear to change upon addition of ICs. Hence these markers may also be useful for identifying macrophage subtypes in patient tissue where these stimuli are found.

Antibodies against proteins from *ALOX15, CCL26, CD200R* and *TGM2* may also be considered here; CCL26 is a secreted chemokine and may be detected in ELISA assays performed on macrophage conditioned media to identify polarisation state of the macrophages. Conversely CD200R is expressed on the surface of cells so may be used as a histology or flow cytometry marker. ALOX15 and TGM2 are localised to the intracellular region/plasma membrane or intracellular/extracellular region respectively, and so may be used in experiments where tissue is lysed or cells are permeablised. However, as with the M1 cells, tissue specificity should be considered. These markers are found to be expressed on other cells and so must be used in conjunction with a macrophage specific marker if used experimentally (Stubbs *et al., 20*10); (Shureiqi *et al., 20*05); (Ai *et al., 20*08). CD200R may be the most appropriate M2a marker discussed here due to its cell surface localization and the fact that its expression is predominantly restricted to cells of myeloid origin (Minas and Liversidge, 2006).

6.4.2. Specificity of novel marker expression on THP-1 cells

Some potential markers were identified from the THP-1 RNA-seq dataset and cross-validated in the PBMC macrophage data which was originally analysed in Chapter 2. It should be noted that in contrast to transcripts identified in Chapter 2, potential markers in Chapter 4 were selected against M0, M2b, M2c, TPP and monocyte conditions. Hence, they may be more specific when considering a larger number of conditions. Here, markers were selected if they were subset-specific in both primary and THP-1 datasets, and if functions were logical for the subset of interest. For instance, potential M1 markers included the ETS variant 7 repressor gene (*ETV7;* coding for a transcription factor that has previously been associated with LPS signalling), the neuralised E3 protein (*NEURL3*; ubiquitin protein ligase gene which undergoes activity

change upon cholesterol accumulation) and *CD276* (a member of the B7 costimulatory family of receptors) (Bobryshev *et al., 20*16); (Baillie *et al., 20*17). According to data available on Protein Atlas (source: https://www.proteinatlas.org), the corresponding protein for the potential M1 marker *NEURL3* is also highly expressed in cell lines derived from B lymphocytes and pancreatic cells (RPMI-8226 and CAPAN-2 respectively) (Thul *et al., 20*17). Hence when considering macrophage polarisation in any diseases where these cell types are also present (e.g. macrophage infiltration in pancreatic cancer, rheumatoid synovium where B cell and macrophages are present), it is important to consider the likelihood of this marker being cross-expressed. ETV7 protein is also expressed in non-hematopoietic cell types in response to inflammatory related stimuli (e.g. in hepatic cells in response to hepatitis C virus) and so is likely to be unreliable if used as a single marker in inflammatory disease tissue (Ignatius Irudayam *et al., 20*15). Additionally, membrane CD276 protein is an important immune checkpoint protein (a member of the B7 and CD28 family) and has been detected on the surface of a number of immune cells (including DCs, monocytes, activated T-cells and some carcinoma cells) and some other cell types (Picarda *et al., 20*16). This must be considered when examining macrophage polarisation in tissues with multiple cell types (Zhang *et al., 20*08).

Some genes that may make useful markers for the M2a polarisation state if validated include *HAS3* which codes for hyaluronan synthase-3, a protein involved in production of hyaluronic acid (Chang *et al., 20*14), *CHN2* (chimerin 2) which codes for a protein involved in proliferation and migration and *LOX* (encodes lectin like LDL receptor 1) which has been found to be associated with atherosclerosis in studies performed on murine macrophages (Ding *et al., 20*13). It should be noted however that expression has also been seen for endothelial cells, smooth muscle cells and fibroblasts which are also present in atherosclerotic (and other disease) tissue (Draude *et al., 19*99). HAS-3 protein was found to be expressed on articular cartilage upon cytokine treatment (Hiscock *et al., 20*00) and so may be problematic as a marker when considering inflamed joint tissue (e.g. in RA).

As discussed previously, M0 and “de-activated” M2c cells were not determined to be significantly different according to DEG analyses, hence markers were identified to represent both of these conditions; *ALOX5* and *VSIG4* were both present M0/M2c cells, but also M1 and M2b phenotypes. Another M0/M2c marker, *EPHB6*, was not induced in M1 and M2b cells but was present for M2a and monocyte subtypes. Hence these markers may be incorporated as a panel to identify these subtypes. In terms of functions, ALOX5 (arachidonate-5 lipoxygenase) has roles in synthesis of leukotrienes.

This gene is specifically expressed in bone marrow derived cells, and mutations in the promoter region have been linked with decreased response to anti-leukotriene drugs in asthma (Mougey *et al., 20*13). *VSIG4* encodes a v-set and immunoglobulin domain containing protein that is structurally related to B7 family of immunoregulatory proteins, which acts as a receptor for C3b and iC3b and may negatively regulate T-cell responses (He *et al., 20*08); (Van Loo *et al., 20*10). EPHB6 is a transmembrane epherin receptor without a functional kinase domain. Downregulation of this gene is seen in metastasis, hence it may inhibit movement of cells when expressed (Wilkinson, 2001). These genes appear to be linked to inflammatory functioning or cell motility and may therefore reflect activity of their relative macrophage subtypes.

All potential M2b markers were also expressed in M1 cells. Hence these markers may be used to identify the M2b polarisation state when used alongside M1 specific markers (e.g. *GBP5*, *CXCL9*). *TNFSF10* and *SERPING1* were identified as most specific in M2b (and M1) THP-1 macrophages along with MDMs. TNFSF10 protein (also known as TRAIL) is a member of the TNF superfamily of cytokines and is credited with inducing apoptosis in transformed tumor macrophages. It also promotes macrophage lipid uptake, supporting foam cell formation (Liu *et al., 20*14). This molecule is secreted and would hence be more useful in biochemical studies compared with histology-based experiments. TNFSF10 is expressed on other immune cells (including NK cells) and may hence be inappropriate in studies performed on whole tissue without a pan macrophage marker. SERPING1 has been discussed previously as an M1 marker; the corresponding protein has been described as a complement activation inhibitor which has clear roles in immune regulation (Wagenaar-Bos and Hack, 2006). According to the Human Protein Atlas (source: http://www.proteinatlas.org/) this protein is predicted to be both secreted and intracellular, and so may be useful in histology studies. However, expression is not specific to macrophages and so co-staining with a pan-macrophage marker would be necessary.

Potential TPP markers included *LMP2* and *CSF2*. *LMP2* codes for the major catalytic immunoproteosome subunit, crucial for MHC I activity (Brucet *et al., 20*04) and *CSF2* codes for GM-CSF, a cytokine which has well documented roles in macrophage (particularly inflammatory related) differentiation (Shi *et al., 20*06). According to the human protein atlas (source: http://www.proteinatlas.org) LMP2 protein is found in the intracellular compartment and so may be used in experiments where cells are permeablised or lysed. However, this protein is expressed in a number of different cell types and would therefore not make a specific marker for this polarisation state in

macrophages. GM-CSF is a secreted protein that is produced by a number of cells (macrophages, NK-cells, T-cells, endothelial cells) and so would not be a reliable histology marker (Shi *et al., 20*06). It may however be used in *in vitro* studies to examine macrophage polarity.

As alluded to previously, in histology studies, it is possible to co-stain a polarisation marker with a pan-macrophage marker if the protein is not specific to macrophages. One frequently used surface marker for this is CD68; this protein has been used reliably in previous investigations (Stöger *et al., 20*12). Expression of the *CD68* appeared to be consistently high in all of the conditions tested in Chapter 5 (when compared to variable expression of *CXCL10*) which supports its use as a pan macrophage marker (Appendix 4, Figure A4.4).

Although RNA-seq analysis provides large amounts of data, quantitative lab-based experiments are often required to validate gene expression in samples of interest prior to practical application. Quantitative PCR is a frequently used tool for this (Rajkumar *et al., 20*15); RNA-seq markers validated using this method are generally confidently applied for downstream experiments. Hence, this may be a useful technique to validate expression of the THP-1 polarisation markers for M0/M2c, M1 M2a and M2b markers identified in this report.

6.4.3. Expression of novel markers in primary monocyte derived macrophages

Although the markers were cross referenced using an MDM dataset, it is also important to validate the expression of these genes in primary macrophage cultures. This would validate the use of these markers in studies performed on human tissue samples and allow them to be applied more confidently.

Overall, a panel of robust macrophage polarisation markers would be beneficial for future research into phenotypes of these cells in human tissue, and a summary of the levels of validation for the markers discussed in this thesis may be found in Appendix 7; Table A7.1 and figure A7.1.

6.5. Transcriptomics as a research method

Next generation sequencing is hailed as a powerful and highly sensitive tool for generating vast amounts of data which can be analysed in a variety of ways to inform us about a biological system. However, is it clear from the data generated in this project that there can be technical limitations when using these techniques and that careful planning is essential to reduce the impact of these factors. One major issue

seen here was batch effect; subtle changes in temperature and gas concentrations in incubators may affect background RNA expression, and so if replicates are not incubated at the same time, this may increase variability between them. Another factor may be variability between different batches of cytokines and HAGG; this would alter the responsiveness of the different samples to stimuli.

If this experiment were to be repeated, all replicates should be prepared on the same day using the same apparatus and kept in the same incubator. To reduce variability between batches of reagents, aliquots of the same substance may be prepared at the same time, pooled, mixed thoroughly and re-aliquotted to ensure consistency between all stocks. These considerations may reduce variability between replicates and prevent masking of biologically relevant changes.

6.6. Influence of Fc gamma receptor ligation on macrophage polarisation

Expression of different FcγRs on monocytes and macrophages (Chapter 5 Figures 5.3.1 and 5.3.2) suggested that these cells were susceptible to IC stimulation. This is corroborated by the changes seen in macrophage and monocyte transcriptomes in Chapter 5, although the differences reported for macrophages were not consistent. For monocytes, enrichment of IRF3 targets in a list of genes which were increased upon IC treatment and increased transcription of genes positively regulating the activity of this protein at the post-translational level suggest FcγR signalling may increase activation of this protein. Overall this may provide insight into potential mechanisms in diseases characterised by macrophage mediated destruction and the presence of IC, such as RA and SLE. Furthering understanding of disease processes is essential when considering novel therapies and management strategies. Interestingly, higher activity of IRF3 has been identified in RA synovial cells with reports of increased regulation of target genes (Angiolilli *et al., 20*16); (Sweeney *et al., 20*10). Circulating pDCs isolated from SLE patients reportedly demonstrated increased expression of IRF3, and a SNP in the corresponding gene has been linked to disease susceptibility (Santana-de *et al., 20*14). Hence this transcription factor appears to have some importance for myeloid cell biology in IC-mediated disease. However, the degree to which IC ligation drives this association remains to be determined.

As stated previously, the TF IRF3 was highlighted as potentially interesting since a significantly increased number of its targets were found to be upregulated upon treatment with IC. To confirm the biological relevance, it would be important to validate the expression of some of these genes using qPCR as discussed previously (for marker validation, Section 7.1) (Rajkumar *et al., 20*15). ERK pathway related

transcription factors E2F1, 4 and 6 were also enriched using this approach; as FcγR signaling was found to induce ERK pathways with subsequent activation of E2F TFs in murine macrophages, these finding could be considered a validation of this approach (Luo *et al., 20*10).

As increased binding of IRF3 to targets was only inferred by RNA-seq data, it will also be useful to demonstrate this interaction occurring experimentally. Chromatin immunoprecipitation assays could be performed for IC treated and non IC treated monocytes to confirm modulation of IRF3-target binding on exposure to ICs, hence relating the changes in gene expression to activity of this protein (Pillai *et al., 20*15).

6.7 Linking Fc-gamma receptor signalling to transcription factor activity in immune complex treated myeloid cells

6.7.1 Examination of promoter sequences for consensus sequences of transcription factor activators which are increased upon IC treatment

As discussed in Chapter 5 (Section 5.3.8), IC treatment was shown to alter the expression of some genes that code for proteins which positively regulate the activity and survival of IFR3 in monocytes. These genes include *PRKDC, HERC5, IKBKE* and *IFIT2*. It would be interesting to examine promotor regions or enhancer elements for these genes to examine whether a common TF is responsible for increasing their transcription and hence an increased IRF3 response. If this is the case then such experiments would inform on how ligation of FcγR with ICs increases IRF3 activity. It should be noted, however, that IRF3 is reportedly activated as a result of TLR signalling (Akira and Takeda, 2004). Hence when studying pathophysiology or diseases with multiple stimuli, it would be essential to determine whether activity of this TF is induced or enhanced by IC binding. As described previously, chromatin immunoprecipitation studies could be used here to prove a difference if IRF3 TF binding to target genes.

6.7.2. Investigating phosphorylation of transcription factors and their activators in immune complex treated monocytes

The respective proteins for *PRKDC* and *IFIT2* genes (described as increased upon IC treatment) reportedly enhance IRF3 phosphorylation (Siegfried *et al., 20*13); (Fitzgerald *et al., 20*03). Hence it would be interesting to measure and compare levels of phosphorylated IRF3 in monocytes treated with IC and unstimulated monocytes. This could be performed using western blotting (with a phosphorylation specific antibody) or

activity assays, and could inform on changes in signalling downstream of FcγR signalling. If these changes can be identified in monocytes, it would be interesting to investigate whether this is also a mechanism observed in M0 macrophages and possibly inflammatory (M1) cells upon IC treatment. If these experiments demonstrate a consistent change, similar experiments could be performed on various M2 macrophage subtypes to determine whether the observations are independent of polarisation state.

If increased activity or phosphorylation of IRF3 or increased transcription of *PRKDC, HERC5, IKBKE* and *IFIT2* can be characterised in monocytic cell lines or PBMC cells, it may be interesting to perform experiments on myeloid cells isolated from RA or SLE patients with autoantibody positive disease versus cells from an inflammatory condition with no ICs present. This may give an indication as to whether ICs induce or contribute to this change in IC-driven inflammatory disease. Additionally, RA patients may be stratified by RF and ACPA status; these subsets of patients are reported to have differences in disease severity, relapse rate and responses to therapy (Aletaha *et al., 20*15; Aletaha and Bluml, 2016; Seegobin *et al., 20*14). Hence it may be informative to examine the IRF3-related changes in macrophages treated with ICs derived from patients with different auto-antibody combinations, or myeloid cells isolated from these individuals.

6.8. Investigating the effects of Fc-gamma receptor blocking agents on effector functions in myeloid cells

Myeloid cells express multiple FcγRs, and ICs formed from IgG1 (used for the experiments in this thesis) will bind to most of these receptors. Hence observations cannot be attributed to the activity of a single FcγR. To dissect activity of individual receptors, gene expression and functional changes in monocytes responding to IC stimulation may be incorporated into an assay using agents designed to block specific FcγRs and subsequent signalling. This method could be used to test contributions of individual FcγRs to the phenotype seen upon treatment with IC, and may have implications for auto-antibody mediated conditions such as RA and SLE.

6.9 Summary

In conclusion, THP-1 cells appear to mimic primary macrophages when generated using the protocol described in this thesis. A number of markers have been identified and validated and so may be used for macrophage polarisation studies in the future. IC treatment appeared to alter the transcriptome of THP-1 monocytes and may increase

activity of TF IRF3, although experimental validation is required to demonstrate this change. RNA-seq datasets contain rich data that could be used in functional studies. Additionally, a number of experiment to validate RNA-seq data generated in this report have been suggested that may validate practical applications of findings in the study of human disease.

Appendix 1: Differentially expressed genes

Table A1.1. Top 100 significantly differentially expressed genes (according to Benjamini-Hotchberg adjusted p-value ordered smallest to largest, maximum threshold set to 0.05) identified through pairwise comparisons between M1 cells and other subsets using Deseq2 package in R (i.e. a negative binomial distribution method)

Monocytes	M0	M2a	M2b	M2c	TPP
IL1B	*CXCL10*	*CXCL10*	*CXCL9*	*ACOD1*	*CXCL10*
CXCL8	*GBP1*	*IDO1*	*UBD*	*GBP1*	*ACOD1*
IGFBP3	*IDO1*	*GBP5*	*ACOD1*	*IDO1*	*GBP1*
PTGS2	*GBP2*	*PDE4B*	*TBX21*	*GBP2*	*CCL8*
MMP1	*HLA-DRA*	*GBP4*	*APOL4*	*GBP5*	*GBP2*
TGM2	*GBP4*	*IRF1*	*IL31RA*	*ANKRD22*	*SECTM1*
THBS1	*RSAD2*	*HAPLN3*	*XIRP1*	*CCL8*	*ANKRD22*
MMP9	*ANKRD22*	*CXCL9*	*HLA-DPB1*	*HLA-DRA*	*CXCL11*
TDO2	*WARS*	*GBP1*	*WARS*	*GBP4*	*IDO1*
PHLDA1	*CCL8*	*P2RX7*	*CD274*	*WARS*	*RSAD2*
IFI30	*GBP5*	*GBP3*	*IRF1*	*CXCL9*	*IFITM1*
ITGB7	*OASL*	*AIM2*	*C1S*	*OASL*	*GBP4*
RND3	*SECTM1*	*IFIT3*	*STAMBPL1*	*IRF1*	*BATF2*
GBP2	*CXCL9*	*IL15RA*	*MNDA*	*CCL2*	*XIRP1*
SPP1	*IRF1*	*CXCL11*	*LZTS1*	*CMPK2*	*LGALS3BP*
GBP1	*IFI44L*	*RIPOR2*	*HAPLN3*	*BATF2*	*WARS*
IDO1	*SLAMF7*	*LIMK2*	*TOP2A*	*IFITM3*	*CMPK2*
CCL20	*CCL2*	*IFIT1*	*IL18BP*	*LGALS3BP*	*OASL*
CXCL1	*IFITM3*	*TNFSF10*	*ACKR4*	*SECTM1*	*C1S*
RSAD2	*STAT1*	*TAP1*	*SCARF1*	*FAM26F*	*FAM26F*
ICAM1	*CD74*	*GBP1P1*	*BIRC5*	*CD74*	*IFITM3*
CCL3L1	*GBP3*	*ANKRD22*	*HLA-DPA1*	*HLA-DQB1*	*ISG15*
CCL3	*LGALS3BP*	*OASL*	*HCAR3*	*ETV7*	*AIM2*
GBP4	*CMPK2*	*IL32*	*CIITA*	*TRIM22*	*GBP3*
CXCL10	*FN1*	*FAM26F*	*IDO1*	*ISG15*	*CCL7*
CCL3L3	*HLA-DPA1*	*GIMAP1-GIMAP5*	*PIM1*	*GBP3*	*IFIT2*
A2M	*FAM26F*	*GIMAP5*	*SLC35F1*	*IFIT3*	*ETV7*
IFIT3	*TRIM22*	*ISG15*	*FAM20A*	*FN1*	*IFIT3*
TSC22D1	*TYMP*	*APOL3*	*SOCS1*	*P2RX7*	*IFI44L*
SOD2	*ETV7*	*EPSTI1*	*HLA-DRA*	*STAT1*	*HAPLN3*
PINLYP	*TAP1*	*SNX10*	*GBP4*	*PTAFR*	*IRF1*
IFI6	*HLA-DQB1*	*DDX58*	*GBP6*	*TAP1*	*STAMBPL1*
MMP8	*HAPLN3*	*TNFSF13B*	*KIF20A*	*APOL1*	*TYMP*
ATF3	*HLA-DRB5*	*F13A1*	*PBK*	*STAMBPL1*	*TAGAP*
CD274	*MX1*	*CFH*	*GBP5*	*HLA-DQA1*	*UBD*
COL22A1	*TNFAIP6*	*RSAD2*	*HIST2H3D*	*TYMP*	*TRIM22*
MMP14	*BATF2*	*MEFV*	*HIST1H2BI*	*MX1*	*CD274*
LRRK2	*ISG15*	*SERPING1*	*ANKRD1*	*IFI35*	*APOL3*
AMPD3	*HLA-DRB1*	*OAS1*	*FAM26F*	*APOL3*	*TAP1*
GIMAP8	*STAMBPL1*	*LOC100419583*	*CCNA2*	*SLAMF7*	*MX1*
PLAUR	*IL10RA*	*PSMB9*	*CDK1*	*CCL5*	*SIGLEC1*
CTSL	*TNFSF10*	*IL23A*	*HIST1H2BB*	*HLA-DRB5*	*STAT1*
MAFF	*APOL1*	*BATF2*	*CEP55*	*TNFSF13B*	*IFIT1*
DUSP4	*SNX10*	*STAT2*	*MKI67*	*MX2*	*TNFSF13B*
GPR68	*EBI3*	*CARD16*	*SHCBP1*	*AIM2*	*EPSTI1*
PHGDH	*APOL3*	*CCL2*	*NUSAP1*	*TNFSF10*	*FN1*

SLAMF8	*CCL5*	*IFIT5*	*PLK1*	*CFH*	*MX2*
CD59	*EPSTI1*	*SDS*	*KIF11*	*OAS1*	*TBX21*
PLEKHO1	*IL32*	*APOL1*	*GBP2*	*IFI44*	*APOL1*
RGS1	*OAS1*	*PLSCR1*	*IL3RA*	*EPSTI1*	*FYB*
TRIB1	*P2RX7*	*TAGAP*	*HLA-DQA1*	*IFIT1*	*LY6E*
CD53	*PSMB8-AS1*	*XIRP1*	*ASPM*	*IL10RA*	*FGL2*
HS3ST3B1	*AIM2*	*CASP1*	*HIST1H4I*	*PSMB8-AS1*	*C1QB*
INHBA	*CCL7*	*ETV7*	*GTSE1*	*APOL2*	*HLA-DPB1*
CSF1	*HLA-DQA1*	*MMP12*	*TTK*	*UBD*	*PSMB8-AS1*
MYB	*TAGAP*	*GIMAP4*	*KIF18B*	*C1QB*	*OAS1*
GBP3	*SAMD9L*	*TIMP3*	*CCNB1*	*LY6E*	*SNX10*
PARM1	*IFIH1*	*IFI44*	*BCAR3*	*HLA-DRB1*	*HLA-DRB5*
IL1RN	*NT5DC2*	*CD80*	*PROCR*	*IL32*	*HLA-DRB1*
CHST15	*SIGLEC1*	*PSMB8-AS1*	*TYMS*	*FBXO6*	*P2RX7*
LGALS3BP	*GIMAP8*	*TNFAIP2*	*ANLN*	*OAS2*	*HLA-DPA1*
P3H2	*SOCS3*	*LAMP3*	*SHISA2*	*IFI27*	*IFI35*
ANPEP	*APOL2*	*GBP7*	*KIF4A*	*TAGAP*	*HLA-DRA*
S100A9	*SOD2*	*UBE2L6*	*EXO1*	*SIGLEC1*	*IFI44*
AZU1	*GBP1P1*	*TNF*	*CENPF*	*IFIH1*	*PTAFR*
FN1	*IFI35*	*WARS*	*CKMT1B*	*SNX10*	*IFI6*
MYO1B	*OAS2*	*IFIT2*	*HIST1H3H*	*IL15RA*	*USP18*
DUSP1	*IFIT1*	*SERPINB7*	*CIT*	*TOP2A*	*LRRK2*
DHRS9	*DDX58*	*UBD*	*KIFC1*	*IL6*	*IFIH1*
SMOX	*MEFV*	*BTN3A3*	*ITK*	*HLA-DPB1*	*PARP9*
TAP1	*MX2*	*HCAR3*	*BUB1*	*C2*	*C2*
SORL1	*PDE4B*	*NAT8L*	*HIST2H3A*	*IRF7*	*UBE2L6*
CDKN1A	*FBXO6*	*MX2*	*HIST2H3C*	*LOC100419583*	*DDX58*
LBH	*LAP3*	*IL6*	*LOC541472*	*ISG20*	*IGFBP5*
C5AR1	*OAS3*	*GBP6*	*LOC100419170*	*XAF1*	*OAS2*
OAS3	*SERPINB7*	*GIMAP8*	*KIF2C*	*OAS3*	*SP110*
CCL4L2	*CFH*	*TRIM69*	*HIST1H1B*	*TRIM69*	*FBXO6*
CCL4L1	*PLSCR1*	*DRAM1*	*HIST1H3F*	*SOCS3*	*SCO2*
PSAT1	*IFI44*	*PARP9*	*IL6*	*CIITA*	*IL32*
GLIS3	*TNFAIP2*	*PTGS2*	*DLGAP5*	*SDS*	*APOL2*
RHOBTB3	*APOL6*	*TRAFD1*	*GBP1*	*SCARF1*	*LAP3*
SRC	*TOP2A*	*NLRC5*	*MMS22L*	*CENPF*	*IFI27*
CCL8	*LIMK2*	*IRF7*	*HIST1H3J*	*FGL2*	*IL18BP*
IFITM1	*STAT2*	*SAMD9*	*CYP27B1*	*PLSCR1*	*SAMD9L*
EMP1	*HELZ2*	*FYB*	*HIST1H2BO*	*TRAFD1*	*C1QC*
ARMC9	*CCL1*	*USP18*	*CCL7*	*IFI6*	*PSMB9*
SLC31A2	*PARP9*	*FRMD4A*	*HIST1H2AJ*	*MEFV*	*GNLY*
HBEGF	*GIMAP5*	*APOL4*	*SMCO4*	*TNFAIP6*	*CCL5*
UPP1	*GIMAP1-GIMAP5*	*SPN*	*MYBL2*	*PDE4B*	*HERC5*
LOC100419170	*HLA-DMA*	*SECTM1*	*HLA-DMA*	*HELZ2*	*MEFV*
SLAMF7	*ISG20*	*APOL2*	*BUB1B*	*SLC31A2*	*CD74*
MTSS1	*STX11*	*STAT1*	*HIST1H2BM*	*SCO2*	*ISG20*
ARID5B	*GCH1*	*SCO2*	*HIST1H2AI*	*NT5DC2*	*MSR1*
SYTL3	*LOC101929319*	*LPL*	*FAM111B*	*DDX58*	*LOC100419583*
IFI44L	*XAF1*	*SAMD9L*	*ZWINT*	*HLA-DMA*	*APOL6*
S100A8	*IL6*	*HELZ2*	*HMMR*	*SAMD9L*	*MSRB1*
CEMIP	*LOC100419170*	*CISH*	*ANKRD22*	*IFIT5*	*APOL4*
CXCL9	*ANKRD1*	*IL3RA*	*HIST1H2BE*	*UBE2L6*	*FABP4*
MET	*IRF5*	*CASP5*	*POLQ*	*PARP9*	*OAS3*
GEM	*IRF7*	*TYMP*	*APOBEC3B*	*USP18*	*IRF7*

Table A1.2. Top 100 significantly differentially expressed genes (according to Benjamini-Hotchberg adjusted p-value ordered smallest to largest, maximum threshold set to 0.05) identified through pairwise comparisons between M0 cells and other subsets using Deseq2 package in R (i.e. a negative binomial distribution method)

Monocytes	M1	M2a	M2b	M2c	TPP
IL1B	*CXCL10*	*ALDH1A2*	*IFI44L*	*N/A*	*CCL1*
SPP1	*GBP1*	*CCL5*	*IFIT1*		*IDO1*
IGFBP3	*IDO1*	*FGL2*	*SNAR-A3*		*IL36G*
FN1	*GBP2*	*TGM2*	*SNAR-A4*		*SERPINB7*
THBS1	*HLA-DRA*	*LOX*	*SNAR-A5*		*SHROOM3*
MMP9	*GBP4*	*IGFBP5*	*SNAR-A7*		*CCL2*
TDO2	*RSAD2*	*FABP4*	*SNAR-A11*		*EBI3*
MMP1	*ANKRD22*	*CD209*	*SNAR-A9*		*CCL22*
CXCL8	*WARS*	*F13A1*	*SNAR-A6*		*SERPINE2*
TGM2	*CCL8*	*FCGR2A*	*SNAR-A8*		*HBB*
COL22A1	*GBP5*	*SLC5A3*	*SNAR-A10*		*CXCL1*
PHLDA1	*OASL*	*CISH*	*SNAR-A14*		*MSR1*
MMP8	*SECTM1*	*THBS1*	*IFITM1*		*CD300A*
CA2	*CXCL9*	*IGFBP3*	*MX1*		*DMP1*
CCL20	*IRF1*	*ANPEP*	*RSAD2*		*ITGA1*
CCL3L1	*IFI44L*	*CD14*	*XAF1*		*PTGS2*
CCL3	*SLAMF7*	*PTGS2*	*CMPK2*		*PCDH17*
ITGB7	*CCL2*	*IL10RA*	*NEURL3*		*FGF2*
MYB	*IFITM3*	*EPAS1*	*HERC5*		*RIN2*
AZU1	*STAT1*	*SERPINE2*	*IFI6*		*SOD2*
PARM1	*CD74*	*GNLY*	*IFIT3*		*FUT7*
MS4A6A	*GBP3*	*KIAA0040*	*CXCL11*		*GFPT2*
HBEGF	*LGALS3BP*	*LIPA*	*SIGLEC1*		*PDE4B*
PINLYP	*CMPK2*	*COL6A2*	*IFI44*		*ITGB8*
ITGB5	*FN1*	*SLC39A8*	*IFI27*		*CFH*
LBH	*HLA-DPA1*	*COL6A1*	*USP18*		*HLA-DRA*
DUSP4	*FAM26F*	*ANKRD1*	*ISG15*		*IL6*
RGS1	*TRIM22*	*SYNJ2*	*HERC6*		*LOXL4*
HS3ST3B1	*TYMP*	*ARRDC4*	*VCAM1*		*SERPINB4*
JAG1	*ETV7*	*VIM*	*HBA2*		*RIPOR2*
MET	*TAP1*	*NPC1*	*SNAR-A1*		*S100A8*
CCR2	*HLA-DQB1*	*FRMD4A*	*SNAR-A2*		*RRAD*
IFI30	*HAPLN3*	*HMOX1*	*SNORD3C*		*SLC7A2*
EMP1	*HLA-DRB5*	*CDKN1A*	*MX2*		*DAZL*
CTSG	*MX1*	*MME*	*OAS3*		*TNFAIP6*
PTGS2	*TNFAIP6*	*S1PR3*	*LAMP3*		*C1orf162*
DHRS9	*BATF2*	*NAT8L*	*OAS2*		*CXCL5*
P3H2	*ISG15*	*DCSTAMP*	*TRIM22*		*STAT4*
MMP14	*HLA-DRB1*	*ALOX5*	*LY6E*		*IL11*
C5AR1	*STAMBPL1*	*SLC7A2*	*OASL*		*CXCL2*
SMOX	*IL10RA*	*AQP9*	*NRIR*		*GALM*
RND3	*TNFSF10*	*DCUN1D3*	*PARP9*		*CD36*
SLAMF8	*APOL1*	*ANTXR1*	*DDX58*		*LOC730338*
MTSS1	*SNX10*	*PFKP*	*OAS1*		*IL1A*
CHST15	*EBI3*	*MATK*	*BATF2*		*GNLY*
ICAM1	*APOL3*	*NDRG2*	*MT2A*		*CSF3*
CNR1	*CCL5*	*FCRLA*	*SAMD9L*		*CD163*
NECTIN3	*EPSTI1*	*SLC38A6*	*HLA-DRA*		*MERTK*
		CTNNAL1			

DDIT4L	*IL32*	*HOPX*	*GBP5*		*NFKBIZ*
CCND1	*OAS1*	*MMRN2*	*IFITM3*		*LOXL2*
PLAUR	*P2RX7*	*VIM-AS1*	*IFIT2*		*CCR7*
ELANE	*PSMB8-AS1*	*TGFBI*	*MT1E*		*BMP2*
GLIS3	*AIM2*	*GPAT3*	*CCR7*		*SPP1*
CXCL1	*CCL7*	*ST6GAL1*	*F13A1*		*SIGLEC11*
RGS16	*HLA-DQA1*	*MFHAS1*	*HBA1*		*BIRC3*
INHBA	*TAGAP*	*MFSD12*	*SNORD3B-1*		*CCL4*
F13A1	*SAMD9L*	*RNASE1*	*SNORD3B-2*		*AMIGO2*
TRIM2	*IFIH1*	*QSOX1*	*AIM2*		*NT5DC2*
CDKN1A	*NT5DC2*	*NCF1*	*MT1X*		*IGFBP5*
PCDH20	*SIGLEC1*	*CD300LB*	*IFIT5*		*SCARB1*
FAM129B	*GIMAP8*	*EMB*	*ISG20*		*NAMPT*
LPL	*SOCS3*	*MRPS6*	*ETV7*		*IL1R2*
GPRIN3	*APOL2*	*GAS2L3*	*CA2*		*INHBA*
AMPD3	*SOD2*	*CTSC*	*ANKRD45*		*ADORA2A*
ITGB3	*GBP1P1*	*NCF1C*	*RUFY4*		*CCL4L1*
TSC22D1	*IFI35*	*ANXA1*	*HLA-DPA1*		*CCL4L2*
MARCKSL1	*OAS2*	*KITLG*	*SNORD3D*		*MIR3142HG*
NRP1	*IFIT1*	*STK38L*	*CCL8*		*MGP*
ATP9A	*DDX58*	*ATP6V1B2*	*SAMD9*		*PIM2*
CD59	*MEFV*	*ARHGAP25*	*CCL13*		*CYFIP2*
PDGFA	*MX2*	*ITGA1*	*GMPR*		*ST14*
LYZ	*PDE4B*	*ITGAM*	*IRF7*		*LAMP3*
MAFF	*FBXO6*	*ATF3*	*EBI3*		*S100A9*
PRTN3	*LAP3*	*TTC9*	*EPSTI1*		*KITLG*
UPP1	*OAS3*	*FAR2*	*CXCL10*		*CXCL3*
A2M	*SERPINB7*	*CCL20*	*IDO1*		*ECE1*
RGCC	*CFH*	*CCDC85A*	*ATP6V0D2*		*ITK*
CD53	*PLSCR1*	*CTSL*	*LOC100419583*		*FLT1*
CCL4L2	*IFI44*	*PTAFR*	*TNFSF10*		*IL24*
CCL4L1	*TNFAIP2*	*FCRLB*	*IFIH1*		*CD22*
CCL3L3	*APOL6*	*IPCEF1*	*GBP1P1*		*CRLF2*
IER3	*TOP2A*	*PCDH20*	*STAP1*		*TRAF1*
BCL2A1	*LIMK2*	*CA2*	*APOBEC3A*		*MTUS1*
PTPN13	*STAT2*	*KLF9*	*RNVU1-18*		*NUDT6*
TMEM158	*HELZ2*	*TDRD9*	*RNU1-3*		*PXDC1*
NRG1	*CCL1*	*CYBB*	*RNU1-4*		*CNR1*
CYTIP	*PARP9*	*CXCL5*	*RNU1-2*		*SLAMF7*
SOX4	*GIMAP5*	*PAPSS2*	*RNU1-1*		*KYNU*
CYP19A1	*GIMAP1-GIMAP5*	*ABCA13*	*SNORD3A*		*FYB*
ABCC3	*HLA-DMA*	*DENND5A*	*ZBP1*		*CCL20*
GEM	*ISG20*	*TMEM123*	*SNORA54*		*WNT5A*
TMTC1	*STX11*	*LRRC8B*	*SNORA63*		*G0S2*
RAI14	*GCH1*	*HS3ST1*	*VSIG4*		*HECW2*
CD14	*LOC101929319*	*ATP13A3*	*STAT1*		*CACNA1E*
ANPEP	*XAF1*	*NCF1B*	*TRIM5*		*NRG1*
GPR84	*IL6*	*VSIG4*	*CFH*		*PYROXD2*
TRIB1	*LOC100419170*	*ATP2B1*	*DHX58*		*CD274*
ADAMTS1	*ANKRD1*	*PLEK*	*IFI35*		*LOC101929319*
NT5E	*IRF5*		*MCOLN2*		*IL23A*
HMOX1	*IRF7*		*FCGBP*		*EREG*

Table A1.3. Top 100 significantly differentially expressed genes (according to Benjamini-Hotchberg adjusted p-value ordered smallest to largest, maximum threshold set to 0.05) identified through pairwise comparisons between Monocytes cells and Monocytes + IC using Deseq2 package in R (i.e. a negative binomial distribution method)

Genes			
STC2	*DDIT4*	*HERPUD1*	*TRIB3*
GPNMB	*CDC20*	*HCK*	*EVI2A*
ASS1	*MYBPH*	*DLGAP5*	*CTSB*
VEGFA	*SEL1L3*	*ZWINT*	*CSF2RA*
MLC1	*RNASE1*	*WARS*	*CDCA2*
CADM1	*CHAC1*	*ATF4*	*SPAG5*
CYBB	*C5AR1*	*TGFBR1*	*BNIP3L*
AOAH	*PSAT1*	*FGL2*	*FASN*
ASAH1	*HLA-DRA*	*LAMP5*	*RRAGD*
LDLRAD4	*PAPPA2*	*SLPI*	*ATF5*
TEX15	*NLRP12*	*GRB10*	*GTSE1*
C1QA	*FRMD3*	*GM2A*	*SYTL1*
SIGLEC6	*SCARNA7*	*CCNA1*	*SLCO2B1*
ALOX5	*P2RX4*	*KIF23*	*MAF*
RPS6KA2	*DNAAF4-PG1*	*CENPE*	*SULF2*
ASNS	*CCPG1*	*SLC11A1*	*CAPG*
MAP3K20	*PRTN3*	*FYN*	*KLHL24*
P2RX7	*FAM84B*	*KDM7A*	*P2RY6*
MKI67	*SLC6A9*	*APOL6*	*PADI2*
CBS	*KIF20A*	*GAS5*	
CBSL	*C6orf48*	*ADAMDEC1*	
PHGDH	*SORL1*	*CCNB1*	
NUPR1	*SNORA103*	*PLK1*	
MRC1	*BUB1*	*ADAMTS1*	
ALDH1L2	*AJUBA*	*WT1*	
F13A1	*DDIT3*	*ADA2*	
C1QC	*PSAP*	*CCNF*	

Table A1.4. Top 300 M1 and M2a genes isolated from Beyer *et al.,* (2012) dataset according to fold change analysis, filtered for genes higher in M0 condition. Genes are ordered by largest to smallest fold change

M1 transcripts		M2a transcripts	
GREM1	*RCAN1*	*DNASE1L3*	*CST7*
EDN1	*ACSL1*	*ALOX15*	*PLTP*
CXCL10	*MSR1*	*DHRS2*	*CPVL*
CP	*SGK1*	*SLC25A48*	*CST3*
HLA-DRB1	*SOD2*	*CCL23*	*MAT2B*
FCGR1B	*RHBDF2*	*CCL26*	*LIPA*
TSC22D1	*ATF3*	*FCER1A*	*MCUR1*
GBP5	*SERPINA1*	*CCL14*	*GCNT1*
GBP5	*TNFSF10*	*FABP4*	*MAF*
VSIG4	*FCAR*	*CD1E*	*CLEC4G*
FCGR1A	*SLC11A1*	*HRH1*	*METTL7A*
CCL7	*CYBB*	*CD1E*	*CTSC*
GBP4	*LYZ*	*HOMER2*	*SCARB1*
CXCL9	*FOSB*	*CD1E*	*NAIP*

APOBEC3A	*LRRK2*	*F13A1*	*CD36*
ANKRD22	*FAM26F*	*CD1A*	*MS4A4A*
CLU	*PDE4B*	*CCL23*	*CYBRD1*
NCOA7	*MT2A*	*MS4A6A*	*NAIP*
IFIT3	*GBP2*	*CCL17*	*ZG16B*
VSIG4	*AQP9*	*CCL13*	*MAF*
GBP1	*PTGS2*	*CCL18*	*KCTD17*
GPC4	*FAM107B*	*CD163L1*	*PTGS1*
CA12	*FPR2*	*CLDN1*	*NAAA*
GCH1	*IL1A*	*ADAM19*	*CAMK1D*
GCH2	*ACSL1*	*MS4A6A*	*Hs.657673*
IFI27	*SLC28A3*	*FOXQ1*	*MS4A4A*
SLAMF7	*LILRA3*	*SLC40A1*	*WDFY4*
CLEC6A	*STAT1*	*GATM*	*RNASE1*
SERPING1	*KYNU*	*PALLD*	*ETV3*
BCL2A1	*CRABP2*	*WNT5B*	*ADAM15*
TNFAIP6	*PIM1*	*STAB1*	*FHOD1*
CA12	*STX11*	*CD1C*	*SEMA4A*
WARS	*SPP1*	*RAMP1*	*EMB*
IFIT2	*SERPINE1*	*MMP12*	*Hs.437365*
CCL8	*DUSP6*	*CD180*	*CLIC2*
IDO1	*MT1H*	*SEPP1*	*CCL22*
SERPING1	*ITGAL*	*CD1E*	*CLEC10A*
F3	*TAP1*	*CLEC4A*	*IRF4*
IL6	*C15orf48*	*ADORA3*	*GPR183*
INHBA	*SOD2*	*MS4A6A*	*TREM2*
SLAMF7	*S100A9*	*GFRA2*	*STK32C*
BHLHE41	*TNFSF14*	*CD200R1*	*RNASE1*
IFIT3	*APOL6*	*MS4A6A*	*MPEG1*
WARS	*SLCO4A1*	*PON2*	*CLEC4A*
OCSTAMP	*C15orf48*	*FOLR2*	*TACSTD2*
CLEC5A	*HBEGF*	*FOLR2*	*SPINT2*
HAPLN3	*ITGAL*	*NDRG2*	*CD302*
ADAMDEC1	*SOCS3*	*MAOA*	*RNASE1*
IRF1	*FOS*	*FAM126A*	*OLFML2B*
BATF2	*ITGB7*	*LGMN*	*ANKH*
GPR84	*DUSP6*	*CTSC*	*LIPA*
CLEC5A	*CXCL2*	*TPM1*	*RGL1*
MSR1	*VAMP5*	*SLC7A8*	*GAS6*
SNX10	*FLT1*	*BLNK*	*FGD2*
IFI27	*PAG1*	*AP2A2*	*VCL*
RARRES3	*TREM1*	*AP2A2*	*JUP*
STAT1	*CEBPB*	*GPD1L*	*EEF2K*
CLEC4E	*ATF3*	*PDGFC*	*KCNK6*
CCL2	*CD82*	-	*IL1R1*
S100A8	*NLRC5*	*TMEM45B*	*ERI1*
WARS	*MT1G*	*AQP3*	*RASSF2*
CYP27B1	*ATF3*	*CD36*	*MAT2A*
APOL3	*FAM26F*	*ARL4C*	*ARPIN*
CLEC12A	*SPINK1*	*TGFBI*	*TMEM71*
CRISPLD2	*OLR1*	*CD1B*	*C10orf128*
SOD2	*FBP1*	*GSTT1*	*WIPF1*
WARS	*MAFF*	*AP1B1*	*FAM198B*
ACSL1	*SERPINA1*	*ST6GAL1*	*ID3*
FAM124A	*P2RX7*	*SUCNR1*	*ENPP2*

CLEC4D	*FLT1*	*SCARB1*	*SNX5*
MT1F	*CCRL2*	*ABCA6*	*CLEC4A*
TM4SF19	*SLC1A4*	*AP1B1*	*GLIPR1*
SERPINA1	*LIMK2*	*SLCO2B1*	*AUH*
TYROBP	*CSF1*	*PLAU*	*AKR1B1*
OLR1	*GIMAP5*	*RNASE1*	*PLCB2*

Table A1.5. Top 300 M1 and M2a genes isolated from Xue *et al.,* (2014) dataset according to fold change analysis, filtered for genes higher in M0 condition. Genes are ordered by largest to smallest fold change

M1 transcripts		**M2a transcripts**	
ADAMDEC1.1	*NA..8681*	*CD1B*	*RGS18*
IL1B	*PLSCR1*	*CD1A*	*CAMK1*
MT1H	*DFNA5*	*HLA.DRB5*	*ITGB5.1*
TNFAIP6	*AQP9*	*NA..60*	*MXD4*
ADAMDEC1	*IFIT3.1*	*CCL22*	*PCED1B*
MT1G	*IRF1*	*FOXQ1*	*FHOD1*
CXCL5	*CTSL.2*	*S100A4.1*	*RAB33A*
SOD2	*ALDH1A1*	*SPP1.1*	*MAP4K1*
CYBB	*FPR2*	*CD1C*	*CEBPA*
GBP5	*C15orf48*	*FCER1A*	*GALNT12*
MT1E	*BTG1*	*SPP1*	*P4HA2.1*
CD14.1	*MT1X*	*ALOX15*	*CPVL.1*
CRISPLD2	*LILRB4*	*MMP12.1*	*CHCHD10*
CXCL8.1	*RILPL2*	*CCL17*	*DTNA.1*
GBP4	*LYSMD2*	*F13A1*	*CLEC10A.1*
ANKRD22.1	*PTGS2*	*MS4A6A.2*	*MAN1C1*
HLA.A.2	*NFS1.1*	*CD1E.1*	*CD1E*
GBP1.1	*ADORA2A*	*MS4A6A*	*RASGRP3*
BHLHE41	*MS4A7.1*	*PALLD*	*NAPSB.1*
GBP1	*MS4A7*	*HOMER2.1*	*RASSF7*
NAMPT	*ALDH1A1.1*	*MMP12*	*CD200R1*
MT1F	*NSUN7*	*IL1R2.1*	*ATP5D.1*
IL1A	*NA..17828*	*TACSTD2*	*NA..1873*
FPR2.1	*FAM20A*	*CD52*	*INF2*
ANKRD22	*CLEC4D*	*LIPA*	*ADAM15.1*
SLC1A3	*IFITM1*	*CCL13*	*TPM2*
CA12	*CD82*	*ESPNL*	*CLEC10A.2*
PDE4B	*C1S.1*	*NFE2*	*LDLR*
OLR1	*IRAK2*	*GPD1L*	*NA..13533*
PCNX	*CTSL.1*	*MS4A6A.1*	*PRDX2.2*
MT2A.1	*CASP4*	*ACOT7.4*	*GALNT18*
MT1A	*MXD1*	*FABP5.1*	*NA..18303*
GPR84	*FTH1*	*GOLGA8B*	*DHRS11*
CXCL8	*ZMYND15*	*NA..17784*	*DUOX1.1*
RHBDF2.2	*G0S2*	*NDRG2.1*	*CHST13*
GCH1	*GK.1*	*QPRT*	*PTRF*
STAT1	*STX11*	*EGR1*	*MAP4K1.1*
CYP27B1	*ISG20*	*TUBA1A*	*MAP1A*
IL7R	*NA..3601*	*PON2.1*	*TPM1.3*
IL2RA	*SEMA6B*	*CMTM8*	*TOP1MT*
LAD1	*MB21D2*	*NA..11983*	*TBC1D10C*

CLEC5A	*HIVEP1*	*SGK223*	*CPVL*
NA..13172	*WARS*	*ACOT7.2*	*DHRS2*
RHBDF2	*PAG1.1*	*NA..3064*	*MKL1*
NAMPT.1	*HIF1A.2*	*SOX8*	*VCL*
CXCL10	*TNFAIP3*	*CTNNAL1*	*RTKN.1*
PTGES	*NLRP3.1*	*RAP1GAP*	*COL9A2*
EXOG	*CXCL9*	*MAOA*	*EIF4G1.2*
CCL5.1	*GK*	*CXCR2P1*	*CBR3*
PSAT1	*LPAR1*	*ATP2B4.1*	*DDIAS*
STAT1.1	*NA..289*	*PON2*	*ANKRD37*
PIM1	*PILRA.2*	*CST3*	*CCL26*
MT1H.1	*KYNU*	*FASN*	*CDR2L*
SNX10	*PILRA*	*CRIP1*	*INSIG1*
CD300LF	*ARID5B*	*HOMER2*	*PDXK*
HBEGF	*APOL3.1*	*GATM*	*GPBAR1.1*
MT1IP	*LILRB3*	*FSCN1*	*MYC*
C1QTNF1.1	*ACKR3*	*GAS6.1*	*NAIP.2*
ORM1	*NINJ1*	*PARM1*	*APBB1IP*
TSC22D1.1	*IRAK3.1*	*PFKP*	*APEX1*
CCL5	*TSC22D1.2*	*GSTT1*	*NA..18577*
WARS.1	*PRKCH*	*SCD*	*GALM*
TMEM176A	*TRAF3IP2.2*	*KIAA1671*	*FAM189A2*
TNFAIP2	*TANK*	*ID2*	*TIFAB*
CD48	*DUSP10.2*	*ATP2B4.2*	*GPT*
DDIT4	*RIPK2*	*ADAM19.1*	*ADCY3*
STOM	*H1F0*	*GAS6*	*NA..18056*
PHGDH	*LRRK2.1*	*PPP1R14A*	*NMNAT3*
DRAM1	*SLC11A1*	*RAB7B*	*RAMP1*
STAT4	*TBC1D9*	*NA..2698*	*MFSD3*
ACSL1	*CES1*	*TSPAN32*	*CARD9*
SLC5A3.1	*PAG1.2*	*HLA.DRB1*	*REPS2.3*
CD14	*NA..17351*	*DCANP1*	*CD93*
ETS2	*MAP1LC3A.2*	*CAMK1D.4*	*SPINT2*
	SLC7A5	*FGD5*	*PIEZO1*
	SLC3A2.2		

Table A1.5. Top 300 M1, M2a, M2b and M2c genes isolated from Xue *et al.,* (2014) dataset according to fold change analysis (versus M0 cells, genes high in any other condition filtered out). Genes are ordered by largest to smallest fold change.

M1	**M2a**	**M2b**	**M2c**
MTG1	*CD1B*	*ACKR3*	*SEPP1*
SOD2	*CD1A*	*ACKR3.1*	*FOLR2*
CYBB	*HLA.DRB5*	*PTGES*	*TMIGD3*
GBP5	*NA..60*	*TNFAIP6*	*CD163L1*
MT1E	*CCL22*	*PTGS2.1*	*GADD45G*
GBP4	*FOXQ1*	*C1QTNF1.1*	*FUCA1*
ANKRD22.1	*S100A4.1*	*LAD1*	*TP53I13*
HLA.A.2	*SPP1.1*	*PTGS2*	*HNRNPA1P33.1*
GBP1.1	*CD1C*	*MUCL1*	*NA..13006*
BHLHE41	*FCER1A*	*MT1H*	*SLC16A5*
GBP1	*SPP1*	*CCL20*	*LILRB5*
NAMPT	*ALOX15*	*IL1A*	*ZNF16*

FPR2.1	*MMP12.1*	*CCL5.1*	*VPS16.1*
ANKRD22	*CCL17*	*TM4SF1*	*MAF.1*
SLC1A3	*F13A1*	*HEY1*	*RASSF2.2*
OLR1	*MS4A6A.2*	*IL2RA*	*HEBP2*
PCNX	*CD1E.1*	*IL6*	*NCF4*
MT2A.1	*MS4A6A*	*G0S2*	*SORL1*
RHBDF2.2	*PALLD*	*CCL5*	*PIK3R2*
GCH1	*HOMER2.1*	*PDE4B*	*ETNK1*
STAT1	*MMP12*	*MT1H.1*	*NUDT1.1*
CYP27B1	*IL1R2.1*	*CRISPLD2*	*SLC18B1*
IL7R	*TACSTD2*	*NFS1.1*	*RN7SK.2*
CLEC5A	*CD52*	*VEGFA*	*CAPN1*
NA..13172	*LIPA*	*STAT4*	*OLFML2B*
RHBDF2	*CCL13*	*MAP1LC3A.2*	*TMEM127*
NAMPT.1	*ESPNL*	*IL1B*	*KLF11.1*
CXCL10	*NFE2*	*NA..3957*	*NENF*
PSAT1	*GPD1L*	*NKG7*	*NA..17082*
STAT1.1	*ACOT7.4*	*PTPRF*	*BLVRB*
PIM1	*FABP5.1*	*MT1IP*	*NA..8737*
CD300LF	*GOLGA8B*	*SIGLEC10*	*HAMP*
ORM1	*NA..17784*	*GPR84*	*PSMD8*
WARS.1	*NDRG2.1*	*IRAK2*	*CCDC106*
TMEM176A	*QPRT*	*MAP3K4.1*	*BATF*
TNFAIP2	*TUBA1A*	*CCR7*	*TPCN2*
DDIT4	*PON2.1*	*CLLU1OS*	*CSF3R.1*
STOM	*CMTM8*	*CA12*	*NA..1181*
PHGDH	*NA..11983*	*NR4A2.1*	*MMP7.1*
DRAM1	*SGK223*	*ADAMDEC1*	*HCFC1R1*
SLC5A3.1	*ACOT7.2*	*MYH11.1*	*SLC37A4*
CD14	*NA..3064*	*ABHD17C*	*PMP22.2*
PLSCR1	*SOX8*	*ADGRE3*	*TLN1*
AQP9	*CTNNAL1*	*ETS2*	*TUBA3D.1*
IFIT3.1	*RAP1GAP*	*EXOG*	*ARSA*
IRF1	*MAOA*	*UPB1*	*MSRB2*
FPR2	*CXCR2P1*	*MT1F*	*LGMN.2*
LILRB4	*ATP2B4.1*	*MT1A*	*GFRA2*
RILPL2	*PON2*	*OSM*	*STAB1*
LYSMD2	*CST3*	*MT1X*	*MIDN*
MS4A7.1	*FASN*	*NA..418*	*SPRYD3*
MS4A7	*CRIP1*	*LRG1*	*TSPAN4*
ALDH1A1.1	*HOMER2*	*SERPINB2*	*GPR34.1*
NSUN7	*GATM*	*SLAMF1*	*NA..5470*
FAM20A	*FSCN1*	*NA..289*	*THOC5*
CLEC4D	*GAS6.1*	*EREG*	*ELANE*
IFITM1	*PARM1*	*THBS1*	*TRPM4*
CD82	*PFKP*	*ADAMDEC1.1*	*NA..8424*
C1S.1	*GSTT1*	*GRAMD1A*	*C20orf27*
CTSL.1	*SCD*	*ADORA2A*	*GABARAP*
CASP4	*KIAA1671*	*NA..12990*	*DPP7.3*
MXD1	*ID2*	*NA..17261*	*CHST13*
ZMYND15	*ATP2B4.2*	*PRDM8*	*ASGR1*
GK.1	*ADAM19.1*	*FOSB*	*SIL1.2*
NA..3601	*GAS6*	*NLRP3*	*PRKDC*
HIVEP1	*PPP1R14A*	*SLC2A6*	*MMP7*
WARS	*RAB7B*	*CXCR5*	*ARMC10.3*
PAG1.1	*NA..2698*	*ETS1*	*CLEC7A*

CXCL9	*TSPAN32*	*NR4A2*	*RHOC.1*
GK	*HLA.DRB1*	*TNIP3*	*NAPRT*
LPAR1	*DCANP1*	*TNFAIP3*	*TMUB2.2*
PILRA.2	*CAMK1D.4*	*PRDM1.3*	*ARL4C*
KYNU	*FGD5*	*TNF*	*TPD52L2.1*
PILRA	*RGS18*	*LAMB3*	*PIP*
ARID5B	*CAMK1*	*TWIST1*	*NA..16839*

Table A1.5. Gene expression by microarray of M1 (IFNγ) and M2a (IL-4) treated genes for different durations of cytokine exposure. Processed data taken from Xue *et al.,* (2014).

M1							
	30min	**1hr**	**2hr**	**6hr**	**12hr**	**24h**	**72hr**
CXCL10	8.622383	11.74963	11.16476	11.60397	14.14067	13.2259	12.13407
CXCL9	7.076647	8.619637	8.156733	10.61023	12.5909	11.05313	10.19115
ANKRD22	8.143827	9.027877	9.357277	10.64953	11.35327	11.17247	10.55137
ANKRD22.	8.320963	9.29633	9.801697	13.00787	11.13893	11.0039	10.7331
GBP5	7.654807	9.93099	10.05694	11.0389	12.41303	12.23887	13.01407
TNFAIP6	6.798347	7.935297	7.814537	6.496573	11.47007	9.54813	10.98807
TNFAIP6.1	6.40316	6.421633	6.408583	6.26342	6.59974	6.24502	6.560133
INHBA	6.295617	6.385097	6.14058	11.53827	6.414727	6.481407	6.40548
IL6	7.1202	8.240917	8.607883	11.53827	9.914383	7.651997	9.609127
M2a							
	30min	**1hr**	**2hr**	**6hr**	**12hr**	**24hr**	**72hr**
CCL17	6.60918	6.445967	10.65853	6.464023	6.519113	6.519113	6.519113
CCL23	8.531047	8.92514	8.995097	10.01211	8.99656	8.99656	8.99656
CCL23.1	10.55905	11.44093	10.98207	11.85957	11.07376	11.07376	11.07376
CCL26	6.439513	6.205127	7.88156	6.444327	6.408263	6.408263	6.408263
ALOX15	6.340073	6.47347	11.0876	6.340313	6.392627	6.392627	6.392627
ALOX15.1	6.358163	6.321583	6.9072	6.546873	6.368393	6.368393	6.368393
ALOX15.2	6.35188	6.393023	7.661347	6.33015	6.30277	6.30277	6.30277
CD200R1	6.439767	6.37568	8.271803	6.518773	6.670263	6.670263	6.670263
CD200R1..	6.416697	6.342137	7.766797	6.35836	6.409573	6.409573	6.409573
HOMER2	6.48212	6.318283	8.747857	6.26168	6.36382	6.36382	6.36382
HOMER2.1	6.66511	6.49117	10.26457	6.492627	6.565813	6.565813	6.565813
MR1	7.762953	8.662087	7.809457	7.543933	7.752213	7.752213	7.752213

Appendix 2: LINUX scripts

Script A2.1. Assessment of read quality using FASTQC

```
mkdir -p /nobackup/NGS_temp/Nikki/reports/
mkdir -p /nobackup/NGS_temp/Nikki/temp/

##runs fastqc software on all fastq files in /raw directory, writes output to /reports directory, uses 4 cores

/nobackup/NGS_Facility/workshop/fastqc/fastqc -o /nobackup/NGS_temp/Nikki/reports/ --threads 4 --dir /nobackup/NGS_temp/Nikki/temp/
/nobackup/NGS_temp/Nikki/*.fastq.gz
```

Script A2.2. Removal of adaptor sequences using CUTADAPT

```
module unload python/3.3.6
module load python/2.7.6
source /home/marc1_a/msjimc/mypython/bin/activate

outDir=/nobackup/NGS_temp/Nikki/trimmed/

mkdir -p $outDir
read1=`sed -n -e "$SGE_TASK_ID p" /nobackup/NGS_temp/Nikki/listOfFiles.txt`

echo $outDir

        read2=$(echo $read1 | sed 's/R1_001/R2_001/g')

        fname=`basename $read1`
        fname2=`basename $read2`

        trimmed_read1=$outDir$fname
        trimmed_read2=$outDir$fname2

        cutadapt -q 10,10 -m 30 -a AGATCGGAAGAGC -A AGATCGGAAGAGC -o $trimmed_read1 -p $trimmed_read2 $read1 $read2
```

Script A2.3. Alignment of reads to reference genome using STAR aligner

```
fastaDir=/nobackup/umaan/data/reference_genomes/hg38_analysis_set
read1=$(ls /nobackup/NGS_temp/Nikki/trimmed/*R1_001.fastq.gz | sed -n -e "$SGE_TASK_ID p")
read2=$(echo $read1 | sed 's/R1_001/R2_001/g')

fname=`basename $read1`

prefix=/nobackup/NGS_temp/Nikki/aligned_stringent/$fname

gtf=/nobackup/umaan/data/reference_genomes/hg38_analysis_set/hg38.gtf


/nobackup/umaan/software/bin/STAR --runMode alignReads --genomeDir $fastaDir --runThreadN 5 --readFilesIn $read1 $read2\
 --outFileNamePrefix $prefix --outSAMtype BAM SortedByCoordinate \
 --outFilterMultimapNmax 50 \
 --outReadsUnmapped Fastx\
 --sjdbGTFfile $gtf --sjdbOverhang 150 --readFilesCommand zcat --outFilterMismatchNmax 1 --outFilterMismatchNoverLmax 0.01
```

Script A2.4. Production of count Tables using subread. # precedes descriptive annotation

```
##install and load required libraries if not already installed

if(!require(Rsubread)){

  source("http://bioconductor.org/biocLite.R")

  biocLite("Rsubread")

}

library(Rsubread)


dir.create("/nobackup/NGS_temp/Nikki/rsubRead", recursive = TRUE)

setwd("/nobackup/NGS_temp/Nikki/rsubRead")


#path to alignment bam files

bams <- c("/nobackup/NGS_temp/Nikki/LPS_1C/LPS_1C_Aligned.sortedByCoord.out.bam",
"/nobackup/NGS_temp/Nikki/LPS_ICR3/LPS_ICR3_Aligned.sortedByCoord.out.bam",

                                "/nobackup/NGS_temp/Nikki/LPS_ICT2/LPS_ICT2_Aligned.sortedByCoord.out.bam",
"/nobackup/NGS_temp/Nikki/LPS/LPS_Aligned.sortedByCoord.out.bam",

                                "/nobackup/NGS_temp/Nikki/LPS3/LPS3_Aligned.sortedByCoord.out.bam",
"/nobackup/NGS_temp/Nikki/LPST2/LPST2_Aligned.sortedByCoord.out.bam",

                                "/nobackup/NGS_temp/Nikki/M1_1C/M1_1C_Aligned.sortedByCoord.out.bam",
"/nobackup/NGS_temp/Nikki/M1_1CT2/M1_1CT2_Aligned.sortedByCoord.out.bam",

                                "/nobackup/NGS_temp/Nikki/M1IC3/M1IC3_Aligned.sortedByCoord.out.bam",
"/nobackup/NGS_temp/Nikki/M1/M1_Aligned.sortedByCoord.out.bam",

                                "/nobackup/NGS_temp/Nikki/M1T2/M1T2_Aligned.sortedByCoord.out.bam",
"/nobackup/NGS_temp/Nikki/M13/M13_Aligned.sortedByCoord.out.bam",

                                "/nobackup/NGS_temp/Nikki/M2a_1C/M2a_1C_Aligned.sortedByCoord.out.bam",
"/nobackup/NGS_temp/Nikki/M2a_1CT2/M2a_1CT2_Aligned.sortedByCoord.out.bam",

                                "/nobackup/NGS_temp/Nikki/M2aIC3/M2aIC3_Aligned.sortedByCoord.out.bam",
"/nobackup/NGS_temp/Nikki/M2a/M2a_Aligned.sortedByCoord.out.bam",

                                "/nobackup/NGS_temp/Nikki/M2a3/M2a3_Aligned.sortedByCoord.out.bam",
"/nobackup/NGS_temp/Nikki/M2aT2/M2aT2_Aligned.sortedByCoord.out.bam",

                                "/nobackup/NGS_temp/Nikki/M2c_1C/M2c_1C_Aligned.sortedByCoord.out.bam",
"/nobackup/NGS_temp/Nikki/M2c_1CT2/M2c_1CT2_Aligned.sortedByCoord.out.bam",

                                "/nobackup/NGS_temp/Nikki/M2cIC3/M2cIC3_Aligned.sortedByCoord.out.bam",
"/nobackup/NGS_temp/Nikki/M2c/M2c_Aligned.sortedByCoord.out.bam",

                                "/nobackup/NGS_temp/Nikki/M2c3/M2c3_Aligned.sortedByCoord.out.bam",
"/nobackup/NGS_temp/Nikki/M2cT2/M2cT2_Aligned.sortedByCoord.out.bam",

                                "/nobackup/NGS_temp/Nikki/MO_1C/MO_1C_Aligned.sortedByCoord.out.bam",
"/nobackup/NGS_temp/Nikki/MO_1CT2/MO_1CT2_Aligned.sortedByCoord.out.bam",

                                "/nobackup/NGS_temp/Nikki/MO_ICR3/MO_ICR3_Aligned.sortedByCoord.out.bam",
"/nobackup/NGS_temp/Nikki/MO/MO_Aligned.sortedByCoord.out.bam",

                                "/nobackup/NGS_temp/Nikki/MO3/MO3_Aligned.sortedByCoord.out.bam",
"/nobackup/NGS_temp/Nikki/MOT2/MOT2_Aligned.sortedByCoord.out.bam",

                                "/nobackup/NGS_temp/Nikki/Mono_1C/Mono_1C_Aligned.sortedByCoord.out.bam",
"/nobackup/NGS_temp/Nikki/Mono_IC3/Mono_IC3_Aligned.sortedByCoord.out.bam",

                                "/nobackup/NGS_temp/Nikki/Mono_ICT2/Mono_ICT2_Aligned.sortedByCoord.out.bam",
"/nobackup/NGS_temp/Nikki/Mono/Mono_Aligned.sortedByCoord.out.bam",

                                "/nobackup/NGS_temp/Nikki/Mono3/Mono3_Aligned.sortedByCoord.out.bam",
"/nobackup/NGS_temp/Nikki/MonoT2/MonoT2_Aligned.sortedByCoord.out.bam",

                                "/nobackup/NGS_temp/Nikki/TPP_1C/TPP_1C_Aligned.sortedByCoord.out.bam",
"/nobackup/NGS_temp/Nikki/TPP_ICR3/TPP_ICR3_Aligned.sortedByCoord.out.bam",

                                "/nobackup/NGS_temp/Nikki/TPP_ICT2/TPP_ICT2_Aligned.sortedByCoord.out.bam",
"/nobackup/NGS_temp/Nikki/TPP/TPP_Aligned.sortedByCoord.out.bam",

                                "/nobackup/NGS_temp/Nikki/TPP3/TPP3_Aligned.sortedByCoord.out.bam",
"/nobackup/NGS_temp/Nikki/TPPT2/TPPT2_Aligned.sortedByCoord.out.bam")


#path to GTF annotation files

gtf <- "/nobackup/NGS_Facility/workshop/star_ref/hg38.gtf"


## will count reads overlapping genes

geneCounts <-featureCounts(bams, annot.ext= gtf, isGTFAnnotationFile = TRUE,

                        useMetaFeatures=TRUE, allowMultiOverlap=TRUE,

                        countMultiMappingReads=TRUE,
```

```
                    fraction=TRUE, nthreads=4, ignoreDup=TRUE)

## will count reads overlapping exons
exonCounts <-featureCounts(bams, annot.ext= gtf, isGTFAnnotationFile = TRUE,
                    useMetaFeatures=FALSE, allowMultiOverlap=TRUE,
                    countMultiMappingReads=TRUE,
                    fraction=TRUE, nthreads=4, ignoreDup=TRUE)

dataGenes <- cbind(geneCounts$annotation, geneCounts$counts)
dataExons <- cbind(exonCounts$annotation, exonCounts$counts)


write.Table(x=as.data.frame(dataGenes), quote=FALSE, sep="\t", file="gene_counts.txt")
```

Appendix 3: R scripts

Script A3.1. Identification of differentially expressed genes and gene ontology and pathway enrichment analysis. Annotation is given in red and preceded by a "#" symbol

```
source("https://bioconductor.org/biocLite.R")
biocLite()
biocLite("org.Hs.eg.db")

## load libraries
library(pheatmap)
library(readr)
library(DESeq2)
library(gplots)
library(clusterProfiler)
library(org.Hs.eg.db)
library(pathview)
library(ReactomePA)
library(reactome.db)

##read in raw count data
counts <- read_delim("C:\\Users\\umnar\\Documents\\RNA_seq\\gene_counts_duplicates.txt","\t", escape_double = FALSE, trim_ws = TRUE)
## read in meta data Table describing the samples
meta_data <- read_delim("~/RNA_seq/meta_data.txt",  "\t", escape_double = FALSE, trim_ws = TRUE)
##convert to data type object
meta_data <- as.data.frame(meta_data)
##rename row names in meta data to correspond to sample names
rownames(meta_data) <- meta_data$Sample_Name
##convert counts Table to data frame
counts <- as.data.frame(counts)
##get sample names
sample_names <- colnames(counts)[8:length(colnames(counts))]
##make sure meta data and counts Table is in the same order by reordering
meta_data <- meta_data[sample_names, ]
##rename rows to have refseq gene identifiers
rownames(counts) <- counts$Refseq
##subset just the raw counts
matrix <- as.matrix(counts[, 8:length(colnames(counts))])
storage.mode(matrix) <- "integer"
```

```
### convert lane from number to factor
meta_data$Lane <- as.factor(meta_data$Lane)

## subset data into indexes e.g. differences between M1 and M2a without ic
indexes <- which(  (meta_data$Subtype == "M0" | meta_data$Subtype == "M2a")  & meta_data$IC == "IC_no" & meta_data$Lane != 5)
dds <- DESeqDataSetFromMatrix(countData = matrix[, indexes ],colData  = meta_data[indexes, ],design = ~ Lane  + Subtype)

##perform actual DE analysis
dds <- DESeq(dds )

##extract results + multiple testing correction
res <- results(dds, pAdjustMethod = "fdr")

## extract log2 normalised counts into a Table
log_norm_counts <- rlog(dds, blind = TRUE)
##actually extract from object to readable Table
norm_counts_Table<- assay(log_norm_counts)
## select significantly changed genes
sig_hits_all <- res[which( res$padj < 0.05 & abs(res$log2FoldChange) > 1 ), ]

## which are DE transcripts at 5% FDR and > 2 fold change
sig_hits<- res[which(res$padj < 0.05 & abs(res$log2FoldChange) > 1), ]
##same, but only up
sig_hits_up<- res[which(res$padj < 0.05 & res$log2FoldChange > 1), ]
##same, but only down
sig_hits_down<- res[which(res$padj < 0.05 & res$log2FoldChange < -1), ]
##select top 100 upregulated
top100_up <- sig_hits_up[order(sig_hits_up$log2FoldChange, decreasing =TRUE), ][1:100, ]
##select top 100 downregulated
top100_down <- sig_hits_down[order(sig_hits_down$log2FoldChange, decreasing =FALSE), ][1:100, ]
## quick visual of top 100 up/down
pheatmap(norm_counts_Table[rownames(top100_up), ], scale="row", display_numbers = TRUE)
##green colour palette
pheatmap(norm_counts_Table[rownames(top100_down), ], scale="row", display_numbers = TRUE, color = redgreen(50))
##check available key types for gene name to identifier mapping
keytypes(org.Hs.eg.db)
##fetch REFSEQ to Gene Symbol mappings from org.hs database
anno<- bitr(rownames(norm_counts_Table), fromType = "REFSEQ",
        toType = c("SYMBOL"),
        OrgDb = org.Hs.eg.db)
##make sure norm counts Table is a data frame type
norm_counts_Table <- as.data.frame(norm_counts_Table)
##add a key refseq column
norm_counts_Table$Refseq <- rownames(norm_counts_Table)
## merged data frame with gene name column at the end
merged <- merge(x=norm_counts_Table, y =anno, by.x = "Refseq", by.y="REFSEQ", all.x=TRUE, all.y = FALSE )

## Make unique row names - incremented gene names with .1 .2, etc
rownames(merged) <- make.names(merged$SYMBOL, unique = TRUE)
##rename for clarity
norm_counts_with_names <- merged
# plot top 100 downregulated genes with gene names
top100_down_gene_names <-norm_counts_with_names[ which(norm_counts_with_names$Refseq %in% rownames(top100_down)), ][,
3:dim(norm_counts_with_names)[2]-1 ]
top100_down_gene_names <- norm_counts_with_names[which(norm_counts_with_names$Refseq %in% rownames(sig_hits_all)), ]
## save this as a file
```

```
png("top100_down_genes_with_names.png", height = 1000, units = "px")
pheatmap(top100_down_gene_names[1:100, 2:5], scale="row", display_numbers = FALSE, color = redgreen(50))
dev.off()

##to save signifcant hits together with normalised values in one big Table, first merge the two Tables as before
sig_hits$Refseq <- rownames(sig_hits)
counts_with_changes <- merge(x=as.data.frame(sig_hits), y =norm_counts_with_names, by.x = "Refseq", by.y="Refseq", all.x=TRUE, all.y = FALSE )
##write Table to file - can open in excel, but maybe not by default
write.Table(counts_with_changes, file="sig_hits.txt", sep="\t", col.names = TRUE, row.names = FALSE, quote=FALSE)

## what are different functions that are over-represented in these DE genes:
## perform erichment for subset of genes for GO domains, biological process, cellular component and molecular function:
DEGs <- unique(counts_with_changes$SYMBOL)
universe <- unique(norm_counts_with_names$SYMBOL)
BP <- enrichGO(keytype = "SYMBOL",
        gene         = DEGs,
        universe     = universe,
        OrgDb        = org.Hs.eg.db,
        ont          = "BP",
        pAdjustMethod = "BH", ## multiple testing correction type, BH == Benjamini-Hotchberg
        pvalueCutoff  = 0.01, ## FDR cutoff  - can change this and p-value together to get more or fewer hits, as required
        qvalueCutoff  = 0.05) ## p-value cutoff
#examine the top hits
head(BP, 50)
#plot top 50 hits as a dot plot
dotplot(BP, 50)
#summarise into a Table
write.Table(BP, file="enriched_BP_test.txt", sep="\t", col.names = TRUE, row.names = FALSE, quote=FALSE)

CC <- enrichGO(keytype = "SYMBOL",
        gene         = DEGs,
        universe     = universe,
        OrgDb        = org.Hs.eg.db,
        ont          = "CC",
        pAdjustMethod = "BH", ## multiple testing correction type, BH == Benjamini-Hotchberg
        pvalueCutoff  = 0.01, ## FDR cutoff  - can change this and p-value together to get more or fewer hits, as required
        qvalueCutoff  = 0.05) ## p-value cutoff
#examine the top hits
head(CC, 50)
#plot top 50 hits as a dot plot
dotplot(CC, 50)
#summarise into a Table
write.Table(CC, file="enriched_CC_test.txt", sep="\t", col.names = TRUE, row.names = FALSE, quote=FALSE)

MF <- enrichGO(keytype = "SYMBOL",
        gene         = DEGs,
        universe     = universe,
        OrgDb        = org.Hs.eg.db,
        ont          = "MF",
        pAdjustMethod = "BH", ## multiple testing correction type, BH == Benjamini-Hotchberg
        pvalueCutoff  = 0.01, ## FDR cutoff  - can change this and p-value together to get more or fewer hits, as required
        qvalueCutoff  = 0.05) ## p-value cutoff
#examine the top hits
head(MF, 50)
#plot top 50 hits as a dot plot
dotplot(MF, 50)
```

```
#summarise into a Table
write.Table(MF, file="enriched_MF_test.txt", sep="\t", col.names = TRUE, row.names = FALSE, quote=FALSE)
### for KEGG pathways, convert gene symbols to ENTREZ
entrez_test<- bitr(DEGs, fromType = "SYMBOL",
            toType = c("ENTREZID"),
            OrgDb = org.Hs.eg.db)
universe <- bitr(universe, fromType = "SYMBOL",
             toType = c("ENTREZID"),
             OrgDb = org.Hs.eg.db)

kegg <- enrichKEGG(use_internal_data = FALSE, ## will fetch latest KEGG annotations
              ##instead of using internal database which may be outdated - set to TRUE if having issues with connection, etc
              qvalueCutoff = 0.05,
              pAdjustMethod = "BH",
              keyType = "ncbi-geneid",
              gene = unique(entrez_test$ENTREZID),
              organism     = 'hsa', ## human
              pvalueCutoff = 0.01,
              universe= unique(universe$ENTREZID))

head(kegg, 10)
#plot top 50 hits as a dot plot
dotplot(kegg, 50)
#summarise into a Table
write.Table(kegg, file="enriched_KEGG_test.txt", sep="\t", col.names = TRUE, row.names = FALSE, quote=FALSE)

##for reactome pathways
reactome <- enrichPathway(gene = unique(entrez_test$ENTREZID),
                    organism = "human",
                    readable = TRUE,
                    pvalueCutoff = 0.05,
                    pAdjustMethod = "BH",
                    qvalueCutoff = 0.05,
                    universe= unique(universe$ENTREZID))
head(reactome, 60)
#plot top 50 hits as a dot plot
dotplot(reactome, 50)
#summarise into a Table
write.Table(reactome, file="enriched_reactome_test.txt", sep="\t", col.names = TRUE, row.names = FALSE, quote=FALSE)
```

Script A3.2. Drawing scatter plots for potential new marker genes. Annotation is given in red and preceded by a “#” symbol

```
## install and load packages
biocLite("reshape2")
library(reshape2)

## change data to long format and change orientation
melted <-t( top100_up_gene_names[1:30, 2:(dim(top100_up_gene_names)[2]-1) ])
## combine Table with meta data
melted <- cbind(melted, meta_data[rownames(melted), ])
## note variable lanes
melted <-melt(melted, id.vars = c ("Sample_Name" ,"Lane",  "Type"  ,  "IC" ,"Subtype"))
## plot as scatter plot
```

```
ggplot(melted, aes(as.numeric(value), variable, colour=factor(m2c), shape=factor(Lane))) + geom_point( size= 3, alpha = 0.7) + theme_light(base_size = 16)+
labs(y="Genes", x = "Log2 count", shape="Sequencer Lane ", colour = " Subtype", title ="Top 25 up-regulated genes: TPP")
```

Script A3.3. Looking at expression of potential new marker genes in publicly available RNA-seq count data. Annotation is given in red and preceded by a "#" symbol

```
# read in counts Table

counts_old <- read_delim("C:\\Users\\umnar\\Documents\\RNA_seq\\RNA_seq_r_project\\old gene counts\\old_data_gene_counts.txt","\t", escape_double =
FALSE, trim_ws = TRUE)

## read in meta data Table describing the samples

meta_data_old <- data.frame(names = c("M1_2", "M1_3", "M2_1", "M2_2", "M2_3", "monocyte_1", "monocyte_2" ,"monocyte_3","THP1_1","THP1_2"
,"THP1_3"),

                    cell_type = c("M1", "M1", "M2a", "M2a", "M2a", "monocyte", "monocyte" ,"monocyte","THP1","THP1" ,"THP1"))

##rename  columns in count Table to be more sensible

##rename row names in meta data to correspond to sample names

rownames(meta_data_old) <- meta_data_old$names

##convert counts Table to data frame

counts_old <- as.data.frame(counts_old)

##get sample names

sample_names <- colnames(counts_old)[8:length(colnames(counts_old))]

##make sure meta data and counts Table is in the same order by reordering

meta_data_old <- meta_data_old[sample_names, ]

##rename rows to have refseq gene identifiers

rownames(counts_old) <- counts_old$Refseq

##subset just the raw counts

matrix_old <- as.matrix(counts_old[, 8:length(colnames(counts_old))])

storage.mode(matrix_old) <- "integer"

ddss_old <- DESeqDataSetFromMatrix(countData = matrix_old,colData  = meta_data_old, design = ~ cell_type)

log_norm_counts_for_pca_old <- rlog(ddss_old, blind = FALSE)

marker_genes_old <- data.frame(Type=c("M1", "M1", "M1","M1","M1","M1","M1", "M1"),

                       symbol=c( "SERPING1", "FAM26F", "CD274","ETV7", "XIRP1", "ACOD1", "GBP5", "LIMP"))

marker_genes_old <- data.frame(Type=c("M2a", "M2a", "M2a","M2a","M2a","M2a","M2a"),

  symbol=c( "CD209", "SPINT2","CHN2","ALOX15","LOX","CHN2","ST8SIA6"))

anno<- bitr(marker_genes_old$symbol, fromType = "SYMBOL",

          toType = c("REFSEQ"),

          OrgDb = org.Hs.eg.db)

markers <- merge(marker_genes_old, anno, by.x="symbol", by.y="SYMBOL", all.x=TRUE, all.y=TRUE)

rownames(markers) <- make.names(markers$symbol, unique= TRUE)

markers_exp <- log_norm_counts_for_pca_old[which(rownames(log_norm_counts_for_pca_old) %in% markers$REFSEQ), ]

markers_exp <- assay(markers_exp)

markers_exp <- as.data.frame(markers_exp)

markers_exp$refseq <- rownames(markers_exp)

markers_exp <- merge(markers_exp, markers, by.x="refseq", by.y="REFSEQ")

# check if duplicates first, if yes run this line

markers_exp <- markers_exp[-which(duplicated(markers_exp)), ]

#markers_exp <- markers_exp[-which(duplicated(markers_exp)), which(meta_data$Lane != 5)]

rownames(markers_exp) <- paste(markers_exp$refseq, markers_exp$symbol, sep=" ")

mat <- markers_exp[ , 2:(dim(markers_exp)[2] -2)]

subset_something <- mat[, (which(meta_data_old$cell_type == "M1"|meta_data_old$cell_type == "M2"|meta_data_old$cell_type == "monocyte"))]

zeroPlus <- subset_something[which(rowSums(subset_something[ ,]) != 0), ]

pheatmap(zeroPlus, display_numbers = TRUE, color= redgreen(50),scale = "row", main = "New M2a markers in MDMs \n")

write.Table(mat, file="newmarkersolddataset.txt",sep="\t", col.names = TRUE, row.names = TRUE, quote=FALSE)
```

Script A3.4. Looking at expression of potential new marker genes in publicly available microarray data. Annotation is given in red and preceded by a "#" symbol

```
#check bioconductor website for correct array probe annotation database:
# https://www.bioconductor.org/packages/3.3/data/annotation/
# in this case, it's 'illuminaHumanv3.db'
# download and load
source("https://bioconductor.org/biocLite.R")
biocLite()
biocLite("illuminaHumanv3.db")
# other packages, if not installed already:
biocLite(c("GenomicFeatures", "AnnotationDbi"))
biocLite("limma")
biocLite("affy")
biocLite("biomaRt")
biocLite("annotate")
package("gplots")
library(limma)# for differential expression analysis
library(affy) # for core expression objects
library(annotate) # probeset annotations - overlaps with biomaRt, can use either
library(gplots) # for plotting functions
library(biomaRt) # for gene and GO annotations
library(illuminaHumanv3.db) # probe annotation db
library(AnnotationDbi)
library(GenomicFeatures)
# set working directory to location of downloaded unpacked files
getwd()
setwd("C:/Users/umnar/Documents/temp/E-GEOD-46903.processed.1 (4)")
# read in data - e.g samples1-3 are from condition 1 and samples 4-6 are from condition 2
sample1 <- read.delim("GSM1140744_sample_Table.txt")
sample2 <- read.delim("GSM1140743_sample_Table.txt")
sample3 <- read.delim("GSM1140742_sample_Table.txt")
sample4 <- read.delim("GSM1140499_sample_Table.txt")
sample5 <- read.delim("GSM1140495_sample_Table.txt")
sample6 <- read.delim("GSM1140443_sample_Table.txt")
sample7 <- read.delim("GSM1140602_sample_Table.txt")
sample8 <- read.delim("GSM1140620_sample_Table.txt")
sample9 <- read.delim("GSM1140622_sample_Table.txt")
sample10 <- read.delim("GSM1140644_sample_Table.txt")
sample11 <- read.delim("GSM1140739_sample_Table.txt")
sample12 <- read.delim("GSM1140740_sample_Table.txt")
sample13 <- read.delim("GSM1140602_sample_Table.txt")
sample14 <- read.delim("GSM1140620_sample_Table.txt")
sample15 <- read.delim("GSM1140622_sample_Table.txt")
sample16 <- read.delim("GSM1140486_sample_Table.txt")
sample17 <- read.delim("GSM1140525_sample_Table.txt")
sample18 <- read.delim("GSM1140530_sample_Table.txt")
sample19 <- read.delim("GSM1140445_sample_Table.txt")
sample20 <- read.delim("GSM1140496_sample_Table.txt")
sample21 <- read.delim("GSM1140500_sample_Table.txt")
# create a single data frame with just expression column
data <- cbind(sample1[, 2], sample2[,2], sample3[,2]
        , sample4[, 2], sample5[, 2], sample6[, 2], sample7[, 2], sample8[,2],
        sample9[,2], sample10[, 2], sample11[, 2], sample12[, 2], sample13[, 2],
        sample14[, 2], sample15[, 2], sample16[, 2], sample17[,2], sample18[,2],
        sample19[, 2], sample20[, 2], sample21[, 2])
```

```
# asign samples as column names and probe ids as row names
names <- paste("Sample", 1:21, sep="")
colnames(data) <- names
rownames(data) <- sample1[, 1]
#convert data frame to matrix
data <- as.matrix(data)
# create meta data matrix
metaData1 <- cbind("hsapiens", c("mon", "mon", "mon", "M0", "M0", "M0", "M1", "M1",
                                 "M1", "M2a", "M2a", "M2a", "M2b", "M2b", "M2b", "M2c", "M2c", "M2c",
                                 "TPP", "TPP", "TPP"))
colnames(metaData1) <-c("Species", "Treatment")
rownames(metaData1) <- paste("Sample", 1:21, sep="")
metaData <- new("AnnotatedDataFrame", data=as.data.frame(metaData1))
#create expression set object for limma input
expressionSet <- ExpressionSet(data, metaData)
###to extract and reformat all data #loop over all treatments, getting the mean expression:
#create empty data frame
results <- data.frame(matrix(ncol = 0, nrow = dim(expressionSet)[1]))
for (treatment in levels(expressionSet$Treatment)){
  sub <-expressionSet[, expressionSet$Treatment == treatment]
  e <- exprs(sub)
  results <- cbind(results, rowMeans(e))
}
#annotate columns and rows
rownames(results) <-make.names(getSYMBOL(rownames(expressionSet), "illuminaHumanv3.db"), unique=TRUE)
colnames(results) <-levels(expressionSet$Treatment)
markers <- data.frame(Type=c("mon", "mon", "mon", "mon"),
                                  symbol=c("MS4A6A", "CLEC12A", "MYB","CCR2"))
an_object <- results[which(rownames(results) %in% markers$symbol), ]
an_object <- an_object[which(rowSums(an_object) != 0), ]
pheatmap(an_object, display_numbers = FALSE, scale="row",
         #annotation_col = meta_data[, c(2, 4,5)],
         color=redgreen(50), show_rownames = TRUE, main = "M2c markers in MDM dataset\n")
write.Table(results, file="NewMarkersXueData.txt", sep="\t", na="NA", row.names=TRUE, col.names=TRUE)
```

Script A3.5. PCA plots and analysis of PCA loadings. Annotation is given in red and preceded by a “#” symbol

```
##PCA stuff:
#### create a dds object for all data to be included in the plot
ddss <- DESeqDataSetFromMatrix(countData = matrix, colData  = meta_data, design = ~ IC + Lane + Subtype)
log_norm_counts_for_pca <- rlog(ddss, blind = FALSE)
log_norm_counts_for_pca_matrix <-assay(log_norm_counts_for_pca)
#### if need to subset, create an index
indexes_for_pca <- which(meta_data$Lane != 5)
## PCA plotting
pca_dat <- plotPCA(log_norm_counts_for_pca[ ,indexes_for_pca ], n = 1000,  intgroup=c("Subtype", "IC"), returnData=TRUE)
ggplot(pca_dat, aes(PC1, PC2, colour=Subtype, label=name)) + geom_point(size=3)  + geom_text_repel(aes(label=name))
library(pcaExplorer)
## preprocessing of data, need a dds and log-transformed
indexes <- which(meta_data$Lane == 5)
dds <- DESeqDataSetFromMatrix(countData = matrix [ ,indexes],
                              colData = meta_data[indexes, ],
```

```
                        #design = ~ Lane + Subtype + IC)
                        design = ~ Subtype + IC)
dds <- DESeq(dds)
rld <- rlog(dds)
## point of entry for these functions, after DESEQ2
## pcaExplorer's plot pca function, generic
pcaplot(rld, intgroup = c("Lane", "Subtype"), ntop = 1000, pcX = 1, pcY = 2, title = "PC1 vs PC2")
##proportion of variance accounted by each PC:
gene_to_refseq<- bitr(rownames(assay(rld)), fromType = "REFSEQ",
                toType = c("SYMBOL"),
                OrgDb = org.Hs.eg.db)

annotated <- as.data.frame(assay(rld))
annotated$REFSEQ <- rownames(annotated)
annotated <- merge(annotated, gene_to_refseq, by.x="REFSEQ", by.y="REFSEQ", all.x=TRUE, all.y=TRUE)
annotated$Name <- paste( annotated$REFSEQ , annotated$SYMBOL,  sep=" \n ")
rownames(annotated) <- annotated$Name
annotated <- annotated[, 2:(dim(annotated)[2]-2)]
pcaobj <- prcomp(t(annotated))
pcascree(pcaobj, type="pev", title="Proportion of explained proportion of variance")
## plot correlation between a principal component and your covariates:
cor <- correlatePCs(pcaobj,colData(dds), pcs =c(1, 2, 3) )
plotPCcorrs(cor, pc=1)
## get top 100 loading genes for a PC
hi_loadings(pcaobj, topN = 10, whichpc = 1)
loading_Table <- hi_loadings(pcaobj, topN = 100, exprTable=annotated, whichpc = 2)
## plot heatmap of genes with highest loadings
pheatmap(loading_Table)

##Refseq genes, can be used as input for GO enrichment, etc/further analysis
##fetch REFSEQ to Gene Symbol mappings from org.hs database
anno<- bitr(rownames(loading_Table), fromType = "REFSEQ",
          toType = c("SYMBOL"),
          OrgDb = org.Hs.eg.db)

BP <- enrichGO(keytype = "SYMBOL",
             gene          = unique(anno$SYMBOL),
             universe      = universe,
             OrgDb         = org.Hs.eg.db,
             ont           = "BP",
             pAdjustMethod = "BH", ## multiple testing correction type, BH == Benjamini-Hotchberg
             pvalueCutoff  = 0.01, ## FDR cutoff  - can change this and p-value together to get more or fewer hits, as required
             qvalueCutoff  = 0.05) ## p-value cutoff
dotplot(BP, showCategory=50)
write.Table(BP, fileName("BP enriched for L5 IC only"))
##make sure norm counts Table is a data frame type
loading_Table <- as.data.frame(loading_Table)
##add a key refseq column
loading_Table$Refseq <- rownames(loading_Table)
## merged data frame with gene name column at the end
merged_loading_Table <- merge(x=loading_Table, y =anno, by.x = "Refseq", by.y="REFSEQ", all.x=TRUE, all.y = FALSE )
rownames(merged_loading_Table) <- make.names(merged_loading_Table$SYMBOL, unique = TRUE)
hi_loadings(merged_loading_Table, topN = 10, whichpc = 1)
```

Script A3.6. Examination of gene signatures and specific markers. Annotation is given in red and preceded by a “#” symbol

```
### for gene signatures
## read in Table of interest
SLE_genes <- read.delim("SLE_genes.txt")
SLE_genes <- as.data.frame(SLE_genes)
## change gene names to refseq identifiers
anno<- bitr(SLE_genes$symbol, fromType = "SYMBOL",
        toType = c("REFSEQ"),
        OrgDb = org.Hs.eg.db)
markers <- merge(SLE_genes, anno, by.x="symbol", by.y="SYMBOL", all.x=TRUE, all.y=TRUE)
# isolate genes of interest from counts Table
markers_exp <- log_norm_counts_for_pca_matrix[which(rownames(log_norm_counts_for_pca_matrix) %in% markers$REFSEQ), ]
markers_exp <- as.data.frame(markers_exp)
## add key refseq column and change rownames to gene names
markers_exp$refseq <- rownames(markers_exp)
merged_SLE <- merge(markers_exp, markers, by.x="refseq", by.y="REFSEQ")
rownames(markers_exp) <- paste(markers_exp$refseq, markers_exp$symbol, sep=" ")
## subset columns wanted and plot as heatmap, removing zero values which do not cluster
merged_SLE <- markers_exp[ , 1:(dim(markers_exp)[2] -1)]
merged_SLE2 <- merged_SLE[which(rowSums(merged_SLE) > 0),which(meta_data$Subtype == "Mono" & meta_data$Lane !=5)]
colnames(merged_SLE2) <- c("Mono_IC_1", "Mono_IC_3", "Mono_1", "Mono_3")
pheatmap(merged_SLE2, display_numbers = FALSE, color= redgreen(50), scale = "row", main = "RA genes", show_rownames = FALSE)


## marker stuff:
## genes
marker_genes2 <- data.frame(Type=c("M1", "M1", "M1", "M1","M1", "M1","M1", "M2a", "M2a","M2a", "M2a","M2a", "M2a","M2a"),
                symbol=c( "GBP5", "ANKRD22", "IL6","TNFAIP6","CXCL9","CXCL10", "IRF1", "TGM2", "HOMER2","ALOX15","CCL17","CD200R1",
"CCL23","CCL26"))
# subset data as required
indexes2 <- which(meta_data$Lane != 5)
# create dds object and log2 normalised counts Table
ddsss <- DESeqDataSetFromMatrix(countData = matrix[ ,indexes2], colData = meta_data[, ], design = ~ IC + Subtype)
log_norm_counts_for_markers <- rlog(ddsss, blind = FALSE)
log_norm_counts_for_markers_matrix <-assay(log_norm_counts_for_markers)
## change gene names to refseq identifiers to isolates genes opf interest from normalised counts Table
anno<- bitr(marker_genes2$symbol, fromType = "SYMBOL",
        toType = c("REFSEQ"),
        OrgDb = org.Hs.eg.db)
markers <- merge(marker_genes2, anno, by.x="symbol", by.y="SYMBOL", all.x=TRUE, all.y=TRUE)
markers_exp <- log_norm_counts_for_pca_matrix[which(rownames(log_norm_counts_for_pca_matrix) %in% markers$REFSEQ), ]
markers_exp <- as.data.frame(markers_exp)
## change row names to gene names
markers_exp$refseq <- rownames(markers_exp)
markers_exp <- merge(markers_exp, markers, by.x="refseq", by.y="REFSEQ")
rownames(markers_exp) <- paste(markers_exp$refseq, markers_exp$symbol, sep=" ")
##subset data as required
mat <- markers_exp[ , 2:(dim(markers_exp)[2] -2)]
## draw heatmap for genes
pheatmap(mat[ , which( meta_data$Lane != 5 & meta_data$IC == "IC_no" )], display_numbers = TRUE, color= redgreen(50),scale = "row", main = "Novel
markers")
## save data into Table
write.Table(mat[ ,(which(mt$IC == "IC_no" & mt$Subtype != LPS & mt$Subtype != TPP) )], file="additional markers basic conditions.txt",sep="\t", col.names =
TRUE, row.names = FALSE, quote=FALSE)
```

Script A3.7. Intersecting and comparing data with publicly available data; Venn diagram and MA plots. Annotation is given in red and preceded by a “#” symbol

```
counts_old <- read_delim("C:\\Users\\umnar\\Documents\\RNA_seq\\RNA_seq_r_project\\old gene counts\\old_data_gene_counts.txt","\t", escape_double =
FALSE, trim_ws = TRUE)
## read in meta data Table describing the samples
meta_data_old <- data.frame(names = c("M1_2", "M1_3", "M2_1", "M2_2", "M2_3", "monocyte_1", "monocyte_2" ,"monocyte_3","THP1_1","THP1_2"
,"THP1_3"),
                            cell_type = c("M1", "M1", "M2a", "M2a", "M2a", "monocyte", "monocyte" ,"monocyte","THP1","THP1" ,"THP1"))
##rename row names in meta data to correspond to sample names
rownames(meta_data_old) <- meta_data_old$names
##convert counts Table to data frame
counts_old <- as.data.frame(counts_old)
##get sample names
sample_names <- colnames(counts_old)[8:length(colnames(counts_old))]
##make sure meta data and counts Table is in the same order by reordering
meta_data_old <- meta_data_old[sample_names, ]
##rename rows to have refseq gene identifiers
rownames(counts_old) <- counts_old$Refseq
##subset just the raw counts
matrix_old <- as.matrix(counts_old[, 8:length(colnames(counts_old))])
storage.mode(matrix_old) <- "integer"
##genes with identifiers in both lists
common_refseq <- rownames(matrix)[which(rownames(matrix) %in% rownames(matrix_old))]
matrix_both <- cbind(matrix[common_refseq, ], matrix_old[common_refseq, ])
##merge metadata Tables
lane <- c(as.character(meta_data$Lane), rep("unknown1", 5), rep("unknown2", 3), rep("unknown3", 3))
ic <- c(as.character(meta_data$IC), rep("IC_no", 11))
name <-  c( as.character(meta_data$Sample_Name), as.character(meta_data_old$names))
subtype <- c(as.character(meta_data$Subtype), as.character(meta_data_old$cell_type))
meta_data_both <- data.frame( name=name,
                              Subtype = subtype ,
                              Lane= lane,
                              IC = ic)
## new stuff:
indexes <- which(meta_data_both$IC == "IC_no" & (meta_data_both$Subtype == "M1" | meta_data_both$Subtype == "M2a")
                 & (meta_data_both$Lane %in% c( "4", "6")))
dds_new <- DESeqDataSetFromMatrix(countData = matrix_both[, indexes],
                                  colData = meta_data_both[indexes, ], design = ~ Subtype)
dds_new <- DESeq(dds_new )
## old stuff:
indexes <- which(meta_data_both$IC == "IC_no" & (meta_data_both$Subtype == "M1" | meta_data_both$Subtype == "M2")
                 & (meta_data_both$Lane == "unknown1"))
dds_old <- DESeqDataSetFromMatrix(countData = matrix_both[, indexes],
                                  colData = meta_data_both[indexes, ], design = ~ Subtype)
dds_old <- DESeq(dds_old )
log_norm_counts_old <- rlog(dds_old, blind = TRUE)
norm_counts_Table_old<- assay(log_norm_counts_old)
norm_counts_not_log <- counts(dds_old, norm=TRUE )

## draw MA plots
setwd("MA_plots")
for ( i in 1: dim(norm_counts_not_log)[2]){
  for ( j in 1: dim(norm_counts_not_log)[2]){

    ma_plot_df <- data.frame(mean =  rowMeans( norm_counts_not_log[, c(i, j )]),
```

```
                    FC = log((norm_counts_not_log[, i ] + 1) / (norm_counts_not_log[, j ] + 1)),
                    sig = rep(FALSE, dim(norm_counts_not_log)[1] ) )
  png(paste(colnames(norm_counts_not_log)[j], colnames(norm_counts_not_log)[i], ".png", sep="_"))
   geneplotter::plotMA(ma_plot_df)
   dev.off()
  }
}
setwd("../")
plotGOgraph(BP)
enrichMap(BP)
res_old <- results(dds_old,  pAdjustMethod = "BH")
res_new <- results(dds_new,  pAdjustMethod = "BH")
r1 <- rownames(res_old[which(res_old$padj < 0.01), ])
r2 <- rownames(res_new[which(res_new$padj < 0.01), ])
a <- calculate.overlap(list(r1, r2))
draw.pairwise.venn(length(a$a1), length(a$a2), length(a$a3), category = c("MDM", "THP-1"),  fill = c("salmon", "light blue") )
overlap <- a$a3
not_overlap_old <- a$a1[-which(a$a1 %in% a$a3)]
not_overlap_new <- a$a2[-which(a$a2 %in% a$a3)]
anno<- bitr(not_overlap_new, fromType = "REFSEQ",
          toType = c("SYMBOL"),
          OrgDb = org.Hs.eg.db)
DEGs <- unique(anno$SYMBOL)
universe <- unique(norm_counts_with_names$SYMBOL)
BP <- enrichGO(keytype = "SYMBOL",
             gene         = DEGs,
             universe     = universe,
             OrgDb        = org.Hs.eg.db,
             ont          = "BP",
             pAdjustMethod = "BH", ## multiple testing correction type, BH == Benjamini-Hotchberg
             pvalueCutoff  = 0.05, ## FDR cutoff  - can change this and p-value together to get more or fewer hits, as required
             qvalueCutoff  = 0.05) ## p-value cutoff
#examine the top hits
head(BP, 50)
dotplot(BP, showCategory=50)
write.Table(BP, file="OLD_VS_NEW_DATASET_M1VM2DEGS.txt", sep="\t", col.names = TRUE, row.names = TRUE, quote=FALSE)
overlap <- a$a3
not_overlap_old <- a$a1[-which(a$a1 %in% a$a3)]
not_overlap_new <- a$a2[-which(a$a2 %in% a$a3)]
```

Script A3.7. Transcription factor analysis. Annotation is given in red and preceded by a "#" symbol

```
###for TF Table
library(readr)
### read in encode Table
TF_Table <- read_delim("~/RNA_seq/RNA_seq_r_project/TF_Table.txt",
                    "\t", escape_double = FALSE, col_names = FALSE,
                    trim_ws = TRUE)
### reformat to gather all non- name columns
TF_tab2 <- tidyr::gather(as.data.frame(TF_Table), key="TF", value="Target",  2:dim(TF_Table)[2] , na.rm = TRUE, convert = FALSE)[, c(1, 3)]
##rename columns
```

```
colnames(TF_tab2) <- c("TF", "Target")
###add a trimmed
TF_tab2$TF_trim <- gsub(TF_tab2$TF, pattern = "_.+", replacement="")
##subset RNA-seq data with names for significant hits in dataset of interest (e.g. genes significantly upregulated in monocytes+IC)
mono_up <-norm_counts_with_names[ which(norm_counts_with_names$Refseq %in% rownames(sig_hits_up)), ]
##subset relevant columns
mono_up <- mono_up[ ,3:dim(mono_up) [2]-1 ]
mono_up <-mdat2
all_regs <- TF_tab2[, 2:3]
some_list_of_interest <-rownames(mono_up)##[1:1000]
all_genes <- rownames(named_counts)
regulators_of_my_list <- unique(all_regs$TF_trim[which(all_regs$Target %in% some_list_of_interest)])
temp <- list()
## Loop over all regulators of gene list to feed data into contingency Table
for ( i in 1:length(regulators_of_my_list)){
  regulator <- regulators_of_my_list[i]
   regs <- all_regs[which(all_regs$TF_trim== regulator),]
   in_universe <- length(unique(regs$Target))
   in_list <- length(which(unique(regs$Target) %in% some_list_of_interest))
   total_universe <- length(unique(all_regs$Target))
   total_list <- length(unique(some_list_of_interest[which(some_list_of_interest %in% all_regs$Target)]))
   matrix(c(1,4,7,4), nrow = 2)
   ratio_list <- in_list / total_list
 ratio_universe <- in_universe / total_universe
   contingency <- matrix(c(in_list, total_list, in_universe, total_universe), nrow = 2)
   fisher <-fisher.test(contingency, alternative = "greater") ##less or greater
   temp[[i]] <- c(regulator, ratio_list, ratio_universe, in_list,  total_list, in_universe, total_universe, fisher$p.value)
 }
## summarise results into data frame
results <- matrix(unlist(temp), nrow=length(temp), byrow=TRUE)
colnames(results) <- c("TF", "ratio_list", "ratio_universe", "in_list",  "total_list", "in_universe", "total_universe", "pvalue")
results <- as.data.frame(results)
##include p-value column
results$pvalue <- as.numeric(as.character(results$pvalue))
##include adjusted p-value column
results$FDR <-p.adjust(results$pvalue, method="BH")
results <- results[ order(results$FDR), ]
results_p <- results[which(results$FDR < 0.05), ]
## plot as a bar chart
ggplot(results_p [1:10,], aes(TF, as.numeric(as.character(ratio_list)), fill=as.numeric(as.character(pvalue)) )) + geom_bar(stat="identity") + labs(fill="P-value",
y="Ratio in Gene set") + coord_flip() + theme_light()
## summarise into a Table and save
write.Table(results, file = ("m2cicTF.txt"), sep="\t", na="NA", row.names=TRUE, col.names=TRUE)
```

Script A3.8. Drawing heatmaps from FPKM files generated from public data

```
#gene Table  with refseq identifiers read in
FPKM <- read.delim("FPKM.txt")
FPKM <- as.data.frame(FPKM)

##fetch REFSEQ to Gene Symbol mappings from org.hs database
anno<- bitr(FPKM$Refseq, fromType = "REFSEQ",
            toType = c("SYMBOL"),
            OrgDb = org.Hs.eg.db)
```

```
## merged data frame with gene name column at the end
merged <- merge(x=FPKM, y =anno, by.x = "Refseq", by.y="REFSEQ", all.x=TRUE, all.y = FALSE )

## two types of unique row names - either incremented gene names with .1 .2, etc, or a combo between refseq and gene name
rownames(merged) <- make.names(merged$SYMBOL, unique = TRUE)

# creates a own color palette from red to white
my_palette <- colorRampPalette(c("red", "yellow", "white"))(n = 299)
#draw heatmap
heatmap.2(merged, margins = c(4, 10),col=my_pallet, trace= "none", dendrogram="row", Colv="NA", cexRow=0.8, cexCol=0.8 )
```

Script A3.9. Drawing heatmaps from count files generated from public data

```
##read in data
xue_data <- read.delim("xuetop300.txt")
## assign gene names as row names
rownames(xue_data) <- make.names(xue_data$gene, unique = TRUE)
# creates a own color palette from red to white
my_palette <- colorRampPalette(c("red", "yellow", "white"))(n = 299)
# draw heatmap
heatmap.2(xue_data, margins = c(4, 10),col=my_pallet, trace= "none", dendrogram="row", Colv="NA", cexRow=0.8, cexCol=0.8 )
```

Appendix 4: Additional Figures

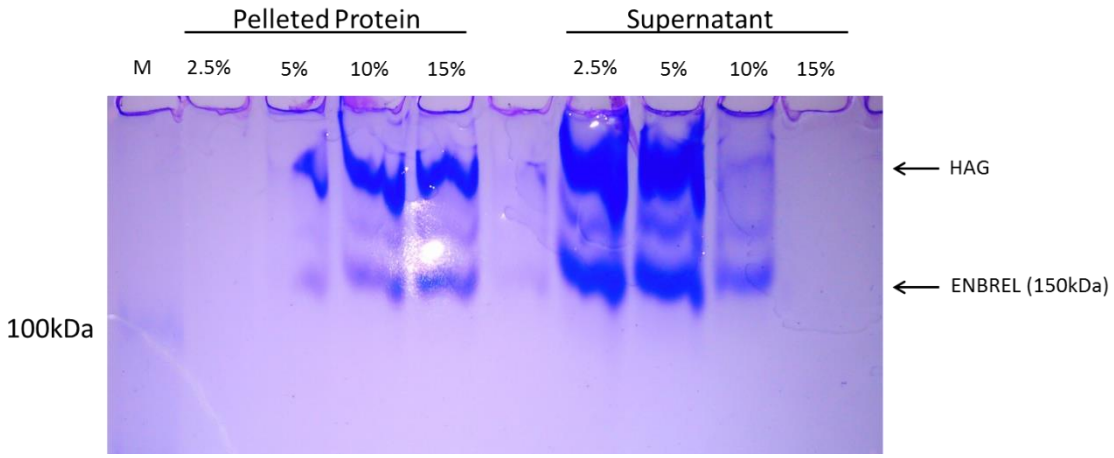

Figure A4.1 This gel was run as part of an experiment by a senior post-doctoral research scientist in the group; fractions of heat aggregated gamma globulin were combined with fractions of EMBREL (as a 150 KDa control) and precipitated with different concentrations of polyethylene glycol (given as percentages on the top of the image), precipitated at 4ºC overnight, centrifuged at 6000xg before samples from both pellet and supernatant were run on a 6% polyacrylamide gel which was stained with coomassie brilliant blue R-250 rapid stain.

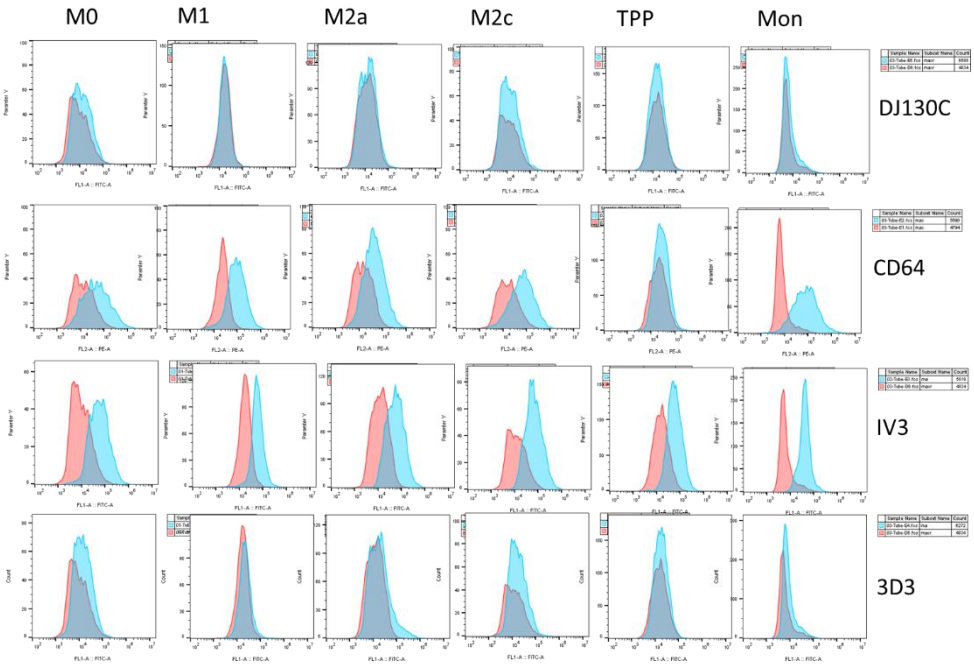

Figure A4.2 Repeat 2 of flow cytometry experiment found in Chapter 5 (Figure 5.3.1). Histograms demonstrate staining antibody (blue) versus isotype control (pink).

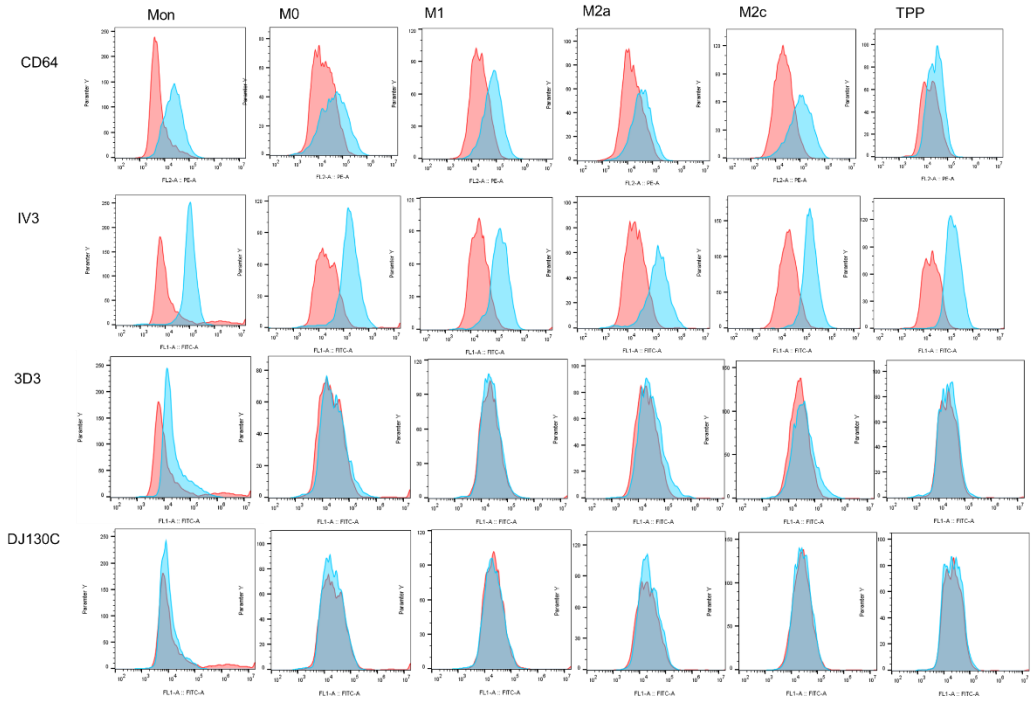

Figure A4.3 Repeat 3 of flow cytometry experiment found in Chapter 5 (Figure 5.3.1). Histograms demonstrate staining antibody (blue) versus isotype control (pink).

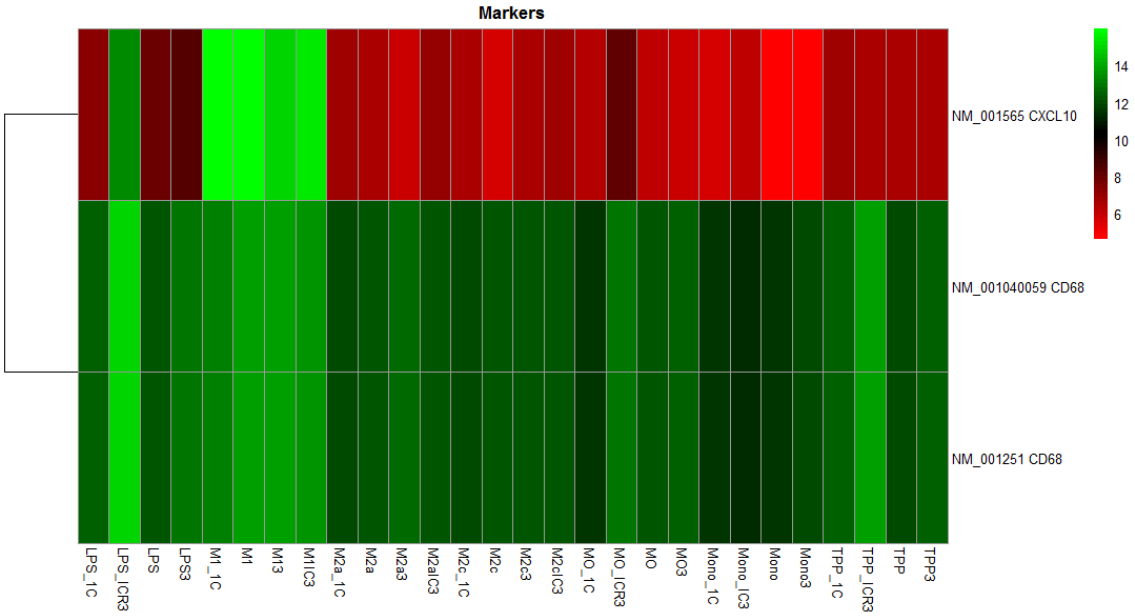

Figure A4.4 Heatmap showing consistently high expression of pan macrophage marker CD68 in all conditions tested, in comparison to M1 marker which is selectively high in one condition only.

Table A4.1: advantages and disadvantages of frequently used macrophage functional assays

Method	Advantages	Disadvantages
Transcriptional markers	High throughput methods available, gross comparisons with primary cells can be made, pathway and functional differences can be inferred	Not ideal for demonstrating macrophage functional differences, transcriptional features do not always translate to protein
Protein markers	More reliable for inferring function than transcript markers, can be used for cellular staining, cytometry and cell lysate analysis	Still not functional assay, not high throughput, some overlap with M2 subtypes
Cytokine and chemokine profile	Demonstrate some functional differences, can be measured quantitatively in numerous ways (ELISA, bead cytometry), can be measured from media	Not high throughput, some overlap with M2 subtypes, secreted so may not be detected by some methods (flow cytometry for instance), some assays have limited detection ranges (ELISA)
Arginine metabolism	Clear functional differences have been recorded between subtypes in mouse macrophages	Disagreement as to whether this translates to human cells
Glucose metabolism	Clear functional differences have been recorded between subtypes in mouse macrophages	Not reported in human cells
Phagocytosis	Well defined macrophage function	Occurs in M1 (bacterial removal) and M2 cells (efferocytosis); differences between activity in different subtypes is not clearly defined
Bacterial killing	Well defined macrophage function	Exposure to bacteria can alter cell phenotype

(Xue at al., 2014); (Ambarus et al., 2012); (Thomas and Mattila, 2014); (Rouzaut et al., 1999); (Babu et al., 2009); (Munder et al., 2005); (O'Neill *et al.,* 2016); (Bartosh and Ylostalo, 2014); (Jetten *et al.,* 2014).

Table A4.2: summary of commonly used monocytic cell lines with advantages and disadvantages of their use

Cell line	Advantages	Disadvantages	References
THP-1	Frequently used in publications and numerous protocols available Show similar morphology, flow cytometry features and protein expression to primary cells Immature (blood derived) cells; confers plasticity Can be differentiated into macrophages and polarised into inflammatory and anti-inflammatory states Demonstrate similar gene expression profiles	Evidence of limited polarisation into the M2 state Mutations in PTEN and CDKs may limit some research Some evidence that CD14 is under-expressed in these cells Numerous protocols available do not corroborate PMA required for differentiation; may induce non-physiological gene expression	(Tsuchiya et al., 1980); (Chanput et al., 2013); (Qin, 2012); (Chanput et al., 2012); (Chanput et al., 2014); (Chanput et al., 2015)
U937	Frequently used in the literature Can be induced into macrophage state Some similarities (e.g. cell surface marker expression) to primary cells	Less similar to primary cells than other cell lines according to flow cytometry, gene expression and protein expression More mature cells (derived from tissue) therefore less plastic	(Qin, 2012); (Chanput et al., 2013); (Chanput et al., 2012).
Mono-Mac 6	Gene/protein expression highly similar to primary cells Can phagocytose opsonised bacteria Isolated from blood so more plastic than tissue derived cell lines	Limited number of studies performed on these cells (fewer than other cell lines) Little evidence of macrophage differentiation or polarisation	(Friedland et al., 1993); (Ziegler-Heitbroc et al., 1988); (Shattock et al., 1994).
HL-60	Immature cells susceptible to stimuli	Cells are promyelocytic and need stimuli to achieve even a monocyte phenotype Resemble banded neutrophils more closely than	(Collins, 1987); (Rovera et al., 1979)
KG-1	Immature cells that can be developed into macrophages	very high p-Syk/Syk so not appropriate for use in studies looking at IC signaling also generate granulocyte like cells	(Hahn et al., 2009).

Appendix 5: FcγR expression experiments

Table A5.1. Counts for specific regions of different FCGR genes, normalised by dividing raw count values by length.

Replicate	Gene	LPS_1	M1_1	M2a_1	M2c_1	M0_1	Mono_1	TPP_1
replicate 1	FCGR2A_part_of_exon3_2	0.0412	0.0448	0.0499	0.0454	0.0463	0.0442	0.0455
replicate 3	FCGR2A_part_of_exon3_3	0.0415	0.0423	0.0495	0.0426	0.0417	0.0426	0.0425
replicate 1	FCGR2B_part_of_exon3_2	0.0264	0.0268	0.0272	0.0267	0.0276	0.0263	0.0275
replicate 3	FCGR2B_part_of_exon3_3	0.0273	0.0264	0.0277	0.0269	0.0266	0.0271	0.0269
replicate 1	FCGR2C_part_of_exon3_2	0.0129	0.0130	0.0129	0.0132	0.0132	0.0129	0.0138
replicate 3	FCGR2C_part_of_exon3_3	0.0129	0.0129	0.0129	0.0130	0.0129	0.0130	0.0129
replicate 1	FCGR3B_last_exon_2	0.0022	0.0023	0.0023	0.0023	0.0022	0.0022	0.0023
replicate 3	FCGR3B_last_exon_3	0.0022	0.0022	0.0022	0.0022	0.0022	0.0022	0.0023
replicate 1	FCGR3A_last_exon_2	0.0049	0.0052	0.0051	0.0054	0.0054	0.0038	0.0060
replicate 3	FCGR3A_last_exon_3	0.0045	0.0046	0.0048	0.0051	0.0049	0.0042	0.0045

Table A5.2. ANOVA output for analysis of FCGR gene expression, using the normalised counts in Table A5.1 with input for each gene being categorised by column.

Anova: Single Facti	FCGR2A									
SUMMARY					ANOVA					
Groups	*Count*	*Sum*	*Average*	*Variance*	*Source of Variation*	*SS*	*df*	*MS*	*F*	*P-value*	*F crit*
Column 1	2	0.082671	0.041335	6.83E-08	Between Groups	7.89E-05	6	1.31E-05	3.937137	0.04789	3.865969
Column 2	2	0.087073	0.043537	3.26E-06	Within Groups	2.34E-05	7	3.34E-06			
Column 3	2	0.099365	0.049682	7.38E-08							
Column 4	2	0.087973	0.043986	3.76E-06	Total	0.000102	13				
Column 5	2	0.087983	0.043991	1.02E-05							
Column 6	2	0.086786	0.043393	1.25E-06							
Column 7	2	0.087985	0.043992	4.72E-06							
Anova: Single Facti	**FCGR2B**									
SUMMARY					ANOVA					
Groups	*Count*	*Sum*	*Average*	*Variance*	*Source of Variation*	*SS*	*df*	*MS*	*F*	*P-value*	*F crit*
Column 1	2	0.053704	0.026852	4.02E-07	Between Groups	1.1E-06	6	1.84E-07	0.791073	0.604478	3.865969
Column 2	2	0.053225	0.026612	7.1E-08	Within Groups	1.63E-06	7	2.32E-07			
Column 3	2	0.054887	0.027444	1.21E-07							
Column 4	2	0.053601	0.0268	5.84E-09	Total	2.73E-06	13				
Column 5	2	0.054233	0.027116	5.32E-07							
Column 6	2	0.05339	0.026695	3.14E-07							
Column 7	2	0.05443	0.027215	1.81E-07							
Anova: Single Facti	**FCGR2C**									
SUMMARY					ANOVA					
Groups	*Count*	*Sum*	*Average*	*Variance*	*Source of Variation*	*SS*	*df*	*MS*	*F*	*P-value*	*F crit*
Column 1	2	0.025844	0.012922	2.06E-14	Between Groups	2.67E-07	6	4.45E-08	0.73054	0.641035	3.865969
Column 2	2	0.025953	0.012977	5.89E-09	Within Groups	4.26E-07	7	6.09E-08			
Column 3	2	0.025844	0.012922	6.79E-15							
Column 4	2	0.026223	0.013112	2E-08	Total	6.93E-07	13				
Column 5	2	0.026136	0.013068	4.26E-08							
Column 6	2	0.025944	0.012972	5.01E-09							
Column 7	2	0.026684	0.013342	3.53E-07							
Anova: Single Facti	**FCGR3A**									
SUMMARY					ANOVA					
Groups	*Count*	*Sum*	*Average*	*Variance*	*Source of Variation*	*SS*	*df*	*MS*	*F*	*P-value*	*F crit*
Column 1	2	0.009479	0.004739	7.75E-08	Between Groups	2.25E-06	6	3.75E-07	1.617559	0.271063	3.865969
Column 2	2	0.009708	0.004854	1.77E-07	Within Groups	1.62E-06	7	2.32E-07			
Column 3	2	0.009927	0.004964	5.98E-08							
Column 4	2	0.010452	0.005226	4.35E-08	Total	3.88E-06	13				
Column 5	2	0.010362	0.005181	1.37E-07							
Column 6	2	0.008033	0.004016	7.14E-08							
Column 7	2	0.010518	0.005259	1.06E-06							
Anova: Single Facti	**FCGR3B**									
SUMMARY					ANOVA					
Groups	*Count*	*Sum*	*Average*	*Variance*	*Source of Variation*	*SS*	*df*	*MS*	*F*	*P-value*	*F crit*
Column 1	2	0.00444	0.00222	1.12E-09	Between Groups	6.45E-09	6	1.08E-09	1.436536	0.321162	3.865969
Column 2	2	0.00448	0.00224	5.52E-10	Within Groups	5.24E-09	7	7.49E-10			
Column 3	2	0.004468	0.002234	5.53E-10							
Column 4	2	0.004448	0.002224	1.5E-09	Total	1.17E-08	13				
Column 5	2	0.004441	0.00222	4.53E-10							
Column 6	2	0.004405	0.002203	6.92E-11							
Column 7	2	0.004552	0.002276	9.9E-10							

Table A5.3. Raw median fluorescent intensity values for flow cytometry staining for various FcγR antibodies on different cell types, an isotype control values for the same cells (top panel), and values normalised by dividing fluorescence by isotype control for each sample. Data used to perform ANOVA tests in Chapter 5 Section 5.3.1.

	monocyte_1	monocyte_2	monocyte_3	M0_1	M0_2	M0_3	M1_1	M1_2	M1_3	M2a_1	M2a_2	M2a_3	M2c_1	M2c_2	M2c_3	TPP_1	TPP_2	TPP_3
	raw values																	
CD64	41967	46885	42181	51566	93830	86877	67090	73728	59426	33941	43566	58611	56566	47161	62331	39539	32478	43700
CD32a	97995	107652	51961	70779	44081	53688	136165	120908	79431	161454	219778	175636	181582	134575	176531	153591	96566	110543
CD32b	16674	9025	13535	23033	20905	20967	21340	38851	16335	25980	52268	42967	33250	33348	33326	22235	29391	25467
CD16	8411	6179	10923	18918	17839	16002	19597	31631	12067	20004	31911	28764	24788	27151	24446	20844	25677	21349
PE-isotype	4800	5366	12540	14696	14653	22631	19198	29478	13898	13857	13615	15001	20063	23859	21106	17997	21018	18433
FITC-isotype	8535	5430	8435	19255	18156	16479	20844	13048	11790	19142	26365	18988	25081	23719	23994	21028	21277	21124
	isotype control corrected (subtracted)																	
CD64	37167	41519	29641	36870	79177	64246	47892	44250	45528	20084	29951	43610	36503	23302	41225	21542	11460	25267
CD32a	89460	102222	43526	51524	25925	37209	115321	107860	67641	142312	193413	156648	156501	110856	152537	132563	75289	89419
CD32b	8139	3595	5100	3778	2749	4488	496	25803	4545	6838	25903	23979	8169	9629	9332	1207	8114	4343
CD16	0	749	2488	0	0	0	0	18583	277	862	5546	9776	0	3432	452	0	4400	225

Table A5.4. Average median fluorescent intensity (normalised by dividing by isotype control) for different proteins on various cell types. Data used to plot bar chart in Chapter 5: Figure 5.3.1, B.

Mean (isotype control corrected)						
	Monocyte	M0	M1	M2a	M2c	TPP
CD64	36109	60097.66667	45890	31215	33676.6667	19423
CD32a	78402.66667	38219.33333	96940.6667	164124.3333	139964.667	99090.33333
CD32b	5611.333333	3671.666667	10281.3333	18906.66667	9043.33333	4554.666667
CD16	1079	0	6286.66667	5394.666667	1294.66667	1541.666667
standard error of mean						
	Monocyte	M0	M1	M2a	M2c	TPP
CD64	3469.449716	12387.85782	1066.82145	6820.714552	5363.44424	4124.153772
CD32a	17823.23922	7407.041252	14807.3122	15217.85925	14599.2486	17226.22792
CD32b	1336.423128	504.813607	7848.35869	6059.839941	445.494607	1996.685949
CD16	736.9330589	0	6148.68664	2574.362402	1076.60289	1430.641853

Appendix 6: STRING network data Tables

Table A6.1 Table containing raw data corresponding to STRING network plot for IRF3 in Chapter 5 (Figure 5.3.14, A) ordered by adjusted p-value. Please note that proteins with a positive fold change are highlighted in salmon as these were the changes focussed on in this report.

Gene name	log2FoldChange	Adjusted p-value (BH)	pvalue
TLR4	-1.995609366	2.77E-16	2.42E-18
PRKDC	1.087345491	9.99E-07	4.12E-08
STAT2	-1.205477352	2.96E-06	1.37E-07
HERC5	1.900882663	1.08E-04	7.57E-06
JUN	-1.161394409	1.87E-04	1.40E-05
IFIT2	1.372495037	0.00106968	1.05E-04
IKBKE	0.970812323	0.001203558	1.21E-04
MX1	0.846372597	0.061201733	0.014747584
ISG15	0.650788027	0.11261446	0.032244172
RSAD2	-0.681480147	0.160884477	0.052558232
RNASEL	-0.386134536	0.264786767	0.105424715
IFIT1	0.548253266	0.381693032	0.18096896
RELA	0.36443476	0.398585623	0.192992581
IRF3	0.286064621	0.408311074	0.199816826
TANK	-0.399825996	0.411367099	0.202026028
TMEM173	-0.284364143	0.431939506	0.217295419
MAVS	-0.240018721	0.504852857	0.277266425
TICAM2	-0.3798007	0.522584139	0.2928093
TRIM21	-0.207366016	0.598023201	0.366909179
TBK1	0.222830389	0.605456601	0.374772769
CREBBP	0.131819792	0.79689822	0.621848935
DDX58	0.064612613	0.921429556	0.832488136
IRF7	-0.062785972	0.922981992	0.835579433
ISG20	0.165752604	0.942831786	0.873065596
IFIH1	-0.043853327	0.946743906	0.879859102
EP300	-0.016385621	0.977356089	0.946607173
TRAF3	0.011680712	0.981981327	0.959998111
TICAM1	-0.010894755	0.99197221	0.980182191
IFNB1	-0.005423675	NA	NA
TLR3	1.843224221	NA	NA
ZBP1	0	NA	NA

Table A6.2 Table containing raw data corresponding to STRING network plot for SP1 in Chapter 5 (Figure 5.3.14, B) ordered by adjusted p-value. Please note that proteins with a positive fold change are highlighted in salmon as these were the changes focussed on in this report.

Gene name	log2FoldChange	Adjusted p-value (BH)	pvalue
JUN	-1.161394409	1.87E-04	1.40E-05
DHFR	0.891682678	2.51E-04	1.94E-05
HDAC1	0.762919706	0.002099221	2.32E-04
HDAC2	0.589096953	0.031957592	0.006390984
MYC	-0.549959533	0.045786901	0.010227087
ETS1	-0.644393895	0.050664922	0.011599877
MMP14	-0.477463959	0.084866868	0.022305619
NFYA	0.485281639	0.16685083	0.055419948
CDKN1A	0.417387698	0.206794738	0.074417604
ARNT	-0.331742001	0.316731151	0.136878515
POU2F1	0.327318895	0.319179561	0.138548669
HIF1A	-0.315149304	0.337459412	0.150182529
TBP	0.370482851	0.377891911	0.178174279
RELA	0.36443476	0.398585623	0.192992581
MAPK1	-0.283282197	0.403725116	0.196570609
SP1	-0.261571364	0.413505427	0.203494935
MAPK14	0.226119257	0.506180117	0.278373451
SREBF2	0.213140571	0.541200614	0.309799081
SMAD3	-0.209494359	0.606817263	0.376237815
NFYB	-0.229765542	0.615797587	0.385604253
SMAD4	-0.144286716	0.723434768	0.520534168
MAPK8	-0.13136004	0.786123853	0.606622338
SMAD2	-0.079420753	0.852755254	0.706061783
SP3	-0.076656973	0.860570055	0.71871762
TP53	-0.183178613	0.878954098	0.747549671
GTF2B	0.074794192	0.885708003	0.761864042
RB1	0.059791247	0.895251611	0.781139496
FOS	0.063200623	0.908582579	0.808169597
EP300	-0.016385621	0.977356089	0.946607173
ESR1	1.826571121	NA	NA
CDKN2B	NA	NA	NA

Appendix 7: Summary of marker specificity in various experiments

Table A7.1 Table of all genes highlighted as potential markers in this thesis. columns refer to specificity of markers in different experiments and analyses in different Chapters. A "✓" indicates specificity for a marker in its given condition(s) in the experiment/analysis, "X" is given for when the marker was not specific for the given condition and "-" for when the marker was not tested in the experiment/analysis. Markers that were specific in every analysis are given in red and markers specific in most analyses and untested in others were given in purple.

Gene	Subtype	Specific in MDM RNAseq/microarray dataset	Specific in THP-1 cells using PCR	Specific in THP-1 RNAseq dataset
CXCL9	M1	✓	✓	✓
CXCL10	M1	✓	✓	✓
IL6	M1	✓	✓	✓
TNFAIP6	M1	✓	✓	✓
GBP5	M1	✓	✓	✓
ANKRD22	M1	✓	✓	✓
STAT1	M1	✓	✓	✓
INHBA	M1	✓	✓	✓
TSC22D1	M1	✓	✓	✓
IRF1	M1	✓	✓	✓
SERPING1	M1/M2b	✓	✓	✓
TNFSF10	M1/M2b	✓	-	✓
ETV7	M1	✓	-	✓
NEURL3	M1	✓	-	✓
CD276	M1	✓	-	✓
ALOX15	M2a	✓	✓	✓
CD200R	M2a	✓	✓	✓
CCL26	M2a	✓	✓	✓
CCL23	M2a	✓	X	X
CCL17	M2a	✓	X	X
HOMER	M2a	✓	✓	X
F13A1	M2a	✓	X	X
CD206	M2a	✓	✓	X
AP2A2	M2a	✓	✓	✓
HAS3	M2a	✓	-	✓
LOX	M2a	✓	-	✓
CHN2	M2a	✓	-	✓
CD163	M2c	✓	X	X
CXCL13	M2c	✓	X	X
SEPP1	M2c	✓	X	X
ALOX5	M2c/M0	✓	-	✓
EPHB6	M2c/M0	✓	-	✓
VSIG4	M2c/M0	✓	-	✓
ABHD	TPP	✓	X	X
STAT4	TPP	✓	X	X
LAMP	TPP	✓	X	X
LMP2	TPP	✓	-	✓
CSF2	TPP	✓	-	✓

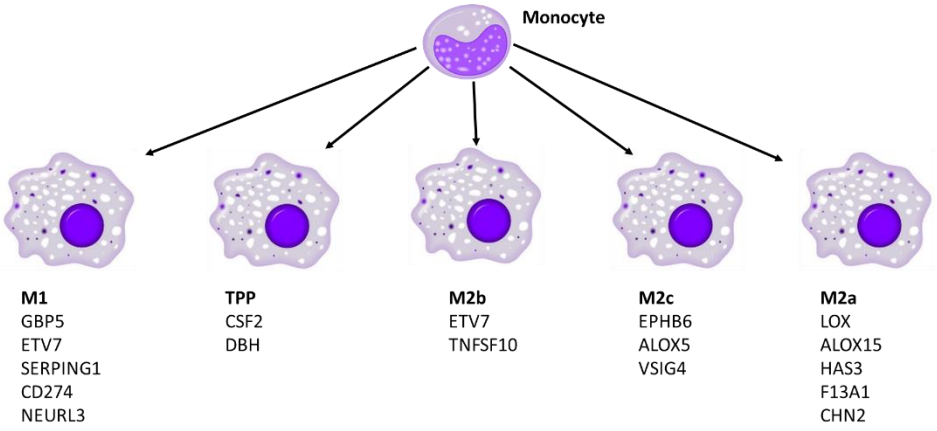

Figure A7.1: summary of macrophage polarisation states tested and markers identified

Bibliography

AALBERSE, R. C., VAN DER GAAG, R. & VAN LEEUWEN, J. 1983. Serologic aspects of IgG4 antibodies. I. Prolonged immunization results in an IgG4-restricted response. The Journal of Immunology, 130, 722-726.

ACKERMAN, M. E., CRISPIN, M., YU, X., BARUAH, K., BOESCH, A. W., HARVEY, D. J., DUGAST, A.-S., HEIZEN, E. L., ERCAN, A. & CHOI, I. 2013. Natural variation in Fc glycosylation of HIV-specific antibodies impacts antiviral activity. The Journal of clinical investigation, 123, 2183.

ADATI, N., HUANG, M.-C., SUZUKI, T., SUZUKI, H. & KOJIMA, T. 2009. High-resolution analysis of aberrant regions in autosomal chromosomes in human leukemia THP-1 cell line. BMC Research Notes, 2, 153-153.

AI, L., KIM, W.-J., DEMIRCAN, B., DYER, L. M., BRAY, K. J., SKEHAN, R. R., MASSOLL, N. A. & BROWN, K. D. 2008. The transglutaminase 2 gene (TGM2), a potential molecular marker for chemotherapeutic drug sensitivity, is epigenetically silenced in breast cancer. Carcinogenesis, 29, 510-518.

ALBRIGHT, A. V. & GONZÁLEZ-SCARANO, F. 2004. Microarray analysis of activated mixed glial (microglia) and monocyte-derived macrophage gene expression. Journal of Neuroimmunology, 157, 27-38.

ALDO, P. B., CRAVEIRO, V., GULLER, S. & MOR, G. 2013. Effect of culture conditions on the phenotype of THP-1 monocyte cell line. American journal of reproductive immunology (New York, N.Y. : 1989), 70, 80-86.

AMBARUS, C. A., SANTEGOETS, K. C. M., VAN BON, L., WENINK, M. H., TAK, P. P., RADSTAKE, T. R. D. J. & BAETEN, D. L. P. 2012. Soluble Immune Complexes Shift the TLR-Induced Cytokine Production of Distinct Polarized Human Macrophage Subsets towards IL-10. PLOS ONE, 7, e35994.

ANDERS, S. & HUBER, W. 2010. Differential expression analysis for sequence count data. Genome Biol, 11.

ANDERSON, C. F. & MOSSER, D. M. 2002. A novel phenotype for an activated macrophage: the type 2 activated macrophage. Journal of Leukocyte Biology, 72, 101-106.

ANDREWS, S. 2010. FastQC: a quality control tool for high throughput sequence data.

ANGELOTTI, F., PARMA, A., CAFARO, G., CAPECCHI, R., ALUNNO, A. & PUXEDDU, I. 2017. One year in review 2017: pathogenesis of rheumatoid arthritis. Clin Exp Rheumatol, 35, 368-378.

ANGIOLILLI, C., GRABIEC, A. M., FERGUSON, B. S., OSPELT, C., FERNANDEZ, B. M., VAN ES, I. E., VAN BAARSEN, L. G., GAY, S., MCKINSEY, T. A. & TAK, P. P. 2016. Inflammatory cytokines epigenetically regulate rheumatoid arthritis fibroblast-like synoviocyte activation by suppressing HDAC5 expression. Annals of the rheumatic diseases, 75, 430-438.

ANTHONY, R. M. & RAVETCH, J. V. 2010. A novel role for the IgG Fc glycan: the anti-inflammatory activity of sialylated IgG Fcs. Journal of clinical immunology, 30, 9-14.

ANTHONY, R. M., URBAN, J. F., ALEM, F., HAMED, H. A., ROZO, C. T., BOUCHER, J.-L., VAN ROOIJEN, N. & GAUSE, W. C. 2006. Memory T(H)2 cells induce alternatively activated macrophages to mediate protection against nematode parasites. Nature medicine, 12, 955-960.

ARANGO DUQUE, G. & DESCOTEAUX, A. 2014. Macrophage Cytokines: Involvement in Immunity and Infectious Diseases. Frontiers in Immunology, 5, 491.

ARNOLD, C. E., GORDON, P., BARKER, R. N. & WILSON, H. M. 2015. The activation status of human macrophages presenting antigen determines the efficiency of Th17 responses. Immunobiology, 220, 10-19.

ARNOLD, L., HENRY, A., PORON, F., BABA-AMER, Y., VAN ROOIJEN, N., PLONQUET, A., GHERARDI, R. K. & CHAZAUD, B. 2007. Inflammatory monocytes recruited after skeletal muscle injury switch into antiinflammatory macrophages to support myogenesis. Journal of Experimental Medicine, 204, 1057-1069.

ARUNACHALAM, L. T. 2014. Autoimmune correlation of rheumatoid arthritis and periodontitis. Journal of Indian Society of Periodontology, 18, 666.

AUFFRAY, C., FOGG, D., GARFA, M., ELAIN, G., JOIN-LAMBERT, O., KAYAL, S., SARNACKI, S., CUMANO, A., LAUVAU, G. & GEISSMANN, F. 2007. Monitoring of Blood Vessels and Tissues by a Population of Monocytes with Patrolling Behavior. Science, 317, 666-670.

AUWERX, J. 1991. The human leukemia cell line, THP-1: A multifacetted model for the study of monocyte-macrophage differentiation. Experientia, 47, 22-31.

AU-YEUNG, N., MANDHANA, R. & HORVATH, C. M. 2013. Transcriptional regulation by STAT1 and STAT2 in the interferon JAK-STAT pathway. JAK-STAT, 2, e23931.

BABU, S., KUMARASWAMI, V. & NUTMAN, T. B. 2009. Alternatively Activated and Immunoregulatory Monocytes in Human Filarial Infections. The Journal of infectious diseases, 199, 1827-1837.

BAETEN, D., DEMETTER, P., CUVELIER, C. A., KRUITHOF, E., VAN DAMME, N., DE VOS, M., VEYS, E. M. & DE KEYSER, F. 2002. Macrophages expressing the scavenger receptor CD163: a link between immune alterations of the gut and synovial inflammation in spondyloarthropathy. The Journal of pathology, 196, 343-350.

BAI, X., KINNEY, W. H., SU, W.-L., BAI, A., OVRUTSKY, A. R., HONDA, J. R., NETEA, M. G., HENAO-TAMAYO, M., ORDWAY, D. J., DINARELLO, C. A. & CHAN, E. D. 2015. Caspase-3-independent apoptotic pathways contribute to interleukin-32γ-mediated control of Mycobacterium tuberculosis infection in THP-1 cells. BMC Microbiology, 15, 39.

BAILLIE, J. K., ARNER, E., DAUB, C., DE HOON, M., ITOH, M., KAWAJI, H., LASSMANN, T., CARNINCI, P., FORREST, A. R. R., HAYASHIZAKI, Y., CONSORTIUM, F., FAULKNER, G. J., WELLS, C. A., REHLI, M., PAVLI, P., SUMMERS, K. M. & HUME, D. A. 2017. Analysis of the human monocyte-derived macrophage transcriptome and response to lipopolysaccharide provides new insights into genetic aetiology of inflammatory bowel disease. PLoS Genetics, 13, e1006641.

BAINTON, D. F., TAKEMURA, R., STENBERG, P. E. & WERB, Z. 1989. Rapid fragmentation and reorganization of Golgi membranes during frustrated phagocytosis

of immobile immune complexes by macrophages. The American journal of pathology, 134, 15.

BARRETT, D. J. & AYOUB, E. M. 1986. IgG2 subclass restriction of antibody to pneumococcal polysaccharides. Clinical and Experimental Immunology, 63, 127-134.

BARRIONUEVO, P., BEIGIER-BOMPADRE, M., FERNANDEZ, G., GOMEZ, S., ALVES-ROSA, M., PALERMO, M. & ISTURIZ, M. 2003. Immune complex–FcγR interaction modulates monocyte/macrophage molecules involved in inflammation and immune response. Clinical & Experimental Immunology, 133, 200-207.

BARROS, M. H. M., HAUCK, F., DREYER, J. H., KEMPKES, B. & NIEDOBITEK, G. 2013. Macrophage Polarisation: an Immunohistochemical Approach for Identifying M1 and M2 Macrophages. PLoS ONE, 8, e80908.

BARROW, A. D. & TROWSDALE, J. 2006. You say ITAM and I say ITIM, let's call the whole thing off: the ambiguity of immunoreceptor signalling. European journal of immunology, 36, 1646-1653.

BARTOSH, T. J. & YLOSTALO, J. H. 2014. Macrophage Inflammatory Assay. Bio-protocol, 4, e1180.

BAUMANN, I., KOLOWOS, W., VOLL, R. E., MANGER, B., GAIPL, U., NEUHUBER, W. L., KIRCHNER, T., KALDEN, J. R. & HERRMANN, M. 2002. Impaired uptake of apoptotic cells into tingible body macrophages in germinal centers of patients with systemic lupus erythematosus. Arthritis & Rheumatology, 46, 191-201.

BEN MKADDEM, S., HAYEM, G., JÖNSSON, F., ROSSATO, E., BOEDEC, E., BOUSSETTA, T., EL BENNA, J., LAUNAY, P., GOUJON, J.-M., BENHAMOU, M., BRUHNS, P. & MONTEIRO, R. C. 2014. Shifting FcγRIIA-ITAM from activation to inhibitory configuration ameliorates arthritis. The Journal of Clinical Investigation, 124, 3945-3959.

BENOIT, M., DESNUES, B. & MEGE, J.-L. 2008. Macrophage Polarization in Bacterial Infections. The Journal of Immunology, 181, 3733-3739.

BERIN, M. C. 2002. The role of TARC in the pathogenesis of allergic asthma. Drug News Perspect, 15, 10-16.

BEYER, M., MALLMANN, M. R., XUE, J., STARATSCHEK-JOX, A., VORHOLT, D., KREBS, W., SOMMER, D., SANDER, J., MERTENS, C. & NINO-CASTRO, A. 2012. High-resolution transcriptome of human macrophages. PloS one, 7, e45466.

BEZBRADICA, J. S., ROSENSTEIN, R. K., DEMARCO, R. A., BRODSKY, I. & MEDZHITOV, R. 2014. A role for the ITAM signaling module in specifying cytokine-receptor functions. Nature immunology, 15, 333-342.

BHATIA, A., BLADES, S., CAMBRIDGE, G. & EDWARDS, J. 1998. Differential distribution of FcgRIIIa in normal human tissues and co-localization with DAF and fibrillin-1: implications for immunological microenvironments. Immunology, 94, 56-63.

BHATIA, S., FEI, M., YARLAGADDA, M., QI, Z., AKIRA, S., SAIJO, S., IWAKURA, Y., VAN ROOIJEN, N., GIBSON, G. A., ST. CROIX, C. M., RAY, A. & RAY, P. 2011. Rapid Host Defense against Aspergillus fumigatus Involves Alveolar Macrophages with a Predominance of Alternatively Activated Phenotype. PLoS ONE, 6, e15943.

BILLADEAU, D. D. & LEIBSON, P. J. 2002. ITAMs versus ITIMs: striking a balance during cell regulation. The Journal of Clinical Investigation, 109, 161-168.

BISWAS, S. K. & MANTOVANI, A. 2010. Macrophage plasticity and interaction with lymphocyte subsets: cancer as a paradigm. Nature immunology, 11, 889-896.

BISWAS, S. K., SICA, A. & LEWIS, C. E. 2008. Plasticity of macrophage function during tumor progression: regulation by distinct molecular mechanisms. The Journal of Immunology, 180, 2011-2017.

BLASZCZYK, K., NOWICKA, H., KOSTYRKO, K., ANTONCZYK, A., WESOLY, J. & BLUYSSEN, H. A. R. 2016. The unique role of STAT2 in constitutive and IFN-induced transcription and antiviral responses. Cytokine & Growth Factor Reviews, 29, 71-81.

BOBRYSHEV, Y. V., IVANOVA, E. A., CHISTIAKOV, D. A., NIKIFOROV, N. G. & OREKHOV, A. N. 2016. Macrophages and their role in atherosclerosis: pathophysiology and transcriptome analysis. BioMed research international, 2016.

BOGDAN, C. 2001. Nitric oxide and the immune response. Nat Immunol, 2, 907-916.

BOLGER, A. M., LOHSE, M. & USADEL, B. 2014. Trimmomatic: a flexible trimmer for Illumina sequence data. Bioinformatics, 30.

BOLLAND, S. & RAVETCH, J. V. 2000. Spontaneous autoimmune disease in FcγRIIB-deficient mice results from strain-specific epistasis. Immunity, 13, 277-285.

BOSSHART, H. & HEINZELMANN, M. 2016. THP-1 cells as a model for human monocytes. Annals of Translational Medicine, 4, 438.

BOURNAZOS, S., WOOF, J. M., HART, S. P. & DRANSFIELD, I. 2009. Functional and clinical consequences of Fc receptor polymorphic and copy number variants. Clinical and Experimental Immunology, 157, 244-254.

BOYD, P. N., LINES, A. C. & PATEL, A. K. 1995. The effect of the removal of sialic acid, galactose and total carbohydrate on the functional activity of Campath-1H. Molecular Immunology, 32, 1311-1318.

BREEDVELD, F. C. & DAYER, J.-M. 2000. Leflunomide: mode of action in the treatment of rheumatoid arthritis. Annals of the Rheumatic Diseases, 59, 841-849.

BRUHNS, P., IANNASCOLI, B., ENGLAND, P., MANCARDI, D. A., FERNANDEZ, N., JORIEUX, S. & DAËRON, M. 2009. Specificity and affinity of human Fcγ receptors and their polymorphic variants for human IgG subclasses. Blood, 113, 3716-3725.

BRYAN, N., AHSWIN, H., SMART, N., BAYON, Y., WOHLERT, S. & HUNT, J. A. 2012. Reactive oxygen species (ROS)–a family of fate deciding molecules pivotal in constructive inflammation and wound healing. Eur Cell Mater, 24, e65.

BURN, G. L., SVENSSON, L., SANCHEZ-BLANCO, C., SAINI, M. & COPE, A. P. 2011. Why is PTPN22 a good candidate susceptibility gene for autoimmune disease? FEBS Letters, 585, 3689-3698.

BURTON, P. R., CLAYTON, D. G., CARDON, L. R., CRADDOCK, N., DELOUKAS, P., DUNCANSON, A., KWIATKOWSKI, D. P., MCCARTHY, M. I., OUWEHAND, W. H. & SAMANI, N. J. 2007. Genome-wide association study of 14,000 cases of seven common diseases and 3,000 shared controls. Nature, 447, 661-678.

BUTTERFIELD, T. A., BEST, T. M. & MERRICK, M. A. 2006. The Dual Roles of Neutrophils and Macrophages in Inflammation: A Critical Balance Between Tissue Damage and Repair. Journal of Athletic Training, 41, 457-465.

CANTAERT, T., DE RYCKE, L., BONGARTZ, T., MATTESON, E. L., TAK, P. P., NICHOLAS, A. P. & BAETEN, D. 2006. Citrullinated proteins in rheumatoid arthritis: crucial… but not sufficient! Arthritis & Rheumatology, 54, 3381-3389.

CARAS, L., TUCUREANU, C., LERESCU, L., PITICA, R., MELINCEANU, L., NEAGU, S. & SALAGEANU, A. 2011. Influence of tumor cell culture supernatants on macrophage functional polarization: in vitro models of macrophage-tumor environment interaction. Tumori, 97, 647.

CARLSON, M. 2016. KEGG. db: A set of annotation maps for KEGG. R package version 3.1. 2.

CARLSON, M. 2017. org.Hs.eg.db: Genome wide annotation for Human. R package version 3.5.0.

CASCAO, R., ROSARIO, H., SOUTO-CARNEIRO, M. & FONSECA, J. 2010. Neutrophils in rheumatoid arthritis: more than simple final effectors. Autoimmunity reviews, 9, 531-535.

CHALUPSKY, K. & CAI, H. 2005. Endothelial dihydrofolate reductase: critical for nitric oxide bioavailability and role in angiotensin II uncoupling of endothelial nitric oxide synthase. Proceedings of the National Academy of Sciences of the United States of America, 102, 9056-9061.

CHAN, G., BIVINS-SMITH, E. R., SMITH, M. S., SMITH, P. M. & YUROCHKO, A. D. 2008. Transcriptome Analysis Reveals Human Cytomegalovirus Reprograms Monocyte Differentiation Towards a M1 Macrophage. Journal of immunology (Baltimore, Md. : 1950), 181, 698-711.

CHANG, M. Y., TANINO, Y., VIDOVA, V., KINSELLA, M. G., CHAN, C. K., JOHNSON, P. Y., WIGHT, T. N. & FREVERT, C. W. 2014. A rapid increase in macrophage-derived versican and hyaluronan in infectious lung disease. Matrix biology : journal of the International Society for Matrix Biology, 35, 162-173.

CHANPUT, W., MES, J. J. & WICHERS, H. J. 2014. THP-1 cell line: An in vitro cell model for immune modulation approach. International Immunopharmacology, 23, 37-45.

CHANPUT, W., MES, J. J., SAVELKOUL, H. F. & WICHERS, H. J. 2013. Characterization of polarized THP-1 macrophages and polarizing ability of LPS and food compounds. Food & function, 4, 266-276.

CHANPUT, W., MES, J., VREEBURG, R. A., SAVELKOUL, H. F. & WICHERS, H. J. 2010. Transcription profiles of LPS-stimulated THP-1 monocytes and macrophages: a tool to study inflammation modulating effects of food-derived compounds. Food & function, 1, 254-261.

CHANPUT, W., PETERS, V. & WICHERS, H. 2015. THP-1 and U937 cells. The Impact of Food Bioactives on Health. Springer.

CHANPUT, W., REITSMA, M., KLEINJANS, L., MES, J. J., SAVELKOUL, H. F. & WICHERS, H. J. 2012. β-Glucans are involved in immune-modulation of THP-1 macrophages. Molecular nutrition & food research, 56, 822-833.

CHAUHAN, A. K., CHEN, C., MOORE, T. L. & DIPAOLO, R. J. 2015. Induced expression of FcγRIIIa (CD16a) on CD4+ T cells triggers generation of IFN-γhigh subset. Journal of Biological Chemistry, 290, 5127-5140.

CHAWLA, A., NGUYEN, K. D. & GOH, Y. P. S. 2011. Macrophage-mediated inflammation in metabolic disease. Nature Reviews. Immunology, 11, 738-749.

CHEN, E. A., SOUAIAIA, T., HERSTEIN, J. S., EVGRAFOV, O. V., SPITSYNA, V. N., REBOLINI, D. F. & KNOWLES, J. A. 2014. Effect of RNA integrity on uniquely mapped reads in RNA-Seq. BMC Research Notes, 7, 753.

CHEN, J., WRIGHT, K., DAVIS, J. M., JERALDO, P., MARIETTA, E. V., MURRAY, J., NELSON, H., MATTESON, E. L. & TANEJA, V. 2016. An expansion of rare lineage intestinal microbes characterizes rheumatoid arthritis. Genome medicine, 8, 43.

CHEN, M., LIN, W.-R., LU, C.-H., CHEN, C.-C., HUANG, Y.-C., LIAO, W.-L. & TSAI, F.-J. 2014. Chimerin 2 genetic polymorphisms are associated with non-proliferative diabetic retinopathy in Taiwanese type 2 diabetic patients. Journal of Diabetes and its Complications, 28, 460-463.

CHINETTI-GBAGUIDI, G. & STAELS, B. 2011. Macrophage polarization in metabolic disorders: functions and regulation. Current Opinion in Lipidology, 22, 365-372.

CHISTIAKOV, D. A., BOBRYSHEV, Y. V. & OREKHOV, A. N. 2015. Changes in transcriptome of macrophages in atherosclerosis. Journal of Cellular and Molecular Medicine, 19, 1163-1173.

CHIZZOLINI, C., REZZONICO, R., DE LUCA, C., BURGER, D. & DAYER, J.-M. 2000. Th2 cell membrane factors in association with IL-4 enhance matrix metalloproteinase-1 (MMP-1) while decreasing MMP-9 production by granulocyte-macrophage colony-stimulating factor-differentiated human monocytes. The Journal of Immunology, 164, 5952-5960.

CHOY, E. 2012. Understanding the dynamics: pathways involved in the pathogenesis of rheumatoid arthritis. Rheumatology, 51, v3-v11.

CHUANG, F. Y., SASSAROLI, M. & UNKELESS, J. C. 2000. Convergence of Fcγ receptor IIA and Fcγ receptor IIIB signaling pathways in human neutrophils. The Journal of Immunology, 164, 350-360.

CICCACCI, C., CONIGLIARO, P., PERRICONE, C., RUFINI, S., TRIGGIANESE, P., POLITI, C., NOVELLI, G., PERRICONE, R. & BORGIANI, P. 2016. Polymorphisms in STAT-4, IL-10, PSORS1C1, PTPN2 and MIR146A genes are associated differently with prognostic factors in Italian patients affected by rheumatoid arthritis. Clinical & Experimental Immunology, 186, 157-163.

CLARK, M. R., STUART, S. G., KIMBERLY, R. P., ORY, P. A. & GOLDSTEIN, I. M. 1991. A single amino acid distinguishes the high-responder from the low-responder form of Fc receptor II on human monocytes. European journal of immunology, 21, 1911-1916.

CLAVEL, C., NOGUEIRA, L., LAURENT, L., IOBAGIU, C., VINCENT, C., SEBBAG, M. & SERRE, G. 2008. Induction of macrophage secretion of tumor necrosis factor α through Fcγ receptor IIa engagement by rheumatoid arthritis–specific autoantibodies to citrullinated proteins complexed with fibrinogen. Arthritis & Rheumatology, 58, 678-688.

CLEMENTS, J. N. 2011. Treatment of rheumatoid arthritis: A review of recommendations and emerging therapy.

COHEN, S. B., DORE, R. K., LANE, N. E., ORY, P. A., PETERFY, C. G., SHARP, J. T., VAN DER HEIJDE, D., ZHOU, L., TSUJI, W. & NEWMARK, R. 2008. Denosumab treatment effects on structural damage, bone mineral density, and bone turnover in rheumatoid arthritis: A twelve-month, multicenter, randomized, double-blind, placebo-controlled, phase II clinical trial. Arthritis & Rheumatology, 58, 1299-1309.

COLLINS, S. J. 1987. The HL-60 promyelocytic leukemia cell line: proliferation, differentiation, and cellular oncogene expression. Blood, 70, 1233-1244.

CONESA, A., MADRIGAL, P., TARAZONA, S., GOMEZ-CABRERO, D., CERVERA, A., MCPHERSON, A., SZCZEŚNIAK, M. W., GAFFNEY, D. J., ELO, L. L., ZHANG, X. & MORTAZAVI, A. 2016. A survey of best practices for RNA-seq data analysis. Genome Biology, 17, 13.

COOPER, D. L., MARTIN, S. G., ROBINSON, J. I., MACKIE, S. L., CHARLES, C. J., NAM, J., ISAACS, J. D., EMERY, P. & MORGAN, A. W. 2012. FcγRIIIa expression on monocytes in rheumatoid arthritis: role in immune-complex stimulated TNF production and non-response to methotrexate therapy. PLoS One, 7, e28918.

CORONEL, A., BOYER, A., FRANSSEN, J. D., ROMET-LEMONNE, J. L., FRIDMAN, W. H. & TEILLAUD, J. L. 2001. Cytokine production and T-cell activation by macrophage–dendritic cells generated for therapeutic use. British journal of haematology, 114, 671-680.

COSTA, C., TRAVES, S. L., TUDHOPE, S. J., FENWICK, P. S., BELCHAMBER, K. B., RUSSELL, R. E., BARNES, P. J. & DONNELLY, L. E. 2016. Enhanced monocyte migration to CXCR3 and CCR5 chemokines in COPD. European Respiratory Journal, ERJ-01642-2015.

COZZOLI, D. K., COURSON, J., CARUANA, A. L., MILLER, B. W., GREENTREE, D. I., THOMPSON, A. B., WROTEN, M. G., ZHANG, P. W., XIAO, B. & HU, J. H. 2012. Nucleus Accumbens mGluR5-Associated Signaling Regulates Binge Alcohol Drinking Under Drinking-in-the-Dark Procedures. Alcoholism: Clinical and Experimental Research, 36, 1623-1633.

CROS, J., CAGNARD, N., WOOLLARD, K., PATEY, N., ZHANG, S.-Y., SENECHAL, B., PUEL, A., BISWAS, S. K., MOSHOUS, D., PICARD, C., JAIS, J.-P., D'CRUZ, D., CASANOVA, J.-L., TROUILLET, C. & GEISSMANN, F. 2010. Human CD14(dim) Monocytes Patrol and Sense Nucleic Acids and Viruses via TLR7 and TLR8 Receptors. Immunity, 33, 375-386.

CUNNINGHAME GRAHAM, D. S., MORRIS, D. L., BHANGALE, T. R., CRISWELL, L. A., SYVÄNEN, A.-C., RÖNNBLOM, L., BEHRENS, T. W., GRAHAM, R. R. & VYSE, T. J. 2011. Association of NCF2, IKZF1, IRF8, IFIH1, and TYK2 with Systemic Lupus Erythematosus. PLoS Genetics, 7, e1002341.

CUTOLO, M., SULLI, A., PIZZORNI, C., SERIOLO, B. & STRAUB, R. H. 2001. Anti-inflammatory mechanisms of methotrexate in rheumatoid arthritis. Annals of the Rheumatic Diseases, 60, 729.

DAHIA, P. L., AGUIAR, R. C., ALBERTA, J., KUM, J. B., CARON, S., SILL, H., MARSH, D. J., RITZ, J., FREEDMAN, A. & STILES, C. 1999. PTEN is inversely

correlated with the cell survival factor Akt/PKB and is inactivated via multiple mechanisms in haematological malignancies. Human molecular genetics, 8, 185-193.

DAI, M., THOMPSON, R. C., MAHER, C., CONTRERAS-GALINDO, R., KAPLAN, M. H., MARKOVITZ, D. M., OMENN, G. & MENG, F. 2010. NGSQC: cross-platform quality analysis pipeline for deep sequencing data. BMC genomics, 11, S7.

DAIGNEAULT, M., PRESTON, J. A., MARRIOTT, H. M., WHYTE, M. K. B. & DOCKRELL, D. H. 2010. The Identification of Markers of Macrophage Differentiation in PMA-Stimulated THP-1 Cells and Monocyte-Derived Macrophages. PLOS ONE, 5, e8668.

DANIELSSON, F., JAMES, T., GOMEZ-CABRERO, D. & HUSS, M. 2015. Assessing the consistency of public human tissue RNA-seq data sets. Briefings in Bioinformatics, 16, 941-949.

DAVID, S. & KRONER, A. 2011. Repertoire of microglial and macrophage responses after spinal cord injury. Nat Rev Neurosci, 12, 388-399.

DAVIS, M. J., TSANG, T. M., QIU, Y., DAYRIT, J. K., FREIJ, J. B., HUFFNAGLE, G. B. & OLSZEWSKI, M. A. 2013. Macrophage M1/M2 polarization dynamically adapts to changes in cytokine microenvironments in Cryptococcus neoformans infection. MBio, 4, e00264-13.

DE ALMEIDA, D. E., LING, S., PI, X., HARTMANN-SCRUGGS, A. M., PUMPENS, P. & HOLOSHITZ, J. 2010. IMMUNE DYSREGULATION BY THE RHEUMATOID ARTHRITIS SHARED EPITOPE. Journal of immunology (Baltimore, Md. : 1950), 185, 1927-1934.

DELGADO, M. D., GUTIÉRREZ, P., RICHARD, C., CUADRADO, M. A., MOREAU-GACHELIN, F. & LEÓN, J. 1998. Spi-1/PU. 1 proto-oncogene induces opposite effects on monocytic and erythroid differentiation of K562 cells. Biochemical and biophysical research communications, 252, 383-391.

DIAZ-GALLO, L.-M. & MARTIN, J. 2012. PTPN22 splice forms: a new role in rheumatoid arthritis. Genome Medicine, 4, 13-13.

DIDONATO, J. A., MERCURIO, F. & KARIN, M. 2012. NF-κB and the link between inflammation and cancer. Immunological reviews, 246, 379-400.

DING, S., LI, F., WANG, J., XU, K. & LI, L. 2008. Interferon gamma receptor 1 gene polymorphism in patients with tuberculosis in China. Scandinavian journal of immunology, 68, 140-144.

DING, Z., MIZERACKI, A. M., HU, C. & MEHTA, J. L. 2013. LOX-1 deletion and macrophage trafficking in atherosclerosis. Biochemical and Biophysical Research Communications, 440, 210-214.

DOBIN, A., DAVIS, C. A., SCHLESINGER, F., DRENKOW, J., ZALESKI, C. & JHA, S. 2013. STAR: ultrafast universal RNA-seq aligner. Bioinformatics, 29.

DONG, S., YING, S., KOJIMA, T., SHIRAIWA, M., KAWADA, A., MÉCHIN, M.-C., ADOUE, V., CHAVANAS, S., SERRE, G., SIMON, M. & TAKAHARA, H. 2008. Crucial Roles of MZF1 and Sp1 in the Transcriptional Regulation of the Peptidylarginine Deiminase Type I Gene (PADI1) in Human Keratinocytes. Journal of Investigative Dermatology, 128, 549-557.

DONLIN, L. T., JAYATILLEKE, A., GIANNOPOULOU, E. G., KALLIOLIAS, G. D. & IVASHKIV, L. B. 2014. Modulation of TNF-induced macrophage polarization by synovial fibroblasts. The Journal of Immunology, 193, 2373-2383.

DRAUDE, G., HRBOTICKY, N. & LORENZ, R. L. 1999. The expression of the lectin-like oxidized low-density lipoprotein receptor (LOX-1) on human vascular smooth muscle cells and monocytes and its down-regulation by lovastatin. Biochemical Pharmacology, 57, 383-386.

DUAN, J., LOU, J., ZHANG, Q., KE, J., QI, Y., SHEN, N., ZHU, B., ZHONG, R., WANG, Z., LIU, L., WU, J., WANG, W., GONG, F. & MIAO, X. 2014. A Genetic Variant rs1801274 in FCGR2A as a Potential Risk Marker for Kawasaki Disease: A Case-Control Study and Meta-Analysis. PLoS ONE, 9, e103329.

DYNAN, W. S., SAZER, S., TJIAN, R. & SCHIMKE, R. T. 1986. Transcription factor Sp1 recognizes a DNA sequence in the mouse dihydrofolate reductase promoter. Nature, 319, 246-248.

EDIN, S., WIKBERG, M. L., RUTEGÅRD, J., OLDENBORG, P.-A. & PALMQVIST, R. 2013. Phenotypic skewing of macrophages in vitro by secreted factors from colorectal cancer cells. PloS one, 8, e74982.

EDWARDS, J. P., ZHANG, X., FRAUWIRTH, K. A. & MOSSER, D. M. 2006. Biochemical and functional characterization of three activated macrophage populations. Journal of leukocyte biology, 80, 1298-1307.

EGESTEN, A., ELIASSON, M., JOHANSSON, H. M., OLIN, A. I., MÖRGELIN, M., MUELLER, A., PEASE, J. E., FRICK, I.-M. & BJÖRCK, L. 2007. The CXC Chemokine MIG/CXCL9 Is Important in Innate Immunity against Streptococcus pyogenes. The Journal of Infectious Diseases, 195, 684-693.

ENGSTRÖM, A., ERLANDSSON, A. N. N., DELBRO, D. & WIJKANDER, J. 2014. Conditioned media from macrophages of M1, but not M2 phenotype, inhibit the proliferation of the colon cancer cell lines HT-29 and CACO-2. International Journal of Oncology, 44, 385-392.

FENG, Y.-H., ZHU, Y.-N., LIU, J., REN, Y.-X., XU, J.-Y., YANG, Y.-F., LI, X.-Y. & ZOU, J.-P. 2004. Differential regulation of resveratrol on lipopolysacchride-stimulated human macrophages with or without IFN-γ pre-priming. International Immunopharmacology, 4, 713-720.

FERNANDES, MARIA J G., ROLLET-LABELLE, E., PARÉ, G., MAROIS, S., TREMBLAY, M.-L., TEILLAUD, J.-L. & NACCACHE, PAUL H. 2006. CD16b associates with high-density, detergent-resistant membranes in human neutrophils. Biochemical Journal, 393, 351-359.

FERRANTE, A., BEARD, L. J. & FELDMAN, R. G. 1990. IgG subclass distribution of antibodies to bacterial and viral antigens. The Pediatric infectious disease journal, 9, 516-524.

FERRANTE, C. J. & LEIBOVICH, S. J. 2012. Regulation of Macrophage Polarization and Wound Healing. Advances in Wound Care, 1, 10-16.

FIRESTEIN, G. S. 2003. Evolving concepts of rheumatoid arthritis. Nature, 423, 356-361.

FITZGERALD, K. A., MCWHIRTER, S. M., FAIA, K. L., ROWE, D. C., LATZ, E., GOLENBOCK, D. T., COYLE, A. J., LIAO, S.-M. & MANIATIS, T. 2003. IKK [straight epsilon] and TBK1 are essential components of the IRF3 signaling pathway. Nature immunology, 4, 491.

FLEETWOOD, A. J., DINH, H., COOK, A. D., HERTZOG, P. J. & HAMILTON, J. A. 2009. GM-CSF-and M-CSF-dependent macrophage phenotypes display differential dependence on type I interferon signaling. Journal of leukocyte biology, 86, 411-421.

FLEIT, H. B. & KOBASIUK, C. D. 1991. The human monocyte-like cell line THP-1 expresses Fc gamma RI and Fc gamma RII. Journal of leukocyte biology, 49, 556-565.

FRATERNALE, A., BRUNDU, S. & MAGNANI, M. 2015. Polarization and repolarization of macrophages. J Clin Cell Immunol, 6, 2.

FRIEDLAND, J. S., SHATTOCK, R. J. & GRIFFIN, G. E. 1993. Phagocytosis of Mycobacterium tuberculosis or particulate stimuli by human monocytic cells induces equivalent monocyte chemotactic protein-1 gene expression. Cytokine, 5, 150-156.

FUJIWARA, Y., HIZUKURI, Y., YAMASHIRO, K., MAKITA, N., OHNISHI, K., TAKEYA, M., KOMOHARA, Y. & HAYASHI, Y. 2016. Guanylate-binding protein 5 is a marker of interferon-γ-induced classically activated macrophages. Clinical & translational immunology, 5, e111.

GALLEGO ROMERO, I., PAI, A. A., TUNG, J. & GILAD, Y. 2014. RNA-seq: impact of RNA degradation on transcript quantification. BMC Biology, 12, 42.

GALON, J., GAUCHAT, J.-F., MAZIÈRES, N., SPAGNOLI, R., STORKUS, W., LÖTZE, M., BONNEFOY, J.-Y., FRIDMAN, W.-H. & SAUTES, C. 1996. Soluble Fcgamma receptor type III (FcgammaRIII, CD16) triggers cell activation through interaction with complement receptors. The Journal of Immunology, 157, 1184-1192.

GARBER, M., GRABHERR, M. G., GUTTMAN, M. & TRAPNELL, C. 2011. Computational methods for transcriptome annotation and quantification using RNA-seq. Nat Methods, 8.

GARRISON, A. R., RADOSHITZKY, S. R., KOTA, K. P., PEGORARO, G., RUTHEL, G., KUHN, J. H., ALTAMURA, L. A., KWILAS, S. A., BAVARI, S., HAUCKE, V. & SCHMALJOHN, C. S. 2013. Crimean–Congo hemorrhagic fever virus utilizes a clathrin- and early endosome-dependent entry pathway. Virology, 444, 45-54.

GEISSMANN, F., JUNG, S. & LITTMAN, D. R. 2003. Blood monocytes consist of two principal subsets with distinct migratory properties. Immunity, 19, 71-82.

GEISSMANN, F., MANZ, M. G., JUNG, S., SIEWEKE, M. H., MERAD, M. & LEY, K. 2010. Development of monocytes, macrophages and dendritic cells. Science (New York, N.Y.), 327, 656-661.

GENIN, M., CLEMENT, F., FATTACCIOLI, A., RAES, M. & MICHIELS, C. 2015. M1 and M2 macrophages derived from THP-1 cells differentially modulate the response of cancer cells to etoposide. BMC Cancer, 15, 577.

GERSTNER, C., DUBNOVITSKY, A., SANDIN, C., KOZHUKH, G., UCHTENHAGEN, H., JAMES, E. A., RÖNNELID, J., YTTERBERG, A. J., PIEPER, J. & REED, E. 2016. Functional and structural characterization of a novel hla-DrB1* 04: 01-restricted α-enolase T cell epitope in rheumatoid arthritis. Frontiers in immunology, 7.

GHAZIZADEH, S., BOLEN, J. & FLEIT, H. 1994. Physical and functional association of Src-related protein tyrosine kinases with Fc gamma RII in monocytic THP-1 cells. Journal of Biological Chemistry, 269, 8878-8884.

GIERUT, A., PERLMAN, H. & POPE, R. M. 2010. Innate immunity and rheumatoid arthritis. Rheumatic Disease Clinics of North America, 36, 271-296.

GORDAN, S., BIBURGER, M. & NIMMERJAHN, F. 2015. bIgG time for large eaters: monocytes and macrophages as effector and target cells of antibody-mediated immune activation and repression. Immunological reviews, 268, 52-65.

GORDON, S. B., IRVING, G. R., LAWSON, R. A., LEE, M. E. & READ, R. C. 2000. Intracellular Trafficking and Killing ofStreptococcus pneumoniae by Human Alveolar Macrophages Are Influenced by Opsonins. Infection and immunity, 68, 2286-2293.

GRATCHEV, A., GUILLOT, P., HAKIY, N., POLITZ, O., ORFANOS, C., SCHLEDZEWSKI, K. & GOERDT, S. 2001. Alternatively Activated Macrophages Differentially Express Fibronectin and Its Splice Variants and the Extracellular Matrix Protein βIG-H3. Scandinavian journal of immunology, 53, 386-392.

GREVERS, L. C., DE VRIES, T. J., EVERTS, V., VERBEEK, J. S., VAN DEN BERG, W. B. & VAN LENT, P. L. 2013. Immune complex-induced inhibition of osteoclastogenesis is mediated via activating but not inhibitory Fcγ receptors on myeloid precursor cells. Annals of the rheumatic diseases, 72, 278-285.

GUILLIAMS, M., BRUHNS, P., SAEYS, Y., HAMMAD, H. & LAMBRECHT, B. N. 2014. The function of Fc [gamma] receptors in dendritic cells and macrophages. Nature reviews. Immunology, 14, 94.

GÜNTHNER, R. & ANDERS, H.-J. 2013. Interferon-regulatory factors determine macrophage phenotype polarization. Mediators of inflammation, 2013.

GUO, S.-X., TAKI, T., OHNISHI, H., PIAO, H.-Y., TABUCHI, K., BESSHO, F., HANADA, R., YANAGISAWA, M. & HAYASHI, Y. 2000. Hypermethylation of p16 and p15 genes and RB protein expression in acute leukemia. Leuk Res, 24.

GUO, Y., SHENG, Q., LI, J., YE, F., SAMUELS, D. C. & SHYR, Y. 2013. Large Scale Comparison of Gene Expression Levels by Microarrays and RNAseq Using TCGA Data. PLOS ONE, 8, e71462.

HAHN, C. K., BERCHUCK, J. E., ROSS, K. N., KAKOZA, R. M., CLAUSER, K., SCHINZEL, A. C., ROSS, L., GALINSKY, I., DAVIS, T. N. & SILVER, S. J. 2009. Proteomic and genetic approaches identify Syk as an AML target. Cancer cell, 16, 281-294.

HAMILTON, T. A., ZHAO, C., PAVICIC, P. G. & DATTA, S. 2014. Myeloid Colony-Stimulating Factors as Regulators of Macrophage Polarization. Frontiers in Immunology, 5, 554.

HARDISON, J. L., WRIGHTSMAN, R. A., CARPENTER, P. M., LANE, T. E. & MANNING, J. E. 2006. The Chemokines CXCL9 and CXCL10 Promote a Protective Immune Response but Do Not Contribute to Cardiac Inflammation following Infection with Trypanosoma cruzi. Infection and Immunity, 74, 125-134.

HARGREAVES, C. E., ROSE-ZERILLI, M. J., MACHADO, L. R., IRIYAMA, C., HOLLOX, E. J., CRAGG, M. S. & STREFFORD, J. C. 2015. Fcγ receptors: genetic variation, function, and disease. Immunological reviews, 268, 6-24.

HARRE, U., GEORGESS, D., BANG, H., BOZEC, A., AXMANN, R., OSSIPOVA, E., JAKOBSSON, P.-J., BAUM, W., NIMMERJAHN, F. & SZARKA, E. 2012. Induction of osteoclastogenesis and bone loss by human autoantibodies against citrullinated vimentin. The Journal of clinical investigation, 122, 1791.

HE, J. Q., WIESMANN, C. & VAN LOOKEREN CAMPAGNE, M. 2008. A role of macrophage complement receptor CRIg in immune clearance and inflammation. Molecular immunology, 45, 4041-4047.

HECHT, C., SCHETT, G. & FINZEL, S. 2014. The impact of rheumatoid factor and ACPA on bone erosion in rheumatoid arthritis. Annals of the rheumatic diseases, annrheumdis-2014-206631.

HEIL, T., VOLKMANN, K., WATAHA, J. & LOCKWOOD, P. 2002. Human peripheral blood monocytes versus THP-1 monocytes for in vitro biocompatibility testing of dental material components. Journal of oral rehabilitation, 29, 401-407.

HINKS, A., BARTON, A., JOHN, S., BRUCE, I., HAWKINS, C., GRIFFITHS, C. E., DONN, R., THOMSON, W., SILMAN, A. & WORTHINGTON, J. 2005. Association between the PTPN22 gene and rheumatoid arthritis and juvenile idiopathic arthritis in a UK population: further support that PTPN22 is an autoimmunity gene. Arthritis & Rheumatology, 52, 1694-1699.

HIRAKATA, M., TOZAWA, R., IMURA, Y. & SUGIYAMA, Y. 2004. Comparison of the effects of pioglitazone and rosiglitazone on macrophage foam cell formation. Biochemical and Biophysical Research Communications, 323, 782-788.

HIRSCH, I., JANOVEC, V., STRANSKA, R. & BENDRISS-VERMARE, N. 2017. Cross Talk between Inhibitory Immunoreceptor Tyrosine-Based Activation Motif-Signaling and Toll-Like Receptor Pathways in Macrophages and Dendritic Cells. Frontiers in Immunology, 8, 394.

HISCOCK, D., CATERSON, B. & FLANNERY, C. 2000. Expression of hyaluronan synthases in articular cartilage. Osteoarthritis and cartilage, 8, 120-126.

HOGARTH, P. M. & PIETERSZ, G. A. 2012. Fc receptor-targeted therapies for the treatment of inflammation, cancer and beyond. Nature reviews Drug discovery, 11, 311-331.

HOLLOX, E. J., DETERING, J.-C. & DEHNUGARA, T. 2009. An integrated approach for measuring copy number variation at the FCGR3 (CD16) locus. Human mutation, 30, 477-484.

HOLOSHITZ, J. 2013. The Quest for Better Understanding of HLA-Disease Association: Scenes from a Road Less Travelled By. Discovery medicine, 16, 93-101.

HÖMIG-HÖLZEL, C., VAN DOORN, R., VOGEL, C., GERMANN, M., CECCHINI, M. G., VERDEGAAL, E. & PEEPER, D. S. 2011. Antagonistic TSC22D1 variants control BRAF E600-induced senescence. The EMBO journal, 30, 1753-1765.

HORIGUCHI, M., OTA, M. & RIFKIN, D. B. 2012. Matrix control of transforming growth factor-β function. Journal of Biochemistry, 152, 321-329.

HU, J. M., LIU, K., LIU, J. H., JIANG, X. L., WANG, X. L., CHEN, Y. Z., LI, S. G., ZOU, H., PANG, L. J., LIU, C. X., CUI, X. B., YANG, L., ZHAO, J., SHEN, X. H., JIANG, J. F., LIANG, W. H., YUAN, X. L. & LI, F. 2017. CD163 as a marker of M2 macrophage,

contribute to predict aggressiveness and prognosis of Kazakh esophageal squamous cell carcinoma. Oncotarget, 8, 21526-21538.

HU, Z. D., WEI, T. T., TANG, Q. Q., MA, N., WANG, L. L., QIN, B. D., YIN, J. R., ZHOU, L. & ZHONG, R. Q. 2016. Gene expression profile of THP-1 cells treated with heat-killed Candida albicans. Ann Transl Med, 4.

HUANG, R., JARITZ, M., GUENZL, P., VLATKOVIC, I., SOMMER, A., TAMIR, I. M., MARKS, H., KLAMPFL, T., KRALOVICS, R., STUNNENBERG, H. G., BARLOW, D. P. & PAULER, F. M. 2011. An RNA-Seq Strategy to Detect the Complete Coding and Non-Coding Transcriptome Including Full-Length Imprinted Macro ncRNAs. PLoS ONE, 6, e27288.

HUMPHREYS, J. H., VAN NIES, J. A., CHIPPING, J., MARSHALL, T., VAN DER HELM-VAN, A. H., SYMMONS, D. P. & VERSTAPPEN, S. M. 2014. Rheumatoid factor and anti-citrullinated protein antibody positivity, but not level, are associated with increased mortality in patients with rheumatoid arthritis: results from two large independent cohorts. Arthritis research & therapy, 16, 483.

IGNATIUS IRUDAYAM, J., CONTRERAS, D., SPURKA, L., SUBRAMANIAN, A., ALLEN, J., REN, S., KANAGAVEL, V., NGUYEN, Q., RAMAIAH, A., RAMAMOORTHY, K., FRENCH, S. W., KLEIN, A. S., FUNARI, V. & ARUMUGASWAMI, V. 2015. Characterization of type I interferon pathway during hepatic differentiation of human pluripotent stem cells and hepatitis C virus infection. Stem Cell Research, 15, 354-364.

IKUTA, K., WAGURI-NAGAYA, Y., KIKUCHI, K., YAMAGAMI, T., NOZAKI, M., AOYAMA, M., ASAI, K. & OTSUKA, T. 2012. The Sp1 transcription factor is essential for the expression of gliostatin/thymidine phosphorylase in rheumatoid fibroblast-like synoviocytes. Arthritis Research & Therapy, 14, R87-R87.

INFANTINO, V., CONVERTINI, P., CUCCI, L., PANARO, M. A., DI NOIA, M. A., CALVELLO, R., PALMIERI, F. & IACOBAZZI, V. 2011. The mitochondrial citrate carrier: a new player in inflammation. Biochemical Journal, 438, 433-436.

IRANI, V., GUY, A. J., ANDREW, D., BEESON, J. G., RAMSLAND, P. A. & RICHARDS, J. S. 2015. Molecular properties of human IgG subclasses and their implications for designing therapeutic monoclonal antibodies against infectious diseases. Molecular Immunology, 67, 171-182.

IVASHKIV, L. B. & DONLIN, L. T. 2014. Regulation of type I interferon responses. Nature reviews. Immunology, 14, 36-49.

IVASHKIV, L. B. 2011. Inflammatory signaling in macrophages: transitions from acute to tolerant and alternative activation states. European journal of immunology, 41, 2477-2481.

JAGUIN, M., HOULBERT, N., FARDEL, O. & LECUREUR, V. 2013. Polarization profiles of human M-CSF-generated macrophages and comparison of M1-markers in classically activated macrophages from GM-CSF and M-CSF origin. Cellular Immunology, 281, 51-61.

JANCAR, S. & CRESPO, M. S. 2005. Immune complex-mediated tissue injury: a multistep paradigm. Trends in immunology, 26, 48-55.

JARVIS, J. N., XU, C., WANG, W., PETTY, H. R., GONZALEZ, M., MORSSY, N., WAXMAN, F. & QUINTERO DEL RIO, A. 1999. Immune Complex Size and Complement Regulate Cytokine Production by Peripheral Blood Mononuclear Cells. Clinical Immunology, 93, 274-282.

JEFFERIES, W. M. 1991. Cortisol and immunity. Medical Hypotheses, 34, 198-208.

JETTEN, N., ROUMANS, N., GIJBELS, M. J., ROMANO, A., POST, M. J., DE WINTHER, M. P. J., VAN DER HULST, R. R. W. J. & XANTHOULEA, S. 2014. Wound Administration of M2-Polarized Macrophages Does Not Improve Murine Cutaneous Healing Responses. PLoS ONE, 9, e102994.

JIANG, G., ESPESETH, A., HAZUDA, D. J. & MARGOLIS, D. M. 2007. c-Myc and Sp1 Contribute to Proviral Latency by Recruiting Histone Deacetylase 1 to the Human Immunodeficiency Virus Type 1 Promoter. Journal of Virology, 81, 10914-10923.

JIANG, M.-X., HONG, X., LIAO, B.-B., SHI, S.-Z., LAI, X.-F., ZHENG, H.-Y., XIE, L., WANG, Y., WANG, X.-L. & XIN, H.-B. 2017. Expression profiling of TRIM protein family in THP1-derived macrophages following TLR stimulation. Scientific Reports, 7.

JIANG, Q., LI, X., CHENG, S., GU, Y., CHEN, G., SHEN, Y., XIE, Y. & CAO, Y. 2016. Combined effects of low levels of palmitate on toxicity of ZnO nanoparticles to THP-1 macrophages. Environmental toxicology and pharmacology, 48, 103-109.

JIANG, Q., LI, X., CHENG, S., GU, Y., CHEN, G., SHEN, Y., XIE, Y. & CAO, Y. 2016a. Combined effects of low levels of palmitate on toxicity of ZnO nanoparticles to THP-1 macrophages. Environmental toxicology and pharmacology, 48, 103-109.

JIANG, X., ASKLING, J., SAEVARSDOTTIR, S., PADYUKOV, L., ALFREDSSON, L., VIATTE, S. & FRISELL, T. 2016b. A genetic risk score composed of rheumatoid arthritis risk alleles, HLA-DRB1 haplotypes, and response to TNFi therapy–results from a Swedish cohort study. Arthritis research & therapy, 18, 288.

JIANG, X., KÄLLBERG, H., CHEN, Z., ÄRLESTIG, L., RANTAPÄÄ-DAHLQVIST, S., DAVILA, S., KLARESKOG, L., PADYUKOV, L. & ALFREDSSON, L. 2016c. An Immunochip-based interaction study of contrasting interaction effects with smoking in ACPA-positive versus ACPA-negative rheumatoid arthritis. Rheumatology, 55, 149-155.

JIANG, Z. & ZHU, L. 2016. Update on the role of alternatively activated macrophages in asthma. Journal of Asthma and Allergy, 9, 101-107.

JIN, L., ZUO, X.-Y., SU, W.-Y., ZHAO, X.-L., YUAN, M.-Q., HAN, L.-Z., ZHAO, X., CHEN, Y.-D. & RAO, S.-Q. 2014. Pathway-based Analysis Tools for Complex Diseases: A Review. Genomics, Proteomics & Bioinformatics, 12, 210-220.

JOHNSON, W. E., RABINOVIC, A. & LI, C. 2007. Adjusting batch effects in microarray expression data using Empirical Bayes methods. Biostatistics, 8.

JOSHI, S., SINGH, A. R., ZULCIC, M., BAO, L., MESSER, K., IDEKER, T., DUTKOWSKI, J. & DURDEN, D. L. 2014. Rac2 controls tumor growth, metastasis and M1-M2 macrophage differentiation in vivo. PloS one, 9, e95893.

JUNGI, T. W. & HAFNER, S. 1986. Quantitative assessment of Fc receptor expression and function during in vitro differentiation of human monocytes to macrophages. Immunology, 58, 131-137.

KADL, A., MEHER, A. K., SHARMA, P. R., LEE, M. Y., DORAN, A. C., JOHNSTONE, S. R., ELLIOTT, M. R., GRUBER, F., HAN, J. & CHEN, W. 2010. Identification of a Novel Macrophage Phenotype That Develops in Response to Atherogenic Phospholipids via Nrf2Novelty and Significance. Circulation research, 107, 737-746.

KAMPHUIS, S., KUIS, W., DE JAGER, W., TEKLENBURG, G., MASSA, M., GORDON, G., BOERHOF, M., RIJKERS, G. T., UITERWAAL, C. S. & OTTEN, H. G. 2005. Tolerogenic immune responses to novel T-cell epitopes from heat-shock protein 60 in juvenile idiopathic arthritis. The Lancet, 366, 50-56.

KAROLCHIK, D., HINRICHS, A. S., FUREY, T. S., ROSKIN, K. M., SUGNET, C. W., HAUSSLER, D. & KENT, W. J. 2004. The UCSC Table Browser data retrieval tool. Nucleic acids research, 32, D493-D496.

KARPOVA, A. Y., TROST, M., MURRAY, J. M., CANTLEY, L. C. & HOWLEY, P. M. 2002. Interferon regulatory factor-3 is an in vivo target of DNA-PK. Proceedings of the National Academy of Sciences of the United States of America, 99, 2818-2823.

KAVAI, M. & SZEGEDI, G. 2007. Immune complex clearance by monocytes and macrophages in systemic lupus erythematosus. Autoimmunity reviews, 6, 497-502.

KAWAI, T. & AKIRA, S. 2010. The role of pattern-recognition receptors in innate immunity: update on Toll-like receptors. Nature immunology, 11, 373-384.

KAWANAKA, N., YAMAMURA, M., AITA, T., MORITA, Y., OKAMOTO, A., KAWASHIMA, M., IWAHASHI, M., UENO, A., OHMOTO, Y. & MAKINO, H. 2002. CD14+, CD16+ blood monocytes and joint inflammation in rheumatoid arthritis. Arthritis & Rheumatology, 46, 2578-2586.

KELLY, B. & O'NEILL, L. A. J. 2015. Metabolic reprogramming in macrophages and dendritic cells in innate immunity. Cell Research, 25, 771-784.

KENNEDY, A., FEARON, U., VEALE, D. J. & GODSON, C. 2011. Macrophages in synovial inflammation. Frontiers in immunology, 2.

KEUSCH, J., LEVY, Y., SHOENFELD, Y. & YOUINOU, P. 1996. Analysis of different glycosylation states in IgG subclasses. Clinica Chimica Acta, 252, 147-158.

KIBE, T., FUJIMOTO, S., ISHIDA, C., TOGARI, H., WADA, Y., OKADA, S., NAKAGAWA, H., TSUKAMOTO, Y. & TAKAHASHI, N. 1996. Glycosylation and placental transport of immunoglobulin G. Journal of clinical biochemistry and nutrition, 21, 57-63.

KINNE, R. W., STUHLMÜLLER, B. & BURMESTER, G.-R. 2007. Cells of the synovium in rheumatoid arthritis. Macrophages. Arthritis Research & Therapy, 9, 224-224.

KITTAN, N. A., ALLEN, R. M., DHALIWAL, A., CAVASSANI, K. A., SCHALLER, M., GALLAGHER, K. A., CARSON IV, W. F., MUKHERJEE, S., GREMBECKA, J. & CIERPICKI, T. 2013. Cytokine induced phenotypic and epigenetic signatures are key to establishing specific macrophage phenotypes. PloS one, 8, e78045.

KLARESKOG, L., CATRINA, A. I. & PAGET, S. 2009. Rheumatoid arthritis. The Lancet, 373, 659-672.

KLARESKOG, L., MALMSTRÖM, V., LUNDBERG, K., PADYUKOV, L. & ALFREDSSON, L. 2011. Smoking, citrullination and genetic variability in the immunopathogenesis of rheumatoid arthritis. Seminars in Immunology, 23, 92-98.

KLEINAU, S. 2003. The impact of Fc receptors on the development of autoimmune diseases. Current pharmaceutical design, 9, 1861-1870.

KOBAYASHI, M., JESCHKE, M. G., SHIGEMATSU, K., ASAI, A., YOSHIDA, S., HERNDON, D. N. & SUZUKI, F. 2010. M2b monocytes predominated in peripheral blood of severely burned patients. The Journal of Immunology, 185, 7174-7179.

KOEFFLER, H. P. 1986. Human acute myeloid leukemia lines: models of leukemogenesis. Semin Hematol, 23.

KOH, T. J. & DIPIETRO, L. A. 2011. Inflammation and wound healing: The role of the macrophage. Expert reviews in molecular medicine, 13, e23-e23.

KOHRO, T., TANAKA, T., MURAKAMI, T., WADA, Y., ABURATANI, H., HAMAKUBO, T. & KODAMA, T. 2004. A comparison of differences in the gene expression profiles of phorbol 12-myristate 13-acetate differentiated THP-1 cells and human monocyte-derived macrophage. Journal of atherosclerosis and thrombosis, 11, 88-97.

KÖLLER, M., ZWÖLFER, B., STEINER, G., SMOLEN, J. S. & SCHEINECKER, C. 2004. Phenotypic and functional deficiencies of monocyte-derived dendritic cells in systemic lupus erythematosus (SLE) patients. International Immunology, 16, 1595-1604.

KONDA MOHAN, V., GANESAN, N., GOPALAKRISHNAN, R. & VENKATESAN, V. 2016. HLA-DRB1 shared epitope alleles in patients with rheumatoid arthritis: relation to autoantibodies and disease severity in a south Indian population. International journal of rheumatic diseases.

KONG, X. & GAO, J. 2017. Macrophage polarization: a key event in the secondary phase of acute spinal cord injury. Journal of cellular and molecular medicine, 21, 941-954.

KORNS, D., FRASCH, S. C., FERNANDEZ-BOYANAPALLI, R., HENSON, P. M. & BRATTON, D. L. 2011. Modulation of Macrophage Efferocytosis in Inflammation. Frontiers in Immunology, 2, 57.

KOZIEL, J., MYDEL, P. & POTEMPA, J. 2014. The link between periodontal disease and rheumatoid arthritis: an updated review. Current rheumatology reports, 16, 408.

KRAUSGRUBER, T., BLAZEK, K., SMALLIE, T., ALZABIN, S., LOCKSTONE, H., SAHGAL, N., HUSSELL, T., FELDMANN, M. & UDALOVA, I. A. 2011. IRF5 promotes inflammatory macrophage polarization and TH1-TH17 responses. Nature immunology, 12, 231-238.

KUKURBA, K. R. & MONTGOMERY, S. B. 2015. RNA Sequencing and Analysis. Cold Spring Harbor protocols, 2015, 951-969.

KUMAR, V., PATEL, S., TCYGANOV, E. & GABRILOVICH, D. I. 2016. The nature of myeloid-derived suppressor cells in the tumor microenvironment. Trends in immunology, 37, 208-220.

KUROSAKI, T. & RAVETCH, J. V. 1989. A single amino acid in the glycosyl phosphatidylinositol attachment domain determines the membrane topology of FcγRIII. Nature, 342, 805-807.

KUTOK, J.L., Yang, X., Folkerth, R. and Adra, C.N., 2011. Characterization of the expression of HTm4 (MS4A3), a cell cycle regulator, in human peripheral blood cells

and normal and malignant tissues. *Journal of cellular and molecular medicine*, *15*(1), pp.86-93.

KWISSA, M., NAKAYA, HELDER I., ONLAMOON, N., WRAMMERT, J., VILLINGER, F., PERNG, GUEY C., YOKSAN, S., PATTANAPANYASAT, K., CHOKEPHAIBULKIT, K., AHMED, R. & PULENDRAN, B. 2014. Dengue Virus Infection Induces Expansion of a CD14+CD16+ Monocyte Population that Stimulates Plasmablast Differentiation. Cell Host & Microbe, 16, 115-127.

KWON, H. J., KIM, S. N., KIM, Y. A. & LEE, Y. H. 2016. The contribution of arachidonate 15-lipoxygenase in tissue macrophages to adipose tissue remodeling. Cell Death Dis, 7, e2285.

LABORDE, E. A., VANZULLI, S., BEIGIER-BOMPADRE, M., ISTURIZ, M. A., RUGGIERO, R. A., FOURCADE, M. G., CATALAN PELLET, A. C., SOZZANI, S. & VULCANO, M. 2007. Immune Complexes Inhibit Differentiation, Maturation, and Function of Human Monocyte-Derived Dendritic Cells. The Journal of Immunology, 179, 673-681.

LABROUSSE, A. M., MEUNIER, E., RECORD, J., LABERNADIE, A., BEDUER, A., VIEU, C., BEN SAFTA, T. & MARIDONNEAU-PARINI, I. 2011. Frustrated Phagocytosis on Micro-Patterned Immune Complexes to Characterize Lysosome Movements in Live Macrophages. Frontiers in Immunology, 2, 51.

LAM, R. S., O'BRIEN-SIMPSON, N. M., HOLDEN, J. A., LENZO, J. C., FONG, S. B. & REYNOLDS, E. C. 2016. Unprimed, M1 and M2 Macrophages Differentially Interact with Porphyromonas gingivalis. PLoS ONE, 11, e0158629.

LANGMEAD, B. & SALZBERG, S. L. 2012. Fast gapped-read alignment with Bowtie 2. Nat Methods, 9.

LARIA, A., LURATI, A., MARRAZZA, M., MAZZOCCHI, D., RE, K. A. & SCARPELLINI, M. 2016a. The macrophages in rheumatic diseases. Journal of inflammation research, 9, 1.

LARIA, A., LURATI, A., MARRAZZA, M., MAZZOCCHI, D., RE, K. A. & SCARPELLINI, M. 2016b. The macrophages in rheumatic diseases. Journal of Inflammation Research, 9, 1-11.

LATHROP, S. K., BINDER, K. A., STARR, T., COOPER, K. G., CHONG, A., CARMODY, A. B. & STEELE-MORTIMER, O. 2015. Replication of Salmonella enterica serovar Typhimurium in human monocyte-derived macrophages. Infection and immunity, 83, 2661-2671.

LAURENT, L., CLAVEL, C., LEMAIRE, O., ANQUETIL, F., CORNILLET, M., ZABRANIECKI, L., NOGUEIRA, L., FOURNIÉ, B., SERRE, G. & SEBBAG, M. 2011. Fcγ receptor profile of monocytes and macrophages from rheumatoid arthritis patients and their response to immune complexes formed with autoantibodies to citrullinated proteins. Annals of the rheumatic diseases, 70, 1052-1059.

LAUZON-JOSET, J., MARSOLAIS, D., LANGLOIS, A. & BISSONNETTE, E. 2014. Dysregulation of alveolar macrophages unleashes dendritic cell–mediated mechanisms of allergic airway inflammation. Mucosal immunology, 7, 155-164.

LEBRE, M. C. & TAK, P. P. 2010. Macrophage subsets in immune-mediated inflammatory disease: Lessons from rheumatoid arthritis, spondyloarthritis, osteoarthitis, behçet's disease and gout. The Open Arthritis Journal, 3.

LEE, Y. & BAE, S. 2016. Intercellular adhesion molecule-1 polymorphisms, K469E and G261R and susceptibility to vasculitis and rheumatoid arthritis: a meta-analysis. Cellular and molecular biology (Noisy-le-Grand, France), 62, 84-90.

LEE, Y. G., JEONG, J. J., NYENHUIS, S., BERDYSHEV, E., CHUNG, S., RANJAN, R., KARPURAPU, M., DENG, J., QIAN, F., KELLY, E. A. B., JARJOUR, N. N., ACKERMAN, S. J., NATARAJAN, V., CHRISTMAN, J. W. & PARK, G. Y. 2015. Recruited Alveolar Macrophages, in Response to Airway Epithelial–Derived Monocyte Chemoattractant Protein 1/CCL2, Regulate Airway Inflammation and Remodeling in Allergic Asthma. American Journal of Respiratory Cell and Molecular Biology, 52, 772-784.

LEE, Y. H., JI, J. D. & SONG, G. G. 2008. Associations between FCGR3A polymorphisms and susceptibility to rheumatoid arthritis: a metaanalysis. The Journal of rheumatology, 35, 2129-2135.

LEEK, J. T., TAUB, M. A. & RASGON, J. L. 2012. A statistical approach to selecting and confirming validation targets in -omics experiments. BMC Bioinformatics, 13.

LI, G., CUNIN, P., WU, D., DIOGO, D., YANG, Y., OKADA, Y., PLENGE, R. M. & NIGROVIC, P. A. 2016. The rheumatoid arthritis risk variant CCR6DNP regulates CCR6 via PARP-1. PLoS genetics, 12, e1006292.

LI, H. & DURBIN, R. 2009. Fast and accurate short read alignment with Burrows-Wheeler transform. Bioinformatics, 25.

LI, H., HANDSAKER, B., WYSOKER, A., FENNELL, T., RUAN, J., HOMER, N., MARTH, G., ABECASIS, G., DURBIN, R. & GENOME PROJECT DATA PROCESSING, S. 2009. The Sequence Alignment/Map format and SAMtools. Bioinformatics, 25, 2078-2079.

LI, P., SCHWARZ, E. M., O'KEEFE, R. J., MA, L., BOYCE, B. F. & XING, L. 2004. RANK Signaling Is Not Required for TNFα-Mediated Increase in CD11bhi Osteoclast Precursors but Is Essential for Mature Osteoclast Formation in TNFα-Mediated Inflammatory Arthritis. Journal of Bone and Mineral Research, 19, 207-213.

LI, X., NAIR, A., WANG, S. & WANG, L. 2015. Quality control of RNA-seq experiments. RNA Bioinformatics, 137-146.

LI, X., WU, J., PTACEK, T., REDDEN, D. T., BROWN, E. E., ALARCÓN, G. S., RAMSEY-GOLDMAN, R., PETRI, M. A., REVEILLE, J. D., KASLOW, R. A., KIMBERLY, R. P. & EDBERG, J. C. 2013. Allelic Dependent Expression of an Activating Fc receptor on B cells Enhances Humoral Immune Responses. Science translational medicine, 5, 216ra175-216ra175.

LIAO, X., SHARMA, N., KAPADIA, F., ZHOU, G., LU, Y., HONG, H., PARUCHURI, K., MAHABELESHWAR, G. H., DALMAS, E., VENTECLEF, N., FLASK, C. A., KIM, J., DOREIAN, B. W., LU, K. Q., KAESTNER, K. H., HAMIK, A., CLÉMENT, K. & JAIN, M. K. 2011. Krüppel-like factor 4 regulates macrophage polarization. The Journal of Clinical Investigation, 121, 2736-2749.

LIAO, Y., SMYTH, G. K. & SHI, W. 2013. The Subread aligner: fast, accurate and scalable read mapping by seed-and-vote. Nucleic acids research, 41, e108-e108.

LIPSKY, P. & ISAKSON, P. 1997. Outcome of specific COX-2 inhibition in rheumatoid arthritis. The Journal of rheumatology. Supplement, 49, 9-14.

LIU, F. F., WU, X., ZHANG, Y., WANG, Y. & JIANG, F. 2014. TRAIL/DR5 Signaling Promotes Macrophage Foam Cell Formation by Modulating Scavenger Receptor Expression. PLOS ONE, 9, e87059.

LIU, Y.-C., ZOU, X.-B., CHAI, Y.-F. & YAO, Y.-M. 2014. Macrophage polarization in inflammatory diseases. International journal of biological sciences, 10, 520.

LIVAK, K. J., WILLS, Q. F., TIPPING, A. J., DATTA, K., MITTAL, R., GOLDSON, A. J., SEXTON, D. W. & HOLMES, C. C. 2013. Methods for qPCR gene expression profiling applied to 1440 lymphoblastoid single cells. Methods (San Diego, Calif.), 59, 71-79.

LONG, E. O. 2008. Negative signalling by inhibitory receptors: the NK cell paradigm. Immunological reviews, 224, 70-84.

LORENZ, M. H., JOACHIM R. KALDEN, HANNS-MARTIN 2001. The pathogenesis of autoimmune diseases. Scandinavian Journal of Clinical and Laboratory Investigation, 61, 16-26.

LOVE, M. I., ANDERS, S. & HUBER, W. 2017. Analyzing RNA-seq data with DESeq2. R package reference manual.

LUMENG, C. N., BODZIN, J. L. & SALTIEL, A. R. 2007. Obesity induces a phenotypic switch in adipose tissue macrophage polarization. Journal of Clinical Investigation, 117, 175-184.

LUMENG, C. N., BODZIN, J. L. & SALTIEL, A. R. 2007a. Obesity induces a phenotypic switch in adipose tissue macrophage polarization. Journal of Clinical Investigation, 117, 175-184.

LUMENG, C. N., DEYOUNG, S. M. & SALTIEL, A. R. 2007b. Macrophages block insulin action in adipocytes by altering expression of signaling and glucose transport proteins. American journal of physiology. Endocrinology and metabolism, 292, E166-E174.

LUND, M. E., TO, J., O'BRIEN, B. A. & DONNELLY, S. 2016. The choice of phorbol 12-myristate 13-acetate differentiation protocol influences the response of THP-1 macrophages to a pro-inflammatory stimulus. Journal of immunological methods, 430, 64-70.

LUO, Y., POLLARD, J.W. and CASADEVALL, A., 2010. Fcγ receptor cross-linking stimulates cell proliferation of macrophages via the ERK pathway. *Journal of Biological Chemistry*, *285*(6), pp.4232-4242.

LUX, A., YU, X., SCANLAN, C. N. & NIMMERJAHN, F. 2013. Impact of Immune Complex Size and Glycosylation on IgG Binding to Human FcγRs. The Journal of Immunology, 190, 4315-4323.

MACHADO, LEE R., HARDWICK, ROBERT J., BOWDREY, J., BOGLE, H., KNOWLES, TIMOTHY J., SIRONI, M. & HOLLOX, EDWARD J. 2012. Evolutionary History of Copy-Number-Variable Locus for the Low-Affinity Fcγ Receptor: Mutation Rate, Autoimmune Disease, and the Legacy of Helminth Infection. American Journal of Human Genetics, 90, 973-985.

MACKAY, C. R. 2008. Moving targets: cell migration inhibitors as new anti-inflammatory therapies. Nat Immunol, 9, 988-998.

MAERE, S., HEYMANS, K. & KUIPER, M. 2005. BiNGO: a Cytoscape plugin to assess overrepresentation of Gene Ontology categories in Biological Networks. Bioinformatics, 21, 3448-3449.

MAEß, M. B., SENDELBACH, S. & LORKOWSKI, S. 2010. Selection of reliable reference genes during THP-1 monocyte differentiation into macrophages. BMC Mol Biol, 11, 90.

MAEß, M. B., WITTIG, B., CIGNARELLA, A. & LORKOWSKI, S. 2014. Reduced PMA enhances the responsiveness of transfected THP-1 macrophages to polarizing stimuli. Journal of Immunological Methods, 402, 76-81.

MAGNUSSON, S. E., WENNERBERG, E., MATT, P., LINDQVIST, U. & KLEINAU, S. 2014. Dysregulated Fc receptor function in active rheumatoid arthritis. Immunology letters, 162, 200-206.

MAHDAVI, M., TAJIK, A. H., EBTEKAR, M., RAHIMI, R., ADIBZADEH, M. M., MOOZARMPOUR, H. R., BEIKVERDI, M. S., OLFAT, S., HASSAN, Z. M. & CHOOPANI, M. 2017. Granulocyte-macrophage colony-stimulating factor, a potent adjuvant for polarization to Th-17 pattern: an experience on HIV-1 vaccine model. Apmis, 125, 596-603.

MAIER, R., WISNIEWSKI, H. G., VILCEK, J. & LOTZ, M. 1996. TSG-6 expression in human articular chondrocytes: Possible implications in joint inflammation and cartilage degradation. Arthritis & Rheumatology, 39, 552-559.

MALHOTRA, R., WORMALD, M. R., RUDD, P. M., FISCHER, P. B., DWEK, R. A. & SIM, R. B. 1995. Glycosylation changes of IgG associated with rheumatooid arthritis can activate complement via the mannose-binding protein. Nature medicine, 1, 237-243.

MAN, S. M., KARKI, R., MALIREDDI, R. K. S., NEALE, G., VOGEL, P., YAMAMOTO, M., LAMKANFI, M. & KANNEGANTI, T.-D. 2015. The transcription factor IRF1 and guanylate-binding proteins target activation of the AIM2 inflammasome by Francisella infection. Nat Immunol, 16, 467-475.

MAO, Y., CHEN, L., WANG, F., ZHU, D., GE, X., HUA, D. & SUN, J. 2017. Cancer cell‐expressed B7‐H3 regulates the differentiation of tumor‐associated macrophages in human colorectal carcinoma. Oncology Letters, 14, 6177-6183.

MARTIN, M. 2011. Cutadapt removes adapter sequences from high-throughput sequencing reads. EMBnet. journal, 17, pp. 10-12.

MARTINEZ, F. O. & GORDON, S. 2014. The M1 and M2 paradigm of macrophage activation: time for reassessment. F1000Prime Reports, 6, 13.

MARTINEZ, F. O., GORDON, S., LOCATI, M. & MANTOVANI, A. 2006. Transcriptional Profiling of the Human Monocyte-to-Macrophage Differentiation and Polarization: New Molecules and Patterns of Gene Expression. The Journal of Immunology, 177, 7303-7311.

MATHIE, S. A., DIXON, K. L., WALKER, S. A., TYRRELL, V., MONDHE, M., O'DONNELL, V. B., GREGORY, L. G. & LLOYD, C. M. 2015b. Alveolar macrophages

are sentinels of murine pulmonary homeostasis following inhaled antigen challenge. Allergy, 70, 80-89.

MATHIE, S., DIXON, K., WALKER, S., TYRRELL, V., MONDHE, M., O'DONNELL, V. B., GREGORY, L. & LLOYD, C. 2015a. Alveolar macrophages are sentinels of murine pulmonary homeostasis following inhaled antigen challenge. Allergy, 70, 80-89.

MATSUMIYA, M., HARRIS, S. A., SATTI, I., STOCKDALE, L., TANNER, R., O'SHEA, M. K., TAMERIS, M., MAHOMED, H., HATHERILL, M., SCRIBA, T. J., HANEKOM, W. A., MCSHANE, H. & FLETCHER, H. A. 2014. Inflammatory and myeloid-associated gene expression before and one day after infant vaccination with MVA85A correlates with induction of a T cell response. BMC Infectious Diseases, 14, 314.

MCINNES , I. B. & SCHETT , G. 2011. The Pathogenesis of Rheumatoid Arthritis. New England Journal of Medicine, 365, 2205-2219.

MELLOR, J. D., BROWN, M. P., IRVING, H. R., ZALCBERG, J. R. & DOBROVIC, A. 2013. A critical review of the role of Fc gamma receptor polymorphisms in the response to monoclonal antibodies in cancer. Journal of Hematology & Oncology, 6, 1-1.

MENDONÇA, M. C., KOLES, N., DOI, S. Q. & SELLITTI, D. F. 2010. Transforming growth factor-β 1 regulation of C-type natriuretic peptide expression in human vascular smooth muscle cells: dependence on TSC22D1. American Journal of Physiology-Heart and Circulatory Physiology, 299, H2018-H2027.

MICHELUCCI, A., CORDES, T., GHELFI, J., PAILOT, A., REILING, N., GOLDMANN, O., BINZ, T., WEGNER, A., TALLAM, A., RAUSELL, A., BUTTINI, M., LINSTER, C. L., MEDINA, E., BALLING, R. & HILLER, K. 2013. Immune-responsive gene 1 protein links metabolism to immunity by catalyzing itaconic acid production. Proceedings of the National Academy of Sciences of the United States of America, 110, 7820-7825.

MILLS, C. 2012. M1 and M2 macrophages: oracles of health and disease. Critical Reviews™ in Immunology, 32.

MINAS, K. & LIVERSIDGE, J. 2006. Is The CD200/CD200 Receptor Interaction More Than Just a Myeloid Cell Inhibitory Signal? Critical reviews in immunology, 26, 213-230.

MITTAR, D., PARAMBAN, R. & MCINTYRE, C. 2011. Flow Cytometry and High-Content Imaging to Identify Markers of Monocyte-Macrophage Differentiation. BD Biosciences, August.

MOORE, K., SHEEDY, F. & FISHER, E. 2013. Macrophages in atherosclerosis: a dynamic balance. Nature reviews. Immunology, 13, 709-721.

MORGAN, A. W., BARRETT, J. H., GRIFFITHS, B., SUBRAMANIAN, D., ROBINSON, J. I., KEYTE, V. H., ALI, M., JONES, E. A., OLD, R. W. & PONCHEL, F. 2005. Analysis of Fcγ receptor haplotypes in rheumatoid arthritis: FCGR3A remains a major susceptibility gene at this locus, with an additional contribution from FCGR3B. Arthritis research & therapy, 8, R5.

MORGAN, A. W., BARRETT, J. H., GRIFFITHS, B., SUBRAMANIAN, D., ROBINSON, J. I., KEYTE, V. H., ALI, M., JONES, E. A., OLD, R. W., PONCHEL, F., BOYLSTON, A. W., SITUNAYAKE, R. D., MARKHAM, A. F., EMERY, P. & ISAACS, J. D. 2006. Analysis of Fcγ receptor haplotypes in rheumatoid arthritis: FCGR3A remains a major

susceptibility gene at this locus, with an additional contribution from FCGR3B. Arthritis Research & Therapy, 8, R5-R5.

MORTAZAVI, A., WILLIAMS, B. A., MCCUE, K., SCHAEFFER, L. & WOLD, B. 2008. Mapping and quantifying mammalian transcriptomes by RNA-Seq. Nat Methods, 5.

MOSSER, D. M. & EDWARDS, J. P. 2008. Exploring the full spectrum of macrophage activation. Nature reviews. Immunology, 8, 958-969.

MOUGEY, E., LANG, J. E., ALLAYEE, H., TEAGUE, W. G., DOZOR, A. J., WISE, R. A. & LIMA, J. J. 2013. ALOX5 Polymorphism Associates with Increased Leukotriene Production and Reduced Lung Function and Asthma Control in Children with Poorly Controlled Asthma. Clinical and experimental allergy : journal of the British Society for Allergy and Clinical Immunology, 43, 512-520.

MUELLER, D., GARCÍA-CUÉLLAR, M.-P., BACH, C., BUHL, S., MAETHNER, E. & SLANY, R. K. 2009. Misguided transcriptional elongation causes mixed lineage leukemia. PLoS biology, 7, e1000249.

MUELLER, M., BARROS, P., WITHERDEN, ABIGAIL S., ROBERTS, AMY L., ZHANG, Z., SCHASCHL, H., YU, C.-Y., HURLES, MATTHEW E., SCHAFFNER, C., FLOTO, R A., GAME, L., STEINBERG, KARYN M., WILSON, RICHARD K., GRAVES, TINA A., EICHLER, EVAN E., COOK, H T., VYSE, TIMOTHY J. & AITMAN, TIMOTHY J. 2013. Genomic Pathology of SLE-Associated Copy-Number Variation at the FCGR2C/FCGR3B/FCGR2B Locus. American Journal of Human Genetics, 92, 28-40.

MULHERIN, D., FITZGERALD, O. & BRESNIHAN, B. 1996. Synovial tissue macrophage populations and articular damage in rheumatoid arthritis. Arthritis & Rheumatology, 39, 115-124.

MUNDER, M., MOLLINEDO, F., CALAFAT, J., CANCHADO, J., GIL-LAMAIGNERE, C., FUENTES, J. M., LUCKNER, C., DOSCHKO, G., SOLER, G. & EICHMANN, K. 2005. Arginase I is constitutively expressed in human granulocytes and participates in fungicidal activity. Blood, 105, 2549-2556.

MURRAY, P. J. & WYNN, T. A. 2011. Obstacles and opportunities for understanding macrophage polarization. Journal of Leukocyte Biology, 89, 557-563.

MURRAY, P. J. & WYNN, T. A. 2011a. Obstacles and opportunities for understanding macrophage polarization. Journal of Leukocyte Biology, 89, 557-563.

MURRAY, P. J. & WYNN, T. A. 2011b. Protective and pathogenic functions of macrophage subsets. Nature reviews. Immunology, 11, 723-737.

MURRAY, P. J., ALLEN, J. E., BISWAS, S. K., FISHER, E. A., GILROY, D. W., GOERDT, S., GORDON, S., HAMILTON, J. A., IVASHKIV, L. B., LAWRENCE, T., LOCATI, M., MANTOVANI, A., MARTINEZ, F. O., MEGE, J.-L., MOSSER, D. M., NATOLI, G., SAEIJ, J. P., SCHULTZE, J. L., SHIREY, K. A., SICA, A., SUTTLES, J., UDALOVA, I., VAN GINDERACHTER, J. A., VOGEL, S. N. & WYNN, T. A. 2014. Macrophage activation and polarization: nomenclature and experimental guidelines. Immunity, 41, 14-20.

NAGALAKSHMI, U., WANG, Z., WAERN, K., SHOU, C., RAHA, D., GERSTEIN, M. & SNYDER, M. 2008. The Transcriptional Landscape of the Yeast Genome Defined by RNA Sequencing. Science (New York, N.Y.), 320, 1344-1349.

NAGASE, H. & MURPHY, G. 2013. Metalloproteinases in cartilage matrix breakdown: the roles in rheumatoid arthritis and osteoarthritis. Proteases: Structure and Function. Springer.

NAGELKERKE, S. Q. & KUIJPERS, T. W. 2014. Immunomodulation by IVIg and the Role of Fc-Gamma Receptors: Classic Mechanisms of Action after all? Frontiers in Immunology, 5, 674.

NAHRENDORF, M., SWIRSKI, F. K., AIKAWA, E., STANGENBERG, L., WURDINGER, T., FIGUEIREDO, J.-L., LIBBY, P., WEISSLEDER, R. & PITTET, M. J. 2007. The healing myocardium sequentially mobilizes two monocyte subsets with divergent and complementary functions. Journal of Experimental Medicine, 204, 3037-3047.

NAKAMURA, R., SENE, A., SANTEFORD, A., GDOURA, A., KUBOTA, S., ZAPATA, N. & APTE, R. S. 2015. IL10-driven STAT3 signalling in senescent macrophages promotes pathological eye angiogenesis. Nature communications, 6.

NARANBHAI, V., FAIRFAX, B. P., MAKINO, S., HUMBURG, P., WONG, D., NG, E., HILL, A. V. S. & KNIGHT, J. C. 2015. Genomic modulators of gene expression in human neutrophils. Nature communications, 6, 7545-7545.

NIGROVIC, P. A. & LEE, D. M. 2007. Synovial mast cells: role in acute and chronic arthritis. Immunological reviews, 217, 19-37.

NIMMERJAHN, F. & RAVETCH, J. V. 2008. Fc[gamma] receptors as regulators of immune responses. Nat Rev Immunol, 8, 34-47.

NIMMERJAHN, F. & RAVETCH, J. V. 2010. FcγRs in health and disease. Negative Co-Receptors and Ligands. Springer.

NOOKAEW, I., PAPINI, M., PORNPUTTAPONG, N., SCALCINATI, G., FAGERBERG, L. & UHLÉN, M. 2012. A comprehensive comparison of RNA-Seq-based transcriptome analysis from reads to differential gene expression and cross-comparison with microarrays: a case study in Saccharomyces cerevisiae. Nucleic Acids Res, 40.

O'NEILL, L. A. & PEARCE, E. J. 2016. Immunometabolism governs dendritic cell and macrophage function. Journal of Experimental Medicine, 213, 15-23.

ODEGAARD, J. I., RICARDO-GONZALEZ, R. R., GOFORTH, M. H., MOREL, C. R., SUBRAMANIAN, V., MUKUNDAN, L., EAGLE, A. R., VATS, D., BROMBACHER, F., FERRANTE, A. W. & CHAWLA, A. 2007. Macrophage-specific PPARγ controls alternative activation and improves insulin resistance. Nature, 447, 1116-1120.

ODERO, M. D., ZELEZNIK-LE, N. J., CHINWALLA, V. & ROWLEY, J. D. 2000. Cytogenetic and molecular analysis of the acute monocytic leukemia cell line THP-1 with an MLL-AF9 translocation. Genes Chromosomes Cancer, 29.

OGAWA, S., HIRANO, N., SATO, N., TAKAHASHI, T., HANGAISHI, A., TANAKA, K., KUROKAWA, M., TANAKA, T., MITANI, K. & YAZAKI, Y. 1994. Homozygous loss of the cyclin-dependent kinase 4-inhibitor (p16) gene in human leukemias. Blood, 84, 2431-2435.

OHTANI, H., JIN, Z., TAKEGAWA, S., NAKAYAMA, T. & YOSHIE, O. 2009. Abundant expression of CXCL9 (MIG) by stromal cells that include dendritic cells and accumulation of CXCR3+ T cells in lymphocyte-rich gastric carcinoma. The Journal of pathology, 217, 21-31.

OKADA, Y., HAN, B., TSOI, LAM C., STUART, PHILIP E., ELLINGHAUS, E., TEJASVI, T., CHANDRAN, V., PELLETT, F., POLLOCK, R., BOWCOCK, ANNE M., KRUEGER, GERALD G., WEICHENTHAL, M., VOORHEES, JOHN J., RAHMAN, P., GREGERSEN, PETER K., FRANKE, A., NAIR, RAJAN P., ABECASIS, GONÇALO R., GLADMAN, DAFNA D., ELDER, JAMES T., DE BAKKER, PAUL I. & RAYCHAUDHURI, S. 2014. Fine Mapping Major Histocompatibility Complex Associations in Psoriasis and Its Clinical Subtypes. American Journal of Human Genetics, 95, 162-172.

OKURA, Y., YAMADA, M., KURIBAYASHI, F., KOBAYASHI, I. & ARIGA, T. 2015. Monocyte/macrophage-specific NADPH oxidase contributes to antimicrobial host defense in X-CGD. Journal of clinical immunology, 35, 158-167.

OLMES, G., BÜTTNER-HEROLD, M., FERRAZZI, F., DISTEL, L., AMANN, K. & DANIEL, C. 2016. CD163+ M2c-like macrophages predominate in renal biopsies from patients with lupus nephritis. Arthritis Research & Therapy, 18, 90.

O'NEILL, L. A. J., KISHTON, R. J. & RATHMELL, J. 2016. A guide to immunometabolism for immunologists. Nat Rev Immunol, 16, 553-565.

OSHLACK, A. & WAKEFIELD, M. J. 2009. Transcript length bias in RNA-seq data confounds systems biology. Biol Direct, 4.

PAGÈS HERVE, C. M., FALCON SETH AND LI NIANHUA 2017. AnnotationDbi: Annotation Database Interface. R package version 1.40.0.

PANAYI, G. S. 2006. Even though T-cell-directed trials have been of limited success, is there reason for optimism? Nature clinical practice Rheumatology, 2, 58-59.

PANMONTHA, W., AMARINTHNUKROWH, P., DAMRONGPHOL, P., DESUDCHIT, T., SUPHAPEETIPORN, K. & SHOTELERSUK, V. 2016. Novel mutations in the FUCA1 gene that cause fucosidosis. Genetics and molecular research: GMR, 15.

PARK, E. K., JUNG, H. S., YANG, H. I., YOO, M. C., KIM, C. & KIM, K. S. 2007. Optimized THP-1 differentiation is required for the detection of responses to weak stimuli. Inflammation Research, 56, 45-50.

PARKHOMCHUK, D., BORODINA, T., AMSTISLAVSKIY, V., BANARU, M., HALLEN, L. & KROBITSCH, S. 2009. Transcriptome analysis by strand-specific sequencing of complementary DNA. Nucleic Acids Res, 37.

PATEL, R. K. & JAIN, M. 2012. NGS QC Toolkit: A Toolkit for Quality Control of Next Generation Sequencing Data. PLOS ONE, 7, e30619.

PERDIGUERO, E. G. & GEISSMANN, F. 2016. Development and maintainance of resident macrophages. Nature immunology, 17, 2-8.

PETRICOIN, E. F., ARDEKANI, A. M., HITT, B. A., LEVINE, P. J., FUSARO, V. A., STEINBERG, S. M., MILLS, G. B., SIMONE, C., FISHMAN, D. A. & KOHN, E. C. 2002. Use of proteomic patterns in serum to identify ovarian cancer. The lancet, 359, 572-577.

PFIRSCH-MAISONNAS, S., ALOULOU, M., XU, T., CLAVER, J., KANAMARU, Y., TIWARI, M., LAUNAY, P., MONTEIRO, R. C. & BLANK, U. 2011. Inhibitory ITAM Signaling Traps Activating Receptors with the Phosphatase SHP-1 to Form Polarized “Inhibisome” Clusters. Science Signaling, 4, ra24-ra24.

PILLAI, S., DASGUPTA, P. & CHELLAPPAN, S. P. 2015. Chromatin immunoprecipitation assays: analyzing transcription factor binding and histone modifications in vivo. Chromatin Protocols, 429-446.

PISKOL, R., RAMASWAMI, G. & LI, JIN B. 2013. Reliable Identification of Genomic Variants from RNA-Seq Data. American Journal of Human Genetics, 93, 641-651.

PLUTA, A., NYMAN, U., JOSEPH, B., ROBAK, T., ZHIVOTOVSKY, B. & SMOLEWSKI, P. 2006. The role of p73 in hematological malignancies. Leukemia, 20.

POITOU, C., DALMAS, E., RENOVATO, M., BENHAMO, V., HAJDUCH, F., ABDENNOUR, M., KAHN, J.-F., VEYRIE, N., RIZKALLA, S. & FRIDMAN, W.-H. 2011. CD14dimCD16+ and CD14+ CD16+ monocytes in obesity and during weight loss. Arteriosclerosis, thrombosis, and vascular biology, 31, 2322-2330.

POLZER, K., BAETEN, D., SOLEIMAN, A., DISTLER, J., GERLAG, D. M., TAK, P. P., SCHETT, G. & ZWERINA, J. 2008. Tumour necrosis factor blockade increases lymphangiogenesis in murine and human arthritic joints. Annals of the rheumatic diseases, 67, 1610-1616.

QIN, Z. 2012. The use of THP-1 cells as a model for mimicking the function and regulation of monocytes and macrophages in the vasculature. Atherosclerosis, 221, 2-11.

RAJAGOPALAN, P. R., ZHANG, Z., MCCOURT, L., DWYER, M., BENKOVIC, S. J. & HAMMES, G. G. 2002. Interaction of dihydrofolate reductase with methotrexate: ensemble and single-molecule kinetics. Proceedings of the National Academy of Sciences, 99, 13481-13486.

RAJKUMAR, A. P., QVIST, P., LAZARUS, R., LESCAI, F., JU, J., NYEGAARD, M., MORS, O., BØRGLUM, A. D., LI, Q. & CHRISTENSEN, J. H. 2015. Experimental validation of methods for differential gene expression analysis and sample pooling in RNA-seq. BMC Genomics, 16, 548.

RATH, M., MÜLLER, I., KROPF, P., CLOSS, E. I. & MUNDER, M. 2014. Metabolism via Arginase or Nitric Oxide Synthase: Two Competing Arginine Pathways in Macrophages. Frontiers in Immunology, 5, 532.

REICHNER, J. S., MESZAROS, A. J., LOUIS, C. A., HENRY, W. L., MASTROFRANCESCO, B., MARTIN, B.-A. & ALBINA, J. E. 1999. Molecular and metabolic evidence for the restricted expression of inducible nitric oxide synthase in healing wounds. The American journal of pathology, 154, 1097-1104.

REINARTZ, S., SCHUMANN, T., FINKERNAGEL, F., WORTMANN, A., JANSEN, J. M., MEISSNER, W., KRAUSE, M., SCHWÖRER, A. M., WAGNER, U. & MÜLLER-BRÜSSELBACH, S. 2014. Mixed-polarization phenotype of ascites-associated macrophages in human ovarian carcinoma: Correlation of CD163 expression, cytokine levels and early relapse. International journal of cancer, 134, 32-42.

REN, Y., TANG, J., MOK, M., CHAN, A. W., WU, A. & LAU, C. 2003. Increased apoptotic neutrophils and macrophages and impaired macrophage phagocytic clearance of apoptotic neutrophils in systemic lupus erythematosus. Arthritis & Rheumatology, 48, 2888-2897.

RICHTER, E., VENTZ, K., HARMS, M., MOSTERTZ, J. & HOCHGRÄFE, F. 2016. Induction of Macrophage Function in Human THP-1 Cells Is Associated with Rewiring

of MAPK Signaling and Activation of MAP3K7 (TAK1) Protein Kinase. Frontiers in Cell and Developmental Biology, 4.

ROBINSON, J. I. 2010. A fine mapping study of the FCGR locus in rheumatoid arthritis. University of Leeds.

ROBINSON, J. I., CARR, I. M., COOPER, D. L., RASHID, L. H., MARTIN, S. G., EMERY, P., ISAACS, J. D., BARTON, A., WILSON, A. G. & BARRETT, J. H. 2012. Confirmation of association of FCGR3B but not FCGR3A copy number with susceptibility to autoantibody positive rheumatoid arthritis. Human mutation, 33, 741-749.

ROBINSON, M. D., MCCARTHY, D. J. & SMYTH, G. K. 2010. edgeR: a Bioconductor package for differential expression analysis of digital gene expression data. Bioinformatics, 26.

RŐSZER, T. 2015. Understanding the mysterious M2 macrophage through activation markers and effector mechanisms. Mediators of inflammation, 2015.

ROUZAUT, A., SUBIRÁ, M. L., DE MIGUEL, C., DOMINGO-DE-MIGUEL, E., GONZÁLEZ, A., SANTIAGO, E. & LÓPEZ-MORATALLA, N. 1999. Co-expression of inducible nitric oxide synthase and arginases in different human monocyte subsets. Apoptosis regulated by endogenous NO. Biochimica et Biophysica Acta (BBA) - Molecular Cell Research, 1451, 319-333.

ROVERA, G., O'BRIEN, T. G. & DIAMOND, L. 1979. Induction of differentiation in human promyelocytic leukemia cells by tumor promoters. Science, 204, 868-870.

SAAG, K. G., KOEHNKE, R., CALDWELL, J. R., BRASINGTON, R., BURMEISTER, L. F., ZIMMERMAN, B., KOHLER, J. A. & FURST, D. E. 1994. Low dose long-term corticosteroid therapy in rheumatoid arthritis: An analysis of serious adverse events. The American Journal of Medicine, 96, 115-123.

SABEH, F., FOX, D. & WEISS, S. J. 2010. Membrane-type I matrix metalloproteinase-dependent regulation of rheumatoid arthritis synoviocyte function. The Journal of Immunology, 184, 6396-6406.

SALMON, J. E., EDBERG, J. C. & KIMBERLY, R. P. 1990. Fc gamma receptor III on human neutrophils. Allelic variants have functionally distinct capacities. Journal of Clinical Investigation, 85, 1287-1295.

SCHER, J. U. & ABRAMSON, S. B. 2011. The microbiome and rheumatoid arthritis. Nature Reviews Rheumatology, 7, 569-578.

SCHETT, G. & GRAVALLESE, E. 2012. Bone erosion in rheumatoid arthritis: mechanisms, diagnosis and treatment. Nature reviews. Rheumatology, 8, 656-664.

SCHETT, G., STACH, C., ZWERINA, J., VOLL, R. & MANGER, B. 2008. How antirheumatic drugs protect joints from damage in rheumatoid arthritis. Arthritis & Rheumatology, 58, 2936-2948.

SCHIFF, M. 2011. Abatacept treatment for rheumatoid arthritis. Rheumatology, 50, 437-449.

SCHILDBERGER, A., ROSSMANITH, E., EICHHORN, T., STRASSL, K. & WEBER, V. 2013. Monocytes, Peripheral Blood Mononuclear Cells, and THP-1 Cells Exhibit Different Cytokine Expression Patterns following Stimulation with Lipopolysaccharide. Mediators of Inflammation, 2013, 10.

SCHROEDER, A., MUELLER, O., STOCKER, S., SALOWSKY, R., LEIBER, M., GASSMANN, M., LIGHTFOOT, S., MENZEL, W., GRANZOW, M. & RAGG, T. 2006. The RIN: an RNA integrity number for assigning integrity values to RNA measurements. BMC Molecular Biology, 7, 3-3.

SCHWENDE, H., FITZKE, E., AMBS, P. & DIETER, P. 1996. Differences in the state of differentiation of THP-1 cells induced by phorbol ester and 1, 25-dihydroxyvitamin D3. Journal of leukocyte biology, 59, 555-561.

SEELING, M., HILLENHOFF, U., DAVID, J. P., SCHETT, G., TUCKERMANN, J., LUX, A. & NIMMERJAHN, F. 2013. Inflammatory monocytes and Fcγ receptor IV on osteoclasts are critical for bone destruction during inflammatory arthritis in mice. Proceedings of the National Academy of Sciences, 110, 10729-10734.

SEYMOUR, H. E., WORSLEY, A., SMITH, J. M. and THOMAS, S. H. L. (2001), Anti-TNF agents for rheumatoid arthritis. British Journal of Clinical Pharmacology, 51: 201–208. doi:10.1046/j.1365-2125.2001.00321.x

SHARIF, O., BOLSHAKOV, V. N., RAINES, S., NEWHAM, P. & PERKINS, N. D. 2007. Transcriptional profiling of the LPS induced NF-κB response in macrophages. BMC immunology, 8, 1.

SHATTOCK, R. J., FRIEDLAND, J. S. & GRIFFIN, G. E. 1994. Phagocytosis of Mycobacterium tuberculosis modulates human immunodeficiency virus replication in human monocytic cells. Journal of general virology, 75, 849-856.

SHAUL, M. E., BENNETT, G., STRISSEL, K. J., GREENBERG, A. S. & OBIN, M. S. 2010. Dynamic, M2-Like Remodeling Phenotypes of CD11c+ Adipose Tissue Macrophages During High-Fat Diet–Induced Obesity in Mice. Diabetes, 59, 1171-1181.

SHENOY, A. R., WELLINGTON, D. A., KUMAR, P., KASSA, H., BOOTH, C. J., CRESSWELL, P. & MACMICKING, J. D. 2012. GBP5 Promotes NLRP3 Inflammasome Assembly and Immunity in Mammals. Science, 336, 481-485.

SHI, H.-X., YANG, K., LIU, X., LIU, X.-Y., WEI, B., SHAN, Y.-F., ZHU, L.-H. & WANG, C. 2010. Positive regulation of interferon regulatory factor 3 activation by Herc5 via ISG15 modification. Molecular and cellular biology, 30, 2424-2436.

SHIELDS, R. L., LAI, J., KECK, R., O'CONNELL, L. Y., HONG, K., MENG, Y. G., WEIKERT, S. H. & PRESTA, L. G. 2002. Lack of fucose on human IgG1 N-linked oligosaccharide improves binding to human FcγRIII and antibody-dependent cellular toxicity. Journal of Biological Chemistry, 277, 26733-26740.

SHIMIZU, H., SAKANO, T., FUJIE, A., NISHIMURA, S. & UEDA, K. 1992. Modulation of C2 and C3 gene expression of human peripheral blood monocytes by interleukin 1β, interferon γ, tumor necrosis factor α and lipopolysaccharide. Cellular and Molecular Life Sciences, 48, 1148-1150.

SHIRATORI, H., FEINWEBER, C., LUCKHARDT, S., LINKE, B., RESCH, E., GEISSLINGER, G., WEIGERT, A. & PARNHAM, M. J. 2017. THP-1 and human peripheral blood mononuclear cell-derived macrophages differ in their capacity to polarize in vitro. Molecular Immunology, 88, 58-68.

SHUREIQI, I., WU, Y., CHEN, D., YANG, X. L., GUAN, B., MORRIS, J. S., YANG, P., NEWMAN, R. A., BROADDUS, R., HAMILTON, S. R., LYNCH, P., LEVIN, B., FISCHER, S. M. & LIPPMAN, S. M. 2005. Critical Role of 15-Lipoxygenase-1 in

Colorectal Epithelial Cell Terminal Differentiation and Tumorigenesis. Cancer research, 65, 11486-11492.

SICA, A. & MANTOVANI, A. 2012. Macrophage plasticity and polarization: in vivo veritas. The Journal of Clinical Investigation, 122, 787-795.

SIEGFRIED, A., BERCHTOLD, S., MANNCKE, B., DEUSCHLE, E., REBER, J., OTT, T., WEBER, M., KALINKE, U., HOFER, M. J. & HATESUER, B. 2013. IFIT2 is an effector protein of type I IFN–mediated amplification of lipopolysaccharide (LPS)-induced TNF-α secretion and LPS-induced endotoxin shock. The Journal of Immunology, 191, 3913-3921.

SIMS, D., SUDBERY, I., ILOTT, N. E., HEGER, A. & PONTING, C. P. 2014. Sequencing depth and coverage: key considerations in genomic analyses. Nat Rev Genet, 15.

SIRONI, M., MARTINEZ, F. O., D'AMBROSIO, D., GATTORNO, M., POLENTARUTTI, N., LOCATI, M., GREGORIO, A., IELLEM, A., CASSATELLA, M. A., VAN DAMME, J., SOZZANI, S., MARTINI, A., SINIGAGLIA, F., VECCHI, A. & MANTOVANI, A. 2006. Differential regulation of chemokine production by Fcγ receptor engagement in human monocytes: association of CCL1 with a distinct form of M2 monocyte activation (M2b, Type 2). Journal of Leukocyte Biology, 80, 342-349.

SMITH, K. G. C. & CLATWORTHY, M. R. 2010. FcγRIIB in autoimmunity and infection: evolutionary and therapeutic implications. Nature reviews. Immunology, 10, 328-343.

SOKOLOVE, J., JOHNSON, D. S., LAHEY, L. J., WAGNER, C. A., CHENG, D., THIELE, G. M., MICHAUD, K., SAYLES, H., REIMOLD, A. M., CAPLAN, L., CANNON, G. W., KERR, G., MIKULS, T. R. & ROBINSON, W. H. 2014. Rheumatoid factor as a potentiator of anti-citrullinated protein antibody mediated inflammation in rheumatoid arthritis. Arthritis & rheumatology (Hoboken, N.J.), 66, 813-821.

SOLBERG, R., SMITH, R., ALMLÖF, M., TEWOLDE, E., NILSEN, H. & JOHANSEN, H. T. 2015. Legumain expression, activity and secretion are increased during monocyte-to-macrophage differentiation and inhibited by atorvastatin. Biological chemistry, 396, 71-80.

SOLER PALACIOS, B., ESTRADA-CAPETILLO, L., IZQUIERDO, E., CRIADO, G., NIETO, C., MUNICIO, C., GONZÁLEZ-ALVARO, I., SÁNCHEZ-MATEOS, P., PABLOS, J. L. & CORBÍ, A. L. 2015. Macrophages from the synovium of active rheumatoid arthritis exhibit an activin A-dependent pro-inflammatory profile. The Journal of pathology, 235, 515-526.

SONG, Y. W. & KANG, E. H. 2010. Autoantibodies in rheumatoid arthritis: rheumatoid factors and anticitrullinated protein antibodies. QJM: An International Journal of Medicine, 103, 139-146.

SONG, Y. W., HAN, C. W., KANG, S. W., BAEK, H. J., LEE, E. B., SHIN, C. H., HAHN, B. H. & TSAO, B. P. 1998. Abnormal distribution of Fcγ receptor type IIa polymorphisms in Korean patients with systemic lupus erythematosus. Arthritis & Rheumatology, 41, 421-426.

SPANO, A., BARNI, S. & SCIOLA, L. 2013. PMA withdrawal in PMA-treated monocytic THP-1 cells and subsequent retinoic acid stimulation, modulate induction of apoptosis and appearance of dendritic cells. Cell proliferation, 46, 328-347.

SPEIR, M. L., ZWEIG, A. S., ROSENBLOOM, K. R., RANEY, B. J., PATEN, B., NEJAD, P., LEE, B. T., LEARNED, K., KAROLCHIK, D., HINRICHS, A. S., HEITNER, S., HARTE, R. A., HAEUSSLER, M., GURUVADOO, L., FUJITA, P. A., EISENHART, C., DIEKHANS, M., CLAWSON, H., CASPER, J., BARBER, G. P., HAUSSLER, D., KUHN, R. M. & KENT, W. J. 2016. The UCSC Genome Browser database: 2016 update. Nucleic Acids Research, 44, D717-D725.

SPENCER, M., YAO-BORENGASSER, A., UNAL, R., RASOULI, N., GURLEY, C. M., ZHU, B., PETERSON, C. A. & KERN, P. A. 2010. Adipose tissue macrophages in insulin-resistant subjects are associated with collagen VI and fibrosis and demonstrate alternative activation. American Journal of Physiology - Endocrinology and Metabolism, 299, E1016-E1027.

SPURRELL, J. C., WIEHLER, S., ZAHEER, R. S., SANDERS, S. P. & PROUD, D. 2005. Human airway epithelial cells produce IP-10 (CXCL10) in vitro and in vivo upon rhinovirus infection. American Journal of Physiology-Lung Cellular and Molecular Physiology, 289, L85-L95.

STAMATOS, N. M., LIANG, F., NAN, X., LANDRY, K., CROSS, A. S., WANG, L. X. & PSHEZHETSKY, A. V. 2005. Differential expression of endogenous sialidases of human monocytes during cellular differentiation into macrophages. The FEBS journal, 272, 2545-2556.

STEFANI, G. & SLACK, F. J. 2008. Small non-coding RNAs in animal development. Nature reviews Molecular cell biology, 9, 219-230.

STÖGER, J. L., GIJBELS, M. J. J., VAN DER VELDEN, S., MANCA, M., VAN DER LOOS, C. M., BIESSEN, E. A. L., DAEMEN, M. J. A. P., LUTGENS, E. & DE WINTHER, M. P. J. 2012. Distribution of macrophage polarization markers in human atherosclerosis. Atherosclerosis, 225, 461-468.

STONE, S. & LA FLAMME, A. C. 2016. Type II Activation of Macrophages and Microglia by Immune Complexes Enhances Th17 Biasing in an IL-6-Independent Manner. PLoS ONE, 11, e0164454.

STOUT, R. D., JIANG, C., MATTA, B., TIETZEL, I., WATKINS, S. K. & SUTTLES, J. 2005. Macrophages Sequentially Change Their Functional Phenotype in Response to Changes in Microenvironmental Influences. The Journal of Immunology, 175, 342-349.

STUBBS, V. E. L., POWER, C. & PATEL, K. D. 2010. Regulation of eotaxin-3/CCL26 expression in human monocytic cells. Immunology, 130, 74-82.

STURM, M., SCHROEDER, C. & BAUER, P. 2016. SeqPurge: highly-sensitive adapter trimming for paired-end NGS data. BMC Bioinformatics, 17, 208.

SU, K., WU, J., EDBERG, J. C., LI, X., FERGUSON, P., COOPER, G. S., LANGEFELD, C. D. & KIMBERLY, R. P. 2004. A promoter haplotype of the immunoreceptor tyrosine-based inhibitory motif-bearing FcγRIIb alters receptor expression and associates with autoimmunity. I. Regulatory FCGR2B polymorphisms and their association with systemic lupus erythematosus. The Journal of Immunology, 172, 7186-7191.

SUN, J., SUN, J., SONG, B., ZHANG, L., SHAO, Q., LIU, Y., YUAN, D., ZHANG, Y. & QU, X. 2016. Fucoidan inhibits CCL22 production through NF-κB pathway in M2 macrophages: a potential therapeutic strategy for cancer. Scientific reports, 6, 35855.

SWEENEY, S. E., KIMBLER, T. B. & FIRESTEIN, G. S. 2010. Synoviocyte innate responses: II. Pivotal role of interferon regulatory factor 3. Journal of immunology (Baltimore, Md. : 1950), 184, 7162-7168.

SZEKANECZ, Z. & KOCH, A. E. 2007. Macrophages and their products in rheumatoid arthritis. Current opinion in rheumatology, 19, 289-295.

SZULZEWSKY, F., PELZ, A., FENG, X., SYNOWITZ, M., MARKOVIC, D., LANGMANN, T., HOLTMAN, I. R., WANG, X., EGGEN, B. J. L., BODDEKE, H. W. G. M., HAMBARDZUMYAN, D., WOLF, S. A. & KETTENMANN, H. 2015. Glioma-Associated Microglia/Macrophages Display an Expression Profile Different from M1 and M2 Polarization and Highly Express Gpnmb and Spp1. PLOS ONE, 10, e0116644.

TACKE, F. & RANDOLPH, G. J. 2006. Migratory fate and differentiation of blood monocyte subsets. Immunobiology, 211, 609-618.

TAKEMURA, R., STENBERG, P. E., BAINTON, D. F. & WERB, Z. 1986. Rapid redistribution of clathrin onto macrophage plasma membranes in response to Fc receptor-ligand interaction during frustrated phagocytosis. The Journal of Cell Biology, 102, 55-69.

TAMURA, T., TAILOR, P., YAMAOKA, K., KONG, H. J., TSUJIMURA, H., O'SHEA, J. J., SINGH, H. & OZATO, K. 2005. IFN Regulatory Factor-4 and -8 Govern Dendritic Cell Subset Development and Their Functional Diversity. The Journal of Immunology, 174, 2573-2581.

TANAKA, H., MATSUSHIMA, H., MIZUMOTO, N. & TAKASHIMA, A. 2009. Classification of chemotherapeutic agents based on their differential in vitro impacts on dendritic cells. Cancer research, 69, 6978-6986.

TANAKA, T., NARAZAKI, M. & KISHIMOTO, T. 2014. IL-6 in Inflammation, Immunity, and Disease. Cold Spring Harbor Perspectives in Biology, 6, a016295.

TANAKA, Y., SUZUKI, Y., TSUGE, T., KANAMARU, Y., HORIKOSHI, S., MONTEIRO, R. C. & TOMINO, Y. 2005. FcγRIIa-131R allele and FcγRIIIa-176V/V genotype are risk factors for progression of IgA nephropathy. Nephrology Dialysis Transplantation, 20, 2439-2445.

TANNAHILL, G. M., CURTIS, A. M., ADAMIK, J., PALSSON-MCDERMOTT, E. M., MCGETTRICK, A. F., GOEL, G., FREZZA, C., BERNARD, N. J., KELLY, B., FOLEY, N. H., ZHENG, L., GARDET, A., TONG, Z., JANY, S. S., CORR, S. C., HANEKLAUS, M., CAFFERY, B. E., PIERCE, K., WALMSLEY, S., BEASLEY, F. C., CUMMINS, E., NIZET, V., WHYTE, M., TAYLOR, C. T., LIN, H., MASTERS, S. L., GOTTLIEB, E., KELLY, V. P., CLISH, C., AURON, P. E., XAVIER, R. J. & O'NEILL, L. A. J. 2013. Succinate is a danger signal that induces IL-1β via HIF-1α. Nature, 496, 238-242.

TARAZONA, S., GARCIA-ALCALDE, F., DOPAZO, J., FERRER, A. & CONESA, A. 2011. Differential expression in RNA-seq: a matter of depth. Genome Res, 21.

TERSTAPPEN, L., NGUYEN, M., LAZARUS, H. M. & MEDOF, M. E. 1992. Expression of the DAF (CD55) and CD59 antigens during normal hematopoietic cell differentiation. Journal of leukocyte biology, 52, 652-660.

THAPA, M., WELNER, R. S., PELAYO, R. & CARR, D. J. J. 2008. CXCL9 and CXCL10 expression are critical for control of genital herpes simplex virus type 2

infection through mobilization of HSV-specific CTL and NK cells to the nervous system. Journal of immunology (Baltimore, Md. : 1950), 180, 1098-1106.

THOMAS, A. C. & MATTILA, J. T. 2014. “Of Mice and Men”: Arginine Metabolism in Macrophages. Frontiers in Immunology, 5, 479.

THUL, P. J., ÅKESSON, L., WIKING, M., MAHDESSIAN, D., GELADAKI, A., BLAL, H. A., ALM, T., ASPLUND, A., BJÖRK, L. & BRECKELS, L. M. 2017. A subcellular map of the human proteome. Science, 356, eaal3321.

TIMMERMAN, K. L., FLYNN, M. G., COEN, P. M., MARKOFSKI, M. M. & PENCE, B. D. 2008. Exercise training-induced lowering of inflammatory (CD14+ CD16+) monocytes: a role in the anti-inflammatory influence of exercise? Journal of leukocyte biology, 84, 1271-1278.

TRAPNELL, C., PACHTER, L. & SALZBERG, S. L. 2009. TopHat: discovering splice junctions with RNA-Seq. Bioinformatics, 25.

TRIPAL, P., BAUER, M., NASCHBERGER, E., MÖRTINGER, T., HOHENADL, C., CORNALI, E., THURAU, M. & STÜRZL, M. 2007. Unique features of different members of the human guanylate-binding protein family. Journal of interferon & cytokine research, 27, 44-52.

TSUCHIYA, S., KOBAYASHI, Y., GOTO, Y., OKUMURA, H., NAKAE, S., KONNO, T. & TADA, K. 1982. Induction of maturation in cultured human monocytic leukemia cells by a phorbol diester. Cancer Res, 42.

TSUCHIYA, S., YAMABE, M., YAMAGUCHI, Y., KOBAYASHI, Y., KONNO, T. & TADA, K. 1980. Establishment and characterization of a human acute monocytic leukemia cell line (THP-1). Int J Cancer, 26.

TULK, S. E., LIAO, K. C., MURUVE, D. A., LI, Y., BECK, P. L. & MACDONALD, J. A. 2015. Vitamin D3 Metabolites Enhance the NLRP3-Dependent Secretion of IL-1β From Human THP-1 Monocytic Cells. Journal of cellular biochemistry, 116, 711-720.

UMAÑA, P., JEAN–MAIRET, J., MOUDRY, R., AMSTUTZ, H. & BAILEY, J. E. 1999. Engineered glycoforms of an antineuroblastoma IgG1 with optimized antibody-dependent cellular cytotoxic activity. Nature biotechnology, 17, 176-180.

VAN DER HEIJDEN, J., BREUNIS, W. B., GEISSLER, J., DE BOER, M., VAN DEN BERG, T. K. & KUIJPERS, T. W. 2012. Phenotypic variation in IgG receptors by nonclassical FCGR2C alleles. The Journal of Immunology, 188, 1318-1324.

VAN LOO, P., TOUSSEYN, T., VANHENTENRIJK, V., DIERICKX, D., MALECKA, A., BEMPT, I. V., VERHOEF, G., DELABIE, J., MARYNEN, P., MATTHYS, P. & DE WOLF-PEETERS, C. 2010. T-cell/histiocyte-rich large B-cell lymphoma shows transcriptional features suggestive of a tolerogenic host immune response. Haematologica, 95, 440-448.

VERDUGO, R. A., ZELLER, T., ROTIVAL, M., WILD, P. S., MÜNZEL, T., LACKNER, K. J., WEIDMANN, H., NINIO, E., TRÉGOUËT, D.-A., CAMBIEN, F., BLANKENBERG, S. & TIRET, L. 2013. Graphical Modeling of Gene Expression in Monocytes Suggests Molecular Mechanisms Explaining Increased Atherosclerosis in Smokers. PLoS ONE, 8, e50888.

VIDARSSON, G., DEKKERS, G. & RISPENS, T. 2014. IgG Subclasses and Allotypes: From Structure to Effector Functions. Frontiers in Immunology, 5, 520.

VILLANI, A.-C., SATIJA, R., REYNOLDS, G., SARKIZOVA, S., SHEKHAR, K., FLETCHER, J., GRIESBECK, M., BUTLER, A., ZHENG, S., LAZO, S., JARDINE, L., DIXON, D., STEPHENSON, E., NILSSON, E., GRUNDBERG, I., MCDONALD, D., FILBY, A., LI, W., DE JAGER, P. L., ROZENBLATT-ROSEN, O., LANE, A. A., HANIFFA, M., REGEV, A. & HACOHEN, N. 2017. Single-cell RNA-seq reveals new types of human blood dendritic cells, monocytes, and progenitors. Science, 356.

VILLIGER, P. M., CRONIN, M. T., AMENOMORI, T., WACHSMAN, W. & LOTZ, M. 1991. IL-6 production by human T lymphocytes. Expression in HTLV-1-infected but not in normal T cells. The Journal of Immunology, 146, 550-559.

VINCIOTTI, V., WIT, E. C., JANSEN, R., DE GEUS, E. J. C. N., PENNINX, B. W. J. H., BOOMSMA, D. I. & 'T HOEN, P. A. C. 2016. Consistency of biological networks inferred from microarray and sequencing data. BMC Bioinformatics, 17, 254.

VITAL, E. M. & EMERY, P. 2006. Abatacept in the treatment of rheumatoid arthritis. Therapeutics and Clinical Risk Management, 2, 365-375.

VOGEL, D. Y. S., GLIM, J. E., STAVENUITER, A. W. D., BREUR, M., HEIJNEN, P., AMOR, S., DIJKSTRA, C. D. & BEELEN, R. H. J. 2014. Human macrophage polarization in vitro: Maturation and activation methods compared. Immunobiology, 219, 695-703.

VOGELPOEL, L. T. C., BAETEN, D. L. P., DE JONG, E. C. & DEN DUNNEN, J. 2015. Control of Cytokine Production by Human Fc Gamma Receptors: Implications for Pathogen Defense and Autoimmunity. Frontiers in Immunology, 6, 79.

VON GUNTEN, S. and Bochner, B.S., 2008. Basic and clinical immunology of Siglecs. *Annals of the New York Academy of Sciences*, *1143*(1), pp.61-82.

WABY, J. S., CHIRAKKAL, H., YU, C., GRIFFITHS, G. J., BENSON, R. S. P., BINGLE, C. D. & CORFE, B. M. 2010. Sp1 acetylation is associated with loss of DNA binding at promoters associated with cell cycle arrest and cell death in a colon cell line. Molecular Cancer, 9, 275-275.

WAGENAAR-BOS, I. G. & HACK, C. E. 2006. Structure and function of C1-inhibitor. Immunology and Allergy Clinics, 26, 615-632.

WALKER, D. G. & LUE, L.-F. 2015. Immune phenotypes of microglia in human neurodegenerative disease: challenges to detecting microglial polarization in human brains. Alzheimer's Research & Therapy, 7, 56.

WANG, C., GONG, B., BUSHEL, P. R., THIERRY-MIEG, J., THIERRY-MIEG, D., XU, J., FANG, H., HONG, H., SHEN, J. & SU, Z. 2014. The concordance between RNA-seq and microarray data depends on chemical treatment and transcript abundance. Nature biotechnology, 32, 926-932.

WANG, C., GONG, B., BUSHEL, P. R., THIERRY-MIEG, J., THIERRY-MIEG, D., XU, J., FANG, H., HONG, H., SHEN, J. & SU, Z. 2014a. The concordance between RNA-seq and microarray data depends on chemical treatment and transcript abundance. Nature biotechnology, 32, 926-932.

WANG, K., SINGH, D., ZENG, Z., COLEMAN, S. J., HUANG, Y. & SAVICH, G. L. 2010a. MapSplice: accurate mapping of RNA-seq reads for splice junction discovery. Nucleic Acids Res, 38.

WANG, N., LIANG, H. & ZEN, K. 2014. Molecular Mechanisms That Influence the Macrophage M1–M2 Polarization Balance. Frontiers in Immunology, 5, 614.

WANG, N., LIANG, H. & ZEN, K. 2014b. Molecular Mechanisms That Influence the Macrophage M1–M2 Polarization Balance. Frontiers in Immunology, 5, 614.

WANG, Q., NI, H., LAN, L., WEI, X., XIANG, R. & WANG, Y. 2010b. Fra-1 protooncogene regulates IL-6 expression in macrophages and promotes the generation of M2d macrophages. Cell research, 20, 701-712.

WANG, Z., GERSTEIN, M. & SNYDER, M. 2009. RNA-Seq: a revolutionary tool for transcriptomics. Nature reviews. Genetics, 10, 57-63.

WEISBERG, S. P., MCCANN, D., DESAI, M., ROSENBAUM, M., LEIBEL, R. L. & FERRANTE, A. W. 2003. Obesity is associated with macrophage accumulation in adipose tissue. Journal of Clinical Investigation, 112, 1796-1808.

WELLS, C. A., RAVASI, T., FAULKNER, G. J., CARNINCI, P., OKAZAKI, Y., HAYASHIZAKI, Y., SWEET, M., WAINWRIGHT, B. J. & HUME, D. A. 2003. Genetic control of the innate immune response. BMC Immunology, 4, 5-5.

WENG, W.-K. & LEVY, R. 2003. Two immunoglobulin G fragment C receptor polymorphisms independently predict response to rituximab in patients with follicular lymphoma. Journal of clinical oncology, 21, 3940-3947.

WERMUTH, P. J. & JIMENEZ, S. A. 2015. The significance of macrophage polarization subtypes for animal models of tissue fibrosis and human fibrotic diseases. Clinical and Translational Medicine, 4, 2.

WHYTE, C. S., BISHOP, E. T., RÜCKERL, D., GASPAR-PEREIRA, S., BARKER, R. N., ALLEN, J. E., REES, A. J. & WILSON, H. M. 2011. Suppressor of cytokine signaling (SOCS) 1 is a key determinant of differential macrophage activation and function. Journal of leukocyte biology, 90, 845-854.

WILHELM, B. T. & LANDRY, J.-R. 2009. RNA-Seq—quantitative measurement of expression through massively parallel RNA-sequencing. Methods, 48, 249-257.

WILKINSON, D. G. 2001. Multiple roles of EPH receptors and ephrins in neural development. Nature Reviews Neuroscience, 2, 155-164.

WILLCOCKS, L. C., LYONS, P. A., CLATWORTHY, M. R., ROBINSON, J. I., YANG, W., NEWLAND, S. A., PLAGNOL, V., MCGOVERN, N. N., CONDLIFFE, A. M., CHILVERS, E. R., ADU, D., JOLLY, E. C., WATTS, R., LAU, Y. L., MORGAN, A. W., NASH, G. & SMITH, K. G. C. 2008. Copy number of FCGR3B, which is associated with systemic lupus erythematosus, correlates with protein expression and immune complex uptake. The Journal of Experimental Medicine, 205, 1573-1582.

WILLEMZE, A., BÖHRINGER, S., KNEVEL, R., LEVARHT, E. N., STOEKEN-RIJSBERGEN, G., HOUWING-DUISTERMAAT, J. J., VAN DER HELM-VAN, A. H., HUIZINGA, T. W., TOES, R. E. & TROUW, L. A. 2012. The ACPA recognition profile and subgrouping of ACPA-positive RA patients. Annals of the rheumatic diseases, 71, 268-274.

WILSON, H. M. 2014. SOCS proteins in macrophage polarization and function. Frontiers in immunology, 5.

WISNIEWSKI, H.-G., HUA, J., POPPERS, D. M., NAIME, D., VILCEK, J. & CRONSTEIN, B. N. 1996. TNF/IL-1-inducible protein TSG-6 potentiates plasmin

inhibition by inter-alpha-inhibitor and exerts a strong anti-inflammatory effect in vivo. The Journal of Immunology, 156, 1609-1615.

WON, J., YIM, J. & KIM, T. K. 2002. Sp1 and Sp3 recruit histone deacetylase to repress transcription of human telomerase reverse transcriptase (hTERT) promoter in normal human somatic cells. Journal of Biological Chemistry, 277, 38230-38238.

WRIGHT, H. L., MOOTS, R. J. & EDWARDS, S. W. 2014. The multifactorial role of neutrophils in rheumatoid arthritis. Nat Rev Rheumatol, 10, 593-601.

WU, W., DIETZE, K. K., GIBBERT, K., LANG, K. S., TRILLING, M., YAN, H., WU, J., YANG, D., LU, M. & ROGGENDORF, M. 2015. TLR ligand induced IL-6 counter-regulates the anti-viral CD8+ T cell response during an acute retrovirus infection. Scientific reports, 5, 10501.

WYNN, T. A., CHAWLA, A. & POLLARD, J. W. 2013. Origins and Hallmarks of Macrophages: Development, Homeostasis, and Disease. Nature, 496, 445-455.

XAUS, J., CARDÓ, M., VALLEDOR, A. F., SOLER, C., LLOBERAS, J. & CELADA, A. 1999. Interferon γ induces the expression of p21 waf-1 and arrests macrophage cell cycle, preventing induction of apoptosis. Immunity, 11, 103-113.

XIE, C., LIU, C., WU, B., LIN, Y., MA, T., XIONG, H., WANG, Q., LI, Z., MA, C. & TU, Z. 2016. Effects of IRF1 and IFN-β interaction on the M1 polarization of macrophages and its antitumor function. International journal of molecular medicine, 38, 148-160.

XUE, J., SCHMIDT, SUSANNE V., SANDER, J., DRAFFEHN, A., KREBS, W., QUESTER, I., DE NARDO, D., GOHEL, TRUPTI D., EMDE, M., SCHMIDLEITHNER, L., GANESAN, H., NINO-CASTRO, A., MALLMANN, MICHAEL R., LABZIN, L., THEIS, H., KRAUT, M., BEYER, M., LATZ, E., FREEMAN, TOM C., ULAS, T. & SCHULTZE, JOACHIM L. Transcriptome-Based Network Analysis Reveals a Spectrum Model of Human Macrophage Activation. Immunity, 40, 274-288.

YAMADA, E., TSUKAMOTO, Y., SASAKI, R., YAGYU, K. & TAKAHASHI, N. 1997. Structural changes of immunoglobulin G oligosaccharides with age in healthy human serum. Glycoconjugate Journal, 14, 401-405.

YANG, I. S. & KIM, S. 2015. Analysis of Whole Transcriptome Sequencing Data: Workflow and Software. Genomics & Informatics, 13, 119-125.

YENDREK, C. R., AINSWORTH, E. A. & THIMMAPURAM, J. 2012. The bench scientist's guide to statistical analysis of RNA-Seq data. BMC Research Notes, 5, 506-506.

YILMAZ-ELIS, A. S., RAMIREZ, J. M., ASMAWIDJAJA, P., VAN DER KAA, J., MUS, A.-M., BREM, M. D., CLAASSENS, J. W., BREUKEL, C., BROUWERS, C. & MANGSBO, S. M. 2014. FcγRIIb on myeloid cells rather than on B cells protects from collagen-induced arthritis. The Journal of Immunology, 192, 5540-5547.

YIN, J., FU, W., DAI, L., JIANG, Z., LIAO, H., CHEN, W., PAN, L. & ZHAO, J. 2017. ANKRD22 promotes progression of non-small cell lung cancer through transcriptional up-regulation of E2F1. Scientific Reports, 7, 4430.

YONA, S., KIM, K.-W., WOLF, Y., MILDNER, A., VAROL, D., BREKER, M., STRAUSS-AYALI, D., VIUKOV, S., GUILLIAMS, M., MISHARIN, A., HUME, D. A., PERLMAN, H., MALISSEN, B., ZELZER, E. & JUNG, S. 2013. Fate mapping reveals

origins and dynamics of monocytes and tissue macrophages under homeostasis. Immunity, 38, 79-91.

YOUNG, M. D., WAKEFIELD, M. J., SMYTH, G. K. & OSHLACK, A. 2010. Gene ontology analysis for RNA-seq: accounting for selection bias. Genome Biol, 11.

YU, G. & HE, Q.-Y. 2016. ReactomePA: an R/Bioconductor package for reactome pathway analysis and visualization. Molecular BioSystems, 12, 477-479.

YU, G. 2012. Statistical analysis and visualization of functional profiles for genes and gene clusters. Journal of Integrative Biology, 16, 284-287.

YU, G., WANG, L.-G., HAN, Y. & HE, Q.-Y. 2012. clusterProfiler: an R package for comparing biological themes among gene clusters. Omics: a journal of integrative biology, 16, 284-287.

YUAN, A., HSIAO, Y.-J., CHEN, H.-Y., CHEN, H.-W., HO, C.-C., CHEN, Y.-Y., LIU, Y.-C., HONG, T.-H., YU, S.-L., CHEN, J. J. W. & YANG, P.-C. 2015. Opposite Effects of M1 and M2 Macrophage Subtypes on Lung Cancer Progression. Scientific Reports, 5, 14273.

YUASA, T., KUBO, S., YOSHINO, T., UJIKE, A., MATSUMURA, K., ONO, M., RAVETCH, J. V. & TAKAI, T. 1999. Deletion of Fcγ receptor IIB renders H-2b mice susceptible to collagen-induced arthritis. Journal of Experimental Medicine, 189, 187-194.

ZASŁONA, Z., PRZYBRANOWSKI, S., WILKE, C., VAN ROOIJEN, N., TEITZ-TENNENBAUM, S., OSTERHOLZER, J. J., WILKINSON, J. E., MOORE, B. B. & PETERS-GOLDEN, M. 2014. Resident Alveolar Macrophages Suppress, whereas Recruited Monocytes Promote, Allergic Lung Inflammation in Murine Models of Asthma. The Journal of Immunology, 193, 4245-4253.

ZENG, C., WANG, W., YU, X., YANG, L., CHEN, S. & LI, Y. 2015. Pathways related to PMA-differentiated THP1 human monocytic leukemia cells revealed by RNA-Seq. Science China Life Sciences, 58, 1282-1287.

ZEYDA, M., FARMER, D., TODORIC, J., ASZMANN, O., SPEISER, M., GYÖRI, G., ZLABINGER, G. & STULNIG, T. 2007. Human adipose tissue macrophages are of an anti-inflammatory phenotype but capable of excessive pro-inflammatory mediator production. International journal of obesity, 31, 1420.

ZHANG, F. X., KIRSCHNING, C. J., MANCINELLI, R., XU, X.-P., JIN, Y., FAURE, E., MANTOVANI, A., ROTHE, M., MUZIO, M. & ARDITI, M. 1999. Bacterial lipopolysaccharide activates nuclear factor-κB through interleukin-1 signaling mediators in cultured human dermal endothelial cells and mononuclear phagocytes. Journal of Biological Chemistry, 274, 7611-7614.

ZHANG, G., HOU, J., SHI, J., YU, G., LU, B. & ZHANG, X. 2008. Soluble CD276 (B7-H3) is released from monocytes, dendritic cells and activated T cells and is detectable in normal human serum. Immunology, 123, 538-546.

ZHAO, S., FUNG-LEUNG, W.-P., BITTNER, A., NGO, K. & LIU, X. 2014. Comparison of RNA-Seq and Microarray in Transcriptome Profiling of Activated T Cells. PLOS ONE, 9, e78644.

ZHOU, D., HUANG, C., LIN, Z., ZHAN, S., KONG, L., FANG, C. & LI, J. 2014. Macrophage polarization and function with emphasis on the evolving roles of coordinated regulation of cellular signaling pathways. Cellular signalling, 26, 192-197.

ZHOU, L., SHEN, L.-H., HU, L.-H., GE, H., PU, J., CHAI, D.-J., SHAO, Q., WANG, L., ZENG, J.-Z. & HE, B. 2010. Retinoid X receptor agonists inhibit phorbol-12-myristate-13-acetate (PMA)-induced differentiation of monocytic THP-1 cells into macrophages. Molecular and cellular biochemistry, 335, 283-289.

ZIEGLER-HEITBROC, H., THIEL, E., FUTTERER, A., HERZOG, V., WIRTZ, A. & RIETHMÜLLER, G. 1988. Establishment of a human cell line (Mono Mac 6) with characteristics of mature monocytes. International Journal of Cancer, 41, 456-461.

ZIZZO, G., HILLIARD, B. A., MONESTIER, M. & COHEN, P. L. 2012. Efficient clearance of early apoptotic cells by human macrophages requires “M2c” polarization and MerTK induction. Journal of immunology (Baltimore, Md. : 1950), 189, 3508-3520.